Université de Montréal

The synthesis and characterisation of new complexes based on novel triazine tridentate and pentadentate ligands.

Par

Elaine Medlycott

Département de chimie

Faculté des aqrts et des sciences

Thèse présentée à la Faculté des études supérieures

en vue de l'obtention du grade de Philosophiæ Doctor (Ph.D.) en chimie

September 2006

Université de Montréal
Faculté des études supérieures

Cette thèse intitulée :

The synthesis and characterisation of new complexes based on novel triazine tridentate and pentadentate ligands.

présentée par :
Elaine Medlycott

a été évaluée par un jury composé des personnes suivantes :

Prof. Christian Reber, président-rapporteur
Prof. Garry Hanan, directeur de recherche
Prof. Frank Schaper, membre du jury
Prof. Michael Ward, examinateur externe
Prof. Christian Reber, représentant du doyen de la FES

Abstract

The versatility of a triazine ring-forming reaction has been explored for the synthesis of two classes of ligands: 2,4-di(2'-pyridyl)-6-(aryl)-1,3,5-triazine and 2,4-bis(α,α-dipyridyl)-6-(aryl)-1,3,5-triazine. The first class of ligands have a tridentate coordination motif and have been applied to the synthesis of Ru(II) complexes in efforts to improve the photophysical properties of the classic Ru(II) complex based on 2,2':6':2''-terpyridine (tpy). The aryl group may be varied, and introducing a bromo-phenyl substituent enables a 'chemistry on the complex' approach to introduce a range of additional chromophores. Alternatively, fused aromatic rings may be introduced directly onto the triazine ring using a modified synthetic approach. The bromo-phenyl substituent in itself offers a means to gain directional control of the aggregation of cations in the solid state through stabilising halogen-halogen interactions. Short Br-Br contacts are observed in a number of complexes of first row metals employing the 2,4-di(2'-pyridyl)-6-(*p*-bromo-phenyl)-1,3,5-triazine ligand.

Substitution of the pyridyl rings whilst maintaining the *p*-bromo-phenyl triazine core provides a means to manipulate the magnetic properties of Fe(II) complexes. Introducing sterically demanding groups adjacent to the coordinating N atom can induce elongated Fe-N bond distances thereby forcing the Fe(II) centre into a high spin configuration.

The second class of triazine ligands allows access to a pentadentate coordinating ligand through the substitution of pyridyl rings with α,α-dipyridyl rings. The electron deficient triazine ring can stabilise Cu(I) cations enabling full characterisation of a dinuclear, helical complex in solution and the solid state.

The photophysical, magnetic, redox and electronic properties have been studied depending on the coordination complexes synthesised. The complexes have been characterised mainly by solution nuclear magnetic resonance spectroscopy (^{1}H and ^{13}C{^{1}H} NMR, mass spectrometry, elemental analyses and, in many cases, analyses in the solid state has been carried out crystallographically by X-ray diffraction.

Key Words: Triazine, tridentate, pentadentate, photophysical properties, magnetic properties, X-ray diffraction, redox.

Résumé

La versatilité d'un ligand triazine pouvant former des réactions a été explorée, dans un but synthétique, pour deux classes de ligands : 2,4-di(2'-pyridyl)-6-(aryl)-1,3,5-triazine et 2,4-bis(α,α-dipyridyl)-6-(aryl)-1.3.5-triazine. La première classe de ligands possède un motif de coordination tridentate et a été utilisée dans la synthèse de complexe de Ru(II) dans le but d'améliorer les propriétés photophysiques du complexe classique de Ru(II) basé sur la 2,2' : 6',2''-terpyridine (tpy). Le groupement aryle peut être variable et l'introduction d'un substituant bromo-phényle rend possible l'approche de la « chimie sur le complexe » dans le but d'introduire une variété de chromophores additionnels. D'un autre côté, des cycles aromatiques fusionnés peuvent être introduits directement sur le cycle de la triazine par une approche synthétique modifiée. Le substituant bromo-phényle offre en soi un moyen de gagner un contrôle directionnel sur l'agrégation de cations dans l'état solide en stabilisant les interactions halogène-halogène. Des contacts Br-Br courts sont observés dans plusieurs complexes de métaux de première rangée employant le ligand 2,4-di(2'-pyridyl)-6-(*p*-bromo-phényl)-1,3,5-triazine.

La substitution des cycles pyridyles tout en maintenant le noyau *p*-bromo-phényl-triazine fournit une méthode permettant la manipulation des propriétés magnétiques pour les complexes de Fe(II). L'introduction d'un groupement demandant, d'un point de vue stérique, en position adjacente à l'atome d'azote, peut induire un allongement de la longueur des liens Fe-N et ainsi forcer le centre de Fe(II) à adopter une configuration à haut spin.

La deuxième classe de ligand triazine permet l'accès à une coordination potentiellement pentavalente par la substitution des cycles pyridyles en α,α-dipyridyles. Le cycle triazine déficient en électron peut stabiliser les cations de Cu(I) et permettre la caractérisation complète d'un complexe dinucléaire hélicoïdale en solution et à l'état solide.

Les propriétés photophysiques, magnétiques, électroniques et d'oxydoréduction ont été observées selon la coordination des complexes synthétisés. Les complexes ont

été caractérisés principalement par spectroscopie de résonance magnétique nucléaire en solution (^{1}H et $^{13}C\{^{1}H\}$ NMR), spectroscopie de masse, analyse élémentaire et, dans certains cas, des analyses cristallographiques à l'état solide ont été faites par diffraction des rayons X.

Mots clés: triazine, tridentate, pentadentate, propriétés photophysiques, propriétés magnétiques, diffraction des rayons X, redox.

Table of contents

List of Figures

List of Schemes

List of Tables

List of abbreviations

Å	Angstrom
Δ	heat
δ	chemical shift
EA	elemental analysis
bpy	2,2'-bipyridine
br	broad
Bu	butyl
cif	crystallographic information file
COSY	correlation spectroscopy
d	doublet
dba	dibenzylideneacetone
DCM	dichloromethane
DMF	N,N-dimethylformamide
DMSO	dimethylsulfoxyde
equiv	equivalents
EtOH	ethanol
Et_2O	diethyl ether
ES	electrospray
Fig.	figure
HOMO	highest occupied molecular orbital
ILCT	intra-ligand charge-transfer
J	coupling constant
L	neutral ligand
LUMO	lowest unoccupied molecular orbital
M	metal
m	multiplet
MC	metal-centred
MLCT	metal-to-ligand charge-transfer
MS	mass spectrometry

m/z	mass /charge
min	minute
Me	methyl
MeCN	acetonitrile
MeOH	methanol
NMR	nuclear magnetic resonance
NOE	nuclear overhauser effect
nBu	n-butyl
ns	nanosecond
o	ortho
OAc	acetate
ORTEP	Oak Ridge thermal ellipsoid program
OSWV	Osteryoung square-wave voltammetry
p	para
Ph	phenyl
ppm	parts per million
py	pyridine
qnpy	2,2‘:6’,2”:6 ”,2”’:6”’,2’”-quinquepyridine
R	Structure factor ($\sum \|\|F_o\| - \|F_c\|\| / \sum \|F_o\|$)
t	triplet
r.t.	room temperature
^{t}Bu	*tert*-butyl
THF	tetrahydrofuran
tpy	2,2’:6’:2’’-terpyridine
trz	triazine
2-tpt	2,4,6-tris(2’-pyridyl)-1,3,5-triazine
4-tpt	2,4,6-tris(4’-pyridyl)-1,3,5-triazine

Acknowledgements

I would like to begin by thanking my supervisor, Professor Garry Hanan for giving me the opportunity to carry out this research towards my PhD. His experience, advice and motivation have been fundamental to the completion of this thesis and an inspiration for the future.

This research would not have been possible with out the financial assistance from the Commonwealth scholarship funded through International Council for Canadian Studies, Université de Montréal and the Comité des études supérieures at the l'Université de Montréal.

I'd like to thank the many graduate students and post doctoral fellows I have had the pleasure to work with in Garry's group including Mike Cooke, Matthew Polson, Elena Ioachim, Joseph Wang, Viviane Friese and more recently Isabelle Theobald, Pierre-Tremblay, Francois Laverdiere and Marie-Pierre Santoni. I wish to thank Mike in particular as his patience, advice and insights have been invaluable over the years.

I would like to thank Francine Bélanger-Gariépy for her patience and advice in the area of crystallography. Her support and knowledge enabled me to advance in the field and improve both my confidence and competence. Additional thanks go to Dr. Michel Simard, Dr. Thierry Maris and Dr. Frank Schaper for their advice in the area of crystallography. I thank the technical services at Université de Montréal including Sylvie Bilodeau and Dr. Tan Phan Viet of the NMR service, Karine Venne and Dr. Alexandra Furtos of the mass spectrometry service and Huguette Dinel of the elemental analysis service.

I was fortunate to be able to carry out an externship in the group of Dr. Gareth Williams in Durham, UK. I would like to thank both Gareth and his group for

welcoming me into their group and for all their assistance in the photophysical experiments performed. Additional thanks go to the groups of Dr. Sebastiano Campagna at the University of Messina, Italy and Prof. Laurie Thompson at Memorial University for their collaborations with photophysical and magnetic measurements.

Finally I would like to thank my family and Daniel for their continued support and confidence throughout this PhD.

Chapter I: Introduction

1.1 General Background

The 1,3,5-triazine motif has become an important molecular component for organic, supramolecular and coordination chemists due to its diverse reactivity and electronic and structural influences.[1] As a consequence, triazine-containing compounds have found applications in catalysis,[2, 3] medicinal chemistry[4] and polymer chemistry[5] as well as contributing significantly to the herbicide industry.[6]

The commercially available compound, 1,3,5-trichloro-2,4,6-triazine (trivially known as cyanuric chloride), is frequently employed as a versatile building block for the synthesis of a range of triazine compounds. Nucleophilic substitution of the chloride atoms proceeds relatively easily using a range of nucleophiles.[7-9] By controlling the temperature, tri-amino substituted triazines can be accessed as outlined in Figure 1.1.[10]

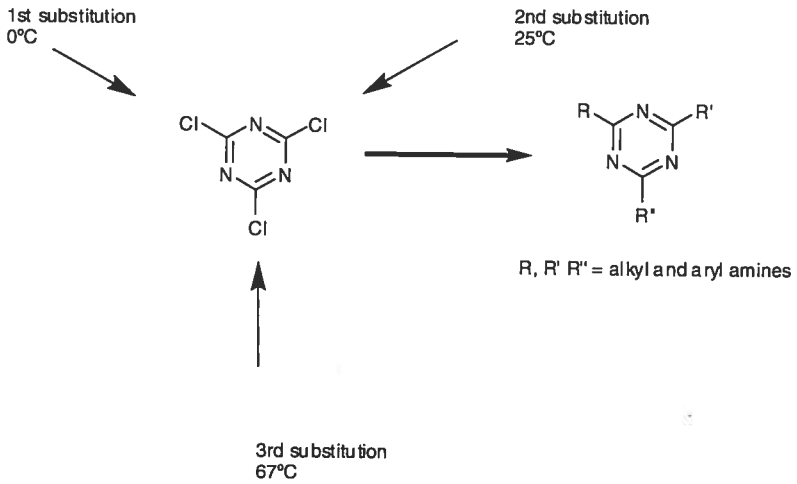

Figure 1.1 Differential reactivity of cyanuric chloride.[10]

The cyanuric chloride core is highly activated compared to alternative aryl cores due to the electropositive character of the N atoms. For this reason organometallic cross coupling reactions may also be employed to allow easy access to unsymmetric aryl-

substituted triazine rings.[11-14] Alternatively, the triazine ring may be generated by using one of two approaches.[15] The first approach is more versatile and allows access to unsymmetrically substituted diaryl and triaryl triazines by reaction of N-cyanoamidines with a chloromethyleniminium salt (Figure 1.2a).[16]

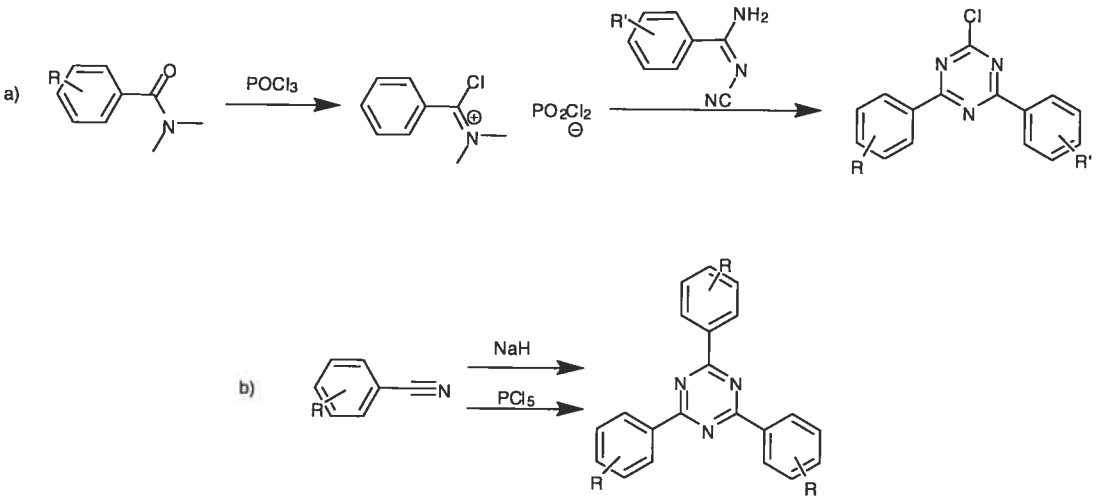

Scheme 1.1 a) Cyclisation reaction of benzonitriles or pyridyl-nitriles, b) the reaction of *N*-cyanoamidines with a chloromethyleniminium salt.

The second approach involves a cyclisation reaction with cyano-containing precursors (Figure 1.2b).[17-21] This has proven to be efficient for the rapid synthesis of aryl-substituted triazines, but is normally limited to symmetric triazines. Despite the limitations, heterocycles can be employed to replace benzonitriles, enabling easy access to ligands such as 2,4,6-tris(4'-pyridyl)-1,3,5-triazine (4-tpt) and 2,4,6-tris(2'-pyridyl)-1,3,5-triazine (2-tpt) which have been extensively used in coordination chemistry and crystal engineering.[18] In addition to the pyridyl-substituted triazine ligands, a 2,2'-bipyridine-based triazine ligand, 2,4,6-tris(6'-α,α-dipyridyl)-1,3,5-triazine (6-tbpt) could be synthesised using the same methodology, however, the coordination chemistry of this ligand remains unexplored due to its limited solubility.[19]

1.2 2,4,6-tris(4'-pyridyl)-1,3,5-triazine (4-tpt)

The (4-tpt) ligand has been used extensively over the last decade in the area of crystal engineering. The first crystallographically characterised coordination polymer using this connector was reported in 1995 by Robson and co-workers.[22] The 4-pyridyl ring permits monodentate coordination to a range of metal ions in which the triazine ring provides the central rigid structure.[23]

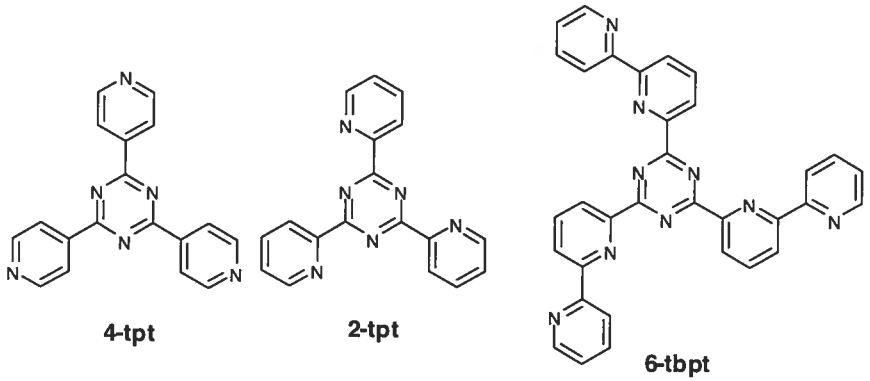

Figure 1.2 Symmetric 4-tpt, 2-tpt and 6-tbpt ligands.

In addition to polymer formation 4-tpt has been used extensively in the synthesis of discrete molecular assemblies suc,h as the coordination cage synthesised by Fujita and co-workers (Figure 1.3).[24]

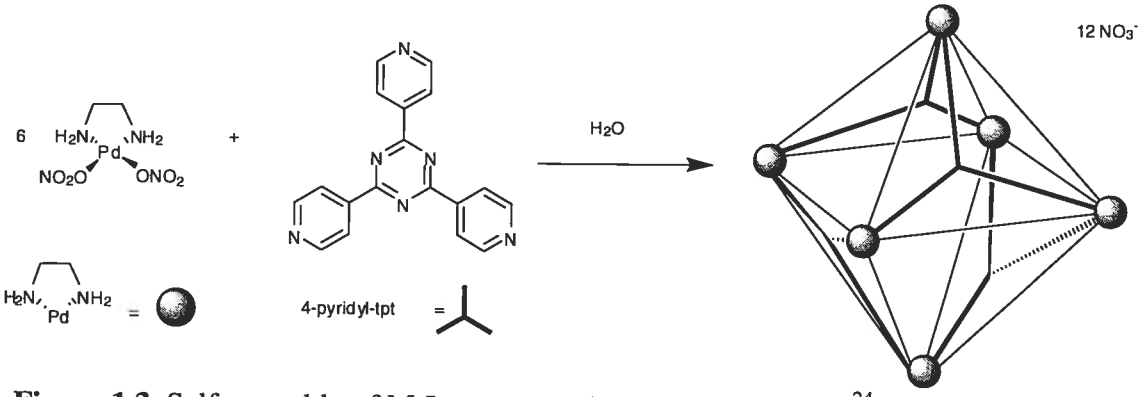

Figure 1.3 Self assembly of M_6L_4 as an octahedral cage in water.[24]

The self assembly of the octahedral cage has been monitored by NMR and shown to be the thermodynamic product, forming even in the presence of excess palladium starting

material. To date, the host-guest chemistry of this coordination cage has been studied extensively.[25-27] It has been shown that the cavity can behave as a 'molecular flask' for carrying out reactions. In particular, the photodimerisation of olefins within this cage show enhanced reaction rates as well as perfect regio- and stereo-selectivity.[28] The catalytic activity observed is a result of the phase transfer properties of the coordination cage, which brings the organic substrates into the aqueous environment where the Pd catalyst can carry out the transformation.

1.3 2,4,6-tris(2'-pyridyl)-1,3,5-triazine (2-tpt)

2-tpt was first synthesised in 1959 and is now commercially available due to its ease of synthesis.[18] The coordinating ability of 2-tpt is more diverse than 4-tpt as the potential exists to display η^1, η^2 or η^3 coordination modes to form mono, bi, tri, or polynuclear complexes.[29-33] The predominant coordination mode is tridentate (Figure 1.4), but a combination of tridetate and bidentate modes is also frequently observed in dinuclear complexes.

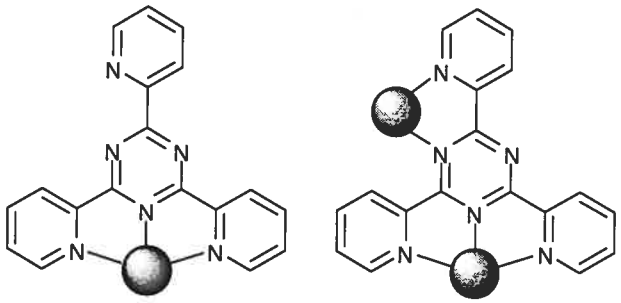

Figure 1.4 The η^3 coordination mode (left), and the η^3- η^2 dinuclear coordination mode (right).[34]

1.3.1 Bidentate chelate complexes of 2-tpt

The bidentate coordination mode of 2-tpt affords complexes with an additional, readily accessible coordination motif for the formation of oligonuclear complexes.[35-37] However, discrete mononuclear complexes with η^2-coordination to 2-tpt often possess

interesting fluxional solution behaviour due to the availability of the adjacent pyridyl rings (Figure 1.5).[38, 39]

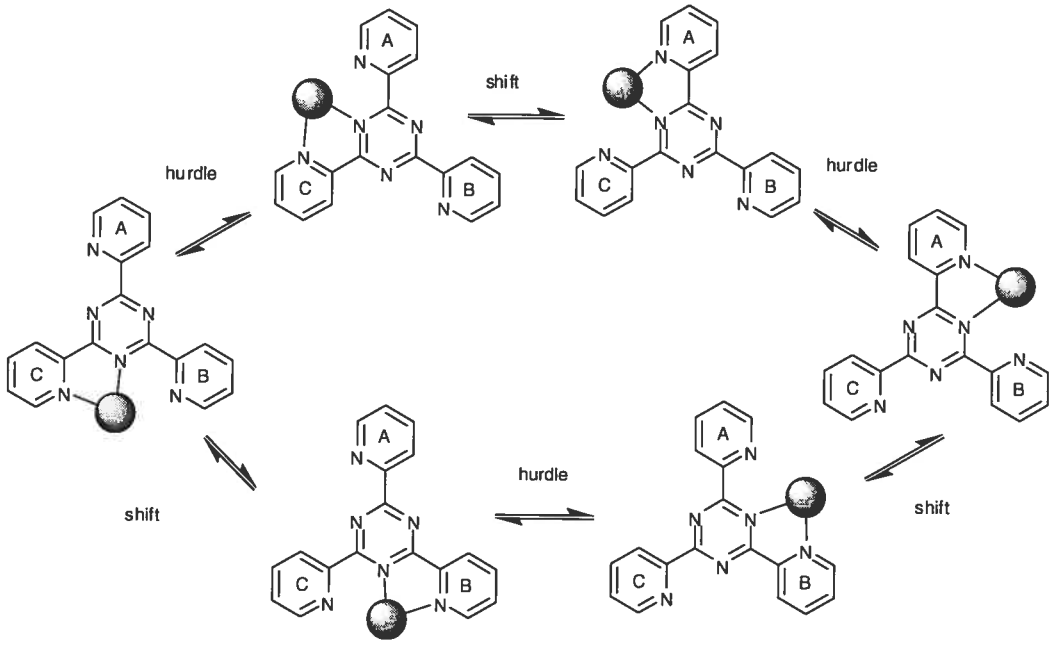

Figure 1.5 The exchange pathways for the dynamic processes in Pt(II) and Pd(II) complexes of 2-tpt.[39]

These processes have been studied by NMR, and it was found that the fluxional behaviour involves "metal hurdling" of a C–C bond followed by the movement of the metal from one edge of the central ligand ring to an adjacent edge, thereby enabling a 1,4-metallotropic shift to coordinate to the adjacent pyridyl ring (Figure 1.5).

1.3.2 Homoleptic Coordination Complexes of 2-tpt: $[M(tpt)_2]^{2+}$

In the tridentate η^3 coordination mode, 2-tpt can behave in the same manner as 2,2':6',2''-terpyridine (tpy) which has been used extensively in many areas of coordination chemistry due to the interesting structural, magnetic, redox and photophysical properties of the bis-terimine systems.[40-42] Tpy was originally synthesized in the 1930's by oxidative coupling of pyridine.[43, 44] However, the synthetic procedures have advanced significantly, giving a range of readily accessible

tpy analogues.[45-49] Despite the structural and geometric diversity displayed by complexes of 2-tpt, the development of more sophisticated systems is limited by the inability to carry out further substitution reactions as is typically performed to develop more evolved tpy-based systems.

The homoleptic $Fe(tpt)_2^{2+}$ and $Co(tpt)_2^{2+}$complexes were initially synthesized in order to study their stability and dissociation kinetics.[50-52] On complexation to Fe(II) an intense purple colour was obtained due to a metal-to-ligand charge-transfer (MLCT) band in the visible region of the spectra. Magnetic studies of this complex indicated that it was low spin at room temperature.[53] The $Fe(tpy)_2^{2+}$ complex is similarly diamagnetic and low spin at room temperature. However, facile modification of the tpy core enables manipulation of the magnetic properties through steric and electronic effects and consequently, high-spin and spin-crossover complexes of the $Fe(tpy)_2^{2+}$-motif can be synthesised.[54, 55]

Ni(II) homoleptic complexes of tpt have been synthesised and characterised in aqueous solution.[32] In contrast to the Cu(II) complexes, the $Ni(tpt)_2^{2+}$ complexes have greater stability in aqueous solution. $Cu(tpt)_2^{2+}$ complexes have been studied in the solid state, but the Cu(II) ion promotes nucleophilic attack and hence hydrolysis of the ligand. Complete hydrolysis of 2-tpt proceeds relatively easily to form the bis(2-pyridylcarbonyl)amine) (bpca) ligand (Figure 1.6). The metal-promoted hydrolysis of tpt was first reported in 1976 by Lippard *et al.*[56] The effect has now been observed with a number of monovalent, divalent and trivalent ions including Cr(III), Fe(II), Fe(III) and Co(III), Ni(II), Zn(II), Re(I), Ru(II), Os(II) and Rh(III).[36, 57-64]

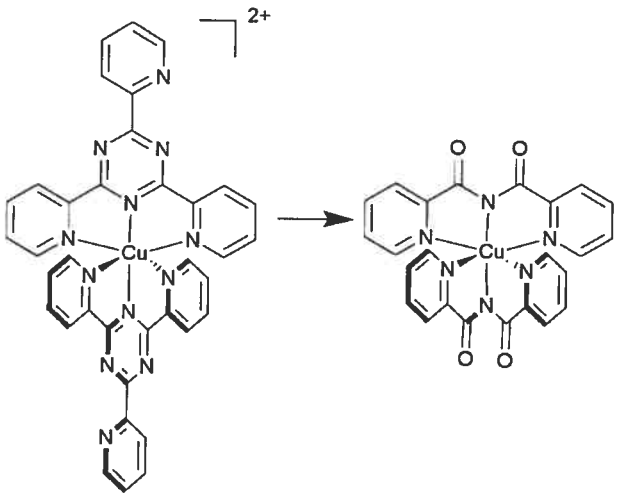

Figure 1.6 Hydrolysis of $Cu(tpt)_2^{2+}$ to $Cu(bpca)_2$.[56]

The rate and ease of hydrolysis is highly dependant on the metal ion and its valency. For monovalent M(I) ions (e.g. Re(I)), the metal promoted hydrolysis will only proceed in dinuclear complexes, $[Re_2tpt]^{2+}$, and requires the presence of alcoholic or aqueous solutions (Figure 1.7).

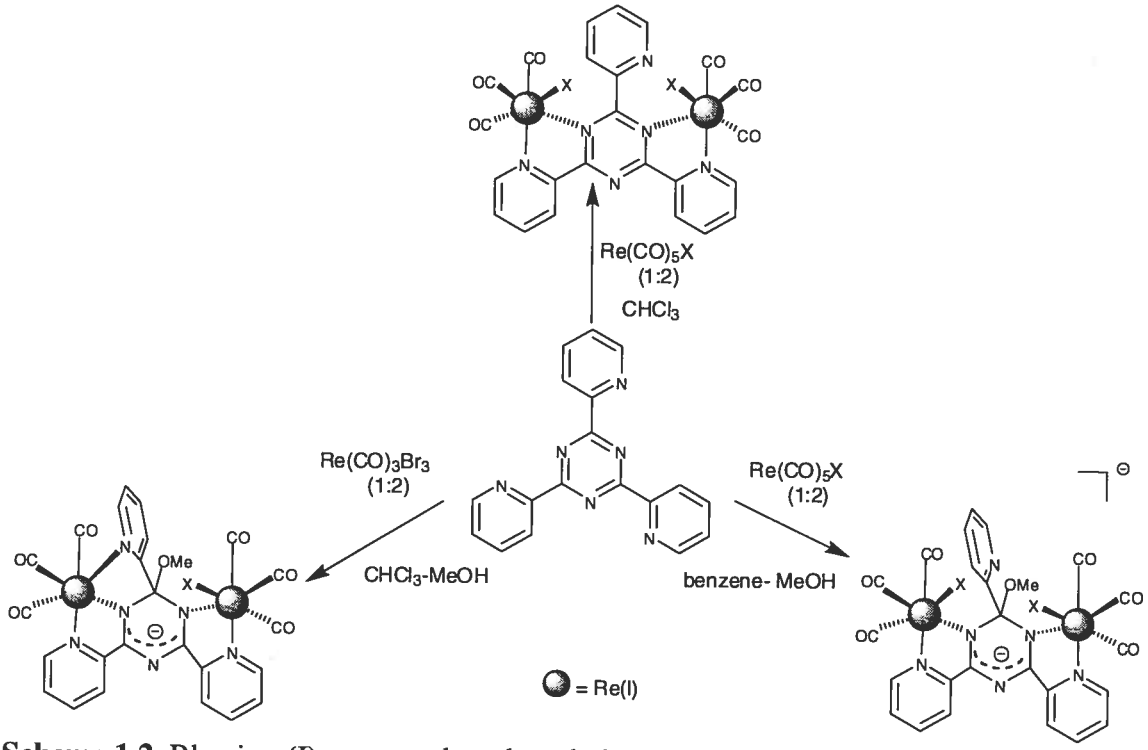

Scheme 1.2 Rhenium(I)-promoted methoxylation of the triazine ring in binuclear complexes.

1.4 Ru (II) complexes of triazine ligands

Ru (II) complexes of polypyridyl ligands have been extensively studied due to their interesting photophysical properties which may be applied for potential light-harvesting applications.[42, 65] Complexes of tridentate tpy-based ligands are structurally favoured over the bidentate polypyridine ligands based on 2,2'-bipyridine (bpy).[42] Despite the interesting properties obtained in complexes of bpy-type ligands,[65-67] rapid synthesis of polymetallic systems can be problematic due to the separation of *facial* and *meridonal* diastereomers.[42] Unfortunately, the photophysical properties of the $Ru(tpy)_2^{2+}$-type complexes are inferior to their bidentate counterparts based on $Ru(bpy)_3^{2+}$. An excited state lifetime of 0.25 ns is observed for $Ru(tpy)_2^{2+}$ at room temperature, while that of $Ru(bpy)_3^{2+}$ has a lifetime near 850 ns.[68] The steric strain resulting from tridentate coordination reduces the ligand field strength of the tpy as compared to the bidentate-bpy analogues. Consequently, deactivation via thermal access to metal-centred (MC), non-emissive states is enhanced at room temperature. Two approaches have been taken to improve the photophysical $Ru(tpy)_2^{2+}$-based complexes: a) Substitution on the tpy ligand thereby maintaining the tpy core, and b) changes in the coordination sphere upon replacement of the pyridyl rings with alternative heterocycles.[68]

As a consequence, Ru(II) complexes of tpt have been studied as tpy analogues for such potential applications as probes for biologically relevant molecules (e.g. DNA).[33, 69] However, manipulation and optimization of the photophyscial properties of $Ru(tpt)_2^{2+}$-type complexes is limited due to the difficulty of substituting the tpt ligand.

A synthetic methodology was previously developed in our laboratory which enables access to asymmetric triazine ligands whilst maintaining the bis-(2-pyridyl)-s-triazine core. Phenyl, toluyl and 4-pyridyl groups were introduced in the pendant positions in an effort to tune the photophysical properties of Ru(II) complexes of tridentate triazine-based ligands (Scheme 1.3).[21, 70]

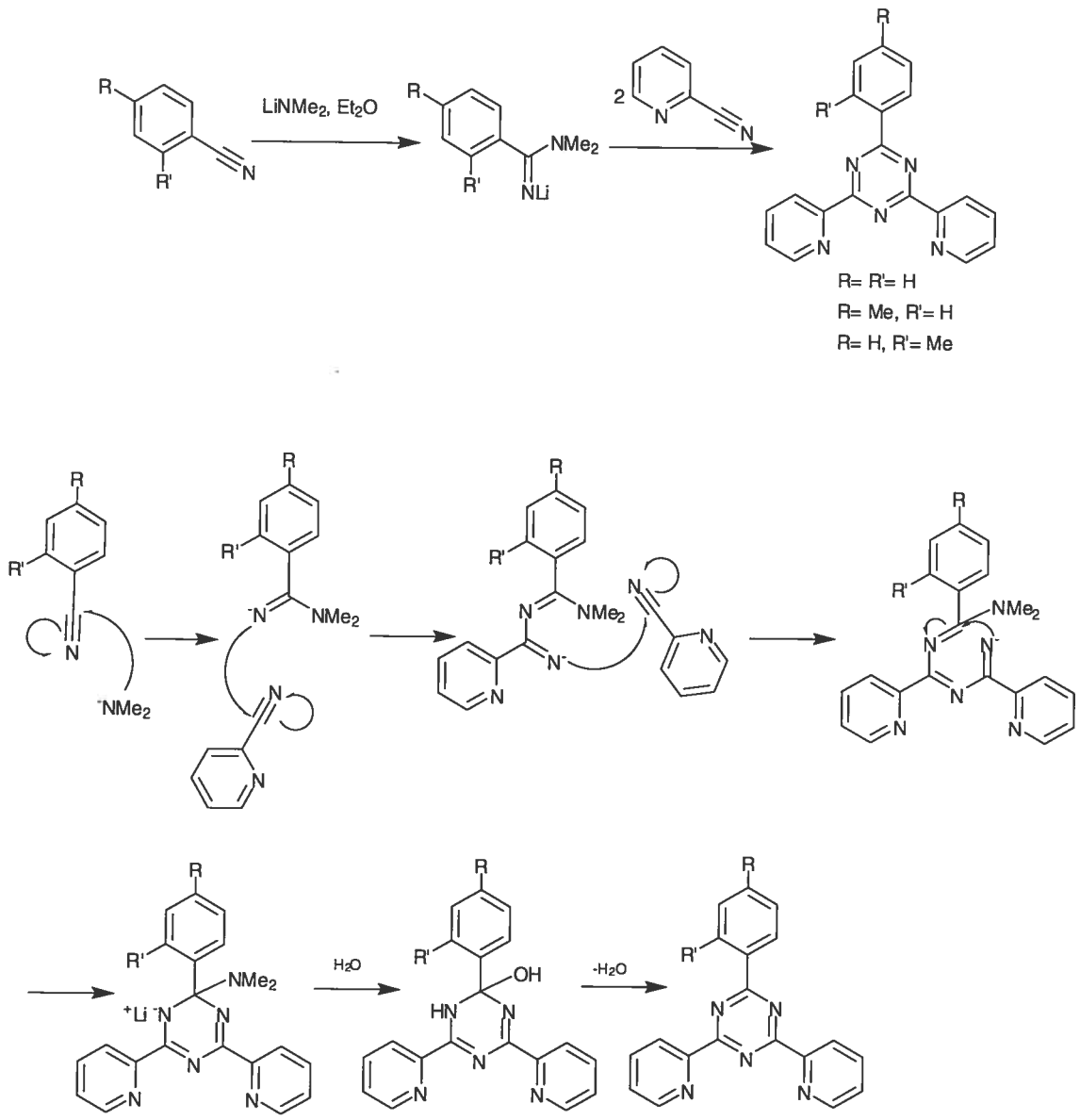

Scheme 1.3 Synthesis of asymmetric triazine ligands (above), mechanism of reaction (below).[21]

This synthetic approach highlighted in scheme 1.2 was successful for 2,4-di(2'-pyridyl)-6-(aryl)-1,3,5-triazine where the aryl group is phenyl-, *o*-toluyl and *p*-toluyl groups. However, efforts to introduce a 4-pyridyl ring onto the pendant position was not successful using this approach.[70] Instead a statistical method was employed using

a 'melt' cyclisation reaction with a mixture of 2-cyanopyridine and 4-cyanopyridine (Scheme 1.4).

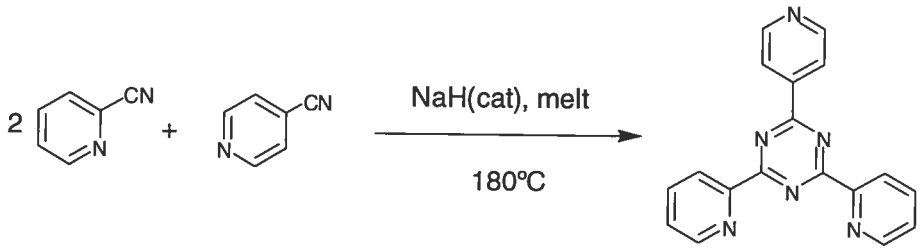

Scheme 1.4 Statistical reaction for the synthesis of 2,4-di(2'-pyridyl)-6-(4'-pyridyl))-1,3,5-triazine.

The homoleptic and heteroleptic-tpy complexes were synthesised for the family of ligands as outlined in scheme 1.5.

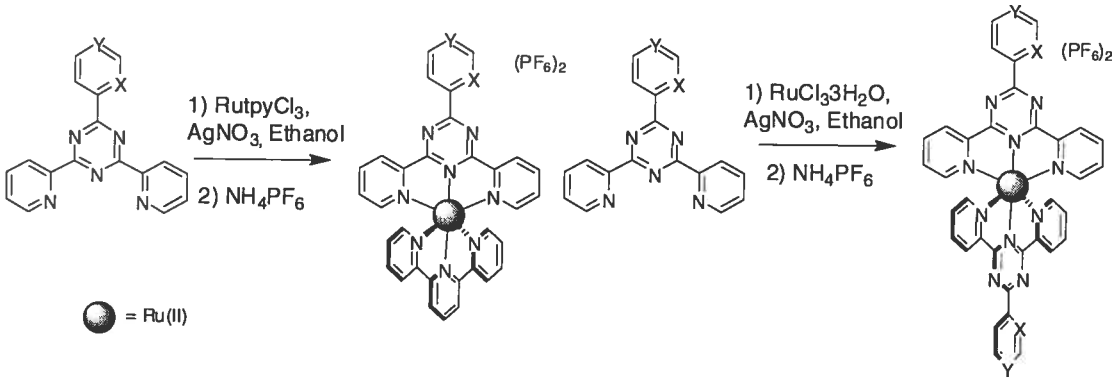

Scheme 1.5 Synthesis of triazine complexes where X =Y=H; X= H, Y= Me; X= Me, Y= H; and X= H, Y= N.[70]

These triazine ligands serve to improve the photophyscial properties of their complexes relative to those of $Ru(tpy)_2^{2+}$, since the electron-deficient triazine ligands stabilize the emissive ^{3}MLCT states through low-lying ligand centred orbitals. Higher energy MC states are unaffected and, thus, the non-emissive MC states are no longer readily accessible at room temperature. The triazine-based complexes emit from their ^{3}MLCT state with lifetimes in the range of 5-15 ns.

1.5 Research Objectives

The coordination chemistry of 2-tpt and related ligands is diverse but limited by the inability to carry out further substitution reactions on the ligand core. Recent developments in the synthesis of 2,4-di(2'-pyridyl)-6-(aryl)-1,3,5-triazine ligands has made possible the synthesis of a range of tridentate triazine ligands. The main objective of this research is to explore the versatility of this reaction and to synthesise triazine ligands with substituted aryl and pyridyl rings. Subtle alterations in these ligands can give rise to disproportionately large changes in the properties of their coordination complexes. These complexes have been characterised by NMR and, in many cases the solid-state structures have been obtained by X-ray diffraction techniques. In addition, the photophysical and magnetic properties have been studied in certain complexes.

Chapter I: This consists of a brief introduction into the applications of triazine ligands to areas of coordination chemistry. This introduction is complementary and serves as a platform to the short introductions given in each chapter and the review reported in chapter II, part A.

Chapter II: The first part of this chapter will introduce synthetic strategies from a published review article previously employed in the synthesis of Ru(II) complexes of tridentate ligands with desirable photophysical properties. The second half of chapter II will report the synthesis of a bromo-substituted triazine ligand and its Ru(II) complexes. The bromo-functionality allows the introduction of a range of organic chromophores by a 'chemistry-on-the-complex' approach or through classical ligand preparation.

Chapter III: This chapter will discuss the solid state and solution properties of Zn(II) and Ru(II) complexes of 2,4-di(2'-pyridyl)-6-(aryl)-1,3,5-triazine ligands in which aryl= naphthyl, phenathryl and pyrenyl substituents. The dependence of the electronic

properties on the fused aromatic ring will be discussed for the Zn(II) complexes and compared to those of Ru(II) complexes.

Chapter IV: This chapter will discuss unpublished work on the synthesis and characterisation of Rh(III) complexes with a bromo-substituted triazine ligand. The electronic properties will be probed by varying the electron-donating properties of the orthogonal ligand.

Chapter V: The first half of this chapter will introduce a family of Co(II) complexes based on triazine ligands for potential applications as redox mediators in dye sensitised solar cells (DSSC's) with particular emphasis on their electrochemical properties. The second half of this chapter discusses the solid state properties of Co(II), Fe (II), Ni(II) and Cu(II) complexes of 2,4-di(2'-pyridyl)-6-(*p*-bromo-phenyl)-1,3,5-triazine and 2,4-di(2'-pyridyl)-6-(*p*-toluyl)-1,3,5-triazine.

Chapter VI: In this chapter, synthesis of triazine ligands will be reported in which the pyridyl rings in 2,4-di(2'-pyridyl)-6-(*p*-bromo-phenyl)-1,3,5-triazine are replaced or substituted. The steric and electronic influence on the magnetic properties of Fe(II) complexes will be reported.

Chapter VII: The synthesis of a pentacoordinate triazine based ligand and its Cu(I) dihelical complex will be described. The solid state and redox properties will be discussed in light of applications as molecular switches.

Chapter VIII: This chapter will review the results and highlight the most important points, as well as discuss future perspectives of the projects reported.

1.6 References

1. P. Gamez and J. Reedijk, *Eur. J. Inorg. Chem.*, 2006, 29.
2. X.-P. Hu, H.-L. Chen and Z. Zheng, *Adv. Synth. Cat.*,, 2005, **347**, 541.
3. V. L. N. Dias, E. N. Fernandes, L. M. S. da Silva, E. P. Marques, J. Zhang and A. L. B. Marques, *J. Power Sources*, 2005, **142**, 10.
4. S. Ronchi, D. Prosperi, F. Compostella and L. Panza, *Synlett*, 2004, 1007.
5. L. M. Pedroso, M. M. C. A. Castro, P. Simoes and A. Portugal, *Polymer,* 2005, **46**, 1766.
6. J. M. Oliva, E. M. D. G. Azenha, H. D. Burrows, R. Coimbra, J. S. S. de Melo, M. L. Canle, M. I. Fernandez, J. A. Santaballa and L. Serrano-Andres, *Chem. Phys. Phys. Chem.*, 2005, **6**, 306.
7. D. Peri, J. S. Alexander, E. Y. Tshuva and A. Melman, *Dalton Trans.*, 2006, 4169.
8. J. Gun, I. Ekeltchik, O. Lev, R. Shelkov and A. Melman, *Chem. Commun.,* 2005, 5319.
9. I. Ekeltchik, J. Gun, O. Lev, R. Shelkov and A. Melman, *Dalton Trans.*, 2006, 1285.
10. P. de Hoog, P. Gamez, W. L. Driessen and J. Reedijk, *Tet. Lett.*, 2002, **43**, 6783.
11. F. Cherioux, L. Guyard and P. Audebert, *Chem. Commun.,* 1998, **2225**.
12. B. Verheyde, W. Maes and W. Dehaen, *Mat. Sc. Eng. C*, 2001, **18**, 243.
13. J. Janietz and M. Bauer, *Synthesis*, 1993, **1**, 33.
14. G. Cooke, H. Augier de Cremiers, V. M. Rotello, B. Tarbit and P. E. Vanderstraeten, *Tetrahedron*, 2001, **57**, 2787.
15. M. Thelakkat and H.-W. Schmidt, *Polym. Adv. Tech.*, 1998, **9**, 429.
16. L. N. Harris, *Synthesis*, 1980, 841.
17. A. H. Hook and D. G. Jones, *J. Chem. Soc.,* 1941, 278.
18. F. H. Case and E. Koft, *J. Am. Chem. Soc.*, 1959, **81**, 905.
19. F. H. Case, *J. Org. Chem.*, 1966, **31**, 2398.

20. S. Yanagida, M. Yokoe, I. Katagiri, M. Ohoka and S. Komori, *Bull. Chem. Soc. Jpn.*, 1973, **46**, 306.

21. M. I. J. Polson, N. J. Taylor and G. S. Hanan, *Chem. Commun.,* 2002, 1356.

22. S. R. Batten, B. F. Hoskins and R. Robson, *Angew. Chem., Int. Ed.,* 1995, **34**, 820.

23. H. L. Anderson and J. K. M. Sanders, *J. Chem. Soc., Chem. Commun.*, 1989, 1714.

24. M. Fujita, D. Oguro, M. Miyazawa, H. Oka and K. Yamaguchi, *Nature*, 1995, **378**, 469.

25. T. Kusukawa and M. Fujita, *J. Am. Chem. Soc.*, 2002, **124**, 13576.

26. S. Tashiro, M. Tominaga, M. Kawano, B. Therrien, T. Ozeki and M. Fujita, *J. Am. Chem. Soc.*, 2005, **127**, 4546.

27. K. Nakabayashi, M. Kawano, M. Yoshizawa, S. Ohkoshi and M. Fujita, *J. Am. Chem. Soc.*, 2004, **126**, 16694–16695.

28. M. Yoshizawa and M. Fujita, *Pure Appl. Chem.*, 2005, **77,** 107–1112.

29. C. Arana, S. Yan, M. Keshavarz-K, K. T. Potts and H. D. Abruña, *Inorg. Chem.*, 1992, **31**, 3680.

30. J. V. Folgado, E. Escriva, A. Beltran-Porter and D. Beltran-Porter, *Trans. Metal Chem.*, 1986, **11**, 485.

31. P. Byers, G. Y. S. Chan, M. G. B. Drew, M. J. Hudson and C. Madic, *Polyhedron*, 1996, **15**, 2845.

32. R. Zibaseresht and R. M. Hartshorn, *Aust. J. Chem.*, 2005, **58**, 345.

33. C. Metcalfe, S. Spey, H. Adams and J. A. Thomas, *J. Chem. Soc. ,Dalton Trans.*, 2002, 4732.

34. T. Glaser, T. Luegger and R. Froehlich, *Eur. J. Inorg. Chem.*, 2004, 394.

35. S. Ghumaan, S. Kar, S. M. Mobin, B. Harish, V. G. Puranik and G. K. Lahiri, *Inorg. Chem.*, 2006, **45**, 2413.

36. X. Chen, F. J. Femia, J. W. Babich and J. A. Zubieta, *Inorg. Chem.*, 2001, **40**, 2769.

37. J. Granifo, *Polyhedron*, 1999, **18**, 1061.

38. A. Gelling, M. D. Olsen, K. G. Orrell, A. G. Osborne and V. Sik, *Inorg. Chim. Acta*, 1997, **264**, 257.
39. A. Gelling, M. Olsen, K. G. Orrell, A. G. Osborne and V. Sik, *Chem. Commun.*, 1997, 587.
40. H. A. Goodwin, *Top. Curr. Chem.*, 2004, **233**, 59.
41. U. S. Schubert and C. Eschbaumer, *Angew. Chem. Int. Ed.*, 2002, **41**, 2892.
42. J. P. Sauvage, J. P. Collin, J. C. Chambron, S. Guillerez, C. Coudret, V. Balzani, F. Barigelletti, L. De Cola and L. Flamigni, *Chem. Rev.*, 1994, **94**, 993.
43. G. Morgan and F. H. Burstall, *J. Chem. Soc., Ab.*, 1937, 1649.
44. G. T. Morgan and F. H. Burstall, *J. Chem. Soc., Ab.*, 1932, 20.
45. D. L. Jameson and L. E. Guise, *Tet. Lett.*, 1991, **32**, 1999.
46. M. Cooke, J. Wang and G. S. Hanan, *Synthetic Commun.*, 2006, 36, 12, 1721.
47. J. Wang and G. S. Hanan, *Synlett*, 2005, 1251.
48. A. M. W. C. Thompson, *Coord. Chem. Rev.*, 1997, **160**, 1.
49. S. Vaduvescu and P. G. Potvin, *Eur. J. Inorg. Chem.*, 2004, 1763.
50. G. K. Pagenkopf and D. W. Margerum, *Inorg. Chem.*, 1968, **7**, 2514.
51. F. H. Fraser, P. Epstein and D. J. Macero, *Inorg. Chem.*, 1972, **11**, 2031.
52. J. Prasad and N. C. Peterson, *Inorg. Chem.*, 1971, **10**, 88.
53. D. Sedney, M. Kahjehnassiri and W. M. Reiff, *Inorg. Chem.*, 1981, **20**, 3476.
54. D. J. Hathcock, K. Stone, J. Madden, S. J. Slattery and *Inorg. Chim. Acta*, 1998, 131.
55. E. C. Constable, G. Baum, E. Bill, R. Dyson, E. Van Eldik, D. Fenske, S. Kaderli, V. Morris, A. Neubrand, M. Neuburger, D. R. Smith, K. Wieghardt, M. Zehnder and A. D. Zuberbuhler, *Chem. Eur. J.*, 1999, **5**, 498.
56. E. I. Lerner and S. J. Lippard, *J. Am. Chem. Soc.*, 1976, **98**, 5397.
57. T. Kajiwara, R. Sensui, T. Noguchi, A. Kamiyama and T. Ito, *Inorg. Chim. Acta*, 2002, **337**, 299.
58. J. M. Rowland, M. M. Olmstead and P. K. Mascharak, *Inorg. Chem.*, 2002, **41**, 2754.
59. P. Paul, B. Tyagi, A. K. Bilakhiya, M. M. Bhadbhade, E. Suresh and G. Ramachandraiah, *Inorg. Chem.*, 1998, **37**, 5733.

60. P. Paul, B. Tyagi, M. M. Bhadbhade and E. Suresh, *J. Chem. Soc., Dalton Trans.*, 1997, 2273.

61. V. M. S. Gil, R. D. Gillard, P. A. Williams, R. S. Vagg and E. C. Watton, *Trans. Metal Chem. (Dordrecht, Netherlands)*, 1979, **4**, 14.

62. J.-V. Folgado, E. Coronado, D. Beltrin-Porter, R. Burriel, A. Fuertes and C. J. Miravitlles, *J. Chem. Soc., Dalton Trans.*, 1988, 3041.

63. P. Paul, B. Tyagi, A. K. Bilakhiya, P. Dastidar and E. Suresh, *Inorg. Chem.*, 2000, **39**, 14.

64. S. Wocadlo, W. Massa and J. V. Folgado, *Inorg. Chim. Acta*, 1993, **207**, 199.

65. V. Balzani, S. Campagna, G. Denti, A. Juris, S. Serroni and M. Venturi, *Acc. Chem. Res.*, 1998, **31**, 26.

66. A. Juris, V. Balzani, F. Barigelletti, S. Campagna, P. Belser and A. Von Zelewsky, *Coord. Chem. Rev.*, 1988, **84**, 85.

67. T. J. Meyer, *Acc. Chem. Res.*, 1989, **22**, 163.

68. E. A. Medlycott and G. S. Hanan, *Coord. Chem. Rev.*, 2006, **250**, 1763.

69. N. Gupta, N. Grover, G. A. Neyhart, P. Singh and H. H. Thorp, *Inorg. Chem.*, 1993, **32**, 310.

70. M. I. J. Polson, E. A. Medlycott, G. S. Hanan, L. Mikelsons, N. J. Taylor, M. Watanabe, Y. Tanaka, F. Loiseau, R. Passalacqua and S. Campagna, *Chem. Eur. J.*, 2004, **10**, 3640.

Chapter II, Part A: Designing tridentate ligands for Ruthenium (II) complexes with prolonged room temperature luminescence lifetimes.

Review 1

Elaine A. Medlycott, Garry S. Hanan*

Département de chimie, Université de Montréal, Montréal, Québec, Canada H3C 3J7

Chemical Society Reviews, **2005**, 34, 133-142.

Abstract

Coordination complexes have been used extensively as the photoactive component of artificial photosynthetic devices. While polynuclear arrays increase the probability of light absorption, the incorporation of the stereogenic Ru(2,2'-bipyridine)$_3^{2+}$ motif gives rise to diastereomeric mixtures whereas the achiral Ru(2,2':6',2''-terpyridine)$_2^{2+}$ motif creates stereopure polynuclear complexes. Thus, polynuclear arrays composed of ruthenium (II) complexes of tridentate ligands are the targets of choice for light-harvesting devices. As Ru(II) complexes of tridentate ligands have short excited-state lifetimes at room temperature (r.t.), considerable effort has focussed on trying to increase their r.t. luminescence lifetime for practical applications. This *tutorial review* will report on the sophisticated synthetic strategies currently in use to enhance the room temperature photophysical properties of Ru (II) complexes of tridentate ligands.

2.1 Introduction

Ruthenium (II) polypyridine complexes have been the focus of considerable attention over the last few decades.[1] Their rich photophysical properties make them attractive candidates for applications as photosensitisers in light-harvesting devices (LHDs) where they replace natural chromophores, such as chlorophyll-*a* and β-carotenoid in photosystem II (PSII). The Ru(II) complexes absorb energy in the visible region of the spectrum giving rise to a singlet metal-to-ligand charge-transfer (^{1}MLCT) excited state, which quickly produces a potentially emitting triplet excited state (^{3}MLCT). The ^{3}MLCT excited state may be sufficiently long-lived to transfer an electron or energy to a suitable acceptor depending on the complex under investigation. In PSII, the excited special pair rapidly transfers an electron through pheophytin to a plastoquinone due to the spatial arrangement of the chromophore and the electron acceptors.[2] Although duplicating the structure of PSII in a LHD would be extremely difficult, artificial systems capable of duplicating its function, that is, generating a charge-separated state,

are of increasing interest.[3] In the absence of the fast electron transfer found in PSII, the excited-state lifetimes of Ru (II) polypyridine complexes must be optimized to permit vectorial electron or energy transfer before excited state deactivation can occur.[3] The luminescence lifetimes may be fine-tuned by manipulating the properties of the excited states which are ultimately dependent on the ligands bonded to the Ru(II) ions.[4] As a greater mechanistic understanding of the processes involved in harnessing light energy may lead to LHDs that replace conventional non-renewable sources of energy with renewable solar energy sources,[5] the design and synthesis of new ligands and their Ru(II) complexes is of critical importance.[6]

The artificial counterparts for the chromophores of PSII have typically been based on the $[Ru(bpy)_3]^{2+}$ motif due to its relatively long-lived excited state at room temperature (1100 ns).[1] However, in larger polynuclear systems based on $[Ru(bpy)_3]^{2+}$, the stereogenic metal centres create diastereomers, and further substitution on the bpy ligands may lead to *facial* and *meridional* isomers.[7] Although methods to create enantiopure complexes based on $[Ru(bpy)_3]^{2+}$ have been developed,[8] attention has turned to synthetically more accessible complexes based on tridentate ligands such as 2,2':6',2''-terpyridine (tpy). $[Ru(tpy)_2]^{2+}$ has a relatively long luminescence lifetime in rigid matrix at 77 K, however, at room temperature its excited state is essentially quenched with a lifetime of only 250 ps.[9] The rigid tridentate ligands create a greater distortion from ideal octahedral geometry in their Ru(II) complexes. Smaller N-Ru-N *trans* angles are found in coordinated tpy (158.6°) as compared to the analogous Ru(II) complexes with bpy (173.0°).[10,11] This gives rise to a weaker ligand field strength, which effectively reduces the energy of the dd metal-centred triplet state (^{3}MC) (Figure 2.1).[12] A consequential decrease in the energy gap between the ^{3}MLCT and ^{3}MC is observed and the ^{3}MC is thermally accessible from the ^{3}MLCT, facilitating non-radiative decay back to the ground state (GS).

The excited-state lifetime of Ru(II) complexes is dependent on the radiative and non-radiative rate constants as given by

$$\tau = \frac{1}{k^o + k^{o\prime} \exp(-Ea/RT)}$$

where $k^o = kr + knr$, the sum of the radiative and non-radiative rate constants, respectively, and relates to a thermally activated crossover process in which Ea is the activation energy barrier to the ^{3}MC state.[13] As Ru(II) polypyridine complexes are weakly emitting, the non-radiative decay constant is the more important factor of the two rate constants.[4] The two major pathways for non-radiative deactivation are through a direct contribution from the ^{3}MLCT state to the GS and through a thermally acessible ^{3}MC state back down to the GS. In order to reduce the overall non-radiative decay constant it is important to diminish the accessibility of the ^{3}MC state from the ^{3}MLCT state. However, if the ^{3}MLCT state is too low in energy, the excited state lifetime may be shortened even more by the direct contribution back to the GS according to the Energy Gap Law.[1,3,4,13] Although tridentate ligands based on the tpy motif have overcome the problems associated with the chirality of $Ru(bpy)_3^{2+}$, it has come at the loss of their excellent photophysical properties.

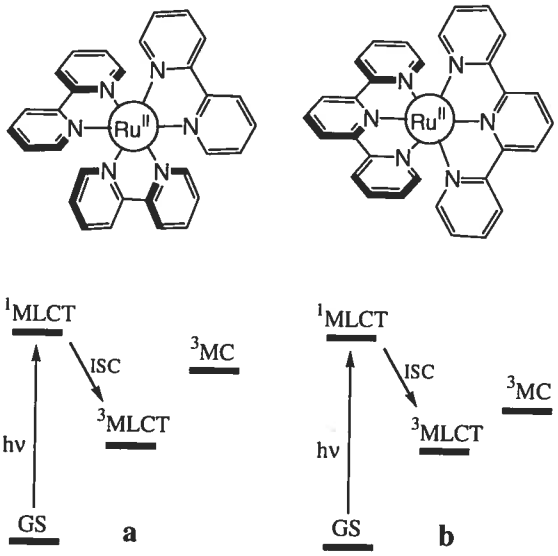

Figure 2.1 a) Photophysically appealing $Ru(bpy)_3^{2+}$ versus b) synthetically appealing $Ru(tpy)_2^{2+}$.

In this tutorial review, the synthetic strategies used to enhance the photophysical properties of Ru(II) complexes of tridentate ligands will be reported. The most popular approach has focused on manipulating the energy difference between ^{3}MLCT and ^{3}MC states of the complex in order to minimise non-radiative decay through the ^{3}MC state to the GS. Destabilisation of the ^{3}MC state or stabilisation of the ^{3}MLCT state, or both, leads to a greater energy gap between the two states. However, stabilisation of the ^{3}MLCT also reduces the energy gap to the ground state which is the usual deactivation pathway for low energy emitting Ru (II) complexes. Alternatively, an additional chromophore may be introduced with a comparable triplet energy to the ^{3}MLCT excited state of the complex, which produces a bichromophoric effect and a substantial increase in the r.t. luminescence lifetime. In the following four sections, we will review the strategies developed to date and highlight the most efficient.

2.2 Ruthenium (II) complexes of functionalised 2,2':6',2''-terpyridine ligands.

a) Direct incorporation of an electron-withdrawing or electron-donating substituent onto tpy.

Complexes of $[Ru(tpy\text{-}X)(tpy\text{-}Y)]^{2+}$ type were synthesised in which X and Y were a wide range of both electron withdrawing and electron donating groups on the 4'-position of the central pyridyl ring.[14] The complexes with electron withdrawing groups (EWGs) were shown to absorb at a lower energy due to greater stabilisation of the ligand-based lowest unoccupied molecular orbital (LUMO) as compared to the metal-based highest occupied molecular orbital (HOMO). The energy of the ^{3}MLCT state was consequently lowered and thermal population of ^{3}MC state was reduced. The luminescence lifetimes were increased and dramatic improvements were observed for complexes with strong EWGs: X = H, Y = SO_2Me: λ_{max} = 679 nm, τ = 36 ns; X = SO_2Me, Y = SO_2Me: λ_{max} = 666 nm, τ = 25 ns. A comparable red shift in the absorption bands were also observed when X or Y were electron donating groups (EDGs) as they destabilise the metal-based HOMO to a greater extent than they

destabilise the ligand-based LUMO. However, the EDGs do not destabilise the ^{3}MC state to a great extent and non-radiative decay back to the GS was facilitated. The longest lifetimes were found for the complexes with mixed EDGs and EWGs: X = OH, Y = SO_2Me: λ_{max} = 706 nm, τ = 50 ns.

When electron withdrawing triarylpyridinium functionalised terpyridines are coordinated to Ru(II), the heteroleptic complexes have a low energy emission (670 nm) and extended r.t. luminescence lifetime of 55 ns.[15] However, the introduction of a phenyl spacer between the tpy and the pyridinium group diminishes the effect of the electron-withdrawing pyridinium substituent and the lifetime is reduced quite significantly to 580 ps, comparable to that of $Ru(tpy)_2^{2+}$. Attaching the relatively electron rich thiophene group directly to the tpy ligand also increases the r.t. luminescence lifetime of Ru(II) complexes, albeit to a lesser extent (<10 ns).[16]

Early pioneering work with acetylene substituents in the 4'-position of the coordinated tpy ligand demonstrated that long excited-state lifetimes could be obtained.[17] The complexes have acetylene groups grafted directly onto the terpyridine core which enhances electron delocalisation and stabilises the ligand-based LUMO (Figure 2.2).[17] The increase in the ^{3}MLCT-^{3}MC energy gap reduces the mixing of the ^{3}MLCT state with the ^{3}MC state. An increase in the number of acetylene units also decreases the emission energy and increases the lifetime of the excited state. The longest r.t. lifetime for acetylene-based complexes corresponds to the acetylene-pyrene complex (580 ns).[17] Although pyrene's triplet state (^{3}Pyr) is higher in energy than the ^{3}MLCT state, it may be populated from the ^{3}MLCT which effectively delays the emission. A similar effect may be responsible for the extended lifetime on the ferrocene-based acetylene complex (Figure 2.2).[18] The strategy of using the equilibrium between triplet states to increase the luminescence lifetime will be discussed in section 3.

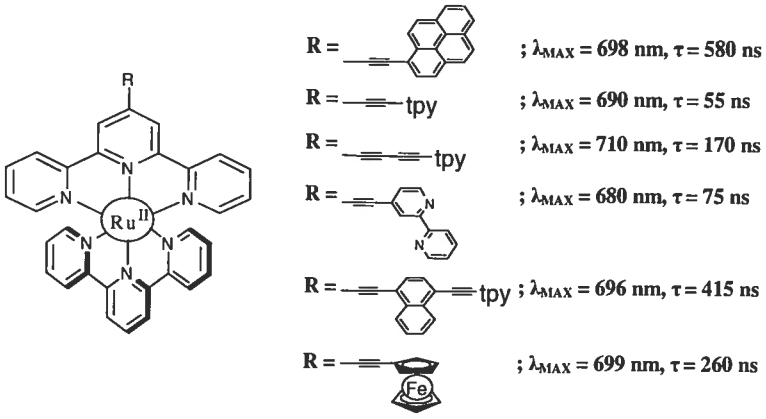

Figure 2.2 Photophysical data for acetylene-substituted $Ru(tpy)_2^{2+}$ complexes.[17-18]

b) Co-planarity of aromatic groups on the tpy ligand

Phenyl substitution in the 4'-position of the tpy gives Ru(II) complexes with photophysical properties that cannot be explained simply in terms of electron donating or withdrawing ability. The Hammett parameter for a phenyl group is essentially the same as hydrogen, therefore, one would expect similar properties to those of $[Ru(tpy)_2]^{2+}$.[14] However, the MLCT absorption band (481 nm) and emission band (715 nm) are at lower energy for $[Ru(Ph\text{-}tpy)_2]^{2+}$ as compared with $[Ru(tpy)_2]^{2+}$, which absorbs and emits as 475 nm and 629 nm, respectively. The ^{3}MLCT state is stabilised by the phenyl substituent to a greater extent than the ^{1}MLCT, an effect that has been observed in a number of similar systems.[19,20] In the ground state the phenyl ring twists away from the central pyridine ring due to unfavourable steric interactions between the hydrogens ortho to the inter-annular bond (Figure 2.3). In the excited state, there is a change in the dihedral angle between the phenyl ring and the central pyridine ring to give a co-planar arrangement. Consequently, the ^{3}MLCT excited state is more stabilised by extended electron delocalisation than the GS. The complex $[Ru(Ph\text{-}tpy)_2]^{2+}$ and its triphenyl-tpy analogue have r.t. luminescence lifetimes of approximately 4 ns.[19] A similar effect is noted for $[Ru(p\text{-toluyl-}tpy)_2]^{2+}$ (0.95 ns).[7] Femtosecond absorption spectroscopy has been used to study a few related systems.[21]

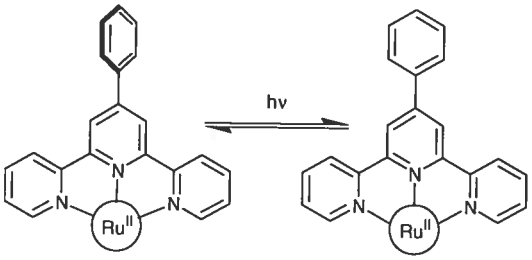

Figure 2.3 Non-planar (left) and co-planar (right) 4'-phenyl-tpy complexes of Ru(II).[19]

A general synthetic approach has been optimised for the synthesis of such ligands in which the substituents are introduced prior to the condensation reaction (Scheme 2.1).[22] Those substituents that are not accessible through this route, may be synthesised by functionalisation of 4'-*p*-toluyl-2,2':6',2'-terpyridine. Electron withdrawing substituents may be substituted on the pendant phenyl ring which further stabilises the ligand LUMO.

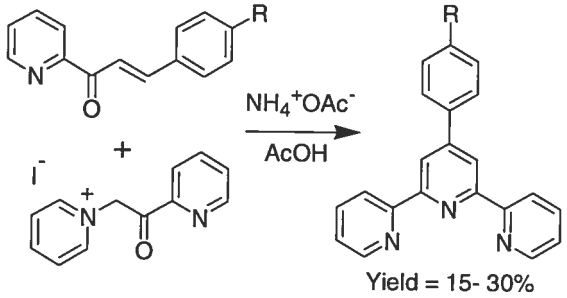

Scheme 2.1 Synthesis of substituted phenyl-terpyridine ligands.[22]

Further studies to improve the effect of co-planar aromatic rings have been carried out by employing a pyrimidyl spacer in place of a phenyl ring. The 2-pyrimidyl substituent lies co-planar to the central terpyridine ring as a result of the intramolecular hydrogen bonding between the N lone pairs on the pyrimidine and H atoms on the central pyridine ring (Figure 2.4).

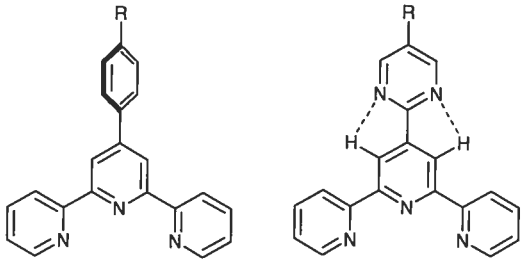

Figure 2.4 Introducing co-planar substituents onto the terpyridine through intramolecular hydrogen bonding.[23]

Further stabilisation of the LUMO can be achieved through substitution of electron-withdrawing groups in the 5-pyrimidyl position.[23] The synthesis involved multiple steps to initially obtain the 4'-amidinate-2,2':6',2''-terpyridine, which is further reacted with substituted trimethinium cations (Scheme 2.2). The heteroleptic Ru(II) complexes were synthesised with a range of electron withdrawing groups (Scheme 2.2).[23] The parent complex, where R = H, has a r.t. luminescence lifetime of 8 ns and all other substituents improve on this value. The cyano-substituted heteroleptic complex has a relatively long-lived r.t. excited state (200 ns). A combination of efficient electron delocalisation over the entire ligand and the electron withdrawing nature of the cyano group contribute to the stabilisation of the ^{3}MLCT state.

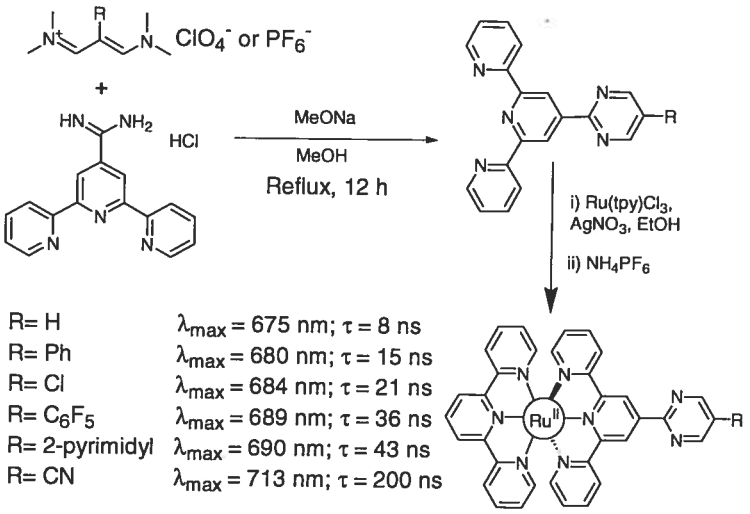

Scheme 2.2 Synthesis of a variety of substituted pyrimidyl terpyridine heteroleptic Ru(II) complexes and their r.t. excited-state lifetimes.[23]

2.3 Bichromophoric Systems

The most successful strategy developed to date is the bichromophore approach, in which an organic chromophore with a non-emissive triplet state is similar in energy to an emissive ^{3}MLCT state and an equilibrium is established between the two states.[24] When a perpendicular arrangement of the organic ligands is favoured on steric grounds, orbital mixing is minimised, which maintains the independence of the two chromophoric units, and consequently favours emission from the ^{3}MLCT state. In some cases, mixing of the organic chromophore triplet state and the ^{3}MLCT state leads to emission from an intraligand state, nonetheless a longer lived excited state is usually obtained.[13] This strategy has been applied extensively to Ru (II) complexes of bidentate ligands to which pyrene is commonly introduced as the additional chromophore.[25,26] As pyrene's triplet state is higher in energy than the ^{3}MLCT state of tpy-based Ru(II) complexes, and anthracene's triplet state (^{3}An) is lower in energy (E^{00}=1.85 eV, 671 nm),[27] the bichromophore approach has not been widely applied to Ru(II) complexes of tridentate ligands. The parent Ru(II) complex has a ligand (tpy-An) consisting of an anthracene moiety directly connected to the 4' position of terpyridine (Figure 2.5).[28] However, $[Ru(tpy\text{-}An)_2]^{2+}$ is not luminescent at room temperature as the energy of the ^{3}MLCT state is significantly higher in energy than the non-emissive ^{3}An state and irreversible energy transfer occurs thereby quenching the excited state.

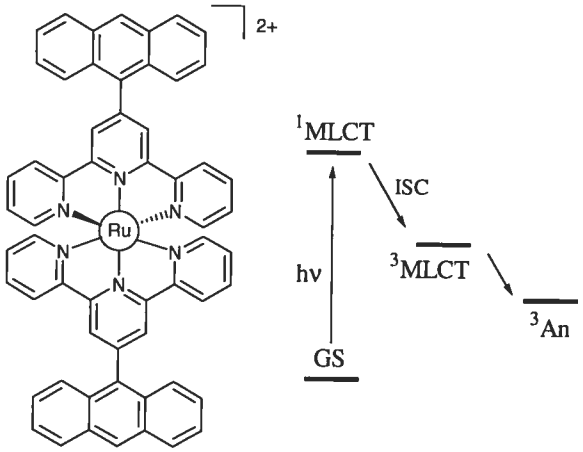

Figure 2.5 Quenching of the ^{3}MLCT excited state of $[Ru(tpy\text{-}An)_2]^{2+}$ due to the low lying non-emissive ^{3}An state.[28]

In order to have efficient energy equilibration in bichromophoric systems, complexes and chromophores with iso-energetic triplet states are required. The pyrimidyl-terpyridine complexes can be used to fine-tune the ^{3}MLCT energy (Scheme 2.2). The anthracene moiety can then be grafted directly onto the 5-pyrimidyl position of the pyrimidyl-terpyridine ligand (Figure 2.6). The terpyridine-based complex with a 5-(9-anthryl)-pyrimid-2-yl substitutent has a ^{3}MLCT energy lower than that of the complex in Figure 2.5.[a] The ^{3}MLCT and the ^{3}An states are now nearly isoenergetic and hence equilibration can occur. The homoleptic complex $[Ru(tpy\text{-}pm\text{-}An)_2]^{2+}$ exhibits biexponential radiative decay back to the GS, with an initial r.t. luminescence lifetime of 6 ns followed by a longer lived component with an r.t. excited-state lifetime of 1806 ns (Figure 2.6).[29] The first component is attributed to the ^{3}MLCT state based on the pyrimidyl-terpyridine unit, and the second component arises from the equilibrium with the ^{3}An state which repopulates the ^{3}MLCT state after the initial emission. The heteroleptic complex $[Ru(tpy\text{-}pm\text{-}An)(tpy)]^{2+}$ also exhibits dual exponential decay with a short-lived first component (5.5 ns) and a longer lived second component (402 ns). In these complexes, the anthracene lies nearly perpendicular to the plane of the pyrimidine ring and, therefore, maintains its own excited state properties. This is an important feature as the secondary chromophore should contribute its independent properties to the final assembly.

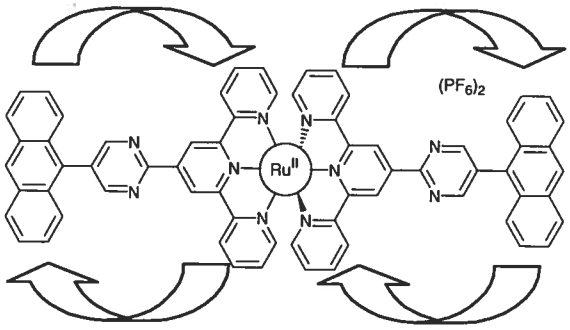

Figure 2.6 The bichromophoric effect in $[Ru(tpy\text{-}pm\text{-}An)_2]^{2+}$: energy transfer from the ^{3}MLCT to the ^{3}An state and back is very efficient.[29]

[a] The chloro-pyrimidyl-terpyridine complex from scheme 2 was coupled with 9-anthrylboronic acid using a Pd(0) catalyst to generate $[Ru(tpy\text{-}pm\text{-}An)_2]^{2+}$.[29]

In all of the bidentate and tridentate bichromophoric systems synthesized to date, the organic chromophore has always been on the same ligand that is involved in the ^{3}MLCT state. Very recently, it has been shown that these two excited states do not have to be involved with the same ligand. The anthryl-terpyridine and pyrimidyl-terpyridine ligands may be synthesized separately and their heteroleptic complexes prepared (Figure 2.7). Even though the spatial separation of the two chromophores exceeds 1 nm, the ^{3}An and the ^{3}MLCT states are almost isoenergetic, which allows equilibration between the two states. A dual exponential decay of the excited state gives two lifetimes at r.t.; 25 ns and 1052 ns (Figure 2.7).[30]

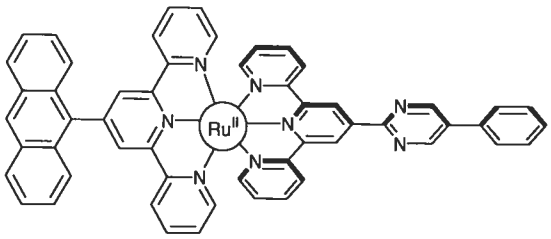

λ_{max} (abs) = 494 nm
λ_{max}(em) = 670 nm
τ = 25 ns and 1052 ns

Figure 2.7 Prolonging r.t. excited-state lifetimes through a long-range multi-chromophore approach.[30]

Two multicomponent systems were reported with a 9-anthryl group introduced into the tridentate ligand (Figure 2.8).[31] The absorption and emission energy of the ^{1}MLCT and ^{3}MLCT states are at significantly longer wavelengths as compared with $Ru(tpy)_2^{2+}$. For the methylated complex (Figure 2.8, left), the ^{1}MLCT and ^{3}MLCT bands are at 530 nm and 730 nm, respectively, and its r.t. luminescence lifetime is 60 ns. The non-methylated complex (Figure 2.8, right) has similar absorption (510 nm) and emission energies (715 nm), but a shorter r.t. excited-state lifetime (30 ns). The emission energy is lower than the energy of the ^{3}An state, which should preclude a bichromophoric effect, suggesting that another process may be operating. The longer lifetime may be a result of the interligand π- π interactions which stabilises the ^{3}MLCT state (cf. section 4).

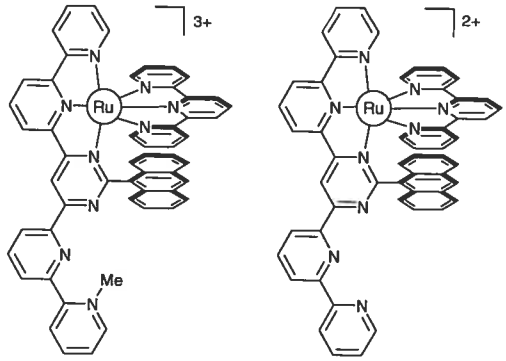

Figure 2.8 Multi component systems that contain Ru^{II}-polypyridine and anthracene chromophores.[31]

More versatile methods have been investigated to incorporate a wider range of organic groups into metal complexes, e.g., the Suzuki-Miyaura cross-coupling reaction with an aryl halide, an arylboronic acid and a Pd(0) catalyst. The conventional synthetic approach for Ru(II) polypyridines is to couple the appropriate organometallic reagent to the halide functionalised Ru(II) complex.[32] However, an alternative approach is to introduce the organometallic reagent onto the complex itself.[33] The Pd(0)-catalysed reaction of a 4'-(*p*-bromophenyl)-tpy complex of Ru(II) with bis(neopentylglycolato)diboron (B_2neo_2), followed by hydrolysis of the corresponding boronate ester gave the boronic acid directly on the complex (Scheme 2.3).

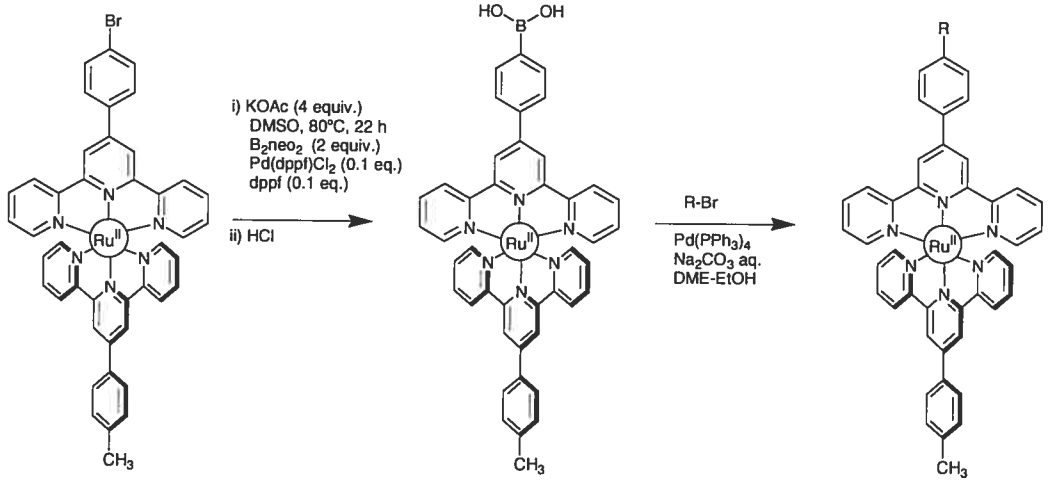

Scheme 2.3 Synthesis of the boronic acid on the metal complex followed by Pd-catalysed coupling reactions.[33]

The cross coupling reactions with a range of aryl halides were carried out using $Pd(PPh_3)_4$ and Na_2CO_3 in DME-EtOH (Scheme 2.3). The coupling reactions are not as efficient as the reactions starting with halosubstituted complexes, however, this alternative approach should allow for the synthesis of complexes that would otherwise not be accessible. Although the complexes prepared by this approach are only weakly emitting, there is considerable potential for new ligands and complexes to be obtained.

2.4 Increasing the energy of the ^{3}MC state

a) σ-Donating ability

As strong σ-donor ligands typically destabilise metal-based orbitals while having a minimal effect on the π^* orbitals of the second tridentate ligand in a heteroleptic complex, they have a great influence over the energies of the molecular orbitals involved in MLCT processes. Consequently, strong σ-donor ligands lower the energy of the ^{1}MLCT and the ^{3}MLCT states effectively reducing surface crossing to the ^{3}MC state. However, if the ^{3}MLCT state is too low in energy, non-radiative decay directly to the GS may occur. The two major ways of increasing σ-donor strength are by cyclometallation and by introducing strong σ-donor heterocycles into the tridentate ligand.

i) Cyclometallation

Cyclometallated complexes are attractive synthetic targets as replacement of a Ru-N bond with Ru-C bond will modify the redox and photophysical properties of the complex and, therefore, offer an alternative means to fine tune orbital energies. Cyclometallating ligands are strong σ-donors and significantly increase the energy gap between the ^{3}MLCT and the ^{3}MC state for heteroleptic complexes with one ligand bound in an N,N,N mode and the cyclometallated ligand in either a N,N,C or N,C,N coordination mode. There are two general synthetic approaches to introduce a cyclometallating group into the Ru(II) coordination sphere: 1) Quaternise a nitrogen

atom and force insertion of Ru in to a CH bond; and 2) Remove a nitrogen atom from the ligand to eliminate the possibility of N,N,N coordination.

The first approach can be more difficult to control and quaternisation of tpy has been found to be synthetically more difficult than expected. *N*-Methyl-2,2':6',2''-terpyridine hexafluorophosphate could be obtained by the reaction of trimethyloxonium tetrafluoroborate in DCM at reflux for 2 hours.[34] Its complexation to $RuCl_3$ then required optimisation of the cyclometallated product over the N,N-bidentate complex in which the vacant coordination site is occupied by a chloride ligand. Although the solvent system plays a vital role in determining the major product, the solvent effect changes from ligand to ligand and was difficult to predict. Quaternisation of 4'-methylthio-terpyridine proceeded more smoothly than for 2,2':6',4''-terpyridine and 2,2':6',3''-terpyridine ligands using CH_3I in DCM.[35]

The second approach, removing a nitrogen from the tpy core, is more commonly employed to synthesise cyclometallated complexes. One pyridyl ring of tpy may be replaced by a pyridine ring substituted in a different position, such as 2,2':6',4''-terpyridine, in which it is impossible to obtain an N,N,N coordination mode (Scheme 2.4).[36]

A red shift is observed for the energy of absorption in the ^{1}MLCT band as compared to $[Ru(tpy)_2]^{2+}$ as would be expected. The HOMO is raised in energy and consequently the HOMO-LUMO energy gap is reduced, as the ^{3}MLCT lies on the non-cyclometallated ligand. Although the effect of one of the non-radiative decay pathways has been reduced, the cyclometallated complex is still only weakly emissive at room temperature (λ_{max} = 790 nm) as the ^{3}MLCT to GS energy gap is very small and non-radiative decay through this alternate route is possible.

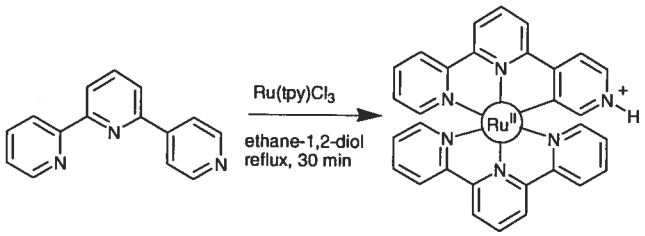

Scheme 2.4 Cyclometallation induced protonation of 2,2':6',4''-terpyridine.[36]

Cyclometallating ligands have also been developed in which a phenyl ring is incorporated into tpy instead of the peripheral or central pyridyl ring to force N,N,C or N,C,N coordination, respectively. The majority of work on mononuclear systems has focused on 6-phenyl-2,2'-bipyridine (bpy-Ph) to obtain an N,N,C coordination motif.[37] The synthesis of the heteroleptic complex, $[Ru(tpy)(bpy\text{-}Ph)]^+$, is highly solvent dependant and a solvent with a high dielectric constant was required to favour the cyclometallated product. The signature for these complexes is the particularly high field signal in the ^1H NMR corresponding to the proton adjacent to the cyclometallating carbon. Complexes incorporating the cyclometallating bpy-Ph ligand all display a red shift of the ^{1}MLCT band in the visible region due to the destabilisation effect of metal based orbitals although emission data for the ^{3}MLCT was not reported.[37]

Substituting peripheral rings in complexes containing the N,N,C mode can lead to optimisation of the synthesis of the cyclometallated product over the bidentate, N,N side-products. Significant improvements in the photophysical properties of Ru(II) complexes may also be observed with substitution on peripheral rings. In the case of complexes displaying the N,N,N coordination mode, *ortho* substitution on peripheral rings leads to greater ring-strain and, therefore, greater distortion from the ideal octahedral coordination geometry. The weaker ligand field strength leads to a lower ^{3}MC state energy and thermally activated surface crossing onto the latter, from which non-radiative decay readily occurs. However, the favourable effects of σ donation counteract the unfavourable effects of steric strain in cyclometallated complexes.[38] Substitution with aromatic groups in the position ortho to the N can also stabilise the ^{3}MLCT state. A crystal structure of $[Ru(mappy)(dtp)]^+$ (Figure 2.9), indicates significant interligand π- π interactions which enhances the delocalisation of the ^{3}MLCT state and as a result increases the r.t. excited-state lifetime to 107 ns.[38]

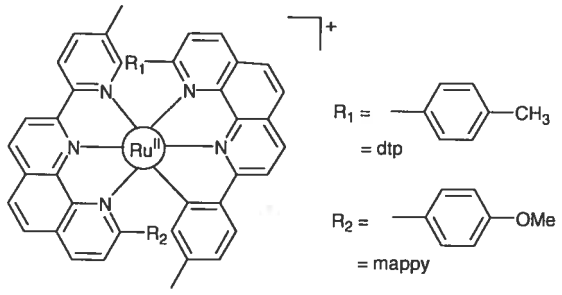

Figure 2.9 Cyclometallated complex $[Ru(mappy)(dtp)]^{+}$.[38]

In contrast to the growing number of publications for Ru(II) complexes with N,N,C coordination, the number of reported N,C,N mononuclear complexes are relatively few. The N,C,N coordination mode has been obtained using the ligand di-1,3-(2-pyridyl)benzene (dpb) which gives the heteroleptic cyclometallated complex $[Ru(ttpy)(dpb)]^{+}$ when reacted with $Ru(ttpy)Cl_3$.[39] The λ_{max} of luminescence at 784 nm is significantly lower in energy than for $[Ru(tpy)_2]^{2+}$.[40] The luminescence lifetime is 4.5 ns, an 18 fold increase on the excited-state lifetime of $[Ru(tpy)_2]^{2+}$. A number of functionalised analogues have been synthesised as synthetic intermediates in the construction of higher nuclearity complexes although their photophysical data are not available.[41] In addition to incorporating phenyl rings in the terpyridine core, thiophene has been introduced to direct the formation of cyclometallated products.[42] The ligand 6-(2-thienyl)-2,2'-bipyridine can be used to increase the σ-donating ability through cyclometallation, or alternatively, to decrease the σ-donating ability through an N,N,S coordination mode. It is interesting to note that the mode of coordination is pH dependent and may be modulated (Figure 2.10). However, the effects of changing coordination modes on the photophysical properties were not reported.[43]

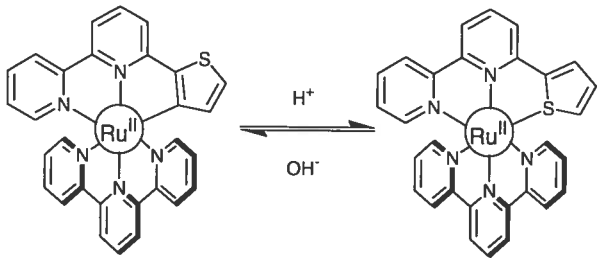

Figure 2.10 Reversible cyclometallation of a thiophene-bipyridine ligand.[43]

ii) Alternative N heterocycles as strong σ donors

The σ-donor strength of the ligand may be increased while maintaining an N,N,N coordination mode by changing the nitrogen containing heterocycle in the tridentate ligand. Deprotonated triazole and tetrazole rings have been incorporated into the tridentate core with great success as the negatively charge ligands are more efficient σ donors than the neutral terpyridine based ligands.[44] The electron density is driven onto the Ru(II) centre which increases the energy gap between the ^{3}MC and ^{3}MLCT states. A mixture of isomers is obtained by introducing a triazole ring due to the inequivalence of N1 and N3 (Figure 2.11). The reaction of Ru(tpy)Cl_3 with 2,6-bis([1,2,4]triazol-3-yl)pyridine ligand yielded all three isomers which were isolated through a combination of column chromatography and semi-preparative HPLC (Figure 2.11a-c). Previous studies on bidentate analogues had shown that the reaction can be directed to favour one isomer over others by introducing sterically demanding substituents in the C5 position. When the reaction was carried out using 2,6-bis(5-phenyl-[1,2,4]triazol-3-yl), the products in Figure 2.11b and Figure 2.11c were isolated and could be separated by column chromatography. In order to eliminate the formation of isomers, the symmetric ligand 2,6-bis([1,2,3,4]tetrazol-5-yl)pyridine was also employed. This was reacted with Ru(tpy)Cl_3 to obtain the heteroleptic complex without the need for column chromatography. All of the complexes are luminescent at room temperature in ethanol and their excited-state lifetimes range from 20 to 80 ns.

On protonation of the non-coordinated N's on the heterocyclic rings, the σ donating strength is diminished and the excited state is quenched.

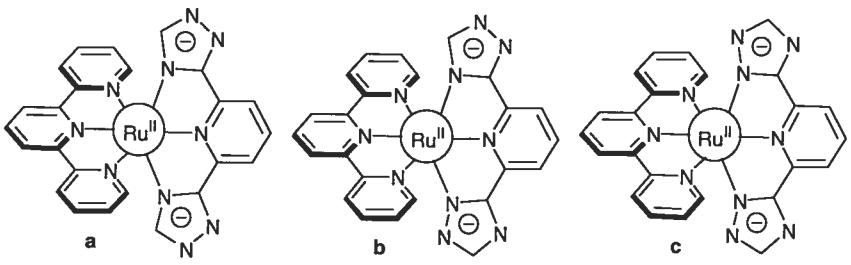

Figure 2.11 Three isomers of a triazole-based Ru(II) complex.[44]

b) Decreasing the steric strain in the tridentate ligand

Another way to increase the ligand field strength is to reduce the angular strain in the tridentate ligands, which in turn increases the energy of the metal-based orbitals. A more flexible ligand was made by introducting a methylene spacer between two of the pyridine rings in tpy (Figure 2.12).[45] The r.t. luminescence lifetime for the homoleptic complex incorporating the 6-(2-picolyl)-2,2'-bipyridine ligand is 17-18 ns, 70 times greater than that of $[Ru(tpy)_2]^{2+}$.

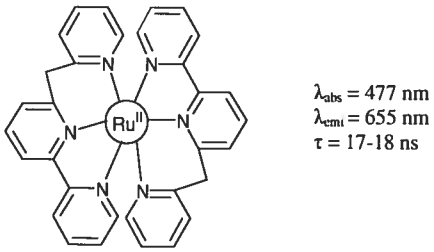

Figure 2.12 Increasing ligand field strength by alleviating steric strain in tridentate ligands.[45]

2.5 π Electron Accepting Ability

It has been shown that σ donor strength can manipulate the energy levels associated primarily with the metal-based orbitals of these complexes. Another approach is to use better π accepting ligands to reduce the energy of the ^{1}MLCT state and consequently the ^{3}MLCT state. The central pyridyl ring of terpyridine can be replaced by a triazine

ring while maintaining a N,N,N coordination mode. An efficient synthetic methodology has been developed for a range of triazine-based ligands (Scheme 2.5).[46]

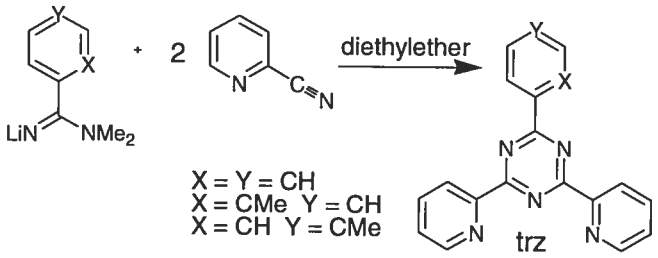

Scheme 2.5 Synthesis of tridentate triazine-based ligands.[46]

The homoleptic complexes $[Ru(trz)_2]^{2+}$ and the heteroleptic complexes $[Ru(trz)(tpy)]^{2+}$ were synthesised by standard procedures.[46] The electronic absorption spectra contain ^{1}MLCT absorption bands which are red-shifted compared to λmax of $[Ru(tpy)_2]^{2+}$ due to greater to the π accepting nature of the tpz ligands. The emission energy is significantly lowered as compared to that of $[Ru(tpy)_2]^{2+}$. The heteroleptic complex $[Ru(trz)(tpy)]^{2+}$, with phenyl group in the pendant position, emits at 740 nm, 2385 cm^{-1} lower in energy than $[Ru(tpy)_2]^{2+}$ and has a lifetime of 9 ns. The stabilisation of the ^{3}MLCT state is also a result of the increased planarity arising from intramolecular H-bonding between the N atoms on the triazine ring with the hydrogens on the pendant phenyl ring. The homoleptic complexes have shorter excited-state lifetimes, presumably due to facilitated non-radiative decay due to solvent interaction with the non-coordinated nitrogen atoms on the triazine ring.[46]

The synthesis and characterisation of a related system in which a pyrazine ring is in the central position has been carried out. In addition to polynuclear complexes, the ligand 2,3,5,6-tetrakis(2-pyridyl)pyrazine has been used in the synthesis of the mononuclear heteroleptic (tpy) and homoleptic complexes (Figure 2.13).[47] Both complexes show some degree of stabilisation of the ^{3}MLCT state with red-shifted emissions at 665 nm and 648 nm and enhanced luminescence lifetimes of 30 and 50 ns for the hetero- and homoleptic complexes, respectively.

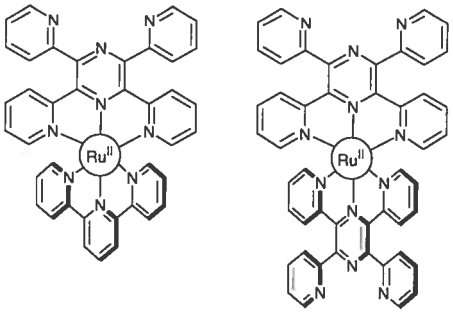

Figure 2.13 Hetero- and homoleptic Ru(II) complexes of 2,3,5,6-tetrakis(2-pyridyl)pyrazine.[47]

The heterocycles in the peripheral position may also be modified. Introducing pyrazine heterocycles into the tridentate ligand should improve the π accepting ability of these ligands. The 2,6-dipyrazinylpyridine ligand was synthesised using a well developed condensation reaction (Scheme 2.6).[48] Lifetime studies were carried out in the solid state and the complexes were shown be weakly emitting at room temperature (τ = 18 ns). The excited state is longer-lived than the toluylterpyridine analogue $[Ru(ttpy)_2]^{2+}$ in the solid state (τ = 10.95 ns).

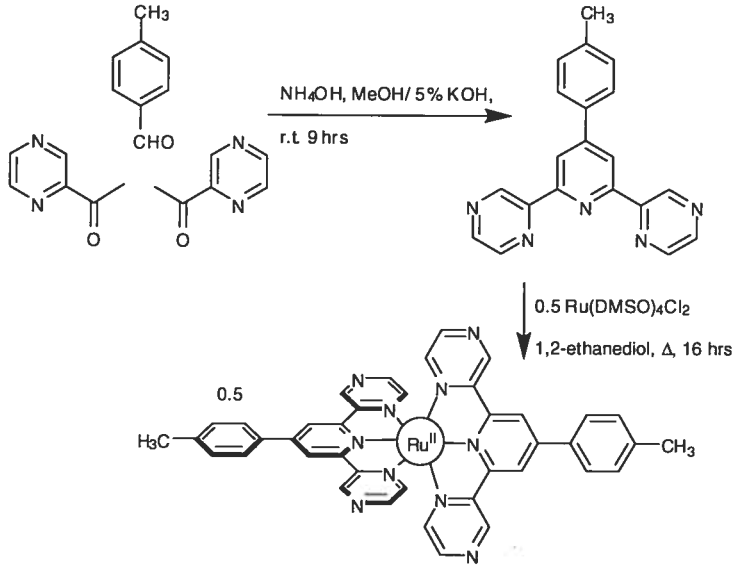

Scheme 2.6 Synthesis of 2,6-dipyrazinylpyridine and its Ru(II) complex.[48]

2.6 Summary and outlook

The optimisation of the photophysical properties of Ru(II) complexes of tridentate ligands is still a developing area of polypyridine chemistry. In this review, the different approaches currently used to synthesise new ligands and complexes as well as to enhance the r.t. excited-state lifetimes of mononuclear complexes have been summarised. To date, the most efficient means of prolonging r.t. luminescence lifetimes is through a bichromophoric system in which emission from the ^{3}MLCT excited state is delayed by equilibration with an isoenergetic triplet state of another chromophore. Figure 2.14 gives a summary of the mononuclear tridentate complexes with the longest reported r.t. excited-state lifetimes. It is clearly apparent from the current literature that considerable potential exists to increase the luminescence lifetimes of Ru (II) complexes of tridentate ligands using a combination of the strategies outlined herein. Considering recent interest in polyruthenium dendrimers and polymers containing tridentate ligands,[49,50] the ability to make them r.t. luminescent bodes well for future applications.

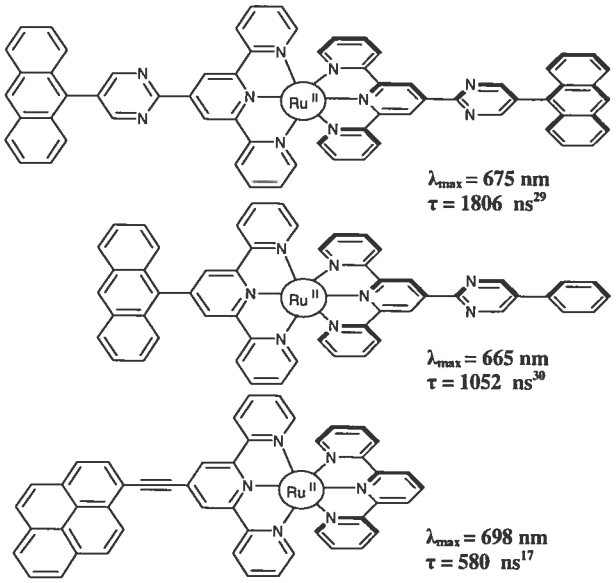

Figure 2.14 Top three complexes with the longest r.t. excited-state lifetimes.

2.7 Acknowledgements

The authors would like to thank the Natural Sciences and Engineering Research Council of Canada and the Université de Montréal for financial support. EAM thanks the Commonwealth Scholarship program. GSH thanks Sebastiano Campagna for a long-standing collaboration for photophysical measurements.

2.8 References

1 A. Juris, V. Balzani, F. Barigelletti, S. Campagna, P. Belser and A. Von Zelewsky, Coord. Chem. Rev., 1988, 84, 85.

2 J. Barber, Quat. Rev. Biophys., 2003, 36, 71.

3 E. Baranoff, J.-P. Collin, L. Flamigni and J.-P. Sauvage, Chem. Soc. Rev., 2004, 147.

4 J. A. Treadway, B. Loeb, R. Lopez, P. A. Anderson, F. R. Keene and T. J. Meyer, Inorg. Chem., 1996, 35, 2242.

5 L. Sun, B. Åkermark and S. Styring, Chem. Soc. Rev., 2001, 30, 36.

6 C. J. Elsevier, J. Reedijk, P. H. Walton and M. D. Ward, Dalton Trans., 2003, 1869.

7 J. P. Sauvage, J. P. Collin, J. C. Chambron, S. Guillerez, C. Coudret, V. Balzani, F. Barigelletti, L. De Cola and L. Flamigni, Chem. Rev., 1994, 94, 993.

8 F. M. MacDonnell, M.-J. Kim, K. L. Wouters and R. Konduri, Coord. Chem. Rev. 2003, 242, 47.

9 J. R. Winkler, T. L. Netzel, C. Creutz and N. Sutin, J. Am.Chem. Soc., 1987, 109, 2381.

10 D. P. Rillema, D. S. Jones, C. Woods and H. A. Levy, Inorg. Chem., 1992, 31, 2935.

11 S. Pyo, E. Perez-Cordero, S. G. Bott and L. Echegoyen, Inorg. Chem., 1999, 38, 3337.

12 J. M. Calvert, J. V. Caspar, R. A. Binstead, T. D. Westmoreland and T. J. Meyer, J. Am. Chem. Soc., 1982, 104, 6620.

13 X.-Y. Xian, A. Del Guerzo and R. H. Schmehl, J. Photochem. Photobio. C, 2004, 5, 55 and references therein.

14 M. Maestri, N. Armaroli, V. Balzani, E. C. Constable and A. M. W. C. Thompson, Inorg. Chem., 1995, 34, 2759.

15 P. Laine, F. Bedioui, E. Amouyal, V. Albin and F. Berruyer-Penaud, Chem. Eur. J., 2002, 8, 3162.

16 E. C. Constable, C. E. Housecroft, E. R. Schofield, S. Encinas, N. Armaroli, F. Barigelletti, L. Flamigni, E. Figgemeier and J. G. Vos, Chem. Commun., 1999, 869.

17 A. Harriman, A. Mayeux, A. De Nicola and R. Ziessel, Phys. Chem. Chem. Phys., 2002, 4, 2229 and references therein.

18 U. Siemeling, J. Vor der Brueggen, U. Vorfeld, B. Neumann, A. Stammler, H.-G. Stammler, A. Brockhinke, R. Plessow, P. Zanello, F. Laschi, F. Fabrizi de Biani, M. Fontani, S. Steenken, M. Stapper and G. Gurzadyan, Chem. Eur. J., 2003, 9, 2819 and references therein.

19 C. R. Hecker, A. K. I. Gushurst and D. R. McMillin, Inorg. Chem., 1991, 30, 538.

20 G. F. Strouse, J. R. Schoonover, R. Duesing, S. Boyde, W. E. Jones Jr. and T. J. Meyer, Inorg. Chem., 1995, 34, 473.

21 J. K. McCusker, Acc. Chem. Res., 2003, 36, 876.

22 F. Kroehnke, Synthesis, 1976, 1.

23 Y.-Q. Fang, N. J. Taylor, G. S. Hanan, F. Loiseau, R. Passalacqua, S. Campagna, H. Nierengarten and A. Van Dorsselaer, J. Am. Chem. Soc., 2002, 124, 7912.

24 A. I. Baba, J. R. Shaw, J. A. Simon, R. P. Thummel and R. H. Schmehl, Coord. Chem. Rev., 1998, 171, 43 and references therein.

25 W. E. Ford and M. A. J. Rodgers, J. Phys. Chem., 1992, 96, 2917.

26 J. A. Simon, S. L. Curry, R. H. Schmehl, T. R. Schatz, P. Piotrowiak, X. Jin and R. P. Thummel, J. Am. Chem. Soc., 1997, 119, 11012.

27 S. L. Murov, I. Carmicheal, and G. L. Hug Handbook of Photochemistry, Marcel Dekker, New York, 1993.

28 G. Albano, V. Balzani, E. C. Constable, M. Maestri and D. R. Smith, Inorg. Chim. Acta, 1998, 277, 225.

29 R. Passalacqua, F. Loiseau, S. Campagna, Y.-Q. Fang and G. S. Hanan, Angew. Chem., Int. Ed., 2003, 42, 1608.

30 J. Wang, G. S. Hanan, F. Loiseau and S. Campagna, Chem. Commun. 2004, accepted for publication.

31 S. Serroni, S. Campagna, R. P. Nascone, G. S. Hanan, G. J. E. Davidson, and J.-M. Lehn, Chem. Eur. J., 1999, 5, 3523.

32 J. C. Chambron, C. Coudret and J. P. Sauvage, New J. Chem., 1992, 16, 361.

33 C. J. Aspley and J. A. G. Williams, New J. Chem., 2001, 25, 1136.

34 D. A. Bardwell, A. M. W. C. Thompson, J. C. Jeffery, J. A. McCleverty and M. D. Ward, J. Chem. Soc., Dalton Trans., 1996, 873.

35 T. Koizumi, T. Tomon and K. Tanaka, Organometallics, 2003, 22, 970.

36 E. C. Constable, A. M. W. Cargill Thompson, J. Cherryman and T. Liddiment, Inorg. Chim. Acta, 1995, 235, 165.

37 E. C. Constable and M. J. Hannon, Inorg. Chim. Acta, 1993, 211, 101.

38 F. Barigelletti, B. Ventura, J.-P. Collin, R. Kayhanian, P. Gavina and J.-P. Sauvage, Eur. J. Inorg. Chem., 2000, 113 and references therein.

39 M. Beley, J. P. Collin and J. P. Sauvage, Inorg. Chem., 1993, 32, 4539.

40 M. Beley, S. Chodorowski, J.-P. Collin, J.-P. Sauvage, L. Flamigni and F. Barigelletti, Inorg. Chem., 1994, 33, 2543.

41 C. Patoux, J.-P. Launay, M. Beley, S. Chodorowski-Kimmes, J.-P. Collin, S. James and J.-P. Sauvage, J. Am. Chem. Soc., 1998, 120, 3717.

42 E. C. Constable, R. P. G. Henney and D. A. Tocher, J. Chem. Soc., Dalton Trans., 1991, 2335 and references therein.

43 E. C. Constable, S. J. Dunne, D. G. F. Rees and C. X. Schmitt, Chem. Commun., 1996, 1169.

44 M. Duatti, S. Tasca, F. C. Lynch, H. Bohlen, J. G. Vos, S. Stagni and M. D. Ward, Inorg. Chem., 2003, 42, 8377.

45 H. Wolpher, O. Johansson, M. Abrahamsson, M. Kritikos, L. Sun and B. Akermark, Inorg. Chem. Commun., 2004, 7, 337.

46 (a) M. I. J. Polson, N. J. Taylor and G. S. Hanan, Chem. Commun., 2002, 1356; (b) M. I. J. Polson, E. A. Medlycott, G. S. Hanan, L. Mikelsons, N. J. Taylor, M. Watanabe, Y. Tanaka, F. Loiseau, R. Passalacqua and S. Campagna., Chem. Eur. J., 2004, 3640.

47 L. M. Vogler, S. W. Jones, G. E. Jensen, R. G. Brewer and K. J. Brewer, Inorg. Chim. Acta, 1996, 250, 155.

48 R. Liegghio, P. G. Potvin and A. B. P. Lever, Inorg. Chem., 2001, 40, 5485.

49 G. R. Newkome, K. S. Yoo, H. J. Kim and C. N. Moorefield, Chem Eur. J., 2003, 9, 3367 and references therein.

50 H. Jiang, S. J. Lee and W. Lin J. Chem. Soc., Dalton Trans., 2002, 3429 and references therein.

Chapter II, Part B: Tuning the excited-state energy of the organic chromophore in bichromophoric systems based on Ru(II) complexes

Article 1

Elaine A. Medlycott,[a] *Garry S. Hanan,**[a] *Frédérique Loiseau,*[b] *Sebastiano Campagna,**[b]

[a] Département de chimie, Université de Montréal, Montréal, Québec, Canada H3C 3J7

[b] Dipartimento di Chimica Inorganica, Chimica Analitica e Chimica Fisica, Università di Messina, 98166 Messina, Italy

Accepted for publication in Chemistry--A European Journal, October 2006

Manuscript Chem.200601376

Abstract

A series of new heteroleptic and homoleptic Ru(II) complexes containing variously substituted bis(pyridyl)triazine ligands have been prepared and their absorption spectra, redox behavior, and luminescence properties (both in fluid solution at room temperature and in rigid matrix at 77 K) have been investigated. For some compounds, X-ray structures have also been determined. The new bis(pyridyl)triazines incorporate additional chromophores such as biphenyl, phenanthrene, anthracene, and bromo-anthracene derivatives, so the Ru(II) species can be considered as multichromophoric species. The absorption spectra and redox properties of all the metal complexes have been assigned to features belonging to specific subunits, suggesting these species can be regarded as multicomponent, supramolecular assemblies from an electronic coupling point of view. Whereas most of the complexes exhibit luminescence properties which can be attributed to metal-to-ligand charge-transfer (MLCT) states involving the metal-based subunit(s), the species containing the anthryl and, even more, the brominated anthryl chromophores, exhibit a complicated luminescence behavior. For example, **2d** (the anthryl-containing heteroleptic metal compound) exhibits MLCT emission at room temperature and emission from the anthracene triplet at 77 K; **2e** (the bromo-substituted anthryl-containing heteroleptic metal compound) exhibits anthryl-based emission at 77 K and MLCT emission at room temperature, but with a prolonged lifetime which suggests equilibration between two triplet states belonging to different chromophores. The equilibration regime between MLCT and aromatic hydrocarbon triplet states is therefore reached by suitable substitution on the organic chromophore.

2.9 Introduction

Ru(II) complexes of polypyridine ligands have been intensely researched as a result of their excellent photophysical properties and promising applications as photo-active devices.[1, 2] The most studied complexes are based on $Ru(bpy)_3^{2+}$ (bpy = 2,2'-bipyridine) as they have been shown to have long-lived excited states at room

temperature originating from their metal-to-ligand charge-transfer (MLCT) state.[3-5] However, bpy-based complexes induce chirality at the metal centre and separation of the diastereomers in polymetallic complexes, although possible,[6] can be complicated, which has turned attention to achiral tridentate 2,2':6',2''-terpyridine (tpy) type ligands.[7] Although tpy is a synthetically appealing target, on coordination to the metal ion, the tridentate ligand imposes a small bite angle and consequently its ligand field strength is lower than that of bpy.[8] This allows thermal access to low-lying non-emissive metal-centred (MC) states and the MLCT excited-state is short lived (0.25 ns for $Ru(tpy)_2^{2+}$).[9] Many strategies have been used to prolong excited state lifetimes of complexes with tridentate ligands, most focusing on the manipulation of the energies of non-emissive MC states relative to emissive MLCT states.[10, 11] One such strategy makes use of electron deficient triazine ligands which function to lower the energy of the ^{3}MLCT state relative to the metal-centred state (Figure 2.15).[12, 13] For this type of complexes, excited-state lifetimes were extended to 8 ns at room temperature, thirty-times greater than that of the parent complex.

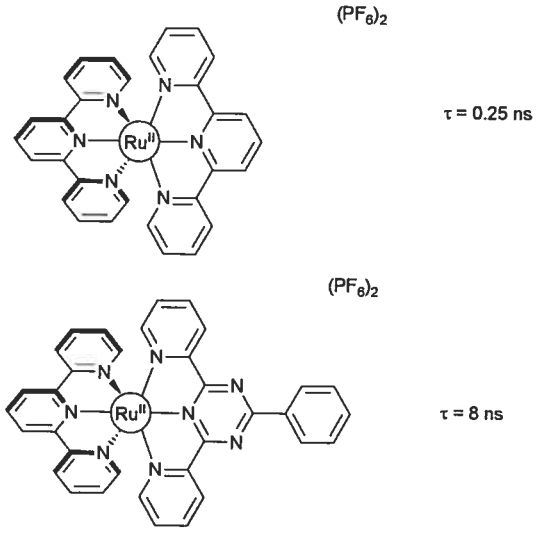

Figure 2.15 Heteroleptic complex incorporating a central triazine ring compared to the parent complex $Ru(tpy)_2^{2+}$.[13]

An alternative strategy has made use of the 'multichromophoric approach',[14] which relies on the presence of additional chromophore(s) with a non-emissive, long-lived triplet state of comparable energy to the ^{3}MLCT state.[14, 15] Reversible

population of the triplet excited state localised on the additional chromophore(s) can occur, thereby delaying emission from the complex and prolonging the MLCT excited state lifetime, with the organic triplet behaving as an excited-state storage element for MLCT emission. Initially this approach was used for Ru(II) complexes of bidentate, bipyridine-type ligands,[15] later it was applied to tridentate tpy-type systems as well.[16, 17] Usually, the organic chromophore triplet is lower in energy than the triplet MLCT level, however, in rare examples the reverse is obtained,[17] although this makes the multichromophoric effect less efficient.

In all the multichromophoric species investigated so far, it is the MLCT state energy which has been modified, by polypyridine ligand substitution or selection, to fit the suitable organic chromophore triplet energy. In this paper, we exploit the possibility of using substituents on the organic chromophore to activate the multichromophoric behaviour. As suitable systems, we selected a family of Ru(II) triazine-based complexes coupled with variously-substituted anthracene or phenanthrene subunits. In such cases the Ru-to-triazine CT level can be lower in energy than the either the phenanthrene or anthracene triplets, so the multichromophoric behaviour is not active in the simplest compounds. However, introduction of the bromo-substituent on anthracene lowers the energy of the anthracene components and the multichromophoric behaviour can take place. Therefore, the systems investigated here belong to the much less explored case where the MLCT level is the lowest-energy state of the two states involved in the equilibration process.[18]

The structural formulae for the studied compounds are shown in Chart 2.1. A bromo-substituent in the 4-position of the pendant phenyl ring allows a 'chemistry-on-the-complex' approach to introduce additional organic components with varying triplet state energies. [16, 19-23]

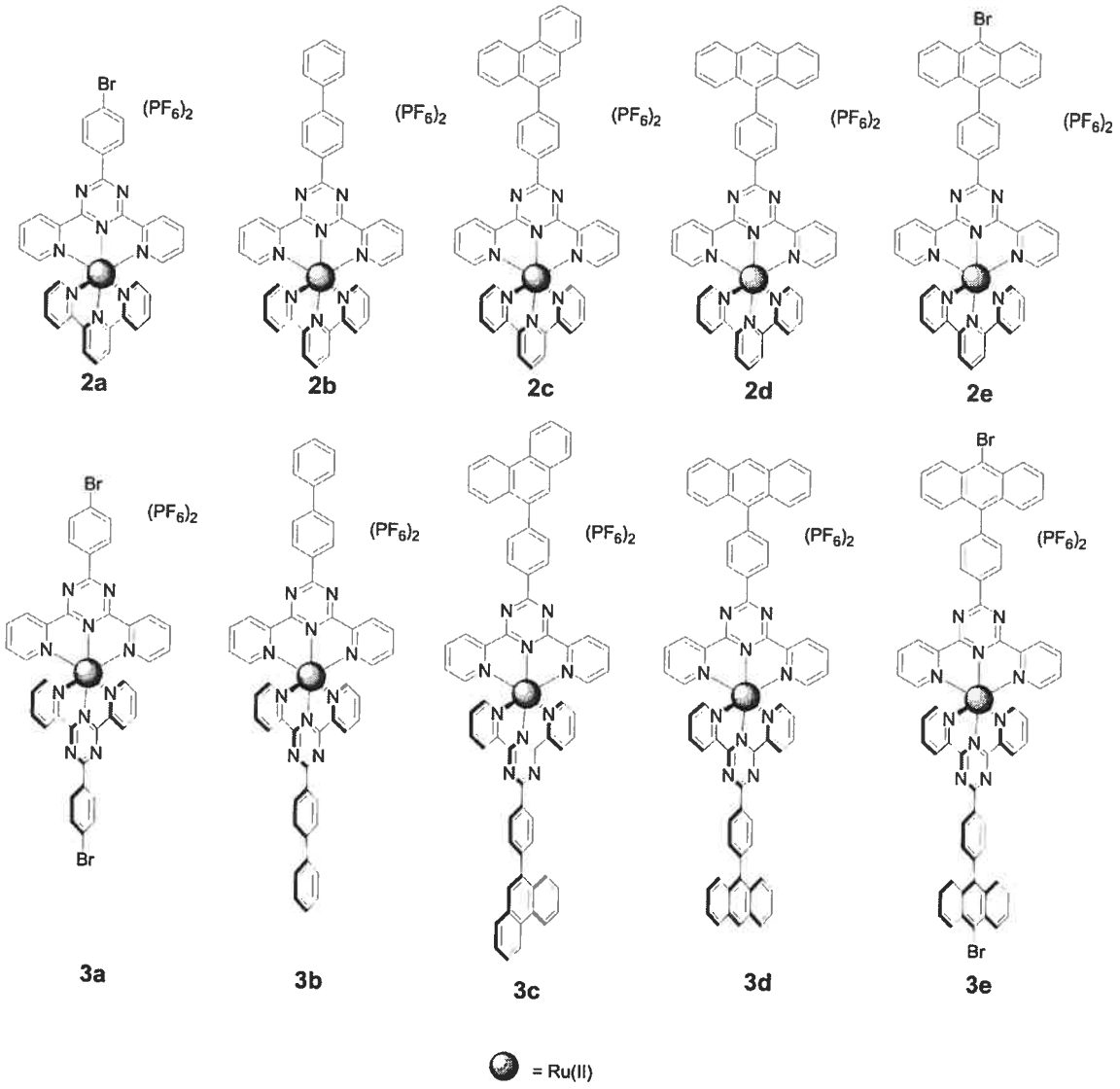

Chart 2.1 Heteroleptic complexes **2a-e** and homoleptic complexes **3a-e** under investigation.

2.10 Experimental Section

Nuclear magnetic resonance (NMR) spectra were recorded in CD_3CN at room temperatutre (r.t.) on a Bruker AV400 spectrometer at 400 MHz for ^1H NMR and at 100 MHz for ^{13}C NMR unless otherwise stated. Chemical shifts are reported in part per million (ppm) relative to residual solvent protons (1.93 ppm for acetonitrile-d_3) and the carbon resonance of the solvent. Absorption spectra and emission spectra were measured in deaerated acetonitrile at r.t. on a Cary 500i UV-Vis-NIR Spectrophotometer and a Cary Eclipse Fluorescence Spectrophotometer, respectively. For the luminescence lifetimes, an Edinburgh OB 900 single-photon-counting spectrometer was used, employing a Hamamatsu PLP2 laser diode as pulse (wavelength output, 408 nm; pulse width, 59 ps). Emission quantum yields were measured at room temperature using the optically dilute method.[24] $[Ru(bpy)_3]^{2+}$ in air-equilibrated aqueous solution and $[((bpy)_2Ru(\mu\text{-}2,3\text{-}dpp))_3Ru]^{8+}$ (2,3-dpp = 2,3-bis(2'-pyridyl)pyrazine) in deaerated acetonitrile solution were used as quantum yield standards, assuming values of 0.028[25] and 0.005,[26]respectively.

Electrochemical measurements were carried out in argon-purged acetonitrile at room temperature with a BAS CV50W multipurpose equipment interfaced to a PC. The working electrode was a Pt electrode. The counter electrode was a Pt wire, and the pseudo-reference electrode was a silver wire. The reference was set using an internal 1 mM ferrocene/ferrocinium sample at 395 mV vs SCE in acetonitrile and 432 mV in DMF. The concentration of the compounds was about 1mM. Tetrabutylammonium hexafluorophosphate (TBAP) was used as supporting electrolyte and its concentration was 0.10 M. Cyclic voltammograms were obtained at scan rates of 50, 100, 200, and 500 mV/s. For irreversible oxidation processes, the cathodic peak was used as E, and the anodic peak was used for irreversible reduction processes. The criteria for reversibility were the separation of 60 mV between cathodic and anodic peaks, the close to unity ratio of the intensities of the cathodic and anodic currents, and the constancy of the peak potential on changing scan rate. The number of exchanged electrons was measured with OSWV, and by taking advantage of the presence of ferrocene used as the internal reference.

Experimental uncertainties are as follows: absorption maxima, ±2 nm; molar absorption coefficient, 10%; emission maxima, ± 5 nm; excited state lifetimes, 10%; luminescence quantum yields, 20%; redox potentials, ± 10 mV.

Compounds **L1** (see later in Scheme 2.7)[27], $Ru(tpy)Cl_3$[28] 9-anthrylboronic acid, 10-bromo-9-anthryl-boronic acid and 9-phenanthryl-boronic acid [29] starting materials were synthesised using previously reported procedures. Solvents were removed under reduced pressure using a rotary evaporator unless otherwise stated.

2a

A suspension of $Ru(tpy)Cl_3$ (100 mg, 0.23 mmol), **L1** (0.23 mmol) and $AgNO_3$ (115 mg, 0.68 mmol) in ethanol (50 mL) was stirred and heated to reflux for four hours. On cooling the solution was filtered to remove the AgCl and the solvent was evaporated. The resulting solid was dissolved in minimal acetonitrile and KPF_6 (5 mL, aq) was added and the solution was diluted with water (100 mL). The precipitate was collected and dissolved in acetonitrile and purified by column chromotography (SiO_2, acetonitrile:aq.KNO_3, 7:1). The nitrate salt was metathesized by extraction of the PF_6 salt in an acetonitrile/DCM mixture in the presence of KPF_6 (aq). The organic extracts were collected and the solvent removed. The solid was dissolved in acetonitrile, and the product precipitated by addition to water. Recrystallisation from acetonitrile/diethyl ether afforded **2a** in 55% yield.

^{1}H NMR (CD_3CN): 9.08 (d, J= 8 Hz, 2H) $H_{3,3''}$; 8.97 (d, J= 9 Hz, 2H) $H_{2''',6'''}$; 8.80 (d, J= 8 Hz, 2H) $H_{T3',T5'}$; 8.52 (d, J= 8 Hz, 2H) $H_{T3,3''}$; 8.49 (t, J= 8 Hz, 1H) $H_{T4'}$; 8.13 (td, J= 1 Hz, 8 Hz, 2H) $H_{4,4''}$; 8.01 (d, J= 9 Hz, 2H) $H_{3''',5'''}$; 7.94 (td, J= 1 Hz, 8 Hz, 2H) $H_{T4,4''}$; 7.60 (d, J= 5 Hz, 2H) $H_{6,6''}$; 7.44 (m, 4H) $H_{T6,6''}$,$H_{5,5''}$; 7.13 (dd, J= 6 Hz, 6 Hz, 2H) $H_{T5,5''}$. ^{13}C NMR (CD_3CN): 124.30, 124.97, 127.79, 128.45, 129.25, 130.97, 131.59, 133.25, 134.48, 137.20, 138.94, 139.09, 153.46, 154.75, 155.68, 158.38 168.55, 170.86. High Res ES-MS: Calcd. for $[M-2PF_6]^{2+}$ 362.0131, found 362.0136; calcd. for $[M-PF_6]^+$ 868.9909, found 868.9916. Anal. Calcd. For $C_{34}H_{23}BrF_{12}N_8P_2Ru.H_2O$: C, 39.55; H, 2.44; N, 10.85. Found C 39.94, H 2.74, N 10.83.

3a

A suspension of $RuCl_3.3H_2O$ (0.10 g, 0.36 mmol), **L1** (0.28 g, 0.73 mmol) and $AgNO_3$ (0.18 g, 1.1 mmol) in DMF (10 mL) was stirred at room temperature for 20 minutes and heated to reflux for one hour. On cooling the solution was filtered to remove the AgCl and the solvent was evaporated. The resulting solid was converted to the PF_6 salt as described above, and purified by column chromotography (SiO_2, acetonitrile:aq.KNO_3, 9:1). The nitrate salt was metathesized to the PF_6 salt as described above to afford **3a** in 86% yield.

^{1}H NMR (CD_3CN, 400 MHz): 9.11 (d, J= 8 Hz, 4H) $H_{3,3''}$; 9.00 (d, J= 8 Hz, 4H), $H_{2''',6'''}$; 8.14, (t, J= 8 Hz, 4H) $H_{4,4''}$; 8.03 (d, J= 8.4 Hz, 4H) $H_{3''',5'''}$; 7.73 (d, J= 5 Hz, 4H) $H_{6,6''}$; 7.40 (dd, J= 6 Hz, 6Hz, 4H) $H_{5,5''}$. ^{13}C NMR (CD_3CN, 100 MHz): 170.62, 165.52, 155.43, 154.44, 139.52, 134.25, 133.33, 131.69, 130.91, 129.59, 128.63. ES-MS: $[M- PF_6]^{2+}$, 441.0. Anal. Calcd. For $C_{38}H_{24}Br_2F_{12}N_{10}P_2Ru$: C, 38.96; H, 2.06; N, 11.96. Found: C, 39.14; H, 1.90; N, 11.87.

General Procedure for Suzuki coupling reactions

Complex **2a** (0.060 g, 0.059 mmol), arylboronic acid (0.41 mmol), $Pd(PPh_3)_4$ (0.027 g, 40 mol%) and K_2CO_3 (0.082g, 0.59 mmol) were added to dry degassed DMF (10 mL) with light excluded. The reaction mixture was heated at 110 °C for 4 h under N_2. The mixture was cooled and poured into deaerated aqueous NH_4PF_6 and filtered through celite and the solid collected in acetonitrile. The residue was chromatographed under subdued lighting on silica gel with 9:1 ACN and aqueous saturated KNO_3 solution as eluent. The nitrate salt was metathesized to the PF_6 salt as described above to afford complexes **2b-d.**

2b (55% yield).

N.B. Yields were improved if DMF degassed by three freeze pump thaw cycles.

^{1}H NMR (CD_3CN): 9.15 (d, J= 9 Hz, 2H) $H_{2''',6'''}$; 9.11 (d, J= 8 Hz, 2H) $H_{3,3'}$; 8.81 (d, J= 8 Hz, 2H) $H_{T3',T5'}$; 8.53 (d, J= 9 Hz, 2H) $H_{T3,3''}$; 8.48 (t, J= 8 Hz, 1H) $H_{T4'}$; 8.14 (m, 4H) $H_{3''',5'''}$, $H_{4,4''}$; 7.94 (td, J= 1 Hz, 8 Hz, 2H), $H_{T4,4''}$; 7.91 (d, J= 7 Hz, 2H) $H_{2'''',6''''}$;

7.60 (m, 4H) $H_{6,6''}$,$H_{3''',5'''}$; 7.53 (d, J= 7 Hz, 1H) $H_{4'''}$; 7.49 (d, J= 6 Hz, 2H) $H_{T6,6''}$; 7.43 (td, J= 1 Hz, 7 Hz, 2H) $H_{5,5''}$; 7.14 (td, J= 1 Hz, 7 Hz, 2H), $H_{T5,5'}$. ^{13}C NMR (CD_3CN): 124.27, 124.94, 127.83, 128.41, 129.17, 129.64, 130.87, 134.17, 137.07, 138.89, 139.07, 139.87, 146.96, 153.44, 154.69, 154.74, 155.72, 158.41, 170.70. High Res ES-MS: Calcd. for $[M\text{-}2PF_6]^{2+}$ 361.0735, found 361.0741; calcd. for $[M\text{-}1PF_6]^{+}$ 867.1117, found 867.1118. Anal. Calcd. For $C_{40}H_{28}F_{12}N_8RuP_2.2H_2O$: C, 45.85; H, 3.08; N, 10.69. Found C, 46.13; H, 3.27; N, 10.81.

2c (40 % yield)

^{1}H NMR (CD_3CN, 400 MHz): 9.23 (d, J= 8 Hz, 2H) $H_{2''',6'''}$; 9.12 (d, J=8 Hz, 2H) $H_{3,3''}$; 8.94 (d, J= 8 Hz, 1H) H_{phenan}; 8.87 (d, J=8 Hz, 1H) H_{phenan}; 8.80 (d, J= 8 Hz, 2H) $H_{T3',5'}$; 8.52 (d, J= 8 Hz, 2H) $H_{T3,3''}$; 8.48 (t, J= 8 Hz, 1H) $H_{T4'}$; 8.13 (t, J= 7 Hz, 2H) $H_{4,4''}$; 8.02-8.08 (m, 4H) $2H_{phenan}$, $H_{3''',5'''}$; 7.91-7.96 (m, 3H) $H_{T4,4''}$, H_{phenan}; 7.69-7.79 (m, 4H) $4H_{phenan}$; 7.58 (d, J= 5 Hz, 2H) $H_{6,6''}$; 7.50 (d, J= 5 Hz, 2H) $H_{T6,6''}$; 7.42 (dd, J= 6 Hz, 6 Hz, 2H) $H_{5,5''}$; 7.15 (dd, J= 7 Hz, 6 Hz, 2H) $H_{T5,5''}$. ^{13}C NMR (CD_3CN, 100 MHz): 124.13, 124.73, 125.22, 125.91, 127.73, 128.42, 128.54, 128.71, 128.73, 129.28, 129.33, 130.24, 131.07, 131.44, 131.68, 131.83, 132.01, 132.58, 132.74, 135.34, 138.03, 138.05, 139.85, 140.02, 148.19, 154.40, 155.62, 155.68, 156.66, 159.34, 159.91, 170.16, 171.73. High Res ESMS: Calcd. for $[M\text{-}2PF_6]^{2+}$ 411.0891, found 411.0890; calcd. for $[M\text{-}PF_6]^{+}$ 967.1430, found 967.1410. Anal. Calcd. For $C_{48}H_{32}F_{12}N_8RuP_2.2H_2O$: C, 50.23; H, 3.16; N, 9.76. Found C, 49.85; H, 3.18; N, 10.10.

2d (29% isolated yield)

^{1}H NMR (CD_3CN): 9.32 (d, J= 9 Hz, 2H) $H_{2''',6'''}$, 9.15 (d, J= 8 Hz, 2H) $H_{3,3''}$; 8.84 (d, J= 8 Hz, 2H) $H_{T3',T5'}$; 8.73 (s, 1H) H_{An}; 8.56 (d, J= 8 Hz, 2H) $H_{T3,3''}$; 8.51 (t, J= 8 Hz, 1H) $H_{T4'}$; 8.21 (d, J= 8 Hz, 2H) $2H_{An}$; 8.15 (td, J= 1 Hz, 8 Hz, 2H) $H_{4,4''}$; 7.96 (td, J= 1 Hz, 8 Hz, 2H) $H_{T4,4''}$; 7.92 (d, J= 9 Hz, 2H) $H_{3''',5'''}$; 7.78 (d, J= 9 Hz, 2H) H_{An}; 7.60 (m, 4H) $H_{6,6''}$ $2H_{An}$; 7.55 (m, 4H) $H_{T6,6''}$, $2H_{An}$; 7.45 (dd, J= 6 Hz, 6 Hz, 2H) $H_{5,5''}$; 7.18 (d, 2H J= 1 Hz, 7 Hz, 2H) $H_{T5,5''}$. ^{13}C NMR (CD_3CN): 170.91, 169.28, 158.44, 155.73, 154.80, 154.70, 153.53, 145.58, 139.11, 138.95, 137.17, 135.92, 134.74,

132.91, 131.83, 130.96, 130.24, 130.19, 129.05, 128.48, 127.82, 127.87, 126.64, 126.45, 125.97, 125.00, 124.32. High Res ES-MS: Calcd. for $[M-2PF_6]^{2+}$ 411.0891, found 411.0901; calcd. for $[M-PF_6]^{+}$ 999.1328, found 99.1359. Anal. Calcd. For $C_{48}H_{32}N_8RuP_2F_{12}.2H_2O$: C, 50.23; H, 3.16; N, 9.76. Found C, 50.63; H, 3.20; N, 9.90.

The same procedure was adopted for the synthesis of the homoleptic complexes but using a larger excess of arylboronic acid (10 equivalents).

3b (65%)

^{1}H NMR (CD_3CN, 400 MHz): 9.18 (d, J= 9 Hz, 4H) $H_{2''',6'''}$; 9.15 (d, J= 8 Hz, 4H) $H_{3,3''}$; 8.16 (t, J= 7 Hz, 4H) $H_{4,4''}$; 8.14 (d, J= 8 Hz, 2H) $H_{3''',5'''}$; 7.92 (d, J= 5 Hz, 4H) $H_{2'''',6''''}$; 7.75 (d, J= 6 Hz, 4H) $H_{6,6''}$; 7.60 (dd, J= 7 Hz, 8 Hz, 4H) $H_{3'''',5''''}$; 7.51 (dd, J= 7 Hz, 7 Hz) 2H) $H_{4''''}$; 7.41 (dd, J= 6 Hz, 7 Hz, 4H) $H_{5,5''}$.
^{13}C NMR (CD_3CN, 100 MHz): 170.56, 170.00, 155.38, 154.76, 147.23, 139.82, 139.48, 133.99, 130.83, 130.75, 129.66, 129.25, 128.51, 128.48, 127.74. ESMS: $[M-2PF_6]^{2+}$, 437.6. Anal. Calcd. For $C_{50}H_{34}F_{12}N_{10}P_2Ru$: C, 51.51; H, 2.94; N, 12.01. Found C 51.45, H 3.30, N 12.02.

3c (54%)

^{1}H NMR (CD_3CN, 400 MHz): 9.27 (d, J= 8Hz, 2H) $H_{2''',6'''}$; 9.17 (d, J= 8Hz, 2H) $H_{3,3''}$; 8.95 (d, J= 8Hz, 1H) H_{phenan}; 8.88 (d, J= 9Hz, 1H) H_{phenan}; 8.18 (t, J= , 2H) $H_{4,4''}$; 8.07 (m, 4H) $H_{3''',5'''}$, $2H_{phenan}$; 7.98 (s, 1H) H_{phenan}; 7.69-7.81 (m, 6H) $H_{6,6''}$, $4H_{phenan}$; 7.43 (dd, J= 6Hz, 6Hz, 2H) $H_{5,5''}$. ESMS: $[M-2PF_6]^{2+}$ 538.5. Anal. Calcd. For $C_{66}H_{42}F_{12}N_{10}P_2Ru$. $2H_2O$: C, 56.54; H, 3.31; N, 9.99. Found C 56.19, H 3.50, N 10.33.

3d (81%)

^{1}H NMR (CD_3CN, 400 MHz): 9.26, (d, J= 8 Hz, 4H) $H_{2'''}$, $H_{6'''}$; 9.22 (d, J= 8 Hz, 4H) $H_{3,3''}$; 8.74 (s, 2H) $2H_{An}$; 8.22 (d, J= 9 Hz, 4H) $4H_{An}$; 8.20 (t, J= 8 Hz, 4H) $H_{4,4''}$; 7.94 (d, J= 8 Hz, 4H) $H_{3''',5'''}$; 7.84 (d, J= 6 Hz, 4H) $H_{6,6''}$; 7.80 (d, J= 9 Hz, 4H) $4H_{An}$; 7.62 (t, J= 7 Hz, 4H) $4H_{An}$; 7.54 (t, J= 9 Hz, 4H) $4H_{An}$; 7.46 (m, 4H) $H_{5,5''}$.

^{13}C NMR (CD_3CN, 100MHz): 125.96, 126.43, 126.64, 127.91, 128.64, 129.05, 130.20, 130.37, 130.93, 131.85, 132.98, 134.56, 135.87, 139.55, 145.94, 154.80, 155.48, 170.25, 170.77. Anal. Calcd. For $C_{66}H_{42}F_{12}N_{10}P_2Ru.\ 3H_2O$: C, 55.82; H, 3.41; N, 9.86. Found C 56.09, H 3.56, N 9.99.

***p*-(10-bromo-anthryl)benzocarbonitrile** (precursor for L2, whose formula is shown in Scheme 2.7) [30]

A mixture of 9,10-dibromoanthracene (4.60 g, 0.014 mol), 4-cyanophenylboronic acid (3.0 g, 0.021 mol), $[Pd(PPh_3)_4]$ (2 mol%), Na_2CO_3 (2 M, 68 mL), degassed THF (125 mL) and toluene (50 mL) was heated at 60°C under N_2 overnight. The mixture was diluted with H_2O and extracted with Et_2O. The combined organic layers were washed with H_2O, brine and dried (Na_2SO_4). The solvent was evaporated and the crude product left was charged on a silica gel column. Elution of the column with 2-10% EtOAc in hexane gave *p*-(10-bromo-anthryl) benzocarbonitrile as a yellow solid (1.91 g, 38 % yield) which was used without any further purification.

^1H NMR ($CDCl_3$, 400 MHz): 8.63 (d, J=8 Hz , 2H); 7.89 (d, J=7 Hz, 2H); 7.61 (t, J=8 Hz, 2H); 7.48-7.53 (m, 4H); 7.42 (m, 2H). ^{13}C NMR ($CDCl_3$, 100MHz): 111.89, 118.69, 123.89, 126.21, 126.37, 127.08, 128.09, 130.09, 130.37, 132.02, 132.27, 135.05, 143.67.

L2: 2,4-di(2'-pyridyl)-6-(*p*-(10-bromo-anthryl)-phenyl)-1,3,5-triazine (Scheme 2.7)

^{n}Butylithium 1.6M (3.1 mL, 4.9 mmol) was added to a stirring solution of dimethylamine 2M (2.5 mL, 4.9 mmol) in anhydrous diethyl ether (100 mL). The mixture was stirred for twenty minutes under nitrogen until a white suspension was visible. After 20 minutes, *p*-(10-bromoanthryl)-benzonitrile (1.6 g, 4.5 mmol) was added and a red colour change was immediately observed. The solution was stirred at room temperature for one hour and 2-cyanopyridine (0.86 mL, 9.0 mmol) was slowly added. A precipitate rapidly formed and the resulting suspension was stirred

overnight. The mixture was stirred in air for a further 30 minutes and the precipitate was filtered. The solid was recystallised from 4:1, ethanol:water and a second recrystallisation was carried out in ethanol alone. On cooling, a precipitate formed, which was washed with diethylether and dried to give **L2** (0.90 g, 35% yield).

^{1}H NMR (300 MHz, $CDCl_3$): 9.03-9.07 (m, 4H) $H_{6,6''}$, $H_{2''',6'''}$; 8.94 (d, J = 8 Hz, 2H), $H_{3,3''}$; 8.68 (d, J = 9 Hz, 2H) H_{anth}; 8.04 (td, J = 1.5, 8 Hz, 2H) $H_{4,4''}$; 7.59-7.75 (m, 4H) $H_{3''',5'''}$, $3H_{anth}$; 7.46, 2H, dd (J = 6 Hz, 8Hz), $H_{5,5''}$. ^{13}C NMR (100 MHz, $CDCl_3$): 121.56, 122.91, 124.62, 125.54, 126.12, 127.62, 129.18, 129.84, 130.33, 131.40, 134.78, 136.37, 136.79, 143.15, 150.16, 153.01, 171.43, 172.52. High Res ESMS: Calcd. for $[M+H]^+$ 566.0974, found 566.0983.

2e: Alternative route (24%)

L2 (228 mg, 0.40 mmol) was added to a stirred solution of $Ru(tpy)Cl_3$ (200 mg, 0.40 mmol) and $AgNO_3$ (206 mg, 1.2 mmol) in ethanol (30 mL) with light excluded. The reaction was heated to reflux for five hours and on cooling the solution was filtered to remove the AgCl and the solvent was evaporated. The resulting solid was dissolved in acetonitrile and purified by column chromotography (SiO_2, acetonitrile:aq.KNO_3, 7:2). The nitrate salt was metathesized to the PF_6 salt as described above to afford **2e** (100 mg, 24%).

^{1}H NMR (CD_3CN, 400 MHz): 9.34 (d, J= 8 Hz, 2H) $H_{2''',6'''}$; 9.17 (d, J= 8 Hz, 2H) $H_{3,3''}$; 8.85 (d, J= 8 Hz, 2H) $H_{T3',T5'}$; 8.71 (d, J= 9 Hz, 2H) $2H_{An}$; 8.57 (d, J= 7 Hz, 2H) $H_{T3,3''}$; 8.53 (t, J= 8 Hz, 1H) $H_{T4'}$; 8.17 (t, J= 8 Hz, 2H) $H_{4,4''}$; 7.98 (t, J= 8 Hz, 2H) $H_{T4,4''}$; 7.92 (d, J= 8 Hz, 2H) $H_{3''',5'''}$; 7.82 (d, J= 9 Hz, 2H), $2H_{An}$; 7.78 (m, 2H) $2H_{An}$; 7.64 (d, J= 6 Hz, 2H) $H_{6,6''}$; 7.60 (m, 2H) $2H_{An}$; 7.55 (m, 2H) $H_{T6,6''}$; 7.47 (m, 2H) $H_{5,5''}$, 7.20 (t, J= 6 Hz, 2H) $H_{T5,5''}$. ^{13}C NMR (CD_3CN, 100MHz): 122.28, 123.54, 124.21, 126.09, 126.54, 127.03, 127.24, 127.33, 127.69, 129.49, 129.75, 129.79, 130.19, 130.22, 131.99, 134.25, 136.41, 138.16, 138.32, 144.15, 152.75, 153.89, 154.02, 154.93, 157.64, 168.36, 170.15. High Res ESMS: Calcd. for $[M-2PF_6]^{2+}$ 450.0443, found 450.0449; calcd. for $[M-1PF_6]^+$ 1045.0.540, found 1045.0530.

3e (Alternative Route 48 %)

L2 (46 mg, 0.082 mmol) was added to a stirred solution of $RuCl_3.3H_2O$ (12 mg, 0.041 mmol) and $AgNO_3$ (21mg, 0.12 mmol) in DMF (10mL) with light excluded. The reaction was heated to reflux for ninety minutes and on cooling the solution was filtered to remove the AgCl and the solvent was evaporated. The resulting solid was dissolved in acetonitrile and purified by column chromotography (SiO_2, acetone: H_2O: aq.KNO_3, 9:0.9:0.1). The nitrate salt was metathesized to the PF_6 salt as described above to afford **3e** (30 mg, 48%).

^{1}H NMR (CD_3CN, 400 MHz): 9.39 (d, J= 8 Hz, 4H) $H_{2''',6'''}$, 9.24 (d, J= 8 Hz, 4H) $H_{3,3''}$; 8.72 (d, J= 9 Hz, 4H) $4H_{An}$; 8.22 (td, J= 1 Hz, 8 Hz, 4H) $H_{4,4''}$; 7.95 (d, J= 8 Hz, 4H) $H_{3''',5'''}$; 7.77-7.87 (m, 12H) $8H_{An}$,$H_{6,6''}$; 7.61 (dd, J= 9 Hz, 9 Hz, 4H) H_{An}; 7.50 (m, 7 Hz, 4H) $H_{5,5''}$. ^{13}C NMR ($CDCl_3$, 100MHz): 122.33, 126.12, 126.56, 127.30, 127.35, 127.87, 129.59, 129.80, 130.15, 130.25, 132.11, 134.04, 136.37, 138.79, 144.58, 153.97, 154.75, 169.32, 169.99. High Res MS: Calcd. for $[M- 2PF_6]^{2+}$ 616.0418, found 616.0430, calcd. for $[M- PF_6]^+$ 1377.0469, found 1377.0476.

2.11 Results and Discussion

Two approaches were applied to the synthesis of complexes **2a-e** and **3a-e** as represented in Figure 2.16. We previously reported a classical synthetic procedure for **3c**, the 'ligand-synthesis' approach (Figure 2.16 a), in which the phenanthryl group was introduced onto the triazine ligand prior to complexation.[31] Alternatively, the brominated ligand **L1** can be complexed to Ru(II) affording an ideal precursor for the 'chemistry-on-the-complex' approach enabling the introduction of organic components using cross coupling reactions (Figure 2.16 b).[16, 19, 20, 23, 32-35]

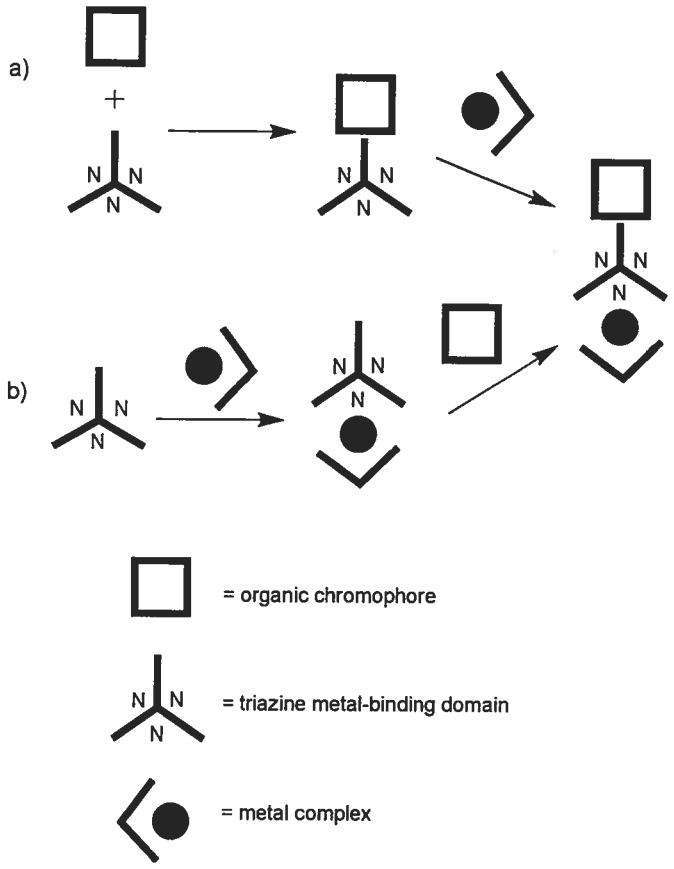

Figure 2.16 Two synthetic approaches to a coordination complex: a) the classical 'ligand-synthesis' approach, and b) the 'chemistry-on-the-complex' approach.

In order to evaluate the effectiveness of the 'chemistry-on-the-complex' approach, we set out to synthesise complexes **2b-e** and **3b-e** in this fashion (Scheme 2.7). Thus, complex **2a** was synthesised by addition of **L1,** synthesised according to a previously

reported procedure,[27] to a suspension of one equivalent of $Ru(tpy)Cl_3$ and three equivalents of $AgNO_3$ in ethanol. After four hours at reflux, the resulting dark solution was cooled, filtered to remove AgCl and dried under reduced pressure. The mixture was solubilised and precipitated on addition to aqueous NH_4PF_6. The precipitate was collected and purified by column chromatography using acetonitrile: KNO_3 (sat), 7:1. The second intense red band was collected and was precipitated as its PF_6^- salt.

It was found that a one-pot synthesis of **3a** was more successful than the two-step approach which would involve the isolation of $Ru(\mathbf{L1})Cl_3$ intermediate. Two equivalents of the ligand were added to one equivalent of $RuCl_3.3H_2O$ and three equivalents of $AgNO_3$ in DMF. The reaction was stirred in DMF at room temperature for 20 minutes and then refluxed for one hour, cooled and purified as for **2a**.

Complexes **2b-d**, and **3b-d** were synthesised using the palladium-catalysed Suzuki-Mayauri reaction in degassed DMF by adapting known procedures (Scheme 2.7).[16] The complexes could be worked up by precipitation in aqueous NH_4PF_6 and then column chromatography on a silica column and elution with 9:1 MeCN:KNO_3(sat). Counter-ion exchange to the PF_6 salts afforded the complexes **2b-d** and **3b-d**.

The synthesis of **2e** was attempted using the 'chemistry-on-the-complex' approach, however, the reaction proceeded slowly and the purification of **2e** was problematic. An alternative approach was taken to introduce the bromo-anthracene substituent into the ligand prior to complexation.[31] A Suzuki-Mayauri reaction afforded *p*-(10-bromoanthryl)-benzonitrile, modifying a published procedure to monosubstitute 9,10-dibromoanthracene using 4-cyanophenylboronic acid. [30, 36] The *p*-(10-bromoanthryl)-benzonitrile could then be used to synthesise the triazine ligand employing the same procedure as **L1**.[27, 31]

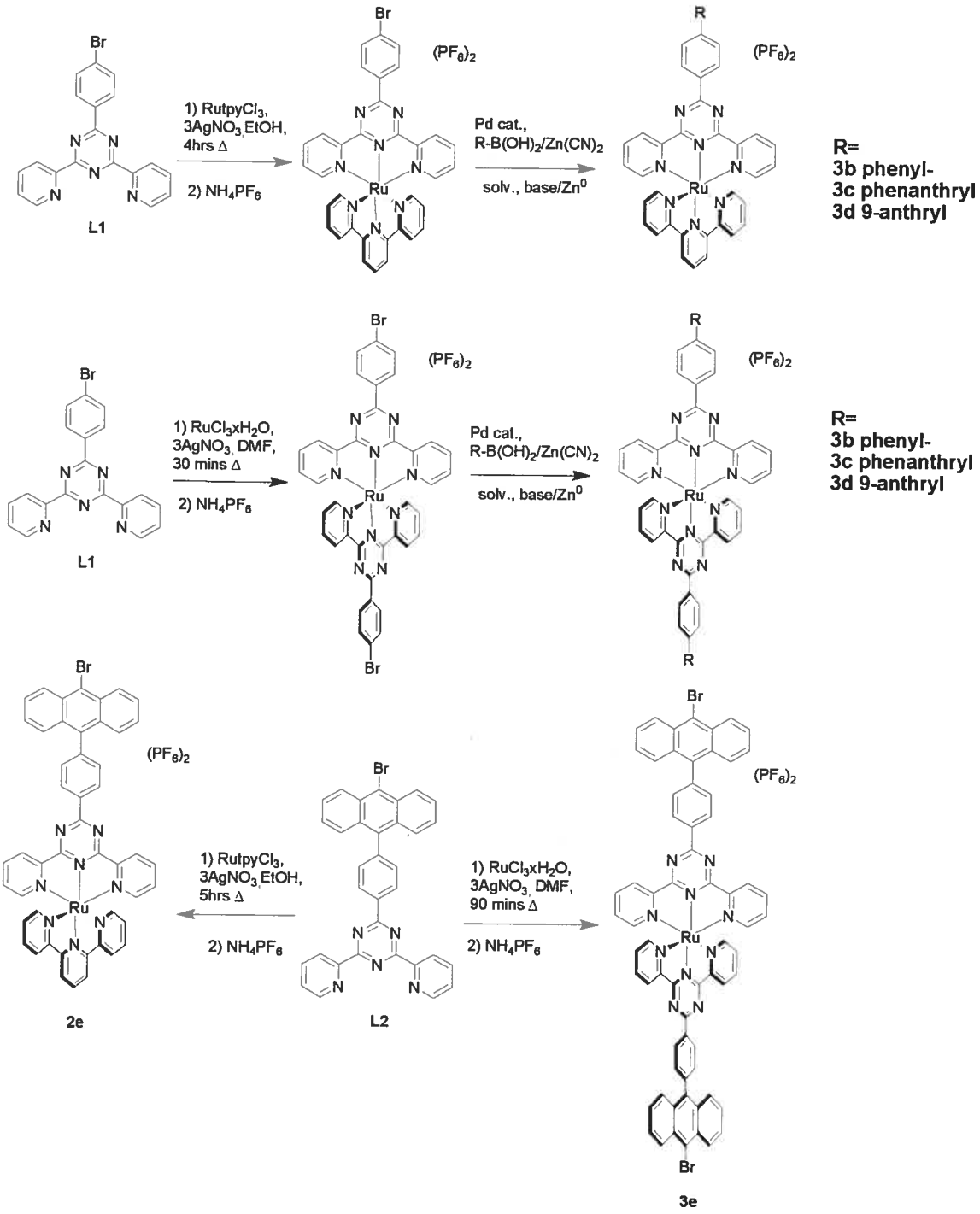

Scheme 2.7 Synthesis of complexes **2a-e** and **3a-e**.

The ^{1}H NMR spectra for complexes **3d** and **3e** are shown in CD_3CN at 400 MHz in Figure 2.17 The bromo-substituent has little effect on the chemical shift of the pyridyl

protons (labelled Figure 2.17) but the signals for the anthracene-based protons in complex **3e** are significantly deshielded with respect to **3d.** The disappearance of the anthracene based singlet at position 10 probes the bromo-substitution of the anthracene moiety.

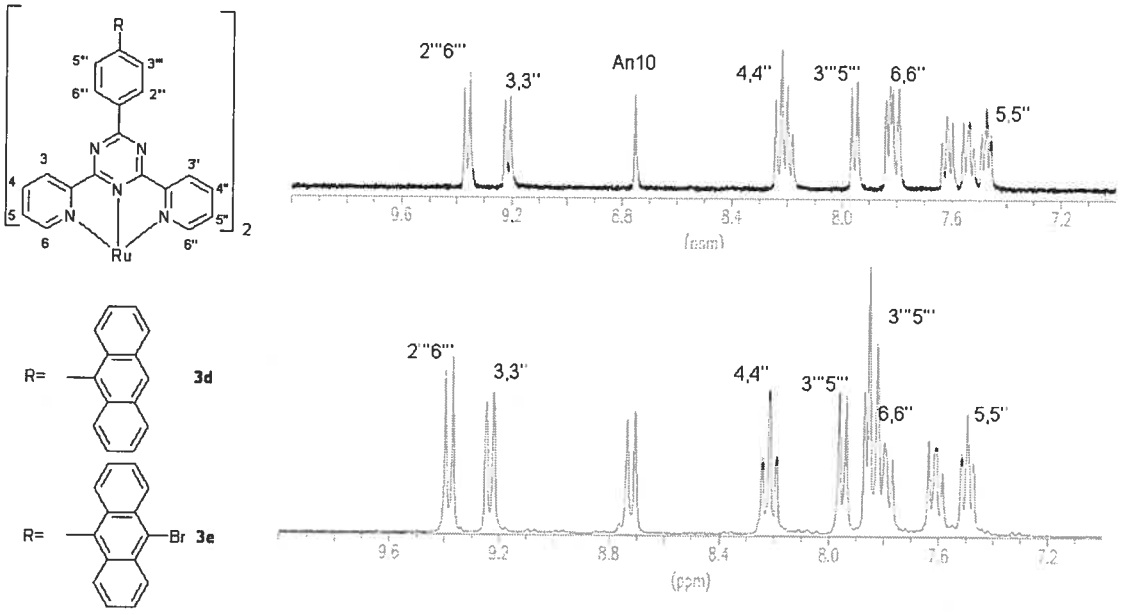

Figure 2.17 ^{1}H NMR of complexes **3d** (top) and **3e** (bottom) at 400 MHz in CD_3CN.

2.11.1 X-Ray crystallography

The solid state structures of ligand **L2** and complexes **2a**, **2b**, **3a** were studied by X-ray diffraction (Figures 2.18 and 2.19). X-Ray quality crystals of **L2** were obtained by slow diffusion of hexane into a concentrated solution of **L2** in chloroform.

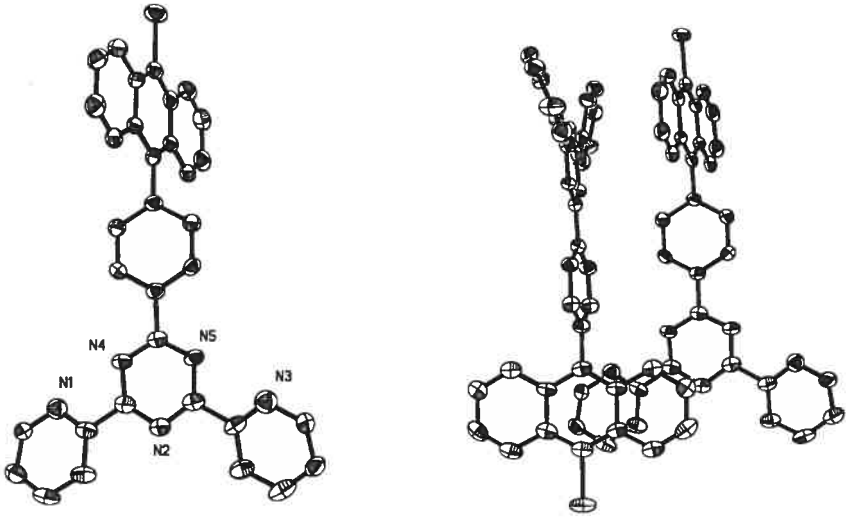

Figure 2.18 X-ray crystal structure of **L2** (left) as an ORTEP representation. Thermal ellipsoids are set at 50%. The π-stacking, face-to-face interactions are shown (right).

The ligand crystallises in the orthorhombic space group $P2_12_12_1$ with four molecules in the unit cell. The two pyridyl and phenyl rings twist away from the triazine ring by 15.6 (2)°, 14.7 (2)°, and 7.0 (2)°, respectively. The pyridyl rings are twisted twice as much as the phenyl ring due to a combination of π-stacking effects between neighbouring molecules and the N-N lone pair repulsions between pyridyl-N atoms and triazine-based N-atoms. The ligand molecules aggregate through continuous π-stacking interactions in the extended lattice between the anthryl-tail of one molecule and the pyridyl head of its neighbour (Figure 2.18). The centroid-centroid distances between the central anthryl ring and the pyridyl rings above and below the plane are 3.30 Å and 4.48 Å.

Crystals of complexes **2a** and **3a** were obtained by slow diffusion of isopropyl ether into a concentrated solution of the complexes in acetonitrile. Complex **2a** crystallised in the triclinic space group $P\bar{1}$ with two cations, four PF_6^- anions and four molecules of acetonitrile in the asymmetric unit. The pendant phenyl rings are twisted by 7.6 (2)° and 9.5 (2)° for both independent cations. The near co-planar configurations are due to intramolecular H-bonding interactions between the lone pairs on the triazine atoms N4 and N5 and the C-H on the phenyl substituent. The slight twist is imposed by edge-to-face interactions of the phenyl ring with the pyridyl ring of a neighbouring cation (H-centroid 2.86 Å and 3.19 Å).

The Ru-N bond distances are reported in Table 2.1. Longer Ru-N bond distances are observed to the pyridyl rings for both triazine and tpy ligands due to the constrained bite-angle imposed by terdentate ligands.[37] The Ru-N (trz) central bond (M- N2/N10) is shorter than the Ru-N7 (tpy) bond distance (M- N7/N15). This is consistent with what has previously been reported for triazine-based complexes and is presumably due to the improved π-acceptor properties in the electron-deficient triazine ligand.[13] The Ru-N (tpy) bond distances are consistent with those previously reported for $Ru(tpy)_2^{2+}$.[38]

Table 2.1 Selected bond distances and angles from the X-ray structures of complexes **2a**, **2b** and **3a.**

	2a		**2b**	**3a**	**$Ru(tpy)_2^{2+}$** [a]
Bond distances (Å)					
M – N1	2.089 (4)	2.106 (4)	2.084 (4)	2.096 (5)	2.07 (1)
M – N2 (trz)	1.957 (4)	1.966 (4)	1.955 (3)	1.972 (5)	1.99 (1)
M – N3	2.101 (4)	2.083 (4)	2.081 (4)	2.085 (5)	2.05 (1)
M – N6	2.065 (4)	2.081 (4)	2.084 (4)		2.09 (1)
M – N7	1.986 (4)	1.985 (4)	1.985 (3)		1.96 (1)
M – N8	2.075 (4)	2.067 (4)	2.054 (4)		2.07 (1)
Bond Angles (°)					
N1– M – N3	155.60 (15)[b]	155.7 (2)[b]	155.60 (16)[b]	155.45 (19)	158.1 (4)
N6 – M – N8	157.34 (16)[c]	157.6 (2)[c]	158.08 (16)[c]		158.2 (4)
Trz-phenyl twist	7.60 (24)	9.47 (24)	4.60 (22)	14.71 (47)	
Phenyl-phenyl twist			26.35 (24)		

[a] Data from reference.[38] [b] N- M- N tridentate bite angle for triazine ligand. [c] N- M- N tridentate bite angle for tpy ligand.

It can be noted that the tridentate bite angles N-M-N in the triazine-based ligands are smaller (155.5-155.6 °) than those in the tpy-based ligands (157.4-158.2 °). The additional N-atoms in the triazine ring distorts the ring angles away from the ideal 120° in benzene significantly more than in the central pyridyl ring of tpy. This will have a negative effect on the ligand field strength thereby facilitating thermal access of metal centred-states (see later).

Complex **3a** crystallises in the monoclinic space group C2/c and was isostructural to the reported Fe(II), Co(II) and Cu(II) complexes of **L1**.[27, 39] Short bromine-bromine contacts are observed in the solid state and these interactions are smaller than the sum of the Van der Waals radii (3.48 Å). In the absence of stabilizing π-stacking interactions these contacts influence the cationic arrangements in the extended lattice.

Efforts to obtain crystals of **2b** as the PF_6^- salt were unsuccessful using a variety of solvent conditions. However, addition of an excess of ammonium tetraphenylborate to the acetonitrile solution allowed salt exchange and the complex was crystallised as a mixed salt containing one PF_6^- and one BPh_4^- anion per cation. The Ru-N bond distances and angles are very similar to those of complex **2a** indicating that the substitution on the periphery has little effect on the metal centre. The phenyl ring closest to the triazine ring is twisted by 4.6 (2)° in a near co-planar interaction. The second phenyl ring is twisted
C-C bond by 26.4 (2)° which is consistant with the twist reported for Ru(II) complexes of biphenyl-tpy type systems.[37] Edge-to-face interactions between biphenyl tails promote the twists about the interannular C-C bond. The inner-phenyl ring face has a short contact with the outer-phenyl edge of a neighbouring cation (H-centroid 2.71 Å). An additional edge-to-face interaction is observed with a short contact of the face of the outer phenyl ring with a neighbouring pyridyl ring (H-centroid 3.10 Å).

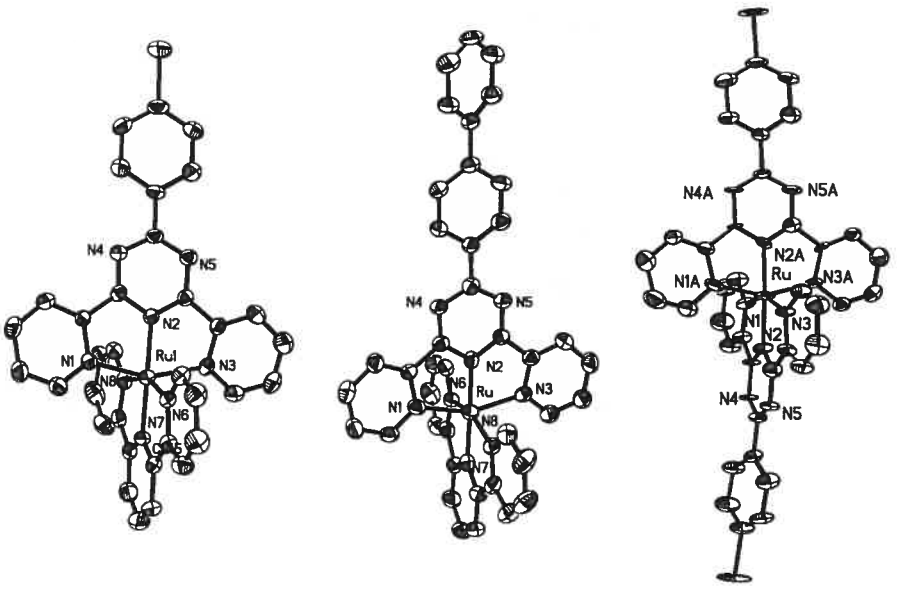

Figure 2.19 X-ray crystal structure of **2a** (left), **2b** (central) and **3a** (right) as an ORTEP representation. Thermal ellipsoids are set at 50%. The anions and H atoms have been omitted for clarity.

2.11.2 Electrochemistry

Table 2.2 Half-Wave Potentials for Ru(II) Complexes **2a-d** and **3a-d.**[a]

	$E_{1/2}$(oxidn)		$E_{1/2}$(redn)			
2a	1.43 (79)		-0.75 (64)	-1.37 (68)	-1.62 (107)	
2b	1.40 (71)		-0.78 (53)	-1.39 (66)	-1.65 (82)	
2c	1.45 (80)		-0.81 (82)	-1.45 (90)	-1.71 (90)	
2d	1.29 (64)	1.43 (98)	-0.77 (48)	-1.39 (62)	-1.64 (70)	
2e	1.43 (91)		-0.77 (74)	-1.40 (79)	-1.66 (80)	
3a	1.53 (76)		-0.71 (50)	-0.87 (55)	-1.51 (70)	-1.71 (128)
3b	1.53 (82)		-0.78 (84)	-0.97 (50)	-1.58 (50)	-1.79 (138)
3c[b]	1.53 (70)		-0.73 (53)	-0.89 (45)	-1.55 (77)	-1.78 (72)
3d	1.32 (42)	1.61 (irr)	-0.74 (48)	-0.91 (50)	-1.55 (64)	-1.80 (61)
3e	1.38 (80)	1.57 (87)	-0.71 (82)	-0.86 (73)	-1.43 (irr)	-1.62 (ads)
$Ru(tpy)_2^{2+}$[c]	1.30		-1.24	-1.49		

[a] Potentials are in volts vs SCE for acetonitrile solutions, 0.1 M in TBAP, recorded at 25 ± 1 C at a sweep rate of 200 mV/s. The difference between cathodic and anodic peak potentials (millivolts) is given in parentheses. [b] Data from reference [31]. [c] Data from reference [40].

Complexes **2a-c** and **2e** all have one reversible oxidation assigned to the Ru(III)/(II) couple as noted for similar complexes.[13] However, complex **2d** has two oxidative processes, the first reversible process is assigned to an anthracene-based oxidation and the second quasi-reversible process is assigned to the Ru(III)/(II) couple. The Ru(III)/(II) couple is at approximately the same potential as in the other complexes indicating the anthracene component is electronically separated from the Ru(II) metal centre. Introduction of the bromo-substituent significantly affects the oxidation potential of the anthracene moiety so that an initial Ru(III)/(II) couple is observed closely followed by the anthracene oxidation. However, the anthracene-based oxidation is highly irreversible and therefore masked by the Ru(III)/(II) couple and cannot be resolved.

All heteroleptic complexes, **2a-e**, have three one-electron reductions which are assignable by comparing them to previously reported results.[13] The first reduction is triazine-based and is observed at a less negative potential than in the parent complex $Ru(tpy)_2^{2+}$ due to the ease of reducing the electron-deficient bis(pyridyl)-triazine ligands compared to tpy.[13] The second reduction is tpy-based and compares well with the reduction of the parent complex $Ru(tpy)_2^{2+}$. The third reduction is assigned to a second one-electron reduction on the triazine ligand.

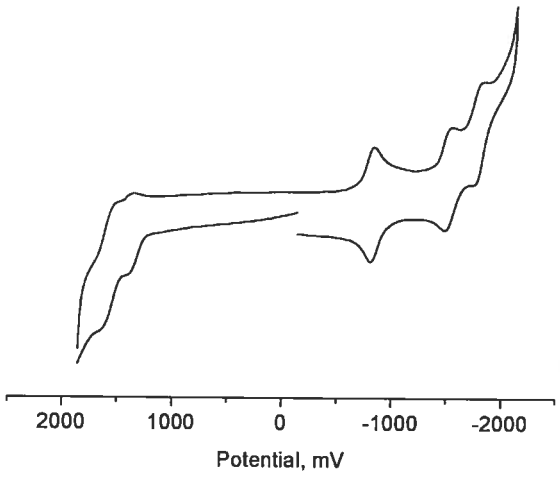

Figure 2.20 Cyclic voltammogram of complex **2d** in acetonitrile with 0.1M $TBAPF_6$.

The homoleptic complexes **3a-b** have reversible Ru(III)/(II) couples at a more positive potential than the heteroleptic complexes as a result of the electron-deficient bis(pyridyl)-triazine ligands drawing electron density away from the Ru(II) metal centres. The anthracene-substituted complex **3d** has an additional oxidation consistent with an anthracene-based oxidation as in **2d**.

Complexes **3** have several reversible ligand-based reductions. There are two one-electron reductions on each triazine to give a total of four reductions. The separation between the second and third reduction processes is in the range 610-660 mV for all of the complexes (leaving aside **3e**, whose irreversible third process makes the comparison impossible), in good agreement with the electron pairing energy in tpy-type ligands.[41]

2.11.3 Absorption spectra and photophysical properties

The electronic absorption and photophysical data of the new complexes are shown in Table 2.3. Representative absorption and emission spectra are shown in Figures 2.21-2.25. The absorption spectra are dominated by ligand-based spin-allowed $\pi \rightarrow \pi^*$ and $n \rightarrow \pi^*$ transitions in the UV region of the spectra and by ^{1}MLCT absorption bands in the visible region (Table 2.3, Figures 2.21 and 2.22). Complexes **2a-e** have a relatively sharp ^{1}MLCT absorption band with the λmax corresponding to the transition involving the tpy ligand. A low energy shoulder corresponds to the singlet MLCT transition involving the bis(pyridyl)triazine ligands.[13] Complexes **2d** and **2e** have additional characteristic sharp, high energy transitions corresponding to the $\pi \rightarrow \pi^*$ transitions associated with the anthracene component (Figure 2.21).[42, 43] The same absorption features are observed in the homoleptic complexes **3d** and **3e**. The ^{1}MLCT bands in the homoleptic complexes are broader and the visible maxima are red-shifted compared with the spectra of complexes **2a-e**, as a consequence of the missing of the higher energy MLCT transitions involving the tpy ligand.[13]

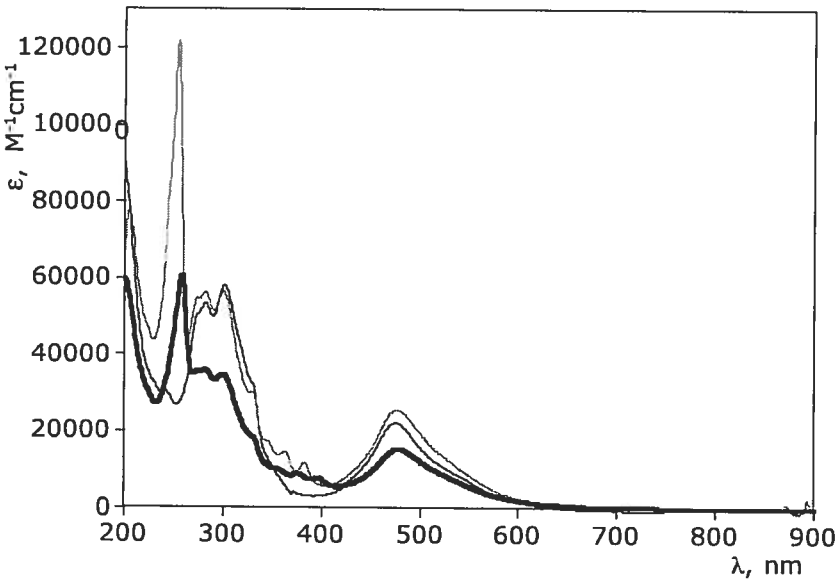

Figure 2.21 Absorption spectra of compounds **2a** (straight line), **2d** (gray line) and **2e** (bold line).

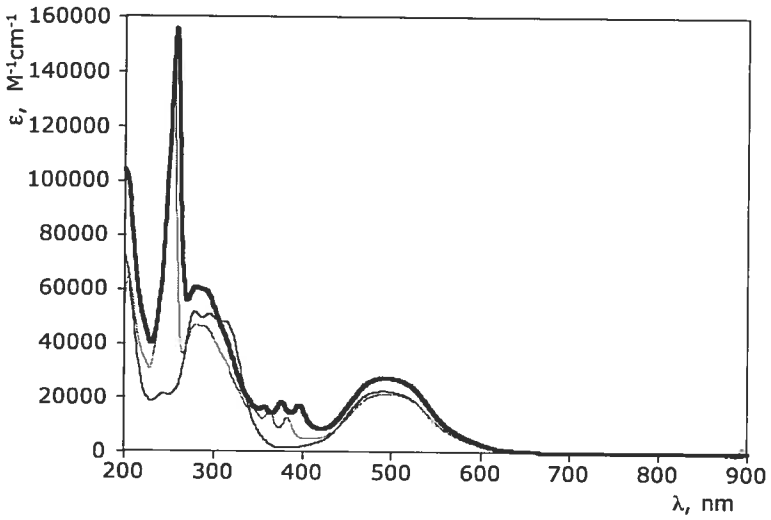

Figure 2.22 Absorption spectra of compounds **3a** (straight line), **3d** (gray line) and **3e** (bold line).

Table 2.3 Spectroscopic and photophysical data of the complexes in deaerated acetonitrile solution (298 K) or in butyronitrile rigid matrix (77 K).

Compound	Absorption 298 K	Luminescence 298 K			Luminescence 77 K	
	λ_{max}, nm (ε, $M^{-1}cm^{-1}$)	λ_{max}, nm	Φ	τ, ns	λ_{max}, nm	τ
2a	282 (53.5); 301 (59.6) 476 (21.7)	739	1.2×10^{-4}	12	693	1.2 μs
2b	273 (59.0); 301 (52.2) 332 (48.6); 478 (27.7	733	1.0×10^{-4}	10	695	1.9 μs
2c	254 (83.1); 273 (79.9) 299 (73.2); 331 (34.3) 477 (26.3)	734	0.9×10^{-4}	13	694	2.0 μs
2d	254 (121.4); 282 (55.7) 299 (56.5); 364 (14.4) 383 (12.3); 477 (25.7)	735	1.0×10^{-4}	13	694	3.4 ms
2e	258 (59.3); 272 (35.7) 281 (36.1); 298 (34.6) 330 (sh); 357 (9.2) 377 (9.1); 397 (8.3) 478 (15.4)	738	0.5×10^{-4}	54	695	3.4 ms
3a	279 (50.9); 295 (50.6) 491 (27.5)	714	$<10^{-5}$	2	676	2.0 μs
3b	276 (64.7); 339 (49.6) 501 (26.5)	____	___	___	682	2.2 μs
3c	206 (86.1); 253 (85.6) 274 (74.7); 328 (sh) 491 (21.1)	717	$<10^{-5}$	6	678	2.2 μs
3d	254 (145.1); 280 (46.7) 346 (16.4); 364 (14.9) 383 (12.9); 494 (20.7)	___	___	___	694	3.5 ms
3e	258 (155.6); 279 (60.7) 357 (15.6); 377 (18.2) 397 (17.3); 493 (26.8)	___	___	___	694	4.2 ms

The room temperature emission of the heteroleptic **2a-e** complexes can be assigned to triplet MLCT states involving the bis(pyridyl)triazine ligands, on the basis of the energies and shapes (Table 2.3, Figures 2.23 and 2.24).[13] As far as the homoleptic **3a-e** species are concerned, only **3a** and **3c** exhibit a sizeable room temperature emission, assigned to the lowest-lying MLCT triplet state, whereas **3b** and **3d-e** do not emit at room temperature. This is probably due to the lowering of the energy of the metal-centered (MC) state, as a consequence of increased distortion in the octahedral geometry exhibited by the homoleptic compounds compared to the heteroleptic species, as supported by comparison between crystallographic data of **2a** and **3a.** Such a lowering of the MC state makes this latter level closer in energy to the MLCT one, so thermal activated surface crossing to the MC state is very efficient and finally leads to very fast radiationless decay which prevents luminescence.

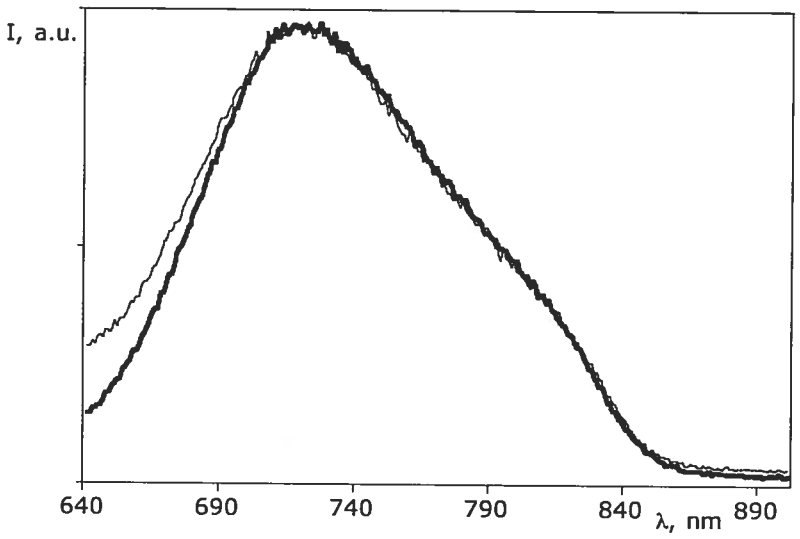

Figure 2.23 Uncorrected emission spectra of compounds **2a** (bold line) and **2e** (straight line) in acetonitrile solutions at room temperature. For corrected maxima values, see Table 2.3.

In the whole series of complexes, varying the substituent in the *para*-position of the phenyl ring has little effect on the energy of the MLCT absorption and emission bands, indicating that the aryl-groups are largely electronically separated from the Ru(II)

centre and the MLCT states associated with it. However, the excited state lifetimes are influenced to a greater extent: in fact, whereas complexes **2a-d** have excited state lifetimes between 10 and 13 ns, approximately fifty-times longer-lived than the parent complex, $Ru(tpy)_2^{2+}$ at room temperature, and well comparable with those of other Ru(II) triazine-based compounds,[13] the excited state lifetime of **2e** is significantly longer (Table 2.3). Indeed, hydrocarbon aromatic chromophores appended to metal complexes can prolong MLCT emission lifetimes.[16, 17] However, biphenyl, phenanthryl, and anthryl groups, which are present in **2b, 2c**, and **2d**, respectively, have no sizeable effect on MLCT lifetime at room temperature. The reason is that the lowest energy MLCT state in these complexes is so low-lying that thermal population of the relevant aromatic organic triplets (whose lowest energy one is that of the 9-aryl-anthracene chromophore, at about 685 nm [16, 42, 43]) is ineffective, also taking in consideration the intrinsic decay rates of aromatic hydrocarbons and MLCT triplets. As far as complex **2e** is concerned, this species bears a brominated anthracene and the electron-withdrawing effect of the bromo substituent lowers the energy of the anthracene-based triplet state. Actually, comparison between the triplet state of anthracene (14870 cm^{-1})[42, 44] and 9-bromo-anthracene (14400 cm^{-1})[43, 45] suggests that a bromo substituent stabilises the anthracene-based triplet state by about 500 cm^{-1}. Assuming the same effect in the present systems, and considering that the triplet state of the aryl-anthracene Ru(II) complexes is at about 685 nm (see above), as also evidenced by the low temperature emission of similar complexes,[16] the triplet state of the bromo-anthryl subunit in **2e** should lie at about 705 nm at room temperature. As a consequence, the lowest energy triplet state of the aromatic anthryl-based chromophore in **2e** becomes low enough to make equilibration between MLCT and anthryl-based triplets effective so that the multichromophoric effect can take place.

On cooling to 77 K in a butyronitrile rigid matrix the excited state lifetimes of complexes **2a-e**, as expected, are prolonged relative to room temperature. This effect is much larger for **2d** and **2e** whose luminescence lifetimes in this condition are three orders of magnitude longer compared to those of **2a-c** (Table 2.3). The shape of the emission is also different for **2d** and **2e** (in particular for the **2d** species, for which the higher-energy band is quite narrow) compared to those of **2a-c** (Figure 2.24). The

lifetime and shape of the emissions clearly indicate that emission of **2a-c** are still from MLCT states, whereas for **2d** and **2e** emission has to be assigned to phosphorescence from the anthracene-based triplet states. In fact, CT states are destabilized on passing from room temperature fluid solution to 77 K rigid matrix,[3, 46, 47] whereas the energy of organic triplets is essentially unperturbed by media conditions: since MLCT and anthryl-based triplet states are relatively close one another in **2d** and **2e**, the energy order of the two states is inverted on passing to 77 K, an already reported behavior for Ru(II) complexes containing anthracene derivatives.[48]

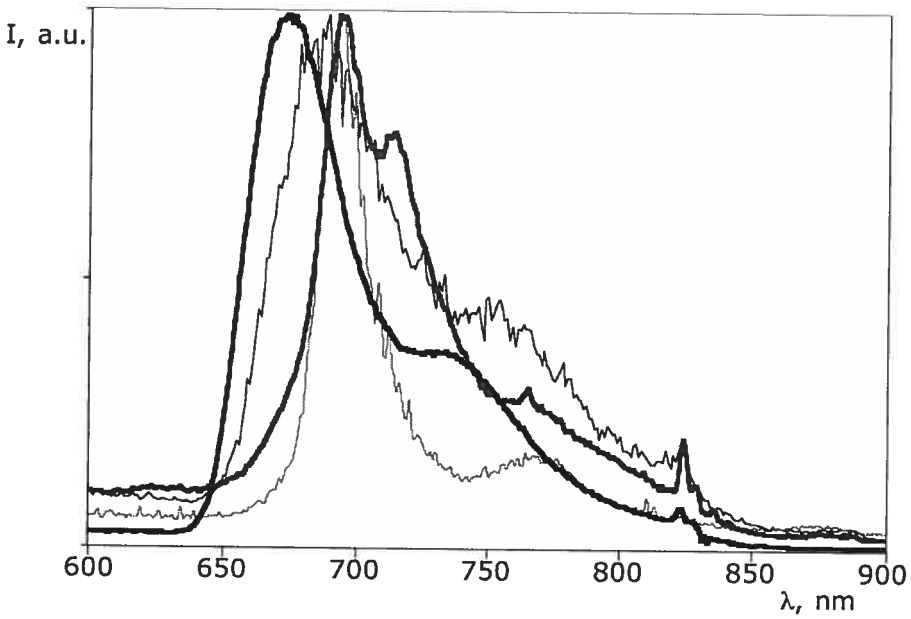

Figure 2.24 Uncorrected emission spectra of compounds **2b** (straight line), **2d** (gray line), **2e** (bold gray line) and **3a** (bold line) in butyronitrile rigid matrix at 77 K.

The 77 K emissions of **2d** and **2e** both maximize at 695 nm. Surprisingly, **2d** and **2e** have the same emission maximum in this condition, suggesting that the presence of the bromo substituent is less important in rigid matrix, as opposed to what happens at room temperature (see above). Indeed, it was expected that the emission energy of **2e** would be slightly lower than that of **2d**: we have no simple explanation for this behavior, we could only infer that potential intermolecular interactions involving the bromine can occur in rigid matrix for **2e** (and **3e**), making the presence of the bromo substituent on the anthracene less effective.

As far as the homoleptic **3a-e** complexes are concerned, all of them exhibit long-lived luminescence at 77 K, similar to the behavior of their heteroleptic counterparts (Table 2.3). The same line of reasoning used for the 77 K emission of **2a-e** allows us to assign the emission of **3a-c** to MLCT states and the emission of **3d** and **3e** to anthracene-based phosphorescence. At 77 K thermal population of the upper-lying MC states is not effective, so allowing luminescence from the homoleptic species. Interestingly, whereas the emission energies of **3d** and **3e** are identical to those of **2d** and **2e**, confirming their common anthryl-based origin and the constant energy level of the relevant aromatic hydrocarbon on passing from hetero- to homo-leptic compounds, the emission energies of **3a-c** are slightly higher than those of the corresponding **2a-c** species, in agreement with the redox potentials and supporting once more their MLCT origin.

2.12 Conclusion

We prepared a series of new hetero- and homoleptic Ru(II) complexes based on bis(pyridyl)triazine ligands and studied their absorption spectra, redox behavior, and luminescence properties, both at room temperature in fluid solution and at 77 K in rigid matrix. In some complexes, anthryl groups are linked to the triazine-based ligands. At room temperature the excited-state lifetimes of the heteroleptic complexes **2a-e** are significantly longer than that of the parent complex, $Ru(tpy)_2^{2+}$ and the homoleptic triazine complexes **3a-e**. The presence of the triazine ligand lowers the energy of the ligand based orbitals and, therefore, MLCT states, whilst the metal-centred states are maintained at higher energy in complexes **2a-e** by the presence of an orthogonal tpy ligand. In homoleptic triazine complexes **3a-e**, the MC states are lower in energy due to the small tridentate N-M-N bite angle as observed in the solid state. As a consequence a minimal improvement is observed in the excited state properties of complexes **3a-e** compared to the parent complex $Ru(tpy)_2^{2+}$.

Introduction of additional chromophores can have an impact on the excited state lifetime when the energy of the organic component is comparable to the energy of the ^{3}MLCT state. This result is obtained by tuning the excited-state energy of the anthracene subunit with the introduction of a bromo substituent. The lowering in

energy of the ^{3}bromo-anthracene excited state, which can then interact with the emissive ^{3}MLCT state in complex **2e**, extends the excited state lifetime to 54 ns at room temperature as compared to an excited state lifetime of 13 ns for complex **2d**, bearing an unsubstituted anthracene. The use of stronger electron-withdrawing (cyano) and electron delocalising (acetylene) groups to further tune the excited-state energy of the anthryl chromophore, and therefore the MLCT luminescence lifetime, will be investigated in due course.

CCDC-619166 – 619169 contains the supplementary crystallographic data for this paper. This data can be obtained free of charge from The Cambridge Crystallographic Data Centre via other *www.ccdc.cam.ac.uk/data_request/cif.*

2.13 Acknowledgments

The authors would like to thank the Natural Sciences and Engineering Research Council of Canada, Université de Montréal, the Centre for Self-Assembled Chemical Systems and the University of Messina for financial support. EAM thanks the ICCS for funding. The authors would also like to thank F. Bélanger-Gariépy for assistance with X-ray analyses. Johnson Matthey PLC is thanked for a loan of $RuCl_3.3H_2O$.

2.14 References and Notes

[1] V. Balzani, A. Juris, M. Venturi, S. Campagna, S. Serroni, *Chem. Rev.* **1996**, *96*, 759.

[2] K. Kalyanasundaram, *Photochemistry of Polypyridine and Porphyrin Complexes*, 1st ed., Academic Press Limited: San Diego, **1992**.

[3] A. Juris, V. Balzani, F. Barigelletti, S. Campagna, P. Belser, A. Von Zelewsky, *Coord. Chem. Rev.* **1998**, *84*, 85.

[4] V. Balzani, S. Campagna, G. Denti, A. Juris, S. Serroni, M. Venturi, *Acc. Chem. Res.* **1998**, *31*, 26.

[5] J. K. McCusker, *Acc. Chem. Res.* **2003**, *36*, 876.

[6] T. J. Rutherford, D. A. Reitsma, F. R. Keene, *J. Chem. Soc., Dalton Trans.* **1994**, 3659.

[7] J. P. Sauvage, J. P. Collin, J. C. Chambron, S. Guillerez, C. Coudret, V. Balzani, F. Barigelletti, L. De Cola, L. Flamigni, *Chem. Rev.* **1994**, *94*, 993.

[8] M. Abrahamsson, M. Jaeger, T. Oesterman, L. Eriksson, P. Persson, H.-C. Becker, O. Johansson, L. Hammarstroem, *J. Am. Chem. Soc. ASAP.*

[9] J. R. Winkler, T. L. Netzel, C. Creutz, N. Sutin, *J. Am. Chem. Soc.* **1987**, *109*, 2381.

[10] E. A. Medlycott, G. S. Hanan, *Chem. Soc. Rev.* **2005**, *34*, 133.

[11] E. A. Medlycott, G. S. Hanan, *Coord. Chem. Rev.* **2006**, *250*, 1763.

[12] M. I. J. Polson, N. J. Taylor, G. S. Hanan, *Chem. Commun.* **2002**, 1356.

[13] M. I. J. Polson, E. A. Medlycott, G. S. Hanan, L. Mikelsons, N. J. Taylor, M. Watanabe, Y. Tanaka, F. Loiseau, R. Passalacqua, S. Campagna, *Chem. Eur. J.* **2004**, *10*, 3640.

[14] N. D. McClenaghan, Y. Leydet, B. Maubert, M. T. Indelli, S. Campagna, *Coord. Chem. Rev.* **2005**, *249*, 1336.

[15] (a) W. E. Ford, M. A. J. Rodgers, *J. Phys. Chem.* **1992**, *96*, 2917. (b) G. J. Wilson, A. Launikonis, W. H. F. Sasse, A. W.-H. Mau, *J. Phys. Chem. A* **1997**, *101*, 4860. (c) J. A. Simon, S. L. Curry, R. H. Schmehl, T. R. Schatz, P. Piotrowiak, X. Jin, R. P. Thummel, *J. Am. Chem. Soc.* **1997**, *119,* 11012. (d) D. S. Tyson, C. R. Luman, X. Zhou, F. N. Castellano, *Inorg. Chem.* **2001**, *40*, 4063. (e) S. Leroy-Lhez, C. Belin, A. D'Aleo, R. Williams, L. De Cola, F. Fages, *Supramol. Chem.* **2003**, *15*, 627. (f) X.Y. Wang, A. Del Guerzo, R.H. Schmehl, *J. Photochem. Photobiol. C: Reviews* **2004**, *5*, 55. (g) J. Wang, Y.-Q. Fang, G. S. Hanan, F. Loiseau, S. Campagna, *Inorg. Chem.* **2005**, *44*, 5.

[16] (a) R. Passalacqua, F. Loiseau, S. Campagna, Y.-Q. Fang, G. S. Hanan, *Angew. Chem. Int. Ed.* **2003**, *42*, 1608. (b) J. Wang, Y.-Q. Fang, L. Bourget-Merle, M. I. J. Polson, G. S. Hanan, A. Juris, F. Loiseau, S. Campagna, *Chem. Eur. J.* **2006**, DOI: 10.1002/chem.200600245. (c) Complex **3c** was previously synthesised employing using an alternative approach as reported in reference [31].

[17] B. Maubert, N. D. McClenaghan, M. T. Indelli, S. Campagna, *J. Phys. Chem. A* **2003**, *107*, 447.

[18] Strictly speaking, the states involved in the equilibration process can be much more than two. In Ru(II) polypyridine complexes such as $Ru(bpy)_3^{2+}$, for example, the lowest-energy ^{3}MLCT manifold is made of three closely spaced levels.[3,46] However, at room temperature as well as at 77 K, these levels are equilibrated and can be considered as a "single" state.

[19] C. J. Aspley, J. A. G. Williams, *New J. Chem.* **2001**, *25*, 1136.

[20] C. Patoux, J.-P. Launay, M. Beley, S. Chodorowski-Kimmes, J.-P. Collin, S. James, J.-P. Sauvage, *J. Am. Chem. Soc.* **1998**, *120*, 3717.

[21] S. J. Dunne, E. C. Constable, *Inorg. Chem. Commun.* **1998**, *1*, 167.

[22] E. C. Constable, A. M. W. Cargill Thompson, S. Greulich, *J. Chem. Soc. Chem. Commun.* **1993**, 1444.

[23] M. Beley, J. P. Collin, R. Louis, B. Metz, J. P. Sauvage, *J. Am. Chem. Soc.* **1991**, *113*, 8521.

[24] G. A. Crosby, J. N. Demas, *J. Phys. Chem.* **1971**, *75*, 991.

[25] N. Nakamaru, *Bull. Chem. Soc. Jpn.* **1982**, *55*, 2697.

[26] S. Campagna, G. Denti, S. Serroni, A. Juris, M. Venturi, V. Ricevuto, V. Balzani, *Chem. Eur. J.* **1995**, *1*, 211.

[27] E. A. Medlycott, I. Theobald, G. S. Hanan, *Eur. J. Inorg. Chem.* **2005**, 1223.

[28] B. P. Sullivan, J. M. Calvert, T. J. Meyer, *Inorg. Chem.* **1980**, *19*, 1404.

[29] M. Baumgarten, L. Gherghel, J. Friedrich, M. Jurczok, W. Rettig, *J. Phys. Chem. A* **2000**, *104*, 1130.

[30] S. Kotha, A. K. Ghosh, K. D. Deodhar, *Synthesis* **2004**, *4*, 594.

[31] E. A. Medlycott, G. S. Hanan, *Submitted for publication.*

[32] K. O. Johansson, J. A. Lotoski, C. C. Tong, G. S. Hanan, *Chem. Commun.* **2000**, 819.

[33] F. Loiseau, R. Passalacqua, S. Campagna, M. I. J. Polson, Y.-Q. Fang, G. S. Hanan, *Photochem. Photobiol. Sci.* **2002**, *1*, 982.

[34] K. J. Arm, J. A. G. Williams, *Chem. Commun.* **2005**, 230.

[35] K. J. Arm, J. A. G. Williams, *Dalton Trans.* **2006**, 2172.

[36] G. J. Pernìa, J. D. Kilburn, J. W. Essex, R. J. Mortishire-Smith, M. Rowley, *J. Am. Chem. Soc.* **1996**, *118*, 10220.

[37] N. W. Alcock, P. R. Barker, J. M. Haider, M. J. Hannon, C. L. Painting, Z. Pikramenou, E. A. Plummer, K. Rissanen, P. Saarenketo, *Dalton Trans.* **2000**, 1447.

[38] S. Pyo, E. Perez-Cordero, S. G. Bott, L. Echegoyen, *Inorg. Chem.* **1999**, *38*, 3337.

[39] E. A. Medlycott, K. A. Udachin, G. S. Hanan, *Submitted for publication.*

[40] M. Beley, J. P. Collin, J. P. Sauvage, H. Sugihara, F. Heisel, A. Miehé, *J. Chem. Soc. Dalton Trans.* **1991**, 3157.

[41] A. Mamo, I. Stefio, M. F. Parisi, A. Credi, M. Venturi, C. Di Pietro, S. Campagna, *Inorg. Chem.* **1997**, *36*, 5947.

[42] S. L. Murov, I. Carmichael, G. L. Hug, in *Handbook of Photochemistry*, Marcel Dekker, New York, **1993**.

[43] *Handbook of Photochemistry*,3rd *Edition, Revised and Expanded*, Eds.: M. Montalti, A. Credi, L. Prodi, M. T. Gandolfi, CRC Press, **2006**.

[44] D. F. Evans, *J. Chem. Soc.* **1957**, 1351.

[45] K. Hamanoue, S. Tai, T. Hikada, T. Nakayama, M. Kimoto, H. Teranashi, *J. Phys. Chem.* **1984**, *88*.

[46] T. J. Meyer, *Pure Appl. Chem.* **1986**, *58*, 1193 and references therein.

[47] P. Chen, T. J. Meyer, *Chem. Rev.* **1998**, *98*, 1439.

[48] (a) S. Serroni, S. Campagna, R. Pistone Nascone, G. S. Hanan, G. J. Davidson, J.-M. Lehn, *Chem. Eur. J.*, **1999**, *5*, 3523. (b) J. Wang, E. A. Medlycott, G. S. Hanan, F. Loiseau, S. Campagna, *Inorg. Chim. Acta*, in press.

Chapter III, Part A: Ru(II) and Zn(II) complexes of multicomponent ligands incorporating triazine-based tridentate ligands

Communication 1

Elaine A. Medlycott,[a] *Garry S. Hanan,*[a]*

[a] Département de chimie, Université de Montréal, Montréal, Québec, Canada H3C 3J7

Accepted for publication in Inorganic Chemistry Communications October, 2006.

Manuscript

Keywords: Triazine ligands / Ruthenium complexes / Zinc complexes / Phenanthrene

Ru(II) and Zn(II) complexes of multicomponent ligands have been synthesised and characterised incorporating triazine-based coordinating motifs with pendant phenanthryl and phenyl-phenanthryl groups. At room temperature the ligands emit from intra-ligand charge-transfer (ILCT) states the energy of which may be lowered significantly by metal-ion coordination (e.g. Zn(II)). The ILCT state is efficiently quenched in the Ru(II) complexes by energy transfer to a low-lying metal-to-ligand charge-transfer ^{3}MLCT state.

Metal complexes of *N*-heterocyclic ligands remain a topic of intense research due to their favourable photophysical properties and promising device applications for the conversion of light into chemical energy.[1-4] Metal complexes of d^6 metal ions are of particular interest as they typically have absorption bands in the visible region of the spectrum due to metal-to-ligand charge-transfer (MLCT) states which may result in an emission from a ^{3}MLCT state. The excited-state lifetimes of such complexes are usually limited, however, by non-radiative deactivation through low-lying metal-centred states, which may be easily populated at room temperature, or by rapid deactivation of low energy ^{3}MLCT states via the energy gap law.[5-7] As a consequence there has been significant attention to the development of ligands with low energy intra-ligand charge-transfer (ILCT) states which give rise to relatively long excited state lifetimes on complexation to metals without non-emissive MC states, e.g. Zn(II).[8-10] Such an approach requires multicomponent ligands that contain a metal-ion binding domain, which also plays the role of an electron acceptor, and an electron-donating motif, which is electronically separated from the acceptor (Figure 3.1). The coordinating motifs are largely based on the tridentate 2,2':6',2''-terpyridine (tpy) or

bidentate 2,2'-bipyridine (bpy) ligands and a relatively facile reduction is an essential prerequisite in order to play the role of electron-acceptor. The role of electron donor can be played by any organic component which is relatively easy to oxidise, and fused polyaromatics have been the components of choice for this role.[9, 11-14]

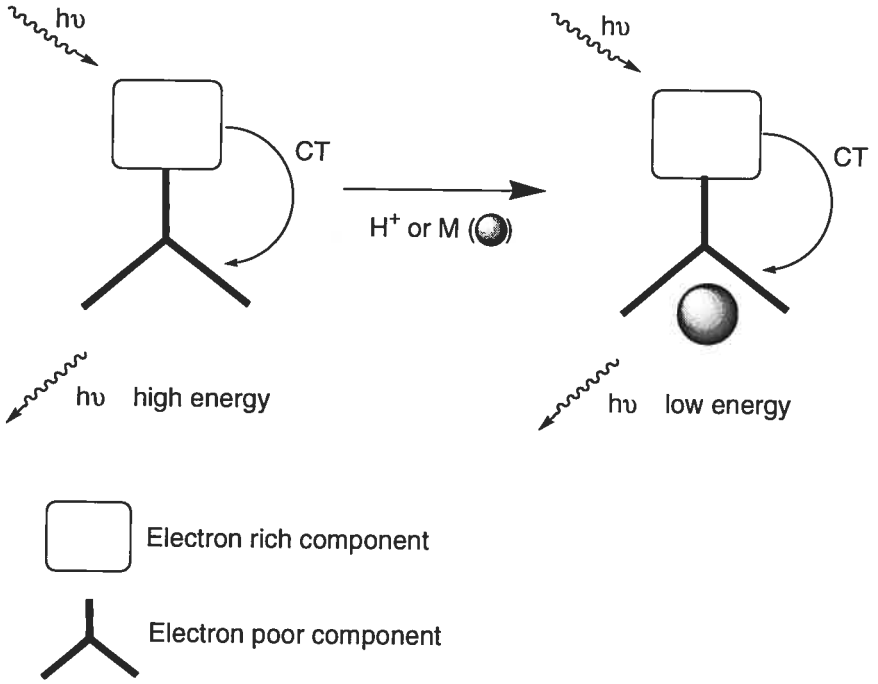

Figure 3.1 The energy of the intra-ligand charge-transfer (ILCT) emission from the ligand can be modulated by metal ion coordination.

In the free ligands, the ILCT-based emission is rarely observed as the coordinating motif has limited electron-accepting capabilities. However, metal coordination or protonation diminishes electron density on the ligand improving its electron-accepting properties. Consequently, the energy of the ^{1}ILCT state is significantly lowered, permitting emission from this state. For example, tpy-based ligands with fused aromatic rings attached to directly to the central pyridine have previously been complexed to Zn(II), Ru(II), Os(II), Ir(III) and Pt(II) metal ions,[9, 12-15] and in the complexed and protonated forms the ^{1}ILCT and ^{3}ILCT emission bands have been observed.

Herein, we report the synthesis and characterization of triazine-based ligands with fused phenanthrene moieties appended directly or through a phenyl spacer to a

tridentate binding motif. The triazine component is significantly easier to reduce than tpy and, consequently, the ILCT state is stabilised and emissive in the case of Zn(II) complexes.

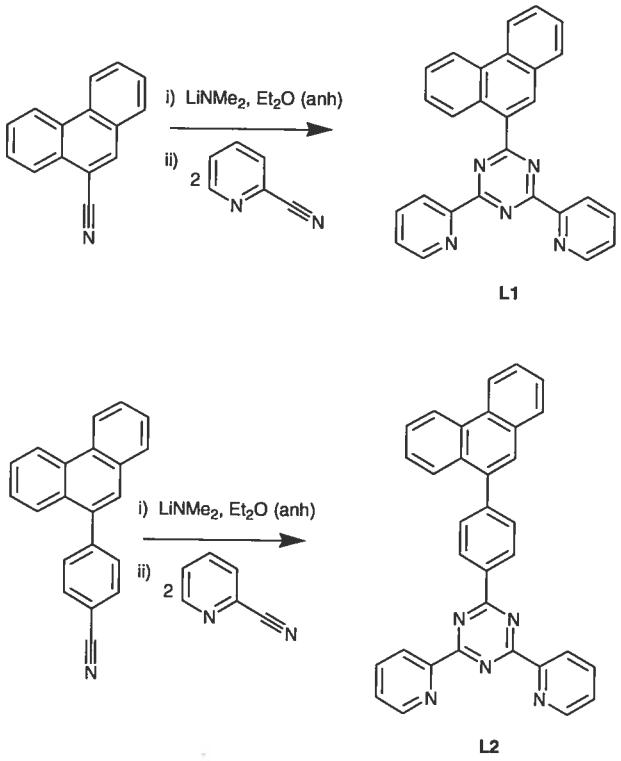

Scheme 1 Synthesis of triazine ligands **L1** and **L2**.

The precursors 9-cyano-phenanthrene or *p*-phenanthryl-benzonitrile were synthesised by modifications of previously published procedures. Ligands **L1** and **L2** were synthesised by a triazine ring-forming reaction.[16, 17] $LiNMe_2$ was generated *in-situ* by slow addition of ^nBuLi to a stirring solution of $HNMe_2$ in anhydrous diethyl ether. On formation of a white suspension, 9-cyano-phenanthrene or *p*-phenanthryl-benzonitrile were added and an amidinate intermediate was formed. Two equivalents of 2-cyanopyridine were added to the reaction mixtures and cyclisation followed by aromatisation yielded **L1** and **L2** in 13% and 42% yield, respectively. The synthesis of **L1** was slower and gave poorer yields on comparison to **L2** due to the steric encumbrance of the peri-hydrogen of the fused benzene ring adjacent to the central cyanated ring. In addition, the amidinate intermediate may be stabilised by a C-H to N

intramolecular H-bonding interaction between the peri-hydrogen and amidinate N, which could influence the cyclisation reaction.

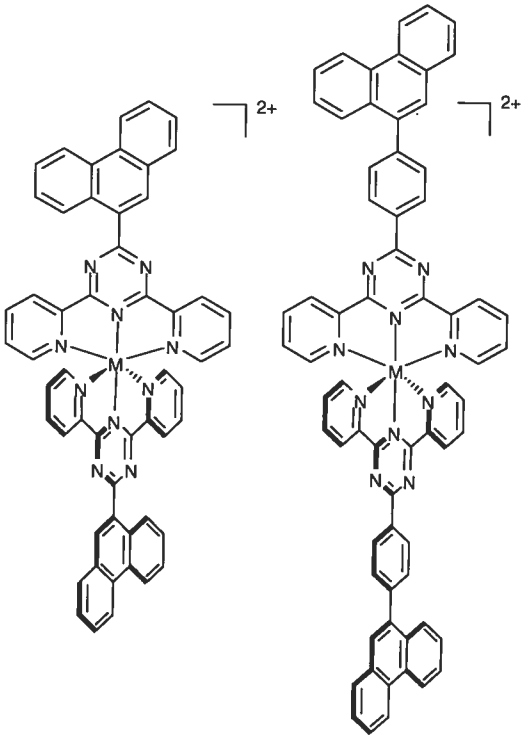

Figure 3.2 The Ru(II) and Zn(II) complexes employed in this study.

The Ru(II) complexes were synthesised from the reaction of $RuCl_3.3H_2O$ in DMF, with two equivalents of the appropriate ligand in the presence of three equivalents of $AgNO_3$ as a dechlorinating agent (Figure 3.2). The mixture was stirred at room temperature for 20 minutes and then heated to reflux for an hour. On cooling, the complexes were converted to the PF_6^- salts and purified by column chromatography using acetone: water: KNO_3 (sat), 9:0.9:0.1. The intense red bands were collected and precipitated as PF_6^- salts to isolate complexes **2a** and **2b** as red solids in 23% and 66% yield, respectively. Complexes **3a** and **3b** were obtained by addition of $Zn(ClO_4)_2.6H_2O$ to two equivalents of the ligand in acetonitrile (Figure 3.2). The mixture was refluxed for 15 minutes and then cooled and the solvent was removed under reduced pressure. Recrystallisation from ethanol, and then acetonitrile/diethyl

ether afforded complexes **3a** and **3b** as yellow solids in 74% and 70% yield, respectively.

The solid state structures of complexes **2a** and **2b** were studied by X-ray diffraction techniques. Crystals were obtained by slow diffusion of isopropyl ether in an acetonitrile solution of the complex. Efforts to obtain crystals of **2a** as the PF_6^- salt were unsuccessful. Addition of excess NBu_4BF_4 in acetonitrile to an acetonitrile solution of **2a**$(PF_6)_2$ enabled anion exchange to occur and red plates suitable for analysis could be obtained.

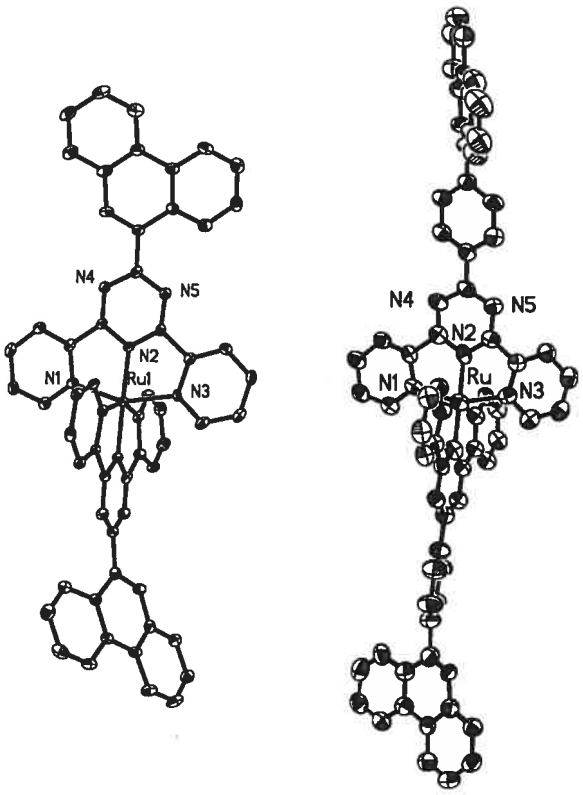

Figure 3.3 X-ray crystal structure of **2a** and **2b** as ORTEP representations. Thermal ellipsoids are set at 30%. The anions and H atoms have been omitted for clarity.

Complex **2a** crystallises in the non-centrosymmetric, orthorhombic space group $Pna2_1$ with four molecules in the unit cell. Face-to-face π -stacking interactions are observed

above and below one of the two phenanthryl rings in complex **2a.** Above the plane, the pendant ring on the phenanthryl group has an offset stacking interaction with a pyridyl ring on a neighbouring cation (centroid-centroid distance 3.42 Å). Face-to-face π-stacking interactions with the second phenanthryl ring on a neighbouring cation are observed below the plane (centroid-centroid distance of 3.63 Å). Complex **2b** crystallises in the monoclinic space group C2/c with 8 molecules in the unit cell. Significant disorder is observed on one of the phenanthryl rings with two favoured orientations of approximately equal occupancy factors (only one orientation is given in Figure 3.3 for clarity). Face-to-face π-stacking interactions are observed for both phenanthryl rings with pyridyl rings of neighbouring cations (centroid-centroid of 3.92 Å and 4.03 Å) similarly to those found in complex **2a**. In both **2a** and **2b** the M-N distances to the central triazine rings are shorter than to the peripheral pyridyl rings. This is expected on comparison to $Ru(tpy)_2^{2+}$-based crystal structures, due to the constrained bite angle observed in the coordination of tridentate ligands.[18] The phenanthryl rings in complex **2a** are twisted by 33.4 (2)° and 31.8 (2)° relative to the triazine rings. In complex **2b** the phenanthyl rings are further twisted relative to the phenyl spacer by 54.6 (3)° or 50.6 (3)° for the disordered rings and 53.1 (2)° for the second phenanthryl ring. This difference is due to unfavourable H-H interactions, *ortho* to the interannular bond in **2b,** whereas *N*-lone pairs in the triazine ring are available to H-bond to the phenanthryl ring in **2a**.

The electrochemistry of the ligands and complexes was studied in acetonitrile. One reversible reduction is observed for **L1** and **L2** at -1.50 V and -1.52 V, respectively, centred principally on the triazine ring. On complexation, significant positive shifts (710-780 mV) are observed for this reduction due to the electron depletion of the triazine by the metal ion. In each complex, four triazine-based reductions are observed corresponding to two reductions on both coordinated triazine ligands. The reduction potentials are not significantly different in the Ru(II) and Zn(II) complexes. In addition to the reductive processes, Ru(II)/(III) couples are observed at similar potentials to those reported for Ru(II) complexes of related triazine ligands.[16]

Table 3.1 Spectroscopic and electrochemical data in CH_3CN solutions at 293K.[a]

	Absorption	Emission	Electrochemistry			
	λ_{max}, nm (ε, $M^{-1}cm^{-1} \times 10^{-3}$)	λ_{max}, nm	$E_{1/2}$(ox)	$E_{1/2}$(red)		
L1	245 (47.8) , 250 (50.5), 268 (30.3), 318 (8.5)	470		-1.50		
L2	254 (54.7), 276 (39.7), 317 (13.4)	477		-1.52		
2a	253 (85.6), 274 (74.7), 334 (18.5), 491 (21.1)	-	1.52	-0.72	-0.89	-1.52	-1.75
2b	206 (86.1), 253 (85.6), 274 (74.7), 328 (sh), 491 (21.1)	-	1.53	-0.73	-0.89	-1.55	-1.78
3a	253 (115.5), 279 (55.4), 290 (53.8), 392 (25.9)	560		-0.74[b]	-0.86	-1.52	-1.72
3b	254 (114.3), 289 (78.5), 366 (20.2)	588		-0.78[b]	-0.91	-1.61[b]	-1.78[b]

[a] Potentials are in volts vs SCE for acetonitrile solutions, 0.1 M in TBAP, recorded at 25 ± 1° C at a sweep rate of 200 mV/s. Unless otherwise stated couples are reversible. [b] Irreversible; potential is given for the cathodic wave.

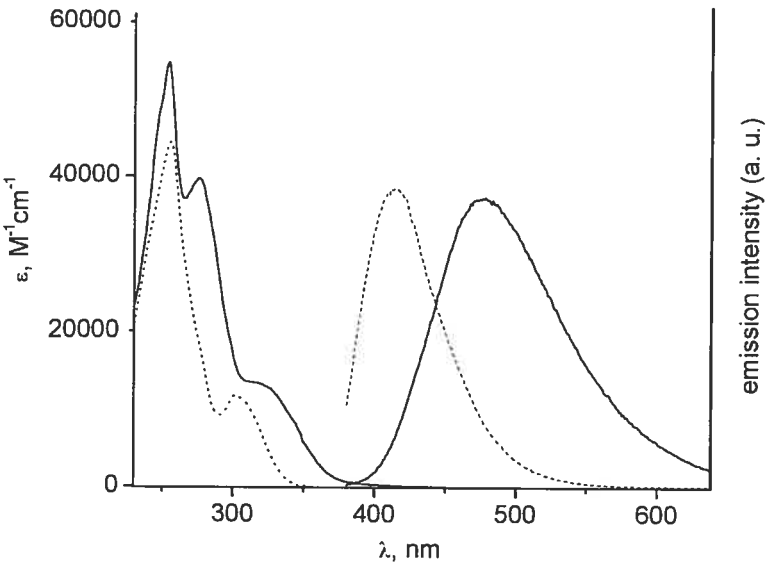

Figure 3.4 Electronic absorption spectra of **L2** (solid line) in acetonitrile and the precursor *p*-phenanthryl-benzonitrile (dotted-line) in DCM (left). Fluorescence

emission spectra of **L2** in air equilibrated acetonitrile (solid line) and toluene (dashed-line) at 295 K (right).

The electronic absorption spectra of **L1** and **L2** consist of high energy absorption bands corresponding to π-π^* transitions on both the dipyridyl-triazine motif and the phenanthrene substituent. In Figure 3.4, the absorption spectra of **L2** and of the precursor *p*-phenanthryl-benzonitrile are compared in DCM. The additional low energy shoulder observed at 317 nm in **L2** (318 nm in **L1**, Table 3.1) contains contributions from an ILCT band, involving electron-donation from the phenanthryl group to the triazine motif, and phenanthryl-based π -π^* transitions as seen by the overlap with the precursor. The triazine ligand should not contribute to this shoulder as n-π^* transitions of a phenyl-substituted triazine ligand lie below 300 nm.[16] Ligand-centred π- π * emissions are observed at 470 nm and 477 nm for **L1** and **L2**, respectively, in air equilibrated acetonitrile, although the bands are broad and featureless, suggesting that they are CT in nature as previously described for related tpy systems.[12] The emission bands shift to longer wavelengths in more polar solvents such as acetonitrile, indicative of charge-transfer behaviour. This emission most likely results from near iso-energetic LC and ^{1}ILCT states.

Excitation into the ^{1}MLCT band of the Ru(II) complexes **2a** and **2b** at room temperature results in weak emissions at approximately 710 nm, presumably weakened by a MC-deactivation of the ^{3}MLCT state.[16] The Zn(II) complexes are emissive at room temperature at 560 and 588 nm for **3a** and **3b,** respectively, when excited into the ILCT absorption band at 330 nm (Figure 3.5). Assuming the phenanthryl rings are electronically separated from the triazine or phenyl-triazine rings, the lower energy excited state of **L2** and complex **3b** may be attributed to the presence of the additional phenyl spacer enhancing delocalisation and stabilising the excited state of the triazine motif. The photophysical properties of Zn(phen-tpy)Cl_2, in which a 9-phenanthryl ring is appended to the 4-position of the central pyridine ring in tpy, has a ILCT-based emission at 466 nm,[12] which is significantly blue shifted in comparison to complex **3a** (560 nm).

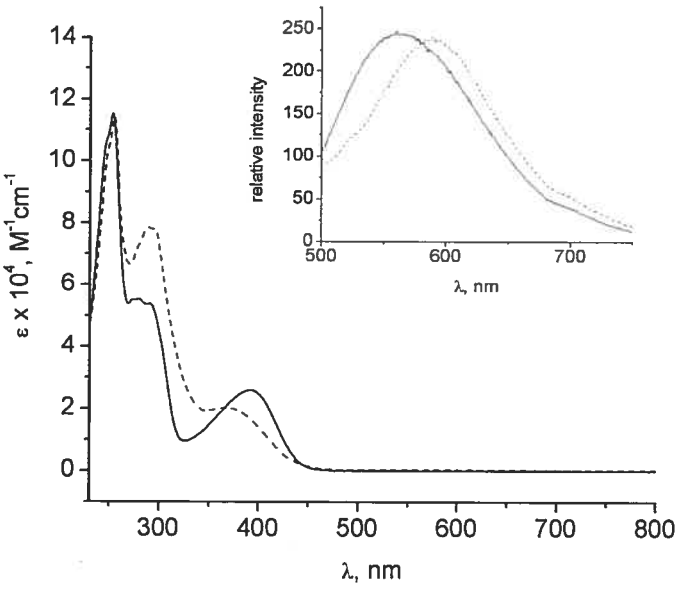

Figure 3.5 Electronic absorption and emission spectra (inset) of complexes **3a** (solid) and **3b** (dashed-line) in aerated acetonitrile.

In summary, two new triazine-based ligands have been synthesised with a phenanthryl group appended directly onto the triazine ring or via a phenyl spacer. The spectroscopic and electrochemical results indicate that the distance between the phenanthryl and triazine group has minimal effect on the spectroscopic properties of the free ligands and the Zn(II) and Ru(II) complexes. The ligands are emissive at room temperature most likely through a combination of LC and ILCT states. The addition of Zn(II) to the ligands increases the acceptor ability of the dipyridyl-triazine core thus lowering the energy of the ILCT state. In the Ru(II) complexes, the ILCT state is quenched by a lower lying ^{3}MLCT state, which may deactivate non-radiatively through metal-centred states. Further experiments are in progress to study the effect of varying the nature of the polyaromatic ring on the photophysical properties of the complexes and will be reported in due course.

CCDC-616592 & 616593 contains the supplementary crystallographic data for this paper. This data can be obtained free of charge from The Cambridge Crystallographic Data Centre via other *www.ccdc.cam.ac.uk/data_request/cif.*

References

[1] J. H. Alstrum-Acevedo, M. K. Brennaman, T. J. Meyer, *Inorg. Chem.* **2005**, *44*, 6802.

[2] V. Balzani, *Photochem. Photobio. Sc.* **2003**, *2*, 459.

[3] V. Balzani, A. Juris, M. Venturi, S. Campagna, S. Serroni, *Chem. Rev.* **1996**, *96*, 759.

[4] V. Balzani, S. Campagna, G. Denti, A. Juris, S. Serroni, M. Venturi, *Acc. Chem. Res.* **1998**, *31*, 26.

[5] J. R. Winkler, T. L. Netzel, C. Creutz, N. Sutin, *J. Am. Chem. Soc.* **1987**, *109*, 2381.

[6] E. M. Kober, J. V. Caspar, R. S. Lumpkin, T. J. Meyer, *J. Phys. Chem.* **1986**, *90*, 3722.

[7] A. Juris, V. Balzani, F. Barigelletti, S. Campagna, P. Belser, A. Von Zelewsky, *Coord. Chem. Rev.* **1998**, *84*, 85.

[8] A. I. Baba, J. R. Shaw, J. A. Simon, R. P. Thummel, R. H. Schmehl, *Coord. Chem. Rev.* **1998**, *171*, 43.

[9] G. Albano, V. Balzani, E. C. Constable, M. Maestri, D. R. Smith, *Inorg. Chim. Acta* **1998**, *277*, 225.

[10] X.-Y. Wang, A. Del Guerzo, R. H. Schmehl, *Chem. Commun.* **2002**, 2344.

[11] X.-y. Wang, A. Del Guerzo, R. H. Schmehl, *J. P.P. C.* **2004**, *5*, 55.

[12] J. F. Michalec, S. A. Bejune, D. G. Cuttell, G. C. Summerton, J. A. Gertenbach, J. S. Field, R. J. Haines, D. R. McMillin, *Inorg. Chemistry* **2001**, *40*, 2193.

[13] W. Leslie, R. A. Poole, P. R. Murray, L. J. Yellowlees, A. Beeby, J. A. G. Williams, *Polyhedron* **2004**, *23*, 2769.

[14] K. K. Patel, E. A. Plummer, M. Darwish, A. Rodger, M. J. Hannon, *J. Inorg. Biochem.* **2002**, *91*, 220.

[15] H. Krass, E. A. Plummer, J. M. Haider, P. R. Barker, N. W. Alcock, Z. Pikramenou, M. J. Hannon, D. G. Kurth, *Angew. Chem., Int. Ed.* **2001**, *40*, 3862.

[16] M. I. J. Polson, E. A. Medlycott, G. S. Hanan, L. Mikelsons, N. J. Taylor, M. Watanabe, Y. Tanaka, F. Loiseau, R. Passalacqua, S. Campagna, *Chem. Eur. J.* **2004**, *10*, 3640.

[17] E. A. Medlycott, I. Theobald, G. S. Hanan, *Eur. J. Inor. Chem.* **2005**, 1223.

[18] S. Pyo, E. Perez-Cordero, S. G. Bott, L. Echegoyen, *Inorg. Chem.* **1999**, *38*, 3337.

Supplementary Material

Ru(II) and Zn(II) complexes of multicomponent ligands incorporating triazine-based tridentate ligands.

Experimental

1) Materials and Instrumentation

Nuclear magnetic resonance (NMR) spectra were recorded in $CDCl_3$ or CD_3CN at room temperature (r.t.) on a Bruker AV400 spectrometer at 400 MHz for ^1H NMR. Chemical shifts are reported in part per million (ppm) relative to residual solvent protons (1.93 ppm for acetonitrile-d_3). Absorption spectra were measured in acetonitrile at r.t. on a Cary 500i UV-Vis-NIR Spectrophotometer and emission spectra in deaerated acetonitrile on a Cary Eclipse Fluorescence Spectrophotometer. Electrochemical measurements were carried out in argon-purged acetonitrile at room temperature with a BAS CV50W multipurpose equipment interfaced to a PC. The working electrode was a Pt electrode. The counter electrode was a Pt wire, and the pseudo-reference electrode was a silver wire. The reference was set using an internal 1 mM ferrocene/ferrocinium sample at 395 mV vs SCE in acetonitrile. The concentration of the compounds was about 1 mM. Tetrabutylammonium hexafluorophosphate (TBAP) was used as supporting electrolyte and its concentration was 0.10 M. Cyclic voltammograms were obtained at scan rates of 50, 100, 200, and 500 mV/s. Experimental uncertainties are as follows: absorption maxima, ±2 nm; molar absorption coefficient, 10%; emission maxima, ± 5 nm; redox potentials, ± 10 mV.

2) Synthesis

Metal salts and other chemicals (Aldrich) were used as supplied. 4-Cyanophenylboronic acid was synthesised according to a literature procedure.[1] The synthesis of 9-cyano-penanthrene and *p*-phenanthryl-benzonitrile was based on previously published procedures.[2,3]

9-cyano-phenanthrene

A mixture of 9-bromo-phenanthrene (2.83 g, 0.011 mol), $K_4[Fe(CN)_6].3H_2O$ (0.99 g, 2.35 mmol), $Pd(OAc)_2$ (12 mg, 0.5 %), Na_2CO_3 (1.13 g, 0.011 mol) and DMA (75 mL) was heated at 120 °C under N_2 for 3 hours. The reaction mixture was cooled and diluted with EtOAc (200 mL). The resulting slurry was extracted 3 times with NH_4OH (5%, aq) and the organic extracts dried over Na_2SO_4. The solvent was removed to afford 9-cyano-phenanthrene as a white solid (1.56 g, 70%)
^1H NMR ($CDCl_3$, 400 MHz): 8.70-8.75 (m, 2H); 8.32 (m, 1H); 8.27 (s, 1H); 7.95 (dt, J= 8 Hz, 1 Hz, 1H); 7.68-7.84 (m, 4H).
The ^1H NMR spectrum corresponded to a previously published spectrum.[4]

***p*-phenanthryl-benzonitrile**

A mixture of 9-bromo-phenanthrene (1.40 g, 9.35 mmol), 4-cyano-phenylboronic acid (2.05 g, 0.014 mol), $[Pd(PPh_3)_4]$ (5 mol%), Na_2CO_3 (2 M, 47 mL),THF (100 mL) and toluene (40 mL) was heated at 85 °C under N_2 overnight. The mixture was diluted with H_2O and extracted with Et_2O. The combined organic layers were washed with H_2O, brine and dried (Na_2SO_4). The solvent was evaporated and the crude product left was charged on a silica gel column. Elution of the column with 2% EtOAc in hexanes gave *p*-phenanthryl-benzonitrile as a white solid (1.00 g, 38% yield).

^1H NMR ($CDCl_3$, 400MHz): 8.80 (d, J = 8 Hz, 1H), 8.74 (d, J = 8 Hz, 1H), 7.91 (dd J = 1 Hz, 8 Hz, 1H), 7.63-7.82 (m, 9H), 7.57 (td, J = 1 Hz, 8 Hz, 1H). $^{13}C\{^1H\}$ NMR ($CDCl_3$, 100MHz): 110.89, 118.60, 122.26, 122.81, 125.83, 126.52, 126.54, 126.80, 126.80, 126.92, 127.59, 128.50, 129.80, 129.88, 130.32, 130.47, 130.77, 131.83, 136.45, 145.36. High Res. ESMS *m/z* calcd for $C_{21}H_{14}N$ $[M+H]^+$: 280.1126; found: 280.1120.

L1

^{n}BuLi (1.6M in hexanes, 5.10 mL, 8.13 mmol) was added dropwise to a stirred solution of $HNMe_2$ (2M in THF, 4.10 mL, 8.13 mmol) in anhydrous Et_2O (150 mL) under an inert atmosphere. The mixture was stirred until a white suspension formed (20 minutes) after which 9-cyano-phenathrene (1.50 g, 7.39 mmol) was added. The mixture was stirred for another 4 hours at which time 2-cyanopyridine (1.44 mL, 15.0 mmol) was added. The reaction mixture was stirred overnight under nitrogen and for a further 30 minutes in air. Et_2O was removed under reduced pressure and the residue was recrystallised three times from water: ethanol (1:3). The solid was collected and washed with Et_2O to afford **L1** as a white powder (0.38 g, 13% yield).

^{1}H NMR ($CDCl_3$, 400 MHz): 8.96-8.92 (m, 3H) $H_{6,6''}$ H_{phenan}; 8.82-8.86 (m, 3H) $H_{3,3''}$ H_{phenan}; 8.75-8.77 (m, 2H) $2H_{phenan}$; 8.09 (d, J = 8 Hz, 1H) H_{phenan}; 7.98 (td, J = 2, 8 Hz, 2H) $H_{4,4''}$; 7.65-7.78 (m, 3H) $3H_{phenan}$; 7.56 (dd, J= 5Hz, 5Hz, 2H) $H_{5,5''}$. ^{13}C {^{1}H} NMR ($CDCl_3$, 100 MHz): 122.33, 122.74, 124.71, 126.18, 126.27, 126.56, 126.68, 126.83, 128.24, 128.98, 129.74, 130.41, 130.68, 131.55, 132.05, 132.73, 136.95, 150.11, 152.87, 171.08, 175.29. Anal. Calcd. For $C_{27}H_{17}N_5.(H_2O)$: C, 75.51; H, 4.46; N, 16.31. Found: C, 76.01; H, 4.38; N, 16.34.

L2

^{n}BuLi (1.6M in hexanes, 2.95 mL, 4.72 mmol) was added dropwise to a stirred solution of $HNMe_2$ (2M in THF, 2.36 mL, 4.72 mmol) in anhydrous Et_2O (150 mL) under an inert atmosphere. The mixture was stirred for 20 minutes until a white suspension formed and *p*-phenanthryl-benzonitrile (1.20 g, 4.29 mmol) was added to the mixture as a solid. The mixture was stirred for one hour further followed by addition of 2-cyanopyridine (0.83 mL, 8.58 mmol). The triazine precipitated immediately and stirring continued for an hour. The reaction was diluted with a 5:1 mixture of water: EtOH (200 mL) and the solution was heated to remove Et_2O. The white precipitate was collected by filtration and washed with EtOH (10 mL) and Et_2O (50 mL) and dried to afford **L2** as a white powder (0.87 g, 42% yield).

^{1}H NMR ($CDCl_3$, 400 MHz): 8.98 (m, 2H) $H_{6,6''}$; 8.95 (d, J = 8 Hz, 2H) $H_{2''',6'''}$; 8.89 (d, J = 8 Hz, 2H) $H_{3,3''}$; 8.80 (d, J = 8 Hz, 1H) H_{phenan}; 8.74 (d, J = 8 Hz, 1H) H_{phenan}; 8.01-7.93 (m, 4H) $H_{4,4''}$, $2H_{phenan}$; 7.79, (d, J = 8 Hz, 2H) $H_{3''',5'''}$; 7.78 (s, 1H) H_{phenan}; 7.62-7.72 (m, 3H) $3H_{phenan}$; 7.54-7.59 (m, 3H) $H_{5,5''}$, H_{phenan}. Anal. Calcd. For $C_{33}H_{21}N_5.½H_2O$: C, 79.82; H, 4.47; N, 14.10. Found: C, 79.59; H, 4.66; N, 14.64.

Complexes 2a and 2b

$RuCl_3.3H_2O$ (0.032 g, 0.12 mmol) was added on stirring to a solution of the appropriate ligand (0.24 mmol) in DMF (15 mL). The mixture was stirred at room temperature for 15 minutes and then heated to reflux for one hour. The mixture was cooled and KPF_6 (5 mL, aq) was added and the solution was diluted with water (100 mL). The resulting solid was collected and dissolved in acetonitrile and purified by column chromotography (SiO2, Acetone: water: KNO_3(aq); 9:0.9:0.1). The nitrate salt was metathesized to the PF_6 salt, and the solvent removed. The solid was dissolved in acetonitrile, and the product precipitated by addition to water. Recrystallisation from acetonitrile/diethyl ether afforded **2a** and **2b** as red solids in 23% and 66% yields, respectively.

2a

^{1}H NMR (CD_3CN, 400 MHz): 9.68 (m, 2H) H_{phenan}; 9.42 (s, 2H) H_{phenan}; 9.17 (d, J = 7 Hz, 4H), $H_{3,3''}$; 9.10 (m, 2H) H_{phenan}; 9.02 (d, J = 8 Hz, 2H) H_{phenan}; 8.40 (d, J = 8 Hz, 2H) H_{phenan}; 8.20 (td, J = 1, 8 Hz, 4H) $H_{4,4''}$, 7.88-8.01 (m, 12H) $4H_{phenan}$, $H_{6,6''}$; 7.50 (dd, J= 6Hz, 6Hz, 4H) $H_{5,5''}$. High Res. ESMS *m/z* calcd. for $C_{54}H_{34}N_{10}Ru$ $[M]^{2+}$: 462.1005; found: 462.10002. Anal. Calcd. For $C_{54}H_{36}F_{12}N_{10}P_2Ru.4H_2O$ C, 50.43, H, 3.29, N, 10.89. Found: C, 50.94; H, 3.32; N, 10.34.

2b

^{1}H NMR (CD_3CN, 400MHz): 9.28 (d, J = 8 Hz, 4H) $H_{2''',6'''}$; 9.19 (d, J= 8 Hz, 4H), $H_{3,3''}$; 8.97 (d, J = 8 Hz, 2H), H_{phenan}; 8.89 (d, J= 8 Hz, 2H), H_{phenan}; 8.18 (td, J = 1 Hz, 8 Hz, 4H) $H_{4,4''}$; 8.07 (d, J= 8 Hz, 4H) $H_{3''',5'''}$; 7.99-8.11 (m, 4H) H_{phenan}; 8.00 (s, 2H) H_{phenan}; 7.80 (d, J = 6 Hz, 4H) $H_{6,6''}$; 7.79-7.81 (m, 4H) H_{phenan}, 7.73 (dd, J= 1Hz, 8Hz, 2H) H_{phenan}; 7.45 (dd, J = 6 Hz, 7 Hz, 4H) $H_{5,5''}$. Anal. Calcd. For $C_{66}H_{42}F_{12}N_{10}P_2Ru.$ $2H_2O$: C, 56.54; H, 3.31; N, 9.99. Found C 56.19, H 3.50, N 10.33.

Complexes 3a and 3b

$Zn(ClO_4)_2.6H_2O$ (0.05 mmol, 0.018 g) was added on stirring to a solution of the appropriate ligand (0.10 mmol) in acetonitrile (15 mL). The mixture was refluxed for 15 minutes, cooled and the solvent removed under reduced pressure. The solid was recrystallised from ethanol, followed by precipitation in acetonitrile/ diethyl ether to afford complexes **3a** and **3b** as yellow solids in 74% and 70% yields, respectively.

3a

^1H NMR (CD_3CN, 400MHz): 9.54 (m, 1H) H_{phen}, 9.43 (s, 1H) H_{phen}; 9.18 (d, J= 8 Hz, 2H) $H_{3,3''}$; 9.08 (m, 1H) H_{phen}; 9.00 (d, J= 9 Hz, 1H) H_{phen}; 8.36-8.43 (m, 5H) $H_{4,4''}$, $H_{6,6''}$, H_{phen}; 7.97-8.04 (m, 3H) $3H_{phen}$; 7.90 (t, J= 7 Hz, 1H) H_{phen}; 7.75 (dd, J = 5 Hz, 6 Hz, 2H) $H_{5,5''}$. Anal. Calcd. For $C_{54}H_{34}C_{l2}N_{10}O_8Zn.5H_2O$: C, 55.09; H, 3.77; N, 11.90. Found C 55.12, H 3.57, N 11.86.

3b

^1H NMR (CD_3CN, 400MHz): 9.27 (d, J= 9Hz, 2H) $H_{2''',6'''}$; 9.25 (d, J= 8 Hz, 2H), $H_{3,3''}$; 8.98 (d, J= 9 Hz, 1H) H_{phen}; 8.91 (d, J= 8 Hz, 1H), H_{phen}; 8.38 (t, J= 8 Hz, 2H) $H_{4,4''}$; 8.34 (d, J= 5 Hz, 2H) $H_{6,6''}$; 8.07-8.12 (m, 4H) $H_{3''',5'''}$,$2H_{phen}$; 8.00 (s, 1H) H_{phen}; 7.71-7.84 (m, 6H) $H_{5,5''}$, $4H_{phen}$. Anal. Calcd. For $C_{66}H_{42}Cl_2N_{10}O_8Zn.2H_2O$: C, 62.15; H, 3.64; N, 10.98. Found C 62.25, H 3.73, N 11.15.

References

[1] G. H. Pernìa, J. D. Kilburn, J. W. Essex, R. J. Mortishire-Smith, M. Rowley, *J. Am. Chem. Soc.* 1996, **118**, 10220.

[2] S. A. Weissman, D. Zewge, C. Chen, *J. Org. Chem.* 2005, **70**, 1508.

[3] S. Kotha, A. K. Ghosh, K. D. Deodhar, *Synthesis* 2004, **4**, 594.

[4] P. H. Gore, F. S. Kamounah, A. Y. Miri, *Tetrahedron* 1979, **35**, 2927.

Chapter III, Part B: Zn(II) and Ru(II) complexes of pyrenyl, phenanthryl and naphthyl appended triazine ligands

3.1 Introduction

In the previous sub-chapter the synthesis and characterisation of Ru(II) and Zn(II) complexes of phenanthryl-appended triazine ligands have been reported. The phenanthryl substituents offer additional chromophoric units which gives rise to emissive Zn(II) complexes through ILCT states in which the phenanthryl group behaves as an electron donor and the triazine motif as an electron acceptor.

In this sub-chapter the influence of the appended aromatic group will be explored. The synthesis and characterisation of Ru(II) and Zn(II) complexes of pyrenyl and naphthyl appended triazine ligands will be discussed and comparisons will be made to complexes of phenyl and phenathryl substituted triazine ligands previously reported.

3.2 Results and Discussion

3.2.1 Synthesis

The ligands **L2** and **L4** were synthesized using the same procedure as reported in the previous sub-chapter. $LiNMe_2$ was generated '*in-situ*' through the slow addition of ^{n}-BuLi to $HNMe_2$ in anhydrous diethyl ether. On addition of the cyano-precursors an amidinate intermediate formed and addition of 2 equivalents of 2-cyanopyridine afforded the triazine ligands on work-up.

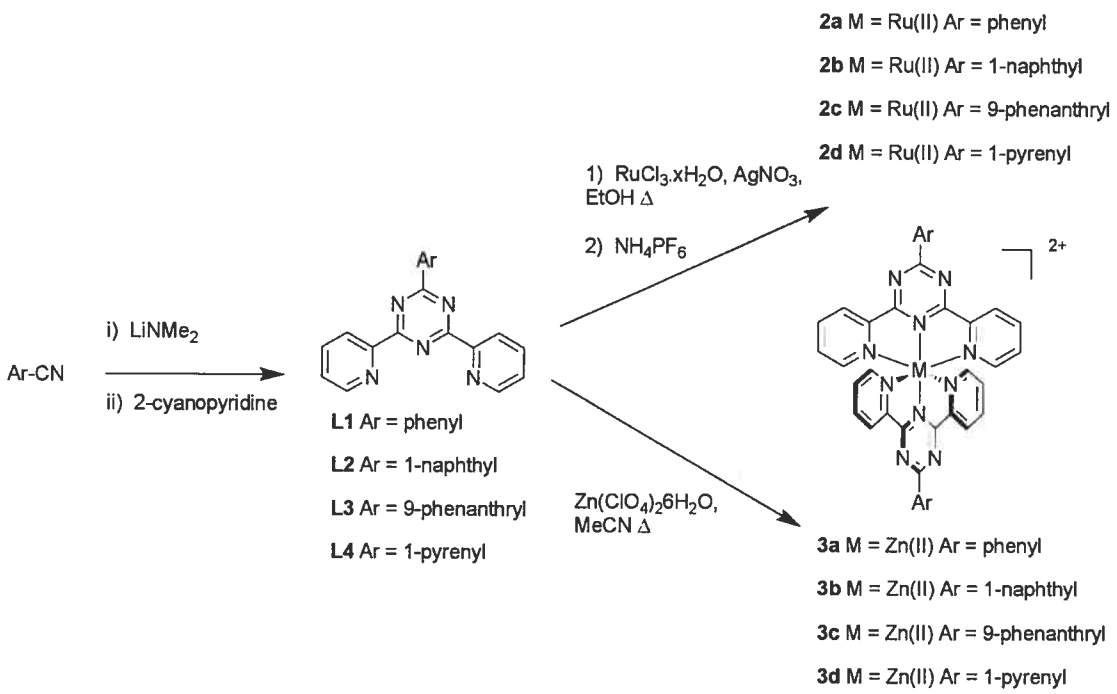

Scheme 3.2 Synthesis of ligands **L1-4**, and the complexation of the ligands to form the Ru(II) complexes **2a-d** and Zn(II) complexes **3a-d**.

Complexes **2b** and **2d** were synthesised by addition of $RuCl_3.3H_2O$ to two equivalents of the ligand, with 3 equivalents of $AgNO_3$ in DMF. The mixture was stirred at room temperature for 15 minutes and then heated to reflux for one hour. The mixture was cooled and filtered to remove AgCl and added to a saturated aqueous solution of KPF_6. The precipitate was collected and column chromatography followed by anion exchange afforded complexes **2b** and **2d** in 56% and 11% yields, respectively. Zn(II) complexes were synthesised by the addition of $Zn(ClO_4)_2.6H_2O$ to a solution of the appropriate ligand in acetonitrile. The mixture was refluxed for 15 minutes and then cooled and the solvent removed by evaporation. Redissolving the residue in ethanol followed by precipitation in diethyl ether afforded complexes **3a-d** in 68%, 55%, 74% and 84% yields, respectively. The complexes were characterised in solution by ^1H NMR and in the solid state by elemental analyses.

The ^{1}H NMR spectra of **L4**, **2d**, and **3d** are shown in Figure 3.6.

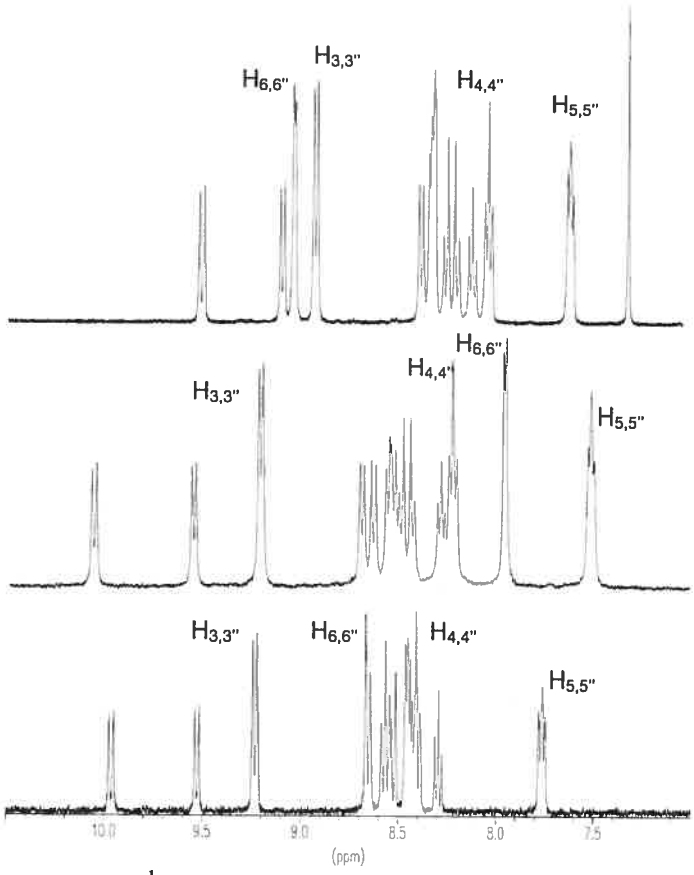

Figure 3.6 ^{1}H NMR spectra of **L4** in $CDCl_3$ (above), **2d** (middle) and **3d** (below) in CD_3CN.

On complexation of **L4** by Ru(II) or Zn(II), the pyridyl and pyrenyl ^{1}H signals are both shifted to lower field in CD_3CN. The Zn(II) ion in complex **3d** has a greater electron-withdrawing effect on the pyridyl protons closest to the metal centre ($H_{5,5''}$ and $H_{6,6''}$) when compared to the Ru(II) complex **2d**. Complex **3d** has limited solubility and reaches its saturation point in solution very rapidly as compared to **2d,** presumably due to aggregation.

3.2.2 Solid State Structures

Crystals suitable for analyses of **L2** were obtained by slow diffusion of hexane in to a concentrated chloroform solution of **L2**. One molecule of water is found in the asymmetric unit with H-bonding to N-pyridyl atoms with N-H distances of 2.15 Å and 2.14 Å. Significant face-to-face π-stacking interactions are observed in the extended lattice with each triazine ring overlaying pyridyl rings above and below the plane with centroid-to-centroid distances of 3.6- 3.8 Å.

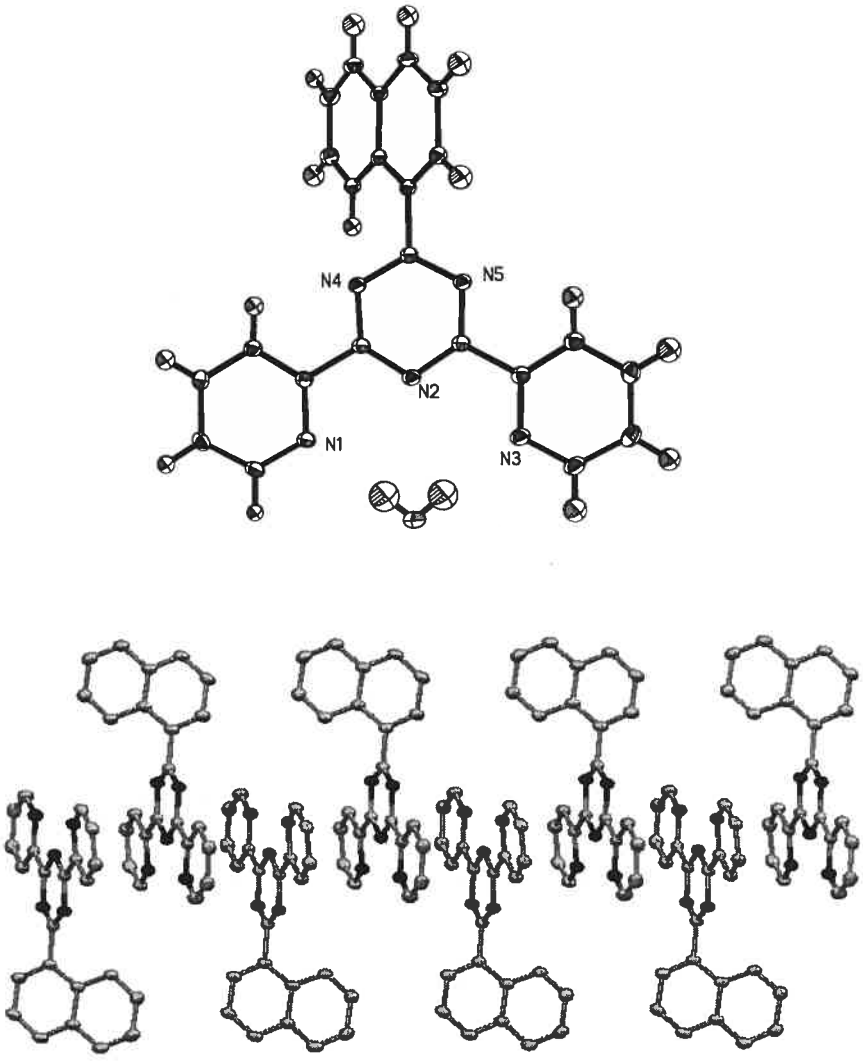

Figure 3.7 ORTEP representation of solid state structure **L2** with H_2O solvent molecule (above). Pyridyl-triazine π-stacking interactions (below), H atoms are omitted for clarity. Thermal ellipsoids are set at 30%.

Slow diffusion of isopropyl ether into acetonitrile solutions of **2b** and **3b** as their PF_6 and ClO_4 salts respectively afforded poor quality crystals. Red crystals of **2b** were eventually obtained by addition of excess NH_4BF_4 in methanol to a concentrated solution of **2b** in acetonitrile followed by slow diffusion of isopropyl ether. The complex crystallised in the monoclinic space group P2(1)/n with two cations, four anions, (three PF_6^- anions and one BF_4^- anion) and four molecules of acetonitrile. The Zn(II) complexes could be synthesised as their PF_6^- salts according to a literature procedure[1] and crystals of **3b** was obtained as the PF_6^- salt by slow diffusion of isopropyl ether into an acetonitrile solution of the complex. Complex **3b** crystallised in the non-centrosymmetric space group P2(1) with two cations, four PF_6 counter-ions and three acetonitrile solvent molecules. In both crystal structures significant π-stacking interactions were observed in the extended lattice between naphthyl groups and coordinating pyridyl rings with centroid-centroid distances of 3.66 Å and 3.71 Å for complex **2b** and 3.89 Å and 3.96 Å in complex **3b** (Figure 3.8).

The use of non-covalent interactions to aggregate functional assemblies through crystal engineering is appealing as conventional, covalent approaches require multistep syntheses.[1-5] Naphthyl-pyridyl, π-stacking interactions were previously observed in naphthyl-appended tpy-based Ru(II) and Fe(II) complexes.[4] In the previous sub-chapter similar interactions in the solid state structure of complex **2c** were observed. The four naphthyl groups in the two cations twist away from the central triazine rings by 16.6°- 36.9° in complex **2b** and 21.5°- 29.1° in complex **3b.** Intramolecular C-H-N (triazine) H-bonding interactions favour minimal twisting of the naphthyl group relative to the triazine ring.

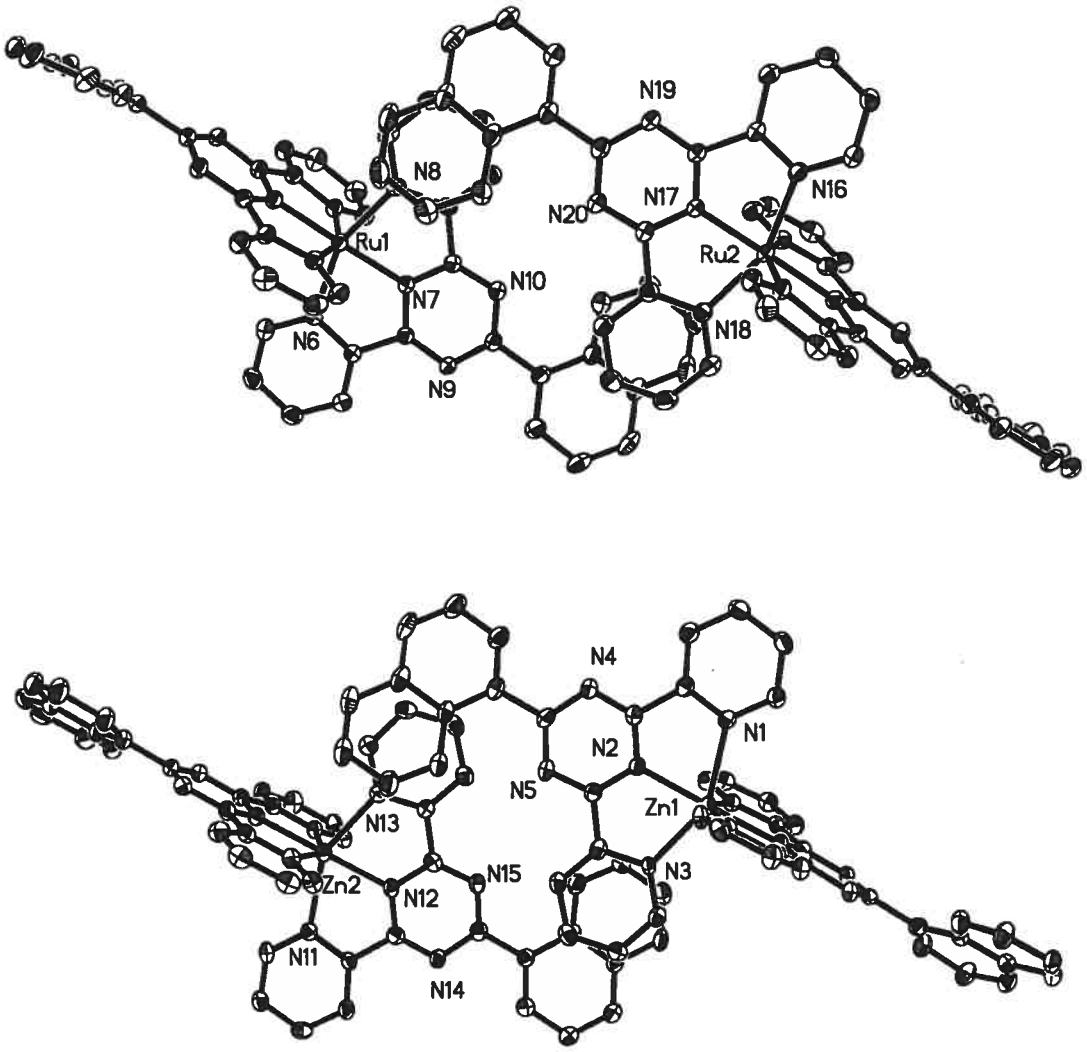

Figure 3.8 ORTEP representations π-stacking interactions in the solid state structures of **2b** and **3b**. Thermal ellipsoids are set at 30%. Anions and solvent molecules of crystallization have been omitted for clarity.

The M-N bond distances in both **2b** and **3b** are shorter to the central triazine ring compared to the terminal pyridyl rings as expected due to the constrained bite angle imposed by tridentate ligands. The Ru-N bond distances, 1.97 -1.98 Å to the central triazine ring and 2.09- 2.11 Å to the terminal pyridyl rings, are in agreement to those previously reported for related Ru(II) complexes of triazine-based ligands.[6, 7]

The Zn-N bond distances are slightly longer and similar to those reported for tpy-type ligands.[1]

3.2.3 Electrochemistry

Table 3.2 Half-Wave Potentials for ligands **L1-4** and complexes **2** and **3**.

Compound	$E_{1/2}$(oxidn)		$E_{1/2}$(redn)			
L1			-1.42 (84)	-2.25 (irr)		
L2			-1.41 (82)	-2.17 (irr)		
L3[b]			-1.42 (86)	-2.15 (irr)		
L4	1.54 (irr)		-1.40 (75)	-1.84 (96)	-2.17(irr)	
2a[a]	1.51(81)		-0.71(65)	-0.88(69)	-1.51(74)	-1.75(78)
2b	1.52(84)		-0.73(63)	-0.89(68)	-1.52 (67)	-1.75(80)
2c[b]	1.52(85)		-0.72(74)	-0.89(77)	-1.52(79)	-1.75(90)
2d	1.46(irr)	1.66(irr)	-0.75(68)	-0.89(69)	-1.51(88)	-1.74(irr)
3a			-0.79 (80)	-0.91((84)	-1.60 (86)	-1.77(78)
3b			-0.80 (67)	-0.91(77)	-1.59(78)	-1.75(74)
3c[b]			-0.81 (irr)	-0.86(104)	-1.52 (103)	-1.73 (108)
3d	1.45 (irr)		-0.76 (68)	-0.87 (76)	-1.52 (irr)	

[a] From reference [6] [b] From reference[7]

The electrochemistry of **L1** was previously reported in acetonitrile.[6] However, due to the limited solubility of **L2-L4**, the electrochemistry of the ligands was carried out in DMF in order to make full comparisons. An initial reversible triazine- based reduction is observed at -1.40 to -1.42 V. The insignificant potential difference between all four ligands indicates that the aryl substituent on the triazine has little influence on this process. A second triazine-based reduction is observed at -2.15 to -2.17 V in **L2-4**. This same reduction shifts to a more negative potential in **L1** (-2.25 V), indicating the LUMO +1 molecular orbital involves significant mixing of the aromatic and triazine motifs. An additional pyrenyl-based reduction is observed in **L4** at -1.84 V. No

oxidative processes are observed in **L1-3** within the solvent limits, however, the pyrene motif is oxidised at 1.54 V in **L4**. As predicted, this is more positive than the tpy-pyrene ligand (1.49 V) due to the electron-deficient triazine ring.[8] However, overall a lower energy HOMO-LUMO gap is observed as estimated from the CV at 2.94 V for **L4** as compared to 3.15 V for tpy-pyrene.[8]

The electrochemistry of complexes **2a-d** and **3a-d** are reported in acetonitrile. The oxidative potentials for the Ru(II)/(III) couple in complexes **2a-c** are in agreement for those previously reported for Ru(II) complexes of triazine ligands.[6, 7] However, in complex **2d**, the pyrene motif is oxidised prior to the Ru(II) centre at 1.46 V and the Ru(II)/(III) couple is consequently at a more positive potential and irreversible. In the Zn(II) complex **3d**, the pyrene motif is oxidised at 1.45 V. The electron-withdrawing effect of metal coordination results in significant positive shifts in the potentials for the triazine-based reductions for both Ru(II) complexes **2a-d** and Zn(II) complexes **3a-d**. Each triazine ligand has two reductions giving a total of four reductions for complexes **2a-d** and **3a-c**.

3.2.4 Spectroscopic Data

At wavelengths below 350 nm ligand based π- π^* and n- π^* transitions dominate the spectra. On complexation to the metal ions, the triazine based transitions shift to lower energy. In Zn(II) complexes **3b-d**, additional transitions are observed in the visible region and are assigned as Ar$\rightarrow$ triazine ^{1}ILCT transitions. This transition is significantly higher in energy in complex **2a** due to the poor electron-donating properties of the phenyl ring relative to the fused-aromatic rings. The ILCT transitions are red-shifted in comparison to Zn(II) tpy complexes with fused-aromatic rings.[3]

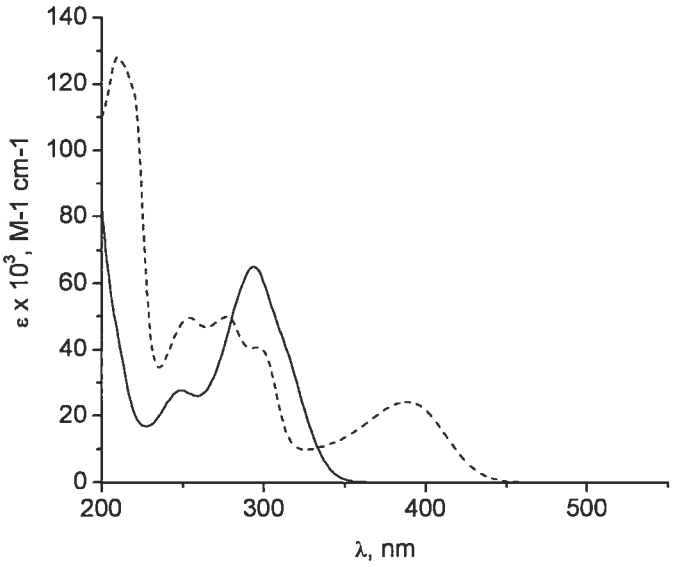

Figure 3.9 Electronic spectra of complexes **3a** and **3b** in acetonitrile.

Table 3.3 Spectroscopic Data in CH_3CN Solutions.

	Absorption[a]	Emission
Compound	λ max, nm (ε, $M^{-1}cm^{-1}$ x 10^{-3})	λ_{max}, nm
L1	276 (40.8) 243 (25.0)	414 (weak)[b]
L2	217 (59.5), 243 (27.9), 277 (20.0), ~312sh (8.1)	454[b]
L3[c]	245 (47.8) , 250 (50.5), 268 (30.3), 318 (8.5)	457[b]
L4	239 (36.1), 281 (21.0), 374 (9.3), 392 (7.5)	459[b]
2a	242(24.4), 284(73.2), 481(24.6)	-
2b	211 (62.0), 274 (26.0), 319 (sh), 487 (8.0)	-
2c[c]	206 (86.1), 253 (85.6), 274 (74.7), 342 (18.5), 491 (21.1)	-
2d	236 (132.5), 273 (116.9), 381 (22.5), 532 (46.6)	-
3a	249 (27.7), 294 (65.1)	378[a]
3b	210 (128.2), 255 (49.5), 278 (50.1), 298 (40.4), 388 (24.2)	560[a]
3c[c]	253 (115.5), 279 (55.4), 290 (53.8), 392 (25.9)	546[a]
3d	237 (108.4), 257 (46.7), 266 (41.1), 281 (44.6), 301 (46.8), 394 (23.1), 457 (38.4)	523, 693[a]

[a] In air equilibrated acetonitrile solutions

[b] In air equilibrated DCM solutions

[c] Previously discussed in chapter III, part A.

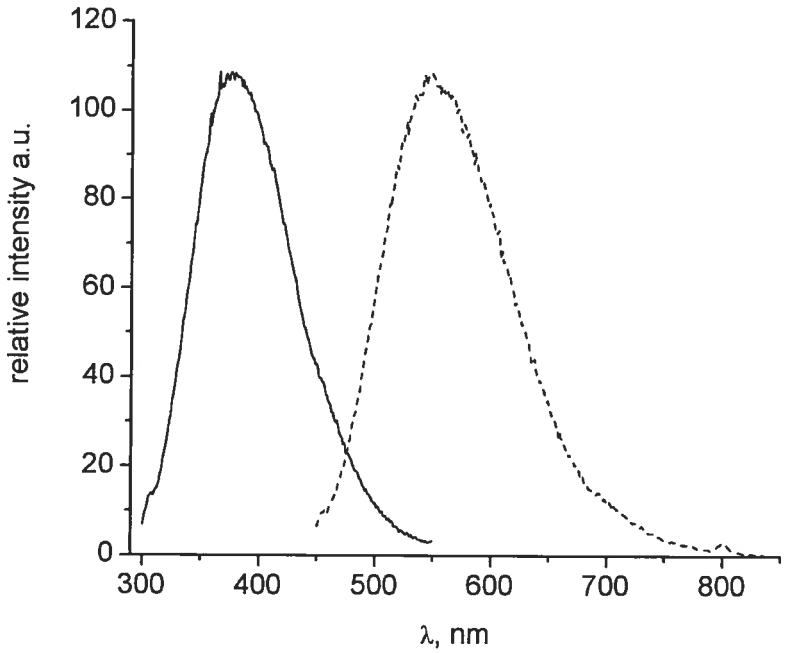

Figure 3.10 Uncorrected emission spectra of **3a** (solid line) and **3b** (dashed-line) in air-equilibrated acetonitrile.

The luminescence data of the ligands were obtained in air equilibrated solutions of the compounds in DCM. The ligands were excited into the π- π* absorption band for **L1** (320 nm), and the ^{1}ILCT absorption bands for **L2-4** (380 nm). **L1** was weakly emissive at room temperature with a band maximum at 414 nm. The intensity was significantly increased in the emission bands of **L2-4** (450-459 nm). The emission profiles for **L2-4** were very broad and negative solvatochromic behaviour indicated that the emissions involve significant charge transfer behaviour. The emissive state most probably has significant ^{1}ILCT character with additional π-π* contributions from the fused aromatic rings.[7] Ru(II) complexes are very weakly emissive at room temperature in air equilibrated acetonitrile presumably due to thermal access of non-emissive metal-centred states. In contrast the Zn(II) complexes are emissive at room temperature. Complex **3a** emits at significantly higher energy (378 nm) when compared to **3b-d** through ligand centred π-π* states. Complexes **3b** emits at 360 nm, consistent with emission from an ^{1}ILCT state as previously discussed for complex **3c**.[7] The emission spectrum is complicated in **3d** due to the presence of two emission

bands at 523 nm and a weaker band at 695 nm. Such dual emissive behaviour has previously been observed in Pt(II) complexes of a pyrenyl-appended tpy ligands.[9]

3.3 Conclusion

Introducing fused-aromatic rings on to the triazine-based tridentate ligands offers a means to stabilise the ILCT band significantly compared to the equivalent systems based on tpy. The ILCT band in tpy-based ligands lies at significantly high energy and the free ligands consequently emit form LC centred states at 77 K. Room temperature emissions studies of **L2-4**, indicate that their emissive excited state has significant charge transfer character from ILCT states. On complexation the ILCT states are red shifted in the Zn(II) complex. In Ru(II) complexes the excited states are quenched by the presence of low-lying metal centred states. The variable temperature photophysical properties are required in order to fully understand the nature of the excited states in pyrenyl-appended complex **3d**.

3.4 Experimental

Nuclear magnetic resonance (NMR) spectra were recorded in $CDCl_3$ and CD_3CN at room temperature (r.t.) on a Bruker AV400 spectrometer at 400 MHz for ^1H NMR and at 100 MHz for ^{13}C NMR. Chemical shifts are reported in part per million (ppm) relative to residual solvent protons (1.93 ppm for acetonitrile-d_3) and the carbon resonance of the solvent. Absorption spectra and emission spectra were measured in acetonitrile at r.t. on a Cary 500i UV-Vis-NIR spectrophotometer and a Cary Eclipse Fluorescence Spectrophotometer, respectively.

Electrochemical measurements were carried out in argon-purged acetonitrile at room temperature with a BAS CV50W multipurpose equipment interfaced to a PC. The working electrode was a Pt electrode. The counter electrode was a Pt wire, and the pseudo-reference electrode was a silver wire. The reference was set using an internal 1 mM ferrocene/ferrocinium sample at 395 mV vs SCE in acetonitrile and 432 mV in DMF. The concentration of the compounds was about 1 mM. Tetrabutylammonium

hexafluorophosphate (TBAP) was used as supporting electrolyte and its concentration was 0.10 M. Cyclic voltammograms were obtained at scan rates of 50, 100, 200, and 500 mV/s. For irreversible oxidation processes, the cathodic peak was used as E, and the anodic peak was used for irreversible reduction processes. The criteria for reversibility were the separation of approximately 60 mV between cathodic and anodic peaks, the close to unity ratio of the intensities of the cathodic and anodic currents, and the constancy of the peak potential on changing scan rate. The number of exchanged electrons was measured with OSWV, and by taking advantage of the presence of ferrocene used as the internal reference.

Experimental uncertainties are as follows: absorption maxima, ±2 nm; molar absorption coefficient, 10%; emission maxima, ± 5 nm; excited state lifetimes, 10%; luminescence quantum yields, 20%; redox potentials, ± 10 mV.

Compounds **L1**, **L3**, **2a**, **2c** and **3c**[6, 7] were synthesised as previously described. Solvents were removed under reduced pressure using a rotary evaporator unless otherwise stated.

L2 and L4

^{n}BuLi (1.6M in hexanes, 5.10 ml, 8.13 mmol) was added dropwise to a stirring solution of $HNMe_2$ (2M in THF, 4.10 ml, 8.13 mmol) in anhydrous Et_2O (150ml) under an inert atmosphere. The mixture was stirred for 20 minutes until a white suspension formed and 1-cyanonaphthalene or 1-cyanopyrene (7.39 mmol) was added to the mixture. The mixture was stirred for 4 hours further followed by addition of 2-cyanopyridine (1.44 ml, 15.0 mmol). The reaction mixture was stirred overnight and worked up by stirring for 30 minutes in air followed by removal of Et_2O. The residue was recrystallised three times from water: ethanol and the solid collected, washed with diethyl ether to yield **L2** as a white solid in 35% yield and **L4** as a yellow solid in 26% yield.

L2

^{1}H NMR (400 MHz, $CDCl_3$): 9.07, d, 1H, 8.6 Hz, H_{nap}; 8.99, dd, 2H, 4.3, 0.5 Hz, $H_{6,6''}$; 8.86, d, 2H, 8.0 Hz, $H_{3,3''}$; 8.58, d, 1H, 7.3 Hz, H_{nap}; 8.09, d, 1H, 8.2 Hz, H_{nap}; 7.99, m, 3H, $H_{4,4''}$,H_{nap}; 7.67, 2H, m, 2H_{nap}; 7.60, 3H, m, $H_{5,5''}$,H_{nap}. ^{13}C NMR (400 MHz, $CDCl_3$): 124.59, 124.80, 125.31, 125.83,126.21, 127.20, 128.42, 130.83, 130.87, 132.35, 132.87, 133.76, 136.92, 150.03, 152.84, 170.95, 175.00. *Anal. Calc.* $C_{23}H_{15}N_5.H_2O$: *Calc.* C 72.8, H 4.5, N 18.5; *Exp.* C 72.6, H 4.6, N 18.5.

L4

^{1}H NMR ($CDCl_3$, 400 MHz): 9.51 (d, J= 10 Hz, 1H) H_{py}; 9.12 (d J= 8 Hz, 1H), H_{py}; 9.06 (d, J = 4 Hz, 2H) $H_{6,6''}$; 8.94 (d, J= 8 Hz, 2H) $H_{3,3''}$; 8.39-8.07 (m, 7H) 7H_{py}; 8.05 (td, J= 2 Hz, 8 Hz, 2H) $H_{4,4''}$; 7.61 (dd, J= 5Hz, 6Hz, 2H) $H_{5,5''}$. ^{13}C NMR (100 MHz, $CDCl_3$): 124.19, 124.49, 124.65, 124.84, 125.56, 125.82, 125.89, 126.09, 127.07, 128.90, 129.07, 129.33, 129.73, 130.27, 130.30, 130.84, 133.63, 136.82, 150.22, 153.13, 171.15, 175.46, 176.75. *Anal. Calc.* $C_{29}H_{18}N_5.0.5H_2O$: *Calc.* C 78.4, H 4.1, N 15.8; *Exp.* C 78.7, H 3.3, N 15.5. ESMS: $[M+H]^+$ 436.3

Ruthenium Triazine Complexes **2b** and **2d**

$RuCl_3.3H_2O$ (0.032 g, 0.12 mmol) was added on stirring to a solution of the appropriate ligand (0.24 mmol) in DMF (15 ml). The mixture was stirred at room temperature for 15 minutes and then heated to reflux for one hour. The reaction mixture was cooled and saturated KPF_6 (aq, 5 ml) was added. The solution was diluted with a 100 ml of water and the red solid thus formed was placed onto a silica column and eluted with acetone:water:KNO_3(sat) 9:0.9:0.1. The nitrate salt was metathesized to the PF_6 salt and the solvent was removed. The residue was dissolved in acetonitrile, precipitated by addition to water, collected and recrystallised from acetonitrile/ether to afford **2b** and **2d** as red solids.

2b (red solid 56%)

^{1}H NMR, (400 MHz, CD_3CN): 9.68 (d, J= 9 Hz, 2H) H_{nap}; 9.11 (d, J= 7 Hz, 4H) $H_{3,3''}$; 9.09 (m, 2H) H_{nap}; 8.40 (d, J= 8 Hz, 2H) H_{nap}; 8.23 (d, J= 8 Hz, 2H) H_{nap}; 8.17 (td, J= 8

Hz, 1 Hz, 4H) $H_{4,4''}$; 7.90-7.98 (m, 4H) H_{nap}; 7.88 (d, J= 6 Hz, 4H) $H_{6,6''}$; 7.81 (t, J= 8 Hz, 2H) H_{nap}; 7.46 (td, J= 6, 2Hz, 4H) $H_{5,5''}$. High Res MS: M^{2+} (-2PF_6) = 462.0845 *Anal. Calc.* $C_{46}H_{30}N_{10}RuP_2F_{12}.4H_2O$: *Calc.* C 46.6, H 3.2, N 11.8; *Exp.* C 46.4, H 2.7, N 11.7.

2d (red solid 11%)

^{1}H NMR, (400 MHz, CD_3CN): 10.03 (d, J= 10 Hz, 2H) H_{pyrene}; 9.52 (d, J= 8.3 Hz, 2H) H_{pyrene}; 9.18 (d, J= 8 Hz, 4H) $H_{3,3''}$; 8.66 (d, J= 8 Hz, 2H) H_{pyrene}; 8.60 (d, J= 9.3 Hz, 2H) H_{pyrene}; 8.38- 8.53 (m, 8H) 4H_{pyrene}; 8.25 (t, J= 7 Hz, 2H) H_{pyrene}; 8.19 (t, J=8 Hz, 4H) $H_{4,4''}$;7.92 (d, J= 5 Hz, 4H) $H_{6,6''}$; 7.47 (dd, J= 6 Hz, 6Hz, 4H) $H_{5,5''}$. *Anal. Calc.* $C_{58}H_{38}N_{10}RuP_2F_{12}.2H_2O$: *Calc.* C 53.7, H 2.9, N 10.8; *Exp.* C 53.7, H 2.4, N 10.2.

Zinc Triazine Complexes **3a, 3b** and **3d**

$Zn(ClO_4)_2.6H_2O$ (0.05 mmol, 0.018 g) was added to a stirred solution of the appropriate ligand (0.1 mmol) in MeCN (15 ml). The mixture was refluxed for 15 minutes, cooled and the solvent removed. The solid was recyrstallised from ethanol, followed by precipitation in acetonitrile/diethyl ether to yield complexes **3a-d.**

3a (white solid 68%)

^{1}H NMR, (400 MHz, CD_3CN): 9.14 (d, J= 8Hz, 2H) $H_{2''',6'''}$; 9.05 (d, J= 7Hz, 2H) $H_{3,3''}$; 8.31 (t, J= 8Hz, 2H) $H_{4,4''}$; 8.24 (d, J= 4Hz, 2H) $H_{6,6''}$; 7.93 (t, J= 7Hz, 1H) $H_{4'''}$; 7.80 (t, J= 7Hz, 2H) $H_{3''',5'''}$; 7.64 (dd, J= 6Hz, 7Hz, 2H) $H_{5,5''}$. *Anal. Calc.* $C_{38}H_{26}Cl_2N_{10}O_8Zn$ Calc: C, 51.5; H, 3.0; N, 15.8. Exp: C, 51.7; H, 3.2, N, 16.1.

3b (yellow solid 55%)

^{1}H NMR, (400 MHz, CD_3CN): 9.50 (d, J= 9Hz, 1H) H_{nap}; 9.09 (d, J= 8Hz, 2H) $H_{3,3''}$; 9.05 (d, J= 7Hz, 1H) H_{nap}; 8.43 (d, J= 8Hz, 1H) H_{nap}; 8.30- 8.34 (m, 4H) $H_{4,4''}$, $H_{6'6''}$; 8.20 (d, J= 8Hz, 1H) H_{nap}; 7.90-7.93 (m, 2H) 2H_{nap}; 7.78 (t, J= 7Hz, 1H) H_{nap}; 7.69 (dd, J= 5Hz, 6Hz, 2H) $H_{5,5''}$. *Anal. Calc.* $C_{46}H_{30}C_{l2}N_{10}O_8Zn.H_2O$: *Calc:* C, 55.0; H, 3.2; N, 13.9. *Exp:* C, 55.1; H, 3.6; N, 14.1

3d (Orange solid 84%)

^{1}H NMR, (400 MHz, CD_3CN): 9.93 (d, J= 9Hz, 1H) H_{pyrene}; 9.49 (d, J= 9Hz, 1H) H_{pyrene}; 9.19 (d, J= 8Hz, 2H) $H_{3,3''}$; 8.60-8.63 (m, 2H) $2H_{pyrene}$; 8.47-8.54 (m, 3H) $3H_{pyrene}$; 8.35-8.41 (m, 5H) H_{pyrene}, $H_{4,4''}$, $H_{6,6''}$; 7.72 (dd, J= 6Hz, 6Hz, 2H) $H_{5,5''}$. *Anal. Calc.* $C_{58}H_{34}Cl_2N_{10}O_8Zn.H_2O$: *Calc:* C, 60.4; H, 3.2; N, 12.2. *Exp:* C, 60.5; H, 3.4; N, 12.3.

3.5 References

[1] N. W. Alcock, P. R. Barker, J. M. Haider, M. J. Hannon, C. L. Painting, Z. Pikramenou, E. A. Plummer, K. Rissanen, P. Saarenketo, *Dalton Trans.* **2000**, 1447.

[2] V. Balzani, S. Campagna, G. Denti, A. Juris, S. Serroni, M. Venturi, *Acc. Chem. Res.* **1998**, *31*, 26.

[3] H. Krass, E. A. Plummer, J. M. Haider, P. R. Barker, N. W. Alcock, Z. Pikramenou, M. J. Hannon, D. G. Kurth, *Angew. Chem., Int. Ed.* **2001**, *40*, 3862.

[4] H.-S. Chow, E. C. Constable, C. E. Housecroft, M. Neuburger, S. Schaffner, *Dalton Trans.* **2006**, 2881.

[5] E. A. Medlycott, *Thesis, Chapter IV* **2006**.

[6] M. I. J. Polson, E. A. Medlycott, G. S. Hanan, L. Mikelsons, N. J. Taylor, M. Watanabe, Y. Tanaka, F. Loiseau, R. Passalacqua, S. Campagna, *Chem. Eur. J.* **2004**, *10*, 3640.

[7] E. A. Medlycott, *Thesis, Chapter III, Part A* **2006**.

[8] W. Leslie, R. A. Poole, P. R. Murray, L. J. Yellowlees, A. Beeby, J. A. G. Williams, *Polyhedron* **2004**, *23*, 2769.

[9] J. F. Michalec, S. A. Bejune, D. G. Cuttell, G. C. Summerton, J. A. Gertenbach, J. S. Field, R. J. Haines, D. R. McMillin, *Inorg. Chem.* **2001**, *40*, 2193.

Chapter IV: Rh (III) complexes of tridentate ligands: Probing their excited state properties by varying ancillary ligands.

4.1 Introduction

Chapters II and III have focussed on the development of Ru(II) complexes as potential sensistisers for light-harvesting applications. In contrast to Ru(II) and Os(II), the use of polypyridine complexes of group 9 metals to applications as sensitisers in light-harvesting devices remains less explored. It has been realised for some time that Ir(III) complexes of tridentate terpyridine-based ligands and cyclometallating polypyridine ligands have promising properties for light harvesting applications due to the long-lived excited state generated from excitation in the visible region.[1-6] The photophysical properties of Ir(III) complexes are highly dependent on the nature of the coordinating polypyridine ligand. The parent complex, $Ir(tpy)_2^{3+}$, is relatively emissive at room temperature in air equilibrated solutions and its photophysical properties are comparable to $Ru(bpy)_3^{2+}$.[7-9] In contrast, Ir(III) complexes of cyclometallating tridentate ligands are highly emissive in degassed solutions and are sensitive to oxygen.[4, 10] The development of such systems has been rather slow due to the kinetic inertness and resulting problems of synthesizing Ir(III) polypyridine complexes. In comparison, Rh(III) polypyridine complexes remain even less studied than their third row counterparts. There have been some initial studies on the photophysical properties of $Rh(bpy)_3^{2+}$ and $Rh(tpy)_2^{2+}$-type systems but the excited-state lifetimes are substantially shorter than the Ir(III) analogues.[11, 12] Despite the limited literature in the use of Rh(tpy)-type systems as potential sensitisers, the $Rh(tpy)_2^{3+}$ motif has been incorporated into Rh(III)– Ru(II) diads in which the $Ru(tpy)_2^{2+}$ complex plays the role of sensitizer and the covalently linked $Rh(tpy)_2^{3+}$-based motif behaves as an electron acceptor (Figure 4.1).[13, 14] At 150 K the electron transfer was monitored from the ^{3}MLCT state of the Ru(II) motif to the Rh(III) domain. The electron transfer process

was found to be distance dependant and was only observed in those diads in which the distances between the Ru(II) and Rh(III) domains is minimized (Figure 4.1).

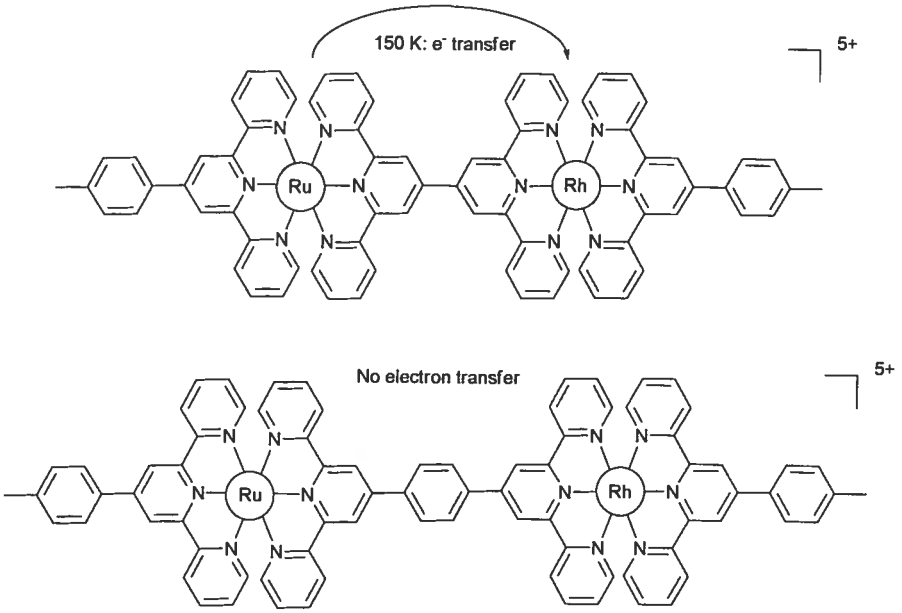

Figure 4.1 Distance dependence of electron transfer in Ru(II)-Rh(III) diads.[14]

The present chapter describes the synthesis of a family of Rh(III) complexes based on a triazine-tridentate ligand, 2,4-di-(2'-pyridyl)-6-(*p*–bromophenyl)-1,3,5-triazine. Four complexes have been synthesised with a second tridentate ligand of variable σ-donating ability in order to probe and understand their excited state properties. The electronic properties are studied as a consequence of the change in the electronic density at the Rh(III) centre.

4.2 Discussion

4.2.1 Synthesis

The triazine ligand **L1** and cyclometallating ligand **L2** were synthesised as previously described.[4, 15] The precursor Rh(**L1**)Cl_3 was obtained by the reaction of $RhCl_3$ with one equivalent of **L1** in refluxing ethanol. After 90 minutes the mixture was cooled and the solid collected. The orange/brown solid was thoroughly washed with water, ethanol and then diethyl ether and dried to yield Rh(**L1**)Cl_3 in 74% yield. The

homoleptic complex, **1a**, could then be synthesised by the reaction of Rh(**L1**)Cl_3 with **L1** in the presence of $AgNO_3$ as a dechlorinating agent in refluxing absolute ethanol. Column chromatography yielded the homoleptic complex in 21% yield. The heteroleptic complex **1b** was synthesised from the reaction of Rh(tpy)Cl_3 with one equivalent of the triazine in anhydrous ethanol and 3 equivalents of $AgSO_3CF_3$ to yield 44% of the heteroleptic complex. Anhydrous solvents were used to avoid the formation of the dicarboxamide from nucleophilic attack of water on the triazine rings.[16, 17] Complex **1c** was synthesized by adopting the previously reported procedure used for Ir(III) complexes of this ligand.[4]

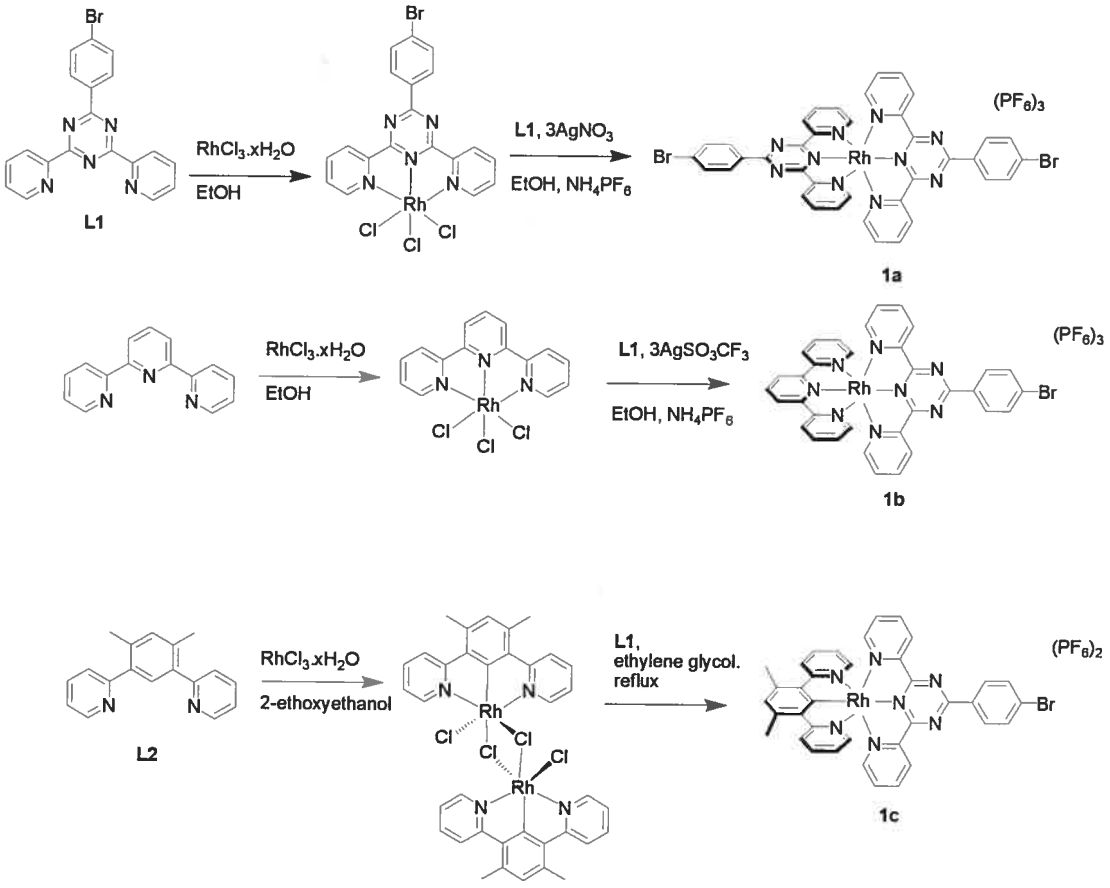

Scheme 4.1 Synthesis of complexes **1a-c**.

4.2.2 Characterisation

The complexes were characterised by ^{1}H NMR, elemental analyses and X-ray diffraction. The ^{1}H NMR spectra of complexes **1a** and **1b** are shown in Figure 4.2.

Complex **1a** has a simplified spectrum with only six signals for the triazine ligand. Evidence of the bis-triazine terdentate complex is observed in the shift of proton H_6, alpha to the coordinating N atom. In the free ligand, H_6 can be observed at 8.99 ppm. However, on complexation H_6 is shielded significantly and shifts to 8.13 ppm, due to the coordination of a second orthogonal ligand. The aromatic region of the ^{1}H NMR of complex **1b** is complicated by the additional signals in the terpyridine ligand. As a consequence two sets of signals are seen for the distal pyridyl rings of both ligands and in each case the signals for **L1** are deshielded with respect to tpy due to the electron deficient nature of the triazine ring.

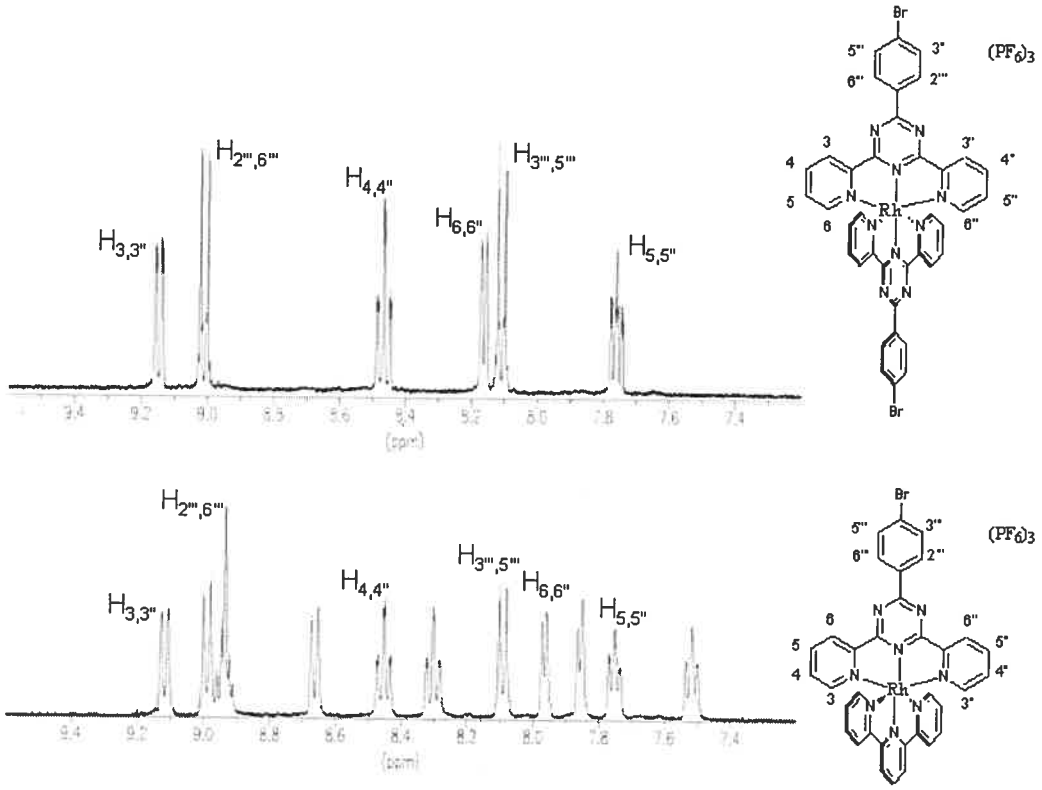

Figure 4.2 ^{1}H NMR of complexes **1a** and **1b** in CD_3CN.

The solid state structures of **1a-c** are shown in Figure 4.3 with bond distances and angles
listed in Table 4.1. X-Ray quality crystals of **1a-c** were obtained by slow diffusion of diethyl ether into a concentrated solution of acetonitrile. Acetonitrile solvent

molecules were observed in the unit cell in all cases. The Rh(III) ion possesses pseudo-octahedral geometry and are bound to a triazine ligand and a second orthogonal tridentate ligand. Complex **1a** crystallises in the monoclinic space group C2/c with half of the cation and one and a half PF_6^- anions found in the asymmetric unit. The cations are arranged to give an offset face-to-face, π-stacking interaction, which is observed between a pyridyl ring and the pendant phenyl ring on a neighbouring cation with a distance of 3.88 Å (centroid-centroid). Relatively short Br-Br distances are observed between neighbouring cations (4.04 Å), similarly to the interactions observed in complexes of first-row metal ions of this ligand.[15, 18] Heteroleptic complex **1b** crystallised in the triclinic space group P-1, with two cations, three PF_6^- anions and three acetonitrile water molecules in the asymmetric unit. The cations are arranged in the extended lattice with long range offset π-stacking interactions between the terminal triazine-based pyridyl ring and the pendant phenyl ring of the neighbouring molecule. Short bromine-bromine interactions are also observed in **1b** with a distance of 3.33Å between neighbouring molecules, less than the sum of the Van der Waals radii.[15, 18]

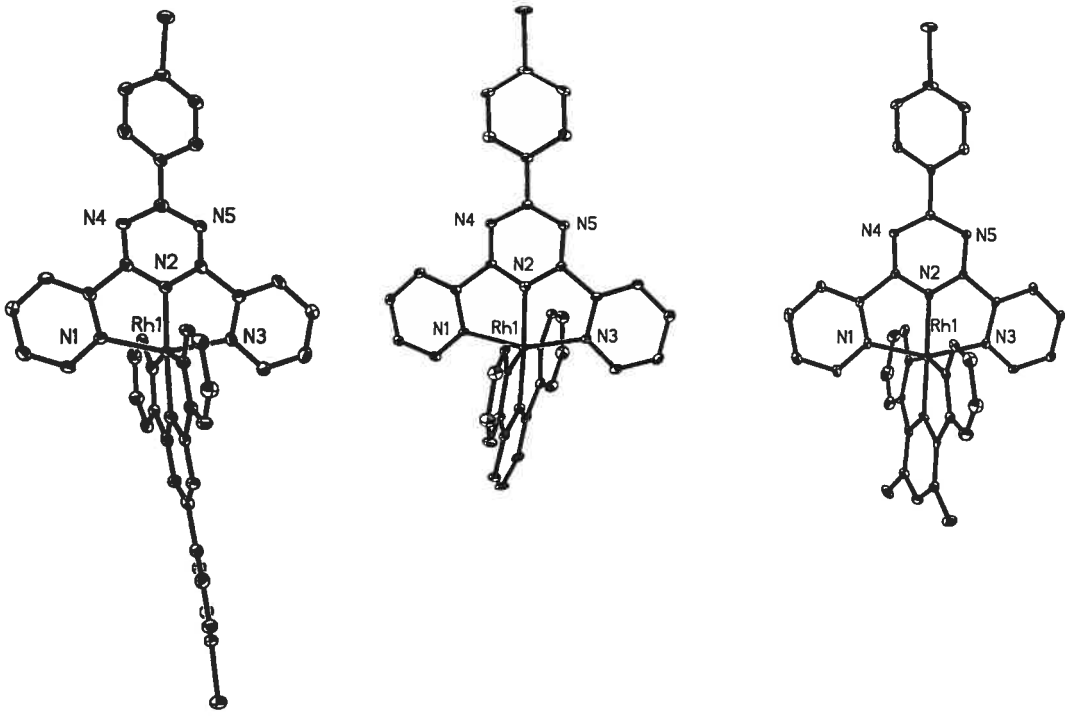

Figure 4.3 ORTEP diagram of **1a-c** shown with 30% thermal ellipsoids. The counter-ions and solvents of crystallisation have been omitted for clarity.

Br-Br interactions were not observed in complex **2c**, however, face-to-face interactions dictate the packing arrangement between a triazine-based pyridyl ring and pendant phenyl ring on a neighbouring cation with a distance of 3.62 Å (centroid to centroid). Additional offset π-stacking interactions are observed between the *meta*-xylene cyclometallating rings and a terpyridine-based terminal pyridyl ring on a neighbouring cation.

Table 4.1 Selected bond distances and angles for complexes **1a-c**.

Bond Distances (Å)	**1a**	**1b**	**1c**
Triazine ligand			
Rh-N_{trz} (terminal)	2.066 (4)	2.066 (4)	2.064 (5)
Rh-N_{trz} (central)	1:964 (4)	1.961 (4)	2.031 (6)
Rh-N_{trz} (terminal)	2.060 (4)	2.074 (4)	2.071 (6)

Second ligand			
Rh-N(terminal)		2.047 (5)	2.045 (6)
Rh-N/C (central)		1.974 (4)	1.955 (7)
Rh-N (terminal)		2.059 (5)	2.045 (6)
Selected Angles (°)			
N1-Rh1-N3	158.2 (2)	158.2 (2)	156.0 (2)
N6-Rh1-N7/N8		160.3 (2)	160.6 (2)
Triazine- phenyl twist	12.64 (0.30)	9.5 (2)	11.4 (4)

Negligible differences are observed in the Rh-N(triazine) bond distances between complexes **1a** and **1b**. An elongation is observed in the Rh-N bond distance to the central triazine ring in the cyclometallated complex **1c**. This is a consequence of the strong *trans*-influence observed *trans* to the cyclometallating *meta*-xylene ring. As predicted, the Rh-C bond distance in **1c** is shorter than the Rh-N(tpy) bond distance to the central pyridyl ring in **1b**.

Table 4.2 Absorption and electrochemical data for complexes **L1** and **1a-c.**

	λ_{max}, nm (ε, $M^{-1}cm^{-1}$)[a]	$E_{1/2}$(redn)[b]				
L1	250 (16.7), 281 (36.3)					
1a	245 (32.4), 302 (47.9), 361 (46.4),	-0.05	-0.28	-0.64	-0.99	-1.43
1b	245 (42.2), 268 (34.6), 298 (37.3), 341 (32.2), 356 (34.6)	-0.22	-0.46	-1.02	-1.50	
1c	247 (44.1), 295 (42.4), 314 (33.2), 354 (22.6)	-0.53 [c]	-1.09	-1.41		

[a] Measured in air equilibrated acetonitrile at r.t..

[b] Measured vs SCE in argon-purged acetonitrile. Reductions are irreversible unless otherwise stated.

[c] Reversible, with 81 mV between the cathodic and anodic waves.

The electrochemistry of complexes **1a-c** were measured in acetonitrile versus $TBAPF_6$ with ferrocene as an internal standard (Table 4.2). In both complexes **1a** and **1b**, an initial irreversible Rh(III)/(I) two-electron reduction was observed at -0.05 V and -0.22 V, which are significantly less negative than Rh(III) homoleptic complexes of tpy-type ligands. Complex **1a** is easier to reduce than **1b** due to the electron deficient nature of the two triazine ligands. The subsequent ligand based reductions are irreversible presumably due to a rearrangement in coordination geometry. Complex **1c,** however, has an initial ligand based reversible reduction corresponding to a one-electron reduction of the triazine ligand. This is due to the electron-donating properties of the cyclometallating ligand resulting in greater electron density at the Rh(III) centre. The Rh(III) centre is subsequently reduced at a significantly more negative potential than complexes **1a-b**, and this is followed by an additional triazine-based reduction.

The electronic absorption spectra of **L1** and **1a-c** were measured in acetonitrile and the data is collected in Table 4.2. Ligand based π-π^* transitions dominate the higher-energy UV region of the spectrum in ligand **L1** (Figure 4.4). On complexation the ligand based transitions are red shifted in complex **1a** as expected.

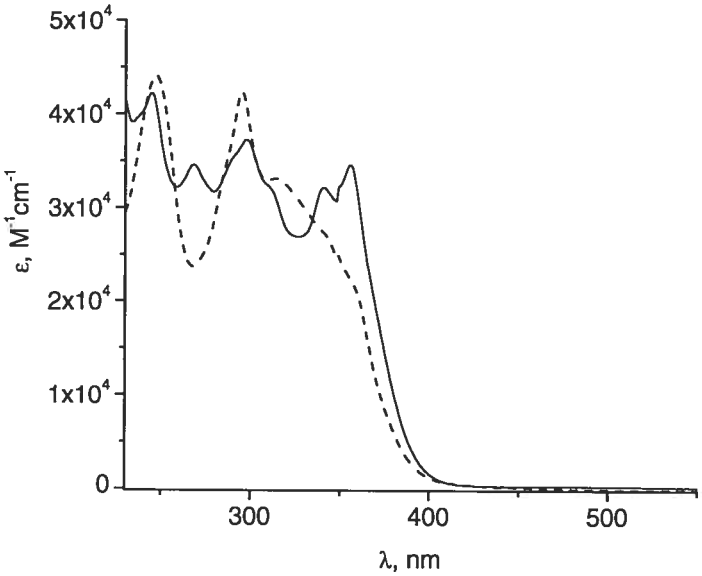

Figure 4.4 Electronic absorption spectra of complexes **1b** and **1c**.

Emission spectra of ligand **L1** and complexes **1a-c** were studied at room temperature in acetonitrile and at 77 K in ethanol/methanol (4:1) glass. Complexes **1a** and **1b** are weakly emissive at room temperature in deaerated acetonitrile solutions giving emission bands with relatively little structure at 536 nm and 541 nm. A similar emission band is observed in **L1** at 469 nm. The bands are blue shifted when measured at 77 K in ethanol:methanol glass 4:1 and are assigned to ligand-centred emissions bands. Contrastingly, complex **1c** has a well-structured emission at room temperature (Figure 4.5) with high O_2 sensitivity and the emission band is blue shifted at 77 K. The O_2 sensitivity indicates charge transfer character and the emission can be considered to have significant ligand-to-ligand charge transfer character between the cyclometallating and triazine ligands. The emission band is further blue-shifted at 77 K to 427 nm.

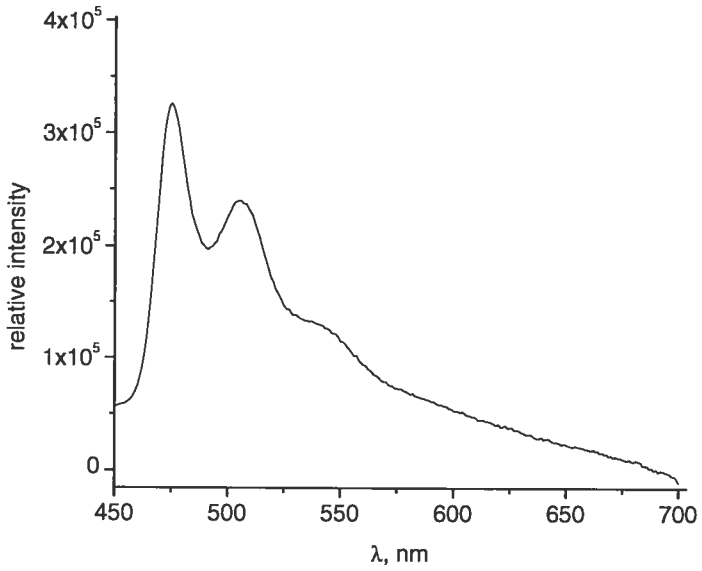

Figure 4.5 The emission spectra of **1c** at room temperature in deaerated acetonitrile.

All complexes and **L1** have an additional low energy structure-less emission band at 77 K. This band is red-shifted with respect to the principle bands observed at room temperature and signicantly red-shifted in the complexes compared to **L1**. Dual emission behaviour was previously reported for a Rh(III) family of complexes incorporating pyridyl triazole-based ligands but the nature of the emitting state was not elucidated.[12] Considering the effect is observed in the ligand as well as the complexes the nature of the emitting state should be ligand based. Triazine ligands have previously been shown to have the potential to display dual emission behaviour due to twisted-intramolecular charge-transfer states (TICT).[19] The pendant bromo-phenyl ring in **L1** has the potential to twist through the interannular bond allowing favourable H-bonding interactions between the triazine-based *N*-lone pairs and C-H ortho to the interannular bond. [20] A TICT band in the triazine ligand may explain the lower energy emissions although the narrow profile of the band shape would not support this assignment. Further experimental studies will be carried out to fully characterize the nature of the emitting state.

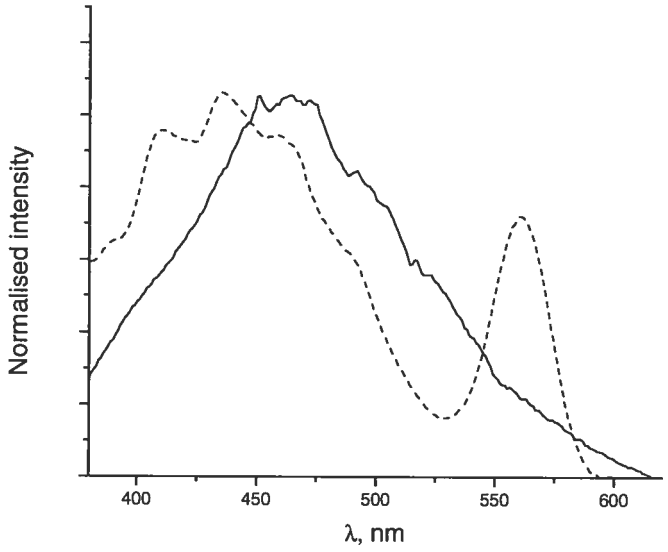

Figure 4.6 Emission profile of **L1** at r.t. (solid line) and 77 K (dashed line).

4.3 Conclusions

A new family of Rh (III) complexes have been synthesised and fully characterised with **L1** and orthogonal ligands with varying σ-donating ability. The complexes are weakly emissive at room temperature in the visible region of the spectrum. The nature of the excited state is dependant on the σ-donating strength of the orthogonal ligand. A cyclometallating ligand is employed in complex **1c** and the emission studies indicate significant inter-ligand charge-transfer character. The orthogonal ligands in **1a** and **1b** are less electron rich and as a consequence the excited state is ligand centred. The introduction of the bromo-functionality in the *para* position of the phenyl ring will allow further chemistry to be carried out on the complex in order to manipulate its photophysical properties.

4.4 Experimental

4.4.1 General Considerations

Nuclear magnetic resonance (NMR) spectra were recorded in CD_3CN at room temperature (r.t.) on a Bruker AV400 spectrometer at 400 MHz for ^1H NMR. Chemical shifts are reported in part per million (ppm) relative to residual solvent protons (1.93 ppm for acetonitrile-d_3). Absorption spectra were measured in acetonitrile at r.t. on a Cary 500i UV-Vis-NIR Spectrophotometer.

The fluorescence excitation and emission spectra of the ligands and complexes 1a-c were recorded using a Jobin Yvon FluoroMax-2 spectrofluorimeter, equipped with a Hamamatsu R928 photomultiplier tube. Samples were degassed via a minimum of three freeze–pump–thaw cycles, base pressure $<10^{-3}$ mbar, in 1 cm pathlength quartz cuvettes, modified to allow connection to the vacuum line. All solvents used were HPLC grade or
pre-distilled.

Electrochemical measurements were carried out in argon-purged acetonitrile at room temperature with a BAS CV50W multipurpose equipment interfaced to a PC. The working electrode was a Pt electrode. The counter electrode was a Pt wire, and the pseudo-reference electrode was a silver wire. The reference was set using an internal 1 mM ferrocene/ferrocinium sample at 395 mV vs SCE in acetonitrile and 432 mV in DMF. The concentration of the compounds was about 1 mM. Tetrabutylammonium hexafluorophosphate (TBAP) was used as supporting electrolyte and its concentration was 0.10 M. Cyclic voltammograms were obtained at scan rates of 50, 100, 200, and 500 mV/s. For irreversible oxidation processes, the cathodic peak was used as E, and the anodic peak was used for irreversible reduction processes. The criteria for reversibility were the separation of 60 mV between cathodic and anodic peaks, the close to unity ratio of the intensities of the cathodic and anodic currents, and the constancy of the peak potential on changing scan rate. The number of exchanged

electrons was measured with OSWV, and by taking advantage of the presence of ferrocene used as the internal reference.

Experimental uncertainties are as follows: absorption maxima, ±2 nm; molar absorption coefficient, 10%; emission maxima, ± 5 nm; excited state lifetimes, 10%; luminescence quantum yields, 20%; redox potentials, ± 10 mV.

$Rh(tpy)Cl_3$[21] and ligands **L1**[15] and **L2**[14] were synthesised as previously described. The precursor $[Rh(\mathbf{L2})Cl_2]_2$ was synthesised according to a procedure developed in the Williams Group, Durham, England.[22] Solvents were removed under reduced pressure using a rotary evaporator unless otherwise stated.

4.4.2 Experimental procedures

$Rh(\mathbf{L1})Cl_3$

A suspension of $RhCl_3$ hydrate (0.28 g, 1.36 mmol) and **L1** (0.53 g, 1.36 mmol) were heated in ethanol (30 mL) for 90 minutes. After cooling to room temperature the precipitate was collected by filtration and washed with ethanol (20 mL), water (20 mL), ethanol (20 mL) and finally diethyl ether (20 mL). The orange solid was collected and dried to afford $Rh(\mathbf{L1})Cl_3$ (0.60 g, 74%).

^1H NMR (d_6-DMSO, 400 MHz): 9.34 (d, J= 5 Hz, 2H) $H_{6,6''}$; 9.05 (d, J= 8 Hz, 2H) $H_{3,3''}$; 8.76 (d, J= 9 Hz, 2H) $H_{2''',6'''}$; 8.56 (t, J= 8 Hz, 2H) $H_{4,4''}$; 8.24 (t, J= 7 Hz, 2H) $H_{5,5''}$; 7.97 (d, J= 9 Hz, 2H) $H_{3''',5'''}$. ^{13}C {^1H} NMR (d_6-DMSO, 100 MHz): 128.64, 130.19, 132.20, 132.34, 132.51, 132.69, 141.37, 154.72, 154.90, 169.81, 172.62.

1a

A suspension of $Rh(\mathbf{L1})Cl_3$ (0.13 g, 0.21 mmol) and $AgNO_3$ (0.11 g, 0.63 mmol) in absolute ethanol (20 mL) was heated to reflux for 3 hours under N_2. Ligand **L1** (0.082 g, 0.21 mmol) was added as a solid and the mixture was refluxed for another four hours. After cooling to room temperature the solution was filtered to remove AgCl and KPF_6 (10 mL, aq.) was added to the filtrate to afford a yellow precipitate. The solid was collected by filtration and purified by column chromotagraphy (silica, acetonitrile:

KNO_3 (sat), 7:1). The nitrate salt was metathesized to the PF_6 salt and the solvent was removed. The residue was dissolved in acetonitrile, precipitated by addition to water, collected and recrystallised from acetonitrile/ether to afford **1a** as a beige solid (26 mg, 15% yield)

^{1}H NMR (CD_3CN, 400MHz): 9.11 (dd, 2H (7.8, 1.1Hz), $H_{3,3''}$; 8.97 (d, 2H) $H_{2''',6'''}$; 8.43 (td, 2H J= 8 Hz, 1Hz, 2H) $H_{4,4''}$; 8.13 (d, J= 6 Hz, 2H) $H_{6,6''}$; 8.07 (d, J= 9 Hz, 2H) $H_{3''',5'''}$; 7.73 (ddd, 6 Hz, 6 Hz, 1 Hz, 2H), $H_{5,5''}$. ^{13}C {^{1}H}NMR (CD_3CN, 100MHz): 130.79, 131.90, 132.40, 132.41, 133.07, 133.24, 143.21, 152.05, 155.66, 168.39, 176.11. High Res. ESMS *m/z* calcd for $C_{38}H_{24}N_{10}Rh$ $[M]^{3+}$: 293.6536; found: 293.6540.

1b

A suspension of $Rh(tpy)Cl_3$ (0.050 g, 0.11 mmol) and $AgSO_3CF_3$ (0.087 g, 0.34 mmol) in ethanol absolute (15 mL),) was heated to reflux for 2 hours under N_2. Ligand **L1** (0.044 g, 0.21 mmol) was then added to the mixture and refluxing continued for four hours. The mixture was cooled and filtered to remove AgCl and KPF_6 (10 mL, aq.) was added to the filtrate to afford a yellow precipitate. The solid was collected by filtration and purified by colunm chromotagraphy (silica, acetonitrile: KNO_3 (sat), 7:1). The nitrate salt was metathesized to the PF_6 salt and the solvent was removed. The residue was dissolved in acetonitrile, precipitated by addition to water, collected and recrystallised from acetonitrile/ether to afford **1b** as a beige solid (40 mg, 30% yield)

^{1}H NMR (CD_3CN, 400 MHz): 9.12 (dd, J = 8 Hz, 2H) $H_{3,3''}$; 8.99 (d, J = 9 Hz, 2H) $H_{2''',6'''}$; 8.94 (m, 5H) $H_{T3',T5'}$ $H_{T4'}$; 8.70, (d, J = 8 Hz, 2H) $H_{T3,3''}$; 8.45 (t, J = 8 Hz, 2H) $H_{4,4''}$; 8.30 (t, J = 8 Hz, 2H) $H_{T4,4''}$; 8.09 (d, J = 9 Hz, 2H) $H_{3''',5'''}$; 7.97 (d, J = 6 Hz, 2H) $H_{6,6''}$; 7.86, (d, J = 6 Hz, 2H) $H_{T6,6''}$; 7.75 (dd, J = 6 Hz, 6 Hz) $H_{5,5''}$; 7.52 (dd, J = 6 Hz, 7 Hz) $H_{T5,5''}$. ^{13}C {^{1}H} NMR (CD_3CN, 75 MHz): 127.65 127.99, 130.54, 131.50, 132.79, 132.88, 133.85, 133.13, 134.90, 143.38, 143.90, 144.83, 152.68, 153.92, 154.60, 155.73, 157.24, 168.99, 176.92. Anal. Calc. for: $C_{34}H_{23}BrN_8Rh(PF_6)_3.2H_2O$: C, 34.11; H, 2.27; N, 9.36. Found: C, 34.08; H, 2.05; N, 9.06.

1c

A suspension of $[Rh(\mathbf{L2})Cl_2]_2$ (0.055g, 0.063mmol) and ligand **L1** (0.049g, 0.126 mmol) in ethylene glycol (3 mL) was heated to 195°C for 15 minutes or until everything dissolved under N_2. The solution was cooled and water (10 mL) added. The mixture was filtered and KPF_6(sat) (10 mL) was added to the filtrate to afford a yellow precipitate. The solid was collected by filtration and washed with water, ethanol and diethyl ether and dried under vacuum to afford the complex 90 mg (69%).

^{1}H NMR (CD_3CN, 400 MHz): 9.05 (d, J = 8 Hz, 2H), $H_{3,3''}$; 9.00 (d, J = 9 Hz, 2H), $H_{2''',6'''}$; 8.32 (d, J = 8.5 Hz, 2H), $H(NCN)_{3,3''}$; 8.29 (t, J = 7.8 Hz, 2H), $H_{4,4''}$; 8.07 (d, J = 9 Hz, 2H), $H_{3''',5'''}$; 7.95 (t, J = 8 Hz, 2H), $H(NCN)_{4,4''}$; 7.66 (d, J = 5 Hz, 2H), $H_{6,6''}$; 7.57 (d, J = 5 Hz, 2H), $H(NCN)_{6,6''}$; 7.54 (t, J = 7 Hz), $H_{5,5''}$, 7.47 (s, 2H), $H(NCN)_{4'}$; 7.02 (t, J = 7 Hz, 2H), $H(NCN)_{5,5''}$, 2.98 (s, 6H) $H(NCN)_{3',5'}$. Anal. Calc. for: $C_{37}H_{27}BrN_7Rh(PF_6)_2.0.5(CH_3CN)$: C, 42.94; H, 2.70; N, 9.88. Found: C, 43.23; H, 2.79; N, 10.27.

4.5 References

1 M. Licini and J. A. G. Williams, *Chem. Commun.*, **1999**, 1943.

2 W. Leslie, R. A. Poole, P. R. Murray, L. J. Yellowlees, A. Beeby, and J. A. G. Williams, *Polyhedron*, **2004**, 23, 2769.

3 I. M. Dixon, J.-P. Collin, J.-P. Sauvage, L. Flamigni, S. Encinas, and F. Barigelletti, *Chem. Soc. Rev.*, **2000**, 29, 385.

4 A. J. Wilkinson, A. E. Goeta, C. E. Foster, and J. A. G. Williams, *Inorg. Chem.*, **2004,** 43, 6513.

5 W. Goodall and J. A. G. Williams, *Dalton Trans.*, **2000**, 2893.

6 K. K.-W. Lo, C.-K. Chung, D. C.-M. Ng, and N. Zhu, *New J. Chem.*, **2002**, 26, 81.

7 N. P. Ayala, C. M. Flynn Jr., L. Sacksteder, J. N. Demas, and B. A. DeGraff, *J. Am. Chem. Soc.*, **1990**, 112, 3837.

8 J.-P. Collin, I. M. Dixon, J.-P. Sauvage, J. A. G. Williams, F. Barigelletti, and L. Flamigni, *J. Am. Chem. Soc.*, **1999**, 121, 5009.

9 A. Juris, V. Balzani, F. Barigelletti, S. Campagna, P. Belser, and A. Von Zelewsky, *Coord. Chem. Rev.*, **1998,** 84, 85.

10 M. Polson, S. Fracasso, V. Bertolasi, M. Ravaglia, and F. Scandola, *Inorg. Chem.*, **2004,** 43, 1950.

11 M. E. Frink, S. D. Sprouse, H. A. Goodwin, R. J. Watts, and P. C. Ford, *Inorg. Chem.*, **1988**, 27, 1283.

12 H. M. Burke, J. F. Gallagher, M. T. Indelli, and J. G. Vos, *Inorg. Chim. Acta*, **2004**, 357, 2989.

13 M. T. Indelli, F. Scandola, J.-P. Collin, J.-P. Sauvage, and A. Sour, *Inorg. Chem.*, **1996,** 35, 303.

14 M. T. Indelli, F. Scandola, L. Flamigni, J.-P. Collin, J.-P. Sauvage, and A. Sour, *Inorg. Chem.,* **1997**, 36, 4247.

15 E. A. Medlycott, *Thesis, Chapter V*, **2006**.

16 P. Paul, B. Tyagi, M. M. Bhadbhade, and E. Suresh, *J. Chem. Soc., Dalton Trans, Inorg. Chem.*, **1997**, 2273.

17 P. Paul, B. Tyagi, A. K. Bilakhiya, M. M. Bhadbhade, E. Suresh, and G. Ramachandraiah, *Inorg. Chem.*, **1998**, 37, 5733.

18 E. A. Medlycott, I. Theobald, and G. S. Hanan, *Eur. J. Inor. Chem.*, **2005**, 1223.

19 G. J. Stueber, M. Kieninger, H. Schettler, W. Busch, B. Goeller, J. Franke, H. E. A. Kramer, H. Hoier, S. Henkel, P. Fischer, H. Port, T. Hirsch, G. Rytz, and J.-L. Birbaum, *J. Phys. Chem.,* **1995**, 99, 10097.

20 M. I. J. Polson, E. A. Medlycott, G. S. Hanan, L. Mikelsons, N. J. Taylor, M. Watanabe, Y. Tanaka, F. Loiseau, R. Passalacqua, and S. Campagna, *Chem. Eur. J.,* **2004**, 10, 3640.

21 I. I. Bhayat and W. R. McWhinnie, *Spectrochim. Acta A*, **1971**, 28, 743.

22 V. Whittle and J. A. G. Williams, *Unpublished Results*, **2006**.

Chapter V, Part A: Co(II) complexes of triazine-based tridentate ligands with positive and attractive Co(II/III) redox couples.

Communication 2

Elaine A. Medlycott, Isabelle Theobald, Garry S. Hanan*

Département de chimie, Université de Montréal, Montréal, Québec, Canada H3C 3J7

European Journal of Inorganic Chemistry, **2005**, *1223-1226.*

5.1 Introduction

Dye-sensitized solar cells (DSSCs) have been intensely studied in the last fifteen years since Grätzel published his landmark work.[1,2] In order to advance the field, many groups have focused their efforts on improving the excited-state properties of the Ru(II) polypyridine complexes that act as the photosensitisers in the Grätzel cell.[3] Much less attention has been paid to the redox mediator, even though it contributes directly to the maximum photocurrent attainable by the DSSC.[2,3] Whereas the classic redox mediator in such systems is the volatile and corrosive I^-/I_3^- couple, its redox potential is fixed and, therefore, cannot be varied to improve the efficiency of the DSSC.[4] Recently, Co(II) complexes of heterocyclic ligands have been shown to be effective redox mediators in DSSCs as they are non-corrosive, non-volatile and modifiable. [5,6,7] Herein we report on a new family of Co(II) complexes based on tridentate triazine ligands that are easily synthesized and modified. Their considerably more positive Co(II/III) redox couples than previously reported Co(II) complexes of polypyridine ligands favours their use in DSSCs.[5,6]

5.2 Results and Discussion

The synthesis of triazines ligands **1a**[8] and **1b**[9] has previously been reported. Ligand **1c** was synthesised by the addition of *p*-bromobenzonitrile to a solution of $LiNMe_2$ in anhydrous diethylether.[9,10] The amidinate intermediate that forms reacts with two equivalents of 2-cyanopyridine to afford ligand **1c** after loss of dimethylamide. A series of homoleptic Co(II) complexes of ligands **1a-c** were synthesised by allowing the ligands to react with $CoCl_2.6H_2O$ followed by precipitation of complexes **2a-c** from the reaction mixture by the addition of NH_4PF_6 (Scheme 5.1a).[11] Heteroleptic complexes **3a-c** may be obtained directly by reacting ligands **1a-c** with one equivalent of $CoCl_2.6H_2O$ in the presence of tetrabutylammonium chloride (NBu_4Cl) (see in (b) Scheme 5.1) or indirectly when NBu_4Cl is introduced into an acetone solution of

complexes **2a-c** (Scheme 5.1c).[12] It has previously been established that an equilibrium exists between the homo- and heteroleptic state of Co(II) complexes of 2,4,6-tripyridyl-s-triazine in acidic solution.[13] In this case, heteroleptic Co(II) complexes **3a-c** could be obtained by the addition of NBu_4Cl to complexes **2a-c**.

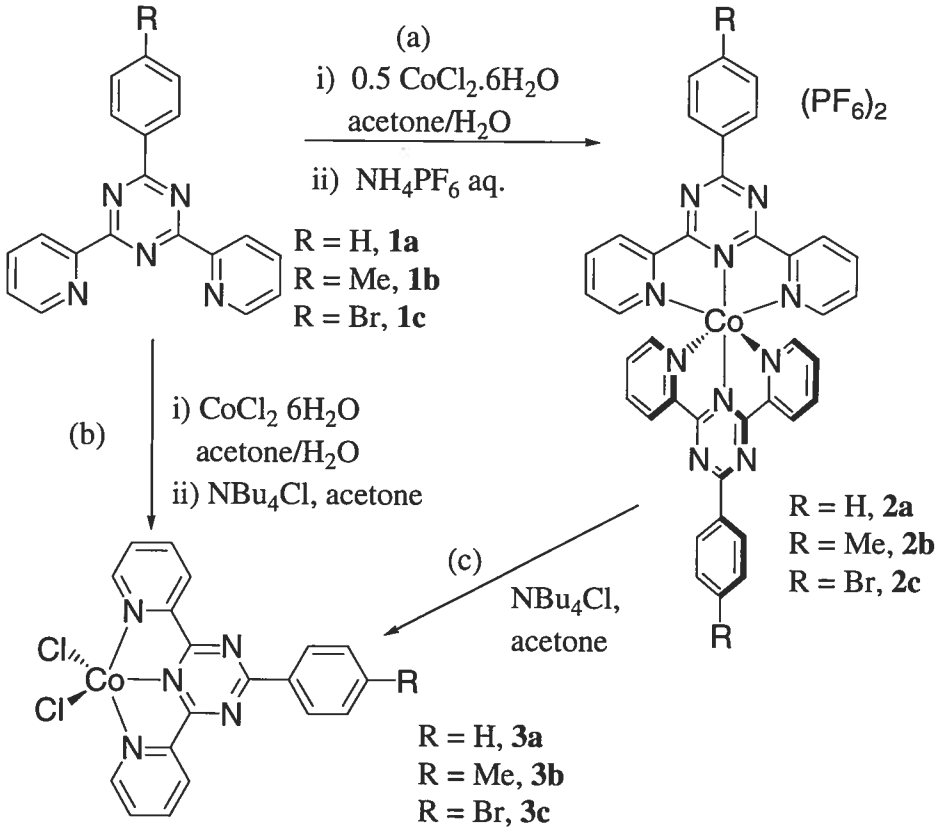

Scheme 5.1 Synthesis of Co(II) homo- and heteroleptic complexes.

The ^1H NMR chemical shifts of the homoleptic complexes are typical of paramagnetic Co(II) complexes that are low spin, with chemical shifts ranging over approximately 110 ppm (Table 5.1).[14] The signals are broadened considerably and therefore no coupling constants could be obtained from the spectra. The greatest shifts are observed for the protons *ortho* to the pyridine N's and, therefore, closest to the paramagnetic Co (II) centre. The protons farthest from the paramagnetic centre, those on the phenyl ring, have the smallest shift as compared to the free ligands.[9]

Table 5.1 ^{1}H NMR chemical shifts of homoleptic complexes **2a**, **2b** and **2c** in CD_3CN.

	δ, ppm						
	Pyridyl				Phenyl		CH_3
1c	8.99	8.87	8.74	7.60	8.74	7.73	
2a	115.08	80.09	37.54	22.87	13.51	6.17	
2b	113.39	78.56	37.13	21.99	13.27	6.13	5.83
2c	111.88	79.38	36.28	22.96	13.36	6.66	

The X-ray crystal structure of **2c** is shown in Figure 5.1. [14] The Co(II) ion is bound by two orthogonal ligands **1c** in a pseudo-octahedral coordination environment as the peripheral pyridines in each ligand pinch in to form N–Co–N angles of 151.79°. The Co–N bond length to the central triazine (1.986 Å) is shorter than the Co–N bond length in homoleptic terpyridine complex (2.022 Å) and the homoleptic triazine complex of 2,4,6-tris(2'-pyridyl)-1,3,5-triazine ligand (2.058 Å). [16,17] The Co–N bond lengths to the peripheral pyridine rings range from 2.134 Å to 2.158 Å, similar to those found in terpyridine complexes of Co(II).

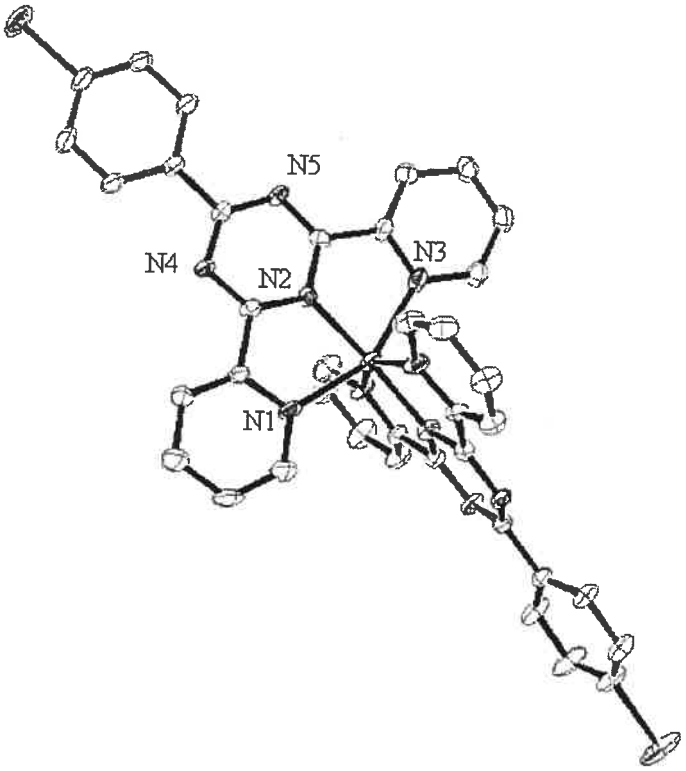

Figure 5.1 ORTEP diagram of **2c** shown with 30% thermal ellipsoids. The counteranions and solvent of crystallisation have been omitted for clarity.

The phenyl ring is twisted by 13.3° relative to the central triazine ring (Figure 5.1). This near planar arrangement is due to favourable N–to–CH hydrogen bonding interactions between the N lone pairs and the H's *ortho* to the interannular bond. The slight twist in the interannular bond is a result of edge-to-face packing between the phenyl rings in different molecules of **2c**, which are separated by 3.514 Å (Figure 5.2). A planar arrangement should easily be adopted in solution which would permit greater electron delocalization between the triazine and the phenyl ring. The two PF_6 counter-ions are found above and below the planes of the triazine rings and do not interfere with the phenyl packing arrangement, consistent with other extended packing arrangements in the solid state.[18] There is also a short Br1–to–Br2' distance of 3.395 Å between adjacent molecules which is indicative of favourable van der Waals

interactions which give rise to a linear one-dimensional tape in the solid state (Figure 5.2).

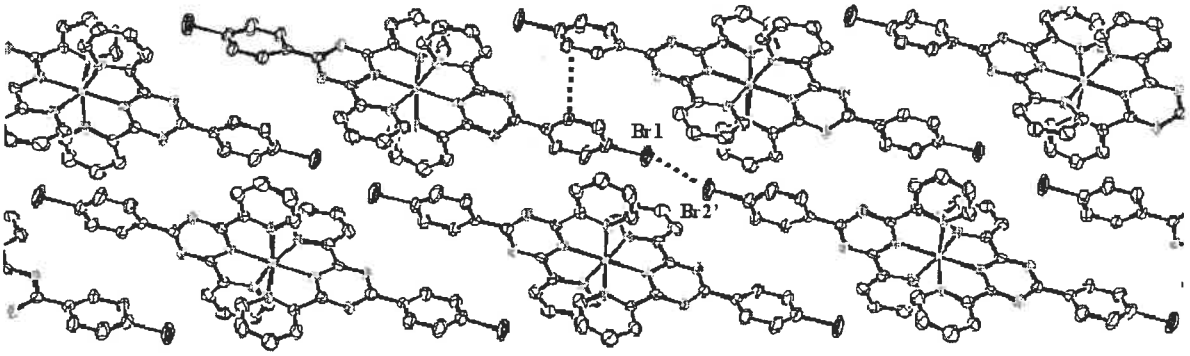

Figure 5.2 Intermolecular packing forces in the solid state structure of **2c:** phenyl-to-phenyl distance = 3.514 Å and the Br1—Br2' distance = 3.395 Å. The PF_6 counteranions and solvent of crystallization have been removed for clarity.

In the electronic spectra of complexes **2a-c**, a very weak metal-centred transition is found at approximately 470 nm (Figure 5.3). The λ_{max} for these d–d transitions are difficult to identify due to the low energy tail from the ligand based transitions but the extinction coefficients are in the order of 500 M^{-1} cm^{-1} for all three complexes. For applications in DSSC, a low extinction coefficient is desirable so as to minimise the competition between the redox mediator and sensitiser for absorption in the visible region. [5–7] Intense ligand based $\pi \rightarrow \pi^*$ transitions are observed in the UV region. Lower energy $\pi \rightarrow \pi^*$ transitions are observed for the Me and Br substituted complexes as compared to the complex R = H. In **2b,** the electron donating methyl groups destabilise the ligand π orbitals to a greater extent than the ligand π^* orbitals. Conversely, in **2c** the ligand π^* orbitals are stabilised to a greater extent than ligand π orbitals due to the electron withdrawing nature of the bromine substituent.

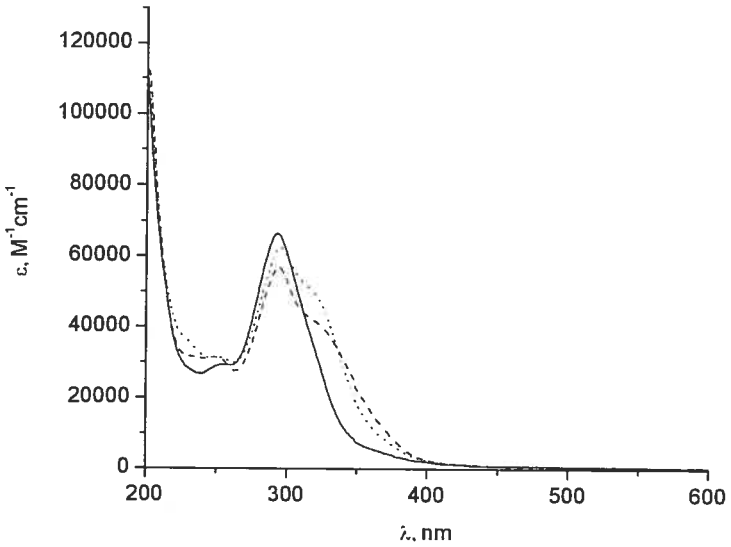

Figure 5.3 Electronic absorption spectra of complexes **2a** (solid line), **2b**(dash line) and **2c** (dot line).

The electrochemistry of complexes **2a, 2b** and **2c** were measured using tetrabutylammonium PF_6 as a supporting electrolyte and a Pt electrode with ferrocene as the internal standard. The data (reported versus SCE) are gathered in Table 5.2. The Co(II)/(III) couples are centred at approximately +0.75 V, which is considerably more positive than previously reported Co(II) of heterocyclic ligands.[5–7] In each case, oxidative processes are irreversible, which may be a result of limited solubility of the Co(III) species. It had previously been noted that irreversibility of the Co(II/III) couple does not necessarily translate into inefficient redox mediators, but sometimes give rise to the most efficient redox mediators.[6] The more positive oxidation potential of **2a-c** as compared to terpyridine complexes of Co(II) is favourable with respect to an increased photocurrent in DSSCs.[7] The Co (II/III) couple is only slightly affected by subsitituent on the phenyl ring, with complex **2c** being the most difficult to oxidise as a result of the electron withdrawing Br substituent and **2b** being the easiest as a result of the electron donating Me substituent. The Co(II/I) couple is also affected by the various substitutents, with **2b** being the hardest to reduce and **2c** the easiest to reduce. The greater variability in the Co(II/I) reduction potential is a reflection of the increased

backbonding of the metal centre to the ligand upon reduction. The two remaining reductions are independent triazine-based reductions and follow the electron withdrawing effect of the substitutents.

Table 5.2 Electrochemical redox potentials for complexes **2a-c** in argon-purged acetonitrile solutions (vs SCE).

$E_{1/2}$ (V) [ΔE_p, (mV)]				
Cpd	Co (II/III)	Co (II/I)	Triazine Reductions	
2a	0.76 [irr]	-0.42 (73)	-1.06 (72)	-1.47 (85)
2b	0.74 [irr]	-0.47 (64)	-1.11 (66)	-1.52 (64)
2c	0.77 [irr]	-0.40 (52)	-1.04 (56)	-1.46 (66)

5.3 Conclusion

Co(II) complexes of tridentate triazine-based ligands, either heteroleptic or homoleptic, are readily synthesized and isolated. The electrochemical properties of the homoleptic complexes indicate that the Co (II/III) redox couples are more positive and more favourable for DSSC than those of Co(II) terpyridine based complexes. The Co(II/III) couple exhibits small shifts in oxidation potential upon modification of the phenyl ring substituents, whereas the Co(II/I) reduction potential is more readily modified. Further modifications to directly substitute electron withdrawing and donating groups directly on the triazine ring will be reported in due course.

Acknowledgements

We thank the Natural Sciences and Engineering Research Council (NSERC) of Canada and the Université de Montréal for financial support. EAM thanks the Canadian Commonwealth Scholarship and Fellowship Program. IT thanks NSERC of Canada for an undergraduate research award.

5.4 References

[1] B. O`Regan, M. Grätzel, *Nature*, **1991**, *353*, 737.

[2] A. Hagfeldt, M. Graetzel, *Acc. Chem. Res.*, **2000**, *33*, 269.

[3] C. A., Bignozzi, E. Argazzi, C. J. Kleverlaan, *Chem. Soc. Rev.*, **2000**, *29*, 87.

[4] M. K. Nazeeruddin, A. Kay, I. Rodicio, R. Humphry-Baker, E. Müller, P. Liska, N. Vlachopoulos, M. Grätzel, *J.Am. Chem. Soc.*, **1993**, *115*, 6382.

[5] H. Nusbaumer, J.-E. Moser, S. M. Zakeeruddin, M. K. Nazeeruddin, M. Grätzel, *J. Phys. Chem. B*, 2001, **105**, 10461.

[6] S. A. Sapp, C. M. Elliott, C. Contado, S. Caramori, C. A. Bignozzi, *J.Am. Chem. Soc.*, **2002**, *124*, 11215.

[7] H. Nusbaumer, S. M. Zakeeruddin, J.-E. Moser, M. Graetzel, *Chem. Eur. J.*, **2003**, *9*, 3756.

[8] M. I. J. Polson, N. J. Taylor, and G. S. Hanan, *Chem. Commun.* **2002**, 1356.

[9] M. I. J. Polson, E. A. Medlycott, G. S. Hanan, L. Mikelsons, N. J. Taylor, M. Watanabe, Y. Tanaka, F. Loiseau, R. Passalacqua, S. Campagna *Chem. Eur. J.* **2004**, *10*, 3640.

[10] Synthesis of 2,4-di-(2'-pyridyl)-6-(*p*-bromophenyl)-1,3,5-triazine **1c:** *Para*-bromobenzonitrile (0.68 g, 3.73 mmol) was added to a stirred mixture of $LiNMe_2$ (0.19 g, 3.73 mmol) in anhydrous diethyl ether. After 30 min, 2-cyanopyridine (0.77 g, 7.46 mmol) was added to the mixture. After an hour the reaction mixture was diluted with H_2O (250 ml) and the precipitate was collected. Recrystallisation of the solid from

ethanol afforded **1c** (0.90 g, 62 %) as a white solid. ^{1}H NMR ($CDCl_3$): 8.99, d, 2H (4.1 Hz); 8.87, d, 2H, (7.8 Hz); 8.74, d, 2H (8.4 Hz); 8.0, t, 2H (7.1 Hz); 7.73, d, 2H (8.4 Hz); 7.60, t, 2H (5.0 Hz).

[11] General procedure for the synthesis of homoleptic Co(II) complexes **2a, 2b, 2c**: The triazine ligand (0.42 mmol) was stirred in acetone (25 ml) and added to a solution of $CoCl_2.6H_2O$ (0.38 mmol, 91 mg). After heating at reflux for 75 min and precipitation in aqueous NH_4PF_6, complexes **2a** (110 mg, 54 %), **2b** (127 mg, 61 %) and **2c** (103 mg, 43 %) were collected.

[12] Synthesis of heteroleptic complexes **3a**, **3b** and **3c** followed the same procedure for complexes **2**. After heating for 75 min the acetone:water mix was removed under reduced pressure and the solution was dissolved in a small amount of acetone and precipitated by the addition of NBu_4Cl. Complexes **3a** (44 %), **3b** (33 %) and **3c** (23 %) were collected. *Anal.* Calc. for **3a.**$2H_2O$: C, 47.82; H, 3.59; N, 14.68. Found: C, 47.67; H, 3.33; N, 14.66. *Anal.* Calc. for **3b.**H_2O : C, 50.76; H, 3.62; N, 14.80. Found: C, 51.38; H, 3.46; N, 15.09. *Anal.* Calc. for **3c.**$4H_2O$: C, 38.54; H, 3.40; N, 11.83. Found: C, 38.55; H, 2.78; N, 11.81.

[13] J. Prasad, N. C. Peterson, *Inorg. Chem.*, **1971**, *10*, 88.

[14] E. C. Constable, C. E. Housecroft, T. Kulke, C. Lazzarini, E. R. Schofield, Y. Zimmermann *J. Chem. Soc., Dalton Trans.*, **2001**, 2864.

[15] Orange crystals of **2c** suitable for X-ray analysis could be grown by slow diffusion of isopropyl ether into a solution of the complex in acetonitrile. Crystal data for **2c**: $C_{38}H_{24}N_{10}Co.2(PF_6)$ was collected on a Bruker APEX at 100 K using Cu-Kα radiation (λ= 1.54178 Å). Full-matrix, least squares refinements on F^2 using all data. 3198 reflections, M = 1129.36, monoclinic, space group C2/c, a = 14.7467(4), b = 20.8588(6), c = 16.6451(5) Å, α = 90 °, β = 96.2640(10) °, γ = 90 °, V = 5089.4(3)Å^3 , Z = 4, R1 [I > 2σ(I)] = 4.28, wR2 = 8.36. CCDC 252138 contains the supplementary crystallographic data for this paper. These data can be obtained free of charge via www.ccdc.cam.ac.uk/data_request/cif, by emailing data_request@ccdc.cam.ac.uk, or

by contacting The Cambridge Crystallographic Data Centre, 12, Union Road, Cambridge CB2 1EZ, UK; fax: +44 1223 336033.

[16] T. Yutaka, I. Mori, M. Kurihara, N. Tamai, H. Nishihara, *Inorg. Chem.* **2003**, *42*, 6306.

[17] B. N. Figgis, E. S. Kucharski, S. Mitra, B. W. Skelton, A. H. White, *Aust. J. Chem.*, **1990**, *43*, 1269.

[18] N. W. Alcock, P. R. Barker, J. M. Haider, M. J. Hannon, C. L. Painting, Z. Pikramenou, E. A. Plummer, K. Rissanen, P. Saarenketo, *J. Chem. Soc., Dalton Trans.* **2000**, 1447.

Chapter V, Part B: Non-covalent polymerisation in the solid-state: halogen-halogen vs methyl-methyl interactions in the complexes of 2,4-di(2-pyridyl)-1,3,5-triazine ligands

Article 2

Elaine A. Medlycott [a], Konstantin A. Udachin [b], Garry S. Hanan [*,a]

a) Département de chimie, Université de Montréal, Montréal, Québec, Canada H3C 3J7

b) Steacie Institute for Molecular Sciences, NRC, Ottawa, Ontario, Canada.

Accepted for publication to Dalton Transactions, October **2006**.

Manuscript B613883G.

Fe (II), Co(II), Ni(II) and Cu(II) complexes based on the triazine ligand 2,4-di(2'-pyridyl)-6-(*p*-bromo-phenyl)-1,3,5-triazine have been synthesised and characterised. Solid state structures of the ligand and the Fe(II), Co(II) and Cu(II) complexes possess Br-Br interactions linking neighbouring molecules to form 1-dimensional tapes. Changing the phenyl substituent from a bromine to a methyl group eliminates the 1-dimensional tape and gives rise to significant π-stacking interactions.

5.5 Introduction

Controlled aggregation of metallic supramolecular assemblies through covalent or non-covalent approaches is of interest for device applications depending on the magnetic,[1-3] redox[4] or luminescent properties[5-7] of the oligo- or poly-nuclear complexes under study. Facile and rapid syntheses of such assemblies is of itself important and as a consequence the synthetically favoured complexes of *N*-heterocyclic tridentate ligands based on 2,2':6':2''-terpyridine (tpy) have been the focus of much attention.[8] Whilst complexes of bidentate ligands such as 2,2'-bipyridine afford interesting properties,[6] rapid synthesis of polymetallic systems can be problematic due to the separation of *facial* and *meridonal* diastereomers.[5]

Three main approaches can be taken to obtain higher nuclearity complexes based on tridentate tpy-type ligands (Figure 5.4). The first involves the synthesis of polytopic ligands that can be applied to the metal-directed assembly of higher nuclear complexes using covalent interactions (Figure 5.4).[8-11] The second and third approaches involve the synthesis of monomeric complexes, which may be polymerised through the use of covalent or non-covalent interactions. Although 'chemistry-on-the-complex' synthetic methods may prove useful to build up polymetallic arrays through covalent interactions,[12, 13] this approach is limited by the solubility of the oligomeric complexes in solution (Figure 5.4b). On the other hand, rapid and controlled aggregation of metal complexes in the solid state can be obtained using non-covalent interactions (Figure 5.4c).[14-16]

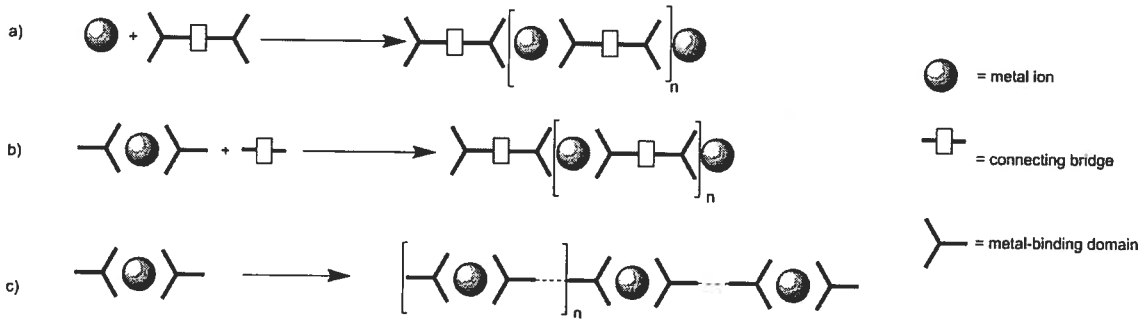

Figure 5.4 Metal-containing polymers assembled by three approaches: a) A classical coordination approach,[17-19] b) A 'chemistry-on-the-complex' approach (including electrochemically),[20-23] and c) the non-covalent assembling approach.[14, 16]

Many synthetic strategies have been developed to improve the properties of complexes with tpy-type ligands.[24] Substitution on the terpyridine core has proved efficient in manipulating both magnetic and photophysical properties through electronic and steric interactions.[25-27] Alternatively, the pyridyl rings can be replaced by different *N*-heterocyclic rings,[28, 29] as we previously reported for a Ru(II) family of complexes based on 2,4-di(2-pyridyl)-6-phenyl-1,3,5-triazine ligand family.[30, 31] The most widely studied triazine containing ligand, however, is the symmetric, commercially available 2,4,6-tris(2'-pyridyl)-1,3,5-triazine (tptz) ligand. Tptz has proved versatile in the synthesis of Fe(II)[32-37], Co(II)[35], Ni(II)[38] and Cu(II)[39-41] complexes with interesting properties and variable coordination modes. However, further substitution of the ligand is difficult and structural and electronic diversity are thus limited. Using the 2,4-di(2-pyridyl)-6-phenyl-1,3,5-triazine ligand family, a range of substituents can be introduced in order to tune and manipulate the photophysical and electrochemical properties of their transition metal complexes.[31, 42]

Herein, we report the synthesis and characterisation of a family of Fe(II), Co(II), Ni(II) and Cu(II) complexes of bromophenyl- and toluyl-substituted tridentate triazine-based ligands. The introduction of pendant Br-atoms enables us to gain directional in the linking of cations in the solid state through non-covalent Van der Waals interactions. These interactions have been exploited in both organic, inorganic and hybrid materials, and the influence of the X-X interaction is highly dependant on

the polarity of a M-X and C-X bond.[43-46] Despite the growing interest in the use of such interactions in crystal engineering, to the best of our knowledge, there are no examples in which this approach has been use to influence the aggregation of linear redox or magnetically active complexes based on tpy or alternative tridentate ligands. Halogen-halogen interactions may be classified into two types depending on the angles θ_1 and θ_2 (figure 5.5a).[46b] In type **I** interactions, the angles θ_1 and θ_2 are essentially equal so that close contacts occur between identical portions of the halogen atom. The interactions are allowed on consideration of the anisotropic behaviour of halogen atoms, allowing short Van der Waals interactions in the equatorial plane. These interactions may be shorter than the reported Van der Waals radii of the halogen in question but are permitted due to the elongation of the electronic distribution giving a non-spherical Van der Waals radii.[46c] Type **II** interactions are considered in terms of 'X atom-polarisation'. In such systems the halogen is polarised positively in the polar region and negatively in the equatorial region with a C-X bond lying perpendicular to the second C-X bond (Figure 5.5b). The Br-Br interactions described in the complexes in this chapter may be considered as type **I** interactions in which the anisotropic electronic distribution permit short Van der Waals contacts. However, the short contacts observed in the ligand may be considered as type **II**.

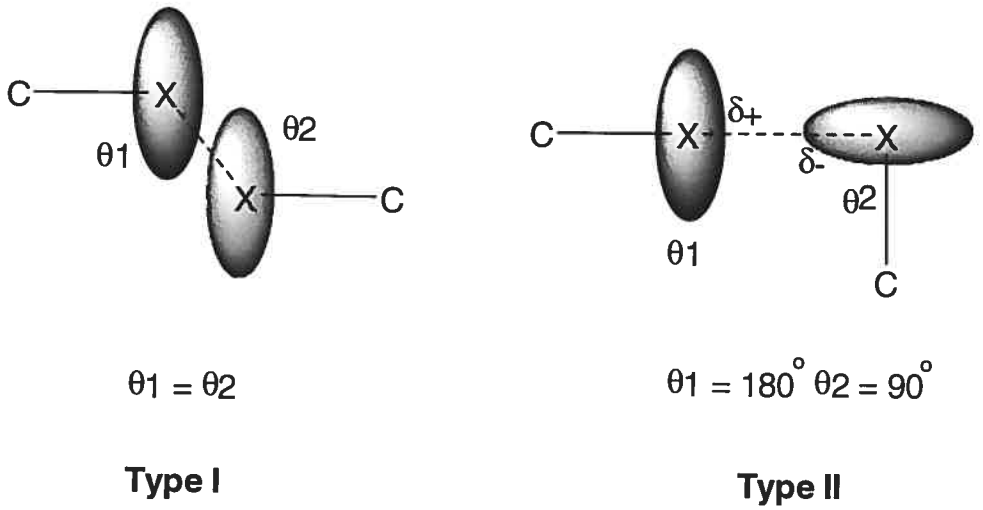

Figure 5.5 a) Type I halogen-halogen interactions (left), b) Type II halogen-halogen interactions (right).

5.6 Results and Discussion

5.6.1 Synthesis

The ligands **L1** and **L2** were synthesised by modified triazine ring-forming reactions (Scheme 5.2).[31, 42] The original method could be improved by generating $LiNMe_2$ '*in-situ*', which proved more reliable than the use of $LiNMe_2$ in the solid state. Subsequent addition of *p*-bromobenzonitrile or tolunitrile afforded an amidinate intermediate which cyclised on addition of 2 equivalents of 2-cyanopyridine to afford the triazine ligands **L1** and **L2**.

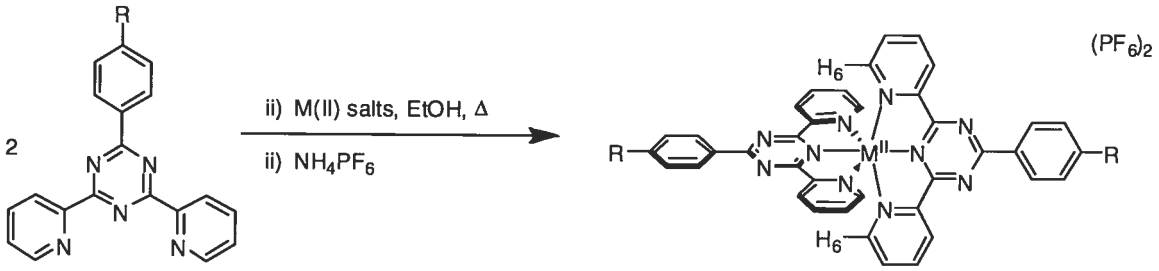

Scheme 5.2 Synthesis of complexes **1a-d** and **2a-d**.

The syntheses of complexes **1a-d** and **2a-d** were carried out in methanol or ethanol (Scheme 1). Anhydrous solvents were employed for the synthesis of Ni(II) and Cu(II) complexes in order to hinder hydrolysis of the triazine ligand which is promoted in aqueous solutions.[47-49] A hot alcoholic solution of the appropriate metal salts was added to an alcoholic solution of the ligand. Colour changes were observed immediately depending on the metal ions used and refluxing was continued for 15-30 minutes. Addition of alcoholic NH_4PF_6 or KPF_6 to the reaction mixture resulted in the precipitation of the complexes as their PF_6^- salts upon cooling which were collected, washed and dried to obtain complexes **1a-d** and **2a-d**.

The ^{1}H NMR spectra were obtained in CD_3CN for all complexes. Complexes **1b-d** and **2b-d** are paramagnetic and the ^{1}H signals are considerably shifted and broadened with respect to typical diamagnetic complexes. All signals were observed in the paramagnetic spectrum for **1b-c** and **2b-c**, however, one peak was missing in complexes **1d** and **2d** due to the broadening of signals. The ^{1}H NMR spectra of **1a** and **2a** resemble that of a low spin diamagnetic Fe (II) complex although broadening of the resonance closest to the metal centre, H_6, is observed. This may indicate a small paramagnetic contribution in the complex for a largely diamagnetic ground state (**Figure 5.6**).

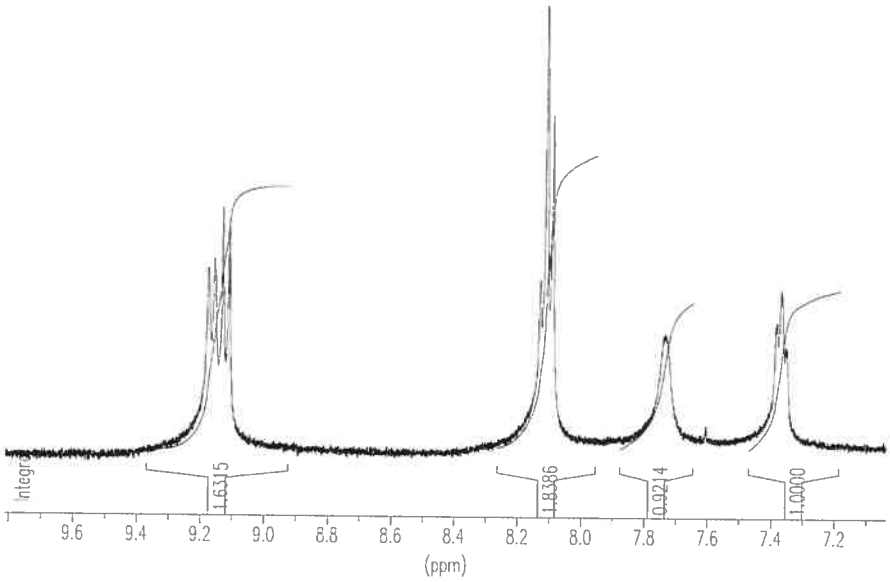

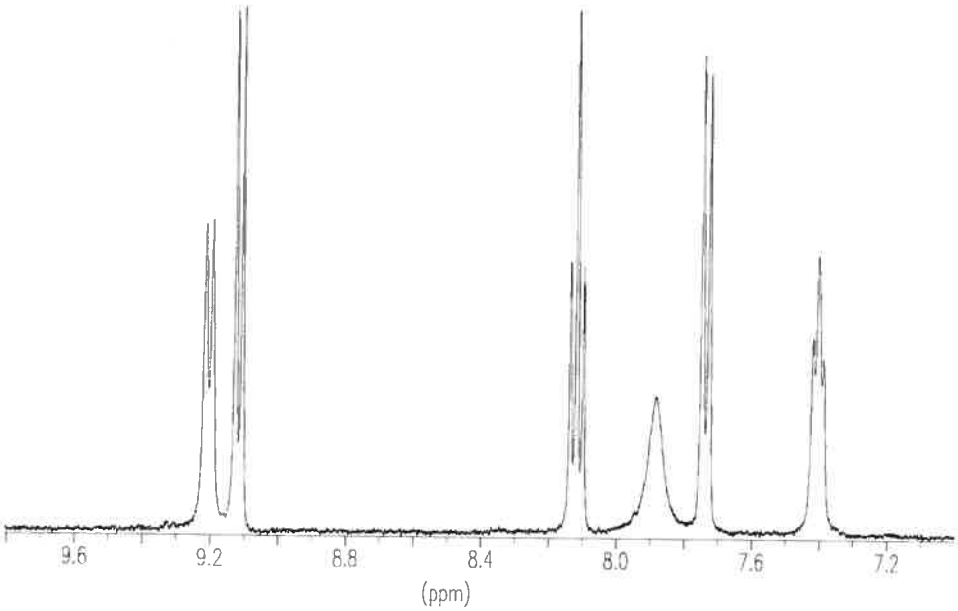

Figure 5.6 ^{1}H NMR of complex **1a** and **2a** in CD_3CN at 400 MHz.

5.6.2 Solid state Structures

Table 5.3 Summary of crystal data and structure refinement for **L1**, **1a**, **1b**, **1c** and **1d**.

Compound	**L1**	**1a Fe**	**1b Co**	**1c Ni**	**1d Cu**	**1d' Cu**
	Colourless	Purple	Orange	green/yellow	Green	green
Formula	$C_{19}H_4BrN_5O$	$C_{38}H_{24}Br_2N_{10}F_{12}FeP_2$	$C_{38}H_{24}Br_2N_{10}CoF_{12}P_2$	$C_{40}H_{27}Br_2N_{11}Ni._2F_{12}P_2$	$C_{40}H_{27}Br_2N_{11}CuF_{12}P_2$	$C_{44}H_{36}Br_2CuF_{12}N_{10}O_2P_2$
Crystal System	Monoclinic	Monoclinic	Monoclinic	Triclinic	Triclinic	Monoclinic
T (K)	150 (2)	100(2)	100(2)	100(2)	100(2)	150(2)
λ (Å)	1.54178	1.54178	1.54178	1.54178	1.54178	1.54178 Å
Space group	$P2_1/c$	C2/c	C2/c	$P\bar{1}$	$P\bar{1}$	C2/c
a (Å)	24.954 (1)	14.4472 (6)	14.7467(4)	8.5536 (2)	8.5175 (2)	14.8156 (2)
b (Å)	3.9351 (2)	21.045 (1)	20.8588 (6)	13.6850 (2)	13.7974 (3)	21.3172 (4)
c (Å)	19.0793 (8)	16.4940 (9)	16.6451 (5)	18.9796 (3)	18.9148 (4)	16.7458 (3)
α (°)	90	90	90	91.086 (1)	89.9110 (1)	90
β (°)	110.007 (2)	99.350 (4)	96.264 (1)	102.348 (1)	78.4970 (1)	95.3930 (10)
γ (°)	90	90	90	91.973 (1)	87.8530 (1)	90
V ($Å^3$)	1760.4 (1)	4948.2 (4)	5089.4 (3)	2168.21 (7)	2176.64 (8)	5265.37 (15)
Z	4	4	4	2	2	4
D (Mg m^{-3})	1.608	1.512	1.474	1.792	1.793	1.577
μ (mm^{-1})	3.406	5.699	5.808	4.392	4.44	3.732
Maximum 2θ (°)						
Number of reflections collected	23442	40326	22391	26398	27217	60135
Number of independent reflections	3232	4826	3198	8310	7620	4823
Data/ restraints/parameters	3232/0/256	4826 / 0 / 361	3198 / 357 / 359	8310 / 2 / 663	7620 / 144 / 790	4823/0/425
R	4.4	9.61	4.28	5.30	3.27	6.17
wR2	12.15	28.9	8.36	15.23	8.67	18.89
Goodness-of-fit on F^2	1.048	1.008	0.925	0.743	1.023	1.046

The solid state structures of the ligand **L1** and its complexes display interesting short-range Br-Br interactions. The starting ligand, **L1**, crystallises in the monoclinic space group $P2_1/c$ with two water molecules associated with each triazine ligand in the asymmetric unit. The pyridyl and phenyl rings lie co-planar to the triazine rings with twists of 2.3 (2) ° and 3.4 (2)° for the pyridyl rings and 1.2 (2)° for the bromo-phenyl ring due to favourable N-to-CH hydrogen bonding interactions between the N lone pairs and the H's *ortho* to the interannular bond. Relatively short Br-Br distances were observed between molecules, with each Br-atom being in close proximity to four others in a zig-zagging arrangement (Figure 5.7).

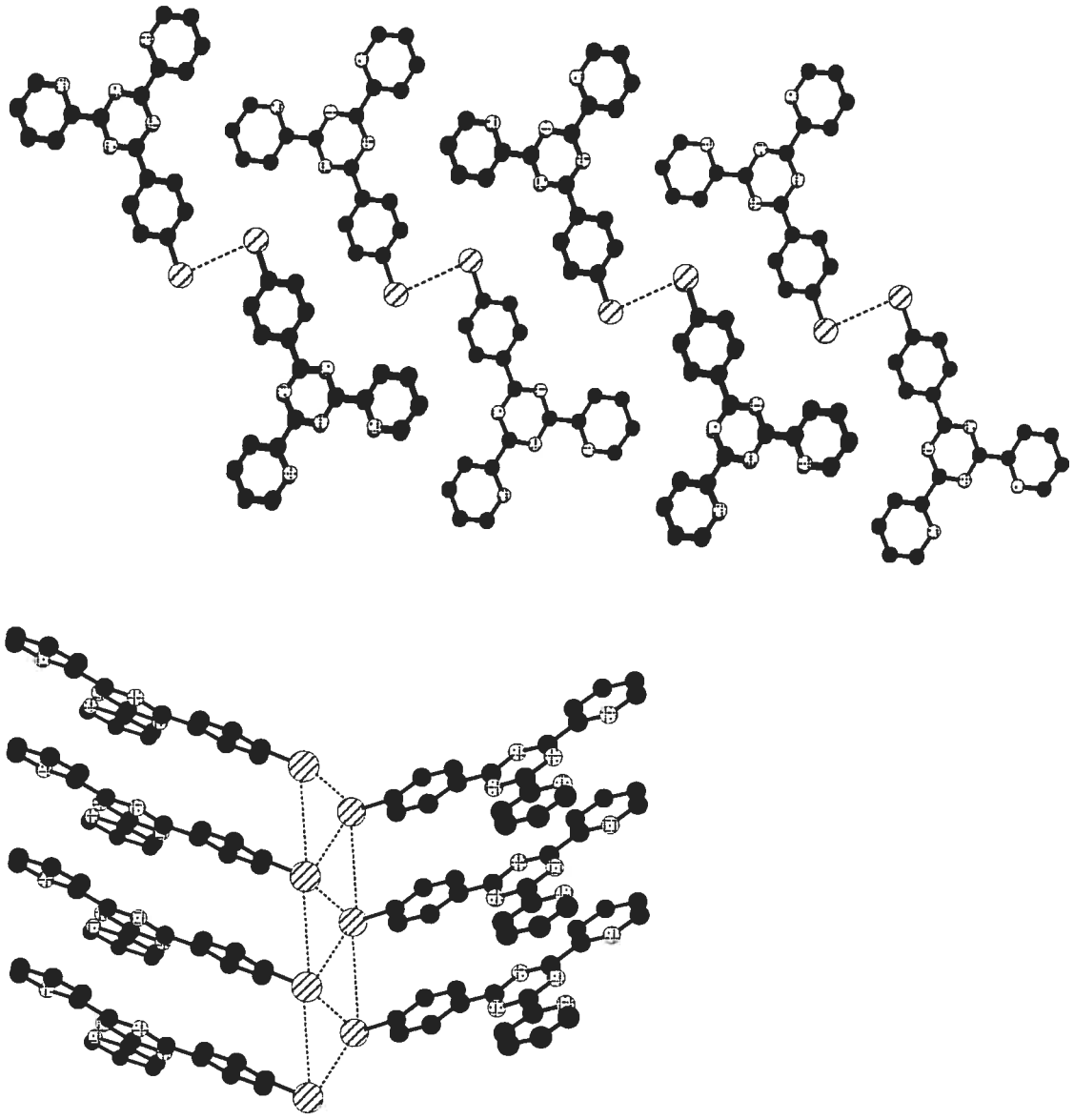

Figure 5.7 The Br-Br interactions observed in **L1**: the *ac* plane (above) and the *ab* plane (below). The H_2O solvent molecules have been omitted for clarity.

The molecules of **L1** stack on top of each other with off-set aromatic face-to-face interactions. Each Br atom is in close proximity to four other Br atoms and distances of 3.94 Å are observed vertically between layers of stacking ligands and 4.14 Å for the diagonal contacts.

The H-atoms on the water molecules were disordered and couldn't be found using electron-density maps but an ideal model was found using Calc-OH.[†] In this model, a water molecule is H-bonded to the N-atoms of the distal pyridyl rings on the ligand. The H-atoms of the second water molecule are H-bonded to the oxygen of the first water molecule and in the extended lattice they form spiraling columns. Ligand **L1** occupies gaps between column pairs.

[†] From the WinGX software suite, version 1.64.04: *J. Appl. Cryst.*, 1999. 32, 563.

Complexes 1a-d

The Fe (II) complex **1a** recrystallises in the monoclinic space group, C2/c and is isostructural to the previously published Co(II) complex **1b**.[42] Purple blocks of **1a** were obtained by slow diffusion of isopropylether into an acetonitrile solution. The Fe(II) metal centre is in a distorted octahedral geometry coordinated to two tridentate ligands as anticipated. Shorter Fe-N bond distances are observed to the central triazine ring compared to the peripheral pyridyl rings due to the constraints imposed by the tridentate ligand. Fe-N distances at 100 K are indicative of low-spin complexes, as expected.[27]

The pendant phenyl rings are twisted by 18.6° in **1a** and 13.3° in **1b** relative to the central triazine ring. The twist in the interannular bond is a result of edge-to-face packing between the phenyl rings in different molecules, which are separated by 3.57 Å and 3.51 Å (Figure 5.8), however, no favourable face-to-face packing interactions were observed.

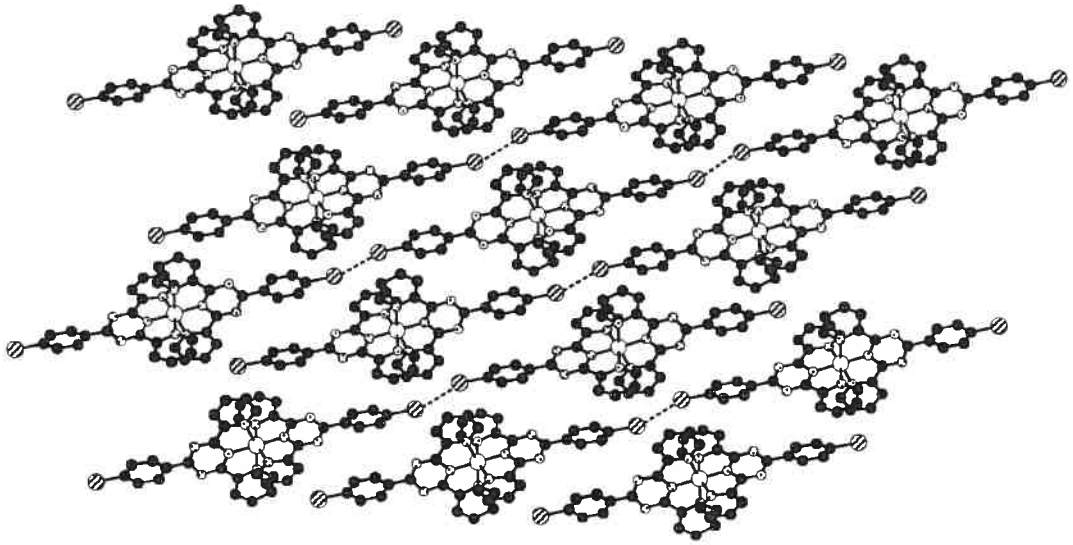

Figure 5.8 Br-Br interactions in the extended lattice in complex **1a**.

Short Br-Br contacts are observed for **1a** and **1b** with a distances of 3.45 Å and 3.40 Å, respectively, between adjacent molecules, indicative of favourable van der Waals interactions which give rise to a linear one-dimensional tape in the solid state (Figure 5.8).[42]

No solvent molecules of crystallisation are observed in the structure of complex **1b** and resolution of solvent in **1a** was not possible.

Table 5.4 Selected bond distances and angles for complexes **1a-d** (trz = triazine, py = pyridine).

	1a	1b	1c		1d		1d'
Bond Distances (Å)							
M - N (trz)	1.872 (5)	1.986 (3)	1.977 (4)	1.992 (4)	1.942 (2)	1.9995 (19)	1.951 (3)
M - N (py)	2.006 (6)	2.158 (4)	2.146 (4)	2.163 (4)	2.152 (2)	2.320 (2)	2.205 (3)
M - N (py')	2.004 (6)	2.134 (3)	2.153 (4)	2.157 (4)	2.149 (2)	2.283 (2)	2.230 (3)
Angles (°)							
N(py)-M-N(py')	159.0 (2)	151.79 (13)	152.83 (14)	152.84 (14)	153.88 (8)	150.14 (7)	153.0 (1)
N(py)-M-N(trz)	79.3 (2)	75.99 (14)	76.89 (14)	76.75 (14)	77.21 (8)	75.79 (7)	76.6 (1)
N(trz)-M-N(py')	79.8 (2)	76.21 (14)	76.07 (14)	76.09 (14)	77.10 (8)	74.36 (7)	76.6 (1)

The Ni (II) and Cu (II) complexes, **1c** and **1d,** were initially recrystallised by slow diffusion of isopropyl ether into acetonitrile solutions. The crystals of **1c** and **1d** are isostructural and recrystallise in the triclinic space group $P\bar{1}$ with a full cation, two PF_6 counter–anions and variable amounts of solvent for either complex in the asymmetric unit. In both complexes the M-N bond distances differ from one ligand to the second but the M-N elongation can be observed more clearly in the Cu(II) complex **1d** (Table 5.4). Cu (II) ions are Jahn-Tellar unstable in a purely octahedral field and despite the distorted octahedral arrangement of the $[Cu(\mathbf{L1})_2]^{2+}$ cation this effect is observed with the elongation of the Cu-N bond distances in complex **1d**, an effect previously reported for tpy-based systems.[39] The asymmetry between the coordinated ligands accounts for the change in the crystal structure system for complexes **1c-d** as compared to the **1a-b** in which both ligands are equivalent.

Unlike complexes **1a-b**, significant face-to-face, π-stacking interactions are observed in **1c-d**, with the shortest contact between the pendant phenyl rings and the distal pyridyl rings being 3.37 Å (Figure 5.9). No short Br-Br contacts are observed

presumably due to greater stabilisation gained from the π-stacking interactions, which inhibit short Br-Br contacts.

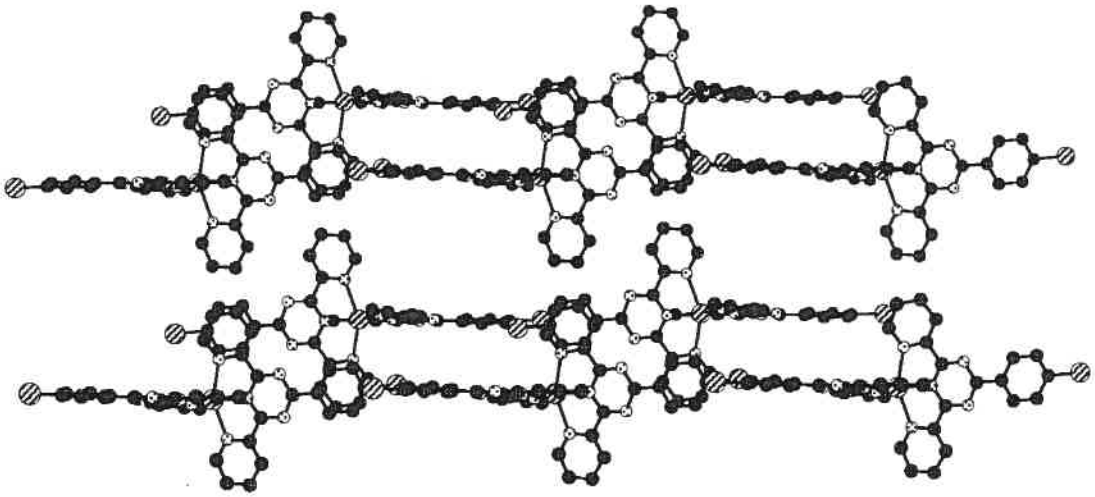

Figure 5.9 π-Stacking interactions in the extended lattice in complex **1d**. The anions and solvent molecules of crystallisation have been omitted for clarity.

The dihedral angle between the triazine ring and phenyl ring on both ligands are 21.00° and 7.31° for **1c** and 19.45° and 7.62° in **1d.** In each case the slightly higher dihedral angle accommodates the face-to-face π-stacking interaction which may preclude the formation of stable Br-Br interactions. Both complexes have two PF_6^- counter ions disordered over three sites.[‡] It was found that crystallisation of **1d** by slow diffusion of isopropyl ether into an acetone solution yielded crystals isostructural to **1a** and **1b**. The shortest Br-Br contacts are observed in **1d'** with a distance of 3.33 Å. There is one molecule of acetone per asymmetric unit which is disordered over two independent sites. It appears that the acetone molecules of crystallisation limits the face-to-face π-stacking interactions observed in **1d**, thereby allowing halogen-halogen interactions to play the determining role of the arrangement of cations in the extended lattice.

[‡] One anion is found on a general position with full occupancy. The remaining anion divided between two sites, one of which is situated on an inversion centre; the other is disordered around an inversion centre.

Complexes 2a-d

Crystals were obtained for complexes **2a-d** by slow diffusion of diethyl ether into an acetonitrile solution yielding thin needle-like blocks for all the crystals.

Table 5.5 Summary of crystal data and structure refinement for **2a**, **2b**, **2c** and **2d**.

Compound	**2a Fe**	**2b Co**	**2c Ni**	**2d Cu**
	Purple	Orange	green/yellow	Green
Formula	$C_{40}H_{30}N_{10}Fe.\ 2(PF_6)$	$C_{40}H_{30}N_{10}Ni.2(PF6)$	$C_{40}H_{30}N_{10}Ni.2(PF6)$	$C_{40}H_{30}N_{10}Cu.2(PF6)$
Crystal System	Monoclinic	Tetragonal	Tetragonal	Tetragonal
T (K)	150(2)	125(2)	150(2)	150(2)
λ (Å)	1.54178	0.71070	1.54178	1.54178
Space group	$P2_1/n$	$I4_1/acd$	$I4_1/acd$	$I4_1/acd$
a (Å)	8.9622 (3)	22.200 (2)	22.2925 (3)	22.598 (4)
b (Å)	33.0144 (8)	22.200 (2)	22.2925 (3)	22.598 (4)
c (Å)	13.3712 (4)	16.819 (3)	16.6862 (4)	17.155 (7)
α (°)	90	90	90	90
β (°)	92.053(2)	90	90	90
γ (°)	90	90	90	90
V ($Å^3$)	3953.8 (2)	8289 (2)	8292.3 (3)	8761 (4)
Z	4	8	8	8
D ($Mg\ m^{-3}$)	1.674	1.602	1.601	1.523
μ (mm^{-1})	4.763	0.591	2.300	2.242
Maximum 2θ (°)	68.97	28.37	68.83	57.24
Number of reflections collected	54135	44078	76131	37122
Number of independent reflections	7253	2517	1928	1494
Data/ restraints/parameters	7253 / 0 / 588	2517/0/152	1928 / 0 / 153	1494 / 0 / 153
R	3.80	3.54	4.16	2.96
wR2	9.88	9.43	11.40	7.97
Goodness-of-fit on F^2	1.002	1.073	1.094	1.022

Table 5.6 Selected bond distances and angles for complexes **2a-d** (trz = triazine, py = pyridine).

	2a		**2b**	**2c**	**2d**
Bond Distances (Å)					
M - N (trz)	1.875 (2)	1.879 (2)	1.962 (2)	1.988 (3)	2.002 (3)
M - N (py)	2.006 (2)	2.009 (2)	2.215 (2)	2.155 (2)	2.261 (2)
M - N (py')	2.008 (2)	2.006 (2)			
Angles (°)					
N(py)-M-N(py')	159.09(8)	159.04(7)	152.92(9)	153.07 (11)	152.89 (11)
N(py)-M-N(trz)	79.70 (8)	79.76 (8)	76.46 (5)	76.53 (6)	76.45 (5)
N(trz)-M-N(py')	79.45 (8)	79.29 (8)			

Complex **2a** recrystallises in the monoclinic space group $P2_1/n$ with one molecule and two PF_6- counter-ions in the asymmetric unit. Intermolecular face-to-edge π-stacking interactions between neighbouring toluyl groups link the cations. Additional offset face-to-face interactions can be found between toluyl and pyridyl groups, but no short contacts exist between the pendant methyl group and methyl groups of neighbouring molecules in the absence of a halogen group.

Complex **2b-d** are isostructural and recrystallise in the tetragonal space group I4(1)/acd. M-N bond distances are in agreement with complexes **1a-d,** although the asymmetric Jahn Tellar distortion observed in **1a** is not observed in **2d** due to high tetragonal symmetry in the cation resulting in both ligands being equivalent. Zig-zagging molecules are linked by face-to-face interactions between toluyl groups of neighbouring molecules which comprise the corners of a square. The cations form layers with each adjacent layer lying perpendicular to the previous (Figure 5.10). The shortest H-H distance between diagonally bisecting toluyl groups is 4.51 Å.

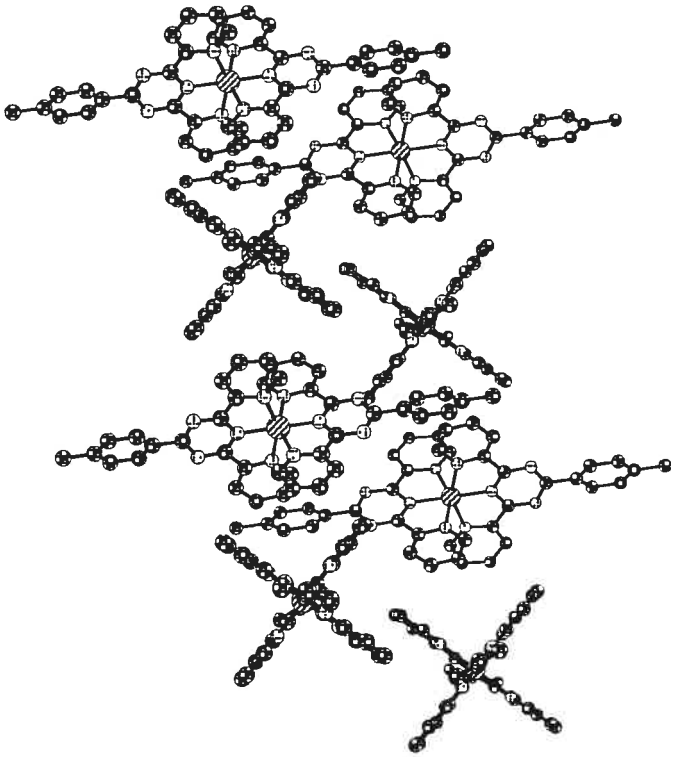

Figure 5.10 Arrangement of cations in the extended lattice of complex **2c**. Counter-ions have been omitted for clarity.

5.6.2 Electronic Spectroscopy and Electrochemistry

The electronic absorption spectra of **L1** and metal complexes **1a-d** were measured in acetonitrile and the data are collected in Table 5.7.

Table 5.7 Spectroscopic data for complexes **L1**, **1a-d**, **L2** and **2a-d**.[a]

	Absorption
	λ_{max}, nm (ε, $M^{-1}cm^{-1} \times 10^{-3}$)
L1	250 (16.7), 281 (36.3)
1a	292 (62.6), 313 (sh), 546 (13.3), 597 (17.8)
1b	295 (54.8), 315 (sh), 421 (0.33), 478 (0.30), 527 (0.26)
1c	295 (67.2), 328 (sh), 848 (0.07)
1d	286 (45.8), 325 (sh), 458 (0.05), 713 (0.07)
L2	246 (17.0), 280 (32.4)
2a	288 (73.5), 321 (sh), 543 (11.7), 595 (14.7)
2b	294 (56.9), 317(sh, 42.3), 429 (0.36), 483 (0.32), 529 (0.27)
2c	295 (73.8), 332 (51.4), 856 (0.05)
2d	297 (57.5), 326 (40.5), 711 (0.09)

[a] In acetonitrile.

All of the complexes have ligand-centred $\pi \rightarrow \pi^*$ and $n \rightarrow \pi^*$ transitions in the UV regions which are red-shifted as compared to the starting ligand. Complexes **1b-d** and **2b-d** are lightly coloured due to weak, forbidden d-d transitions in the visible and near IR region of their spectra (Figure 5.11). Complexes **1a** and **2a,** however, are intensely purple due to an allowed metal-to-ligand charge-transfer (^{1}MLCT) band in the low energy visible region (Figure 5.12). This is characteristic for low-spin, predominantly diamagnetic complexes of d^6 metal ions. The ^{1}MLCT band can be resolved into two bands, which may be explained by the presence of ligand-based LUMO and LUMO +1 resulting in MLCT transitions to two ligand-based molecular orbitals.

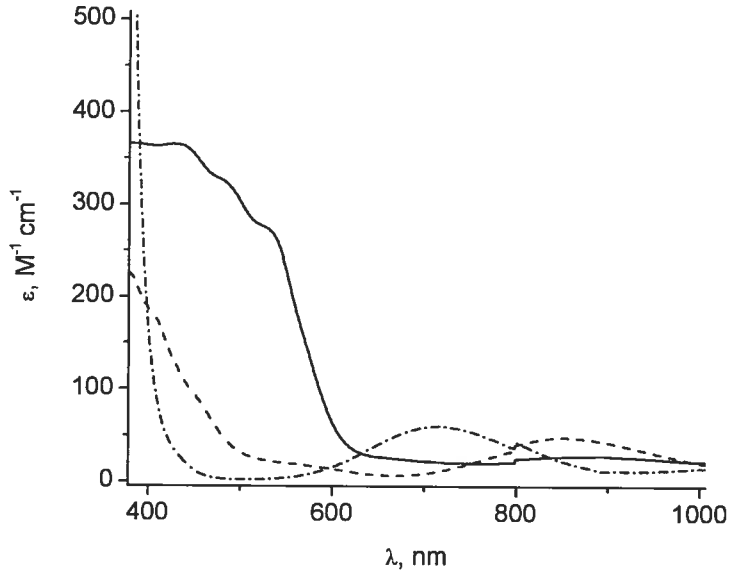

Figure 5.11 d-d transitions in the visible region of the spectra for complexes **2b-d**. Solid line = **2b**, dashed line = **2c**, dotted line = **2d**.

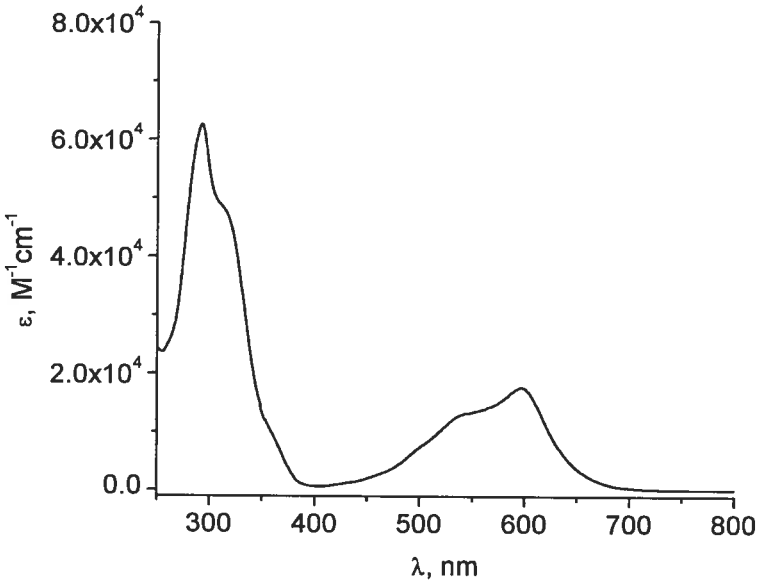

Figure 5.12 The UV-visible spectrum for complex **1a** in acetonitrile.

The electrochemistry of complexes **1a-d** were measured in acetonitrile versus $TBAPF_6$ using a Pt electrode and ferrocene as the internal standard. The cyclic voltammogram

of **1a** is shown in Figure 5.13. The anodic region has a reversible Fe(II)/(III) couple at 1.40 V. The cathodic region is rich with reversible ligand-based reductions involving two one-electron reductions observed on each triazine ligand which can be compared to the previously reported electrochemistry of **1b**, in which only two ligand-based reductions were observed after the Co(II)/ (I) couple in the anodic region.[42]

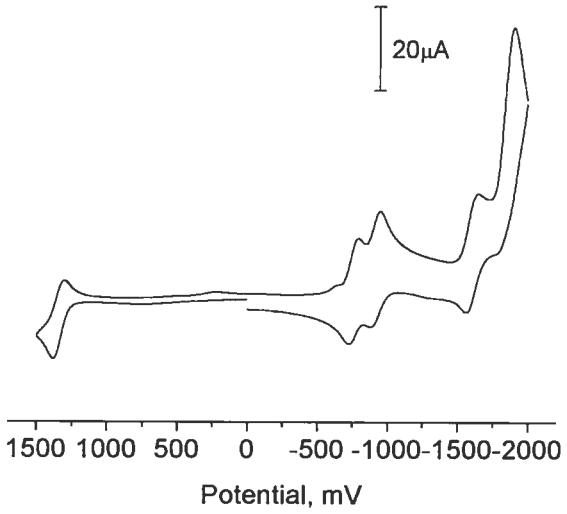

Figure 5.13 Cyclic voltammogram in acetonitrile with 0.1 M $TBAPF_6$ of complex **1a** 200 mVs^{-1}.

The same Fe(II)/(III) couple and ligand-based reductive processes are observed for **2a**, although a shift to more negative potential is observed due to the electron-donating effect of the methyl substituent as compared to Br in **1a**. The ligand-based reductions of **2a** occur at the same potentials as $[Ru(\mathbf{L2})_2](PF_6)_2$ (Table 5.8), suggesting that the nature of the coordinating d^6 metal has little effect on the relative energies of the ligand-based orbitals. However, the Fe(II/III) couple is 100 mV less positive when compared to the Ru(II)/(III) couple. This result supports those from the UV-visible spectrum of **2a**, which indicates a red shift in the MLCT band relative to $[Ru(\mathbf{L2})_2](PF_6)_2$.[31]

Table 5.8 Electrochemical redox potentials vs SCE for complexes in argon-purged acetonitrile solutions.[a]

	$E_{1/2}$ (V) [ΔE_p, (mV)]					
Complex	M (II/III)					
1a $[Fe(\mathbf{L1})_2](PF_6)_2$	+1.40 (77)	-0.69 (65)	-0.85 (62)	-1.53 (79)	-1.76 (irr)	
2a $[Fe(\mathbf{L2})_2](PF_6)_2$	+1.36 (97)	-0.75 (62)	-0.91(75)	-1.56 (99)	-1.82 (irr)	
$[Ru(\mathbf{L2})_2](PF_6)_2$ [b]	+1.50 (101)	-0.74 (64)	-0.90 (70)	-1.53 (84)	-1.78 (87)	
1b $[Co(\mathbf{L1})_2](PF_6)_2$ [c]	+0.77 (irr)	-0.40 (52)	-1.04 (56)	-1.46 (66)		
2b $[Co(\mathbf{L2})_2](PF_6)_2$ [c]	+0.74 (irr)	-0.47 (64)	-1.11 (66)	-1.52 (64)		
1c $[Ni(\mathbf{L1})_2](PF_6)_2$		-0.76 (72)	-0.88 (76)	-1.46 (irr)	-1.64 (irr)	-1.76 (90)
2c $[Ni(\mathbf{L2})_2](PF_6)_2$		-0.87 (42)	-1.00 (46)	-1.70 (71)		
1d $[Cu(\mathbf{L1})_2](PF_6)_2$		-0.11 (irr)	-1.28 (irr)	-1.56 (irr)		
2d $[Cu(\mathbf{L2})_2](PF_6)_2$		-0.50 (irr)	-1.12 (irr)	-1.53 (100)		

[a] Using ferrocene as an internal standard, [b] from reference [31], [c] from reference [42].

For the Ni(II) complex **1c**, no metal-based oxidative processes are observed due to the effect of the electron-deficient triazine rings on the Ni(II) centre. The first two reversible reductions are ligand based followed by an irreversible metal-centred reduction. As in the Fe(II) complexes, a second reduction is observed on each triazine ligand. For the Ni(II) complexes the difference between the toluyl- and bromo-phenyl-substituted triazine ligands is more significant. The first ligand-based reduction for **1c** is 110 mV less negative as compared to **2c** due to the electron-withdrawing nature of the bromo-substituent.

Highly irreversible, extremely broad reductive signals were observed for Cu(II) complexes **1d** and **2d** at -0.11 V and -0.50 V, respectively, followed by adsorption spikes at -1.28 V and -1.12 V, respectively. These are consistent with a reduction of Cu(II) followed by adsorption of Cu^0 to the electrode.[14] Despite the large difference reported for the initial reductive process between complexes **1d** and **2d**, the broadness of both signals makes the difference less significant. An additional triazine-based reduction is then observed for both complexes **1d** and **2d**.

5.7 Conclusion

A bromo-functionalised triazine ligand has been synthesised and displays two-dimensional Br-Br interactions in the solid state. When complexed to Fe(II), Co(II) and Cu(II) cations, halogen-halogen interactions are present in the solid state structure to give linear one-dimensional tapes in the extended lattice depending on the solvent of crystallisation. The presence of solvent can modify the formation of the one-dimensional tape as exemplified by the Cu(II) complex **1d**. Additional edge-to-face π-stacking interactions and Br-to face interactions are observed in complexes **1a-b** and **1d**. However, similar favourable π-interactions in complexes **2a-d** do not require short Me-Me contacts. The one-dimensional tape of Ni(II) complex **1c** have not been obtained as yet. Initial ^{1}H NMR studies of the Fe(II) complex indicate that these complexes may have a paramagnetic contribution to the diamagnetic ground state. Further magnetic measurements will be carried out to elucidate the nature of their spin cross-over properties.

Acknowledgments

The authors thank the Natural Sciences and Engineering Research Council of Canada and the Université de Montréal for financial support. EAM thanks the ICCS for funding. The authors thank F. Bélanger-Gariépy for assistance with X-ray analyses.

5.8 Experimental

Materials and Instrumentation

Nuclear magnetic resonance (NMR) spectra were recorded in CD_3CN at room temperature (r.t.) on a Bruker AV400 spectrometer at 400 MHz for ^1H NMR and at 100 MHz for ^{13}C NMR. Chemical shifts are reported in part per million (ppm) relative to residual solvent protons (1.93 ppm for acetonitrile-d_3) and the carbon resonance of the solvent. Absorption spectra were measured in air equilibrated acetonitrile at r.t. on a Cary 500i UV-Vis-NIR spectrophotometer.

Electrochemical measurements were carried out in argon-purged acetonitrile at room temperature with a BAS CV50W multipurpose equipment interfaced to a PC. The working electrode was a Pt electrode. The counter electrode was a Pt wire, and the pseudo-reference electrode was a silver wire. The reference was set using an internal 1 mM ferrocene/ferrocinium sample at 395 mV vs SCE in acetonitrile and 432 mV in DMF. The concentration of the compounds was 1 mM. Tetrabutylammonium hexafluorophosphate (TBAP) was used as supporting electrolyte and its concentration was 0.10 M. Cyclic voltammograms were obtained at scan rates of 50, 100, 200, and 500 mV/s. For irreversible oxidation processes, the cathodic peak was used as E, and the anodic peak was used for irreversible reduction processes. The criteria for reversibility were the separation of 60 mV between cathodic and anodic peaks, the close to unity ratio of the intensities of the cathodic and anodic currents, and the constancy of the peak potential on changing scan rate. The number of exchanged electrons was measured with OSWV, and by taking advantage of the presence of ferrocene used as the internal reference.

Experimental uncertainties are as follows: absorption maxima, ± 2 nm; molar absorption coefficient, 10%; redox potentials, ± 10 mV.

Crystal Structure Determination

X-ray crystallographic data for **1a-d** were collected from a single crystal sample, which was mounted on a loop fiber. Data were collected using a Bruker Platform diffractometer, equipped with a Bruker SMART 2K Charged-Coupled Device (CCD)

Area Detector using the program SMART and normal focus sealed tube source graphite monochromated Cu-Kα radiation.

X-ray crystallographic data for **L1**, **2a**, **2c** and **2d** were collected from a single crystal sample, which was mounted on a loop fiber. Data were collected using a Bruker Platform diffractometer, equipped with a Bruker SMART 4K Charged-Coupled Device (CCD) Area Detector using the program SMART and a rotating anode source Cu-Kα radiation.

X-ray crystallographic data for **2b** was collected with Mo $K\alpha$ radiation (λ=0.71073 Å, $2\theta_{max}$= 57.5°, ω scan mode) on a Bruker SMART CCD diffractometer, at 125 K. Empirical adsorption corrections were applied using the SADABS program.

The structures were solved by direct method and refined using full-matrix least squares on F^2 using the SHELXTL suite of programs.[50] The H atoms were generated geometrically and were included in the refinement in the riding model approximation.

CCDC numbers 611625 – 611633 contain supplementary crystallographic data for this paper. These data can be obtained free of charge from The Cambridge Crystallographic Data Centre via www.ccdc.cam.ac.uk/data_request/cif.

Metal salts and other chemicals (Aldrich) were used as supplied. **L1** and **L2** were synthesised by a modified literature method.[42] Complexes **1b** and **2b** were prepared according to literature methods.[42]

L1

^{n}BuLi (1.6M in hexanes, 5.10 mL, 8.13 mmol) was added dropwise to a stirred solution of $HNMe_2$ (2M in THF, 4.10 mL, 8.13 mmol) in anhydrous Et_2O (150 mL) under an inert atmosphere. The mixture was stirred for 20 minutes until a white suspension formed and *p*-bromo-benzonitrile (1.35 g, 7.39 mmol) was added. The triazine precipitated immediately and stirring continued for an hour. The reaction was diluted with 5:1 mixture of water: EtOH (200 mL) and the solution was heated to remove Et_2O. The white precipitate was collected by filtration and washed with EtOH

(10 mL) and Et_2O (50 mL) and dried to afford **L1** as a white powder (1.96 g, 68% yield).

^1H NMR ($CDCl_3$, 400 MHz): 8.99 (d, J= 4 Hz, 2H) $H_{6,6''}$; 8.87 (d, J= 8 Hz, 2H) $H_{3,3''}$; 8.74 (d, J= 8 Hz, 2H) $H_{2''',6'''}$; 8.0 (t, J= 7 Hz, 2H) $H_{4,4''}$; 7.73 (d, J= 8 Hz, 2H) $H_{3''',5'''}$; 7.60 (t, J= 5 Hz, 2H) $H_{5,5''}$. Consistent with a previously published spectrum.[42]

$[Fe(L)_2](PF_6)_2$ (1a and 2a)

$FeCl_2.H_2O$ (0.046 g, 0.23 mmol) dissolved in ethanol (5 mL) was added to a stirred solution of the ligand (0.46 mmol) in ethanol (15 mL). The solution immediately turned intense purple and was heated to reflux for 20 minutes. On cooling, saturated KPF_6 (aq, 5 mL) was added and the product precipitated. The solid was collected and washed with water, ethanol and diethyl ether to yield complexes **1a** (0.24 g, 91%) and **2a** (0.15 g, 67%).

1a: ^1H NMR (CD_3CN, 400 MHz): 9.16, d, 2H (8 Hz), $H_{3,3''}$; 9.12, d, 2H (8 Hz), $H_{2''',6'''}$; 8.11, d, 2H (8 Hz), $H_{3''',5'''}$; 8.11, t, 2H (8 Hz), $H_{4,4''}$; 7.74, s (br), 2H, $H_{6,6''}$; 7.37, t, 2H (6 Hz), $H_{5,5''}$. ESMS: M^{2+}- 418.3. Calc. Anal. $C_{38}H_{24}N_{10}Br_2FeP_2F_{12}.2H_2O$: *Calc:*C, 39.27; H, 2.43; N, 12.05. *Exp:* C, 39.34; H, 2.22; N, 11.49.

2a: ^1H NMR (CD_3CN, 400 MHz): 9.21, d, 2H (8 Hz), $H_{3,3''}$; 9.12, d, 2H (8 Hz), $H_{2''',6'''}$; 8.12, t, 2H (8 Hz), $H_{4,4''}$; 7.88, s (br), 2H, $H_{6,6''}$; 7.74, d, 2H (8 Hz), $H_{3''',5'''}$; 7.41, t, 2H (6 Hz), $H_{5,5''}$; 2.64, s, 3H, H_{Me}. ESMS: M^{2+}-353.5. Anal. Calc. $C_{40}H_{30}N_{10}FeP_2F_{12}$: *Calc:*C, 48.21; H, 3.03; N, 14.06. *Exp:* C, 48.23; H, 3.32; N, 14.21.

$[Ni(L)_2](PF_6)_2$ (1c and 2c)

$Ni(OAc)_2$ (0.038 g, 0.15 mmol) dissolved in ethanol (15 mL) was added to a stirred solution of the ligand (0.30 mmol) in ethanol (30 mL). The mixture turned green/yellow immediately and was heated to reflux for 15 minutes. On cooling, ethanolic KPF_6 was added and the green precipitate was collected and washed with water, ethanol and diethyl ether to yield complexes **1c** (0.12 g, 68%) and **2c** (0.085 g, 56%).

1c: ^{1}H NMR (CD_3CN, 400 MHz): 7.78, 12.42, 13.86, 43.22, 71.95, ~124(br).
Anal. Calc. $C_{38}H_{24}N_{10}NiP_2F_{12}$: *Calc:*C, 40.42; H, 2.14; N, 12.41. *Exp:* C, 40.66; H, 2.43; N, 12.48.
2c: ^{1}H NMR (CD_3CN, 400 MHz): 0.14, 7.46, 12.53, 13.80, 43.12, 71.70, 123 (br).
Anal. Calc. $C_{40}H_{30}N_{10}NiP_2F_{12}$: *Calc:* C, 48.07; H, 3.03; N, 14.02. *Exp:* C, 48.42; H, 3.02; N, 13.83.

$[Cu(L)_2](PF_6)_2$ (1d and 2d)
$Cu(NO_3)_2.H_2O$ (0.14 g, 0.62 mmol) dissolved in ethanol (15 mL) was added to a stirred solution of the ligand (1.23 mmol) in ethanol (30 mL). The mixture turned green immediately and was heated to reflux for 15 minutes. On cooling, ethanolic KPF_6 was added and the green precipitate collected and washed with water, ethanol and diethyl ether to yield complexes **1d** (0.55 g, 79%) and **2d** (0.42 g, 68%).
1d: ^{1}H NMR (CD_3CN, 400 MHz): 7.41, 9.30, 10.22, ~25 (br), ~37 (v br), 1 peak missing.
Anal. Calc. $C_{38}H_{24}N_{10}Br_2CuP_2F_{12}.H_2O$: *Calc:*C 39.62, H 2.27, N12.16 *Exp:* C39.46, H 1.58, N 12.03.

2d: ^{1}H NMR (CD_3CN, 400 MHz): 1.00, 7.04, 9.40, 10.19, ~25 (br), ~38 (v br), 1 peak missing. Anal. Calcd. $C_{40}H_{30}N_{10}CuP_2F_{12}$: *Calc:*C 47.84, H 3.01, N13.95 *Exp:* C48.01, H 2.64, N 13.88.

5.9 References

1. H. A. Goodwin, *Top. Curr. Chem.*, 2004, **233**, 59.
2. A. B. Gaspar, V. Ksenofontov, M. Seredyuk and P. Guetlich, *Coord. Chem. Rev.*, 2005, **249**, 2661.
3. Y. Bodenthin, U. Pietsch, H. Moehwald and D. G. Kurth, *J. Am. Chem. Soc.*, 2005, **127**, 3110.
4. M. W. Cooke, G. S. Hanan, F. Loiseau, S. Campagna, M. Watanabe and Y. Tanaka, *Angew. Chem. Int. Ed.*, 2005, **44**, 4881.
5. J. P. Sauvage, J. P. Collin, J. C. Chambron, S. Guillerez, C. Coudret, V. Balzani, F. Barigelletti, L. De Cola and L. Flamigni, *Chem. Rev.*, 1994, **94**, 993.
6. V. Balzani, S. Campagna, G. Denti, A. Juris, S. Serroni and M. Venturi, *Acc. Chem. Res.*, 1998, **31**, 26.
7. A. Harriman and R. Ziessel, *Coord. Chem. Rev.*, 1998, **171**, 331.
8. U. S. Schubert and C. Eschbaumer, *Angew. Chem. Int. Ed.*, 2002, **41**, 2892.
9. E. C. Constable, A. M. W. C. Thompson, D. A. Tocher and M. A. M. Daniels, *New J. Chem.*, 1992, **16**, 855.
10. G. R. Newkome, T. J. Cho, C. N. Moorefield, R. Cush, P. S. Russo, G. A. Godìnez, M. J. Saunders and P. P. Mohapatra, *Chem. Eur. J.*, 2002, **8**, 2946.
11. G. R. Newkome, T. J. Cho, C. N. Moorefield, P. P. Mohapatra and G. A. Godìnez, *Chem. Eur J.*, 2004, **10**, 1493.
12. C. J. Aspley and J. A. G. Williams, *New J. Chem.*, 2001, **25**, 1136.
13. R. Passalacqua, F. Loiseau, S. Campagna, Y.-Q. Fang and G. S. Hanan, *Angew. Chem., Int. Ed.*, 2003, **42**, 1608.
14. N. W. Alcock, P. R. Barker, J. M. Haider, M. J. Hannon, C. L. Painting, Z. Pikramenou, E. A. Plummer, K. Rissanen and P. Saarenketo, *Dalton Trans.*, 2000, 1447.
15. H.-S. Chow, E. C. Constable, C. E. Housecroft, M. Neuburger and S. Schaffner, *Dalton Trans.*, 2006, 2881.
16. M. Pascu, G. J. Clarkson, M. K. Benson and M. J. Hannon, *Dalton Trans.*, 2006, 2635.

17. D. G. Kurth, J. Pitarch Lopez and W.-F. Dong, *Chem. Commun.*, 2005, 2119.
18. D. G. Kurth and R. Osterhout, *Langmuir*, 1999, **15**, 4842.
19. S.-C. Yu, C.-C. Kwok, W.-K. Chan and C.-M. Che, *Adv. Mater. (Weinheim, Ger.)*, 2003, **15**, 1643.
20. J. Hjelm, R. W. Handel, A. Hagfeldt, E. C. Constable, C. E. Housecroft and R. J. Forster, *Inorg. Chem.*, 2005, **44**, 1073.
21. S. Kelch and M. Rehahn, *Macromolecules*, 1999, **32**, 5818.
22. S. Kelch and M. Rehahn, *Chemical Communications (Cambridge, United Kingdom)*, 1999, 1123.
23. B. J. Holliday and T. M. Swager, *Chemical Communications (Cambridge, United Kingdom)*, 2005, 23.
24. E. A. Medlycott and G. S. Hanan, *Coord. Chem. Rev.*, 2006, **250**, 1763.
25. M. Maestri, N. Armaroli, V. Balzani, E. C. Constable and A. M. W. C. Thompson, *Inorg. Chem.*, 1995, **34**, 2759.
26. D. J. Hathcock, K. Stone, J. Madden and S. J. Slattery, *Inorg. Chim. Acta*, 1998, 131.
27. E. C. Constable, G. Baum, E. Bill, R. Dyson, E. Van Eldik, D. Fenske, S. Kaderli, V. Morris, A. Neubrand, M. Neuburger, D. R. Smith, K. Wieghardt, M. Zehnder and A. D. Zuberbuhler, *Chem. Eur. J.*, 1999, **5**, 498.
28. R. Liegghio, P. G. Potvin and A. B. P. Lever, *Inorg. Chem.*, 2001, 5485.
29. M. A. Halcrow, *Coord. Chem. Rev.*, 2005, **249**, 2880.
30. M. I. J. Polson, N. J. Taylor and G. S. Hanan, *Chem. Commun.*, 2002, 1356.
31. M. I. J. Polson, E. A. Medlycott, G. S. Hanan, L. Mikelsons, N. J. Taylor, M. Watanabe, Y. Tanaka, F. Loiseau, R. Passalacqua and S. Campagna, *Chem. Eur. J.*, 2004, **10**, 3640.
32. G. K. Pagenkopf and D. W. Margerum, *Inorg. Chem.*, 1968, **7**, 2514.
33. F. H. Fraser, P. Epstein and D. J. Macero, *Inorg. Chem.*, 1972, **11**, 2031.
34. D. Sedney, M. Kahjehnassiri and W. M. Reiff, *Inorg. Chem.*, 1981, **20**, 3476.
35. C. Arana, S. Yan, M. Keshavarz-K, K. T. Potts and H. D. Abruña, *Inorg. Chem.*, 1992, **31**, 3680.

36. P. G. Hela, R. N. Reddy, N. R. Anipindi, K. I. Priyadarsini and T. Mukherjib, *React. Kinet. Catal. Lett.*, 2005, **85**, 79.

37. M. Barbosa, C. Díaz, M. Ines Toral, J. Retuert and Y. Martinez, *J. Mater. Chem.*, 2005, **15**, 1360.

38. R. Zibaseresht and R. M. Hartshorn, *Aust. J. Chem.*, 2005, **58**, 345.

39. J.-V. Folgado, W. Henke, R. Allmann, H. Stratemeier, D. Beltrin-Porter, T. Rojo and D. Reinen, *Inorg. Chem.*, 1990, **29**, 2035.

40. V. L. N. Dias, E. N. Fernandes, L. M. S. da Silva, E. P. Marques, J. Zhang and A. L. Brandes Marquesa, *J. Power Sources*, 2005, **142**, 10.

41. R. N. Patel, N. Singh, K. K. Shukla, V. L. N. Gundla and U. K. Chauhan, *Spectrochim. Acta Part A*, 2005, **63**, 21.

42. E. A. Medlycott, I. Theobald and G. S. Hanan, *Eur. J. Inorg. Chem.*, 2005, 1223.

43. O. Navon, J. Bernstein and V. Khodorkovsky, *Angew. Chem., Int. Ed. Eng.*, 1997, **36**, 601.

44. H. F. Lieberman, R. J. Davey and D. M. T. Newsham, *Chem. Mater.*, 2000, 490.

45. A. Matsumoto, T. Tanaka, T. Tsubouchi, K. Tashiro, S. Saragai and S. Nakamoto, *J. Am. Chem. Soc.*, 2002, **124**, 8891.

46. a) F. Zordan, L. Brammer and P. Sherwood, *J. Am. Chem. Soc.*, 2005, **127**, 5979. b) G. R. Desiraju, R. Parthasarathy, *J. Am. Chem. Soc.,* 1989, **111**, 8725. c) C. Malla Reddy, M. T. Kirchner, R. C. Gundakaram, K. Anantha Padmanabhan, G. R. Desiraju, *Chem. Eur. J.,* 2006, **12**, 2222.

47. E. I. Lerner and S. J. Lippard, *J. Am. Chem. Soc.*, 1976, **98**, 5397.

48. V. M. S. Gil, R. D. Gillard, P. A. Williams, R. S. Vagg and E. C. Watton, *Transition Met. Chem. (London)*, 1979, **4**, 14.

49. J.-V. Folgado, E. Coronado, D. Beltrin-Porter, R. Burriel, A. Fuertes and C. J. Miravitlles, *J. Chem. Soc., Dalton Trans.*, 1988, 3041.

50. G. M. Sheldrick, *SHELXTL,*2001 and 1997, Bruker Analytical X-Ray Systems, Madison, WI.

Chapter VI: Tridentate triazine-containing ligands as flexible platforms for spin cross-over complexes of Fe(II)

Article 3

Elaine A. Medlycott,[a] Garry S. Hanan,[a] Tareque S.M. Abedin[b] and Laurence K. Thompson[b]*

a) Département de Chimie, Université de Montréal, Montréal, Québec, H3T-1J4, Canada.

b) Department of Chemistry, Memorial University, St. John's, Newfoundland, A1B 3X7, Canada.

Submitted to Dalton Transactions, September 2006.

Manuscript B613885C

Key words: tridentate N ligands / transition metal complexes / halogen-halogen interactions / structure elucidation / ligand design

Fe (II) complexes based on ligands containing a 1,3,5-triazine core have been synthesised and characterized and their electrochemical, spectroscopic and magnetic properties have also been investigated. The incorporation of various substituted metal-binding heterocycles into the 2,4-positions of the triazine allows the properties of the complexes to be varied considerably. Whereas the magnetic moments of the pyridyl (**1b**: 2.4 B. M.) and pyrazyl (**1c**: 4.2 B. M.) substituents lead to spin cross-over complexes, the 6-picolyl (**1d**: 5.4 B. M.) substituent is a pure Curie paramagnet at 300 K. Interestingly, the Fe(II) complex of bromo-phenyl-2,2':6'',2'''-terpyridine (**1a**) displays significant anion effects in the solid-state, with the ClO_4 salt exhibiting diamagnetic behaviour (2.1 B. M. at 300 K) and the PF_6 salt spin cross-over properties (3.5 B. M. at 300 K). The Fe-N bond distances observed in the 6-picolyl complex $[Fe(\mathbf{1d})_2](ClO_4)_2$ for both the central rings 2.084 (5) Å and the distal rings 2.254 (4) Å and 2.369 (4) Å are significantly longer than those of the pyridyl complex $[Fe(\mathbf{1b})_2](ClO_4)_2$ (centre: 1.869 (4) Å; distal: 1.992 (4) Å; distal: 2.005 (4) Å) due to steric strain and the high-spin nature of $[Fe(\mathbf{1d})_2](ClO4)_2$.

6.1 Introduction

The ability to control and fine-tune the magnetic and electronic properties of transition metal complexes is fundamental to the development of efficient molecular electronic devices based on metal ions.[1] Transition metal complexes with the potential to undergo a change of spin state are particularly good targets for development towards molecular

switches as the optical, magnetic and geometric properties may change significantly following a change in spin state.[2] In this regard, complexes with d^6 to d^7 electronic configurations are of great interest as they are able to undergo spin transitions between their low-spin and high-spin states and, consequently Fe(II) and Co(II) coordination complexes have been studied extensively.[2-5]

In general, Fe(II) complexes incorporating polypyridine ligands are low spin and diamagnetic at room temperature which allows temperature-induced changes in spin state to be monitored by NMR spectroscopy.[6] The spin state may also be manipulated by incorporating electron-donating or -accepting groups onto the framework and through the introduction of steric bulk, steric strain, or mechanical strain within the ligand.[7-10] These modifications allow access of high and low spin complexes as well as complexes in which Fe(II) cation is intermediate between the two states which are termed spin cross-over complexes. Another approach to alter the magnetic behaviour of the complexes involves substitution of the pyridyl rings within the tpy-motif with different heterocycles[11-19] as the substitution of distal pyridyl rings in the tpy core is relatively facile. However, there are fewer examples of Fe(II) complexes of tridentate ligands in which the central ring has been substituted.[20, 21] One example of such a ligand is 2,4,6-tris(2'-pyridyl)-1,3,5-triazine (tpt) which is readily synthesised and commercially available.[22] The $Fe(tpt)_2^{2+}$ complex is diamagnetic and stable at room temperature,[23-26] although due to the nature of the tridentate ligand, further functionalisation is difficult.

We have previously synthesised a family of triazine ligands based on 2,4-di(2'-pyridyl)-6-(phenyl)-1,3,5-triazine. The pendant phenyl ring can be readily substituted, thus enabling fine tuning of electronic and redox properties in Ru(II) and Co(II) complexes.[27-30] For example, if a bromophenyl-functionalised triazine ligand is employed we are able to gain directional control of the arrangement of cations in the solid state through non-covalent, halogen-halogen interactions (Fig. 6.1).[29, 31]

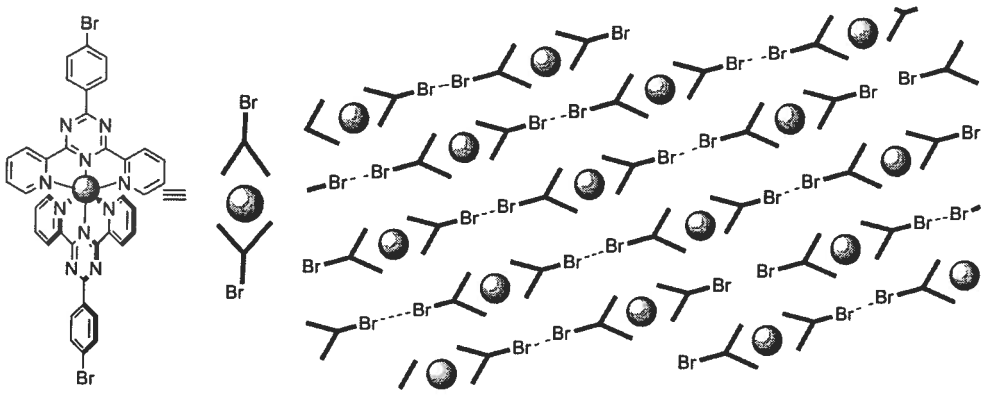

Figure 6.1 Halogen-halogen interactions in Ru(II), Fe(II), Co(II) and Cu(II) complexes of bromine-substituted triazine ligands.[31]

Herein, we report the synthesis, electronic and magnetic properties of a series of triazine-based Fe(II) complexes. Whilst substitution on the pendant phenyl ring has proved effective in the fine tuning of the electronic properties, substitution on the pyridyl rings provides coarse changes in the electronic, redox and magnetic properties of the assembled complexes.

6.2 Results and Discussion

6.2.1 Synthesis

In order to develop spin cross-over properties in a series of Fe(II) complexes, we required a flexible synthetic strategy to obtain various ligands. Triazine appeared to be the best choice for incorporation into the ligand design as it has a weaker ligand field strength as compared to pyridine, which should favour spin cross-over complexes. Thus, in a similar fashion to the one-step synthesis of tpy (Fig. 6.2a), we examined a triazine ring-forming reaction to afford variably substituted ligands (Fig. 6.2b).

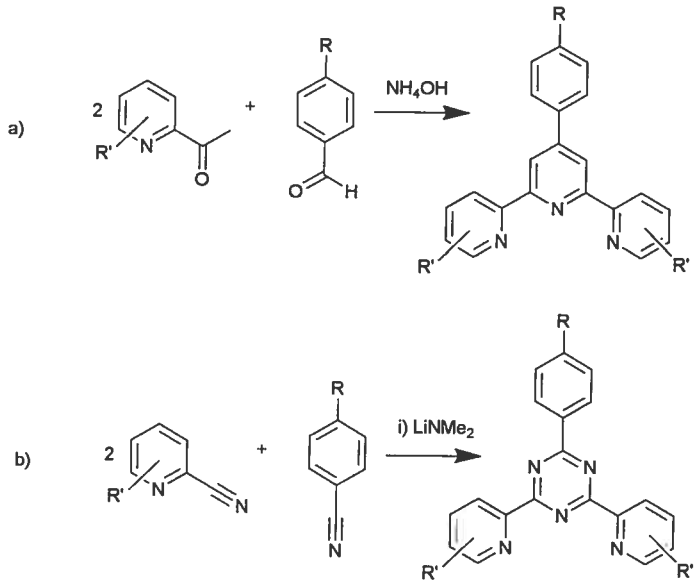

Figure 6.2 a) One-step terpyridine synthesis (above),[32] b) Triazine ring-forming reaction (below).[27-29, 33]

The synthetic procedure reported for triazine ligands, Fig. 6.2b, is general for a range of R groups substituted on the phenyl ring. As seen in Fig. 6.3, we were interested in retaining the bromo-phenyl pendant ring and in examining the versatility of this reaction by methyl substitution on the distal pyridyl rings (Fig. 6.3, **1c**) or replacing the pyridyl rings with an alternative heterocycle (pyrazine, Fig. 6.3, **1d**). For the synthesis of **1c** and **1d**, bromobenzonitrile was added to a stirred solution of $LiNMe_2$ in anhydrous diethyl ether. The amidinate intermediate that forms reacts with two equivalents of 2-cyanopyrazine or 2-cyano-6-methylpyridine and cyclisation affords ligands **1c** and **1d**, respectively, on work-up.

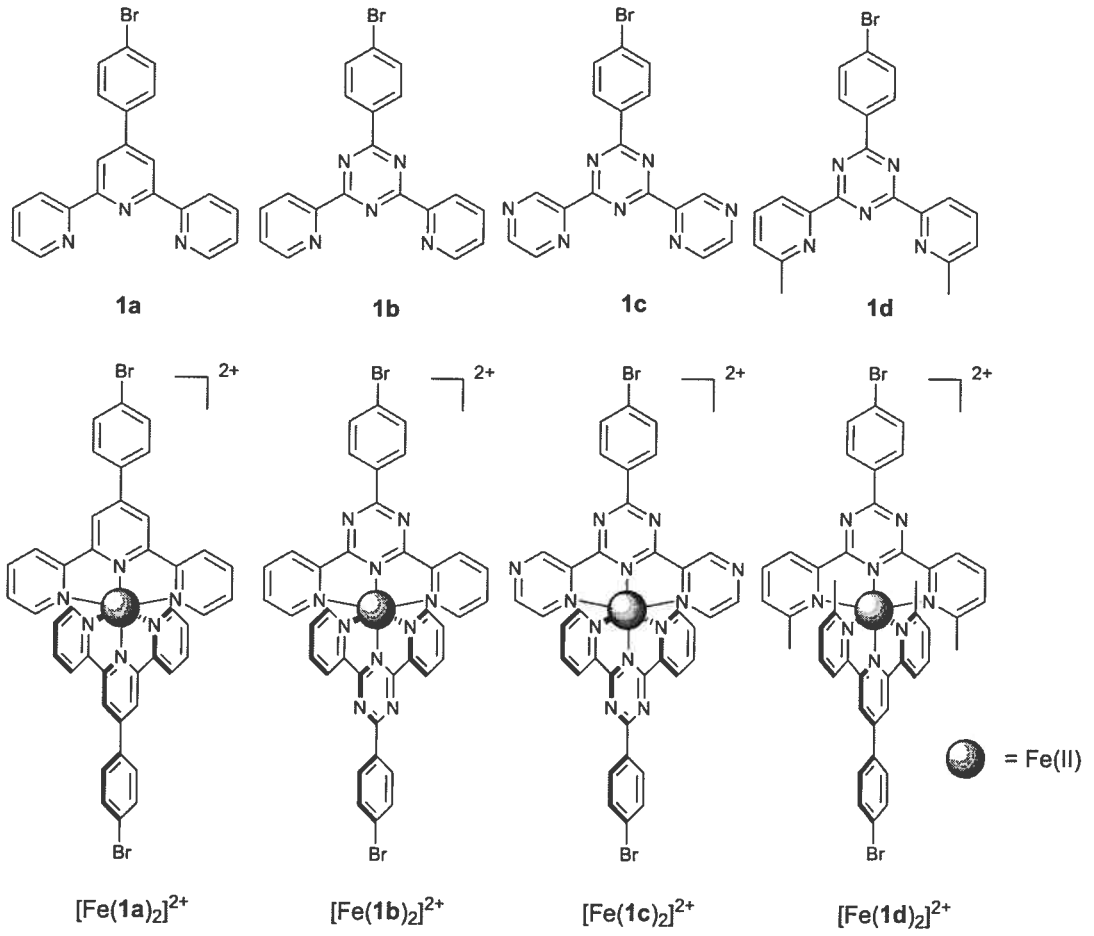

Figure 6.3 The brominated terpyridine and triazine ligands and their Fe(II) complexes used in this study.

Fe(II) complexes of ligands **1a** and **1b** could be synthesised as both the PF_6^- and ClO_4^- salts, however, complexes of ligands **1c** and **1d** were only isolated as perchlorate salts due to the instability of the complexes on counter-ion exchange. Complexes $[Fe(\mathbf{1a})_2](PF_6)_2$ and $[Fe(\mathbf{1b})_2](PF_6)_2$ were synthesised by adapting a reported procedure.[31] Complexes of the type $Fe(L)_2(ClO_4)_2$ were synthesised by addition of $Fe(ClO_4)_2.6H_2O$ in acetonitrile to a stirred solution of the ligand in acetonitrile. After 20 minutes of heating, the solvent was removed under reduced pressure and the mixture was taken up in a small amount of acetonitrile and precipitated in Et_2O. The purple or red product was isolated by filtration and dried.

The ligands and complexes were characterised by ^{1}H NMR and their chemical shifts are shown in Table 6.1. The variable temperature spectra of complex $[Fe(\mathbf{1b})_2](PF_6)_2$ are shown in Fig. 6.4 and the paramagnetic spectrum for complex $[Fe(\mathbf{1d})_2](ClO_4)_2$ in Fig. 6.5.

Complexes $[Fe(\mathbf{1a})_2]^{2+}$, $[Fe(\mathbf{1b})_2]^{2+}$ and $[Fe(\mathbf{1c})_2]^{2+}$ showed signals in the 7-11 ppm range at room temperature indicating the presence of low-spin complexes. However, less resolution was observed for the ^{1}H signals closest to the coordinating *N*-atom in $[Fe(\mathbf{1b})_2]^{2+}$ and $[Fe(\mathbf{1c})_2]^{2+}$ as their PF_6^- and ClO_4^- salts. Increasing the temperature resulted in the loss of signal structure of the next closest signals, H_3 and H_5, followed by H_4, being furthest from the coordinating site (Fig. 6.4). The phenyl protons maintained their doublet character without any broadening as they are furthest from the metal centre.

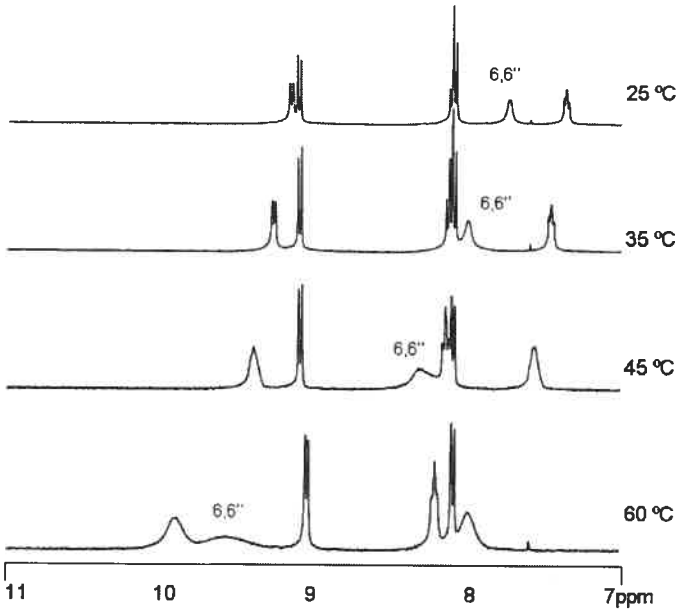

Figure 6.4 Variable temperature ^{1}H NMR spectra $[Fe(\mathbf{1b})_2]^{2+}$ as the PF_6^- salt in CD_3CN at 400 MHz.

The shift to low field of H_6 is unexpected as compared to structurally similar paramagnetic complexes based on the $Fe(tpy)_2^{2+}$ motif in which a high-field shift is observed into the negative ppm range.[9] In addition, other complexes showing spin-crossover properties had ^{1}H NMR spectra with paramagnetic signals corresponding to

the high-spin complex and diamagnetic sub-spectrum as a result of slow exchange of the two states. However, no clear sub-spectrum or paramagnetic spectrum was observed for $[Fe(\mathbf{1b})_2](PF_6)_2$ indicating that the exchange of spin states is occurring faster than the NMR time scale. The room temperature spectrum is more characteristic of a low spin complex despite the broadening observed, suggesting that the diamagnetic contribution is greater in the equilibrium between spin states.

Table 6.1 ^{1}H NMR signals obtained in CD_3CN at room temperature for **1c**, **1d** and the Fe(II) complexes of **1a-d** as their perchlorate salts.

Cpd	3, 3"	4, 4"	5, 5"	6, 6"	3', 5'	3"', 5"'	2"', 6"'	Me
1c	9.98		8.94	8.87		7.77	8.69	
1d	8.63	7.85	7.41			7.71	8.67	2.80
$[Fe(\mathbf{1a})_2]^{2+}$	8.63	7.93	7.11	7.20	9.19	8.02	8.26	-
$[Fe(\mathbf{1b})_2]^{2+}$	9.16	8.10	7.37	7.76	-	8.10	9.11	-
$[Fe(\mathbf{1c})_2]^{2+}$	10.26		8.71	8.32	-	8.12	9.11	
$[Fe(\mathbf{1d})_2]^{2+}$	52.5/53.8	13.08	52.5/53.8	-	-	7.66	3.33	-1.56

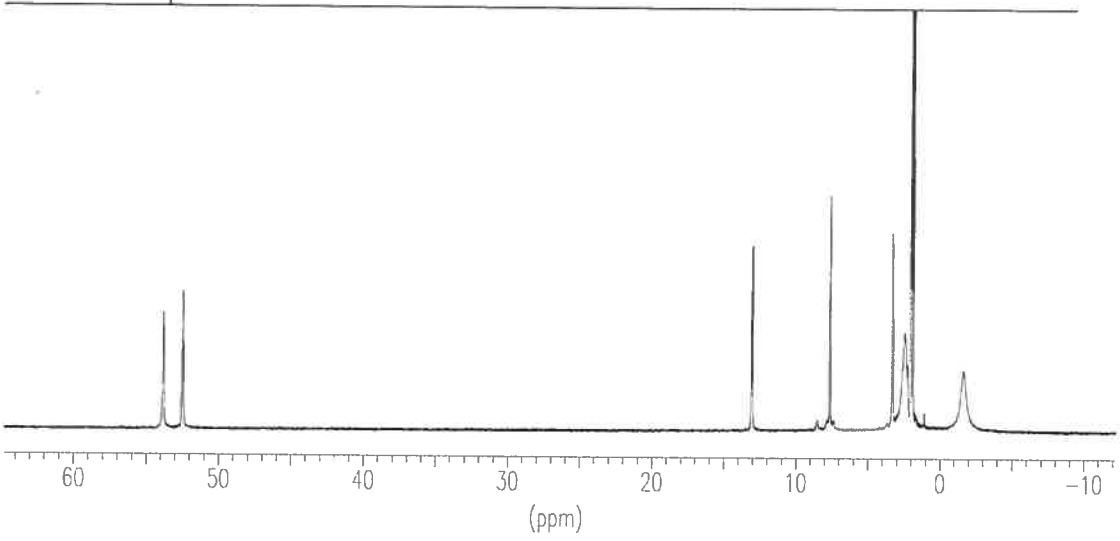

Figure 6.5 The paramagnetic spectrum of complex $[Fe(\mathbf{1d})_2]^{2+}$ (300 MHz).

6.2.2 X-ray Crystallography

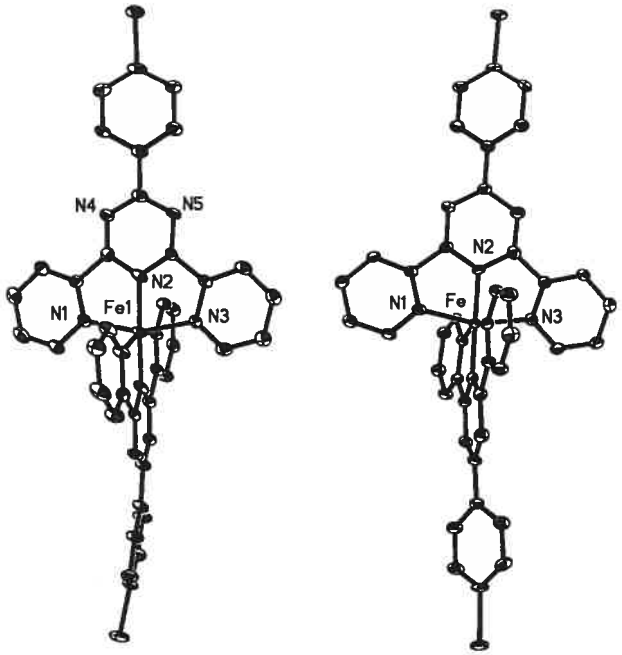

Figure 6.6 X-ray crystal structures of complexes $[Fe(\mathbf{1a})_2](PF_6)_2$ and $[Fe(\mathbf{1b})_2](ClO_4)_2$ as ORTEP representations. Thermal ellipsoids are set at 50%. The anions and solvent molecules of crystallisation have been omitted for clarity.

Table 6.2 Summary of crystal data and structure refinement for Fe(II) complexes of ligands **1a-d**.

Compound	$[Fe(\mathbf{1a})_2](PF_6)_2$	$[Fe(\mathbf{1b})_2](ClO_4)_2$	$[Fe(\mathbf{1c})_2](ClO_4)(PF_6)$	$[Fe(\mathbf{1d})_2](ClO_4)_2$
Formula	$C_{46}\ H_{34}\ Br_2\ F_{12}\ Fe\ N_8\ P_2$	$C_{44}\ H_{33}\ Br_2\ Cl_2\ Fe\ N_{13}\ O_8$	$C_{42}\ H_{32}\ Br_2\ Cl\ F_6\ Fe\ N_{18}\ O_4\ P$	$C_{46}\ H_{38}\ Br_2\ Cl_2\ Fe\ N_{12}\ O_8$
Crystal System	Triclinic	Triclinic	Monoclinic	Monoclinic
T (K)	100 (2)	100 (2)	100 (2)	150(2)
λ (Å)	1.54178	1.54178	1.54178	1.54178
Space group	$P\bar{1}$	$P\bar{1}$	C2/c	C2/c
a (Å)	10.1585 (2)	10.7253 (9)	27.0294 (15)	19.4190 (4)
b (Å)	11.4649 (2)	15.1165 (11)	9.2400 (5)	10.2896 (2)
c (Å)	22.6626 (3)	15.5248 (10)	39.652 (2)	24.4899 (5)
α (°)	93.4240 (10)	74.638 (5)		
β (°)	100.5180 (10)	73.791 (5)	106.461 (3)	98.8900 (10)
γ (°)	113.1240 (10)	89.096 (5)		
V (Å^3)	2361.24 (7)	2326.0 (3)	9497.3 (9)	4834.63 (17)
Z	2	2	8	4
D (Mg m^{-3})	1.694	1.654	1.747	1.612
μ (mm^{-1})	6.003	6.254	6.135	6.019
Maximum 2θ (°)	73.02	73.34	55.13	58.20
Number of reflections collected	29279	27650	38944	20606
Number of independent reflections	9061	8842	5939	3342
Data/ restraints/parameters	9061/0/642	8842/0/634	5939/0/641	3342/69/387
R	0.0515	0.0711	0.0779	0.0603
wR2	0.1366	0.2312	0.2373	0.1700
Goodness-of-fit on F^2	1.035	1.023	1.011	0.951

Purple crystals of $[Fe(\mathbf{1b})_2](ClO_4)_2$ and $[Fe(\mathbf{1d})_2](ClO_4)_2$ were obtained by slow diffusion of isopropyl ether into acetonitrile solutions of the complexes. Efforts to obtain crystals of $[Fe(\mathbf{1c})_2](ClO_4)_2$ were unsuccessful but addition of excess NH_4PF_6 to the acetonitrile solution followed by filtration and crytallisation by slow diffusion yielded purple crystals as the mixed salt. Attempts to crystallise $[Fe(\mathbf{1a})_2](ClO_4)_2$ were also unsuccessful, but acceptable crystals were obtained as the PF_6^- salt.

Both complexes $[Fe(\mathbf{1a})_2](PF_6)_2$ and $[Fe(\mathbf{1b})_2](ClO_4)_2$ crystallised in the triclinic space group $P\bar{1}$ with one complete molecule, 2 counter-ions and two or three acetonitrile solvent molecules in the asymmetric unit. Complexes $[Fe(\mathbf{1c})_2](ClO_4)(PF_6)$ and $[Fe(\mathbf{1d})_2](ClO_4)_2$ crystallised in the monoclinic space group C2/c.

The Fe-N (centre) bond distances in all the complexes are shorter than the Fe-N (distal) bond distances. The Fe-N bond distances of $[Fe(\mathbf{1a})_2](PF_6)_2$ were unexceptional for Fe(tpy)-type complexes and those for complex $[Fe(\mathbf{1b})_2](ClO_4)_2$ were similar to those found in the previously reported structure reported as the PF_6^- salt.[31] The Fe-N bond distances in $[Fe(\mathbf{1c})_2](ClO_4)(PF_6)$ were lengthened to the central triazine ring as compared to $[Fe(\mathbf{1b})_2](ClO_4)_2$, but shorter to the peripheral pyrazine rings when compared to the pyridyl rings of $[Fe(\mathbf{1b})_2](ClO_4)_2$.

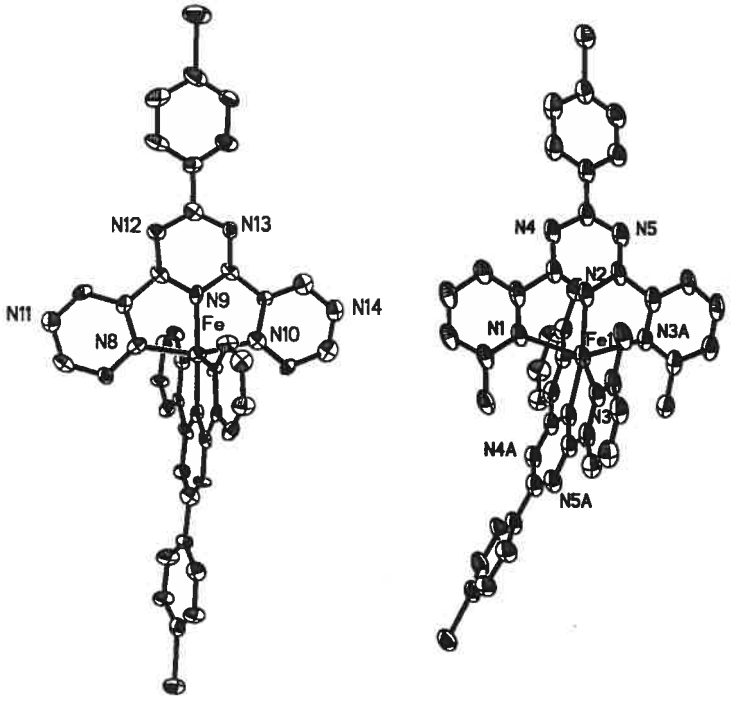

Figure 6.7 X-ray crystal structures of complexes $[Fe(\mathbf{1c})_2](ClO_4)(PF_6)$ and $[Fe(\mathbf{1d})_2](ClO_4)_2$ as ORTEP representations. Thermal ellipsoids are set at 50%. The anions and solvent molecules of crystallisation have been omitted for clarity.

A significant elongation of Fe-N bond distances is observed in complex $[Fe(\mathbf{1d})_2](ClO_4)_2$ for both the central rings and the distal rings due to a combination of the steric strain imposed by the methyl substituents and the consequential occupation of anti-bonding metal-based orbitals in the high spin complex. This is consistent with the formation of a high-spin complex. Smaller bite angles (72-73°) are reported for the high-spin complex due to the elongation of the Fe-N bonds consistent with observations made from high-spin tpy-based complexes.[9]

Table 6.3 Selected bond distances and angles for the Fe(II) complexes of **1a-d**.

	$[Fe(\mathbf{1a})_2](PF_6)_2$	$[Fe(\mathbf{1b})_2](ClO_4)_2$	$[Fe(\mathbf{1c})_2](ClO_4)(PF_6)$	$[Fe(\mathbf{1d})_2](ClO_4)_2$
Bond Distances (Å)				
Fe-N (centre)	1.876 (3)	1.869 (4)	1.879 (9)	2.084 (5)
Fe-N	1.970 (4)	1.986 (4)	1.983 (8)	2.254 (4)
Fe-N	1.972 (3)	2.005 (4)	1.987 (8)	2.369 (4)
Fe-N (centre)	1.877 (3)	1.870 (4)	1.876 (9)	
Fe-N	1.974 (3)	1.996 (4)	1.982 (9)	
Fe-N	1.974 (3)	2.006 (4)	1.993 (9)	
Selected Angles (°)				
Trz-phenyl twist	30.6 (2)/ 28.30 (2)	14.3 (3)/ 10.6 (3)	7.9 (3)/ 11.7 (4)	11.9 (3)
Trz-pyridyl twist	9.8 (2)/ 2.8 (3)	2.4 (4)/ 8.7 (3)	3.7 (3)/ 3.2 (3)	10.2 (3)/ 3.6 (1)
N(trz)-Fe-N(trz) (ϕ)	178.8 (1)	175.9 (2)	178.0 (4)	169.1 (2)
N(py)-Fe-(Npy) bite angle	162.1 (1)/ 162.2 (1)	159.6 (2)/ 159.1 (2)	159.9(4)/ 159.5 (4)	146.7 (2)

Intermolecular Br-Br interactions are observed in all of the complexes in the extended lattice similar to those reported for Co(II) complexes of related ligands.[29, 31] Intermolecular Br-Br distances of 3.46 Å, 3.42 Å and 3.55 Å are observed for $[Fe(\mathbf{1a})_2](PF_6)_2$, $[Fe(\mathbf{1b})_2](ClO_4)_2$ and $[Fe(\mathbf{1d})_2](ClO_4)_2$, respectively, which are all shorter than the sum of the Van der Waals Br radii giving rise to 1-dimensional tapes running throughout the lattice (Fig. 6.8). In complex $[Fe(\mathbf{1c})_2](ClO_4)(PF_6)$, the Br-Br contacts have lengthened to 4.26 Å.

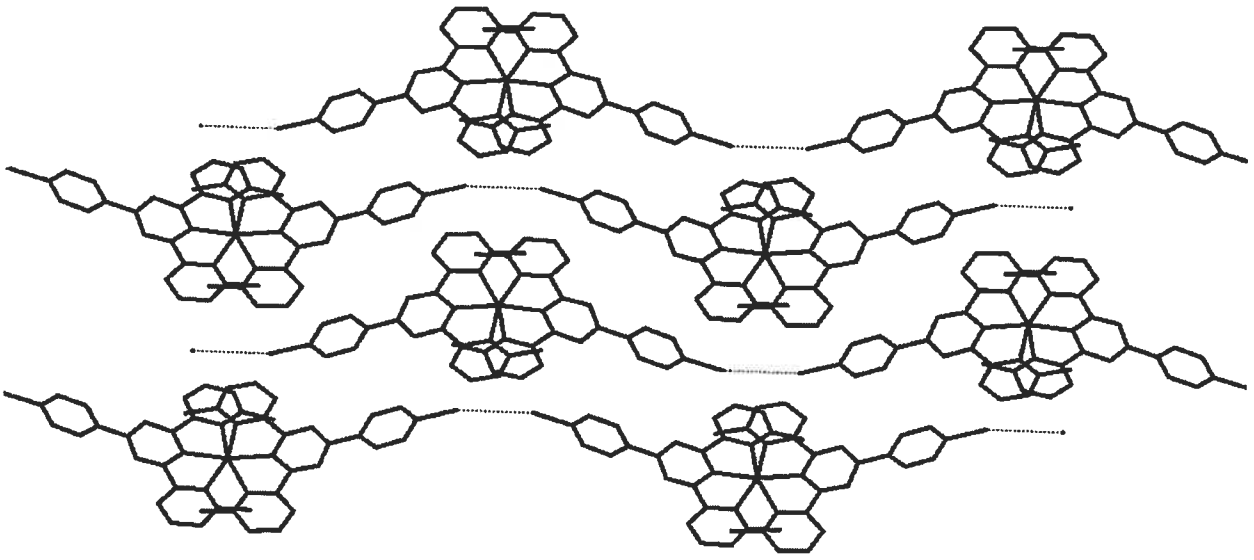

Figure 6.8 Short Br-Br contacts in the extended lattice of complex $[Fe(\mathbf{1d})_2](ClO_4)_2$. Anions and acetonitrile solvent molecules have been omitted for clarity.

6.2.3 Electrochemistry and Electronic Spectroscopy

The redox potentials for the Fe(II) complexes as their ClO_4^- salts are shown in Table 6.4.

Table 6.4 Electrochemical data in CH_3CN solutions at 293K.[a]

	$E_{1/2}$(ox)	$E_{1/2}$(red)			
$[Fe(\mathbf{1a})_2]^{2+}$	1.11 (75)	-1.20 (68)	-1.32 (57)		
$[Fe(\mathbf{1b})_2]^{2+}$	1.38 (106)	-0.69 (66)	-0.84 (67)	-1.52 (82)	-1.82 (irr)
$[Fe(\mathbf{1c})_2]^{2+}$	1.89 (irr)	-0.42 (69)	-0.51 (69)	-1.13 (82)	-1.40 (55)
$[Fe(\mathbf{1d})_2]^{2+}$	1.62 (irr)	-0.51 (54)	-0.78 (76)	-1.62 (irr)	-1.80 (irr)
$[Fe(tpy)_2]^{2+}$ [c]	1.10 (70)	-1.13 (70)	-1.27 (60)	-1.94 (70)	

[a] Potentials are in volts vs SCE for acetonitrile solutions, 0.1 M in TBAP, recorded at 25 ± 1° C at a sweep rate of 200 mV/s. Unless otherwise stated couples are reversible. [b] Irreversible; potential is given for the cathodic wave. (ΔE_p in parentheses (mV)). [c] From reference 26.

The Fe(II)/(III) couples dominate the anodic region and ligand-based reductions dominate the cathodic region of the cyclic voltammograms. The Fe(II)/(III) couples of the triazine-based complexes are irreversible as their ClO_4^- salts, although the same couple of $[Fe(\mathbf{1b})_2](PF_6)_2$ is reversible, presumably due to the improved solubility of the PF_6^- salts in acetonitrile solution.[31] The metal-based oxidation of $[Fe(\mathbf{1a})_2](ClO_4)_2$ is observed at +1.11 V, which is in agreement of the parent complex $[Fe(tpy)_2]^{2+}$ (+1.10 V) indicating that bromophenyl substitution of the tpy core has a minimal effect on the metal-based orbitals. The same Fe(II)/(III) couple in the triazine-based complexes occurs at a significantly more positive potential (1.38- 1.89 V) due the electron-deficient nature of the triazine ligands as compared to the tpy ligand. Similarly, the triazine based complexes are easier to reduce than the terpyridine complexes. In complex $[Fe(\mathbf{1a})_2](ClO_4)_2$, a one-electron reduction of one terpyridine is observed followed by a second one-electron reduction of the second terpyridine ligand with a peak separation of 120 mV between reductions. The separation between the reductions of the first and second triazine-based ligand in $[Fe(\mathbf{1b})_2](ClO_4)_2$ is 150 mV, which indicates greater sensitivity of the triazine ligands to reductive processes. An additional triazine-based reduction is observed on both ligands to give a total of four reductions for the complexes of triazine ligands.

The Fe(II) centres of complexes $[Fe(\mathbf{1c})_2](ClO_4)_2$ and $[Fe(\mathbf{1d})_2](ClO_4)_2$ are significantly more difficult to oxidise and the ligands significantly easier to reduce than triazine complex $[Fe(\mathbf{1b})_2](ClO_4)_2$. The pyrazine rings are more electron deficient than the pyridyl rings in $[Fe(\mathbf{1b})_2](ClO_4)_2$ thereby withdrawing more electron-density away from the metal centre. The positive shift, despite the introduction of electron-donating methyl groups in $[Fe(\mathbf{1d})_2](ClO_4)_2$, is a consequence of the high spin-state and weaker ligand field imposed by the elongation of the Fe-N bond distances.

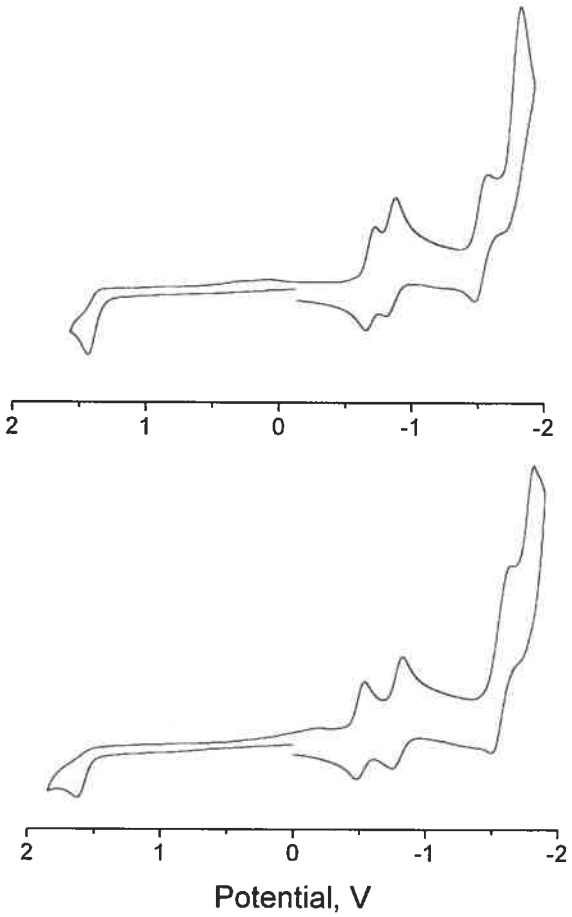

Figure 6.9 Cyclic voltammograms of (above) $[Fe(\mathbf{1b})_2](ClO_4)_2$ and $[Fe(\mathbf{1d})_2](ClO_4)_2$ (below) in CH_3CN at room temperature.

Table 6.5 Spectroscopic data in CH_3CN solutions at 293K.

	Absorption λ_{max}, nm (ε, $M^{-1}cm^{-1} \times 10^{-3}$)
$[Fe(\mathbf{1a})_2]^{2+}$	286 (67.3), 319 (42.7), 359 (7.2, sh), 568 (19.3)
$[Fe(\mathbf{1b})_2]^{2+}$	288 (67.1), 316 (40.3, sh), 548 (10.5), 597 (13.8)
$[Fe(\mathbf{1c})_2]^{2+}$	285 (71.3), 326 (43.4, sh), 533 (11.5), 576 (15.4)
$[Fe(\mathbf{1d})_2]^{2+}$	290 (52.9), 328 (26.9, sh), 400 (1.2, sh), 507 (0.4)

The absorption spectra of $[Fe(\mathbf{1a})_2](ClO_4)_2$, $[Fe(\mathbf{1b})_2](ClO_4)_2$ and $[Fe(\mathbf{1d})_2](ClO_4)_2$ are shown in Figure 6.10.

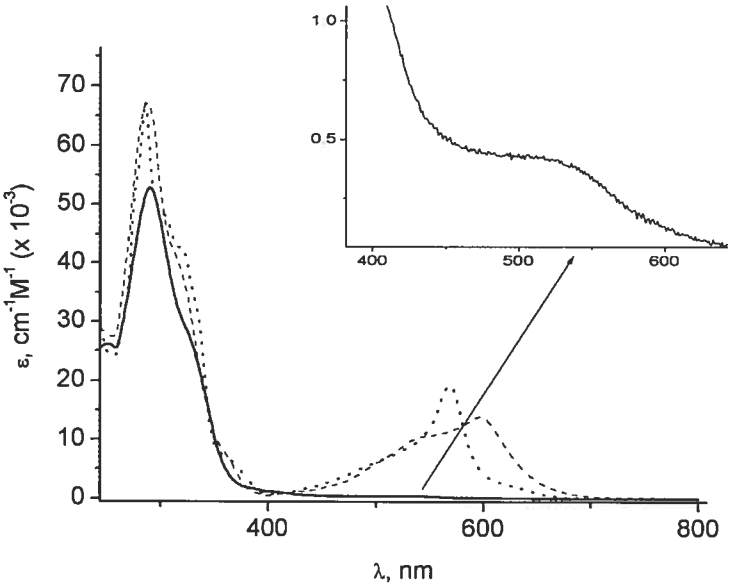

Figure 6.10 Electronic spectra in acetonitrile for complexes $[Fe(\mathbf{1a})_2](ClO_4)_2$ (dotted-line), $[Fe(\mathbf{1b})_2](ClO_4)_2$ (dashed-line) and $[Fe(\mathbf{1d})_2](ClO_4)_2$ (straight line). $[Fe(\mathbf{1d})_2](ClO_4)_2$ is expanded in the visible region in the inset.

The UV regions of the electronic spectra for all of the Fe(II) complexes are dominated by ligand-centred $\pi \rightarrow \pi^*$ and $n \rightarrow \pi^*$ transitions. The visible regions are dominated by MLCT bands albeit they are much less intense in the high-spin complex $[Fe(\mathbf{1d})_2](ClO_4)_2$ compared to the remaining complexes. The change in intensity may

be as a result of poor overlap between the ligand and metal orbitals due to the elongated bond distances. The ^{1}MLCT absorption band in complex $[Fe(\mathbf{1a})_2](ClO_4)_2$ is relatively sharp (569 nm) with a high energy shoulder. The transition is red-shifted compared to the parent complex $[Fe(tpy)_2)]^{2+}$ (552 nm) as the bromophenyl substituent lowers the energy of the ligand based LUMO.[35] The triazine complex, $[Fe(\mathbf{1b})_2](ClO_4)_2$, has two resolved MLCT bands at 542 and 597 nm, which may be a consequence of transitions to a triazine-based LUMO and a low-lying, triazine-based LUMO+1 orbital in the ligand. The two transitions may be considered as MLCT transitions to the ligand-based LUMO and LUMO +1.

6.2.4 Magnetic measurements

The magnetism of the complexes was studied in solution at room temperature using the modified Evan's method and in the solid state using a SQUID magnetometer from 2-300 K. In solution, it was confirmed that $[Fe(\mathbf{1a})_2]^{2+}$ is diamagnetic at room temperature, consistent with the diamagnetic solution behaviour previously reported for an Fe(II) complex of a tolyl-tpy ligand.[7] The parent complex, $[Fe(tpy)_2]^{2+}$, is considered low spin at room temperature irrespective of its counter-anion.[34] In contrast, $[Fe(\mathbf{1a})_2](PF_6)_2$ has significant paramagnetic contributions to the magnetic moment (3.5 B. M.) at 300 K in the solid state, whereas the perchlorate salt remains largely diamagnetic (Fig. 6.11).[7] The magnetic moment of complex $[Fe(\mathbf{1b})_2]^{2+}$ as both the PF_6^- and ClO_4^- salts differ marginally between 2-300 K (Fig. 6.11), with the PF_6^- salt having slightly greater paramagnetic contribution (2.5 B. M.) and slow spin cross-over properties up to room temperature. Complex $[Fe(\mathbf{1c})_2](ClO_4)_2$ shows behaviour similar to complex $[Fe(\mathbf{1b})_2](ClO_4)_2$ with a magnetic moment of 4.2 B. M. at 300 K, more characteristic of a high-spin complex.

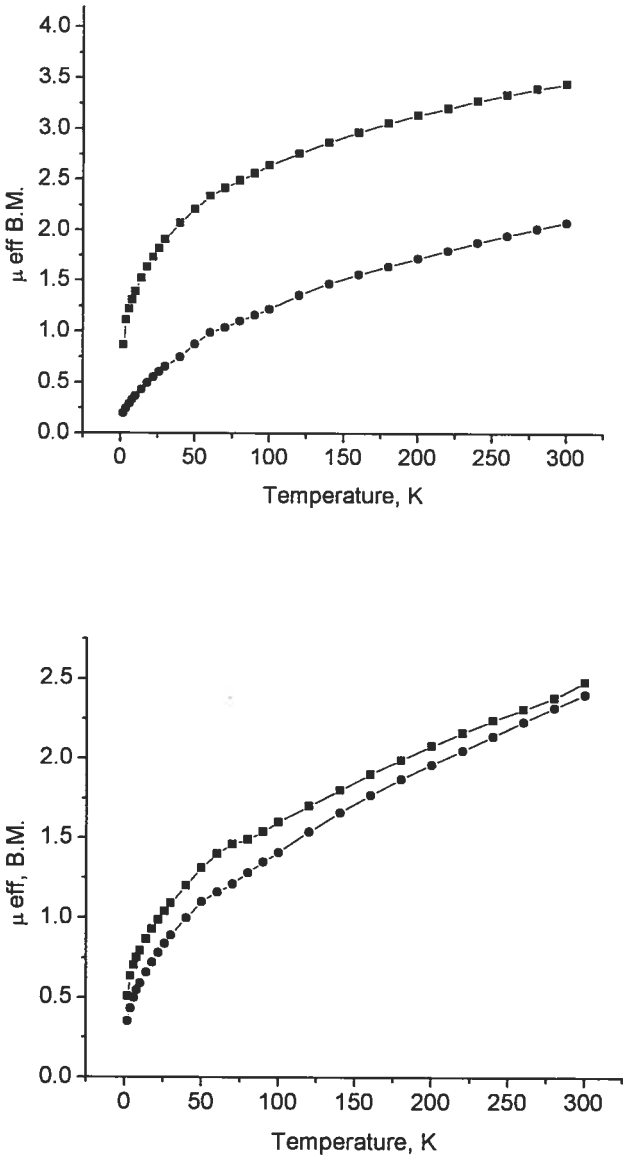

Figure 6.11 Variable temperature magnetic susceptibility data for $[Fe(\mathbf{1a})_2]^{2+}$ (above) and $[Fe(\mathbf{1b})_2]^{2+}$ (below) as the PF_6^- salts (-■-) and ClO_4^- salts (-●-).

A plot of $1/\chi$ vs temperature for complex $[Fe(\mathbf{1d})_2](ClO_4)_2$ indicates a zero value for the Weiss constant, thereby suggesting that complex $[Fe(\mathbf{1d})_2](ClO_4)_2$ is a pure Curie paramagnet. The magnetic moment measured between 20-300 K corresponds to a high-spin Fe(II) complex (S= 2), with 5.4 B. M. measured at 340 K.

Below 20K there is a reduction in the magnetic moment, down to 3.9 B.M. at 4 K, associated with zero-field splitting of the spin quintet state.

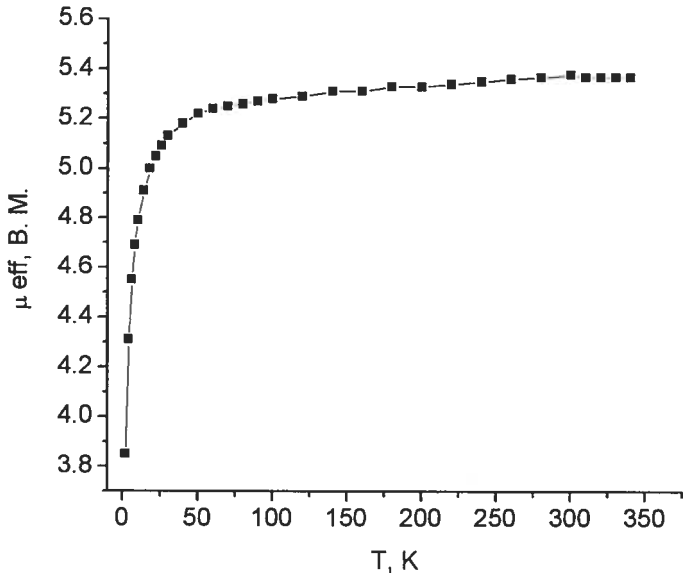

Figure 6.12 Plot of the variable temperature magnetic moment of $[Fe(\mathbf{1d})_2](ClO_4)_2$.

6.3 Conclusions

In solution complex $[Fe(\mathbf{1a})_2]^{2+}$ is low spin, with no evidence of a paramagnetic contribution. The solid-state measurements indicate significant high-spin contributions as the PF_6^- salt which are absent in the ClO_4^- salts. The solution and solid state magnetic data for complexes $[Fe(\mathbf{1b})_2](ClO_4)_2$ and $[Fe(\mathbf{1c})_2](ClO_4)_2$, on the other hand, indicate a small paramagnetic contribution to a largely diamagnetic ground state, due to the weaker ligand field strength of the triazine containing ligands. Modification of complex $[Fe(\mathbf{1b})_2](ClO_4)_2$ with methyl substituents in the 6-position of the pyridyl rings induce sufficient steric strain to force a high spin configuration over the temperature range 20-300 K. These results indicate that steric strain invokes a greater spin cross-over effect than variations in the electronic properties due to heterocyclic

substitution. We are currently undertaking further investigations of phenyl-tpy type ligands and the effects of substitution at other positions on the ligands.

CCDC-619603 & 619606 contains the supplementary crystallographic data for this paper. This data can be obtained free of charge from The Cambridge Crystallographic Data Centre via other *www.ccdc.cam.ac.uk/data_request/cif.*

Acknowledgements

GSH and LKT thank the Natural Sciences and Engineering Research Council of Canada and GSH thanks the Université de Montréal for financial support. EAM thanks the Commonwealth Scholarship Programme for a doctoral scholarship and Francine Belanger for assistance with crystallography.

6.4 Experimental

Materials and Instrumentation

Nuclear magnetic resonance (NMR) spectra were recorded in CD_3CN at room temperature (r.t.) on a Bruker AV400 spectrometer at 400 MHz for ^1H NMR and at 100 MHz for ^{13}C NMR. Chemical shifts are reported in part per million (ppm) relative to residual solvent protons (1.93 ppm for acetonitrile-d_3) and the carbon resonance of the solvent. Absorption spectra were measured in deaerated acetonitrile at r.t. on a Cary 500i UV-Vis-NIR Spectrophotometer.

Electrochemical measurements were carried out in argon-purged acetonitrile at room temperature with a BAS CV50W multipurpose equipment interfaced to a PC. The working electrode was a Pt electrode. The counter electrode was a Pt wire, and the pseudo-reference electrode was a silver wire. The reference was set using an internal 1 mM ferrocene/ferrocinium sample at 395 mV vs SCE in acetonitrile and 432 mV in DMF. The concentration of the compounds was 1 mM. Tetrabutylammonium hexafluorophosphate (TBAP) was used as supporting electrolyte and its concentration was 0.10 M. Cyclic voltammograms were obtained at scan rates of 50, 100, 200, and 500 mV/s. For irreversible oxidation processes, the cathodic peak was used as E, and

the anodic peak was used for irreversible reduction processes. The criteria for reversibility were the separation of 60 mV between cathodic and anodic peaks, the close to unity ratio of the intensities of the cathodic and anodic currents, and the constancy of the peak potential on changing scan rate. The number of exchanged electrons was measured with OSWV, and by taking advantage of the presence of ferrocene used as the internal reference.

Variable temperature magnetic data were obtained with a Quantum Design MPMS5S Squid magnetometer operating in DC mode. Samples were prepared in gelatine capsules or aluminium cups, and measured data were corrected for sample holder response, and underlying sample diamagnetism using Pascal corrections.

Experimental uncertainties are as follows: absorption maxima, ±2 nm; molar absorption coefficient, 10%; redox potentials, ± 10 mV.

Synthetic Procedures

1a, **1b** and $Fe(L)_2(PF_6)_2$ complexes were synthesised as previously described.[29, 31, 32]

1c

^{n}BuLi (1.6M in hexanes, 11.0 mL, 0.018 mol) was added dropwise to a stirring solution of $HNMe_2$ (2M in THF, 8.8 mL, 0.018 mmol) in anhydrous Et_2O (150 mL) under an inert atmosphere. The mixture was stirred until a white suspension formed (20 minutes) and *p*-bromo-benzonitrile (3.00 g, 0.016 mol) was added to the mixture as a solid. The mixture was stirred for one hour, followed by addition of 2-cyanopyrazine (3.47 g, 0.033 mol). The reaction was stirred under N_2 for four hours and in air for a further 30 minutes. The solid was collected by filtration, recrystallised from ethanol:water 1:2, washed with diethyl ether and dried to afford **1c** as a white powder (1.00 g, 16% yield).

^{1}H NMR (400 MHz, $CDCl_3$): 9.98, d, 2H, (J= 1 Hz), $H_{3,3''}$; 8.94 (t, J= 2 Hz, 2H) $H_{5,5''}$; 8.87 (d, J= 2 Hz, 2H) $H_{6,6''}$; 8.69 (d, J= 9 Hz, 2H) $H_{2''',6'''}$; 7.77 (d, J= 9 Hz, 2H) $H_{3''',5'''}$. ^{13}C {^{1}H} NMR (100 MHz, $CDCl_3$): 128.65, 130.56, 131.97, 133.21, 144.65, 145.87, 147.01, 148.02, 170.37, 172.12. High Res ESMS *m/z* calcd for $C_{17}H_{11}N_7Br$: $[M+H]^+$ 392.02594; Found: 392.02582.

1d

^{n}BuLi (1.6M in hexanes, 1.45 mL, 2.32 mmol) was added dropwise to a stirring solution of $HNMe_2$ (2M in THF, 1.16 mL, 2.32 mmol) in anhydrous Et_2O (30 mL) under an inert atmosphere. The mixture was stirred until a white suspension formed (20 minutes) and *p*-bromo-benzonitrile (0.38 g, 2.11 mmol) was added to the mixture as a solid. The mixture was stirred for one hour, followed by addition of 2-cyano-6-methylpyridine (0.50 g, 4.23 mmol). The reaction was stirred under N_2 overnight and in air for a further 30 minutes. The solid was collected by filtration, recrystallised from ethanol:water 1:2, washed with diethyl ether and dried to afford **1d** as a white powder (333 mg, 38% yield).

^{1}H NMR ($CDCl_3$, 400 MHz): 8.67 (d, J= 9 Hz, 2H) $H_{2''',6'''}$; 8.63 (d, J 8 Hz, 2H) $H_{3,3''}$; 7.85 (t, J= 8 Hz, 2H) $H_{4,4''}$; 7.71 (d, J= 9 Hz, 2H) $H_{3''',5'''}$; 7.41 (d, J= 7 Hz, 2H) $H_{5,5''}$; 2.80 (s, 6H) $H_{6,6''}$. ^{13}C {^{1}H} NMR ($CDCl_3$, 100 MHz): 23.90, 121.84, 126.37, 127.71, 130.29, 131.63, 133.95, 137.09, 151.96, 159.14, 171.11, 171.17.Anal. Calc. For $C_{21}H_{16}BrN_5$: C, 60.30; H, 3.86; N, 16.74. Found C 59.87; H, 3.88; N, 16.52.

$[Fe(\mathbf{1a})_2](ClO_4)_2$: **1a** (198 mg, 0.51 mmol) was dissolved in acetonitrile (30 mL) and heated gently. In a separate flask, the $Fe(ClO_4)_2.6H_2O$ (65 mg, 0.26 mmol) was heated in acetonitrile (5 mL) and was then added on stirring to the ligand solution. An intense purple colour was immediately observed and stirring and heating were continued for a further 10 minutes. The solution was filtered, cooled and the solvent removed. The solid was dissolved in a minimum amount of acetonitrile and added to diethyl ether (200 mL). The solid was collected and dried to afford $[Fe(\mathbf{1a})_2](ClO_4)_2$ as a purple powder (150 mg, 57% yield).

^{1}H NMR (CD_3CN): 9.19 (s, 2H) $H_{3',5'}$; 8.63 (d, J= 2H, 8 Hz) $H_{3,3''}$; 8.26 (d, J= 8Hz, 2H) $H_{2''',6'''}$; 8.02 (d, J= 9 Hz, 2H) $H_{3''',5'''}$; 7.91 (td, J= 8 Hz, 1 Hz) $H_{4,4''}$; 7.20 (d, J= 6 Hz, 2H) $H_{6,6''}$; 7.11 (td, J= 6 Hz, 1Hz, 2H) $H_{5,5''}$. ESMS: M^{2+}- 416.4. *Anal.* Calcd for: $C_{42}H_{28}N_6Br_2Fe_1(ClO_4)_2.H_2O$: C, 48.08; H, 2.88; N, 8.01. Found: C, 47.94; H, 2.37; N, 7.89.

$[Fe(\mathbf{1b})_2](ClO_4)_2$: The same method of preparation was used as $[Fe(\mathbf{1a})_2](ClO_4)_2$, starting with $Fe(ClO_4)_2.6H_2O$ (65 mg, 0.26 mmol) and **1b** (199 mg, 0.51 mmol). $[Fe(\mathbf{1b})_2](ClO_4)_2$ was isolated as a purple powder (115 mg, 44% yield).
^1H NMR (CD_3CN): 9.16 (d, J= 8 Hz, 2H) $H_{3,3''}$; 9.11 (d, J= 9 Hz, 2H) $H_{2''',6'''}$; 8.10 (m, 4H) $H_{3''',5'''}$, $H_{4,4''}$; 7.76 (s, broad, 2H) $H_{6,6''}$; 7.37 (t, J= 6 Hz, 2H) $H_{5,5''}$. ESMS: M^{2+}- 418.3. *Anal.* Calcd for: $C_{38}H_{24}N_{10}Br_2Fe_1.(ClO_4)_2$: C , 44.09; H, 2.34; N, 13.53. Found: C, 43.77; H, 1.86; N, 13.41.

$[Fe(\mathbf{1c})_2](ClO_4)_2$: The same method of preparation was used as $[Fe(\mathbf{1a})_2](ClO_4)_2$, starting with $Fe(ClO_4)_2.6H_2O$ (65 mg, 0.26 mmol) and **1c** (200 mg, 0.51 mmol). $[Fe(\mathbf{1c})_2](ClO_4)_2$ was isolated as a purple powder (162 mg, 56% yield).
^1H NMR (CD_3CN): 10.26 (s, broad, 2H) $H_{3,3''}$; 9.11 (d, J= 9 Hz, 2H) $H_{2''',6'''}$; 8.71 (s (broad), 2H) $H_{5,5''}$; 8.32 (s, broad, 2H) $H_{6,6''}$; 8.12 (d, J= 9 Hz, 2H) $H_{3''',5'''}$. High Res ESMS *m/z* calcd for $C_{34}H_{20}N_{14}Br_2Fe$: $[M]^{2+}$ 419.9845; found: 419.9846. *Anal.* Calcd for: $C_{34}H_{20}N_{14}Br_2Fe_1(ClO_4)_2.0.5(H_2O)$: C, 38.96; H, 2.02; N, 18.71. Found: C, 39.30; H, 1.94; N, 18.87.

$[Fe(\mathbf{1d})_2](ClO_4)_2$: The same method of preparation was used as $[Fe(\mathbf{1d})_2](ClO_4)_2$, starting with $Fe(ClO_4)_2.6H_2O$ (30 mg, 0.12 mmol) and **1d** (100 mg, 0.24 mmol). $[Fe(\mathbf{1d})_2](ClO_4)_2$ was isolated as a red solid (80 mg, 61% yield).
^1H NMR (CD_3CN): 53.83, 52.49, 13.08, 7.66, 3.33, -1.56. High Res ESMS *m/z* calcd for $C_{34}H_{20}N_{14}Br_2Fe$: $[M]^{2+}$ 445.0263; found: 445.0270. *Anal.* Calcd for: $C_{42}H_{32}N_{10}Br_2Fe_1(ClO_4)_2.H_2O$: C, 45.47; H, 3.09; N, 12.63. Found: C, 45.72; H, 2.64; N, 12.81.

6.5 References

1. A. Juris, V. Balzani, F. Barigelletti, S. Campagna, P. Belser and A. Von Zelewsky, *Coord. Chem. Rev.*, 1988, **84**, 85.
2. P. Gütlich, Y. Garcia and H. A. Goodwin, *Chem. Soc. Rev.*, 2000, **29**, 419.
3. H. A. Goodwin, *Coord. Chem. Rev.*, 1976, **18**, 293.
4. P. Gütlich, *Structure and Bonding*, 1981, **44**, 83.

5. P. Gütlich, P. J. an Koningsbruggen and F. Renz, *Structure and Bonding*, 2004, **107**, 27.
6. H. A. Goodwin, *Top. Curr. Chem.*, 2004, **233**, 59.
7. J. Chambers, B. Eaves, D. Parker, R. Claxton, P. S. Ray and S. J. Slattery, *Inorg. Chim. Acta*, 2006, **359**, 2400.
8. D. J. Hathcock, K. Stone, J. Madden and S. J. Slattery, *Inorg. Chim. Acta*, 1998, **282**, 131.
9. E. C. Constable, G. Baum, E. Bill, R. Dyson, R. Van Eldik, D. Fenske, S. Kaderli, D. Morris, A. Neubrand, M. Neuburger, D. R. Smith, K. Wieghardt, M. Zehnder and A. D. Zuberbuhler, *Chem. Eur. J.*, 1999, **5**, 498.
10. Y. Bodenthin, U. Pietsch, H. Moehwald and D. G. Kurth, *J. Am. Chem. Soc.*, 2005, **127**, 3110.
11. C. A. Kilner and M. A. Halcrow, *Polyhedron*, 2006, **25**, 235.
12. P. Manikandan, K. Padmakumar, K. R. Justin Thomas, B. Varghese, H. Onodera and M. P. T., *Inorg. Chem.*, 2001, **40**, 6930.
13. J. M. Holland, J. A. McAllister, C. A. Kilner, M. Thornton-Pett, A. J. Bridgeman and M. A. Halcrow, *J. Chem. Soc., Dalton Trans.*, 2002, 548.
14. D. L. Reger, J. R. Gardinier, M. D. Smith, A. M. Shahin, G. J. Long, L. Rebbouh and F. Grandjean, *Inorg. Chem.*, 2005, **44**, 1852.
15. J. Elhaïk, D. J. Evans, C. A. Kilnera and M. A. Halcrow, *Dalton Trans.*, 2005, 1693.
16. C. Enachescu, J. Linares, F. Varret, K. Boukheddaden, E. Codjovi, S. G. Salunke and R. Mukherjee, *Inorg. Chem.*, 2004, **43**, 4880.
17. T. Ayers, R. Turk, C. Lane, J. Goins, D. L. Jameson and S. J. Slattery, *Inorg. Chim. Acta*, 2004, **357**, 202.
18. M. A. Halcrow, *Coord. Chem. Rev.*, 2005, **249**, 2880.
19. J. M. Holland, J. A. McAllister, C. A. Kilner, M. Thornton-Pett, A. J. Bridgeman and M. A. Halcrow, *J. Chem. Soc., Dalton Trans.*, 2002, 548.
20. V. A. Money, J. Elhaik, I. R. Evans, M. A. Halcrow and J. A. K. Howard, *Dalton Trans.*, 2004, 65.

21. J. Elhaik, V. A. Money, S. A. Barrett, C. A. Kilner, I. R. Evans and M. A. Halcrow, *Dalton Trans.*, 2003, 2053.

22. F. H. Case and E. Koft, *J. Am. Chem. Soc.*, 1959, **81**, 905.

23. G. K. Pagenkopf and D. W. Margerum, *Inorg. Chem.*, 1968, **7**, 2514.

24. D. Sedney, M. Kahjehnassiri and W. M. Reiff, *Inorg. Chem.*, 1981, **20**.

25. F. H. Fraser, P. Epstein and D. J. Macero, *Inorg. Chem.*, 1972, **11**, 2031.

26. C. Arana, S. Yan, M. Keshavarz-K, K. T. Potts, and H. D. Abruña, *Inorg. Chem.,* 1992, **31**, 3680.

27. M. I. J. Polson, N. J. Taylor and G. S. Hanan, *Chem. Commun.,* 2002, 1356.

28. M. I. J. Polson, E. A. Medlycott, G. S. Hanan, L. Mikelsons, N. J. Taylor, M. Watanabe, Y. Tanaka, F. Loiseau, R. Passalacqua and S. Campagna, *Chem. Eur. J.*, 2004, **10**, 3640.

29. E. A. Medlycott, I. Theobald and G. S. Hanan, *Eur. J. Inorg. Chem.*, 2005, 1223.

30. E. A. Medlycott and G. S. Hanan, *Submitted for publication to Eur. J. Inorg. Chem.*, 2006.

31. E. A. Medlycott, K. A. Udachin and G. S. Hanan, *Submitted for publication to Dalton Trans.*, 2006.

32. J. Wang and G. S. Hanan, *Synlett*, 2005, 1251.

33. E. A. Medlycott, G. S. Hanan, F. Loiseau and S. Campagna, *Submitted for publication to Chem. Eur. J.*, 2006.

34. E. C. Constable and M. D. Ward, *Inorg. Chim. Acta*, 1988, **141**, 201.

35. J. M. Rao, D. Macero and M. Hughes, *Inorg. Chim. Acta,* 1980, **41**, 221.

Chapter VII: Minimal reorganisation in the electrochemically driven oxidation of a binuclear, double helical Cu(I) complex of a triazine-based pentadentate ligand

7.1 Introduction

The redox-controlled reversible reorganisation of molecular assemblies is an attractive concept towards their application as molecular switches.[1, 2] Transition metal ions are excellent candidates for molecular switches as external perturbation of their physical environment can change the molecular geometry through changes in the electronic requirements and properties of their metal complexes.[3] The bistability, speed and reversiblity of a molecular switch is highly dependant on the translational motion, the coordination geometry of the metal ion and the ligand requirements.[4] In this regard, Cu(I)/Cu(II) complexes of polypyidine ligands have been of particular interest for applications as molecular switches due to the differences in topological preferences between Cu(I) and Cu(II) cations.[5, 6] Cu(I) complexes of rigid pentadentate ligands such as 2,2':6',2":6 ",2"':6"',2"'-quinquepyridine (qnpy) have previously been employed to assemble dinuclear or trinuclear, double-stranded helical-type structures under inert conditions (Figure 7.1).[7, 8]

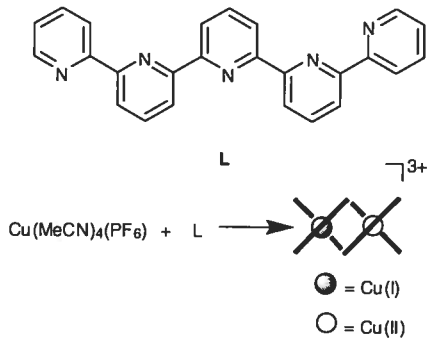

Figure 7.1 Synthesis of a mixed valence $[CuL]_2^{3+}$ complex based on qnpy.[7]

These complexes are highly sensitive in solution and rapidly oxidise to the mixed valence form.[7, 8] The mixed valent and homovalent Cu(II) complexes are stabilised as both metal and ligand requirements are satisfied through pentadentate coordination of the Cu(II) cation. To date, Cu(I) complexes of rigid pentadentate polypyridine ligands based on qnpy have not been characterised in the solid state due to the instability of the Cu(I) ion on crystallisation. In contrast, many crystal structures have been obtained from multinuclear Cu(I) complexes of rigid polypyridine ligands in which there are four or six of coordinating atoms within the ligand as both ligand and metal preferences are satisfied by tetracoordinate complexation of the metal ions.[6]
Herein, the synthesis, solid state structure and electrochemical properties of a $[CuL1]_2^{2+}$ -type complex will be discussed where **L1** is a pentadentate, triazine-based heterocyclic ligand. The electron deficient triazine ring can stabilise the Cu(I) ion favouring tetrahedral geometry.

7.2 Results and discussion

7.2.1 Synthesis and solution studies

The synthesis of ligand **L1** was carried out by a triazine ring-forming reaction in which two equivalents of 6-cyano-2,2'-bipyridine were reacted with *p*-bromobenzoamidinate.[9] $[CuL1]_2^{2+}$ was synthesised by addition of $Cu(MeCN)_4(PF_6)$ to a stirred solution of **L1** in acetonitrile under inert conditions. After 15 minutes of stirring, the mixture was filtered and precipitated as a brown solid on addition of diethyl ether. The precipitate was collected and dried to afford the complex as a brown solid in 80% yield.

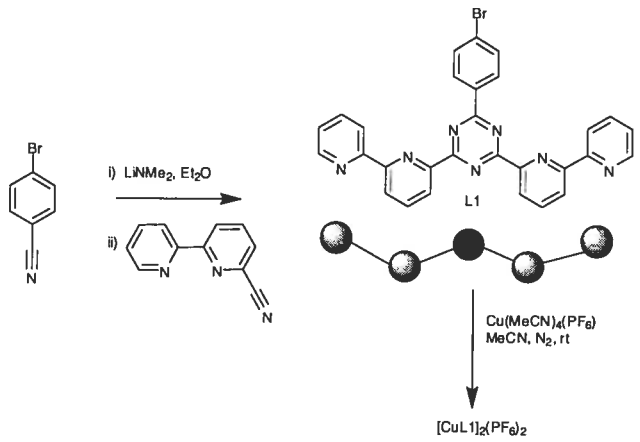

Scheme 7.1 Synthesis of binuclear, helical complex $[CuL1]_2^{2+}$.

In contrast to Cu(I) qnpy-type complexes,[7, 8] the homovalent Cu(I) complex was stable in the solid state and solution for weeks. The ^{1}H NMR spectrum of $[CuL1]_2^{2+}$ supported a symmetric complex (Figure 7.2), and the presence of a binuclear Cu(I) complex with two pentadentate ligands was confirmed by high res. ESMS.

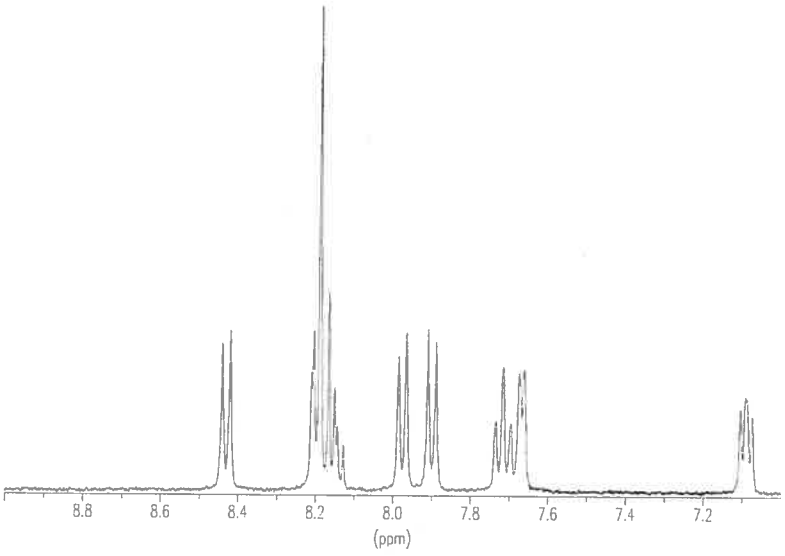

Figure 7.2 The ^{1}H NMR spectrum of $[CuL1]_2^{2+}$ in CD_3CN at 400 MHz.

The initial evidence in solution suggested that the Cu(I) centres would be bound through the peripheral 2,2'-bipyridine (bpy) motifs in a pseudo tetrahedral arrangement which would retain symmetry leaving the triazine rings unbound (Figure 7.3). If the molecules were static in solution in the symmetric configuration, the most stable orientation would

be one in which one ligand would shift relative to the other resulting in both phenyl rings pointing to the outside of the helix and the triazine would behave as a *m*-phenylene unit.[10, 11] A model complex was generated based on the published crystal structure of a dihelical Cu(I) complex incorporating bpy substituted biphenylene unit (Figure 7.3).[10, 12]

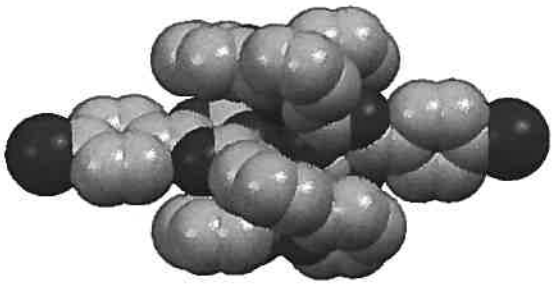

Figure 7.3 Space-fillng model of a calculated symmetric complex based on $[Cu\mathbf{L1}]_2^{2+}$.

7.2.2 Solid state structure

Brown crystals of $[Cu\mathbf{L1}]_2^{2+}$ were obtained on slow diffusion of diethyl ether into a concentrated solution of the complex in acetonitrile. The dinuclear complex crystallises in the monoclinic space group $P2_1/c$ with both helical enantiomers in the unit cell. The solid state structure indicates the ligands are in fact asymmetric, with bpy-type coordination to one Cu(I) ion and triazine-pyridine coordination to the second Cu(I) centre (Figure 7.4).

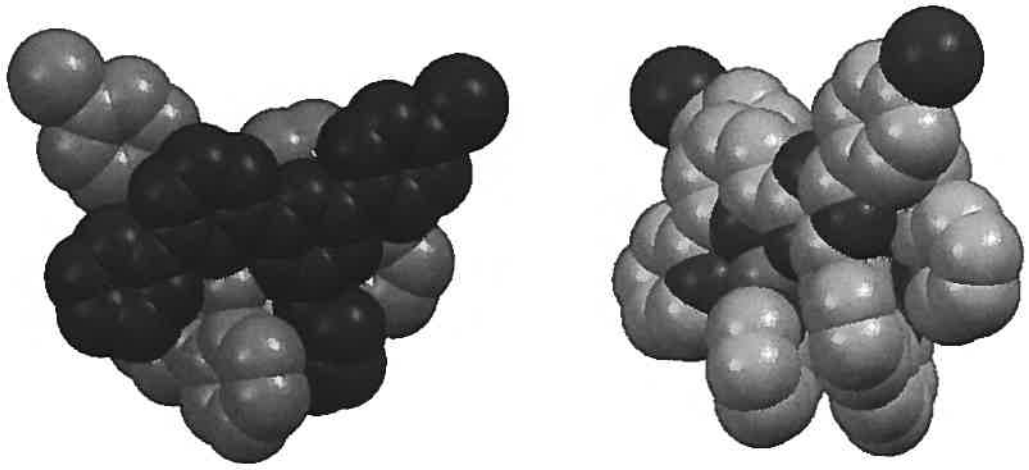

Figure 7.4 Solid state structure of $[Cu\mathbf{L1}]_2^{2+}$ as a space filling model. Ligands differentiated (left).

In each ligand strand a pendant pyridyl ring is positioned with its N-pyridyl atoms pointing towards the Cu(I) centres at distances of 2.69 Å and 2.51 Å. The remaining Cu-N distances are 2.04-2.23 Å. As expected the Cu-N distances are longer to the triazine rings than the pyridyl rings.

Variable temperature ^{1}H NMR studies were carried out in efforts to observe dynamic processes in solution. Such discrepancies in the solid state and solution behaviour were previously observed in helical Cu (I) complexes of 2,2':6':2''-terpyridine derivatives but dynamic processes were not observed in solution down to -80°C in deuterated acetone.[13] The ^{1}H signals of $[Cu\mathbf{L1}]_2^{2+}$ remained well resolved at low temperature within the limits of the deuterated solvents employed (CD_3CN and CD_3NO_2). In the solid state structure of $[Cu\mathbf{L1}]_2^{2+}$, face-to-face π-stacking interactions are observed between the pendant phenyl ring on one ligand and the pyridyl ring adjacent to the triazine on the second, (centroid-centroid distances of 3.59 Å and 3.62 Å). This interaction should be absent in solution for a static symmetric model (Figure 7.3). One and two-dimensional NOE experiments indicated that these protons are in fact in close proximity suggesting dynamic processes are occurring in solution with a symmetric intermediate (Figure 7.5). Moreover, the electronic

absorption spectrum in acetonitrile has an absorption band trailing out to 800 nm ascribed to a Cu(I)-to-triazine ^{1}MLCT band, whereas the Cu(I) ^{1}MLCT transition to bpy is around 450 nm with tailings to 600 nm, thus supporting triazine coordination to the Cu(I) ion.

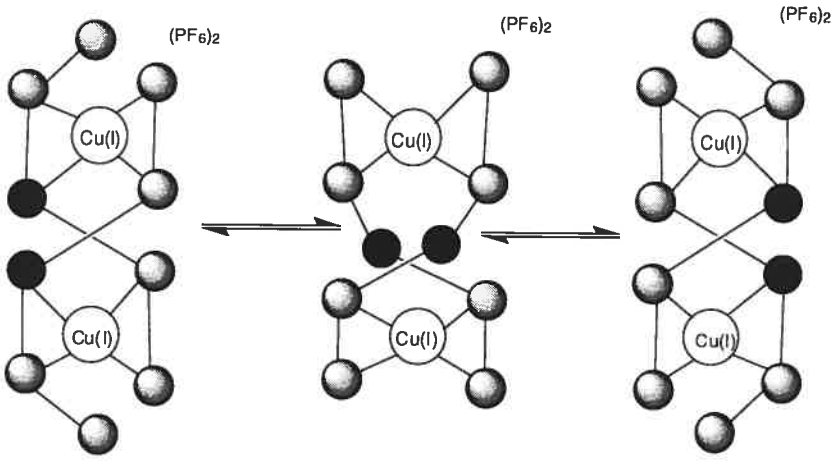

Figure 7.5 A side view of the dynamic processes occuring in solution.

7.2.3 Electrochemistry

Electrochemical measurements were carried out in anhydrous acetonitrile using the SCE versus ferrocene as an internal reference with 0.1 M $TBAPF_6$. In the anodic region, two initial ligand-based reversible reductions were observed at -0.92 V and -1.15 V. This was followed by an irreversible reduction of Cu(I) to Cu(0) which was plating on the electrode at -1.70 V. In the cathodic region, an initial oxidation corresponding to the formation of the mixed valence complex $[CuL]_2^{3+}$ is observed at 0.24 V. This was studied at variable scan rates with each scan commencing at -100 mV (Figure 7.6). At 5 Vs^{-1}, the anodic/cathodic peak separation is 92 mv and this is reduced to 62 mV at a scan rate of 25 mVs^{-1}. A second reversible oxidation is observed at 0.72 V at 25 mVs^{-1}, corresponding to the formation of the homovalent binuclear $[Cu\mathbf{L1}]_2^{4+}$ complex. The reversible behaviour of $[Cu\mathbf{L1}]_2^{2+}$ at variable scan rates supports the solid state evidence in that minimal rearrangement is required to satisfy Cu(II) ion in a pseudo square pyramidal geometry. A positive shift is observed for the initial oxidation (+0.24 V) compared to $[Cu_3L_2]^{3+}$ where L is a qnpy-type

complexes (-0.04 V).[8] The positive shift and increased stabilisation is a consequence of the stabilising electron deficient triazine motif.

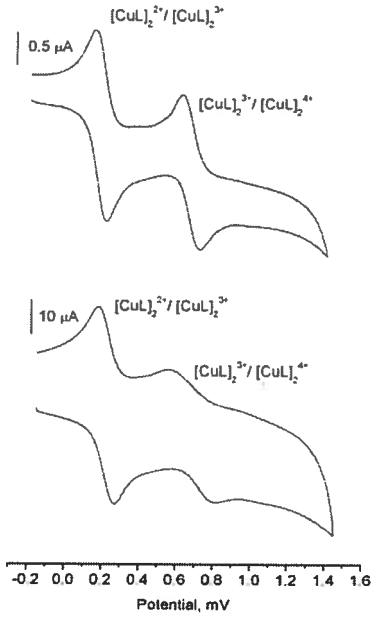

Figure 7.6 Cyclic voltammogram in the cathodic region of $[CuL1]_2^{2+}$ at 3000 mVs^{-1} and 25 mVs^{-1}.

7.2.4 Cu(II) promoted hydrolysis

Efforts to chemically oxidise $[CuL1]_2^{2+}$ were unsuccessful employing $NOBF_4$ as an oxidising agent. Following the process by electronic spectroscopy indicated that there was more than one product in solution due to the absence of an isobestic point. However, $NOBF_4$ is hygroscopic and traces of water can promote the hydrolysis of the ligand as observed previously in Cu(II) complexes of 2,4,6-tris(2'-pyridyl)-1,3,5-triazine.[14] If an acetonitrile solution of $[CuL1]_2^{2+}$ is left to crystallise over an extended period of time, the complex oxidises to a Cu(II) containing compound as indicated by the green crystals that were observed. The solid state structure of the oxidised species was determined by X-ray diffraction (Figure 7.7).

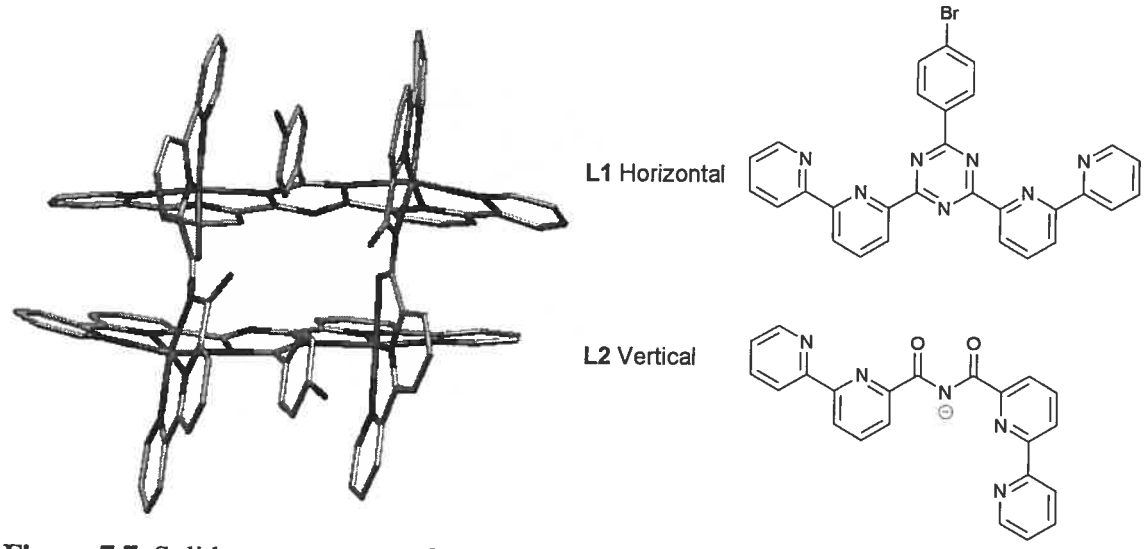

Figure 7.7 Solid state structure of [2 x 2] grid incorporating **L1** and and hydrolysed ligand **L2**.

The formation of a [2 x 2] grid proceeds via oxidation of the homovalent Cu(I) complex $[Cu\mathbf{L1}]_2^{2+}$ to $[Cu\mathbf{L1}]_2^{4+}$. The electrochemical evidence indicates that minimal rearrangement is required on oxidation to stabilise the homovalent Cu(II) complex, suggesting that in the absence of water a homovalent dihelical Cu(II) complex is obtained. In the presence of water, the Cu(II) complex promotes hydrolysis of ligand **L1**. The helix can then dissassemble and subsequently self assemble to form a grid with four Cu(II) cations, two unhydrolysed ligands **L1** (horizontally arranged) and two hydrolysed ligands **L2** (vertically arranged) (Figure 7.7). The Cu(II) ions are in a pseudo octahedral environment, with each Cu(II) centre coordinating in a tridentate, bpy-triazine mode to the unhydrolysed ligand and either bpy, N (amido) or bpy, C=O (amido) to the hydrolysed ligand **L2**. The Cu-N/O bond distances in **L2** are typical for tridentate coordination with the shortest bond lengths observed to the central pyridyl ring (1.94-1.97 Å) due to the constrained bite angle on tridentate coordiantion. The Cu-O (amido) bond distances (2.21-2.23 Å) are longer than the Cu-N (amido) bond distances (2.05-2.09 Å). The Cu-N triazine bond distances are elongated in the unhydrolysed ligand **L1** (2.21-2.42 Å), whilst the Cu(II)-N bpy are significantly shorter (1.95-2.06 Å to the central pyridine and 2.10-2.26 Å to the peripheral pyridine).

The direct synthesis of the homovalent complex from Cu(II) starting materials was attempted with a number of Cu(II) salts, all of which afforded mixtures of hydrolysed products due to traces of water in the starting salts. Large green, block crystals of the fully hydrolysed complex were isolated by slow diffusion of isopropylether into an acetonitrile solution of the Cu(II) complex.

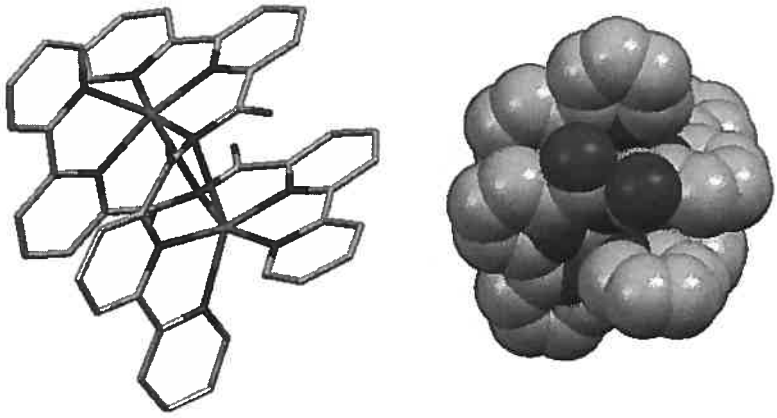

Figure 7.8 Dihelical structure of the fully hydrolysed complex $[CuL2]^{2+}$.

The helical complex crystallised in the triclinic space group P-1 with the two helical enantiomers in the unit cell. Each Cu(II) ion is in pseudo trigonal bipyrimidal geometry with each Cu(II) ion coordinated to two bpy motifs from both ligands and the N(amido) occupying the fifth coordination site. Elongated Cu-N (amido) distances (2.70 Å) are observed to the amido group on the second ligand. Unlike the [2 x 2] grid, the C=O (amido) groups are not involved in coordination and point to the exterior of the helix. Short intra-molecular, face-to-face, π-stacking interactions are observed between the pyridyl rings adjacent to the amido group on each ligand (centroid-centroid distances of 3.37 and 3.62 Å).

The potential interconvesion of the Cu(I)/ Cu(II) complexes discussed so far are presented in Scheme 2. It is proposed that on formation of the Cu(II) dihelical structure the ligand becomes susceptible to nucleophilic attack. Hydrolysis of one ligand renders the second ligand more labile. When one Cu(II) ion is fully bound and

the second partially bound to the hydrolysed ligand, a corner building block is created for the formation of the [2 x 2] grid incorporating bot **L1** and **L2**. The unhydrolysed ligand **L1**, eventually hydrolyses but a fully hydrolysed [2 x 2] grid has not been observed. The formation of the dihelical complex, $[Cu\mathbf{L2}]^{2+}$, is presumably sterically favoured as significant distortion of **L2** would be required in order to form a [2 x 2] grid.

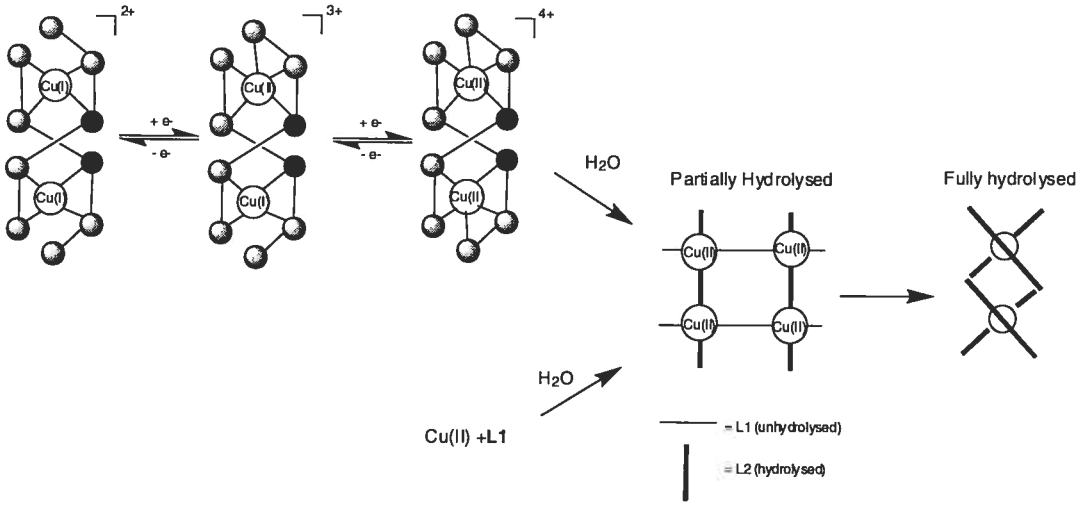

Scheme 7.2 Proposed interconversion of Cu(I) and Cu(II) complexes and access of the hydrolysed complexes.

7.3 Conclusions

A Cu(I) dihelical complex is synthesised with **L1** and is found to be significantly more stable to oxidation than the related complexes based on qnpy. The electron deficient triazine ring stabilises the low oxidation state and offers flexibility through dynamic processes in solution. The complex can be electrochemically oxidised to the homovalent Cu(II) dihelical complex. To date, it has not been possible to chemically synthesise this complex by either chemical oxidation of $[Cu\mathbf{L1}]_2^{2+}$ or directly from Cu(II) salts. Traces of water result in nucleophillic attack of **L1** to form the hydrolysed ligand **L2**. Partial hydrolysis results in the self assembly of [2 x 2] grids with two hydrolysed and 2 unhydrolysed ligands. The unhydrolysed ligands in the grid are then susceptible to nucleophilic attack and can rearrange to for the $[Cu\mathbf{L2}]^{2+}$ (Scheme 7.2).

7.4 Experimental

General Considerations

Electrochemical measurements were carried out in argon-purged acetonitrile at room temperature with a BAS CV50W multipurpose equipment interfaced to a PC. The working electrode was a Pt electrode. The counter electrode was a Pt wire, and the pseudo-reference electrode was a silver wire. The reference was set using an internal 1 mM ferrocene/ferrocinium sample at 395 mV vs SCE in acetonitrile and 432 mV in DMF. The concentration of the compounds was 1 mM. Tetrabutylammonium hexafluorophosphate (TBAP) was used as supporting electrolyte and its concentration was 0.10 M. Cyclic voltammograms were obtained at scan rates of 50, 100, 200, 500, 3000 and 5000 mV/s. For irreversible oxidation processes, the cathodic peak was used as E, and the anodic peak was used for irreversible reduction processes. The criteria for reversibility were the separation of approximately 60 mV between cathodic and anodic peaks, the close to unity ratio of the intensities of the cathodic and anodic currents, and the constancy of the peak potential on changing scan rate.

Synthetic procedures

L1: ^{n}BuLi (1.6M in hexanes, 1.90 mL, 3.04 mmol) was added dropwise to a stirred solution of $HNMe_2$ (2M in THF, 1.52 mL, 3.04 mmol) in anhydrous Et_2O (150 mL) under an inert atmosphere. The mixture was stirred for 20 minutes until a white suspension formed and *p*-bromobenzonitrile (0.50 g, 2.76 mmol) was added to the mixture. The solution was stirred for one hour at which time 6-cyano-2,2'-bipyridine (1.00 g, 5.52 mmol) was added. The triazine precipitated immediately and the mixture was stirred for a further five hours. The flask was opened to air and the mixture stirred for 30 minutes. The precipitate was collected by filtration and the solid was recrystallised from ethanol:water (100 mL). The precipitate was collected as a white solid and washed with diethylether (50 mL) and dried to yield **L1** as a white solid (0.62 g, 41%).

^{1}H NMR ($CDCl_3$, 400 MHz): 8.88-8.92 (m, 4H); 8.81 (d, J = 9 Hz, 2H); 8.74-8.76 (m, 4H); 8.16 (t , J = 8 Hz, 2H); 7.98 (t, J = 8 Hz, 2H); 7.80 (d, J = 8 Hz, 2H); 7.41-7.44 (m, 2H). ^{13}C {^{1}H} NMR ($CDCl_3$, 100 MHz): 171.86, 171.27, 156.38, 155.29, 152.27, 148.84, 137.72, 136.65, 134.24, 131.72, 130.48, 127.81, 124.62, 123.85, 123.52, 121.31. Anal. Calcd. For $C_{29}H_{18}N_7Br$: C, 63.98; H, 3.33; N, 18.01. Found C, 63.64; H, 3.70; N, 17.70.

$[Cu(L1)]_2^{2+}$: Ligand **L1** (54 mg, 0.099 mmol) was added to a colourless solution of $[Cu(MeCN)_4][PF_6]$ (37 mg, 0.099 mmol) in deoxygenated acetonitrile (30 mL) under N_2. The colourless solution immediately turned brown, indicative of complex formation. The mixture was stirred at room temperature for 30 minutes. Anhydrous diethyl ether (100 mL) was added and the product precipitated. The precipitate was collected and dried to afford $[Cu(\mathbf{L1})]_2$ as a brown solid (61 mg, 80% yield).

^{1}H NMR (400 MHz, CD_3CN): 8.42 (d, J= 9 Hz, 2H); 8.12-8.21 (m, 6H); 7.97 (d, J= 8 Hz, 2H); 7.90 (d, J = 8 Hz, 2H); 7.71 (td, J = 2Hz, 8 Hz, 2H); 7.66 (d, J = 5 Hz, 2H); 7.08 (dd, J = 5Hz, 1 Hz, 2H). ^{13}C NMR (100 MHz, CD_3CN): 122.10, 125.00, 125.05, 125.96, 128.27, 130.49, 132.13, 132.91, 137.29, 138.77, 147.42, 148.51, 150.62, 151.79, 169.44, 170.10. High Res ES-MS: $[M\text{-}PF_6]^+$: Calcd, 1356.9842. Found,

1356.98439. Anal. Calc. for $C_{58}H_{36}Br_2CuN_{14}(PF_6)_2.½(H_2O)$: C, 45.71; H, 2.51; N, 12.87 Found C, 45.66; H, 2.70; N, 13.02.

7.5 References

1. J.-P. Collin, V. Heitz and J.-P. Sauvage, *Top. Curr. Chem.*, 2005, **262**, 29.
2. J.-P. Sauvage, *Acc. Chem. Res.*, 1998, **31**, 611.
3. M. D. Ward, *Chem. Soc. Rev.*, 1995, **24**, 121.
4. A. M. Brouwer, C. Frochot, F. G. Gatti, D. A. Leigh, L. Mottier, F. Paolucci, S. Roffia and G. W. H. Wurpel, *Science*, 2001, **291**, 2124.
5. J. P. Collin, C. Dietrich-Buchecker, P. Gavina, M. C. Jimenez-Molero and J.-P. Sauvage, *Acc. Chem. Res.*, 2001, **34**, 477.
6. V. Amendola, L. Fabbrizzi and P. Pallavicini, *Coord. Chem. Rev.*, 2001, **216-217**, 435.
7. M. Barley, E. C. Constable, S. A. Corr, R. C. S. McQueen, J. C. Nutkins, M. D. Ward and M. G. B. Drew, *J. Chem. Soc., Dalton Trans.*,1988, 2655.
8. K. T. Potts, M. Keshavarz-K, F. S. Tham, H. D. Abruna and C. R. Arana, *Inorg. Chem.*, 1993, **32**, 4422.
9. E. A. Medlycott, I. Theobald and G. S. Hanan, *Eur. J. Inorg. Chem.*, 2005, 1223.
10. C. Dietrich-Buchecker, G. Rapenne, J.-P. Sauvage, A. De Cian and J. Fischer, *Chem. Eur. J.*, 1999, **5**, 1432.
11. E. C. Constable, M. J. Hannon and D. A. Tocher, *J. Chem. Soc., Dalton Trans.*, 1993, 1883.
12. PM3 energy minimized structure, Chem 3D.
13. K. T. Potts, M. Keshavarz-K, F. S. Tham, H. D. Abruna and C. Arana, *Inorg. Chem.*, 1993, **32**, 4450.
14. E. I. Lerner and S. J. Lippard, *J. Am. Chem. Soc.*, 1976, **98**, 5397.

Chapter VIII: Conclusions and Future Perspectives

There are many coordination complexes in the literature incorporating the 2,4,6-tris(2'-pyridyl)-1,3,5-triazine (2-tpt) ligand in a variety of coordination modes. Despite interesting structural, magnetic and photophysical properties, difficulties in functionalising this ligand limit optimisation of the properties associated with its complexes. In order to overcome these limitations, tridentate ligands based on the 2,4-di-(2'-pyridyl)-1,3,5-triazine core were developed with appended phenyl groups.[1, 2] The core objective of this thesis was to explore the varying properties of the functionalised triazine ligands and their coordination complexes. The subjects covered within this thesis are considerably varied but the synthetic procedure employed to obtain the triazine ligands is central to every chapter.

This chapter will serve as a summary for the important points discussed in chapters II-VII. Future perspectives within the context of each chapter will be discussed.

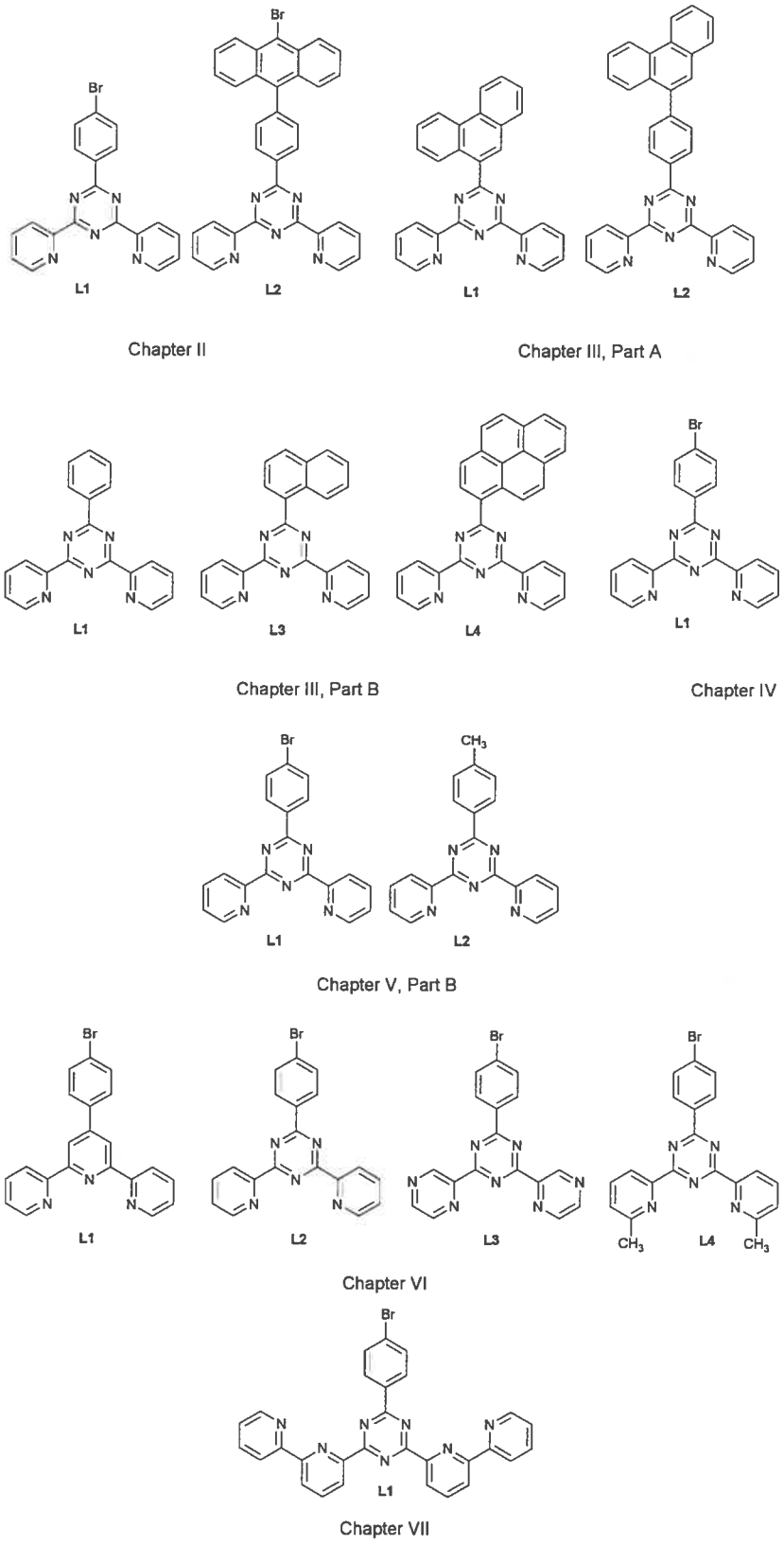

Chart 8.1 Triazine ligands synthesized throughout this thesis.

Chapter II describes the approaches previously taken to try and improve the photophysical properties of Ru(II) complexes of tridentate, tpy-based ligands. In part B, the synthesis and characterisation of the Ru(II) complex of the 2,4-di(2'-pyridyl)-6-(*p*-bromo-phenyl)-1,3,5-triazine (Br-dpt) ligand is reported.[3] 'Chemistry-on-the-complex' methodology is utilised in the synthesis of multichromophoric complexes incorporating secondary aromatic components. Interaction between the ^{3}MLCT state of the complex and the triplet state of the organic chromophore may be tuned through functionalisation. Introduction of a bromo-substitutent onto the anthracene chromophore lowers the energy of its triplet state, decreasing the energy difference between its triplet state and the ^{3}MLCT state of the complex. Subsequent mixing of the anthracene and ^{3}MLCT excited states prolongs the excited state lifetime to 54 ns from 13 ns at r.t. The heavy atom effect from the bromine in complex **2e** may comprimise the advantage of a multichromophoric effect by promoting access to the non-emissive anthracene triplet state. However, further modification of the anthracene unit by incorporating acetylene or cyano electron-withdrawing groups by a 'chemistry-on-the-complex' approach, may diminish this quenching process and improve photophysical properties significantly.

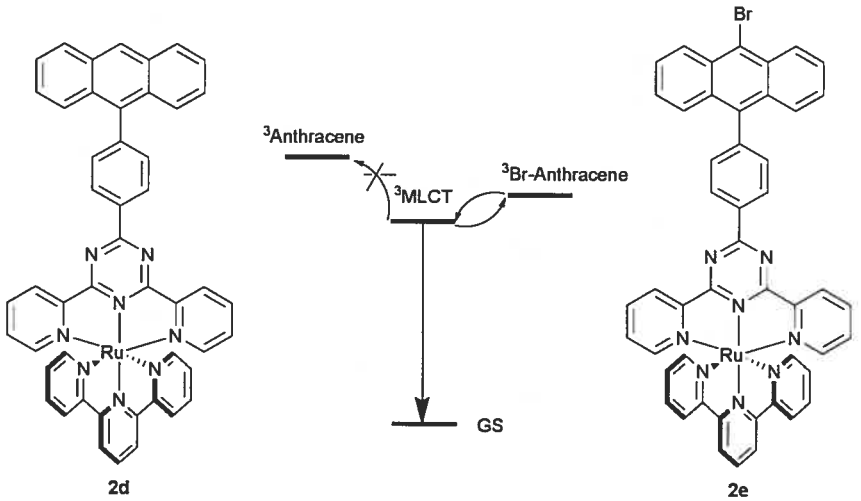

Figure 8.1 Emission from the triplet excited states of complexes **2d** and **2e**, chapter II, part B.

Poly-aromatics such as naphthyl-, phenanthryl- and pyrenyl- have been appended to the 2,4-di-(2'-pyridyl)-1,3,5-triazine core (chapter III).[4] The triazine ligands are emissive at room temperature in aerated solutions through ILCT emitting states (Figure 8.2). In contrast, the tpy-based ligands with appended polyaromatics are emissive through ligand-centred (LC) π- π^* states.[5] The Zn(II) complexes of the triazine ligands are emissive through ILCT states which are red-shifted compared to the ligands alone due to the enhanced electron-accepting capabilities of the triazine core upon metal-ion complexation. The ILCT excited states of the Ru(II) complexes are quenched by low-lying MLCT states.

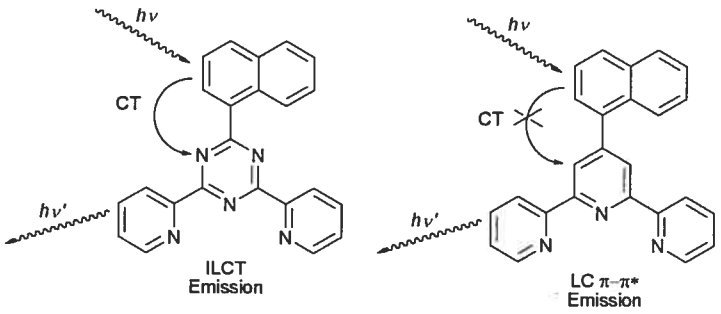

Figure 8.2 ILCT emission in naphthyl-based triazine ligands in contrast to the π- π^* LC emission in tpy-based complexes.[6]

Studies of Rh(III) complexes as potential sensitizers for light-harvesting applications are rare, primarily because they absorb mainly in the UV region and little in the visible.[7] Ru(II) complexes of triazine ligands absorb and emit at significantly lower energy than their tpy-based counter-parts,[2] and it was considered that the same low energy shift may be observed in Rh(III) complexes of triazine ligands. This could potentially pull the absorption energy into the visible region. The absorption energy of Rh(III) complexes of triazine-based ligands do in fact lie at lower energy than their tpy-analogues, with lower energy bands trailing into the visible region. The emission from Rh(III) complexes incorporating Br-dpt is dependant on the orthogonal ligand in heteroleptic complexes (Chapter IV). Excitation of heteroleptic complexes incorporating Br-tpt and an electron-poor, second orthogonal ligand gives rise to ligand centred excited states (LC π- π^* emissions). Excitation of a complex in which a

cyclometallating ligand is introduced orthogonal to Br-dpt results in an excited state with significant charge transfer character. However, all of the complexes are very weakly emissive with properties inferior to those reported for polypyridine complexes of Ir(III).[8] The synthesis of Ir(III) complexes incorporating the same ligand family may prove more effective in the quest for complexes with prolonged excited states (Figure 8.3).

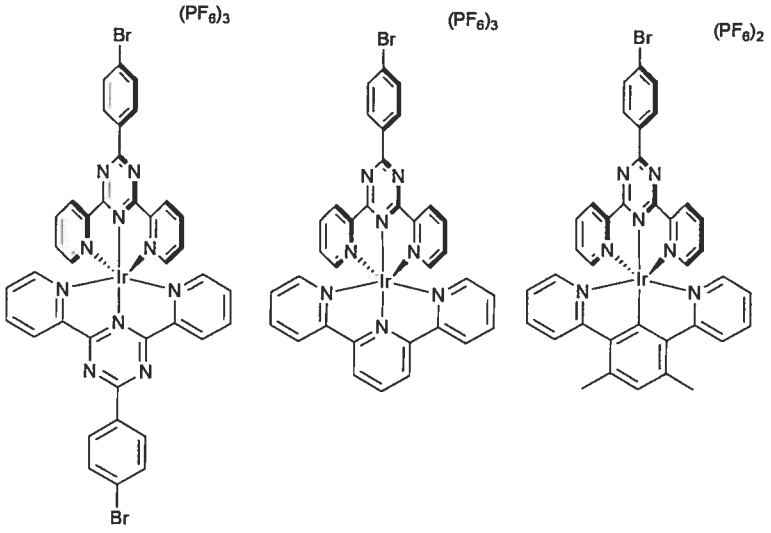

Figure 8.3 Ir(III) complexes of Br-dpt, analogous to the Rh(III) complexes synthesised in chapter IV.

The *p*-bromo-phenyl motif provides a method to gain directional control of cations in the solid state, as discussed in chapter V.[9] One-dimensional tapes form upon crystallisation of Fe(II), Co(II), Cu(II), Ru(II) and Rh(III) complexes incorporating Br-dpt. In Chapter VI, it was confirmed that the stabilising halogen-halogen interactions are not specific to this ligand and are observed in variations of the triazine ligand as well as in equivalent tpy-based systems. Removal of the Br-atom, as observed in complexes of the *p*-toluyl substituted triazine ligand, eliminates the one-dimensional arrangement. The formation of the polymeric arrangement of complexes incorporating Br-dpt is dependant on both the cation and solvent of crystallisation. Further solid state studies could be undertaken to gain an insight into how this aggregation could influence the solid state properties.

Aside from the Fe(II) complexes, the first row metal-complexes of Br-dpt examined in this work were paramagnetic in solution as determined by ^{1}H NMR. In solution, a broadening of ^{1}H signals closest to the metal-centre in the Fe(II) complex was observed indicating paramagnetic contributions to the largely diamagnetic ground state.[10] The solid state analysis indicated that the spin cross-over process was very gradual over the temperature range 4- 300 K and that the counter-ion had little effect on the magnetic properties when comparisons were made between PF_6^- and ClO_4^- salts. In order to apply such systems to the area of molecular switches, sharper spin cross-over behaviour is required. This may be achieved electronically or sterically. A sterically demanding ligand **(L4)** was developed with methyl substitution adjacent to the coordinating N atom. An elongation of the Fe-N distances force the Fe(II) cation into a high spin configuration, giving a complex with properties intermediate of $[Fe(\mathbf{L2})_2]^{2+}$ and $[Fe(\mathbf{L4})_2]^{2+}$ which may be ideal for applications as molecular switches. Substituting further from the site of coordination may also result in favourable spin cross-over behaviour. Alternatively, asymmetry in the 2,4-di-(2'-pyridyl)-1,3,5-triazine core may improve the spin cross-over behaviour (Figure 8.4, ligand E). However, a synthetic approach would need to be developed in order to obtain such asymmetric ligands as the current method may only be applied to symmetric ligands.

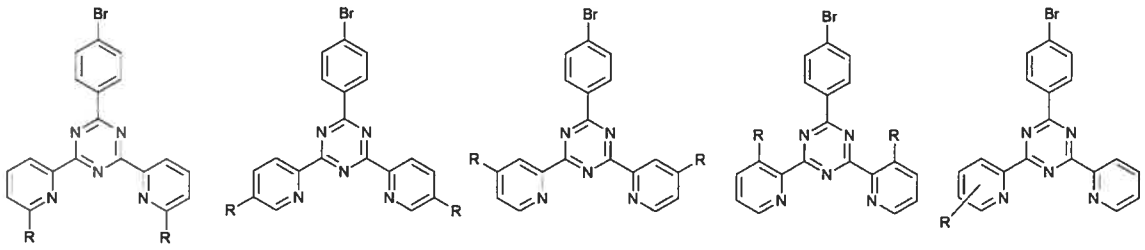

Figure 8.4 Triazine ligands with potentially improved spin cross-over properties.

The ^{1}H signals of the Fe(II) complex of *p*-bromophenyl-2,2':6':2''-terpyridine (Br-tpy) complexes were well resolved, indicating that the complex is low spin at room temperature. The solid state analyses indicated that the magnetic moment was highly dependant on the anion, with significantly greater paramagnetic contribution as the PF_6^- salt compared to the ClO_4^- salt. Cation-dependent magnetic moments were

previously observed in Fe(II) complexes of pyrazoyl-based tridentate ligands.[11] $Fe(tpy)_2^{2+}$ and its related complexes substituted on the 4'-position have always been considered diamagnetic and low spin at room temperature.[12, 13] Further solution and solid state studies are required to determine whether or not this effect is exclusive to Fe(II) complexes of (Br-tpy) (Figure 8.5).

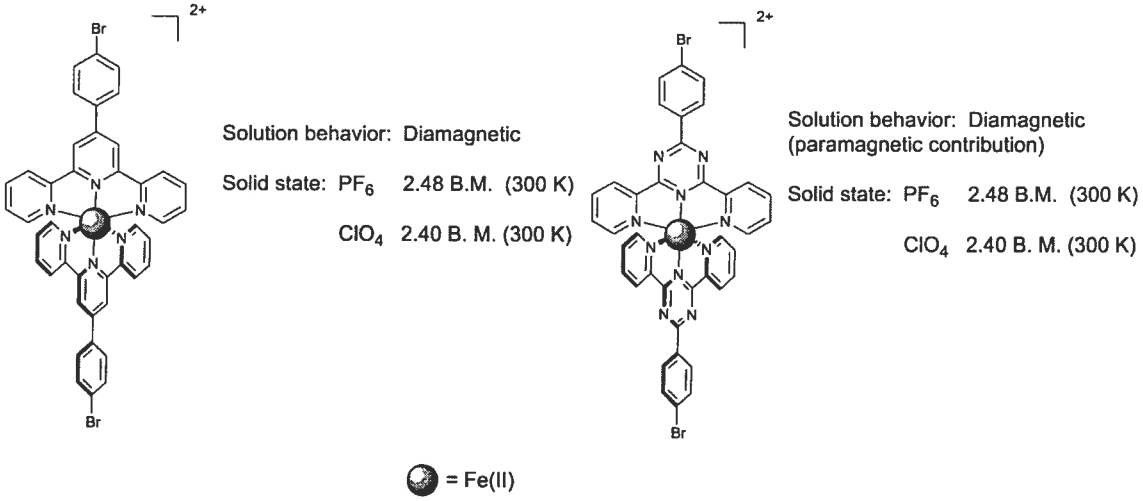

Figure 8.5 Summary of the magnetic properties of **1a** and **1b**, chapter VI.

Chapters II-VI discuss the properties of complexes synthesised with tridentate triazine-based ligands. In chapter VII, the synthesis of a potentially pentadentate coordinating ligand is discussed. However, the triazine-based ligand has potentially variable coordination modes, as outlined in Figure 8.6.

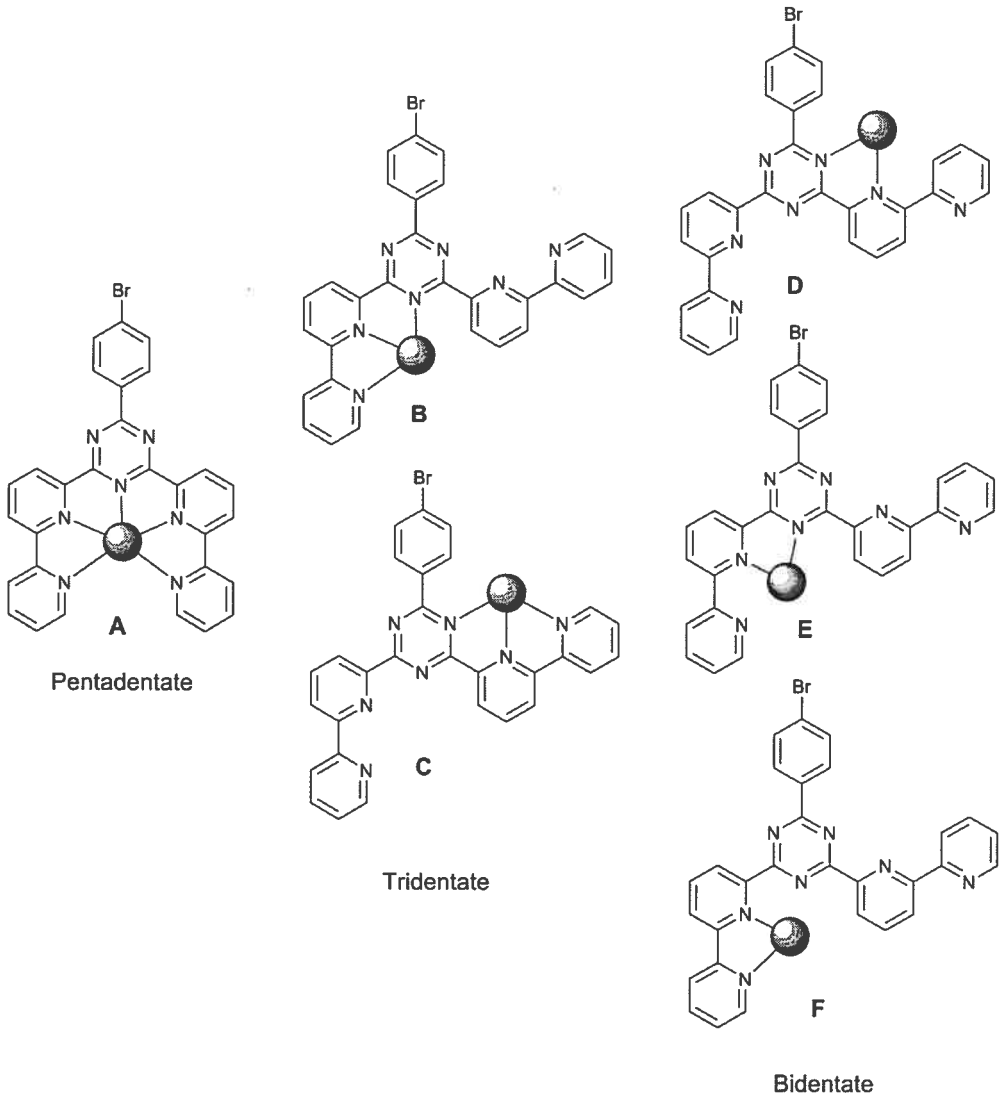

Figure 8.6 Potential coordination modes of the bppt ligand employed in chapter VII.

Complexation of the bis-(bipyridyl)-triazine (bppt) ligand with Cu(I) results in the formation of a dihelical, binuclear complex $[CuL]_2^{2+}$. The ^1H NMR indicated that the complex was bound in a symmetric fashion, suggesting that each Cu(I) ion coordinates to both ligands through bpy-type coordination (bidentate mode F, Figure 8.6). However, in the solid state, both bidentate coordination modes E and F were observed for each ligand in an asymmetric conformation. NOE experiments carried out in solution provided evidence of dynamic processes in which the solid state structure is the intermediate between the two symmetric conformations (Figure 8.7).

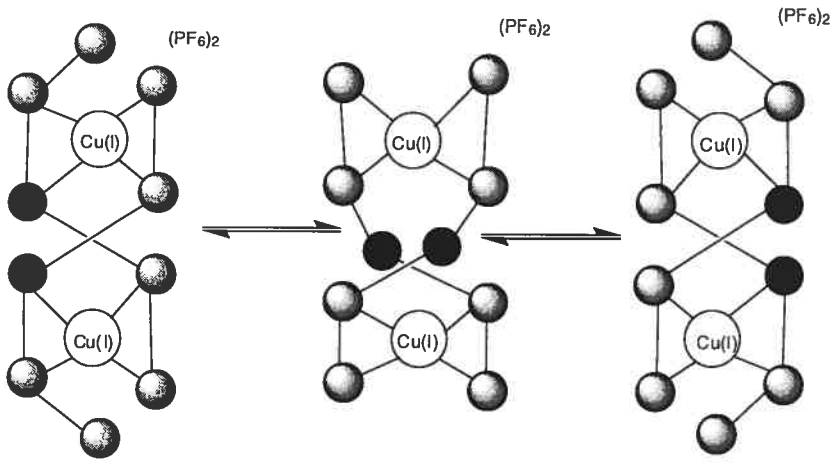

Figure 8.7 Dynamic processes in acetonitrile solutions of $[CuL]_2^{2+}$.

Cu(I) is considered a relatively unstable cation and can readily undergo oxidation to Cu(II) as observed with the synthesis of Cu(I) complexes of qnpy.[14] The presence of an electron deficient triazine ring in the complex $[CuL]_2^{2+}$ stabilises the electron rich Cu(I) cation enabling characterisation in solution and in the solid state. The dihelical complex undergoes two reversible oxidations to the Cu(II) homovalent complex. The reversibility suggests that these processes involve minimal reorganisation, so the ligand arrangement stays intact. However, chemical synthesis of the complex was not possible starting with a Cu(II) salt, as hydrolysis of the ligand is promoted in the presence of water. Partial hydrolysis yielded a [2 x 2] grid which then rearranges on full hydrolysis to form a binuclear, dihelical structure. Isolation of the ligand **L2** would offer a variety of coordination modes through *N,N*-bpy, *N*-amido and C=O-amido sites. Consequently, the application of this ligand offers huge scope to many areas of coordination chemistry.

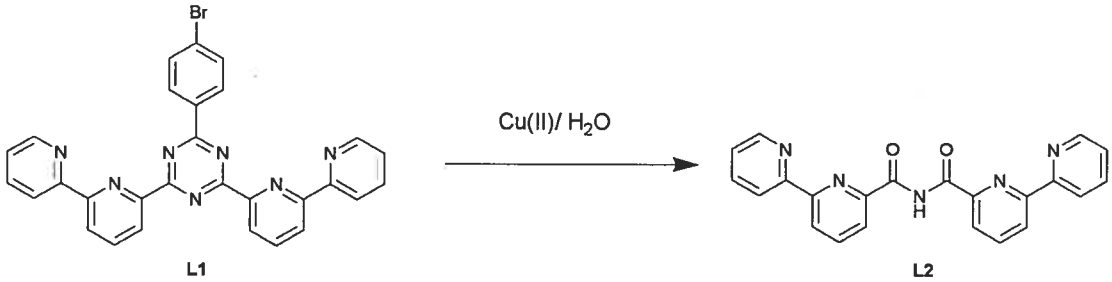

Figure 8.8 Cu(II) promoted hydrolysis of **L1** to **L2**

In summary, this thesis describes the synthesis and characterisation of a range of tridentate and pentadentate triazine-based ligands. The triazine ligand-forming reaction employed is both versatile and flexible. Changing the coordinated metal-ion provides a method to introduce gross changes in the properties of the complexes studied and determines the magnetic, photophysical or redox properties. Varying the triazine ligand has provided a means to fine-tune the magnetic, photophysical and redox properties of interest.

8.1` References

1. M. I. J. Polson, N. J. Taylor and G. S. Hanan, *Chem. Commun.*, 2002, 1356.
2. M. I. J. Polson, E. A. Medlycott, G. S. Hanan, L. Mikelsons, N. J. Taylor, M. Watanabe, Y. Tanaka, F. Loiseau, R. Passalacqua and S. Campagna, *Chem. Eur. J.*, 2004, **10**, 3640.
3. E. A. Medlycott, G. S. Hanan, F. Loiseau and S. Campagna, *Chem. Eur. J. Submitted for publication*, 2006.
4. E. A. Medlycott, G. S. Hanan, *Eur. J. Inorg. Chem., Submitted for publication*, 2006.
5. J. F. Michalec, S. A. Bejune, D. G. Cuttell, G. C. Summerton, J. A. Gertenbach, J. S. Field, R. J. Haines and D. R. McMillin, *Inorg. Chem.*, 2001, **40**, 2193.
6. M. E. Frink, S. D. Sprouse, H. A. Goodwin, R. J. Watts and P. C. Ford, *Inorg. Chem.*, 1988, **27**, 1283.
7. E. Baranoff, J.-P. Collin, L. Flamigni and J.-P. Sauvage, *Chem. Soc. Rev.*, 2004, **33**, 147.
8. E. A. Medlycott, G. S. Hanan, F. Loiseau and S. Campagna, *Manuscript in preparation*, 2006.
9. E. A. Medlycott, K. A. Udachin, G. S. Hanan, *Dalton Trans., Submitted for publication*, 2006.
10. E. A. Medlycott, G. S. Hanan, T. S.M. Abedin and L. K. Thompson, *Dalton Trans., Submitted for publication*, 2006.

11. V. A. Money, J. Elhaik, I. R. Evans, M. A. Halcrow and J. A. K. Howard, *Dalton Trans.*, 2004, 65.

12. E. C. Constable, G. Baum, E. Bill, R. Dyson, R. Van Eldik, D. Fenske, S. Kaderli, D. Morris, A. Neubrand, M. Neuburger, D. R. Smith, K. Wieghardt, M. Zehnder and A. D. Zuberbuhler, *Chem. Eur. J.*, 1999, **5**, 498.

13. J. Chambers, B. Eaves, D. Parker, R. Claxton, P. S. Ray and S. J. Slattery, *Inorg. Chim. Acta*, 2006, **359**, 2400.

14. M. Barley, E. C. Constable, S. A. Corr, R. C. S. McQueen, J. C. Nutkins, M. D. Ward and M. G. B. Drew, *J. Chem. Soc., Dalton Trans.*,1988, 2655.

Appendix

Appendix 1: CCDC N°'s for chapters II, III-part A, V and VI.

The crystallographic reports and cif files of the structures listed below are available from the Cambridge Crystallographic Data Centre (CCDC) and may be downloaded electronically from the internet site: www.ccdc.cam.ac.uk/data_request/cif. Alternatively, requests can be made by email at the following address: data_request@ccdc.cam.ac.uk.

Chapter	Complex/ Ligand	CCDC N°
Chapter II, Part B	**L2** $\{C_{33}H_{20}BrN_5\}$	**619166**
	2a $\{C_{38}H_{29}BrF_{12}N_{10}P_2Ru\}$	**619167**
	2b $\{C_{70}H_{57}BF_6N_{11}PRu\}$	**619168**
	3a $\{C_{38}H_{24}Br_2F_{12}N_{10}P_2Ru\}$	**619169**
Chapter III, Part A	**2a** $\{C_{58}H_{40}B_2F_8N_{12}Ru\}$	**616593**
	3a $\{C_{66}H_{42}F_{12}N_{10}P_2Ru\}$	**616592**
Chapter V	**L1** $\{C_{19}H_{16}BrN_5O_2\}$	**611633**
	1a $\{C_{38}H_{24}Br_2F_{12}FeN_{10}P_2\}$	**611625**
	1c $\{C_{40}H_{27}Br_2F_{12}N_{11}NiP_2\}$	**611626**
	1d $\{C_{40}H_{27}Br_2CuF_{12}N_{11}P_2\}$	**611627**
	1d' $\{C_{44}H_{36}Br_2CuF_{12}N_{10}O_2P_2\}$	**611628**
	2a $\{C_{40}H_{30}F_{12}FeN_{10}P_2\}$	**611629**
	2b $\{C_{40}H_{30}CoF_{12}N_{10}P_2\}$	**611630**
	2c $\{C_{40}H_{30}F_{12}N_{10}NiP_2\}$	**611631**
	2d $\{C_{40}H_{30}CuF_{12}N_{10}P_2\}$	**611632**
Chapter VI	$[Fe(\mathbf{1a})_2](PF_6)_2$ $\{C_{46}H_{34}Br_2F_{12}FeN_8P_2\}$	**619603**
	$[Fe(\mathbf{1b})_2](ClO_4)_2$ $\{C_{44}H_{33}Br_2Cl_2FeN_{13}O_8\}$	**619605**
	$[Fe(\mathbf{1c})_2](PF_6)(ClO_4)$ $\{C_{42}H_{32}Br_2ClF_6FeN_{18}O_4P\}$	**619604**
	$[Fe(\mathbf{1d})_2](ClO_4)_2$ $\{C_{46}H_{38}Br_2Cl_2FeN_{12}O_8\}$	**619606**

Appendix 2: Bromine and methyl contacts in Chapter V, part B.

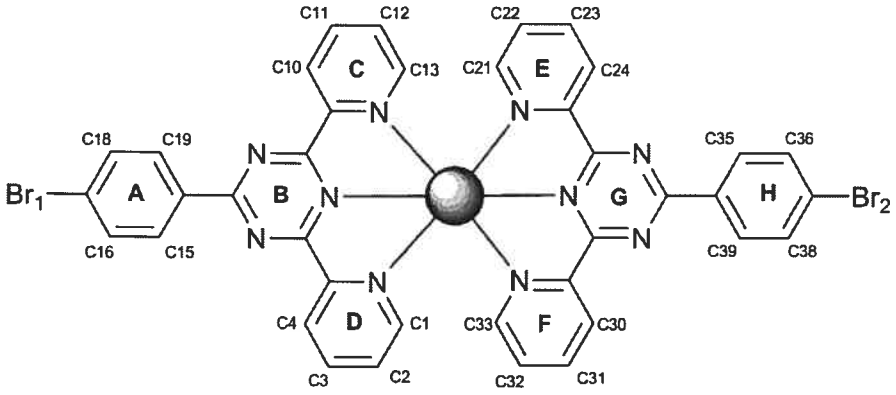

	1a	1c	1d	1d'
		Bond distances (Å)		
Br-Br	3.45	5.99	6.00	3.33
Br1 contacts	3.90 (C)	3.81 (C23)	3.95 (C32)	3.87 (C)
	3.93 (D)	3.50 (C, MeCN)	3.43 (C, MeCN)	3.94 (D)
	3.66 (C1)	3.15 (F, PF_6)	3.07 (F, PF_6)	3.82 (C13)
		3.71 (C12)	3.71 (C2)	3.59 (O, acetone)
Br2 contacts		3.99 (C)	3.94 (F)	
		3.88 (C15)	3.86 (C19)	
		3.34 (F, PF_6)	3.34 (F, PF_6)	
		3.67 (C22)	3.50 (C21)	

Table 1. Short Br contacts observed in complexes **1a-d** (centroid distances indicated by letter, edge contacts indicated by atom number and atom contacts indicated by name).

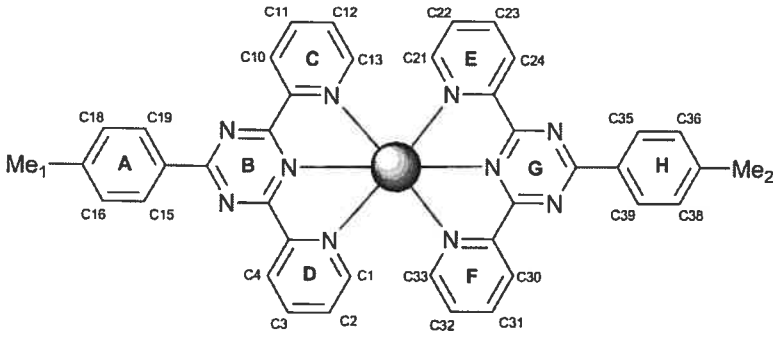

	1a	1b	1c	1d
	Bond distances (Å)			
Me-Me	6.22	5.52	5.49	5.64
Me1 contacts	3.59 (C30)	3.27 (F, PF_6)	3.27 (F, PF_6)	3.31 (F, PF_6)
	3.82 (N10)	3.85 (C)	3.87 (C)	3.90 (C)
	3.59 (C30)			
Me2 contacts	3.68 (C19)			

Table 2. Short Me contacts observed in complexes **1a-d** (centroid distances indicated by letter, edge contacts indicated by atom number and atom contacts indicated by name).

Appendix 3: Supplementary information for chapter II, part B.

Table 1. Crystal data and structure refinement for **L2 Chapter II, Part B.**

Empirical formula	C33 H20 Br N5
Formula weight	566.45
Temperature	100(2)K
Wavelength	1.54178 Å
Crystal system	Orthorhombic
Space group	P212121
Unit cell dimensions	a = 10.8718(3) Å α = 90° b = 15.0504(4) Å β = 90° c = 15.4806(5) Å γ = 90°
Volume	2533.01(13)Å^3
Z	4
Density (calculated)	1.485 g/cm^3
Absorption coefficient	2.471 mm^{-1}
F(000)	1152
Crystal size	0.22 x 0.12 x 0.08 mm
Theta range for data collection	4.10 to 58.94°
Index ranges	$-11 \le h \le 11$, $-16 \le k \le 16$, $-16 \le \ell \le 17$
Reflections collected	34701
Independent reflections	3599 [R_{int} = 0.044]
Absorption correction	Semi-empirical from equivalents
Max. and min. transmission	0.8600 and 0.8600
Refinement method	Full-matrix least-squares on F^2
Data / restraints / parameters	3599 / 0 / 352
Goodness-of-fit on F^2	1.004
Final R indices [I>2sigma(I)]	R1 = 0.0392, wR_2 = 0.0963
R indices (all data)	R1 = 0.0460, wR_2 = 0.1008
Absolute structure parameter	-0.052(19)
Largest diff. peak and hole	0.498 and -0.371 e/Å^3

Table 2. Bond lengths [Å] and angles [°] for **L2 Chapter II, Part B.**

Br(1)-C(27)	1.916(4)
N(1)-C(5)	1.329(5)
N(1)-C(1)	1.336(5)
N(2)-C(6)	1.334(5)
N(2)-C(8)	1.352(5)
N(3)-C(9)	1.331(5)
N(3)-C(13)	1.331(5)
N(4)-C(6)	1.327(4)
N(4)-C(7)	1.343(5)
N(5)-C(8)	1.322(4)
N(5)-C(7)	1.355(5)
C(1)-C(2)	1.373(6)
C(2)-C(3)	1.368(6)
C(3)-C(4)	1.379(6)
C(4)-C(5)	1.398(5)
C(5)-C(6)	1.489(5)
C(7)-C(14)	1.484(5)
C(8)-C(9)	1.500(5)
C(9)-C(10)	1.389(5)
C(10)-C(11)	1.372(6)
C(11)-C(12)	1.369(6)
C(12)-C(13)	1.374(6)
C(14)-C(15)	1.383(5)
C(14)-C(19)	1.388(5)
C(15)-C(16)	1.376(5)
C(16)-C(17)	1.411(5)
C(17)-C(18)	1.397(5)
C(17)-C(20)	1.497(5)
C(18)-C(19)	1.382(5)
C(20)-C(33)	1.404(5)
C(20)-C(21)	1.410(5)
C(21)-C(22)	1.426(5)
C(21)-C(26)	1.451(5)
C(22)-C(23)	1.359(5)
C(23)-C(24)	1.415(6)
C(24)-C(25)	1.349(6)
C(25)-C(26)	1.429(6)
C(26)-C(27)	1.386(6)
C(27)-C(28)	1.396(6)
C(28)-C(29)	1.414(6)
C(28)-C(33)	1.449(5)
C(29)-C(30)	1.354(6)
C(30)-C(31)	1.423(6)
C(31)-C(32)	1.359(6)
C(32)-C(33)	1.428(5)
C(5)-N(1)-C(1)	117.8(4)
C(6)-N(2)-C(8)	114.6(3)
C(9)-N(3)-C(13)	116.3(3)
C(6)-N(4)-C(7)	114.6(3)
C(8)-N(5)-C(7)	115.0(3)
N(1)-C(1)-C(2)	123.9(4)
C(3)-C(2)-C(1)	118.1(4)
C(2)-C(3)-C(4)	119.5(4)
C(3)-C(4)-C(5)	118.6(4)
N(1)-C(5)-C(4)	122.1(3)
N(1)-C(5)-C(6)	117.5(3)
C(4)-C(5)-C(6)	120.4(4)
N(4)-C(6)-N(2)	125.9(3)
N(4)-C(6)-C(5)	117.2(3)
N(2)-C(6)-C(5)	116.9(3)
N(4)-C(7)-N(5)	124.7(3)
N(4)-C(7)-C(14)	118.0(3)
N(5)-C(7)-C(14)	117.3(3)
N(5)-C(8)-N(2)	125.0(3)
N(5)-C(8)-C(9)	117.8(3)
N(2)-C(8)-C(9)	117.2(3)
N(3)-C(9)-C(10)	123.4(4)
N(3)-C(9)-C(8)	116.2(3)
C(10)-C(9)-C(8)	120.4(4)
C(11)-C(10)-C(9)	118.1(4)
C(12)-C(11)-C(10)	119.7(4)
C(11)-C(12)-C(13)	117.7(4)
N(3)-C(13)-C(12)	124.7(4)
C(15)-C(14)-C(19)	118.6(3)
C(15)-C(14)-C(7)	120.4(3)
C(19)-C(14)-C(7)	120.9(3)
C(16)-C(15)-C(14)	121.8(3)
C(15)-C(16)-C(17)	119.7(4)
C(18)-C(17)-C(16)	118.6(4)
C(18)-C(17)-C(20)	121.2(3)
C(16)-C(17)-C(20)	120.2(3)
C(19)-C(18)-C(17)	120.4(4)
C(18)-C(19)-C(14)	120.9(3)
C(33)-C(20)-C(21)	121.1(3)
C(33)-C(20)-C(17)	119.8(3)
C(21)-C(20)-C(17)	119.1(3)
C(20)-C(21)-C(22)	122.4(3)
C(20)-C(21)-C(26)	119.6(3)
C(22)-C(21)-C(26)	118.0(3)
C(23)-C(22)-C(21)	121.5(4)
C(22)-C(23)-C(24)	120.1(4)
C(25)-C(24)-C(23)	121.1(4)
C(24)-C(25)-C(26)	121.2(4)
C(27)-C(26)-C(25)	124.3(4)
C(27)-C(26)-C(21)	117.7(4)
C(25)-C(26)-C(21)	118.0(4)
C(26)-C(27)-C(28)	124.3(3)
C(26)-C(27)-BR1	118.2(3)
C(28)-C(27)-BR1	117.5(3)
C(27)-C(28)-C(29)	124.1(4)
C(27)-C(28)-C(33)	117.6(4)
C(29)-C(28)-C(33)	118.2(4)
C(30)-C(29)-C(28)	121.6(4)
C(29)-C(30)-C(31)	120.9(4)
C(32)-C(31)-C(30)	119.6(4)
C(31)-C(32)-C(33)	121.6(4)
C(20)-C(33)-C(32)	122.3(3)
C(20)-C(33)-C(28)	119.6(4)
C(32)-C(33)-C(28)	118.1(4)

Table 1. Crystal data and structure refinement for **2a, Chapter II, Part B.**

Empirical formula	C38 H29 Br F12 N10 P2 Ru
Formula weight	1096.63
Temperature	220(2)K
Wavelength	1.54178 Å
Crystal system	Triclinic
Space group	P-1
Unit cell dimensions	a = 9.2785(2) Å α = 98.7180(10)° b = 12.6372(3) Å β = 91.8380(10)° c = 36.1243(6) Å γ = 92.405(2)°
Volume	4179.93(15)Å^3
Z	4
Density (calculated)	1.743 g/cm^3
Absorption coefficient	5.761 mm^{-1}
F(000)	2176
Crystal size	0.70 x 0.07 x 0.07 mm
Theta range for data collection	1.24 to 72.99°
Index ranges	$-10 \le h \le 8$, $-15 \le k \le 15$, $-44 \le \ell \le 44$
Reflections collected	50892
Independent reflections	16008 [R_{int} = 0.036]
Absorption correction	Semi-empirical from equivalents
Max. and min. transmission	0.7500 and 0.4300
Refinement method	Full-matrix least-squares on F^2
Data / restraints / parameters	16008 / 135 / 1209
Goodness-of-fit on F^2	0.914
Final R indices [I>2sigma(I)]	R_1 = 0.0522, wR_2 = 0.0637
R indices (all data)	R_1 = 0.1060, wR_2 = 0.0702
Largest diff. peak and hole	0.833 and -0.713 e/Å^3

Table 2. Bond lengths [Å] and angles [°] for **2a, Chapter II, Part B.**

Ru(1)-N(2)	1.957(4)	Ru(2)-N(14)	2.081(4)
Ru(1)-N(7)	1.986(4)	Ru(2)-N(11)	2.083(4)
Ru(1)-N(6)	2.065(4)	Ru(2)-N(9)	2.106(4)
Ru(1)-N(8)	2.075(4)	N(9)-C(35)	1.320(5)
Ru(1)-N(1)	2.089(4)	N(9)-C(39)	1.371(5)
Ru(1)-N(3)	2.101(4)	N(10)-C(42)	1.338(5)
N(1)-C(1)	1.321(5)	N(10)-C(40)	1.357(5)
N(1)-C(5)	1.377(5)	N(11)-C(47)	1.325(5)
N(2)-C(6)	1.339(5)	N(11)-C(43)	1.381(5)
N(2)-C(8)	1.341(5)	N(12)-C(40)	1.315(5)
N(3)-C(13)	1.327(5)	N(12)-C(41)	1.354(5)
N(3)-C(9)	1.371(5)	N(13)-C(42)	1.323(5)
N(4)-C(6)	1.316(5)	N(13)-C(41)	1.346(5)
N(4)-C(7)	1.353(5)	N(14)-C(54)	1.335(5)
N(5)-C(8)	1.332(5)	N(14)-C(58)	1.371(5)
N(5)-C(7)	1.347(5)	N(15)-C(63)	1.340(6)
N(6)-C(20)	1.326(5)	N(15)-C(59)	1.361(6)
N(6)-C(24)	1.365(5)	N(16)-C(68)	1.321(6)
N(7)-C(25)	1.340(5)	N(16)-C(64)	1.371(5)
N(7)-C(29)	1.355(5)	C(35)-C(36)	1.395(6)
N(8)-C(34)	1.332(5)	C(36)-C(37)	1.382(6)
N(8)-C(30)	1.379(5)	C(37)-C(38)	1.386(6)
C(1)-C(2)	1.388(6)	C(38)-C(39)	1.380(6)
C(2)-C(3)	1.379(6)	C(39)-C(40)	1.478(6)
C(3)-C(4)	1.388(6)	C(41)-C(48)	1.490(6)
C(4)-C(5)	1.380(5)	C(42)-C(43)	1.471(6)
C(5)-C(6)	1.477(6)	C(43)-C(44)	1.368(6)
C(7)-C(14)	1.475(5)	C(44)-C(45)	1.382(6)
C(8)-C(9)	1.464(6)	C(45)-C(46)	1.369(6)
C(9)-C(10)	1.375(6)	C(46)-C(47)	1.380(6)
C(10)-C(11)	1.365(6)	C(48)-C(53)	1.378(6)
C(11)-C(12)	1.375(6)	C(48)-C(49)	1.381(6)
C(12)-C(13)	1.388(6)	C(49)-C(50)	1.391(6)
C(14)-C(19)	1.380(6)	C(50)-C(51)	1.371(6)
C(14)-C(15)	1.387(6)	C(51)-C(52)	1.383(6)
C(15)-C(16)	1.374(6)	C(51)-Br(2)	1.906(5)
C(16)-C(17)	1.355(6)	C(52)-C(53)	1.378(6)
C(17)-C(18)	1.375(6)	C(54)-C(55)	1.378(6)
C(17)-Br(1)	1.891(5)	C(55)-C(56)	1.384(6)
C(18)-C(19)	1.380(6)	C(56)-C(57)	1.362(6)
C(20)-C(21)	1.384(6)	C(57)-C(58)	1.390(6)
C(21)-C(22)	1.372(6)	C(58)-C(59)	1.447(6)
C(22)-C(23)	1.379(6)	C(59)-C(60)	1.385(6)
C(23)-C(24)	1.369(6)	C(60)-C(61)	1.363(7)
C(24)-C(25)	1.469(6)	C(61)-C(62)	1.388(7)
C(25)-C(26)	1.401(6)	C(62)-C(63)	1.391(6)
C(26)-C(27)	1.376(6)	C(63)-C(64)	1.461(7)
C(27)-C(28)	1.366(6)	C(64)-C(65)	1.384(6)
C(28)-C(29)	1.381(6)	C(65)-C(66)	1.379(7)
C(29)-C(30)	1.463(6)	C(66)-C(67)	1.364(6)
C(30)-C(31)	1.385(6)	C(67)-C(68)	1.386(6)
C(31)-C(32)	1.373(6)	P(1)-F(12)	1.588(3)
C(32)-C(33)	1.375(6)	P(1)-F(16)	1.596(3)
C(33)-C(34)	1.387(6)	P(1)-F(14)	1.597(3)
Ru(2)-N(10)	1.966(4)	P(1)-F(15)	1.597(3)
Ru(2)-N(15)	1.985(4)	P(1)-F(11)	1.599(3)
Ru(2)-N(16)	2.067(4)	P(1)-F(13)	1.606(3)

P(2)-F(25)	1.553(3)	C(25)-N(7)-RU1	119.3(4)
P(2)-F(24)	1.558(3)	C(29)-N(7)-RU1	118.9(4)
P(2)-F(21)	1.561(3)	C(34)-N(8)-C(30)	118.5(5)
P(2)-F(22)	1.575(3)	C(34)-N(8)-RU1	127.6(4)
P(2)-F(26)	1.577(4)	C(30)-N(8)-RU1	113.8(4)
P(2)-F(23)	1.585(3)	N(1)-C(1)-C(2)	122.7(5)
P(3)-F(35)	1.587(3)	C(3)-C(2)-C(1)	119.6(5)
P(3)-F(33)	1.589(3)	C(2)-C(3)-C(4)	118.6(5)
P(3)-F(34)	1.594(3)	C(5)-C(4)-C(3)	119.1(5)
P(3)-F(32)	1.596(3)	N(1)-C(5)-C(4)	122.0(5)
P(3)-F(36)	1.601(3)	N(1)-C(5)-C(6)	114.8(4)
P(3)-F(31)	1.604(3)	C(4)-C(5)-C(6)	123.1(5)
P(4)-F(44)	1.43(11)	N(4)-C(6)-N(2)	123.8(5)
P(4)-F(45)	1.54(13)	N(4)-C(6)-C(5)	124.3(5)
P(4)-F(43)	1.57(13)	N(2)-C(6)-C(5)	111.8(4)
P(4)-F(46)	1.59(13)	N(5)-C(7)-N(4)	125.2(5)
P(4)-F(41)	1.63(12)	N(5)-C(7)-C(14)	118.0(5)
P(4)-F(42)	1.70(11)	N(4)-C(7)-C(14)	116.7(5)
P(5)-F(51)	1.45(11)	N(5)-C(8)-N(2)	123.0(5)
P(5)-F(55)	1.53(11)	N(5)-C(8)-C(9)	123.9(5)
P(5)-F(54)	1.54(12)	N(2)-C(8)-C(9)	113.0(5)
P(5)-F(53)	1.58(11)	N(3)-C(9)-C(10)	121.7(5)
P(5)-F(52)	1.62(12)	N(3)-C(9)-C(8)	113.9(5)
P(5)-F(56)	1.71(11)	C(10)-C(9)-C(8)	124.4(5)
N(71)-C(72)	1.064(9)	C(11)-C(10)-C(9)	120.0(5)
C(72)-C(73)	1.443(8)	C(10)-C(11)-C(12)	118.9(5)
N(81)-C(82)	1.080(15)	C(11)-C(12)-C(13)	119.0(5)
C(82)-C(83)	1.466(11)	N(3)-C(13)-C(12)	123.0(5)
N(91)-C(92)	1.108(7)	C(19)-C(14)-C(15)	117.6(5)
C(92)-C(93)	1.470(7)	C(19)-C(14)-C(7)	121.1(5)
C(101)-C(102)	1.443	C(15)-C(14)-C(7)	121.1(5)
C(102)-N(103)	1.1405	C(16)-C(15)-C(14)	121.0(5)
N(2)-RU1-N(7)	177.00(17)	C(17)-C(16)-C(15)	120.0(5)
N(2)-RU1-N(6)	104.44(15)	C(16)-C(17)-C(18)	120.9(5)
N(7)-RU1-N(6)	78.48(17)	C(16)-C(17)-BR1	118.7(4)
N(2)-RU1-N(8)	98.18(16)	C(18)-C(17)-BR1	120.4(4)
N(7)-RU1-N(8)	78.92(17)	C(17)-C(18)-C(19)	118.8(5)
N(6)-RU1-N(8)	157.34(16)	C(18)-C(19)-C(14)	121.6(5)
N(2)-RU1-N(1)	78.16(15)	N(6)-C(20)-C(21)	122.9(5)
N(7)-RU1-N(1)	102.60(15)	C(22)-C(21)-C(20)	118.8(6)
N(6)-RU1-N(1)	91.06(15)	C(21)-C(22)-C(23)	119.0(6)
N(8)-RU1-N(1)	92.39(15)	C(24)-C(23)-C(22)	119.7(5)
N(2)-RU1-N(3)	77.68(15)	N(6)-C(24)-C(23)	121.5(5)
N(7)-RU1-N(3)	101.70(15)	N(6)-C(24)-C(25)	114.7(5)
N(6)-RU1-N(3)	91.69(15)	C(23)-C(24)-C(25)	123.8(5)
N(8)-RU1-N(3)	94.33(14)	N(7)-C(25)-C(26)	120.0(5)
N(1)-RU1-N(3)	155.60(15)	N(7)-C(25)-C(24)	113.0(5)
C(1)-N(1)-C(5)	118.0(4)	C(26)-C(25)-C(24)	127.0(5)
C(1)-N(1)-RU1	128.4(4)	C(27)-C(26)-C(25)	118.3(5)
C(5)-N(1)-RU1	113.5(3)	C(28)-C(27)-C(26)	120.7(5)
C(6)-N(2)-C(8)	117.6(4)	C(27)-C(28)-C(29)	119.7(6)
C(6)-N(2)-RU1	121.2(3)	N(7)-C(29)-C(28)	119.4(5)
C(8)-N(2)-RU1	121.0(3)	N(7)-C(29)-C(30)	113.1(5)
C(13)-N(3)-C(9)	117.5(4)	C(28)-C(29)-C(30)	127.5(6)
C(13)-N(3)-RU1	128.3(4)	N(8)-C(30)-C(31)	121.1(5)
C(9)-N(3)-RU1	114.2(3)	N(8)-C(30)-C(29)	115.2(5)
C(6)-N(4)-C(7)	115.1(4)	C(31)-C(30)-C(29)	123.6(5)
C(8)-N(5)-C(7)	115.2(4)	C(32)-C(31)-C(30)	118.5(6)
C(20)-N(6)-C(24)	118.1(5)	C(31)-C(32)-C(33)	121.2(6)
C(20)-N(6)-RU1	127.3(4)	C(32)-C(33)-C(34)	117.7(6)
C(24)-N(6)-RU1	114.5(4)	N(8)-C(34)-C(33)	122.9(5)
C(25)-N(7)-C(29)	121.7(5)	N(10)-RU2-N(15)	174.00(17)

N(10)-RU2-N(16)	104.64(16)	C(50)-C(51)-C(52)	121.9(5)
N(15)-RU2-N(16)	78.59(18)	C(50)-C(51)-BR2	118.6(5)
N(10)-RU2-N(14)	97.80(16)	C(52)-C(51)-BR2	119.5(4)
N(15)-RU2-N(14)	79.04(17)	C(53)-C(52)-C(51)	118.3(5)
N(16)-RU2-N(14)	157.55(16)	C(48)-C(53)-C(52)	120.8(5)
N(10)-RU2-N(11)	78.67(16)	N(14)-C(54)-C(55)	124.0(5)
N(15)-RU2-N(11)	96.40(15)	C(54)-C(55)-C(56)	117.8(6)
N(16)-RU2-N(11)	89.92(15)	C(57)-C(56)-C(55)	119.5(6)
N(14)-RU2-N(11)	94.31(15)	C(56)-C(57)-C(58)	120.4(6)
N(10)-RU2-N(9)	77.26(16)	N(14)-C(58)-C(57)	120.5(5)
N(15)-RU2-N(9)	107.84(15)	N(14)-C(58)-C(59)	116.0(5)
N(16)-RU2-N(9)	92.69(15)	C(57)-C(58)-C(59)	123.5(6)
N(14)-RU2-N(9)	92.45(15)	N(15)-C(59)-C(60)	118.8(5)
N(11)-RU2-N(9)	155.67(16)	N(15)-C(59)-C(58)	113.3(5)
C(35)-N(9)-C(39)	118.5(5)	C(60)-C(59)-C(58)	127.9(6)
C(35)-N(9)-RU2	127.3(4)	C(61)-C(60)-C(59)	120.4(6)
C(39)-N(9)-RU2	114.2(3)	C(60)-C(61)-C(62)	120.0(6)
C(42)-N(10)-C(40)	117.1(4)	C(61)-C(62)-C(63)	118.9(6)
C(42)-N(10)-RU2	120.3(3)	N(15)-C(63)-C(62)	119.9(6)
C(40)-N(10)-RU2	122.4(3)	N(15)-C(63)-C(64)	113.1(5)
C(47)-N(11)-C(43)	117.7(4)	C(62)-C(63)-C(64)	127.0(6)
C(47)-N(11)-RU2	129.1(4)	N(16)-C(64)-C(65)	120.6(6)
C(43)-N(11)-RU2	113.1(3)	N(16)-C(64)-C(63)	115.0(5)
C(40)-N(12)-C(41)	115.1(5)	C(65)-C(64)-C(63)	124.4(6)
C(42)-N(13)-C(41)	114.6(4)	C(66)-C(65)-C(64)	120.4(6)
C(54)-N(14)-C(58)	117.9(5)	C(67)-C(66)-C(65)	118.6(6)
C(54)-N(14)-RU2	129.0(4)	C(66)-C(67)-C(68)	118.6(6)
C(58)-N(14)-RU2	113.1(4)	N(16)-C(68)-C(67)	124.0(6)
C(63)-N(15)-C(59)	122.1(5)	F(12)-P(1)-F(16)	90.40(17)
C(63)-N(15)-RU2	119.0(4)	F(12)-P(1)-F(14)	179.9(2)
C(59)-N(15)-RU2	118.2(4)	F(16)-P(1)-F(14)	89.49(17)
C(68)-N(16)-C(64)	117.7(5)	F(12)-P(1)-F(15)	90.47(18)
C(68)-N(16)-RU2	128.4(4)	F(16)-P(1)-F(15)	90.55(18)
C(64)-N(16)-RU2	113.9(4)	F(14)-P(1)-F(15)	89.45(18)
N(9)-C(35)-C(36)	122.8(5)	F(12)-P(1)-F(11)	89.94(17)
C(37)-C(36)-C(35)	118.4(5)	F(16)-P(1)-F(11)	178.9(2)
C(36)-C(37)-C(38)	119.7(5)	F(14)-P(1)-F(11)	90.18(17)
C(39)-C(38)-C(37)	118.5(5)	F(15)-P(1)-F(11)	90.44(17)
N(9)-C(39)-C(38)	122.0(5)	F(12)-P(1)-F(13)	89.57(18)
N(9)-C(39)-C(40)	115.4(5)	F(16)-P(1)-F(13)	88.77(17)
C(38)-C(39)-C(40)	122.6(5)	F(14)-P(1)-F(13)	90.50(17)
N(12)-C(40)-N(10)	123.3(5)	F(15)-P(1)-F(13)	179.3(2)
N(12)-C(40)-C(39)	126.1(5)	F(11)-P(1)-F(13)	90.23(17)
N(10)-C(40)-C(39)	110.6(5)	F(25)-P(2)-F(24)	89.8(2)
N(13)-C(41)-N(12)	125.7(5)	F(25)-P(2)-F(21)	91.6(2)
N(13)-C(41)-C(48)	116.4(5)	F(24)-P(2)-F(21)	89.7(2)
N(12)-C(41)-C(48)	117.9(5)	F(25)-P(2)-F(22)	91.3(2)
N(13)-C(42)-N(10)	124.1(5)	F(24)-P(2)-F(22)	179.0(3)
N(13)-C(42)-C(43)	123.6(5)	F(21)-P(2)-F(22)	90.4(2)
N(10)-C(42)-C(43)	112.3(5)	F(25)-P(2)-F(26)	89.6(2)
C(44)-C(43)-N(11)	121.9(5)	F(24)-P(2)-F(26)	90.4(2)
C(44)-C(43)-C(42)	122.9(5)	F(21)-P(2)-F(26)	178.8(3)
N(11)-C(43)-C(42)	115.1(5)	F(22)-P(2)-F(26)	89.5(2)
C(43)-C(44)-C(45)	118.7(5)	F(25)-P(2)-F(23)	178.5(3)
C(46)-C(45)-C(44)	119.8(5)	F(24)-P(2)-F(23)	91.2(2)
C(45)-C(46)-C(47)	118.8(5)	F(21)-P(2)-F(23)	89.5(2)
N(11)-C(47)-C(46)	123.0(5)	F(22)-P(2)-F(23)	87.8(2)
C(53)-C(48)-C(49)	120.2(5)	F(26)-P(2)-F(23)	89.2(2)
C(53)-C(48)-C(41)	120.0(5)	F(35)-P(3)-F(33)	179.7(2)
C(49)-C(48)-C(41)	119.8(5)	F(35)-P(3)-F(34)	89.55(17)
C(48)-C(49)-C(50)	119.6(5)	F(33)-P(3)-F(34)	90.14(18)
C(51)-C(50)-C(49)	119.0(5)	F(35)-P(3)-F(32)	90.44(17)

F(33)-P(3)-F(32)	89.87(17)	F(43)-P(4)-F(42)	86(6)
F(34)-P(3)-F(32)	179.7(2)	F(46)-P(4)-F(42)	86(6)
F(35)-P(3)-F(36)	89.96(17)	F(41)-P(4)-F(42)	83(5)
F(33)-P(3)-F(36)	90.07(18)	F(51)-P(5)-F(55)	93(6)
F(34)-P(3)-F(36)	90.47(17)	F(51)-P(5)-F(54)	97(6)
F(32)-P(3)-F(36)	89.23(17)	F(55)-P(5)-F(54)	93(6)
F(35)-P(3)-F(31)	90.43(18)	F(51)-P(5)-F(53)	93(6)
F(33)-P(3)-F(31)	89.53(17)	F(55)-P(5)-F(53)	170(8)
F(34)-P(3)-F(31)	89.37(17)	F(54)-P(5)-F(53)	92(6)
F(32)-P(3)-F(31)	90.94(17)	F(51)-P(5)-F(52)	92(7)
F(36)-P(3)-F(31)	179.6(2)	F(55)-P(5)-F(52)	88(6)
F(44)-P(4)-F(45)	95(7)	F(54)-P(5)-F(52)	171(8)
F(44)-P(4)-F(43)	93(7)	F(53)-P(5)-F(52)	85(6)
F(45)-P(4)-F(43)	170(8)	F(51)-P(5)-F(56)	175(9)
F(44)-P(4)-F(46)	98(7)	F(55)-P(5)-F(56)	89(5)
F(45)-P(4)-F(46)	92(6)	F(54)-P(5)-F(56)	87(6)
F(43)-P(4)-F(46)	91(7)	F(53)-P(5)-F(56)	84(5)
F(44)-P(4)-F(41)	93(7)	F(52)-P(5)-F(56)	84(5)
F(45)-P(4)-F(41)	90(7)	N(71)-C(72)-C(73)	178.20(14)
F(43)-P(4)-F(41)	84(6)	N(81)-C(82)-C(83)	176.40(17)
F(46)-P(4)-F(41)	168(8)	N(91)-C(92)-C(93)	179.3(9)
F(44)-P(4)-F(42)	176(9)	N(103)-C(102)-C(101)	178.9
F(45)-P(4)-F(42)	86(6)		

Table 1. Crystal data and structure refinement for **2b, Chapter II, Part B.**

Empirical formula	C70 H57 B F6 N11 P Ru
Formula weight	1309.12
Temperature	220(2)K
Wavelength	1.54178 Å
Crystal system	Monoclinic
Space group	P21/c
Unit cell dimensions	a = 27.1833(7) Å α = 90° b = 9.0685(3) Å β = 110.5550(10)° c = 26.3648(7) Å γ = 90°
Volume	6085.5(3)Å^3
Z	4
Density (calculated)	1.429 g/cm^3
Absorption coefficient	2.934 mm^{-1}
F(000)	2688
Crystal size	0.34 x 0.08 x 0.06 mm
Theta range for data collection	1.74 to 55.15°
Index ranges	$-28 \le h \le 28$, $-9 \le k \le 9$, $-27 \le \ell \le 27$
Reflections collected	50898
Independent reflections	7651 [R_{int} = 0.048]
Absorption correction	Semi-empirical from equivalents
Max. and min. transmission	0.9000 and 0.7100
Refinement method	Full-matrix least-squares on F^2
Data / restraints / parameters	7651 / 45 / 843
Goodness-of-fit on F^2	1.016
Final R indices [I>2sigma(I)]	R_1 = 0.0483, wR_2 = 0.0635
R indices (all data)	R_1 = 0.0946, wR_2 = 0.0692
Largest diff. peak and hole	1.134 and -0.520 e/Å^3

Table 2. Bond lengths [Å] and angles [°] for **2b, Chapter II, Part B.**

Ru-N(2)	1.955(3)	C(37)-C(38)	1.372(6)
Ru-N(7)	1.985(3)	C(38)-C(39)	1.381(6)
Ru-N(8)	2.054(4)	C(39)-C(40)	1.385(5)
Ru-N(3)	2.081(4)	P-F(4)	1.559(3)
Ru-N(6)	2.084(4)	P-F(1)	1.585(3)
Ru-N(1)	2.084(4)	P-F(2)	1.593(3)
N(1)-C(1)	1.347(5)	P-F(6)	1.594(3)
N(1)-C(5)	1.366(5)	P-F(3)	1.595(3)
N(2)-C(8)	1.339(5)	P-F(5)	1.600(3)
N(2)-C(6)	1.352(5)	B-C(41)	1.620(7)
N(3)-C(13)	1.328(5)	B-C(61)	1.639(7)
N(3)-C(9)	1.382(5)	B-C(71)	1.641(7)
N(4)-C(6)	1.322(5)	B-C(51)	1.649(7)
N(4)-C(7)	1.352(5)	C(41)-C(42)	1.391(6)
N(5)-C(8)	1.323(5)	C(41)-C(46)	1.395(6)
N(5)-C(7)	1.355(5)	C(42)-C(43)	1.385(6)
N(6)-C(26)	1.324(5)	C(43)-C(44)	1.364(6)
N(6)-C(30)	1.375(5)	C(44)-C(45)	1.395(6)
N(7)-C(31)	1.350(5)	C(45)-C(46)	1.395(6)
N(7)-C(35)	1.350(5)	C(51)-C(56)	1.372(6)
N(8)-C(40)	1.337(5)	C(51)-C(52)	1.390(6)
N(8)-C(36)	1.383(5)	C(52)-C(53)	1.404(6)
C(1)-C(2)	1.379(5)	C(53)-C(54)	1.346(7)
C(2)-C(3)	1.378(6)	C(54)-C(55)	1.342(7)
C(3)-C(4)	1.386(5)	C(55)-C(56)	1.394(7)
C(4)-C(5)	1.366(5)	C(61)-C(66)	1.402(6)
C(5)-C(6)	1.477(5)	C(61)-C(62)	1.412(5)
C(7)-C(14)	1.472(6)	C(62)-C(63)	1.377(6)
C(8)-C(9)	1.468(6)	C(63)-C(64)	1.378(6)
C(9)-C(10)	1.384(5)	C(64)-C(65)	1.372(6)
C(10)-C(11)	1.382(5)	C(65)-C(66)	1.379(6)
C(11)-C(12)	1.380(5)	C(71)-C(76)	1.377(6)
C(12)-C(13)	1.376(6)	C(71)-C(72)	1.386(6)
C(14)-C(15)	1.377(5)	C(72)-C(73)	1.382(6)
C(14)-C(19)	1.382(5)	C(73)-C(74)	1.365(7)
C(15)-C(16)	1.381(5)	C(74)-C(75)	1.361(7)
C(16)-C(17)	1.392(5)	C(75)-C(76)	1.402(6)
C(17)-C(18)	1.391(5)	C(81)-C(82)	1.448(7)
C(17)-C(20)	1.490(6)	C(82)-N(83)	1.119(6)
C(18)-C(19)	1.379(5)	C(91)-C(92)	1.415(18)
C(20)-C(21)	1.378(5)	C(92)-N(93)	1.137(18)
C(20)-C(25)	1.383(5)	C(101)-C(102)	1.395(17)
C(21)-C(22)	1.387(6)	C(102)-N(103)	1.117(18)
C(22)-C(23)	1.383(6)	C(111)-C(112)	1.486(8)
C(23)-C(24)	1.361(6)	C(112)-N(113)	1.126(7)
C(24)-C(25)	1.383(5)	N(2)-RU-N(7)	177.40(18)
C(26)-C(27)	1.390(6)	N(2)-RU-N(8)	98.19(16)
C(27)-C(28)	1.378(6)	N(7)-RU-N(8)	79.34(18)
C(28)-C(29)	1.369(6)	N(2)-RU-N(3)	77.73(16)
C(29)-C(30)	1.376(6)	N(7)-RU-N(3)	103.03(15)
C(30)-C(31)	1.460(6)	N(8)-RU-N(3)	91.06(13)
C(31)-C(32)	1.401(6)	N(2)-RU-N(6)	103.58(15)
C(32)-C(33)	1.374(6)	N(7)-RU-N(6)	78.93(17)
C(33)-C(34)	1.381(6)	N(8)-RU-N(6)	158.08(16)
C(34)-C(35)	1.392(6)	N(3)-RU-N(6)	91.08(13)
C(35)-C(36)	1.462(6)	N(2)-RU-N(1)	77.93(16)
C(36)-C(37)	1.381(6)	N(7)-RU-N(1)	101.36(15)

N(8)-RU-N(1)	94.03(13)	C(23)-C(24)-C(25)	120.2(5)
N(3)-RU-N(1)	155.60(16)	C(24)-C(25)-C(20)	121.5(5)
N(6)-RU-N(1)	92.98(13)	N(6)-C(26)-C(27)	122.1(5)
C(1)-N(1)-C(5)	116.8(4)	C(28)-C(27)-C(26)	119.4(5)
C(1)-N(1)-RU	128.1(3)	C(29)-C(28)-C(27)	118.3(5)
C(5)-N(1)-RU	114.9(3)	C(28)-C(29)-C(30)	120.9(5)
C(8)-N(2)-C(6)	116.7(4)	N(6)-C(30)-C(29)	120.3(5)
C(8)-N(2)-RU	122.2(3)	N(6)-C(30)-C(31)	115.7(5)
C(6)-N(2)-RU	120.9(3)	C(29)-C(30)-C(31)	124.0(5)
C(13)-N(3)-C(9)	117.6(4)	N(7)-C(31)-C(32)	118.7(5)
C(13)-N(3)-RU	128.6(3)	N(7)-C(31)-C(30)	113.2(5)
C(9)-N(3)-RU	113.8(3)	C(32)-C(31)-C(30)	128.1(5)
C(6)-N(4)-C(7)	115.1(4)	C(33)-C(32)-C(31)	119.5(5)
C(8)-N(5)-C(7)	115.0(4)	C(32)-C(33)-C(34)	120.8(5)
C(26)-N(6)-C(30)	119.0(4)	C(33)-C(34)-C(35)	118.6(5)
C(26)-N(6)-RU	127.7(4)	N(7)-C(35)-C(34)	119.8(5)
C(30)-N(6)-RU	113.2(3)	N(7)-C(35)-C(36)	113.5(5)
C(31)-N(7)-C(35)	122.7(4)	C(34)-C(35)-C(36)	126.7(5)
C(31)-N(7)-RU	119.0(3)	C(37)-C(36)-N(8)	121.2(4)
C(35)-N(7)-RU	118.4(4)	C(37)-C(36)-C(35)	124.0(5)
C(40)-N(8)-C(36)	116.8(4)	N(8)-C(36)-C(35)	114.7(5)
C(40)-N(8)-RU	129.1(3)	C(38)-C(37)-C(36)	120.4(5)
C(36)-N(8)-RU	114.0(3)	C(37)-C(38)-C(39)	118.9(5)
N(1)-C(1)-C(2)	122.3(4)	C(38)-C(39)-C(40)	118.4(5)
C(3)-C(2)-C(1)	119.9(5)	N(8)-C(40)-C(39)	124.1(5)
C(2)-C(3)-C(4)	118.8(5)	F(4)-P-F(1)	90.15(17)
C(5)-C(4)-C(3)	118.5(5)	F(4)-P-F(2)	179.8(2)
N(1)-C(5)-C(4)	123.7(4)	F(1)-P-F(2)	89.85(16)
N(1)-C(5)-C(6)	113.9(4)	F(4)-P-F(6)	90.84(17)
C(4)-C(5)-C(6)	122.4(5)	F(1)-P-F(6)	178.96(18)
N(4)-C(6)-N(2)	123.9(4)	F(2)-P-F(6)	89.16(15)
N(4)-C(6)-C(5)	123.9(5)	F(4)-P-F(3)	90.94(18)
N(2)-C(6)-C(5)	112.2(4)	F(1)-P-F(3)	89.62(16)
N(4)-C(7)-N(5)	125.1(4)	F(2)-P-F(3)	89.31(17)
N(4)-C(7)-C(14)	116.7(5)	F(6)-P-F(3)	90.68(16)
N(5)-C(7)-C(14)	118.3(5)	F(4)-P-F(5)	90.43(18)
N(5)-C(8)-N(2)	124.2(4)	F(1)-P-F(5)	90.49(16)
N(5)-C(8)-C(9)	124.6(5)	F(2)-P-F(5)	89.32(17)
N(2)-C(8)-C(9)	111.2(4)	F(6)-P-F(5)	89.19(16)
N(3)-C(9)-C(10)	120.9(4)	F(3)-P-F(5)	178.62(19)
N(3)-C(9)-C(8)	114.9(4)	C(41)-B-C(61)	110.9(4)
C(10)-C(9)-C(8)	124.2(5)	C(41)-B-C(71)	106.1(4)
C(11)-C(10)-C(9)	120.3(5)	C(61)-B-C(71)	110.7(4)
C(12)-C(11)-C(10)	118.0(5)	C(41)-B-C(51)	111.5(4)
C(13)-C(12)-C(11)	119.5(5)	C(61)-B-C(51)	108.4(4)
N(3)-C(13)-C(12)	123.6(5)	C(71)-B-C(51)	109.3(4)
C(15)-C(14)-C(19)	118.7(4)	C(42)-C(41)-C(46)	113.6(5)
C(15)-C(14)-C(7)	120.5(5)	C(42)-C(41)-B	127.0(5)
C(19)-C(14)-C(7)	120.7(5)	C(46)-C(41)-B	119.3(5)
C(14)-C(15)-C(16)	120.2(4)	C(43)-C(42)-C(41)	124.1(5)
C(15)-C(16)-C(17)	121.8(5)	C(44)-C(43)-C(42)	120.7(5)
C(18)-C(17)-C(16)	117.1(4)	C(43)-C(44)-C(45)	118.1(5)
C(18)-C(17)-C(20)	121.5(5)	C(44)-C(45)-C(46)	119.8(5)
C(16)-C(17)-C(20)	121.3(5)	C(45)-C(46)-C(41)	123.6(5)
C(19)-C(18)-C(17)	121.0(5)	C(56)-C(51)-C(52)	113.7(5)
C(18)-C(19)-C(14)	121.0(5)	C(56)-C(51)-B	121.3(5)
C(21)-C(20)-C(25)	117.2(5)	C(52)-C(51)-B	124.9(5)
C(21)-C(20)-C(17)	120.9(5)	C(51)-C(52)-C(53)	122.8(5)
C(25)-C(20)-C(17)	121.9(5)	C(54)-C(53)-C(52)	120.2(6)
C(20)-C(21)-C(22)	121.9(5)	C(55)-C(54)-C(53)	119.1(7)
C(23)-C(22)-C(21)	119.2(5)	C(54)-C(55)-C(56)	120.4(7)
C(24)-C(23)-C(22)	119.9(5)	C(51)-C(56)-C(55)	123.7(6)

C(66)-C(61)-C(62)	113.5(4)	C(73)-C(72)-C(71)	123.7(5)
C(66)-C(61)-B	125.7(5)	C(74)-C(73)-C(72)	119.9(6)
C(62)-C(61)-B	120.7(5)	C(75)-C(74)-C(73)	119.4(6)
C(63)-C(62)-C(61)	123.7(5)	C(74)-C(75)-C(76)	119.1(6)
C(62)-C(63)-C(64)	119.9(5)	C(71)-C(76)-C(75)	123.9(5)
C(65)-C(64)-C(63)	118.8(5)	N(83)-C(82)-C(81)	178.4(7)
C(64)-C(65)-C(66)	120.7(5)	N(93)-C(92)-C(91)	169(3)
C(65)-C(66)-C(61)	123.3(5)	N(103)-C(102)-C(101)	178(4)
C(76)-C(71)-C(72)	113.9(5)	N(113)-C(112)-C(111)	178.0(9)
C(76)-C(71)-B	125.2(5)		
C(72)-C(71)-B	120.8(5)		

Table 1. Crystal data and structure refinement for **3a, Chapter II, Part B** WITH SQUEEZE.

Empirical formula	C38 H24 Br2 F12 N10 P2 Ru
Formula weight	1171.50
Temperature	220(2)K
Wavelength	1.54178 Å
Crystal system	Monoclinic
Space group	C2/c
Unit cell dimensions	a = 14.0743(7) Å α = 90° b = 16.9533(8) Å β = 102.873(4)° c = 21.0567(10) Å γ = 90°
Volume	4898.0(4)Å^3
Z	4
Density (calculated)	1.589 g/cm^3
Absorption coefficient	5.880 mm^{-1}
F(000)	2296
Crystal size	0.75 x 0.13 x 0.07 mm
Theta range for data collection	4.14 to 72.86°
Index ranges	$-17 \le h \le 17$, $-20 \le k \le 20$, $-25 \le \ell \le 25$
Reflections collected	19889
Independent reflections	4841 [R_{int} = 0.035]
Absorption correction	Semi-empirical from equivalents
Max. and min. transmission	0.7400 and 0.3800
Refinement method	Full-matrix least-squares on F^2
Data / restraints / parameters	4841 / 0 / 294
Goodness-of-fit on F^2	1.089
Final R indices [I>2sigma(I)]	R_1 = 0.0727, wR_2 = 0.2274
R indices (all data)	R_1 = 0.0794, wR_2 = 0.2346
Largest diff. peak and hole	1.964 and -2.585 e/Å^3

Table 2. Bond lengths [Å] and angles [°] for **3a, Chapter II, Part B** WITH SQUEEZE.

Ru-N(2)#1	1.972(5)	C(1)-N(1)-C(5)	117.5(5)
Ru-N(2)	1.972(5)	C(1)-N(1)-RU	127.9(4)
Ru-N(3)#1	2.085(5)	C(5)-N(1)-RU	114.6(4)
Ru-N(3)	2.085(5)	C(8)-N(2)-C(6)	118.2(5)
Ru-N(1)	2.096(5)	C(8)-N(2)-RU	120.2(4)
Ru-N(1)#1	2.096(5)	C(6)-N(2)-RU	121.2(4)
N(1)-C(1)	1.344(8)	C(13)-N(3)-C(9)	117.0(5)
N(1)-C(5)	1.383(7)	C(13)-N(3)-RU	128.5(4)
N(2)-C(8)	1.339(8)	C(9)-N(3)-RU	114.4(4)
N(2)-C(6)	1.358(7)	C(6)-N(4)-C(7)	115.7(5)
N(3)-C(13)	1.345(8)	C(8)-N(5)-C(7)	115.1(5)
N(3)-C(9)	1.372(8)	N(1)-C(1)-C(2)	123.0(6)
N(4)-C(6)	1.326(8)	C(3)-C(2)-C(1)	118.8(6)
N(4)-C(7)	1.344(8)	C(4)-C(3)-C(2)	119.7(6)
N(5)-C(8)	1.319(8)	C(5)-C(4)-C(3)	119.2(6)
N(5)-C(7)	1.349(8)	C(4)-C(5)-N(1)	121.8(6)
C(1)-C(2)	1.382(10)	C(4)-C(5)-C(6)	123.7(6)
C(2)-C(3)	1.38(1)	N(1)-C(5)-C(6)	114.5(5)
C(3)-C(4)	1.379(10)	N(4)-C(6)-N(2)	122.0(5)
C(4)-C(5)	1.378(9)	N(4)-C(6)-C(5)	125.7(5)
C(5)-C(6)	1.453(8)	N(2)-C(6)-C(5)	112.3(5)
C(7)-C(14)	1.484(8)	N(4)-C(7)-N(5)	125.6(5)
C(8)-C(9)	1.477(8)	N(4)-C(7)-C(14)	119.2(5)
C(9)-C(10)	1.373(9)	N(5)-C(7)-C(14)	115.2(5)
C(10)-C(11)	1.377(9)	N(5)-C(8)-N(2)	123.3(5)
C(11)-C(12)	1.377(10)	N(5)-C(8)-C(9)	123.6(6)
C(12)-C(13)	1.379(10)	N(2)-C(8)-C(9)	113.0(5)
C(14)-C(19)	1.39(1)	N(3)-C(9)-C(10)	123.0(5)
C(14)-C(15)	1.391(9)	N(3)-C(9)-C(8)	114.0(5)
C(15)-C(16)	1.414(9)	C(10)-C(9)-C(8)	123.1(6)
C(16)-C(17)	1.367(11)	C(9)-C(10)-C(11)	118.6(6)
C(17)-C(18)	1.372(10)	C(12)-C(11)-C(10)	119.4(6)
C(17)-Br	1.907(6)	C(11)-C(12)-C(13)	119.5(6)
C(18)-C(19)	1.392(9)	N(3)-C(13)-C(12)	122.5(6)
P-F(2)	1.574(5)	C(19)-C(14)-C(15)	120.8(6)
P-F(5)	1.577(5)	C(19)-C(14)-C(7)	118.5(6)
P-F(1)	1.589(5)	C(15)-C(14)-C(7)	120.7(6)
P-F(4)	1.600(5)	C(14)-C(15)-C(16)	119.1(6)
P-F(6)	1.603(5)	C(17)-C(16)-C(15)	118.5(6)
P-F(3)	1.606(5)	C(16)-C(17)-C(18)	123.1(6)
N(2)#1-RU-N(2)	175.7(3)	C(16)-C(17)-BR	120.2(5)
N(2)#1-RU-N(3)#1	78.2(2)	C(18)-C(17)-BR	116.6(5)
N(2)-RU-N(3)#1	98.7(2)	C(17)-C(18)-C(19)	118.7(7)
N(2)#1-RU-N(3)	98.7(2)	C(14)-C(19)-C(18)	119.8(6)
N(2)-RU-N(3)	78.2(2)	F(2)-P-F(5)	91.3(3)
N(3)#1-RU-N(3)	87.9(3)	F(2)-P-F(1)	90.9(3)
N(2)#1-RU-N(1)	105.8(2)	F(5)-P-F(1)	90.8(3)
N(2)-RU-N(1)	77.3(2)	F(2)-P-F(4)	176.7(3)
N(3)#1-RU-N(1)	95.2(2)	F(5)-P-F(4)	91.5(3)
N(3)-RU-N(1)	155.45(19)	F(1)-P-F(4)	90.8(3)
N(2)#1-RU-N(1)#1	77.30(19)	F(2)-P-F(6)	89.3(3)
N(2)-RU-N(1)#1	105.8(2)	F(5)-P-F(6)	89.7(3)
N(3)#1-RU-N(1)#1	155.45(19)	F(1)-P-F(6)	179.4(3)
N(3)-RU-N(1)#1	95.2(2)	F(4)-P-F(6)	88.9(3)
N(1)-RU-N(1)#1	92.0(3)	F(2)-P-F(3)	90.0(3)

F(5)-P-F(3)	178.7(3)	F(6)-P-F(3)	90.1(3)
F(1)-P-F(3)	89.4(3)		
F(4)-P-F(3)	87.2(3)		

Appendix 4: Supplementary information for chapter III, part A.

Table 1. Crystal data and structure refinement for **2a, Chapter III, Part A.**

Empirical formula	C58 H40 B2 F8 N12 Ru
Formula weight	1179.71
Temperature	150(2)K
Wavelength	1.54178 Å
Crystal system	Orthorhombic
Space group	Pna21
Unit cell dimensions	a = 26.1672(4) Å α = 90° b = 13.6435(2) Å β = 90° c = 13.9456(2) Å γ = 90°
Volume	4978.75(13)Å^3
Z	4
Density (calculated)	1.574 Mg/m^3
Absorption coefficient	3.285 mm^{-1}
F(000)	2392
Crystal size	0.30 x 0.10 x 0.06 mm
Theta range for data collection	3.38 to 72.97°
Index ranges	$-31 \le h \le 32$, $-16 \le k \le 16$, $-15 \le \ell \le 17$
Reflections collected	60536
Independent reflections	9034 [R_{int} = 0.062]
Absorption correction	Semi-empirical from equivalents
Max. and min. transmission	0.8700 and 0.5500
Refinement method	Full-matrix least-squares on F^2
Data / restraints / parameters	9034 / 1 / 732
Goodness-of-fit on F^2	0.942
Final R indices [I>2sigma(I)]	R_1 = 0.0537, wR_2 = 0.1163
R indices (all data)	R_1 = 0.0745, wR_2 = 0.1235
Absolute structure parameter	0.013(11)
Largest diff. peak and hole	0.859 and -0.573 e/Å^3

Table 2. Bond lengths [Å] and angles [°] for **2a, Chapter III, Part A.**

Ru(1)-N(2)	1.960(4)	C(34)-C(41)	1.464(9)
Ru(1)-N(7)	1.988(4)	C(35)-C(36)	1.472(8)
Ru(1)-N(6)	2.082(5)	C(36)-C(37)	1.382(7)
Ru(1)-N(8)	2.088(5)	C(37)-C(38)	1.370(8)
Ru(1)-N(3)	2.089(4)	C(38)-C(39)	1.367(8)
Ru(1)-N(1)	2.096(5)	C(39)-C(40)	1.394(8)
N(1)-C(1)	1.324(8)	C(41)-C(42)	1.363(9)
N(1)-C(5)	1.378(7)	C(41)-C(54)	1.477(9)
N(2)-C(6)	1.349(6)	C(42)-C(43)	1.395(10)
N(2)-C(8)	1.358(7)	C(43)-C(44)	1.412(9)
N(3)-C(13)	1.343(7)	C(43)-C(48)	1.430(9)
N(3)-C(9)	1.367(8)	C(44)-C(45)	1.365(9)
N(4)-C(6)	1.318(7)	C(45)-C(46)	1.378(9)
N(4)-C(7)	1.364(7)	C(46)-C(47)	1.379(9)
N(5)-C(8)	1.301(7)	C(47)-C(48)	1.415(8)
N(5)-C(7)	1.361(6)	C(48)-C(49)	1.446(8)
N(6)-C(28)	1.334(6)	C(49)-C(54)	1.406(8)
N(6)-C(32)	1.370(7)	C(49)-C(50)	1.420(9)
N(7)-C(33)	1.324(7)	C(50)-C(51)	1.358(8)
N(7)-C(35)	1.344(7)	C(51)-C(52)	1.398(9)
N(8)-C(40)	1.332(7)	C(52)-C(53)	1.368(9)
N(8)-C(36)	1.384(7)	C(53)-C(54)	1.420(8)
N(9)-C(33)	1.314(7)	B(1)-F(11)	1.370(7)
N(9)-C(34)	1.365(7)	B(1)-F(13)	1.383(8)
N(10)-C(35)	1.302(7)	B(1)-F(14)	1.388(7)
N(10)-C(34)	1.361(8)	B(1)-F(12)	1.394(9)
C(1)-C(2)	1.382(8)	B(2)-F(24)	1.311(10)
C(2)-C(3)	1.382(8)	B(2)-F(21)	1.355(10)
C(3)-C(4)	1.389(9)	B(2)-F(23)	1.367(9)
C(4)-C(5)	1.387(7)	B(2)-F(22)	1.408(10)
C(5)-C(6)	1.467(8)	C(61)-C(62)	1.482(14)
C(7)-C(14)	1.482(8)	C(62)-N(63)	1.121(10)
C(8)-C(9)	1.492(8)	C(71)-C(72)	1.430(9)
C(9)-C(10)	1.375(9)	C(72)-N(73)	1.141(8)
C(10)-C(11)	1.371(8)	N(2)-RU1-N(7)	177.63(19)
C(11)-C(12)	1.376(9)	N(2)-RU1-N(6)	100.46(19)
C(12)-C(13)	1.386(9)	N(7)-RU1-N(6)	77.73(19)
C(14)-C(15)	1.343(9)	N(2)-RU1-N(8)	103.7(2)
C(14)-C(27)	1.462(9)	N(7)-RU1-N(8)	78.18(19)
C(15)-C(16)	1.429(10)	N(6)-RU1-N(8)	155.86(19)
C(16)-C(17)	1.404(10)	N(2)-RU1-N(3)	77.82(19)
C(16)-C(21)	1.41(1)	N(7)-RU1-N(3)	100.74(18)
C(17)-C(18)	1.361(10)	N(6)-RU1-N(3)	94.97(17)
C(18)-C(19)	1.409(10)	N(8)-RU1-N(3)	90.95(19)
C(19)-C(20)	1.375(9)	N(2)-RU1-N(1)	77.89(19)
C(20)-C(21)	1.401(8)	N(7)-RU1-N(1)	103.61(19)
C(21)-C(22)	1.470(9)	N(6)-RU1-N(1)	91.42(18)
C(22)-C(23)	1.404(10)	N(8)-RU1-N(1)	92.77(17)
C(22)-C(27)	1.420(8)	N(3)-RU1-N(1)	155.6(2)
C(23)-C(24)	1.383(9)	C(1)-N(1)-C(5)	117.5(5)
C(24)-C(25)	1.369(9)	C(1)-N(1)-RU1	128.9(4)
C(25)-C(26)	1.376(9)	C(5)-N(1)-RU1	113.7(4)
C(26)-C(27)	1.410(8)	C(6)-N(2)-C(8)	117.4(5)
C(28)-C(29)	1.388(8)	C(6)-N(2)-RU1	121.6(4)
C(29)-C(30)	1.374(8)	C(8)-N(2)-RU1	121.0(4)
C(30)-C(31)	1.373(8)	C(13)-N(3)-C(9)	115.9(5)
C(31)-C(32)	1.411(8)	C(13)-N(3)-RU1	128.2(4)
C(32)-C(33)	1.473(7)	C(9)-N(3)-RU1	115.6(4)

C(6)-N(4)-C(7)	116.0(5)	C(30)-C(29)-C(28)	119.2(5)
C(8)-N(5)-C(7)	116.6(5)	C(31)-C(30)-C(29)	120.0(6)
C(28)-N(6)-C(32)	117.7(5)	C(30)-C(31)-C(32)	118.0(6)
C(28)-N(6)-RU1	128.7(4)	N(6)-C(32)-C(31)	122.1(5)
C(32)-N(6)-RU1	113.6(4)	N(6)-C(32)-C(33)	115.9(5)
C(33)-N(7)-C(35)	118.0(5)	C(31)-C(32)-C(33)	121.9(5)
C(33)-N(7)-RU1	121.4(4)	N(9)-C(33)-N(7)	123.7(5)
C(35)-N(7)-RU1	120.6(4)	N(9)-C(33)-C(32)	124.9(5)
C(40)-N(8)-C(36)	118.2(5)	N(7)-C(33)-C(32)	111.4(5)
C(40)-N(8)-RU1	128.2(4)	N(10)-C(34)-N(9)	124.2(5)
C(36)-N(8)-RU1	113.5(4)	N(10)-C(34)-C(41)	116.5(5)
C(33)-N(9)-C(34)	115.0(5)	N(9)-C(34)-C(41)	118.9(6)
C(35)-N(10)-C(34)	115.3(5)	N(10)-C(35)-N(7)	123.6(5)
N(1)-C(1)-C(2)	123.5(6)	N(10)-C(35)-C(36)	124.4(5)
C(3)-C(2)-C(1)	119.0(6)	N(7)-C(35)-C(36)	112.0(5)
C(2)-C(3)-C(4)	119.1(5)	C(37)-C(36)-N(8)	120.6(6)
C(5)-C(4)-C(3)	118.5(6)	C(37)-C(36)-C(35)	123.9(5)
N(1)-C(5)-C(4)	122.3(6)	N(8)-C(36)-C(35)	115.4(5)
N(1)-C(5)-C(6)	115.1(4)	C(38)-C(37)-C(36)	120.4(6)
C(4)-C(5)-C(6)	122.6(5)	C(39)-C(38)-C(37)	118.7(6)
N(4)-C(6)-N(2)	123.1(5)	C(38)-C(39)-C(40)	119.8(6)
N(4)-C(6)-C(5)	125.1(5)	N(8)-C(40)-C(39)	122.0(6)
N(2)-C(6)-C(5)	111.7(5)	C(42)-C(41)-C(34)	118.3(6)
N(5)-C(7)-N(4)	123.5(5)	C(42)-C(41)-C(54)	117.9(6)
N(5)-C(7)-C(14)	119.4(5)	C(34)-C(41)-C(54)	123.3(6)
N(4)-C(7)-C(14)	116.9(5)	C(41)-C(42)-C(43)	124.3(7)
N(5)-C(8)-N(2)	123.2(5)	C(42)-C(43)-C(44)	122.6(7)
N(5)-C(8)-C(9)	124.5(5)	C(42)-C(43)-C(48)	119.2(6)
N(2)-C(8)-C(9)	112.3(5)	C(44)-C(43)-C(48)	118.1(6)
N(3)-C(9)-C(10)	123.8(6)	C(45)-C(44)-C(43)	122.4(7)
N(3)-C(9)-C(8)	113.1(6)	C(44)-C(45)-C(46)	119.5(7)
C(10)-C(9)-C(8)	123.1(6)	C(45)-C(46)-C(47)	120.9(6)
C(11)-C(10)-C(9)	118.9(6)	C(46)-C(47)-C(48)	121.2(7)
C(10)-C(11)-C(12)	118.8(6)	C(47)-C(48)-C(43)	117.9(6)
C(11)-C(12)-C(13)	119.5(6)	C(47)-C(48)-C(49)	123.8(6)
N(3)-C(13)-C(12)	123.1(6)	C(43)-C(48)-C(49)	118.3(6)
C(15)-C(14)-C(27)	120.4(6)	C(54)-C(49)-C(50)	118.3(5)
C(15)-C(14)-C(7)	116.4(6)	C(54)-C(49)-C(48)	121.0(6)
C(27)-C(14)-C(7)	123.0(6)	C(50)-C(49)-C(48)	120.8(5)
C(14)-C(15)-C(16)	122.5(7)	C(51)-C(50)-C(49)	121.7(6)
C(17)-C(16)-C(21)	119.5(7)	C(50)-C(51)-C(52)	119.6(6)
C(17)-C(16)-C(15)	120.9(7)	C(53)-C(52)-C(51)	120.8(6)
C(21)-C(16)-C(15)	119.6(7)	C(52)-C(53)-C(54)	120.2(6)
C(18)-C(17)-C(16)	121.1(8)	C(49)-C(54)-C(53)	119.1(6)
C(17)-C(18)-C(19)	119.4(7)	C(49)-C(54)-C(41)	118.7(6)
C(20)-C(19)-C(18)	120.7(7)	C(53)-C(54)-C(41)	122.2(6)
C(19)-C(20)-C(21)	120.4(7)	F(11)-B(1)-F(13)	110.8(5)
C(20)-C(21)-C(16)	118.8(6)	F(11)-B(1)-F(14)	110.4(6)
C(20)-C(21)-C(22)	122.7(7)	F(13)-B(1)-F(14)	109.8(6)
C(16)-C(21)-C(22)	118.4(6)	F(11)-B(1)-F(12)	108.2(7)
C(23)-C(22)-C(27)	117.8(6)	F(13)-B(1)-F(12)	108.9(6)
C(23)-C(22)-C(21)	122.1(6)	F(14)-B(1)-F(12)	108.6(5)
C(27)-C(22)-C(21)	120.0(6)	F(24)-B(2)-F(21)	113.3(8)
C(24)-C(23)-C(22)	122.4(6)	F(24)-B(2)-F(23)	113.1(8)
C(25)-C(24)-C(23)	119.0(7)	F(21)-B(2)-F(23)	110.8(7)
C(24)-C(25)-C(26)	121.3(6)	F(24)-B(2)-F(22)	105.7(7)
C(25)-C(26)-C(27)	120.7(6)	F(21)-B(2)-F(22)	103.1(7)
C(26)-C(27)-C(22)	118.8(6)	F(23)-B(2)-F(22)	110.1(7)
C(26)-C(27)-C(14)	122.9(6)	N(63)-C(62)-C(61)	178.7(8)
C(22)-C(27)-C(14)	118.3(6)	N(73)-C(72)-C(71)	176.7(9)
N(6)-C(28)-C(29)	122.9(5)		

Table 1. Crystal data and structure refinement for **2b, Chapter III, Part A.**

Empirical formula	C66 H42 F12 N10 P2 Ru
Formula weight	1366.11
Temperature	220(2)K
Wavelength	1.54178 Å
Crystal system	Monoclinic
Space group	C2/c
Unit cell dimensions	a = 20.4809(9) Å α = 90° b = 14.6002(6) Å β = 94.887(2)° c = 44.9325(18) Å γ = 90°
Volume	13387.1(10)Å^3
Z	8
Density (calculated)	1.356 g/cm^3
Absorption coefficient	3.043 mm^{-1}
F(000)	5520
Crystal size	0.46 x 0.25 x 0.06 mm
Theta range for data collection	1.97 to 55.18°
Index ranges	$-21 \le h \le 21$, $-15 \le k \le 15$, $-47 \le \ell \le 47$
Reflections collected	55963
Independent reflections	8429 [R_{int} = 0.053]
Absorption correction	Semi-empirical from equivalents
Max. and min. transmission	0.8700 and 0.5600
Refinement method	Full-matrix least-squares on F^2
Data / restraints / parameters	8429 / 1338 / 1005
Goodness-of-fit on F^2	0.920
Final R indices [I>2sigma(I)]	R_1 = 0.0674, wR_2 = 0.1563
R indices (all data)	R_1 = 0.1416, wR_2 = 0.1764
Largest diff. peak and hole	0.676 and -0.324 e/Å^3

Table 2. Bond lengths [Å] and angles [°] for **2b, Chapter III, Part A.**

Ru-N(7)	1.937(5)	C(38)-C(39)	1.465(8)
Ru-N(2)	1.941(6)	C(39)-N(9)	1.328(7)
Ru-N(1)	2.064(6)	C(39)-N(7)	1.358(7)
Ru-N(3)	2.084(6)	N(7)-C(41)	1.347(7)
Ru-N(6)	2.087(5)	C(41)-N(10)	1.324(7)
Ru-N(8)	2.113(5)	C(41)-C(42)	1.449(8)
N(1)-C(1)	1.331(7)	N(10)-C(40)	1.358(7)
N(1)-C(5)	1.370(7)	C(40)-N(9)	1.349(7)
C(1)-C(2)	1.394(8)	C(40)-C(47)	1.440(8)
C(2)-C(3)	1.361(7)	C(42)-N(8)	1.372(6)
C(3)-C(4)	1.382(7)	C(42)-C(43)	1.377(7)
C(4)-C(5)	1.345(7)	N(8)-C(46)	1.346(7)
C(5)-C(6)	1.481(8)	C(46)-C(45)	1.373(8)
C(6)-N(4)	1.338(7)	C(45)-C(44)	1.348(8)
C(6)-N(2)	1.355(8)	C(44)-C(43)	1.384(8)
N(2)-C(8)	1.332(7)	C(47)-C(48)	1.363(8)
C(8)-N(5)	1.324(7)	C(47)-C(52)	1.390(8)
C(8)-C(9)	1.470(8)	C(48)-C(49)	1.376(9)
N(5)-C(7)	1.357(7)	C(49)-C(50)	1.386(9)
C(7)-N(4)	1.345(7)	C(50)-C(51)	1.364(8)
C(7)-C(14)	1.470(8)	C(50)-C(53)	1.469(13)
C(9)-C(10)	1.363(8)	C(50)-C(68)	1.480(15)
C(9)-N(3)	1.383(7)	C(51)-C(52)	1.377(8)
N(3)-C(13)	1.352(7)	C(53)-C(54)	1.291(16)
C(13)-C(12)	1.376(8)	C(53)-C(67)	1.421(16)
C(12)-C(11)	1.351(8)	C(54)-C(55)	1.411(17)
C(11)-C(10)	1.379(8)	C(55)-C(56)	1.414(18)
C(14)-C(15)	1.358(8)	C(55)-C(60)	1.422(18)
C(14)-C(19)	1.409(8)	C(56)-C(57)	1.369(17)
C(15)-C(16)	1.400(8)	C(57)-C(58)	1.388(15)
C(16)-C(17)	1.379(8)	C(58)-C(59)	1.347(14)
C(17)-C(18)	1.387(8)	C(59)-C(60)	1.427(18)
C(17)-C(20)	1.470(8)	C(60)-C(61)	1.446(18)
C(18)-C(19)	1.377(8)	C(61)-C(67)	1.413(17)
C(20)-C(21)	1.300(8)	C(61)-C(62)	1.440(17)
C(20)-C(33)	1.436(9)	C(62)-C(63)	1.35(2)
C(21)-C(22)	1.419(9)	C(63)-C(64)	1.39(2)
C(22)-C(23)	1.408(10)	C(64)-C(66)	1.367(16)
C(22)-C(27)	1.42(1)	C(66)-C(67)	1.388(16)
C(23)-C(24)	1.378(11)	C(68)-C(81)	1.42(3)
C(24)-C(25)	1.411(12)	C(68)-C(69)	1.45(4)
C(25)-C(26)	1.371(12)	C(69)-C(70)	1.46(3)
C(26)-C(27)	1.430(11)	C(70)-C(75)	1.38(3)
C(27)-C(28)	1.451(11)	C(70)-C(71)	1.41(4)
C(28)-C(33)	1.412(10)	C(71)-C(72)	1.34(3)
C(28)-C(29)	1.458(11)	C(72)-C(73)	1.39(2)
C(29)-C(30)	1.347(12)	C(73)-C(74)	1.34(2)
C(30)-C(31)	1.398(12)	C(74)-C(75)	1.42(3)
C(31)-C(32)	1.363(10)	C(75)-C(76)	1.46(4)
C(32)-C(33)	1.376(9)	C(76)-C(77)	1.38(3)
N(6)-C(34)	1.338(7)	C(76)-C(81)	1.52(4)
N(6)-C(38)	1.365(7)	C(77)-C(78)	1.30(4)
C(34)-C(35)	1.387(8)	C(78)-C(79)	1.40(3)
C(35)-C(36)	1.364(8)	C(79)-C(80)	1.28(3)
C(36)-C(37)	1.369(8)	C(80)-C(81)	1.40(3)
C(37)-C(38)	1.376(8)	P(1)-F(13)	1.502(16)

P(1)-F(12)	1.503(12)	N(3)-C(13)-C(12)	121.5(7)
P(1)-F(11)	1.571(12)	C(11)-C(12)-C(13)	120.5(7)
P(1)-F(16)	1.590(11)	C(12)-C(11)-C(10)	120.3(7)
P(1)-F(14)	1.599(12)	C(9)-C(10)-C(11)	117.4(7)
P(1)-F(15)	1.615(14)	C(15)-C(14)-C(19)	117.2(7)
P(2)-F(23)	1.49(2)	C(15)-C(14)-C(7)	123.3(7)
P(2)-F(22)	1.50(2)	C(19)-C(14)-C(7)	119.2(7)
P(2)-F(21)	1.578(18)	C(14)-C(15)-C(16)	121.6(6)
P(2)-F(24)	1.59(2)	C(17)-C(16)-C(15)	122.1(7)
P(2)-F(26)	1.601(17)	C(16)-C(17)-C(18)	115.5(6)
P(2)-F(25)	1.61(2)	C(16)-C(17)-C(20)	122.4(7)
P(3)-F(33)	1.543(5)	C(18)-C(17)-C(20)	122.1(7)
P(3)-F(34)	1.564(7)	C(19)-C(18)-C(17)	123.3(7)
P(3)-F(35)	1.565(6)	C(18)-C(19)-C(14)	120.2(7)
P(3)-F(36)	1.589(6)	C(21)-C(20)-C(33)	120.9(7)
P(3)-F(31)	1.600(7)	C(21)-C(20)-C(17)	119.6(7)
P(3)-F(32)	1.603(7)	C(33)-C(20)-C(17)	119.4(7)
N(7)-RU-N(2)	176.8(2)	C(20)-C(21)-C(22)	125.1(8)
N(7)-RU-N(1)	101.2(2)	C(23)-C(22)-C(21)	123.4(9)
N(2)-RU-N(1)	78.2(3)	C(23)-C(22)-C(27)	120.2(9)
N(7)-RU-N(3)	102.9(2)	C(21)-C(22)-C(27)	116.4(9)
N(2)-RU-N(3)	77.7(3)	C(24)-C(23)-C(22)	121.5(1)
N(1)-RU-N(3)	155.8(3)	C(23)-C(24)-C(25)	118.50(12)
N(7)-RU-N(6)	78.1(2)	C(26)-C(25)-C(24)	121.40(12)
N(2)-RU-N(6)	98.8(2)	C(25)-C(26)-C(27)	121.00(11)
N(1)-RU-N(6)	93.41(19)	C(22)-C(27)-C(26)	117.3(1)
N(3)-RU-N(6)	89.15(19)	C(22)-C(27)-C(28)	119.9(9)
N(7)-RU-N(8)	77.5(2)	C(26)-C(27)-C(28)	122.9(1)
N(2)-RU-N(8)	105.6(2)	C(33)-C(28)-C(27)	119.5(8)
N(1)-RU-N(8)	93.68(19)	C(33)-C(28)-C(29)	118.0(9)
N(3)-RU-N(8)	93.87(19)	C(27)-C(28)-C(29)	122.5(1)
N(6)-RU-N(8)	155.5(2)	C(30)-C(29)-C(28)	120.7(1)
C(1)-N(1)-C(5)	115.9(6)	C(29)-C(30)-C(31)	120.0(1)
C(1)-N(1)-RU	128.4(5)	C(32)-C(31)-C(30)	120.0(1)
C(5)-N(1)-RU	115.7(5)	C(31)-C(32)-C(33)	122.8(9)
N(1)-C(1)-C(2)	123.1(7)	C(32)-C(33)-C(28)	118.5(8)
C(3)-C(2)-C(1)	119.1(7)	C(32)-C(33)-C(20)	123.3(8)
C(2)-C(3)-C(4)	118.7(7)	C(28)-C(33)-C(20)	118.2(8)
C(5)-C(4)-C(3)	119.2(6)	C(34)-N(6)-C(38)	117.4(6)
C(4)-C(5)-N(1)	124.0(6)	C(34)-N(6)-RU	128.1(5)
C(4)-C(5)-C(6)	123.2(7)	C(38)-N(6)-RU	114.4(4)
N(1)-C(5)-C(6)	112.8(7)	N(6)-C(34)-C(35)	122.2(7)
N(4)-C(6)-N(2)	123.6(6)	C(36)-C(35)-C(34)	119.5(7)
N(4)-C(6)-C(5)	123.8(7)	C(35)-C(36)-C(37)	119.5(7)
N(2)-C(6)-C(5)	112.3(7)	C(36)-C(37)-C(38)	118.9(7)
C(8)-N(2)-C(6)	116.9(6)	N(6)-C(38)-C(37)	122.5(6)
C(8)-N(2)-RU	122.0(5)	N(6)-C(38)-C(39)	114.1(6)
C(6)-N(2)-RU	121.0(5)	C(37)-C(38)-C(39)	123.2(7)
N(5)-C(8)-N(2)	124.0(7)	N(9)-C(39)-N(7)	123.0(6)
N(5)-C(8)-C(9)	123.0(7)	N(9)-C(39)-C(38)	124.7(7)
N(2)-C(8)-C(9)	112.7(7)	N(7)-C(39)-C(38)	112.3(7)
C(8)-N(5)-C(7)	115.6(6)	C(41)-N(7)-C(39)	117.0(6)
N(4)-C(7)-N(5)	124.9(6)	C(41)-N(7)-RU	122.0(5)
N(4)-C(7)-C(14)	116.6(8)	C(39)-N(7)-RU	121.0(5)
N(5)-C(7)-C(14)	118.5(7)	N(10)-C(41)-N(7)	123.6(6)
C(6)-N(4)-C(7)	114.9(6)	N(10)-C(41)-C(42)	124.1(7)
C(10)-C(9)-N(3)	123.9(7)	N(7)-C(41)-C(42)	112.2(6)
C(10)-C(9)-C(8)	123.0(7)	C(41)-N(10)-C(40)	115.9(6)
N(3)-C(9)-C(8)	113.1(7)	N(9)-C(40)-N(10)	124.2(6)
C(13)-N(3)-C(9)	116.4(6)	N(9)-C(40)-C(47)	116.4(7)
C(13)-N(3)-RU	129.0(5)	N(10)-C(40)-C(47)	119.5(7)
C(9)-N(3)-RU	114.6(5)	C(39)-N(9)-C(40)	116.2(6)

N(8)-C(42)-C(43)	120.4(6)	C(70)-C(75)-C(76)	119(2)
N(8)-C(42)-C(41)	115.1(6)	C(74)-C(75)-C(76)	123(2)
C(43)-C(42)-C(41)	124.5(7)	C(77)-C(76)-C(75)	125(3)
C(46)-N(8)-C(42)	118.8(6)	C(77)-C(76)-C(81)	117(3)
C(46)-N(8)-RU	128.0(5)	C(75)-C(76)-C(81)	118(3)
C(42)-N(8)-RU	113.1(4)	C(78)-C(77)-C(76)	123(3)
N(8)-C(46)-C(45)	121.8(6)	C(77)-C(78)-C(79)	120(3)
C(44)-C(45)-C(46)	119.5(7)	C(80)-C(79)-C(78)	122(3)
C(45)-C(44)-C(43)	120.1(7)	C(79)-C(80)-C(81)	123(3)
C(42)-C(43)-C(44)	119.2(7)	C(80)-C(81)-C(68)	120(2)
C(48)-C(47)-C(52)	116.0(7)	C(80)-C(81)-C(76)	115(2)
C(48)-C(47)-C(40)	122.6(8)	C(68)-C(81)-C(76)	125(2)
C(52)-C(47)-C(40)	121.3(8)	F(13)-P(1)-F(12)	91.0(9)
C(47)-C(48)-C(49)	122.7(8)	F(13)-P(1)-F(11)	92.1(1)
C(48)-C(49)-C(50)	120.7(8)	F(12)-P(1)-F(11)	93.7(8)
C(51)-C(50)-C(49)	117.3(7)	F(13)-P(1)-F(16)	90.5(1)
C(51)-C(50)-C(53)	127.10(13)	F(12)-P(1)-F(16)	93.5(8)
C(49)-C(50)-C(53)	114.90(13)	F(11)-P(1)-F(16)	172.2(9)
C(51)-C(50)-C(68)	116.40(18)	F(13)-P(1)-F(14)	93.4(9)
C(49)-C(50)-C(68)	125.60(18)	F(12)-P(1)-F(14)	175.2(1)
C(53)-C(50)-C(68)	19.90(15)	F(11)-P(1)-F(14)	84.1(8)
C(50)-C(51)-C(52)	121.4(7)	F(16)-P(1)-F(14)	88.5(8)
C(51)-C(52)-C(47)	121.8(7)	F(13)-P(1)-F(15)	175.9(9)
C(54)-C(53)-C(67)	124.90(14)	F(12)-P(1)-F(15)	92.8(8)
C(54)-C(53)-C(50)	120.30(14)	F(11)-P(1)-F(15)	89.2(8)
C(67)-C(53)-C(50)	114.40(13)	F(16)-P(1)-F(15)	87.7(8)
C(53)-C(54)-C(55)	120.10(16)	F(14)-P(1)-F(15)	82.9(7)
C(54)-C(55)-C(56)	121.80(15)	F(23)-P(2)-F(22)	91.10(19)
C(54)-C(55)-C(60)	119.20(15)	F(23)-P(2)-F(21)	94.40(17)
C(56)-C(55)-C(60)	119.00(14)	F(22)-P(2)-F(21)	90.60(17)
C(57)-C(56)-C(55)	120.00(17)	F(23)-P(2)-F(24)	92.90(17)
C(56)-C(57)-C(58)	121.30(15)	F(22)-P(2)-F(24)	176(2)
C(59)-C(58)-C(57)	120.40(13)	F(21)-P(2)-F(24)	87.10(14)
C(58)-C(59)-C(60)	121.10(15)	F(23)-P(2)-F(26)	89.10(18)
C(55)-C(60)-C(59)	118.20(15)	F(22)-P(2)-F(26)	92.40(14)
C(55)-C(60)-C(61)	118.90(14)	F(21)-P(2)-F(26)	175(2)
C(59)-C(60)-C(61)	122.70(16)	F(24)-P(2)-F(26)	89.70(15)
C(67)-C(61)-C(62)	117.30(15)	F(23)-P(2)-F(25)	175(2)
C(67)-C(61)-C(60)	119.20(14)	F(22)-P(2)-F(25)	94.20(17)
C(62)-C(61)-C(60)	123.50(16)	F(21)-P(2)-F(25)	86.90(15)
C(63)-C(62)-C(61)	122.70(18)	F(24)-P(2)-F(25)	81.90(16)
C(62)-C(63)-C(64)	118.50(19)	F(26)-P(2)-F(25)	89.30(16)
C(66)-C(64)-C(63)	120.40(15)	F(33)-P(3)-F(34)	92.5(4)
C(64)-C(66)-C(67)	122.50(16)	F(33)-P(3)-F(35)	178.9(4)
C(66)-C(67)-C(61)	117.90(15)	F(34)-P(3)-F(35)	87.7(4)
C(66)-C(67)-C(53)	125.10(15)	F(33)-P(3)-F(36)	91.4(3)
C(61)-C(67)-C(53)	116.90(13)	F(34)-P(3)-F(36)	89.9(4)
C(81)-C(68)-C(69)	109.60(18)	F(35)-P(3)-F(36)	87.5(3)
C(81)-C(68)-C(50)	124(2)	F(33)-P(3)-F(31)	90.6(3)
C(69)-C(68)-C(50)	126(2)	F(34)-P(3)-F(31)	93.9(5)
C(68)-C(69)-C(70)	128(3)	F(35)-P(3)-F(31)	90.5(3)
C(75)-C(70)-C(71)	120(3)	F(36)-P(3)-F(31)	175.6(5)
C(75)-C(70)-C(69)	119(2)	F(33)-P(3)-F(32)	85.8(3)
C(71)-C(70)-C(69)	120(3)	F(34)-P(3)-F(32)	178.4(4)
C(72)-C(71)-C(70)	118(3)	F(35)-P(3)-F(32)	93.9(4)
C(71)-C(72)-C(73)	122(2)	F(36)-P(3)-F(32)	90.1(4)
C(74)-C(73)-C(72)	120.10(17)	F(31)-P(3)-F(32)	86.1(4)
C(73)-C(74)-C(75)	120.30(19)		
C(70)-C(75)-C(74)	118(2)		

Appendix 5: Supplementary information for chapter III, part B.

Table 1. Crystal data and structure refinement for **L2, Chapter III,Part B.**

Empirical formula	C23 H17 N5 O
Formula weight	379.42
Temperature	100(2)K
Wavelength	1.54178 Å
Crystal system	Monoclinic
Space group	P21/c
Unit cell dimensions	a = 8.9102(5) Å α = 90° b = 23.1288(10) Å β = 108.705(3)° c = 9.3172(4) Å γ = 90°
Volume	1818.69(15)Å^3
Z	4
Density (calculated)	1.386 g/cm^3
Absorption coefficient	0.714 mm^{-1}
F(000)	792
Crystal size	0.62 x 0.43 x 0.23 mm
Theta range for data collection	3.82 to 72.87°
Index ranges	$-8 \le h \le 10$, $-27 \le k \le 27$, $-11 \le \ell \le 11$
Reflections collected	14499
Independent reflections	3462 [R_{int} = 0.044]
Absorption correction	Semi-empirical from equivalents
Max. and min. transmission	0.8900 and 0.8800
Refinement method	Full-matrix least-squares on F^2
Data / restraints / parameters	3462 / 2 / 285
Goodness-of-fit on F^2	0.998
Final R indices [I>2sigma(I)]	R_1 = 0.0539, wR_2 = 0.1493
R indices (all data)	R_1 = 0.0581, wR_2 = 0.1530
Largest diff. peak and hole	0.229 and -0.273 e/Å^3

Table 2. Atomic coordinates (x 10^4) and equivalent isotropic displacement parameters ($Å^2$ x 10^3) for **L2, Chapter III,Part B.**

U_{eq} is defined as one third of the trace of the orthogonalized Uij tensor.

	x	y	z	U_{eq}
N(1)	6625(2)	74(1)	7053(2)	28(1)
N(2)	7604(2)	33(1)	4555(2)	25(1)
N(3)	9117(2)	-917(1)	3941(2)	31(1)
N(4)	6587(2)	980(1)	3890(2)	25(1)
N(5)	7922(2)	502(1)	2399(2)	26(1)
C(1)	6195(2)	108(1)	8296(2)	30(1)
C(2)	5390(2)	574(1)	8638(2)	31(1)
C(3)	4986(2)	1030(1)	7628(2)	32(1)
C(4)	5431(2)	1004(1)	6330(2)	29(1)
C(5)	6259(2)	526(1)	6101(2)	25(1)
C(6)	6837(2)	505(1)	4764(2)	24(1)
C(7)	7165(2)	955(1)	2730(2)	25(1)
C(8)	8108(2)	54(1)	3349(2)	25(1)
C(9)	8943(2)	-460(1)	3007(2)	26(1)
C(10)	9507(2)	-453(1)	1787(2)	30(1)
C(11)	10283(3)	-937(1)	1497(2)	33(1)
C(12)	10470(2)	-1408(1)	2444(2)	34(1)
C(13)	9876(3)	-1376(1)	3641(2)	35(1)
C(14)	7006(2)	1476(1)	1755(2)	26(1)
C(15)	5537(2)	1774(1)	1150(2)	26(1)
C(16)	4098(2)	1589(1)	1356(2)	28(1)
C(17)	2718(3)	1884(1)	713(2)	33(1)
C(18)	2679(3)	2379(1)	-186(2)	37(1)
C(19)	4034(3)	2567(1)	-414(2)	34(1)
C(20)	5489(2)	2273(1)	233(2)	28(1)
C(21)	6898(3)	2460(1)	-22(2)	33(1)
C(22)	8283(3)	2161(1)	566(2)	33(1)
C(23)	8337(2)	1663(1)	1450(2)	29(1)
O(51)	1867(1)	1043(1)	3311(2)	40(1)

Table 3. Hydrogen coordinates (x 10^4) and isotropic displacement parameters ($Å^2$ x 10^3) for **L2, Chapter III,Part B.**

	x	y	z	U_{eq}
H(1)	6459	-205	8992	22(5)
H(2)	5116	578	9543	25(5)
H(3)	4424	1354	7819	33(6)
H(4)	5164	1308	5608	30(5)
H(10)	9360	-122	1155	36(6)
H(11)	10678	-943	662	47(7)
H(12)	10997	-1746	2280	37(6)
H(13)	10019	-1700	4297	43(7)
H(16)	4095	1254	1945	30(6)
H(17)	1771	1756	873	45(7)
H(18)	1710	2579	-631	32(6)
H(19)	4002	2901	-1017	45(7)
H(21)	6878	2799	-607	35(6)
H(22)	9215	2289	376	42(7)
H(23)	9302	1455	1842	42(7)
H(51B)	2200(30)	713(6)	3190(40)	75(10)
H(51A)	1590(30)	987(14)	4080(18)	74(10)

Table 4. Anisotropic parameters ($Å^2$ x 10^3) for **L2, Chapter III,Part B.**

The anisotropic displacement factor exponent takes the form:

$$-2\pi^2 [h^2 a^{*2} U_{11} + ... + 2 h k a^* b^* U_{12}]$$

	U11	U22	U33	U23	U13	U12
N(1)	35(1)	24(1)	22(1)	1(1)	6(1)	-3(1)
N(2)	33(1)	20(1)	21(1)	0(1)	5(1)	-2(1)
N(3)	38(1)	22(1)	31(1)	2(1)	9(1)	1(1)
N(4)	36(1)	19(1)	20(1)	0(1)	6(1)	0(1)
N(5)	35(1)	19(1)	23(1)	0(1)	8(1)	-2(1)
C(1)	40(1)	27(1)	20(1)	3(1)	7(1)	-5(1)
C(2)	39(1)	32(1)	21(1)	-4(1)	10(1)	-8(1)
C(3)	39(1)	26(1)	28(1)	-6(1)	9(1)	-3(1)
C(4)	39(1)	23(1)	23(1)	0(1)	6(1)	-2(1)
C(5)	33(1)	21(1)	19(1)	-1(1)	4(1)	-4(1)
C(6)	31(1)	19(1)	18(1)	-1(1)	3(1)	-4(1)
C(7)	34(1)	20(1)	19(1)	-1(1)	5(1)	-3(1)
C(8)	30(1)	21(1)	20(1)	-1(1)	4(1)	-4(1)
C(9)	30(1)	20(1)	24(1)	-1(1)	4(1)	-3(1)
C(10)	37(1)	24(1)	26(1)	-1(1)	6(1)	-2(1)
C(11)	38(1)	30(1)	32(1)	-7(1)	11(1)	-2(1)
C(12)	37(1)	24(1)	39(1)	-8(1)	9(1)	1(1)
C(13)	45(1)	21(1)	37(1)	1(1)	10(1)	3(1)
C(14)	41(1)	17(1)	19(1)	-2(1)	10(1)	-2(1)
C(15)	42(1)	17(1)	17(1)	-4(1)	7(1)	-2(1)
C(16)	40(1)	21(1)	22(1)	1(1)	9(1)	-1(1)
C(17)	38(1)	31(1)	28(1)	0(1)	6(1)	-2(1)
C(18)	43(1)	31(1)	30(1)	2(1)	2(1)	4(1)
C(19)	50(1)	23(1)	23(1)	2(1)	4(1)	-2(1)
C(20)	43(1)	18(1)	19(1)	-2(1)	6(1)	-3(1)
C(21)	50(1)	20(1)	28(1)	4(1)	12(1)	-4(1)
C(22)	47(1)	23(1)	32(1)	0(1)	17(1)	-6(1)
C(23)	41(1)	22(1)	26(1)	-1(1)	12(1)	-1(1)
O(51)	52(1)	31(1)	41(1)	13(1)	20(1)	8(1)

Table 5. Bond lengths [Å] and angles [°] for C23 H17 N5 O

N(1)-C(1)	1.334(2)	C(3)-C(2)-C(1)	118.50(17)
N(1)-C(5)	1.344(2)	C(3)-C(2)-H(2)	120.7
N(2)-C(6)	1.335(2)	C(1)-C(2)-H(2)	120.8
N(2)-C(8)	1.339(2)	C(2)-C(3)-C(4)	118.39(18)
N(3)-C(13)	1.336(3)	C(2)-C(3)-H(3)	120.8
N(3)-C(9)	1.346(2)	C(4)-C(3)-H(3)	120.8
N(4)-C(7)	1.339(2)	C(5)-C(4)-C(3)	118.95(17)
N(4)-C(6)	1.344(2)	C(5)-C(4)-H(4)	120.4
N(5)-C(7)	1.335(2)	C(3)-C(4)-H(4)	120.6
N(5)-C(8)	1.339(2)	N(1)-C(5)-C(4)	123.27(17)
C(1)-C(2)	1.386(3)	N(1)-C(5)-C(6)	116.73(16)
C(1)-H(1)	0.9502	C(4)-C(5)-C(6)	119.97(15)
C(2)-C(3)	1.383(3)	N(2)-C(6)-N(4)	125.00(17)
C(2)-H(2)	0.9501	N(2)-C(6)-C(5)	118.58(15)
C(3)-C(4)	1.389(3)	N(4)-C(6)-C(5)	116.37(15)
C(3)-H(3)	0.9500	N(5)-C(7)-N(4)	125.03(15)
C(4)-C(5)	1.383(3)	N(5)-C(7)-C(14)	116.78(16)
C(4)-H(4)	0.9501	N(4)-C(7)-C(14)	118.16(15)
C(5)-C(6)	1.492(2)	N(2)-C(8)-N(5)	125.46(16)
C(7)-C(14)	1.487(2)	N(2)-C(8)-C(9)	118.39(15)
C(8)-C(9)	1.489(3)	N(5)-C(8)-C(9)	116.15(16)
C(9)-C(10)	1.383(3)	N(3)-C(9)-C(10)	122.86(17)
C(10)-C(11)	1.386(3)	N(3)-C(9)-C(8)	116.77(16)
C(10)-H(10)	0.9500	C(10)-C(9)-C(8)	120.37(16)
C(11)-C(12)	1.378(3)	C(9)-C(10)-C(11)	119.20(17)
C(11)-H(11)	0.9502	C(9)-C(10)-H(10)	120.3
C(12)-C(13)	1.381(3)	C(11)-C(10)-H(10)	120.5
C(12)-H(12)	0.9499	C(12)-C(11)-C(10)	118.55(19)
C(13)-H(13)	0.9502	C(12)-C(11)-H(11)	120.8
C(14)-C(23)	1.375(3)	C(10)-C(11)-H(11)	120.7
C(14)-C(15)	1.426(3)	C(11)-C(12)-C(13)	118.44(18)
C(15)-C(16)	1.422(3)	C(11)-C(12)-H(12)	120.9
C(15)-C(20)	1.427(2)	C(13)-C(12)-H(12)	120.7
C(16)-C(17)	1.365(3)	N(3)-C(13)-C(12)	124.20(18)
C(16)-H(16)	0.9499	N(3)-C(13)-H(13)	117.7
C(17)-C(18)	1.412(3)	C(12)-C(13)-H(13)	118.1
C(17)-H(17)	0.9498	C(23)-C(14)-C(15)	120.61(16)
C(18)-C(19)	1.363(3)	C(23)-C(14)-C(7)	117.45(17)
C(18)-H(18)	0.9500	C(15)-C(14)-C(7)	121.94(17)
C(19)-C(20)	1.416(3)	C(16)-C(15)-C(14)	123.65(16)
C(19)-H(19)	0.9501	C(16)-C(15)-C(20)	117.93(17)
C(20)-C(21)	1.419(3)	C(14)-C(15)-C(20)	118.37(17)
C(21)-C(22)	1.368(3)	C(17)-C(16)-C(15)	121.00(17)
C(21)-H(21)	0.9502	C(17)-C(16)-H(16)	119.5
C(22)-C(23)	1.408(3)	C(15)-C(16)-H(16)	119.5
C(22)-H(22)	0.9499	C(16)-C(17)-C(18)	120.8(2)
C(23)-H(23)	0.9499	C(16)-C(17)-H(17)	119.7
O(51)-H(51B)	0.8400	C(18)-C(17)-H(17)	119.5
O(51)-H(51A)	0.8400	C(19)-C(18)-C(17)	119.81(19)
C(1)-N(1)-C(5)	116.81(16)	C(19)-C(18)-H(18)	120.1
C(6)-N(2)-C(8)	114.69(15)	C(17)-C(18)-H(18)	120.1
C(13)-N(3)-C(9)	116.76(17)	C(18)-C(19)-C(20)	121.05(18)
C(7)-N(4)-C(6)	114.99(15)	C(18)-C(19)-H(19)	119.5
C(7)-N(5)-C(8)	114.80(15)	C(20)-C(19)-H(19)	119.5
N(1)-C(1)-C(2)	124.03(17)	C(19)-C(20)-C(21)	121.33(17)
N(1)-C(1)-H(1)	118.0	C(19)-C(20)-C(15)	119.38(18)
C(2)-C(1)-H(1)	118.0	C(21)-C(20)-C(15)	119.28(18)

C(22)-C(21)-C(20)	120.73(17)	C(14)-C(23)-C(22)	120.57(19)
C(22)-C(21)-H(21)	119.7	C(14)-C(23)-H(23)	119.7
C(20)-C(21)-H(21)	119.6	C(22)-C(23)-H(23)	119.7
C(21)-C(22)-C(23)	120.42(19)	H(51B)-O(51)-H(51A)	101(3)
C(21)-C(22)-H(22)	119.8		
C(23)-C(22)-H(22)	119.8		

Table 1. Crystal data and structure refinement for **2b, chapter III, part B.**

Empirical formula	C100 H72 B F22 N24 P3 Ru2
Formula weight	2333.68
Temperature	220(2)K
Wavelength	1.54178 Å
Crystal system	Monoclinic
Space group	P21/n
Unit cell dimensions	a = 19.4728(3) Å α = 90° b = 22.3984(3) Å β = 100.8690(10)° c = 22.8983(3) Å γ = 90°
Volume	9808.1(2)Å^3
Z	4
Density (calculated)	1.580 g/cm^3
Absorption coefficient	3.867 mm^{-1}
F(000)	4704
Crystal size	0.28 x 0.28 x 0.10 mm
Theta range for data collection	2.74 to 72.96°
Index ranges	$-23 \le h \le 22$, $-27 \le k \le 27$, $-28 \le \ell \le 28$
Reflections collected	119340
Independent reflections	19369 [R_{int} = 0.038]
Absorption correction	Semi-empirical from equivalents
Max. and min. transmission	0.7500 and 0.4200
Refinement method	Full-matrix least-squares on F^2
Data / restraints / parameters	19369 / 174 / 1368
Goodness-of-fit on F^2	0.911
Final R indices [I>2sigma(I)]	R_1 = 0.0510, wR_2 = 0.1350
R indices (all data)	R_1 = 0.0820, wR_2 = 0.1484
Largest diff. peak and hole	1.081 and -0.881 e/Å^3

Table 2. Atomic coordinates (x 10^4) and equivalent isotropic displacement parameters ($Å^2$ x 10^3) for **2b, chapter III, part B.**

U_{eq} is defined as one third of the trace of the orthogonalized Uij tensor.

	x	y	z	U_{eq}
Ru(1)	2487(1)	2461(1)	7246(1)	32(1)
N(1)	2337(2)	3216(2)	6689(2)	34(1)
N(2)	1522(2)	2352(2)	6810(2)	33(1)
N(3)	2192(2)	1669(2)	7612(2)	35(1)
N(4)	610(2)	2645(2)	6040(2)	34(1)
N(5)	508(2)	1772(2)	6616(2)	36(1)
N(6)	2366(2)	2950(2)	7998(2)	34(1)
N(7)	3457(2)	2522(1)	7685(1)	32(1)
N(8)	3041(2)	2003(2)	6693(2)	35(1)
N(9)	4239(2)	2822(2)	8538(2)	34(1)
N(10)	4634(2)	2256(2)	7777(2)	35(1)
C(1)	2775(2)	3674(2)	6663(2)	44(1)
C(2)	2600(2)	4149(2)	6273(2)	51(1)
C(3)	1965(2)	4163(2)	5897(2)	51(1)
C(4)	1504(2)	3694(2)	5910(2)	41(1)
C(5)	1699(2)	3234(2)	6307(2)	36(1)
C(6)	1237(2)	2732(2)	6375(2)	33(1)
C(7)	254(2)	2161(2)	6179(2)	34(1)
C(8)	1148(2)	1877(2)	6914(2)	34(1)
C(9)	1527(2)	1492(2)	7385(2)	35(1)
C(10)	1241(2)	981(2)	7586(2)	41(1)
C(11)	1644(2)	649(2)	8030(2)	47(1)
C(12)	2311(2)	822(2)	8257(2)	46(1)
C(13)	2577(2)	1331(2)	8038(2)	41(1)
C(14)	-465(2)	2080(2)	5844(2)	33(1)
C(15)	-783(2)	2584(2)	5569(2)	40(1)
C(16)	-1487(2)	2588(2)	5303(2)	45(1)
C(17)	-1882(2)	2085(2)	5322(2)	41(1)
C(18)	-1576(2)	1554(2)	5570(2)	33(1)
C(19)	-1983(2)	1028(2)	5565(2)	45(1)
C(20)	-1701(2)	515(2)	5789(2)	53(1)
C(21)	-983(2)	482(2)	6030(2)	51(1)
C(22)	-574(2)	974(2)	6052(2)	42(1)
C(23)	-852(2)	1534(2)	5835(2)	33(1)
C(24)	1775(2)	3158(2)	8129(2)	43(1)
C(25)	1757(2)	3475(2)	8642(2)	49(1)
C(26)	2375(2)	3587(2)	9034(2)	49(1)
C(27)	2992(2)	3365(2)	8909(2)	44(1)
C(28)	2982(2)	3052(2)	8390(2)	34(1)
C(29)	3609(2)	2798(2)	8218(2)	32(1)
C(30)	4746(2)	2548(2)	8302(2)	33(1)
C(31)	3986(2)	2250(2)	7485(2)	33(1)
C(32)	3750(2)	1959(2)	6905(2)	35(1)
C(33)	4196(2)	1674(2)	6597(2)	41(1)
C(34)	3925(3)	1427(2)	6050(2)	51(1)
C(35)	3226(3)	1469(2)	5834(2)	51(1)
C(36)	2791(2)	1748(2)	6163(2)	43(1)
C(37)	5455(2)	2555(2)	8664(2)	38(1)
C(38)	5510(2)	2522(2)	9272(2)	45(1)
C(39)	6164(3)	2482(2)	9648(2)	54(1)

C(40)	6766(2)	2483(2)	9418(2)	54(1)
C(41)	6740(2)	2520(2)	8805(2)	47(1)
C(42)	7354(2)	2536(2)	8558(3)	62(2)
C(43)	7339(3)	2616(3)	7981(3)	78(2)
C(44)	6701(3)	2688(3)	7593(3)	72(2)
C(45)	6080(2)	2657(2)	7801(2)	53(1)
C(46)	6079(2)	2570(2)	8409(2)	40(1)
Ru(2)	2432(1)	9959(1)	2281(1)	30(1)
N(11)	2345(2)	10731(1)	1756(2)	32(1)
N(12)	1468(2)	9904(1)	1821(2)	31(1)
N(13)	2074(2)	9163(2)	2600(2)	34(1)
N(14)	604(2)	10259(2)	1049(2)	33(1)
N(15)	416(2)	9371(2)	1585(2)	36(1)
N(16)	2329(2)	10451(2)	3044(1)	32(1)
N(17)	3401(2)	9986(1)	2728(1)	30(1)
N(18)	2978(2)	9490(1)	1727(2)	33(1)
N(19)	4197(2)	10297(2)	3572(2)	35(1)
N(20)	4578(2)	9720(2)	2807(2)	35(1)
C(47)	2820(2)	11165(2)	1752(2)	39(1)
C(48)	2696(2)	11652(2)	1386(2)	42(1)
C(49)	2065(2)	11713(2)	1003(2)	44(1)
C(50)	1573(2)	11268(2)	996(2)	38(1)
C(51)	1720(2)	10790(2)	1368(2)	32(1)
C(52)	1224(2)	10305(2)	1398(2)	29(1)
C(53)	211(2)	9782(2)	1150(2)	34(1)
C(54)	1058(2)	9440(2)	1903(2)	33(1)
C(55)	1395(2)	9024(2)	2352(2)	35(1)
C(56)	1076(2)	8512(2)	2506(2)	43(1)
C(57)	1446(3)	8134(2)	2925(2)	48(1)
C(58)	2126(2)	8269(2)	3165(2)	46(1)
C(59)	2421(2)	8782(2)	2993(2)	41(1)
C(60)	-495(2)	9727(2)	777(2)	38(1)
C(61)	-747(2)	10230(2)	463(2)	46(1)
C(62)	-1433(2)	10266(2)	135(2)	51(1)
C(63)	-1870(2)	9793(2)	120(2)	48(1)
C(64)	-1634(2)	9258(2)	423(2)	43(1)
C(65)	-2099(2)	8770(2)	397(2)	54(1)
C(66)	-1887(3)	8246(3)	668(2)	61(2)
C(67)	-1186(3)	8182(2)	963(3)	64(2)
C(68)	-729(2)	8654(2)	1009(2)	52(1)
C(69)	-937(2)	9209(2)	749(2)	41(1)
C(70)	1745(2)	10689(2)	3171(2)	38(1)
C(71)	1744(2)	11001(2)	3690(2)	40(1)
C(72)	2363(2)	11076(2)	4096(2)	44(1)
C(73)	2971(2)	10843(2)	3962(2)	39(1)
C(74)	2941(2)	10532(2)	3438(2)	33(1)
C(75)	3561(2)	10265(2)	3253(2)	31(1)
C(76)	4703(2)	10021(2)	3326(2)	36(1)
C(77)	3924(2)	9722(2)	2520(2)	33(1)
C(78)	3680(2)	9440(2)	1935(2)	34(1)
C(79)	4125(2)	9159(2)	1618(2)	42(1)
C(80)	3853(2)	8927(2)	1060(2)	48(1)
C(81)	3142(3)	8972(2)	858(2)	49(1)
C(82)	2716(2)	9246(2)	1197(2)	41(1)
C(83)	5422(2)	10040(2)	3681(2)	38(1)
C(84)	5488(2)	10075(2)	4285(2)	48(1)
C(85)	6146(2)	10057(2)	4667(2)	54(1)
C(86)	6735(3)	10010(2)	4434(2)	56(1)
C(87)	6701(2)	10005(2)	3812(2)	50(1)
C(88)	7318(2)	9992(2)	3567(3)	67(2)
C(89)	7291(3)	10019(3)	2986(3)	85(2)
C(90)	6647(3)	10068(3)	2588(3)	81(2)

C(91)	6032(2)	10061(2)	2800(2)	57(1)
C(92)	6043(2)	10023(2)	3413(2)	42(1)
P(1)	4683(1)	4211(1)	7523(1)	52(1)
F(11)	4025(2)	4331(2)	7801(2)	101(1)
F(12)	4955(2)	4867(2)	7652(2)	103(1)
F(13)	4242(2)	4408(1)	6893(1)	74(1)
F(14)	4425(2)	3544(1)	7382(2)	73(1)
F(15)	5122(1)	4009(2)	8146(1)	72(1)
F(16)	5336(1)	4088(2)	7218(1)	78(1)
P(2)	4763(1)	1650(1)	2468(1)	62(1)
F(21)	4080(2)	1808(2)	2723(2)	86(1)
F(22)	5048(2)	2309(2)	2586(2)	95(1)
F(23)	4351(2)	1835(1)	1829(1)	74(1)
F(24)	4485(2)	991(1)	2348(2)	86(1)
F(25)	5170(2)	1460(2)	3097(2)	97(1)
F(26)	5431(2)	1483(2)	2183(2)	80(1)
P(3)	4109(1)	8436(1)	4392(1)	86(1)
F(31)	4511(4)	7876(3)	4553(3)	275(5)
F(32)	3451(2)	8091(3)	4077(2)	170(2)
F(33)	4341(2)	8462(3)	3771(2)	170(2)
F(34)	4744(2)	8796(3)	4700(2)	180(3)
F(35)	3791(3)	8449(3)	4959(2)	187(3)
F(36)	3701(3)	9039(2)	4169(2)	147(2)
B(4)	806(3)	6078(3)	5789(2)	45(1)
F(41)	1276(2)	6526(2)	5761(2)	148(2)
F(42)	676(2)	6178(2)	6355(2)	138(2)
F(43)	1154(3)	5599(2)	5795(3)	165(2)
F(44)	234(2)	6150(2)	5404(2)	123(2)
C(101)	4580(4)	3143(3)	5938(3)	102(2)
C(102)	3841(4)	3058(3)	5699(3)	81(2)
N(103)	3288(4)	3002(3)	5517(3)	115(2)
C(111)	5050(4)	4053(3)	9627(3)	100(2)
C(112)	5738(5)	3997(4)	10023(4)	104(3)
N(113)	6227(4)	3940(4)	10322(5)	177(4)
C(121)	9426(4)	2617(4)	9162(4)	137(3)
C(122)	9129(4)	2035(5)	9172(4)	94(3)
N(123)	8893(4)	1561(4)	9183(4)	128(3)
C(131)	4815(3)	547(3)	927(3)	97(2)
C(132)	4062(3)	520(2)	838(3)	63(2)
N(133)	3477(3)	497(2)	772(2)	83(2)

Table 3. Hydrogen coordinates (x 10^4) and isotropic displacement parameters ($Å^2$ x 10^3) for **2b, chapter III, part B.**

	x	y	z	U_{eq}
H(1)	3214	3673	6918	52
H(2)	2920	4462	6267	61
H(3)	1843	4486	5635	62
H(4)	1067	3690	5653	50
H(10)	782	863	7422	50
H(11)	1458	305	8177	57
H(12)	2589	597	8559	55
H(13)	3041	1444	8192	50
H(15)	-517	2933	5561	48
H(16)	-1690	2934	5111	54
H(17)	-2365	2096	5166	49
H(19)	-2463	1042	5399	53
H(20)	-1984	174	5784	64
H(21)	-785	117	6179	61
H(22)	-94	943	6214	50
H(24)	1353	3086	7863	51
H(25)	1330	3614	8724	58
H(26)	2375	3811	9381	59
H(27)	3416	3427	9175	53
H(33)	4676	1648	6756	49
H(34)	4220	1233	5829	62
H(35)	3037	1308	5460	62
H(36)	2307	1760	6013	51
H(38)	5103	2526	9436	54
H(39)	6191	2456	10062	64
H(40)	7202	2457	9676	65
H(42)	7789	2488	8812	75
H(43)	7758	2624	7835	94
H(44)	6693	2758	7187	86
H(45)	5653	2696	7533	64
H(47)	3255	11133	2010	46
H(48)	3043	11945	1396	51
H(49)	1971	12048	753	53
H(50)	1139	11295	736	45
H(56)	612	8423	2328	52
H(57)	1234	7789	3044	58
H(58)	2389	8013	3446	55
H(59)	2890	8866	3160	49
H(61)	-450	10561	468	56
H(62)	-1587	10617	-73	61
H(63)	-2332	9820	-92	58
H(65)	-2561	8809	189	64
H(66)	-2204	7928	659	73
H(67)	-1030	7812	1130	77
H(68)	-268	8606	1218	63
H(70)	1323	10643	2899	45
H(71)	1325	11161	3769	48
H(72)	2368	11281	4454	53
H(73)	3399	10895	4225	47
H(79)	4605	9125	1779	50
H(80)	4145	8746	828	57
H(81)	2944	8815	483	59
H(82)	2232	9262	1053	50

H(84)	5083	10112	4451	57
H(85)	6177	10076	5081	65
H(86)	7172	9981	4690	68
H(88)	7755	9963	3822	80
H(89)	7708	10006	2836	102
H(90)	6638	10105	2177	97
H(91)	5602	10082	2533	68
H(10A)	4812	3289	5626	153
H(10B)	4787	2766	6087	153
H(10C)	4636	3431	6260	153
H(11A)	4686	3939	9841	150
H(11B)	5033	3792	9286	150
H(11C)	4979	4463	9493	150
H(12A)	9413	2738	8753	206
H(12B)	9907	2610	9373	206
H(12C)	9160	2898	9353	206
H(13A)	5008	153	1033	146
H(13B)	4989	826	1245	146
H(13C)	4955	678	563	146

Table 4. Anisotropic parameters ($Å^2$ x 10^3) for **2b, chapter III, part B.**

The anisotropic displacement factor exponent takes the form:

$$-2\pi^2 [h^2 a^{*2} U_{11} + ... + 2 h k a^* b^* U_{12}]$$

	U11	U22	U33	U23	U13	U12
Ru(1)	26(1)	37(1)	33(1)	0(1)	2(1)	-3(1)
N(1)	29(2)	35(2)	37(2)	0(2)	4(2)	-2(2)
N(2)	28(2)	35(2)	34(2)	1(2)	3(1)	-2(1)
N(3)	32(2)	36(2)	34(2)	0(2)	4(2)	-3(2)
N(4)	31(2)	36(2)	33(2)	1(2)	1(1)	-3(1)
N(5)	30(2)	38(2)	39(2)	0(2)	3(2)	-6(2)
N(6)	33(2)	36(2)	32(2)	-1(2)	6(2)	-2(2)
N(7)	27(2)	38(2)	32(2)	-4(2)	5(1)	-1(1)
N(8)	36(2)	36(2)	33(2)	-1(2)	4(2)	-3(2)
N(9)	28(2)	42(2)	32(2)	0(2)	3(1)	-1(2)
N(10)	30(2)	41(2)	35(2)	-2(2)	6(2)	-2(2)
C(1)	39(3)	43(3)	47(3)	-5(2)	3(2)	-9(2)
C(2)	53(3)	40(3)	59(3)	0(2)	10(2)	-15(2)
C(3)	51(3)	41(3)	60(3)	14(2)	6(2)	-3(2)
C(4)	38(3)	40(3)	44(3)	3(2)	5(2)	-1(2)
C(5)	36(2)	34(2)	37(2)	-1(2)	7(2)	-2(2)
C(6)	30(2)	32(2)	36(2)	2(2)	5(2)	1(2)
C(7)	28(2)	39(2)	33(2)	-4(2)	3(2)	-4(2)
C(8)	32(2)	38(2)	32(2)	0(2)	8(2)	-4(2)
C(9)	33(2)	38(2)	33(2)	2(2)	2(2)	0(2)
C(10)	38(3)	40(3)	45(3)	2(2)	4(2)	-4(2)
C(11)	58(3)	36(3)	48(3)	8(2)	10(2)	-2(2)
C(12)	50(3)	48(3)	36(3)	8(2)	-1(2)	6(2)
C(13)	36(3)	47(3)	38(3)	2(2)	-2(2)	3(2)
C(14)	29(2)	37(2)	31(2)	-2(2)	2(2)	1(2)
C(15)	37(3)	37(2)	44(3)	0(2)	3(2)	-3(2)
C(16)	38(3)	43(3)	48(3)	0(2)	-3(2)	8(2)
C(17)	29(2)	55(3)	36(2)	-7(2)	0(2)	0(2)
C(18)	29(2)	42(3)	28(2)	-1(2)	4(2)	-5(2)
C(19)	34(3)	60(3)	36(3)	3(2)	-2(2)	-10(2)
C(20)	50(3)	55(3)	48(3)	10(2)	-6(2)	-22(2)
C(21)	51(3)	41(3)	54(3)	9(2)	-5(2)	-8(2)
C(22)	36(3)	43(3)	43(3)	4(2)	-2(2)	-3(2)
C(23)	29(2)	41(2)	28(2)	-3(2)	5(2)	-3(2)
C(24)	33(2)	45(3)	49(3)	4(2)	7(2)	1(2)
C(25)	43(3)	54(3)	51(3)	2(2)	15(2)	16(2)
C(26)	52(3)	56(3)	40(3)	-5(2)	10(2)	14(2)
C(27)	39(3)	56(3)	36(3)	-2(2)	4(2)	3(2)
C(28)	32(2)	37(2)	32(2)	0(2)	7(2)	1(2)
C(29)	31(2)	35(2)	29(2)	2(2)	6(2)	-1(2)
C(30)	30(2)	33(2)	35(2)	2(2)	3(2)	0(2)
C(31)	31(2)	32(2)	35(2)	1(2)	5(2)	1(2)
C(32)	39(2)	32(2)	33(2)	-2(2)	8(2)	-5(2)
C(33)	43(3)	38(3)	41(3)	-3(2)	6(2)	3(2)
C(34)	65(3)	44(3)	46(3)	-11(2)	15(2)	8(2)
C(35)	65(3)	45(3)	39(3)	-12(2)	-2(2)	4(2)
C(36)	44(3)	41(3)	38(3)	-3(2)	-5(2)	-2(2)
C(37)	34(2)	41(3)	37(2)	-4(2)	-1(2)	1(2)
C(38)	44(3)	52(3)	37(3)	0(2)	1(2)	1(2)
C(39)	56(3)	54(3)	41(3)	0(2)	-15(2)	4(2)

C(40)	40(3)	51(3)	61(3)	-3(3)	-20(2)	6(2)
C(41)	34(2)	39(3)	64(3)	-13(2)	-6(2)	4(2)
C(42)	29(3)	61(4)	93(5)	-20(3)	2(3)	2(2)
C(43)	33(3)	106(5)	101(5)	-39(4)	24(3)	-8(3)
C(44)	50(3)	104(5)	68(4)	-16(4)	27(3)	-10(3)
C(45)	36(3)	72(4)	52(3)	-5(3)	8(2)	-2(2)
C(46)	29(2)	44(3)	45(3)	-3(2)	1(2)	3(2)
Ru(2)	25(1)	33(1)	29(1)	1(1)	-1(1)	-2(1)
N(11)	27(2)	34(2)	33(2)	3(2)	4(1)	0(1)
N(12)	28(2)	34(2)	30(2)	0(2)	5(1)	-4(1)
N(13)	34(2)	34(2)	32(2)	0(2)	6(2)	-1(2)
N(14)	27(2)	39(2)	32(2)	-2(2)	2(1)	-2(1)
N(15)	27(2)	37(2)	42(2)	0(2)	2(2)	-4(1)
N(16)	26(2)	38(2)	30(2)	2(2)	1(1)	0(1)
N(17)	27(2)	34(2)	29(2)	1(2)	0(1)	1(1)
N(18)	31(2)	30(2)	34(2)	-1(2)	2(1)	-1(1)
N(19)	27(2)	40(2)	35(2)	-1(2)	-2(2)	-2(2)
N(20)	29(2)	38(2)	36(2)	2(2)	0(2)	1(2)
C(47)	30(2)	44(3)	41(3)	-2(2)	3(2)	-5(2)
C(48)	36(3)	36(3)	56(3)	-1(2)	9(2)	-9(2)
C(49)	53(3)	33(3)	48(3)	5(2)	16(2)	0(2)
C(50)	35(2)	40(3)	37(2)	3(2)	4(2)	2(2)
C(51)	26(2)	38(2)	30(2)	-4(2)	3(2)	0(2)
C(52)	26(2)	35(2)	26(2)	-1(2)	3(2)	0(2)
C(53)	27(2)	41(2)	33(2)	-6(2)	2(2)	-4(2)
C(54)	30(2)	34(2)	34(2)	-5(2)	4(2)	-6(2)
C(55)	38(2)	34(2)	32(2)	-3(2)	5(2)	-5(2)
C(56)	44(3)	43(3)	44(3)	2(2)	12(2)	-8(2)
C(57)	62(3)	38(3)	47(3)	1(2)	17(2)	-4(2)
C(58)	57(3)	39(3)	40(3)	6(2)	7(2)	5(2)
C(59)	46(3)	40(3)	36(2)	3(2)	1(2)	3(2)
C(60)	27(2)	46(3)	38(2)	-11(2)	0(2)	1(2)
C(61)	38(3)	55(3)	42(3)	-5(2)	-3(2)	-3(2)
C(62)	43(3)	58(3)	44(3)	-4(2)	-12(2)	2(2)
C(63)	30(2)	71(4)	40(3)	-14(2)	-4(2)	-3(2)
C(64)	29(2)	57(3)	41(3)	-15(2)	3(2)	-3(2)
C(65)	33(3)	77(4)	47(3)	-21(3)	-2(2)	-11(2)
C(66)	45(3)	70(4)	66(4)	-20(3)	4(3)	-25(3)
C(67)	55(3)	51(3)	81(4)	-5(3)	1(3)	-7(3)
C(68)	33(3)	51(3)	68(4)	-10(3)	1(2)	-12(2)
C(69)	32(2)	48(3)	40(3)	-13(2)	5(2)	-4(2)
C(70)	29(2)	41(3)	41(3)	7(2)	3(2)	-2(2)
C(71)	36(2)	40(3)	44(3)	-1(2)	7(2)	5(2)
C(72)	49(3)	45(3)	37(3)	-4(2)	5(2)	5(2)
C(73)	37(2)	40(3)	37(2)	0(2)	-1(2)	2(2)
C(74)	29(2)	34(2)	34(2)	1(2)	0(2)	-2(2)
C(75)	28(2)	33(2)	32(2)	2(2)	1(2)	-2(2)
C(76)	29(2)	36(2)	42(3)	6(2)	2(2)	-3(2)
C(77)	27(2)	34(2)	35(2)	1(2)	2(2)	0(2)
C(78)	35(2)	32(2)	34(2)	2(2)	4(2)	3(2)
C(79)	37(3)	41(3)	43(3)	-4(2)	-1(2)	5(2)
C(80)	54(3)	38(3)	52(3)	-8(2)	10(2)	9(2)
C(81)	60(3)	46(3)	38(3)	-8(2)	-1(2)	5(2)
C(82)	40(3)	41(3)	40(3)	-3(2)	-2(2)	0(2)
C(83)	31(2)	37(2)	43(3)	2(2)	-4(2)	3(2)
C(84)	38(3)	56(3)	46(3)	-2(2)	0(2)	4(2)
C(85)	45(3)	57(3)	52(3)	-3(3)	-11(2)	2(2)
C(86)	43(3)	44(3)	69(4)	-4(3)	-21(2)	3(2)
C(87)	31(2)	42(3)	70(4)	-8(3)	-5(2)	4(2)
C(88)	27(3)	73(4)	95(5)	-26(4)	-5(3)	7(2)
C(89)	34(3)	115(6)	109(6)	-43(5)	23(3)	-7(3)
C(90)	52(4)	123(6)	71(4)	-27(4)	19(3)	-6(4)

C(91)	36(3)	72(4)	63(4)	-13(3)	11(2)	-3(2)
C(92)	31(2)	35(2)	57(3)	-9(2)	0(2)	1(2)
P(1)	39(1)	54(1)	58(1)	10(1)	-1(1)	-6(1)
F(11)	53(2)	156(4)	95(3)	-7(3)	19(2)	21(2)
F(12)	116(3)	65(2)	111(3)	-4(2)	-20(2)	-24(2)
F(13)	64(2)	67(2)	80(2)	19(2)	-16(2)	0(2)
F(14)	67(2)	54(2)	87(2)	20(2)	-11(2)	-11(2)
F(15)	50(2)	107(3)	53(2)	18(2)	-2(1)	-9(2)
F(16)	45(2)	123(3)	63(2)	12(2)	5(2)	-10(2)
P(2)	43(1)	63(1)	73(1)	15(1)	-4(1)	-6(1)
F(21)	46(2)	124(3)	87(3)	-4(2)	7(2)	1(2)
F(22)	75(2)	72(2)	128(3)	-6(2)	-9(2)	-20(2)
F(23)	62(2)	81(2)	71(2)	17(2)	-8(2)	-4(2)
F(24)	67(2)	60(2)	120(3)	27(2)	-10(2)	-10(2)
F(25)	55(2)	140(3)	86(3)	38(2)	-10(2)	-4(2)
F(26)	44(2)	104(3)	89(3)	-2(2)	6(2)	-5(2)
P(3)	63(1)	108(2)	89(1)	-19(1)	17(1)	-5(1)
F(31)	279(7)	243(7)	240(8)	-96(6)	-111(6)	206(6)
F(32)	119(3)	243(5)	143(4)	-12(3)	11(3)	-21(3)
F(33)	119(3)	243(5)	143(4)	-12(3)	11(3)	-21(3)
F(34)	81(3)	280(7)	175(5)	-67(5)	14(3)	-58(4)
F(35)	178(5)	246(6)	169(5)	58(5)	115(4)	21(5)
F(36)	188(5)	77(3)	147(4)	-2(3)	-40(4)	8(3)
B(4)	25(3)	61(4)	49(3)	6(3)	12(2)	6(2)
F(41)	98(3)	186(5)	148(4)	67(4)	-10(3)	-42(3)
F(42)	85(3)	245(6)	86(3)	-22(3)	23(2)	0(3)
F(43)	148(4)	139(5)	191(6)	-47(4)	-13(4)	21(4)
F(44)	71(3)	189(5)	99(3)	-48(3)	-7(2)	8(3)
C(101)	121(7)	67(5)	119(7)	-1(4)	28(5)	0(4)
C(102)	108(6)	61(4)	80(5)	-7(4)	32(5)	-6(4)
N(103)	121(6)	122(6)	103(6)	-3(4)	24(5)	-15(5)
C(111)	113(6)	119(6)	79(5)	2(5)	45(5)	-4(5)
C(112)	110(7)	114(7)	91(6)	-30(5)	29(5)	-3(6)
N(113)	120(7)	191(9)	198(10)	-65(8)	-26(6)	-7(7)
C(121)	88(6)	173(10)	145(9)	10(8)	8(6)	13(6)
C(122)	58(5)	118(7)	103(6)	-24(6)	7(4)	15(5)
N(123)	106(6)	144(7)	138(7)	-29(6)	29(5)	26(5)
C(131)	54(4)	130(6)	108(6)	20(5)	17(4)	-7(4)
C(132)	57(4)	59(4)	69(4)	7(3)	-1(3)	-5(3)
N(133)	64(3)	89(4)	92(4)	6(3)	1(3)	-4(3)

Table 5. Bond lengths [Å] and angles [°] for **2b, chapter III, part B.**

Ru(1)-N(2)	1.970(3)	C(34)-C(35)	1.361(6)
Ru(1)-N(7)	1.971(3)	C(35)-C(36)	1.385(6)
Ru(1)-N(8)	2.081(3)	C(37)-C(38)	1.378(6)
Ru(1)-N(3)	2.089(3)	C(37)-C(46)	1.444(6)
Ru(1)-N(6)	2.091(3)	C(38)-C(39)	1.399(6)
Ru(1)-N(1)	2.104(3)	C(39)-C(40)	1.373(7)
N(1)-C(1)	1.341(5)	C(40)-C(41)	1.396(7)
N(1)-C(5)	1.379(5)	C(41)-C(42)	1.417(7)
N(2)-C(8)	1.336(5)	C(41)-C(46)	1.432(5)
N(2)-C(6)	1.348(5)	C(42)-C(43)	1.327(8)
N(3)-C(13)	1.346(5)	C(43)-C(44)	1.394(7)
N(3)-C(9)	1.361(5)	C(44)-C(45)	1.382(6)
N(4)-C(6)	1.329(5)	C(45)-C(46)	1.406(6)
N(4)-C(7)	1.357(5)	Ru(2)-N(17)	1.971(3)
N(5)-C(8)	1.325(5)	Ru(2)-N(12)	1.977(3)
N(5)-C(7)	1.347(5)	Ru(2)-N(18)	2.086(3)
N(6)-C(24)	1.328(5)	Ru(2)-N(13)	2.095(3)
N(6)-C(28)	1.375(5)	Ru(2)-N(11)	2.096(3)
N(7)-C(31)	1.349(5)	Ru(2)-N(16)	2.107(3)
N(7)-C(29)	1.351(5)	N(11)-C(47)	1.343(5)
N(8)-C(36)	1.346(5)	N(11)-C(51)	1.370(5)
N(8)-C(32)	1.378(5)	N(12)-C(52)	1.341(5)
N(9)-C(29)	1.307(5)	N(12)-C(54)	1.346(5)
N(9)-C(30)	1.358(5)	N(13)-C(59)	1.328(5)
N(10)-C(31)	1.312(5)	N(13)-C(55)	1.373(5)
N(10)-C(30)	1.351(5)	N(14)-C(52)	1.319(5)
C(1)-C(2)	1.391(6)	N(14)-C(53)	1.358(5)
C(2)-C(3)	1.366(6)	N(15)-C(54)	1.331(5)
C(3)-C(4)	1.386(6)	N(15)-C(53)	1.361(5)
C(4)-C(5)	1.379(6)	N(16)-C(70)	1.336(5)
C(5)-C(6)	1.465(5)	N(16)-C(74)	1.365(5)
C(7)-C(14)	1.476(5)	N(17)-C(75)	1.338(5)
C(8)-C(9)	1.466(5)	N(17)-C(77)	1.341(5)
C(9)-C(10)	1.389(5)	N(18)-C(82)	1.341(5)
C(10)-C(11)	1.379(6)	N(18)-C(78)	1.365(5)
C(11)-C(12)	1.361(6)	N(19)-C(75)	1.315(5)
C(12)-C(13)	1.385(6)	N(19)-C(76)	1.370(5)
C(14)-C(15)	1.382(5)	N(20)-C(77)	1.319(5)
C(14)-C(23)	1.434(5)	N(20)-C(76)	1.347(5)
C(15)-C(16)	1.390(5)	C(47)-C(48)	1.368(6)
C(16)-C(17)	1.370(6)	C(48)-C(49)	1.376(6)
C(17)-C(18)	1.402(6)	C(49)-C(50)	1.380(5)
C(18)-C(19)	1.419(5)	C(50)-C(51)	1.367(5)
C(18)-C(23)	1.427(5)	C(51)-C(52)	1.462(5)
C(19)-C(20)	1.335(6)	C(53)-C(60)	1.480(5)
C(20)-C(21)	1.405(6)	C(54)-C(55)	1.450(5)
C(21)-C(22)	1.355(6)	C(55)-C(56)	1.382(5)
C(22)-C(23)	1.419(5)	C(56)-C(57)	1.375(6)
C(24)-C(25)	1.379(6)	C(57)-C(58)	1.368(6)
C(25)-C(26)	1.381(6)	C(58)-C(59)	1.375(6)
C(26)-C(27)	1.380(6)	C(60)-C(61)	1.377(6)
C(27)-C(28)	1.377(6)	C(60)-C(69)	1.439(6)
C(28)-C(29)	1.465(5)	C(61)-C(62)	1.404(6)
C(30)-C(37)	1.471(5)	C(62)-C(63)	1.357(6)
C(31)-C(32)	1.474(5)	C(63)-C(64)	1.416(6)
C(32)-C(33)	1.373(5)	C(64)-C(65)	1.414(6)
C(33)-C(34)	1.380(6)	C(64)-C(69)	1.424(5)

C(65)-C(66)	1.355(7)	N(2)-RU1-N(6)	103.69(13)
C(66)-C(67)	1.412(7)	N(7)-RU1-N(6)	77.85(13)
C(67)-C(68)	1.374(6)	N(8)-RU1-N(6)	155.60(13)
C(68)-C(69)	1.405(6)	N(3)-RU1-N(6)	91.80(13)
C(70)-C(71)	1.378(6)	N(2)-RU1-N(1)	77.46(13)
C(71)-C(72)	1.386(6)	N(7)-RU1-N(1)	105.32(13)
C(72)-C(73)	1.379(6)	N(8)-RU1-N(1)	93.25(13)
C(73)-C(74)	1.379(6)	N(3)-RU1-N(1)	155.31(13)
C(74)-C(75)	1.480(5)	N(6)-RU1-N(1)	93.09(13)
C(76)-C(83)	1.483(5)	C(1)-N(1)-C(5)	117.0(4)
C(77)-C(78)	1.475(5)	C(1)-N(1)-RU1	128.6(3)
C(78)-C(79)	1.382(5)	C(5)-N(1)-RU1	114.4(3)
C(79)-C(80)	1.390(6)	C(8)-N(2)-C(6)	118.2(4)
C(80)-C(81)	1.378(6)	C(8)-N(2)-RU1	120.6(3)
C(81)-C(82)	1.382(6)	C(6)-N(2)-RU1	121.1(3)
C(83)-C(84)	1.367(6)	C(13)-N(3)-C(9)	118.2(4)
C(83)-C(92)	1.455(6)	C(13)-N(3)-RU1	127.7(3)
C(84)-C(85)	1.408(6)	C(9)-N(3)-RU1	114.1(3)
C(85)-C(86)	1.358(7)	C(6)-N(4)-C(7)	115.9(3)
C(86)-C(87)	1.412(7)	C(8)-N(5)-C(7)	116.5(4)
C(87)-C(88)	1.420(7)	C(24)-N(6)-C(28)	118.7(4)
C(87)-C(92)	1.427(6)	C(24)-N(6)-RU1	127.4(3)
C(88)-C(89)	1.322(8)	C(28)-N(6)-RU1	113.8(3)
C(89)-C(90)	1.409(8)	C(31)-N(7)-C(29)	117.6(3)
C(90)-C(91)	1.375(6)	C(31)-N(7)-RU1	121.0(3)
C(91)-C(92)	1.403(7)	C(29)-N(7)-RU1	121.2(3)
P(1)-F(11)	1.557(3)	C(36)-N(8)-C(32)	117.1(4)
P(1)-F(12)	1.571(3)	C(36)-N(8)-RU1	128.0(3)
P(1)-F(15)	1.585(3)	C(32)-N(8)-RU1	114.9(3)
P(1)-F(16)	1.587(3)	C(29)-N(9)-C(30)	115.8(4)
P(1)-F(14)	1.589(3)	C(31)-N(10)-C(30)	115.9(3)
P(1)-F(13)	1.596(3)	N(1)-C(1)-C(2)	122.2(4)
P(2)-F(25)	1.567(3)	C(3)-C(2)-C(1)	120.4(4)
P(2)-F(24)	1.577(3)	C(2)-C(3)-C(4)	118.8(4)
P(2)-F(22)	1.582(3)	C(5)-C(4)-C(3)	118.8(4)
P(2)-F(23)	1.586(3)	C(4)-C(5)-N(1)	122.9(4)
P(2)-F(21)	1.590(3)	C(4)-C(5)-C(6)	123.0(4)
P(2)-F(26)	1.606(3)	N(1)-C(5)-C(6)	114.1(4)
P(3)-F(31)	1.488(5)	N(4)-C(6)-N(2)	122.6(4)
P(3)-F(34)	1.533(4)	N(4)-C(6)-C(5)	124.6(4)
P(3)-F(35)	1.540(5)	N(2)-C(6)-C(5)	112.8(4)
P(3)-F(32)	1.552(5)	N(5)-C(7)-N(4)	124.0(4)
P(3)-F(33)	1.571(5)	N(5)-C(7)-C(14)	119.1(4)
P(3)-F(36)	1.600(4)	N(4)-C(7)-C(14)	116.9(4)
B(4)-F(43)	1.269(6)	N(5)-C(8)-N(2)	122.7(4)
B(4)-F(44)	1.293(6)	N(5)-C(8)-C(9)	124.7(4)
B(4)-F(41)	1.366(6)	N(2)-C(8)-C(9)	112.6(4)
B(4)-F(42)	1.385(6)	N(3)-C(9)-C(10)	121.7(4)
C(101)-C(102)	1.453(8)	N(3)-C(9)-C(8)	114.9(4)
C(102)-N(103)	1.085(8)	C(10)-C(9)-C(8)	123.4(4)
C(111)-C(112)	1.474(9)	C(11)-C(10)-C(9)	118.8(4)
C(112)-N(113)	1.071(10)	C(12)-C(11)-C(10)	119.8(4)
C(121)-C(122)	1.429(10)	C(11)-C(12)-C(13)	119.5(4)
C(122)-N(123)	1.158(10)	N(3)-C(13)-C(12)	122.0(4)
C(131)-C(132)	1.444(7)	C(15)-C(14)-C(23)	120.1(4)
C(132)-N(133)	1.121(6)	C(15)-C(14)-C(7)	115.9(4)
N(2)-RU1-N(7)	176.82(14)	C(23)-C(14)-C(7)	123.8(4)
N(2)-RU1-N(8)	100.69(13)	C(14)-C(15)-C(16)	121.7(4)
N(7)-RU1-N(8)	77.74(13)	C(17)-C(16)-C(15)	119.6(4)
N(2)-RU1-N(3)	77.87(13)	C(16)-C(17)-C(18)	120.8(4)
N(7)-RU1-N(3)	99.36(13)	C(17)-C(18)-C(19)	120.4(4)
N(8)-RU1-N(3)	92.20(13)	C(17)-C(18)-C(23)	120.7(4)

C(19)-C(18)-C(23)	118.9(4)	C(47)-N(11)-C(51)	117.1(4)
C(20)-C(19)-C(18)	121.6(4)	C(47)-N(11)-RU2	128.3(3)
C(19)-C(20)-C(21)	120.2(4)	C(51)-N(11)-RU2	114.6(3)
C(22)-C(21)-C(20)	120.5(4)	C(52)-N(12)-C(54)	118.7(3)
C(21)-C(22)-C(23)	121.5(4)	C(52)-N(12)-RU2	121.0(3)
C(22)-C(23)-C(18)	117.3(4)	C(54)-N(12)-RU2	120.1(3)
C(22)-C(23)-C(14)	125.8(4)	C(59)-N(13)-C(55)	117.5(4)
C(18)-C(23)-C(14)	116.9(4)	C(59)-N(13)-RU2	128.5(3)
N(6)-C(24)-C(25)	122.4(4)	C(55)-N(13)-RU2	114.0(3)
C(24)-C(25)-C(26)	119.2(4)	C(52)-N(14)-C(53)	116.2(4)
C(27)-C(26)-C(25)	119.1(4)	C(54)-N(15)-C(53)	115.9(3)
C(28)-C(27)-C(26)	119.5(4)	C(70)-N(16)-C(74)	118.3(4)
N(6)-C(28)-C(27)	121.1(4)	C(70)-N(16)-RU2	127.5(3)
N(6)-C(28)-C(29)	115.4(4)	C(74)-N(16)-RU2	114.2(3)
C(27)-C(28)-C(29)	123.5(4)	C(75)-N(17)-C(77)	117.5(3)
N(9)-C(29)-N(7)	123.1(4)	C(75)-N(17)-RU2	121.3(3)
N(9)-C(29)-C(28)	125.2(4)	C(77)-N(17)-RU2	121.2(3)
N(7)-C(29)-C(28)	111.7(3)	C(82)-N(18)-C(78)	117.9(4)
N(10)-C(30)-N(9)	124.5(4)	C(82)-N(18)-RU2	127.2(3)
N(10)-C(30)-C(37)	118.9(4)	C(78)-N(18)-RU2	114.9(3)
N(9)-C(30)-C(37)	116.5(4)	C(75)-N(19)-C(76)	114.9(4)
N(10)-C(31)-N(7)	123.0(4)	C(77)-N(20)-C(76)	115.8(4)
N(10)-C(31)-C(32)	124.8(4)	N(11)-C(47)-C(48)	122.5(4)
N(7)-C(31)-C(32)	112.2(3)	C(47)-C(48)-C(49)	120.3(4)
C(33)-C(32)-N(8)	122.8(4)	C(48)-C(49)-C(50)	117.9(4)
C(33)-C(32)-C(31)	123.2(4)	C(51)-C(50)-C(49)	119.8(4)
N(8)-C(32)-C(31)	114.0(4)	C(50)-C(51)-N(11)	122.3(4)
C(32)-C(33)-C(34)	118.8(4)	C(50)-C(51)-C(52)	123.2(4)
C(35)-C(34)-C(33)	119.1(4)	N(11)-C(51)-C(52)	114.5(4)
C(34)-C(35)-C(36)	120.5(4)	N(14)-C(52)-N(12)	122.9(4)
N(8)-C(36)-C(35)	121.8(4)	N(14)-C(52)-C(51)	124.7(4)
C(38)-C(37)-C(46)	119.9(4)	N(12)-C(52)-C(51)	112.5(3)
C(38)-C(37)-C(30)	117.0(4)	N(14)-C(53)-N(15)	124.0(4)
C(46)-C(37)-C(30)	123.0(4)	N(14)-C(53)-C(60)	117.4(4)
C(37)-C(38)-C(39)	120.9(5)	N(15)-C(53)-C(60)	118.6(4)
C(40)-C(39)-C(38)	120.5(5)	N(15)-C(54)-N(12)	122.2(4)
C(39)-C(40)-C(41)	120.9(4)	N(15)-C(54)-C(55)	124.5(4)
C(40)-C(41)-C(42)	122.0(5)	N(12)-C(54)-C(55)	113.3(4)
C(40)-C(41)-C(46)	120.0(4)	N(13)-C(55)-C(56)	121.8(4)
C(42)-C(41)-C(46)	118.0(5)	N(13)-C(55)-C(54)	114.8(4)
C(43)-C(42)-C(41)	122.6(5)	C(56)-C(55)-C(54)	123.4(4)
C(42)-C(43)-C(44)	120.0(5)	C(57)-C(56)-C(55)	119.2(4)
C(45)-C(44)-C(43)	120.4(6)	C(58)-C(57)-C(56)	118.9(4)
C(44)-C(45)-C(46)	120.9(5)	C(57)-C(58)-C(59)	119.6(4)
C(45)-C(46)-C(41)	118.0(4)	N(13)-C(59)-C(58)	123.0(4)
C(45)-C(46)-C(37)	124.2(4)	C(61)-C(60)-C(69)	118.9(4)
C(41)-C(46)-C(37)	117.8(4)	C(61)-C(60)-C(53)	115.7(4)
N(17)-RU2-N(12)	178.02(13)	C(69)-C(60)-C(53)	125.2(4)
N(17)-RU2-N(18)	77.50(13)	C(60)-C(61)-C(62)	122.4(5)
N(12)-RU2-N(18)	100.77(13)	C(63)-C(62)-C(61)	119.8(5)
N(17)-RU2-N(13)	101.22(13)	C(62)-C(63)-C(64)	120.3(4)
N(12)-RU2-N(13)	77.78(13)	C(65)-C(64)-C(63)	119.2(4)
N(18)-RU2-N(13)	91.46(12)	C(65)-C(64)-C(69)	120.1(5)
N(17)-RU2-N(11)	103.77(13)	C(63)-C(64)-C(69)	120.7(4)
N(12)-RU2-N(11)	77.23(13)	C(66)-C(65)-C(64)	120.9(5)
N(18)-RU2-N(11)	93.53(12)	C(65)-C(66)-C(67)	119.4(5)
N(13)-RU2-N(11)	155.00(12)	C(68)-C(67)-C(66)	120.8(5)
N(17)-RU2-N(16)	77.58(12)	C(67)-C(68)-C(69)	121.1(5)
N(12)-RU2-N(16)	104.16(13)	C(68)-C(69)-C(64)	117.5(4)
N(18)-RU2-N(16)	155.07(12)	C(68)-C(69)-C(60)	124.8(4)
N(13)-RU2-N(16)	93.81(13)	C(64)-C(69)-C(60)	117.7(4)
N(11)-RU2-N(16)	91.91(12)	N(16)-C(70)-C(71)	122.0(4)

C(70)-C(71)-C(72)	119.7(4)	F(11)-P(1)-F(13)	88.75(19)
C(73)-C(72)-C(71)	118.7(4)	F(12)-P(1)-F(13)	90.91(19)
C(74)-C(73)-C(72)	119.1(4)	F(15)-P(1)-F(13)	179.4(2)
N(16)-C(74)-C(73)	122.1(4)	F(16)-P(1)-F(13)	89.33(18)
N(16)-C(74)-C(75)	114.5(4)	F(14)-P(1)-F(13)	88.90(17)
C(73)-C(74)-C(75)	123.4(4)	F(25)-P(2)-F(24)	90.3(2)
N(19)-C(75)-N(17)	124.0(4)	F(25)-P(2)-F(22)	89.7(2)
N(19)-C(75)-C(74)	123.6(4)	F(24)-P(2)-F(22)	179.4(2)
N(17)-C(75)-C(74)	112.4(3)	F(25)-P(2)-F(23)	179.4(2)
N(20)-C(76)-N(19)	124.3(4)	F(24)-P(2)-F(23)	89.23(19)
N(20)-C(76)-C(83)	119.5(4)	F(22)-P(2)-F(23)	90.76(19)
N(19)-C(76)-C(83)	116.1(4)	F(25)-P(2)-F(21)	92.1(2)
N(20)-C(77)-N(17)	123.3(4)	F(24)-P(2)-F(21)	89.4(2)
N(20)-C(77)-C(78)	124.5(4)	F(22)-P(2)-F(21)	91.2(2)
N(17)-C(77)-C(78)	112.1(3)	F(23)-P(2)-F(21)	88.19(18)
N(18)-C(78)-C(79)	122.7(4)	F(25)-P(2)-F(26)	90.15(19)
N(18)-C(78)-C(77)	114.3(4)	F(24)-P(2)-F(26)	89.4(2)
C(79)-C(78)-C(77)	123.0(4)	F(22)-P(2)-F(26)	90.0(2)
C(78)-C(79)-C(80)	119.1(4)	F(23)-P(2)-F(26)	89.56(19)
C(81)-C(80)-C(79)	117.7(4)	F(21)-P(2)-F(26)	177.5(2)
C(80)-C(81)-C(82)	121.0(4)	F(31)-P(3)-F(34)	89.3(4)
N(18)-C(82)-C(81)	121.6(4)	F(31)-P(3)-F(35)	94.8(4)
C(84)-C(83)-C(92)	120.1(4)	F(34)-P(3)-F(35)	91.1(3)
C(84)-C(83)-C(76)	117.1(4)	F(31)-P(3)-F(32)	92.6(4)
C(92)-C(83)-C(76)	122.8(4)	F(34)-P(3)-F(32)	178.0(4)
C(83)-C(84)-C(85)	121.8(5)	F(35)-P(3)-F(32)	88.5(3)
C(86)-C(85)-C(84)	119.7(5)	F(31)-P(3)-F(33)	91.6(4)
C(85)-C(86)-C(87)	121.0(4)	F(34)-P(3)-F(33)	93.0(3)
C(86)-C(87)-C(88)	121.1(5)	F(35)-P(3)-F(33)	172.5(3)
C(86)-C(87)-C(92)	120.7(4)	F(32)-P(3)-F(33)	87.2(3)
C(88)-C(87)-C(92)	118.2(5)	F(31)-P(3)-F(36)	175.3(4)
C(89)-C(88)-C(87)	121.4(5)	F(34)-P(3)-F(36)	90.6(3)
C(88)-C(89)-C(90)	121.2(5)	F(35)-P(3)-F(36)	89.9(3)
C(91)-C(90)-C(89)	119.9(6)	F(32)-P(3)-F(36)	87.4(3)
C(90)-C(91)-C(92)	120.4(5)	F(33)-P(3)-F(36)	83.8(3)
C(91)-C(92)-C(87)	118.9(4)	F(43)-B(4)-F(44)	120.1(6)
C(91)-C(92)-C(83)	124.3(4)	F(43)-B(4)-F(41)	105.0(5)
C(87)-C(92)-C(83)	116.6(4)	F(44)-B(4)-F(41)	112.0(5)
F(11)-P(1)-F(12)	92.0(2)	F(43)-B(4)-F(42)	108.6(5)
F(11)-P(1)-F(15)	91.56(19)	F(44)-B(4)-F(42)	109.4(4)
F(12)-P(1)-F(15)	89.56(19)	F(41)-B(4)-F(42)	99.6(5)
F(11)-P(1)-F(16)	178.0(2)	N(103)-C(102)-C(101)	179.0(1)
F(12)-P(1)-F(16)	88.5(2)	N(113)-C(112)-C(111)	177.30(13)
F(15)-P(1)-F(16)	90.36(17)	N(123)-C(122)-C(121)	179.40(12)
F(11)-P(1)-F(14)	89.6(2)	N(133)-C(132)-C(131)	179.4(8)
F(12)-P(1)-F(14)	178.3(2)		
F(15)-P(1)-F(14)	90.62(17)		
F(16)-P(1)-F(14)	89.83(19)		

Table 1. Crystal data and structure refinement for **3b, chapter III, part B.**

Empirical formula	C49 H34.50 F12 N11.50 P2 Zn
Formula weight	1139.69
Temperature	150(2)K
Wavelength	1.54178 Å
Crystal system	Monoclinic
Space group	P21
Unit cell dimensions	a = 8.7117(5) Å α = 90° b = 25.7595(15) Å β = 96.872(3)° c = 21.8696(12) Å γ = 90°
Volume	4872.5(5)Å^3
Z	4
Density (calculated)	1.554 Mg/m^3
Absorption coefficient	2.171 mm^{-1}
F(000)	2308
Crystal size	0.26 x 0.08 x 0.02 mm
Theta range for data collection	2.03 to 68.99°
Index ranges	$-9 \le h \le 10$, $-30 \le k \le 31$, $-26 \le \ell \le 25$
Reflections collected	66693
Independent reflections	17438 [R_{int} = 0.046]
Absorption correction	Semi-empirical from equivalents
Max. and min. transmission	0.9700 and 0.6900
Refinement method	Full-matrix least-squares on F^2
Data / restraints / parameters	17438 / 4 / 1363
Goodness-of-fit on F^2	0.978
Final R indices [I>2sigma(I)]	R_1 = 0.0496, wR_2 = 0.1153
R indices (all data)	R_1 = 0.0874, wR_2 = 0.1335
Absolute structure parameter	0.35(2)
Largest diff. peak and hole	0.565 and -0.657 e/Å^3

Table 2. Atomic coordinates (x 10^4) and equivalent isotropic displacement parameters ($Å^2$ x 10^3) for **3b, chapter III, part B.**

U_{eq} is defined as one third of the trace of the orthogonalized Uij tensor.

	x	y	z	U_{eq}
Zn(1)	3695(1)	7505(1)	7631(1)	34(1)
N(1)	2890(5)	6754(2)	8033(2)	35(1)
N(2)	3181(5)	6999(2)	6899(2)	33(1)
N(3)	4226(5)	7938(2)	6819(2)	31(1)
N(4)	2423(5)	6175(2)	6527(2)	40(1)
N(5)	3135(5)	6833(2)	5842(2)	38(1)
N(6)	1523(5)	7941(2)	7715(2)	34(1)
N(7)	4179(5)	7999(2)	8378(2)	32(1)
N(8)	6146(5)	7332(2)	8023(2)	31(1)
N(9)	3414(5)	8677(2)	8990(2)	33(1)
N(10)	5976(5)	8341(2)	9164(2)	34(1)
C(1)	2759(7)	6653(2)	8634(3)	44(2)
C(2)	2194(7)	6188(2)	8819(3)	46(2)
C(3)	1708(7)	5815(2)	8383(3)	49(2)
C(4)	1869(7)	5913(2)	7771(3)	45(2)
C(5)	2462(6)	6374(2)	7618(2)	37(1)
C(6)	2696(6)	6521(2)	6976(2)	35(1)
C(7)	2657(6)	6347(2)	5962(3)	37(1)
C(8)	3419(6)	7141(2)	6334(2)	34(1)
C(9)	4016(6)	7670(2)	6276(2)	35(1)
C(10)	4412(6)	7879(2)	5738(2)	40(1)
C(11)	5047(7)	8371(2)	5746(3)	46(2)
C(12)	5232(6)	8642(2)	6284(3)	42(1)
C(13)	4806(6)	8423(2)	6810(2)	39(1)
C(14)	2302(7)	5970(2)	5447(3)	41(1)
C(15)	1191(7)	5612(2)	5522(3)	51(2)
C(16)	726(8)	5243(3)	5074(3)	64(2)
C(17)	1384(8)	5241(3)	4536(3)	62(2)
C(18)	2534(7)	5602(3)	4430(3)	49(2)
C(19)	3209(8)	5607(3)	3867(3)	58(2)
C(20)	4368(9)	5944(3)	3772(3)	61(2)
C(21)	4895(9)	6299(3)	4241(3)	61(2)
C(22)	4248(7)	6323(2)	4785(3)	48(2)
C(23)	3054(7)	5982(2)	4895(3)	41(1)
C(24)	163(6)	7882(2)	7363(2)	36(1)
C(25)	-1139(6)	8168(2)	7456(3)	43(1)
C(26)	-1054(6)	8517(2)	7929(3)	41(1)
C(27)	351(6)	8584(2)	8301(2)	38(1)
C(28)	1582(6)	8291(2)	8180(2)	31(1)
C(29)	3122(6)	8335(2)	8542(2)	32(1)
C(30)	4880(6)	8671(2)	9291(2)	31(1)
C(31)	5561(6)	8005(2)	8706(2)	32(1)
C(32)	6682(6)	7617(2)	8527(2)	31(1)
C(33)	8096(5)	7536(3)	8852(2)	39(1)
C(34)	9047(6)	7157(2)	8655(2)	43(1)
C(35)	8519(6)	6871(2)	8136(2)	42(1)
C(36)	7062(6)	6972(2)	7832(2)	36(1)
C(37)	5185(6)	9064(2)	9783(2)	37(1)
C(38)	4284(7)	9492(2)	9735(3)	46(1)
C(39)	4440(7)	9897(3)	10168(3)	52(2)
C(40)	5496(7)	9841(2)	10677(3)	47(2)

C(41)	6452(6)	9405(2)	10761(2)	40(1)
C(42)	7597(7)	9373(2)	11286(3)	46(2)
C(43)	8624(7)	8984(2)	11347(3)	47(2)
C(44)	8583(7)	8598(3)	10887(3)	54(2)
C(45)	7465(7)	8604(2)	10392(3)	48(2)
C(46)	6366(6)	9008(2)	10301(2)	37(1)
Zn(2)	1379(1)	7537(1)	2638(1)	36(1)
N(11)	2187(5)	8286(2)	2245(2)	35(1)
N(12)	1720(5)	8062(2)	3361(2)	34(1)
N(13)	766(5)	7112(2)	3450(2)	34(1)
N(14)	2408(5)	8888(2)	3739(2)	38(1)
N(15)	1651(5)	8234(2)	4414(2)	37(1)
N(16)	3583(5)	7122(2)	2601(2)	38(1)
N(17)	970(5)	7029(2)	1909(2)	34(1)
N(18)	-1052(5)	7686(2)	2222(2)	34(1)
N(19)	1852(5)	6350(2)	1324(2)	42(1)
N(20)	-730(5)	6670(2)	1099(2)	38(1)
C(47)	2425(6)	8389(2)	1667(2)	39(1)
C(48)	3013(7)	8844(2)	1466(3)	43(1)
C(49)	3364(7)	9233(2)	1906(3)	47(2)
C(50)	3107(7)	9140(2)	2509(2)	44(1)
C(51)	2533(6)	8673(2)	2660(2)	36(1)
C(52)	2225(6)	8545(2)	3295(2)	37(1)
C(53)	2114(6)	8718(2)	4309(2)	40(1)
C(54)	1416(6)	7916(2)	3933(2)	38(1)
C(55)	840(6)	7387(2)	3977(2)	34(1)
C(56)	322(6)	7194(2)	4502(2)	40(1)
C(57)	-293(7)	6699(2)	4494(3)	46(2)
C(58)	-362(7)	6414(2)	3960(3)	45(2)
C(59)	196(6)	6630(2)	3446(3)	40(1)
C(60)	2394(6)	9095(2)	4815(2)	36(1)
C(61)	3454(7)	9474(2)	4761(3)	48(2)
C(62)	3915(8)	9830(3)	5234(3)	55(2)
C(63)	3239(7)	9806(3)	5765(3)	53(2)
C(64)	2144(7)	9435(2)	5846(3)	40(1)
C(65)	1431(8)	9417(3)	6406(3)	50(2)
C(66)	321(9)	9083(3)	6477(3)	62(2)
C(67)	-178(8)	8723(3)	6015(3)	58(2)
C(68)	468(7)	8719(3)	5468(3)	49(2)
C(69)	1670(6)	9065(2)	5380(3)	40(1)
C(70)	4902(6)	7198(2)	2972(3)	45(1)
C(71)	6208(7)	6901(3)	2918(3)	51(2)
C(72)	6154(7)	6519(3)	2475(3)	52(2)
C(73)	4807(6)	6436(2)	2096(3)	46(1)
C(74)	3536(6)	6744(2)	2171(2)	40(1)
C(75)	2051(7)	6703(2)	1777(3)	39(1)
C(76)	443(7)	6347(2)	999(2)	39(1)
C(77)	-390(6)	7002(2)	1563(2)	36(1)
C(78)	-1541(6)	7385(2)	1721(2)	35(1)
C(79)	-2981(6)	7434(3)	1394(2)	42(1)
C(80)	-3962(7)	7813(3)	1581(3)	53(2)
C(81)	-3481(7)	8119(2)	2091(3)	47(2)
C(82)	-2020(6)	8040(2)	2391(2)	38(1)
C(83)	189(7)	5950(2)	508(3)	46(2)
C(84)	1172(8)	5528(3)	585(3)	60(2)
C(85)	1102(9)	5119(3)	153(4)	75(2)
C(86)	-8(9)	5138(3)	-337(3)	68(2)
C(87)	-1014(8)	5557(3)	-445(3)	59(2)
C(88)	-2088(10)	5581(3)	-969(3)	73(2)
C(89)	-3181(10)	5969(3)	-1054(3)	75(2)
C(90)	-3196(10)	6359(3)	-619(3)	75(2)
C(91)	-2093(8)	6370(3)	-105(3)	63(2)

C(92)	-961(7)	5972(3)	-2(3)	53(2)
P(1)	2486(2)	7520(1)	122(1)	44(1)
F(11)	3109(4)	8088(1)	314(2)	62(1)
F(12)	1720(5)	7731(2)	-529(2)	83(1)
F(13)	4042(5)	7417(2)	-171(2)	92(2)
F(14)	3236(6)	7312(2)	765(2)	96(2)
F(15)	949(5)	7628(2)	411(2)	89(1)
F(16)	1883(4)	6957(1)	-65(1)	56(1)
P(2)	6776(2)	8298(1)	4078(1)	58(1)
F(21)	7328(4)	7780(2)	3775(2)	70(1)
F(22)	8322(4)	8581(2)	3918(2)	74(1)
F(23)	5923(4)	8473(2)	3409(2)	72(1)
F(24)	5199(4)	8022(2)	4206(2)	68(1)
F(25)	7600(4)	8123(2)	4731(2)	71(1)
F(26)	6210(5)	8818(2)	4374(2)	74(1)
P(3)	8078(2)	6860(1)	6142(1)	47(1)
F(31)	8531(4)	6338(2)	5819(2)	63(1)
F(32)	9625(4)	7138(2)	5979(2)	62(1)
F(33)	7166(4)	7052(2)	5508(1)	59(1)
F(34)	6525(4)	6583(2)	6325(2)	60(1)
F(35)	8984(4)	6664(2)	6785(1)	62(1)
F(36)	7609(4)	7377(1)	6477(2)	60(1)
P(4)	5678(2)	9788(1)	7873(1)	63(1)
F(41)	6501(6)	9487(2)	7360(2)	90(1)
F(42)	6894(7)	9542(2)	8393(2)	133(2)
F(43)	6795(5)	10260(2)	7823(2)	91(1)
F(44)	4481(5)	10059(2)	7367(2)	111(2)
F(45)	4585(9)	9309(2)	7921(2)	156(3)
F(46)	4887(6)	10084(2)	8389(2)	96(2)
C(101)	9230(10)	4898(3)	1867(4)	90(3)
C(102)	9365(8)	5416(3)	2084(3)	60(2)
N(103)	9432(7)	5835(2)	2235(3)	66(2)
C(111)	7155(11)	9710(4)	3388(5)	128(4)
C(112)	8395(11)	9603(5)	3101(5)	125(5)
N(113)	9421(11)	9569(4)	2806(4)	130(4)
C(121)	7420(20)	5407(4)	6583(6)	219(9)
C(122)	6484(16)	5483(4)	7059(5)	113(4)
N(123)	5801(11)	5538(3)	7454(4)	108(3)

Table 3. Hydrogen coordinates (x 10^4) and isotropic displacement parameters ($Å^2$ x 10^3) for C49 **3b, chapter III, part B.**

	x	y	z	U_{eq}
H(1)	3067	6911	8935	52
H(2)	2136	6123	9243	55
H(3)	1272	5498	8502	59
H(4)	1566	5661	7463	54
H(10)	4251	7687	5365	48
H(11)	5352	8517	5381	55
H(12)	5653	8983	6294	50
H(13)	4923	8619	7181	47
H(15)	720	5614	5892	62
H(16)	-44	4995	5141	77
H(17)	1058	4990	4229	74
H(19)	2843	5370	3551	69
H(20)	4811	5940	3396	73
H(21)	5718	6528	4181	73
H(22)	4613	6571	5089	57
H(24)	89	7636	7038	43
H(25)	-2079	8121	7194	51
H(26)	-1939	8712	8005	49
H(27)	446	8827	8630	46
H(33)	8422	7737	9209	47
H(34)	10042	7094	8871	51
H(35)	9149	6608	7990	50
H(36)	6709	6777	7474	44
H(38)	3508	9520	9393	56
H(39)	3827	10202	10107	63
H(40)	5585	10105	10982	57
H(42)	7630	9632	11596	56
H(43)	9378	8968	11698	56
H(44)	9340	8331	10922	65
H(45)	7426	8329	10101	58
H(47)	2166	8125	1368	47
H(48)	3174	8893	1048	52
H(49)	3773	9556	1793	57
H(50)	3330	9400	2814	52
H(56)	387	7398	4866	48
H(57)	-662	6559	4850	55
H(58)	-786	6073	3941	54
H(59)	172	6429	3081	48
H(61)	3904	9499	4388	58
H(62)	4683	10083	5186	66
H(63)	3530	10049	6085	63
H(65)	1766	9652	6730	59
H(66)	-147	9085	6848	75
H(67)	-966	8481	6078	70
H(68)	100	8481	5152	59
H(70)	4944	7461	3279	54
H(71)	7135	6961	3184	61
H(72)	7043	6314	2433	63
H(73)	4745	6174	1789	55
H(79)	-3296	7217	1051	50
H(80)	-4959	7862	1360	64
H(81)	-4143	8376	2228	56
H(82)	-1688	8251	2738	46

H(84)	1916	5512	940	72
H(85)	1812	4838	203	89
H(86)	-103	4855	-618	82
H(88)	-2067	5322	-1277	88
H(89)	-3923	5969	-1410	90
H(90)	-3968	6621	-672	90
H(91)	-2095	6647	181	76
H(10A)	9016	4898	1417	135
H(10B)	8382	4725	2044	135
H(10C)	10198	4712	1992	135
H(11A)	6250	9529	3179	192
H(11B)	6965	10085	3377	192
H(11C)	7343	9593	3817	192
H(12A)	8115	5113	6686	328
H(12B)	8027	5721	6535	328
H(12C)	6760	5334	6197	328

Table 4. Anisotropic parameters ($Å^2$ x 10^3) for **3b, chapter III, part B.**

The anisotropic displacement factor exponent takes the form:

$$-2\pi^2 [h^2 a^{*2} U_{11} + ... + 2 h k a^* b^* U_{12}]$$

	U11	U22	U33	U23	U13	U12
Zn(1)	36(1)	39(1)	27(1)	-5(1)	3(1)	0(1)
N(1)	36(3)	32(3)	36(3)	-4(2)	4(2)	2(2)
N(2)	38(3)	33(3)	27(2)	-3(2)	1(2)	0(2)
N(3)	36(2)	38(3)	20(2)	-1(2)	4(2)	0(2)
N(4)	46(3)	42(3)	33(3)	-7(2)	6(2)	-3(2)
N(5)	42(3)	43(3)	28(2)	-8(2)	0(2)	3(2)
N(6)	32(2)	35(3)	36(3)	0(2)	3(2)	0(2)
N(7)	30(2)	35(3)	30(2)	-5(2)	4(2)	0(2)
N(8)	27(2)	43(3)	25(2)	-1(2)	4(2)	3(2)
N(9)	39(3)	34(3)	27(2)	-3(2)	8(2)	0(2)
N(10)	37(2)	38(3)	27(2)	-5(2)	4(2)	4(2)
C(1)	51(4)	45(4)	33(3)	0(3)	2(3)	-1(3)
C(2)	56(4)	50(4)	33(3)	5(3)	11(3)	2(3)
C(3)	59(4)	41(4)	50(4)	5(3)	20(3)	2(3)
C(4)	50(4)	40(4)	47(4)	-8(3)	11(3)	-1(3)
C(5)	33(3)	39(3)	38(3)	-5(3)	0(2)	2(2)
C(6)	29(3)	43(4)	32(3)	-4(3)	3(2)	3(2)
C(7)	31(3)	38(3)	41(3)	-12(3)	1(2)	-2(2)
C(8)	33(3)	36(3)	34(3)	-2(3)	4(2)	3(2)
C(9)	34(3)	38(4)	31(3)	-3(2)	-3(2)	7(2)
C(10)	46(3)	46(4)	28(3)	-1(3)	0(2)	1(3)
C(11)	52(4)	49(4)	36(3)	7(3)	9(3)	5(3)
C(12)	41(3)	41(4)	43(4)	4(3)	6(2)	-2(3)
C(13)	42(3)	40(4)	34(3)	-4(3)	-2(2)	1(3)
C(14)	42(3)	41(4)	40(3)	-12(3)	2(3)	7(3)
C(15)	46(4)	53(4)	54(4)	-15(3)	5(3)	-8(3)
C(16)	59(4)	67(5)	65(5)	-27(4)	3(3)	-16(4)
C(17)	64(4)	66(5)	51(4)	-32(4)	-11(3)	2(4)
C(18)	51(4)	51(4)	41(4)	-14(3)	-10(3)	13(3)
C(19)	65(5)	68(5)	36(4)	-14(3)	-6(3)	17(4)
C(20)	82(5)	63(5)	36(4)	-8(3)	1(3)	19(4)
C(21)	80(5)	55(5)	48(4)	-9(3)	13(3)	9(4)
C(22)	56(4)	50(4)	36(3)	-8(3)	3(3)	6(3)
C(23)	47(4)	44(4)	29(3)	-9(3)	-6(2)	9(3)
C(24)	30(3)	42(3)	35(3)	1(2)	-1(2)	4(2)
C(25)	26(3)	49(4)	51(4)	6(3)	0(2)	1(2)
C(26)	37(3)	41(3)	46(3)	0(3)	9(2)	6(3)
C(27)	37(3)	41(3)	36(3)	-2(2)	8(2)	4(2)
C(28)	35(3)	31(3)	27(3)	0(2)	6(2)	3(2)
C(29)	36(3)	32(3)	29(3)	1(2)	9(2)	-1(2)
C(30)	40(3)	25(3)	27(3)	0(2)	5(2)	-3(2)
C(31)	37(3)	35(3)	24(3)	4(2)	6(2)	0(2)
C(32)	36(3)	30(3)	27(3)	-3(2)	5(2)	1(2)
C(33)	36(3)	49(3)	32(3)	-7(3)	2(2)	4(3)
C(34)	36(3)	52(4)	39(3)	-5(3)	-1(2)	8(3)
C(35)	42(3)	48(4)	37(3)	2(3)	13(2)	6(3)
C(36)	38(3)	46(4)	25(3)	-5(2)	5(2)	9(3)
C(37)	35(3)	38(3)	39(3)	-4(2)	8(2)	-2(2)
C(38)	51(4)	44(4)	43(3)	-13(3)	3(3)	8(3)
C(39)	57(4)	44(4)	53(4)	-14(3)	-3(3)	8(3)

C(40)	52(4)	45(4)	45(3)	-16(3)	7(3)	0(3)
C(41)	42(3)	44(3)	34(3)	0(3)	9(2)	-4(3)
C(42)	53(4)	53(4)	32(3)	-4(3)	1(3)	-3(3)
C(43)	63(4)	47(4)	29(3)	-2(3)	-4(3)	-6(3)
C(44)	59(4)	55(4)	43(4)	-4(3)	-16(3)	10(3)
C(45)	61(4)	48(4)	34(3)	-3(3)	0(3)	4(3)
C(46)	43(3)	39(3)	30(3)	0(2)	9(2)	-3(3)
Zn(2)	34(1)	41(1)	31(1)	-2(1)	2(1)	1(1)
N(11)	32(2)	40(3)	31(3)	1(2)	0(2)	0(2)
N(12)	33(2)	43(3)	26(2)	-1(2)	1(2)	1(2)
N(13)	35(3)	34(3)	34(3)	3(2)	6(2)	0(2)
N(14)	45(3)	41(3)	27(2)	-2(2)	-2(2)	1(2)
N(15)	38(3)	43(3)	28(2)	0(2)	1(2)	3(2)
N(16)	38(3)	41(3)	35(3)	3(2)	1(2)	6(2)
N(17)	33(2)	35(3)	35(2)	-3(2)	4(2)	2(2)
N(18)	31(2)	40(3)	29(2)	0(2)	1(2)	5(2)
N(19)	42(3)	43(3)	41(3)	-2(2)	10(2)	-1(2)
N(20)	42(3)	38(3)	35(3)	-3(2)	8(2)	-2(2)
C(47)	41(3)	49(4)	27(3)	-5(3)	6(2)	8(3)
C(48)	53(4)	44(4)	34(3)	2(3)	7(3)	8(3)
C(49)	55(4)	34(4)	54(4)	10(3)	6(3)	-1(3)
C(50)	62(4)	41(4)	27(3)	1(3)	5(3)	1(3)
C(51)	41(3)	41(3)	27(3)	2(3)	7(2)	-1(3)
C(52)	32(3)	43(4)	35(3)	3(3)	-2(2)	-1(3)
C(53)	37(3)	46(4)	35(3)	-1(3)	0(2)	1(3)
C(54)	32(3)	45(4)	36(3)	6(3)	3(2)	6(2)
C(55)	31(3)	35(4)	36(3)	-2(2)	1(2)	4(2)
C(56)	45(3)	40(3)	34(3)	6(3)	4(2)	8(3)
C(57)	55(4)	49(4)	33(3)	12(3)	8(3)	10(3)
C(58)	43(4)	39(4)	52(4)	8(3)	2(3)	-1(3)
C(59)	38(3)	40(4)	42(4)	1(3)	5(2)	5(3)
C(60)	37(3)	38(3)	31(3)	1(3)	-4(2)	1(3)
C(61)	54(4)	47(4)	45(4)	-5(3)	12(3)	-7(3)
C(62)	61(4)	54(4)	51(4)	-11(3)	10(3)	-16(3)
C(63)	61(4)	52(4)	46(4)	-14(3)	11(3)	-13(3)
C(64)	49(4)	36(3)	33(3)	1(3)	0(2)	0(3)
C(65)	73(4)	48(4)	27(3)	-8(3)	1(3)	3(3)
C(66)	98(6)	58(5)	33(3)	-3(3)	16(3)	-10(4)
C(67)	77(5)	56(4)	44(4)	-2(3)	20(3)	-25(4)
C(68)	60(4)	47(4)	38(4)	-5(3)	-2(3)	-5(3)
C(69)	43(3)	40(4)	35(3)	0(3)	-3(2)	1(3)
C(70)	35(3)	57(4)	42(3)	3(3)	2(2)	2(3)
C(71)	36(3)	58(4)	58(4)	9(3)	1(3)	4(3)
C(72)	40(4)	56(4)	61(4)	10(3)	8(3)	9(3)
C(73)	41(3)	39(3)	58(4)	-2(3)	10(3)	6(3)
C(74)	43(3)	42(3)	36(3)	6(3)	7(2)	-2(3)
C(75)	46(3)	37(3)	36(3)	-1(3)	10(3)	3(3)
C(76)	51(4)	33(3)	34(3)	-6(2)	9(2)	-6(3)
C(77)	43(3)	36(3)	30(3)	0(2)	3(2)	-4(2)
C(78)	31(3)	41(4)	35(3)	0(2)	8(2)	0(2)
C(79)	40(3)	52(4)	34(3)	-6(3)	0(2)	-1(3)
C(80)	34(3)	74(5)	48(4)	-5(3)	-6(3)	8(3)
C(81)	43(3)	61(4)	37(3)	1(3)	8(3)	14(3)
C(82)	32(3)	48(4)	34(3)	-1(3)	4(2)	6(3)
C(83)	55(4)	42(4)	45(4)	-11(3)	18(3)	-4(3)
C(84)	68(5)	58(4)	59(4)	-19(3)	23(3)	2(4)
C(85)	79(5)	73(5)	76(5)	-28(4)	27(4)	-2(4)
C(86)	69(5)	70(5)	70(5)	-33(4)	27(4)	-23(4)
C(87)	68(5)	65(5)	46(4)	-16(3)	20(3)	-18(4)
C(88)	93(6)	92(6)	40(4)	-21(4)	26(4)	-51(5)
C(89)	93(6)	77(6)	53(5)	9(4)	-1(4)	-31(5)
C(90)	106(6)	68(5)	48(4)	3(4)	-7(4)	-17(5)

C(91)	87(5)	62(5)	37(4)	-3(3)	-10(3)	-8(4)
C(92)	56(4)	65(5)	39(4)	-19(3)	12(3)	-20(3)
P(1)	57(1)	48(1)	27(1)	-1(1)	4(1)	-12(1)
F(11)	88(3)	56(2)	39(2)	-1(2)	5(2)	-23(2)
F(12)	120(3)	69(3)	52(2)	16(2)	-27(2)	-40(2)
F(13)	64(3)	107(4)	110(3)	-43(3)	36(2)	-21(3)
F(14)	150(4)	73(3)	52(2)	21(2)	-41(2)	-38(3)
F(15)	91(3)	86(4)	101(3)	-29(3)	52(2)	-21(3)
F(16)	76(2)	54(2)	37(2)	-5(2)	6(2)	-23(2)
P(2)	46(1)	85(1)	41(1)	-5(1)	-1(1)	6(1)
F(21)	61(2)	87(3)	60(2)	-12(2)	0(2)	18(2)
F(22)	49(2)	106(3)	68(3)	-4(2)	4(2)	-3(2)
F(23)	55(2)	113(3)	44(2)	-1(2)	-6(2)	24(2)
F(24)	51(2)	101(3)	52(2)	-6(2)	6(2)	-5(2)
F(25)	59(2)	109(3)	41(2)	8(2)	-10(2)	-1(2)
F(26)	77(3)	88(3)	57(2)	-15(2)	14(2)	11(2)
P(3)	41(1)	64(1)	36(1)	-7(1)	0(1)	4(1)
F(31)	79(3)	61(2)	49(2)	-6(2)	15(2)	16(2)
F(32)	47(2)	87(3)	51(2)	-3(2)	9(2)	-9(2)
F(33)	58(2)	74(3)	40(2)	-1(2)	-8(2)	3(2)
F(34)	50(2)	83(3)	47(2)	-4(2)	8(2)	-6(2)
F(35)	52(2)	99(3)	34(2)	0(2)	0(2)	17(2)
F(36)	51(2)	68(3)	58(2)	-21(2)	-4(2)	9(2)
P(4)	92(1)	51(1)	49(1)	-2(1)	17(1)	-3(1)
F(41)	136(4)	65(3)	78(3)	-19(2)	51(3)	-11(3)
F(42)	185(6)	127(5)	83(3)	17(3)	0(3)	79(4)
F(43)	92(3)	76(3)	106(3)	-18(3)	19(3)	-20(3)
F(44)	99(4)	161(5)	67(3)	-2(3)	-13(2)	-13(3)
F(45)	285(8)	81(4)	128(4)	-50(3)	130(5)	-91(4)
F(46)	134(4)	96(4)	63(3)	-16(2)	30(3)	15(3)
C(101)	118(7)	46(5)	110(7)	-13(5)	35(5)	-1(5)
C(102)	74(5)	55(5)	56(4)	-9(4)	19(3)	7(4)
N(103)	73(4)	62(4)	65(4)	-12(3)	19(3)	6(3)
C(111)	105(8)	114(9)	159(11)	-47(7)	-14(7)	27(7)
C(112)	69(7)	181(12)	114(8)	-88(8)	-29(6)	38(7)
N(113)	138(8)	176(10)	73(6)	-5(6)	-7(5)	49(7)
C(121)	460(30)	61(7)	176(13)	-4(7)	195(16)	8(11)
C(122)	196(12)	62(6)	88(7)	-7(5)	49(8)	17(6)
N(123)	140(8)	98(6)	90(6)	-8(5)	27(5)	20(5)

Table 5. Bond lengths [Å] and angles [°] for **3b, chapter III, part B.**

Zn(1)-N(2)	2.073(4)	C(35)-C(36)	1.385(7)
Zn(1)-N(7)	2.074(4)	C(37)-C(38)	1.349(8)
Zn(1)-N(3)	2.192(4)	C(37)-C(46)	1.443(8)
Zn(1)-N(6)	2.226(4)	C(38)-C(39)	1.405(8)
Zn(1)-N(8)	2.249(4)	C(39)-C(40)	1.365(8)
Zn(1)-N(1)	2.272(5)	C(40)-C(41)	1.398(8)
N(1)-C(5)	1.354(7)	C(41)-C(46)	1.428(8)
N(1)-C(1)	1.359(7)	C(41)-C(42)	1.430(8)
N(2)-C(6)	1.319(7)	C(42)-C(43)	1.340(8)
N(2)-C(8)	1.329(6)	C(43)-C(44)	1.412(8)
N(3)-C(13)	1.349(7)	C(44)-C(45)	1.366(8)
N(3)-C(9)	1.366(6)	C(45)-C(46)	1.414(8)
N(4)-C(6)	1.326(7)	Zn(2)-N(17)	2.061(4)
N(4)-C(7)	1.351(7)	Zn(2)-N(12)	2.075(4)
N(5)-C(8)	1.337(7)	Zn(2)-N(13)	2.206(4)
N(5)-C(7)	1.354(7)	Zn(2)-N(16)	2.208(4)
N(6)-C(24)	1.342(6)	Zn(2)-N(18)	2.236(4)
N(6)-C(28)	1.354(6)	Zn(2)-N(11)	2.258(4)
N(7)-C(31)	1.326(6)	N(11)-C(47)	1.333(6)
N(7)-C(29)	1.342(6)	N(11)-C(51)	1.357(7)
N(8)-C(36)	1.322(6)	N(12)-C(52)	1.332(7)
N(8)-C(32)	1.359(6)	N(12)-C(54)	1.362(6)
N(9)-C(29)	1.319(6)	N(13)-C(59)	1.335(7)
N(9)-C(30)	1.366(6)	N(13)-C(55)	1.349(7)
N(10)-C(30)	1.333(6)	N(14)-C(52)	1.310(7)
N(10)-C(31)	1.340(6)	N(14)-C(53)	1.373(7)
C(1)-C(2)	1.373(8)	N(15)-C(54)	1.329(7)
C(2)-C(3)	1.383(8)	N(15)-C(53)	1.339(7)
C(3)-C(4)	1.386(8)	N(16)-C(70)	1.340(6)
C(4)-C(5)	1.352(8)	N(16)-C(74)	1.350(7)
C(5)-C(6)	1.492(7)	N(17)-C(75)	1.319(7)
C(7)-C(14)	1.491(8)	N(17)-C(77)	1.329(6)
C(8)-C(9)	1.468(8)	N(18)-C(82)	1.325(6)
C(9)-C(10)	1.375(7)	N(18)-C(78)	1.368(6)
C(10)-C(11)	1.381(8)	N(19)-C(75)	1.339(7)
C(11)-C(12)	1.361(8)	N(19)-C(76)	1.344(7)
C(12)-C(13)	1.374(7)	N(20)-C(77)	1.331(7)
C(14)-C(15)	1.362(8)	N(20)-C(76)	1.356(7)
C(14)-C(23)	1.442(9)	C(47)-C(48)	1.372(8)
C(15)-C(16)	1.389(8)	C(48)-C(49)	1.396(8)
C(16)-C(17)	1.369(9)	C(49)-C(50)	1.384(7)
C(17)-C(18)	1.407(9)	C(50)-C(51)	1.358(8)
C(18)-C(19)	1.426(9)	C(51)-C(52)	1.484(7)
C(18)-C(23)	1.443(8)	C(53)-C(60)	1.471(8)
C(19)-C(20)	1.367(10)	C(54)-C(55)	1.458(8)
C(20)-C(21)	1.409(9)	C(55)-C(56)	1.378(7)
C(21)-C(22)	1.377(8)	C(56)-C(57)	1.382(8)
C(22)-C(23)	1.403(9)	C(57)-C(58)	1.375(8)
C(24)-C(25)	1.387(7)	C(58)-C(59)	1.393(8)
C(25)-C(26)	1.366(8)	C(60)-C(61)	1.358(8)
C(26)-C(27)	1.397(8)	C(60)-C(69)	1.454(8)
C(27)-C(28)	1.363(7)	C(61)-C(62)	1.404(8)
C(28)-C(29)	1.479(7)	C(62)-C(63)	1.365(8)
C(30)-C(37)	1.479(7)	C(63)-C(64)	1.378(8)
C(31)-C(32)	1.483(7)	C(64)-C(69)	1.420(8)
C(32)-C(33)	1.363(7)	C(64)-C(65)	1.438(8)
C(33)-C(34)	1.383(8)	C(65)-C(66)	1.319(9)
C(34)-C(35)	1.385(8)	C(66)-C(67)	1.402(9)

C(67)-C(68)	1.380(8)	N(3)-ZN1-N(8)	97.31(15)
C(68)-C(69)	1.407(8)	N(6)-ZN1-N(8)	147.81(15)
C(70)-C(71)	1.389(8)	N(2)-ZN1-N(1)	73.38(16)
C(71)-C(72)	1.379(9)	N(7)-ZN1-N(1)	105.16(16)
C(72)-C(73)	1.369(8)	N(3)-ZN1-N(1)	148.33(16)
C(73)-C(74)	1.387(8)	N(6)-ZN1-N(1)	95.36(16)
C(74)-C(75)	1.470(8)	N(8)-ZN1-N(1)	90.31(15)
C(76)-C(83)	1.481(8)	C(5)-N(1)-C(1)	117.5(5)
C(77)-C(78)	1.477(7)	C(5)-N(1)-ZN1	115.4(4)
C(78)-C(79)	1.373(7)	C(1)-N(1)-ZN1	127.1(4)
C(79)-C(80)	1.391(8)	C(6)-N(2)-C(8)	117.7(5)
C(80)-C(81)	1.388(8)	C(6)-N(2)-ZN1	122.1(4)
C(81)-C(82)	1.376(7)	C(8)-N(2)-ZN1	120.1(4)
C(83)-C(84)	1.381(9)	C(13)-N(3)-C(9)	117.9(4)
C(83)-C(92)	1.407(8)	C(13)-N(3)-ZN1	126.7(3)
C(84)-C(85)	1.413(9)	C(9)-N(3)-ZN1	115.4(3)
C(85)-C(86)	1.355(10)	C(6)-N(4)-C(7)	115.1(5)
C(86)-C(87)	1.392(10)	C(8)-N(5)-C(7)	115.2(5)
C(87)-C(88)	1.392(10)	C(24)-N(6)-C(28)	117.2(5)
C(87)-C(92)	1.440(9)	C(24)-N(6)-ZN1	126.6(4)
C(88)-C(89)	1.378(11)	C(28)-N(6)-ZN1	116.2(3)
C(89)-C(90)	1.384(11)	C(31)-N(7)-C(29)	117.1(4)
C(90)-C(91)	1.388(9)	C(31)-N(7)-ZN1	121.3(3)
C(91)-C(92)	1.421(9)	C(29)-N(7)-ZN1	121.6(3)
P(1)-F(15)	1.572(4)	C(36)-N(8)-C(32)	118.2(4)
P(1)-F(14)	1.572(4)	C(36)-N(8)-ZN1	126.9(3)
P(1)-F(16)	1.579(4)	C(32)-N(8)-ZN1	114.8(3)
P(1)-F(13)	1.590(4)	C(29)-N(9)-C(30)	115.9(4)
P(1)-F(12)	1.594(4)	C(30)-N(10)-C(31)	115.6(4)
P(1)-F(11)	1.600(4)	N(1)-C(1)-C(2)	121.7(6)
P(2)-F(25)	1.585(4)	C(1)-C(2)-C(3)	119.6(5)
P(2)-F(21)	1.589(4)	C(2)-C(3)-C(4)	118.7(6)
P(2)-F(26)	1.592(4)	C(5)-C(4)-C(3)	119.0(6)
P(2)-F(24)	1.601(4)	C(4)-C(5)-N(1)	123.4(5)
P(2)-F(22)	1.606(4)	C(4)-C(5)-C(6)	123.6(5)
P(2)-F(23)	1.623(4)	N(1)-C(5)-C(6)	112.9(5)
P(3)-F(31)	1.592(4)	N(2)-C(6)-N(4)	124.3(5)
P(3)-F(33)	1.593(3)	N(2)-C(6)-C(5)	116.0(5)
P(3)-F(36)	1.596(4)	N(4)-C(6)-C(5)	119.7(5)
P(3)-F(32)	1.603(4)	N(4)-C(7)-N(5)	124.3(5)
P(3)-F(35)	1.609(4)	N(4)-C(7)-C(14)	115.9(5)
P(3)-F(34)	1.621(4)	N(5)-C(7)-C(14)	119.7(5)
P(4)-F(45)	1.569(5)	N(2)-C(8)-N(5)	123.3(5)
P(4)-F(43)	1.570(5)	N(2)-C(8)-C(9)	115.6(5)
P(4)-F(46)	1.587(4)	N(5)-C(8)-C(9)	121.1(5)
P(4)-F(42)	1.589(5)	N(3)-C(9)-C(10)	121.6(5)
P(4)-F(44)	1.589(5)	N(3)-C(9)-C(8)	113.9(5)
P(4)-F(41)	1.601(4)	C(10)-C(9)-C(8)	124.4(5)
C(101)-C(102)	1.416(9)	C(9)-C(10)-C(11)	119.3(5)
C(102)-N(103)	1.128(8)	C(12)-C(11)-C(10)	119.3(5)
C(111)-C(112)	1.341(11)	C(11)-C(12)-C(13)	119.8(6)
C(112)-N(113)	1.166(11)	N(3)-C(13)-C(12)	122.1(5)
C(121)-C(122)	1.409(14)	C(15)-C(14)-C(23)	121.1(5)
C(122)-N(123)	1.115(11)	C(15)-C(14)-C(7)	115.9(5)
N(2)-ZN1-N(7)	178.50(18)	C(23)-C(14)-C(7)	123.0(5)
N(2)-ZN1-N(3)	74.97(16)	C(14)-C(15)-C(16)	122.0(6)
N(7)-ZN1-N(3)	106.50(17)	C(17)-C(16)-C(15)	119.5(7)
N(2)-ZN1-N(6)	105.93(17)	C(16)-C(17)-C(18)	121.2(6)
N(7)-ZN1-N(6)	73.77(16)	C(17)-C(18)-C(19)	121.5(6)
N(3)-ZN1-N(6)	94.29(16)	C(17)-C(18)-C(23)	120.2(6)
N(2)-ZN1-N(8)	106.06(16)	C(19)-C(18)-C(23)	118.3(6)
N(7)-ZN1-N(8)	74.16(16)	C(20)-C(19)-C(18)	121.7(6)

C(19)-C(20)-C(21)	119.0(7)	C(51)-N(11)-ZN2	115.3(3)
C(22)-C(21)-C(20)	121.7(7)	C(52)-N(12)-C(54)	117.4(5)
C(21)-C(22)-C(23)	120.6(6)	C(52)-N(12)-ZN2	123.0(4)
C(22)-C(23)-C(14)	125.2(5)	C(54)-N(12)-ZN2	119.6(4)
C(22)-C(23)-C(18)	118.7(6)	C(59)-N(13)-C(55)	118.3(5)
C(14)-C(23)-C(18)	116.1(6)	C(59)-N(13)-ZN2	125.7(4)
N(6)-C(24)-C(25)	122.4(5)	C(55)-N(13)-ZN2	115.7(4)
C(26)-C(25)-C(24)	119.3(5)	C(52)-N(14)-C(53)	116.0(5)
C(25)-C(26)-C(27)	119.1(5)	C(54)-N(15)-C(53)	117.4(5)
C(28)-C(27)-C(26)	118.3(5)	C(70)-N(16)-C(74)	118.8(5)
N(6)-C(28)-C(27)	123.6(5)	C(70)-N(16)-ZN2	126.3(4)
N(6)-C(28)-C(29)	113.8(4)	C(74)-N(16)-ZN2	114.9(3)
C(27)-C(28)-C(29)	122.5(5)	C(75)-N(17)-C(77)	116.9(5)
N(9)-C(29)-N(7)	123.4(5)	C(75)-N(17)-ZN2	120.8(4)
N(9)-C(29)-C(28)	122.1(5)	C(77)-N(17)-ZN2	122.3(4)
N(7)-C(29)-C(28)	114.5(4)	C(82)-N(18)-C(78)	117.8(4)
N(10)-C(30)-N(9)	123.9(5)	C(82)-N(18)-ZN2	127.4(3)
N(10)-C(30)-C(37)	121.2(5)	C(78)-N(18)-ZN2	114.7(3)
N(9)-C(30)-C(37)	114.8(4)	C(75)-N(19)-C(76)	115.2(5)
N(7)-C(31)-N(10)	123.9(5)	C(77)-N(20)-C(76)	114.5(5)
N(7)-C(31)-C(32)	115.7(4)	N(11)-C(47)-C(48)	125.5(6)
N(10)-C(31)-C(32)	120.4(4)	C(47)-C(48)-C(49)	116.8(5)
N(8)-C(32)-C(33)	122.8(5)	C(50)-C(49)-C(48)	119.1(6)
N(8)-C(32)-C(31)	114.0(4)	C(51)-C(50)-C(49)	119.3(5)
C(33)-C(32)-C(31)	123.2(5)	N(11)-C(51)-C(50)	123.2(5)
C(32)-C(33)-C(34)	118.9(5)	N(11)-C(51)-C(52)	114.3(5)
C(33)-C(34)-C(35)	118.6(5)	C(50)-C(51)-C(52)	122.6(5)
C(34)-C(35)-C(36)	119.2(5)	N(14)-C(52)-N(12)	124.2(5)
N(8)-C(36)-C(35)	122.2(5)	N(14)-C(52)-C(51)	121.6(5)
C(38)-C(37)-C(46)	119.8(5)	N(12)-C(52)-C(51)	114.2(5)
C(38)-C(37)-C(30)	116.8(5)	N(15)-C(53)-N(14)	123.0(5)
C(46)-C(37)-C(30)	123.5(5)	N(15)-C(53)-C(60)	120.8(5)
C(37)-C(38)-C(39)	123.1(6)	N(14)-C(53)-C(60)	116.1(5)
C(40)-C(39)-C(38)	118.2(6)	N(15)-C(54)-N(12)	121.8(5)
C(39)-C(40)-C(41)	121.7(6)	N(15)-C(54)-C(55)	123.1(5)
C(40)-C(41)-C(46)	120.2(5)	N(12)-C(54)-C(55)	115.1(5)
C(40)-C(41)-C(42)	119.9(5)	N(13)-C(55)-C(56)	122.4(5)
C(46)-C(41)-C(42)	119.8(5)	N(13)-C(55)-C(54)	114.7(5)
C(43)-C(42)-C(41)	121.0(6)	C(56)-C(55)-C(54)	122.8(5)
C(42)-C(43)-C(44)	119.8(5)	C(55)-C(56)-C(57)	119.2(5)
C(45)-C(44)-C(43)	120.8(6)	C(58)-C(57)-C(56)	118.9(5)
C(44)-C(45)-C(46)	121.8(6)	C(57)-C(58)-C(59)	119.1(6)
C(45)-C(46)-C(41)	116.8(5)	N(13)-C(59)-C(58)	122.2(5)
C(45)-C(46)-C(37)	126.3(5)	C(61)-C(60)-C(69)	118.7(5)
C(41)-C(46)-C(37)	116.9(5)	C(61)-C(60)-C(53)	117.5(5)
N(17)-ZN2-N(12)	178.00(17)	C(69)-C(60)-C(53)	123.7(5)
N(17)-ZN2-N(13)	105.72(17)	C(60)-C(61)-C(62)	122.9(6)
N(12)-ZN2-N(13)	74.76(18)	C(63)-C(62)-C(61)	118.9(6)
N(17)-ZN2-N(16)	74.58(17)	C(62)-C(63)-C(64)	121.1(6)
N(12)-ZN2-N(16)	107.35(17)	C(63)-C(64)-C(69)	121.3(5)
N(13)-ZN2-N(16)	94.82(16)	C(63)-C(64)-C(65)	120.5(5)
N(17)-ZN2-N(18)	74.08(16)	C(69)-C(64)-C(65)	118.2(5)
N(12)-ZN2-N(18)	103.96(16)	C(66)-C(65)-C(64)	121.3(6)
N(13)-ZN2-N(18)	95.94(16)	C(65)-C(66)-C(67)	121.0(6)
N(16)-ZN2-N(18)	148.57(16)	C(68)-C(67)-C(66)	120.4(6)
N(17)-ZN2-N(11)	106.29(16)	C(67)-C(68)-C(69)	120.1(6)
N(12)-ZN2-N(11)	73.19(17)	C(68)-C(69)-C(64)	118.9(5)
N(13)-ZN2-N(11)	147.95(16)	C(68)-C(69)-C(60)	123.8(5)
N(16)-ZN2-N(11)	95.06(16)	C(64)-C(69)-C(60)	117.1(5)
N(18)-ZN2-N(11)	91.28(15)	N(16)-C(70)-C(71)	121.2(6)
C(47)-N(11)-C(51)	116.1(5)	C(72)-C(71)-C(70)	119.7(6)
C(47)-N(11)-ZN2	128.5(4)	C(73)-C(72)-C(71)	119.4(6)

C(72)-C(73)-C(74)	118.6(6)	F(12)-P(1)-F(11)	90.8(2)
N(16)-C(74)-C(73)	122.3(5)	F(25)-P(2)-F(21)	90.6(2)
N(16)-C(74)-C(75)	114.3(5)	F(25)-P(2)-F(26)	90.1(2)
C(73)-C(74)-C(75)	123.3(5)	F(21)-P(2)-F(26)	179.3(2)
N(17)-C(75)-N(19)	124.1(5)	F(25)-P(2)-F(24)	91.2(2)
N(17)-C(75)-C(74)	115.3(5)	F(21)-P(2)-F(24)	90.5(2)
N(19)-C(75)-C(74)	120.6(5)	F(26)-P(2)-F(24)	89.3(2)
N(19)-C(76)-N(20)	124.6(5)	F(25)-P(2)-F(22)	91.4(2)
N(19)-C(76)-C(83)	115.9(5)	F(21)-P(2)-F(22)	89.3(2)
N(20)-C(76)-C(83)	119.5(5)	F(26)-P(2)-F(22)	90.9(2)
N(17)-C(77)-N(20)	124.7(5)	F(24)-P(2)-F(22)	177.4(2)
N(17)-C(77)-C(78)	114.5(5)	F(25)-P(2)-F(23)	179.4(3)
N(20)-C(77)-C(78)	120.8(5)	F(21)-P(2)-F(23)	89.2(2)
N(18)-C(78)-C(79)	122.8(5)	F(26)-P(2)-F(23)	90.1(2)
N(18)-C(78)-C(77)	114.3(4)	F(24)-P(2)-F(23)	88.3(2)
C(79)-C(78)-C(77)	122.9(5)	F(22)-P(2)-F(23)	89.1(2)
C(78)-C(79)-C(80)	117.9(5)	F(31)-P(3)-F(33)	90.0(2)
C(81)-C(80)-C(79)	119.8(5)	F(31)-P(3)-F(36)	178.8(2)
C(82)-C(81)-C(80)	118.2(5)	F(33)-P(3)-F(36)	90.7(2)
N(18)-C(82)-C(81)	123.5(5)	F(31)-P(3)-F(32)	91.1(2)
C(84)-C(83)-C(92)	120.1(6)	F(33)-P(3)-F(32)	90.7(2)
C(84)-C(83)-C(76)	114.7(6)	F(36)-P(3)-F(32)	89.9(2)
C(92)-C(83)-C(76)	125.1(6)	F(31)-P(3)-F(35)	90.1(2)
C(83)-C(84)-C(85)	121.9(7)	F(33)-P(3)-F(35)	179.4(2)
C(86)-C(85)-C(84)	118.1(8)	F(36)-P(3)-F(35)	89.19(19)
C(85)-C(86)-C(87)	122.5(7)	F(32)-P(3)-F(35)	89.8(2)
C(86)-C(87)-C(88)	121.4(7)	F(31)-P(3)-F(34)	89.8(2)
C(86)-C(87)-C(92)	119.5(7)	F(33)-P(3)-F(34)	90.42(19)
C(88)-C(87)-C(92)	119.1(7)	F(36)-P(3)-F(34)	89.2(2)
C(89)-C(88)-C(87)	121.9(7)	F(32)-P(3)-F(34)	178.5(2)
C(88)-C(89)-C(90)	119.8(7)	F(35)-P(3)-F(34)	89.0(2)
C(89)-C(90)-C(91)	120.5(8)	F(45)-P(4)-F(43)	179.1(3)
C(90)-C(91)-C(92)	121.0(7)	F(45)-P(4)-F(46)	90.6(3)
C(83)-C(92)-C(91)	124.8(6)	F(43)-P(4)-F(46)	90.1(3)
C(83)-C(92)-C(87)	117.7(7)	F(45)-P(4)-F(42)	89.8(4)
C(91)-C(92)-C(87)	117.5(6)	F(43)-P(4)-F(42)	89.6(3)
F(15)-P(1)-F(14)	89.1(3)	F(46)-P(4)-F(42)	89.5(3)
F(15)-P(1)-F(16)	89.7(2)	F(45)-P(4)-F(44)	92.3(4)
F(14)-P(1)-F(16)	90.5(2)	F(43)-P(4)-F(44)	88.3(3)
F(15)-P(1)-F(13)	179.3(3)	F(46)-P(4)-F(44)	88.8(3)
F(14)-P(1)-F(13)	91.2(3)	F(42)-P(4)-F(44)	177.3(3)
F(16)-P(1)-F(13)	90.9(2)	F(45)-P(4)-F(41)	89.6(3)
F(15)-P(1)-F(12)	90.6(3)	F(43)-P(4)-F(41)	89.6(2)
F(14)-P(1)-F(12)	179.7(4)	F(46)-P(4)-F(41)	179.1(3)
F(16)-P(1)-F(12)	89.5(2)	F(42)-P(4)-F(41)	89.6(3)
F(13)-P(1)-F(12)	89.0(3)	F(44)-P(4)-F(41)	92.1(3)
F(15)-P(1)-F(11)	90.6(2)	N(103)-C(102)-C(101)	177.1(9)
F(14)-P(1)-F(11)	89.2(2)	N(113)-C(112)-C(111)	171.10(15)
F(16)-P(1)-F(11)	179.6(3)	N(123)-C(122)-C(121)	176.90(16)
F(13)-P(1)-F(11)	88.9(2)		

Appendix 6: Supplementary information for chapter IV.

Table 1. Crystal data and structure refinement for **1a, chapter IV.**

Identification code	gary47
Empirical formula	C42 H30 Br2 F18 N12 P3 Rh
Formula weight	1400.42
Temperature	100(2)K
Wavelength	1.54178 Å
Crystal system	Monoclinic
Space group	C2/c
Unit cell dimensions	a = 14.7120(2) Å α = 90° b = 16.1234(2) Å β = 106.0500(10)° c = 21.0927(3) Å γ = 90°
Volume	4808.32(11)Å^3
Z	4
Density (calculated)	1.935 g/cm^3
Absorption coefficient	6.853 mm^{-1}
F(000)	2752
Crystal size	0.29 x 0.17 x 0.12 mm
Theta range for data collection	4.16 to 72.88°
Index ranges	$-18 \le h \le 18$, $-19 \le k \le 19$, $-25 \le \ell \le 22$
Reflections collected	20344
Independent reflections	4705 [R_{int} = 0.037]
Absorption correction	Semi-empirical from equivalents
Max. and min. transmission	0.5800 and 0.4100
Refinement method	Full-matrix least-squares on F^2
Data / restraints / parameters	4705 / 0 / 354
Goodness-of-fit on F^2	0.955
Final R indices [I>2sigma(I)]	R_1 = 0.0489, wR_2 = 0.1222
R indices (all data)	R_1 = 0.0833, wR_2 = 0.1329
Largest diff. peak and hole	1.714 and -0.573 e/Å^3

Table 2. Atomic coordinates (x 10^4) and equivalent isotropic displacement parameters ($Å^2$ x 10^3) for **1a, chapter IV.**

U_{eq} is defined as one third of the trace of the orthogonalized Uij tensor.

	x	y	z	U_{eq}
Rh(1)	10000	3000(1)	2500	22(1)
N(1)	9294(3)	3884(3)	2891(2)	25(1)
N(2)	8733(3)	2950(3)	1875(2)	26(1)
N(3)	10204(3)	2102(3)	1858(2)	24(1)
N(4)	7145(3)	3316(3)	1628(2)	27(1)
N(5)	7698(3)	2248(3)	1025(2)	26(1)
C(1)	9639(4)	4385(4)	3404(3)	31(1)
C(2)	9085(4)	4944(4)	3623(3)	35(2)
C(3)	8135(4)	4998(4)	3299(3)	35(2)
C(4)	7757(4)	4495(4)	2757(3)	30(1)
C(5)	8354(4)	3950(3)	2562(3)	27(1)
C(6)	8021(4)	3397(3)	1989(3)	24(1)
C(7)	7011(4)	2722(4)	1150(3)	28(1)
C(8)	8547(4)	2376(4)	1400(3)	27(1)
C(9)	9399(4)	1915(3)	1369(3)	26(1)
C(10)	9393(4)	1320(4)	902(3)	31(1)
C(11)	10220(4)	913(4)	915(3)	33(1)
C(12)	11025(4)	1100(4)	1403(3)	36(2)
C(13)	11000(4)	1698(4)	1874(3)	28(1)
C(14)	6053(4)	2583(4)	731(3)	28(1)
C(15)	5302(4)	3126(4)	715(3)	34(1)
C(16)	4415(4)	2985(4)	304(3)	34(1)
C(17)	4267(4)	2284(4)	-101(3)	31(1)
C(18)	4974(4)	1730(4)	-86(3)	32(1)
C(19)	5868(4)	1874(4)	323(3)	31(1)
Br(1)	3069(1)	2085(1)	-708(1)	40(1)
P(2)	7783(1)	4945(1)	491(1)	32(1)
F(21)	6749(2)	4658(2)	500(2)	42(1)
F(22)	7443(3)	5881(2)	403(2)	48(1)
F(23)	7518(2)	4818(2)	-290(2)	43(1)
F(24)	8133(2)	4004(2)	604(2)	43(1)
F(25)	8074(2)	5064(2)	1283(2)	40(1)
F(26)	8827(2)	5219(2)	487(2)	43(1)
P(3)	5000	4506(2)	2500	43(1)
F(31)	4267(2)	5209(2)	2148(2)	50(1)
F(32)	5467(3)	4512(2)	1904(2)	56(1)
F(33)	4262(3)	3810(3)	2140(2)	79(2)
C(21)	5852(5)	1846(4)	3319(3)	55(2)
C(22)	6376(5)	1782(4)	2826(4)	45(2)
N(23)	6764(4)	1741(4)	2429(3)	50(2)

Table 3. Hydrogen coordinates (x 10^4) and isotropic displacement parameters ($Å^2$ x 10^3) for **1a, chapter IV.**

	x	y	z	U_{eq}
H(1)	10294	4355	3628	37
H(2)	9355	5289	3992	42
H(3)	7743	5376	3447	42
H(4)	7105	4525	2526	36
H(10)	8825	1191	573	37
H(11)	10233	507	591	40
H(12)	11601	822	1419	43
H(13)	11561	1821	2212	33
H(15)	5409	3600	994	40
H(16)	3911	3357	295	41
H(18)	4851	1249	-356	39
H(19)	6363	1492	330	38
H(21A)	5538	2387	3281	82
H(21B)	6289	1788	3761	82
H(21C)	5375	1405	3247	82

Table 4. Anisotropic parameters ($Å^2$ x 10^3) for **1a, chapter IV.**

The anisotropic displacement factor exponent takes the form:

$$-2\pi^2 [h^2 a^{*2} U_{11} + ... + 2 h k a^* b^* U_{12}]$$

	U11	U22	U33	U23	U13	U12
Rh(1)	18(1)	30(1)	16(1)	0	3(1)	0
N(1)	21(2)	31(3)	22(2)	2(2)	5(2)	3(2)
N(2)	23(2)	34(3)	19(2)	1(2)	5(2)	1(2)
N(3)	28(2)	26(3)	19(2)	-2(2)	9(2)	2(2)
N(4)	21(2)	36(3)	21(2)	1(2)	3(2)	0(2)
N(5)	22(2)	34(3)	22(2)	-3(2)	6(2)	-1(2)
C(1)	25(3)	42(4)	21(3)	0(3)	0(2)	-1(3)
C(2)	39(4)	37(4)	25(3)	-4(3)	5(3)	0(3)
C(3)	32(3)	40(4)	34(3)	-6(3)	10(3)	5(3)
C(4)	21(3)	39(4)	26(3)	2(3)	1(2)	1(3)
C(5)	31(3)	31(3)	19(3)	-1(2)	7(2)	-1(3)
C(6)	24(3)	29(3)	18(3)	2(2)	7(2)	-4(2)
C(7)	30(3)	31(3)	23(3)	5(3)	6(2)	1(3)
C(8)	32(3)	29(3)	19(3)	0(2)	9(2)	-1(3)
C(9)	23(3)	33(3)	22(3)	4(3)	9(2)	0(2)
C(10)	36(3)	38(4)	18(3)	-3(3)	7(2)	-8(3)
C(11)	35(3)	36(4)	29(3)	-4(3)	10(3)	0(3)
C(12)	35(3)	39(4)	36(4)	5(3)	16(3)	9(3)
C(13)	27(3)	36(3)	22(3)	6(3)	10(2)	0(3)
C(14)	26(3)	38(4)	19(3)	0(3)	6(2)	0(3)
C(15)	35(3)	39(4)	27(3)	-2(3)	12(3)	-3(3)
C(16)	23(3)	44(4)	33(3)	1(3)	6(2)	4(3)
C(17)	20(3)	45(4)	26(3)	5(3)	2(2)	-4(3)
C(18)	31(3)	38(4)	26(3)	-3(3)	6(3)	-9(3)
C(19)	27(3)	39(4)	28(3)	1(3)	8(2)	-1(3)
Br(1)	28(1)	53(1)	34(1)	-1(1)	-1(1)	-4(1)
P(2)	28(1)	39(1)	26(1)	0(1)	4(1)	2(1)
F(21)	32(2)	56(2)	39(2)	-9(2)	10(2)	-7(2)
F(22)	53(2)	41(2)	45(2)	7(2)	7(2)	7(2)
F(23)	46(2)	56(2)	26(2)	-2(2)	7(2)	-6(2)
F(24)	50(2)	42(2)	42(2)	5(2)	23(2)	8(2)
F(25)	43(2)	49(2)	26(2)	-4(2)	5(2)	1(2)
F(26)	33(2)	55(2)	38(2)	13(2)	4(2)	1(2)
P(3)	42(1)	42(2)	49(2)	0	21(1)	0
F(31)	46(2)	57(3)	49(2)	6(2)	17(2)	5(2)
F(32)	53(2)	67(3)	56(3)	-12(2)	26(2)	1(2)
F(33)	72(3)	66(3)	111(4)	-36(3)	47(3)	-27(2)
C(21)	46(4)	66(5)	48(5)	-2(4)	7(3)	6(4)
C(22)	38(4)	42(4)	48(5)	-2(3)	1(3)	-2(3)
N(23)	32(3)	67(4)	49(4)	4(3)	7(3)	-2(3)

Table 5. Bond lengths [Å] and angles [°] for **1a, chapter IV.**

Rh(1)-N(2)#1	1.964(4)	N(3)#1-RH1-N(1)#1	158.19(17)
Rh(1)-N(2)	1.964(4)	N(2)#1-RH1-N(1)	104.41(17)
Rh(1)-N(3)	2.060(4)	N(2)-RH1-N(1)	78.91(18)
Rh(1)-N(3)#1	2.060(4)	N(3)-RH1-N(1)	158.19(17)
Rh(1)-N(1)#1	2.066(4)	N(3)#1-RH1-N(1)	92.40(17)
Rh(1)-N(1)	2.066(4)	N(1)#1-RH1-N(1)	92.7(2)
N(1)-C(1)	1.333(7)	C(1)-N(1)-C(5)	118.0(5)
N(1)-C(5)	1.369(7)	C(1)-N(1)-RH1	128.4(4)
N(2)-C(8)	1.335(7)	C(5)-N(1)-RH1	113.5(4)
N(2)-C(6)	1.347(7)	C(8)-N(2)-C(6)	119.7(5)
N(3)-C(13)	1.332(7)	C(8)-N(2)-RH1	119.5(4)
N(3)-C(9)	1.372(6)	C(6)-N(2)-RH1	120.0(4)
N(4)-C(6)	1.310(6)	C(13)-N(3)-C(9)	118.8(5)
N(4)-C(7)	1.365(7)	C(13)-N(3)-RH1	127.9(4)
N(5)-C(8)	1.298(7)	C(9)-N(3)-RH1	113.3(3)
N(5)-C(7)	1.350(7)	C(6)-N(4)-C(7)	114.6(5)
C(1)-C(2)	1.377(8)	C(8)-N(5)-C(7)	115.9(5)
C(2)-C(3)	1.378(7)	N(1)-C(1)-C(2)	122.7(5)
C(3)-C(4)	1.386(7)	C(1)-C(2)-C(3)	119.3(6)
C(4)-C(5)	1.384(7)	C(2)-C(3)-C(4)	119.5(6)
C(5)-C(6)	1.472(7)	C(5)-C(4)-C(3)	118.3(5)
C(7)-C(14)	1.460(7)	N(1)-C(5)-C(4)	122.2(5)
C(8)-C(9)	1.474(7)	N(1)-C(5)-C(6)	115.5(5)
C(9)-C(10)	1.374(7)	C(4)-C(5)-C(6)	122.3(5)
C(10)-C(11)	1.376(8)	N(4)-C(6)-N(2)	122.2(5)
C(11)-C(12)	1.370(7)	N(4)-C(6)-C(5)	126.0(5)
C(12)-C(13)	1.392(8)	N(2)-C(6)-C(5)	111.8(5)
C(14)-C(15)	1.404(8)	N(5)-C(7)-N(4)	125.4(5)
C(14)-C(19)	1.412(8)	N(5)-C(7)-C(14)	116.3(5)
C(15)-C(16)	1.371(7)	N(4)-C(7)-C(14)	118.2(5)
C(16)-C(17)	1.398(8)	N(5)-C(8)-N(2)	122.1(5)
C(17)-C(18)	1.364(8)	N(5)-C(8)-C(9)	125.4(5)
C(17)-Br(1)	1.898(5)	N(2)-C(8)-C(9)	112.5(5)
C(18)-C(19)	1.378(7)	N(3)-C(9)-C(10)	121.7(5)
P(2)-F(22)	1.584(4)	N(3)-C(9)-C(8)	115.1(5)
P(2)-F(23)	1.597(3)	C(10)-C(9)-C(8)	123.2(5)
P(2)-F(21)	1.597(3)	C(9)-C(10)-C(11)	119.2(5)
P(2)-F(24)	1.599(4)	C(12)-C(11)-C(10)	119.1(6)
P(2)-F(26)	1.599(3)	C(11)-C(12)-C(13)	120.0(6)
P(2)-F(25)	1.618(3)	N(3)-C(13)-C(12)	121.1(5)
P(3)-F(32)	1.592(4)	C(15)-C(14)-C(19)	118.2(5)
P(3)-F(32)#2	1.592(4)	C(15)-C(14)-C(7)	122.7(5)
P(3)-F(31)#2	1.598(4)	C(19)-C(14)-C(7)	119.0(5)
P(3)-F(31)	1.598(4)	C(16)-C(15)-C(14)	121.1(6)
P(3)-F(33)	1.600(4)	C(15)-C(16)-C(17)	118.8(5)
P(3)-F(33)#2	1.600(4)	C(18)-C(17)-C(16)	121.7(5)
C(21)-C(22)	1.461(10)	C(18)-C(17)-BR1	117.7(5)
C(22)-N(23)	1.138(8)	C(16)-C(17)-BR1	120.5(4)
N(2)#1-RH1-N(2)	175.3(3)	C(17)-C(18)-C(19)	119.6(6)
N(2)#1-RH1-N(3)	97.38(17)	C(18)-C(19)-C(14)	120.5(6)
N(2)-RH1-N(3)	79.28(18)	F(22)-P(2)-F(23)	91.4(2)
N(2)#1-RH1-N(3)#1	79.28(18)	F(22)-P(2)-F(21)	90.4(2)
N(2)-RH1-N(3)#1	97.38(17)	F(23)-P(2)-F(21)	90.73(19)
N(3)-RH1-N(3)#1	90.7(2)	F(22)-P(2)-F(24)	178.1(2)
N(2)#1-RH1-N(1)#1	78.92(18)	F(23)-P(2)-F(24)	90.5(2)
N(2)-RH1-N(1)#1	104.41(17)	F(21)-P(2)-F(24)	89.4(2)
N(3)-RH1-N(1)#1	92.40(17)	F(22)-P(2)-F(26)	90.6(2)

F(23)-P(2)-F(26)	89.59(19)	F(31)#2-P(3)-F(31)	89.7(3)
F(21)-P(2)-F(26)	179.0(2)	F(32)-P(3)-F(33)	90.8(2)
F(24)-P(2)-F(26)	89.62(19)	F(32)#2-P(3)-F(33)	89.7(2)
F(22)-P(2)-F(25)	89.5(2)	F(31)#2-P(3)-F(33)	179.3(3)
F(23)-P(2)-F(25)	178.7(2)	F(31)-P(3)-F(33)	89.7(2)
F(21)-P(2)-F(25)	90.13(18)	F(32)-P(3)-F(33)#2	89.7(2)
F(24)-P(2)-F(25)	88.60(19)	F(32)#2-P(3)-F(33)#2	90.8(2)
F(26)-P(2)-F(25)	89.54(19)	F(31)#2-P(3)-F(33)#2	89.7(2)
F(32)-P(3)-F(32)#2	179.3(3)	F(31)-P(3)-F(33)#2	179.3(3)
F(32)-P(3)-F(31)#2	88.8(2)	F(33)-P(3)-F(33)#2	90.9(4)
F(32)#2-P(3)-F(31)#2	90.7(2)	N(23)-C(22)-C(21)	178.2(8)
F(32)-P(3)-F(31)	90.7(2)		
F(32)#2-P(3)-F(31)	88.82(19)		

Table 1. Crystal data and structure refinement for **1b, Chapter IV.**

Identification code	gary49
Empirical formula	C40 H32 Br F18 N11 P3 Rh
Formula weight	1284.50
Temperature	100(2)K
Wavelength	1.54178 Å
Crystal system	Triclinic
Space group	P-1
Unit cell dimensions	a = 12.1567(9) Å α = 88.563(4)° b = 13.2319(8) Å β = 85.257(5)° c = 14.8553(9) Å γ = 84.843(5)°
Volume	2371.4(3)Å^3
Z	2
Density (calculated)	1.799 g/cm^3
Absorption coefficient	5.923 mm^{-1}
F(000)	1272
Crystal size	0.44 x 0.32 x 0.14 mm
Theta range for data collection	2.99 to 72.65°
Index ranges	$-14 \le h \le 13$, $-16 \le k \le 16$, $-17 \le \ell \le 18$
Reflections collected	27576
Independent reflections	8972 [R_{int} = 0.029]
Absorption correction	Semi-empirical from equivalents
Max. and min. transmission	0.5800 and 0.3200
Refinement method	Full-matrix least-squares on F^2
Data / restraints / parameters	8972 / 0 / 670
Goodness-of-fit on F^2	1.116
Final R indices [I>2sigma(I)]	R_1 = 0.0572, wR_2 = 0.1653
R indices (all data)	R_1 = 0.0653, wR_2 = 0.1997
Largest diff. peak and hole	2.350 and -1.970 e/Å^3

Table 2. Atomic coordinates (x 10^4) and equivalent isotropic displacement parameters ($Å^2$ x 10^3) for **1b, Chapter IV.**

U_{eq} is defined as one third of the trace of the orthogonalized Uij tensor.

	x	y	z	U_{eq}
Rh(1)	1918(1)	2221(1)	2615(1)	15(1)
N(1)	1510(4)	3605(3)	3226(3)	18(1)
N(2)	2265(3)	1869(3)	3857(3)	15(1)
N(3)	2517(4)	710(3)	2486(3)	18(1)
N(4)	2461(4)	2434(3)	5294(3)	20(1)
N(5)	3050(4)	707(3)	4873(3)	19(1)
N(6)	310(4)	1876(3)	2625(3)	23(1)
N(7)	1578(4)	2668(3)	1383(3)	18(1)
N(8)	3444(4)	2661(3)	2147(3)	23(1)
C(1)	1168(4)	4494(4)	2844(3)	20(1)
C(2)	991(5)	5377(4)	3338(4)	24(1)
C(3)	1145(5)	5346(4)	4254(4)	22(1)
C(4)	1507(4)	4423(4)	4656(3)	20(1)
C(5)	1693(4)	3581(4)	4127(3)	19(1)
C(6)	2140(4)	2592(4)	4475(3)	17(1)
C(7)	2895(4)	1479(4)	5470(3)	19(1)
C(8)	2723(4)	941(4)	4064(3)	16(1)
C(9)	2870(4)	272(4)	3273(3)	17(1)
C(10)	3320(4)	-714(4)	3307(3)	20(1)
C(11)	3405(5)	-1292(4)	2528(4)	25(1)
C(12)	3029(5)	-846(4)	1742(4)	25(1)
C(13)	2589(4)	153(4)	1743(3)	18(1)
C(14)	3200(4)	1277(4)	6403(3)	20(1)
C(15)	2900(5)	2006(4)	7054(4)	29(1)
C(16)	3186(6)	1842(5)	7932(4)	34(1)
C(17)	3776(4)	937(5)	8145(3)	24(1)
C(18)	4099(5)	209(4)	7506(4)	26(1)
C(19)	3808(5)	369(4)	6625(4)	23(1)
C(20)	-268(5)	1360(4)	3277(3)	22(1)
C(21)	-1326(4)	1112(4)	3163(4)	22(1)
C(22)	-1812(5)	1385(4)	2379(4)	28(1)
C(23)	-1225(5)	1916(4)	1700(4)	29(1)
C(24)	-156(4)	2159(4)	1842(3)	20(1)
C(25)	539(5)	2666(4)	1167(3)	21(1)
C(26)	246(5)	3142(4)	360(3)	25(1)
C(27)	1063(6)	3582(4)	-198(3)	29(1)
C(28)	2141(5)	3553(4)	43(3)	25(1)
C(29)	2392(5)	3091(4)	858(3)	21(1)
C(30)	3466(5)	3033(4)	1275(3)	23(1)
C(31)	4446(5)	3326(4)	856(4)	27(1)
C(32)	5400(5)	3257(5)	1318(4)	32(1)
C(33)	5347(5)	2897(5)	2199(4)	29(1)
C(34)	4335(5)	2587(4)	2599(3)	25(1)
Br(1)	4180(1)	712(1)	9348(1)	41(1)
P(1)	2725(1)	6253(1)	1018(1)	24(1)
F(11)	2156(3)	6942(3)	1819(2)	38(1)
F(12)	3072(3)	5383(3)	1737(2)	37(1)
F(13)	1581(3)	5764(3)	938(2)	36(1)
F(14)	2378(3)	7125(3)	290(2)	38(1)
F(15)	3869(3)	6756(3)	1094(3)	38(1)

F(16)	3309(4)	5552(3)	221(2)	44(1)
P(2)	493(1)	8387(1)	4089(1)	21(1)
F(21)	727(3)	9206(2)	3292(2)	25(1)
F(22)	-558(3)	9106(2)	4498(2)	28(1)
F(23)	-288(3)	7846(3)	3473(2)	33(1)
F(24)	1530(3)	7654(2)	3693(2)	26(1)
F(25)	1286(3)	8922(2)	4709(2)	27(1)
F(26)	247(3)	7569(2)	4898(2)	27(1)
P(3)	8026(1)	4848(1)	2527(1)	28(1)
F(31)	8798(4)	4149(4)	3164(3)	57(1)
F(32)	8737(5)	5792(4)	2624(5)	80(2)
F(33)	8845(5)	4521(4)	1703(4)	86(2)
F(34)	7305(5)	3940(4)	2463(4)	80(2)
F(35)	7258(5)	5232(5)	3399(3)	73(2)
F(36)	7251(3)	5558(3)	1912(2)	41(1)
C(41)	4734(8)	5932(6)	3258(6)	56(2)
C(42)	4458(6)	5002(6)	3735(5)	41(2)
N(43)	4225(6)	4277(5)	4102(5)	51(2)
C(51)	9890(7)	8833(7)	1435(5)	52(2)
C(52)	9249(6)	9118(5)	674(4)	34(1)
N(53)	8751(6)	9334(5)	73(4)	48(2)
C(61)	6894(6)	3142(5)	4663(5)	38(1)
C(62)	6074(6)	2420(5)	4586(4)	35(1)
N(63)	5430(6)	1840(4)	4524(5)	47(2)

Table 3. Hydrogen coordinates (x 10^4) and isotropic displacement parameters ($Å^2$ x 10^3) for **1b, Chapter IV.**

	x	y	z	U_{eq}
H(1)	1043	4520	2221	23
H(2)	765	6002	3051	28
H(3)	1007	5943	4602	27
H(4)	1622	4380	5281	24
H(10)	3571	-1001	3854	24
H(11)	3714	-1978	2535	29
H(12)	3074	-1228	1205	29
H(13)	2333	452	1202	22
H(15)	2494	2624	6896	34
H(16)	2981	2341	8379	41
H(18)	4519	-399	7667	32
H(19)	4018	-131	6180	28
H(20)	61	1166	3821	27
H(21)	-1719	751	3628	26
H(22)	-2540	1214	2298	33
H(23)	-1545	2109	1153	34
H(26)	-494	3165	193	30
H(27)	875	3906	-749	35
H(28)	2697	3843	-342	30
H(31)	4469	3575	250	32
H(32)	6077	3456	1032	39
H(33)	5984	2857	2533	35
H(34)	4297	2322	3200	30
H(41A)	5235	5763	2721	85
H(41B)	5097	6352	3657	85
H(41C)	4054	6307	3073	85
H(51A)	9438	8469	1890	78
H(51B)	10117	9444	1701	78
H(51C)	10550	8392	1230	78
H(61A)	7502	3014	4193	57
H(61B)	7185	3065	5259	57
H(61C)	6548	3834	4588	57

Table 4. Anisotropic parameters ($Å^2$ x 10^3) for **1b, chapter IV.**

The anisotropic displacement factor exponent takes the form:

$$-2\pi^2 [h^2 a^{*2} U_{11} + ... + 2 h k a^* b^* U_{12}]$$

	U11	U22	U33	U23	U13	U12
Rh(1)	23(1)	15(1)	7(1)	0(1)	-3(1)	0(1)
N(1)	28(2)	18(2)	8(2)	0(2)	-4(2)	3(2)
N(2)	13(2)	18(2)	15(2)	2(2)	0(2)	-7(2)
N(3)	26(2)	17(2)	11(2)	-1(2)	-3(2)	2(2)
N(4)	29(2)	18(2)	13(2)	1(2)	-5(2)	0(2)
N(5)	20(2)	20(2)	15(2)	1(2)	-2(2)	0(2)
N(6)	38(3)	18(2)	11(2)	-6(2)	-11(2)	11(2)
N(7)	20(2)	18(2)	14(2)	1(2)	1(2)	-3(2)
N(8)	40(3)	18(2)	9(2)	0(2)	-3(2)	5(2)
C(1)	24(3)	17(2)	17(2)	6(2)	-5(2)	-3(2)
C(2)	32(3)	18(2)	21(3)	3(2)	-7(2)	2(2)
C(3)	30(3)	17(2)	19(2)	-3(2)	-2(2)	1(2)
C(4)	23(3)	22(2)	15(2)	-1(2)	-1(2)	-3(2)
C(5)	22(3)	21(2)	12(2)	3(2)	-1(2)	1(2)
C(6)	21(2)	21(2)	10(2)	2(2)	0(2)	0(2)
C(7)	23(3)	19(2)	15(2)	0(2)	-5(2)	-1(2)
C(8)	16(2)	19(2)	14(2)	-2(2)	-2(2)	-2(2)
C(9)	18(2)	22(2)	12(2)	-1(2)	-4(2)	-1(2)
C(10)	25(3)	20(2)	15(2)	1(2)	-5(2)	-3(2)
C(11)	33(3)	19(2)	22(3)	-1(2)	-4(2)	0(2)
C(12)	35(3)	22(2)	17(2)	-6(2)	-2(2)	-2(2)
C(13)	16(2)	24(2)	16(2)	-2(2)	-2(2)	-7(2)
C(14)	22(3)	24(2)	15(2)	2(2)	-7(2)	-3(2)
C(15)	33(3)	30(3)	22(3)	1(2)	-7(2)	2(2)
C(16)	46(4)	41(3)	13(3)	-3(2)	-10(2)	9(3)
C(17)	17(2)	44(3)	13(2)	11(2)	-5(2)	-7(2)
C(18)	30(3)	26(3)	24(3)	9(2)	-10(2)	-3(2)
C(19)	25(3)	23(3)	22(3)	4(2)	-3(2)	-6(2)
C(20)	39(3)	17(2)	8(2)	-2(2)	-2(2)	7(2)
C(21)	17(2)	26(3)	25(3)	2(2)	1(2)	-14(2)
C(22)	23(3)	33(3)	29(3)	3(2)	-5(2)	-9(2)
C(23)	36(3)	30(3)	21(3)	1(2)	-16(2)	3(2)
C(24)	27(3)	21(2)	11(2)	0(2)	-6(2)	3(2)
C(25)	30(3)	19(2)	13(2)	-5(2)	-5(2)	2(2)
C(26)	36(3)	25(3)	15(2)	0(2)	-10(2)	1(2)
C(27)	55(4)	25(3)	8(2)	4(2)	-13(2)	1(2)
C(28)	42(3)	22(2)	12(2)	0(2)	-2(2)	-3(2)
C(29)	35(3)	18(2)	9(2)	-2(2)	-1(2)	-2(2)
C(30)	37(3)	15(2)	15(2)	-1(2)	1(2)	1(2)
C(31)	32(3)	29(3)	18(3)	2(2)	4(2)	-10(2)
C(32)	32(3)	33(3)	32(3)	2(2)	1(2)	-7(2)
C(33)	22(3)	35(3)	30(3)	3(2)	-2(2)	-6(2)
C(34)	36(3)	24(3)	15(2)	0(2)	-5(2)	5(2)
Br(1)	39(1)	69(1)	13(1)	8(1)	-9(1)	10(1)
P(1)	35(1)	23(1)	15(1)	-1(1)	-2(1)	-4(1)
F(11)	50(2)	33(2)	29(2)	-9(1)	10(2)	-9(2)
F(12)	39(2)	38(2)	32(2)	12(2)	-3(2)	-2(2)
F(13)	39(2)	40(2)	33(2)	8(2)	-10(2)	-17(2)
F(14)	53(2)	33(2)	30(2)	11(1)	-9(2)	-5(2)
F(15)	38(2)	40(2)	37(2)	0(2)	-1(2)	-10(2)

F(16)	73(3)	30(2)	27(2)	-7(1)	12(2)	-7(2)
P(2)	30(1)	17(1)	14(1)	-1(1)	-3(1)	0(1)
F(21)	31(2)	24(2)	21(2)	6(1)	-6(1)	-3(1)
F(22)	30(2)	21(2)	34(2)	-1(1)	1(1)	-2(1)
F(23)	45(2)	33(2)	23(2)	-4(1)	-9(1)	-9(2)
F(24)	38(2)	22(2)	18(2)	-2(1)	1(1)	2(1)
F(25)	40(2)	27(2)	15(1)	-5(1)	-6(1)	-3(1)
F(26)	39(2)	22(2)	18(2)	1(1)	2(1)	-1(1)
P(3)	30(1)	29(1)	23(1)	2(1)	-2(1)	-4(1)
F(31)	38(2)	59(3)	70(3)	29(2)	-6(2)	4(2)
F(32)	58(3)	45(3)	146(6)	8(3)	-44(3)	-16(2)
F(33)	116(5)	69(3)	55(3)	21(3)	45(3)	40(3)
F(34)	94(4)	64(3)	95(4)	20(3)	-52(4)	-41(3)
F(35)	90(4)	95(4)	25(2)	5(2)	-1(2)	38(3)
F(36)	47(2)	54(2)	21(2)	9(2)	-6(2)	1(2)
C(41)	60(5)	45(4)	61(5)	12(4)	3(4)	4(4)
C(42)	38(4)	44(4)	40(4)	-6(3)	-5(3)	13(3)
N(43)	47(4)	42(3)	58(4)	3(3)	11(3)	9(3)
C(51)	60(5)	71(5)	27(3)	5(3)	-22(3)	-1(4)
C(52)	40(3)	39(3)	25(3)	-4(2)	-11(3)	0(3)
N(53)	59(4)	57(4)	31(3)	5(3)	-19(3)	-4(3)
C(61)	41(4)	36(3)	37(3)	6(3)	-7(3)	-5(3)
C(62)	51(4)	31(3)	22(3)	-1(2)	-13(3)	9(3)
N(63)	61(4)	29(3)	54(4)	1(3)	-25(3)	1(3)

Table 5. Bond lengths [Å] and angles [°] for **1b, Chapter IV.**

Rh(1)-N(2)	1.961(4)	P(1)-F(12)	1.603(4)
Rh(1)-N(7)	1.974(4)	P(1)-F(15)	1.608(4)
Rh(1)-N(6)	2.046(5)	P(1)-F(14)	1.613(4)
Rh(1)-N(8)	2.056(5)	P(2)-F(23)	1.596(3)
Rh(1)-N(1)	2.066(4)	P(2)-F(24)	1.600(3)
Rh(1)-N(3)	2.074(4)	P(2)-F(25)	1.607(3)
N(1)-C(1)	1.340(6)	P(2)-F(22)	1.609(3)
N(1)-C(5)	1.374(6)	P(2)-F(21)	1.610(3)
N(2)-C(6)	1.332(6)	P(2)-F(26)	1.624(3)
N(2)-C(8)	1.342(6)	P(3)-F(33)	1.557(5)
N(3)-C(13)	1.335(6)	P(3)-F(34)	1.558(5)
N(3)-C(9)	1.374(6)	P(3)-F(36)	1.596(4)
N(4)-C(6)	1.314(6)	P(3)-F(35)	1.598(5)
N(4)-C(7)	1.353(6)	P(3)-F(32)	1.598(5)
N(5)-C(8)	1.318(6)	P(3)-F(31)	1.605(4)
N(5)-C(7)	1.360(6)	C(41)-C(42)	1.456(11)
N(6)-C(20)	1.356(7)	C(42)-N(43)	1.139(10)
N(6)-C(24)	1.365(6)	C(51)-C(52)	1.449(8)
N(7)-C(25)	1.329(7)	C(52)-N(53)	1.137(8)
N(7)-C(29)	1.360(7)	C(61)-C(62)	1.454(10)
N(8)-C(34)	1.315(7)	C(62)-N(63)	1.155(9)
N(8)-C(30)	1.373(6)	N(2)-RH1-N(7)	176.28(16)
C(1)-C(2)	1.386(7)	N(2)-RH1-N(6)	102.07(16)
C(2)-C(3)	1.387(7)	N(7)-RH1-N(6)	79.44(17)
C(3)-C(4)	1.397(7)	N(2)-RH1-N(8)	97.59(16)
C(4)-C(5)	1.370(7)	N(7)-RH1-N(8)	81.03(17)
C(5)-C(6)	1.470(7)	N(6)-RH1-N(8)	160.29(17)
C(7)-C(14)	1.475(7)	N(2)-RH1-N(1)	79.58(16)
C(8)-C(9)	1.478(6)	N(7)-RH1-N(1)	96.96(16)
C(9)-C(10)	1.371(7)	N(6)-RH1-N(1)	94.22(17)
C(10)-C(11)	1.394(7)	N(8)-RH1-N(1)	90.78(17)
C(11)-C(12)	1.387(8)	N(2)-RH1-N(3)	78.77(16)
C(12)-C(13)	1.381(7)	N(7)-RH1-N(3)	104.64(16)
C(14)-C(15)	1.387(8)	N(6)-RH1-N(3)	92.13(17)
C(14)-C(19)	1.400(7)	N(8)-RH1-N(3)	90.20(17)
C(15)-C(16)	1.384(8)	N(1)-RH1-N(3)	158.27(16)
C(16)-C(17)	1.383(8)	C(1)-N(1)-C(5)	118.5(4)
C(17)-C(18)	1.378(8)	C(1)-N(1)-RH1	128.4(3)
C(17)-Br(1)	1.902(5)	C(5)-N(1)-RH1	112.9(3)
C(18)-C(19)	1.390(8)	C(6)-N(2)-C(8)	120.0(4)
C(20)-C(21)	1.380(8)	C(6)-N(2)-RH1	119.1(3)
C(21)-C(22)	1.376(8)	C(8)-N(2)-RH1	120.6(3)
C(22)-C(23)	1.398(8)	C(13)-N(3)-C(9)	119.2(4)
C(23)-C(24)	1.400(8)	C(13)-N(3)-RH1	127.2(3)
C(24)-C(25)	1.449(7)	C(9)-N(3)-RH1	113.6(3)
C(25)-C(26)	1.397(7)	C(6)-N(4)-C(7)	115.2(4)
C(26)-C(27)	1.399(9)	C(8)-N(5)-C(7)	114.8(4)
C(27)-C(28)	1.384(9)	C(20)-N(6)-C(24)	119.9(5)
C(28)-C(29)	1.387(7)	C(20)-N(6)-RH1	127.3(4)
C(29)-C(30)	1.486(8)	C(24)-N(6)-RH1	112.7(4)
C(30)-C(31)	1.380(8)	C(25)-N(7)-C(29)	124.1(4)
C(31)-C(32)	1.391(9)	C(25)-N(7)-RH1	118.2(3)
C(32)-C(33)	1.381(8)	C(29)-N(7)-RH1	117.0(3)
C(33)-C(34)	1.411(8)	C(34)-N(8)-C(30)	121.5(5)
P(1)-F(11)	1.591(4)	C(34)-N(8)-RH1	125.7(4)
P(1)-F(13)	1.600(4)	C(30)-N(8)-RH1	112.8(4)
P(1)-F(16)	1.601(4)	N(1)-C(1)-C(2)	121.5(5)

C(1)-C(2)-C(3)	119.8(5)	C(33)-C(32)-C(31)	118.9(6)
C(2)-C(3)-C(4)	119.0(5)	C(32)-C(33)-C(34)	119.2(5)
C(5)-C(4)-C(3)	118.4(5)	N(8)-C(34)-C(33)	120.7(5)
C(4)-C(5)-N(1)	122.6(4)	F(11)-P(1)-F(13)	89.9(2)
C(4)-C(5)-C(6)	122.4(4)	F(11)-P(1)-F(16)	179.2(3)
N(1)-C(5)-C(6)	114.9(4)	F(13)-P(1)-F(16)	90.5(2)
N(4)-C(6)-N(2)	122.2(4)	F(11)-P(1)-F(12)	89.9(2)
N(4)-C(6)-C(5)	124.3(4)	F(13)-P(1)-F(12)	89.8(2)
N(2)-C(6)-C(5)	113.4(4)	F(16)-P(1)-F(12)	89.4(2)
N(4)-C(7)-N(5)	125.7(4)	F(11)-P(1)-F(15)	89.9(2)
N(4)-C(7)-C(14)	115.7(4)	F(13)-P(1)-F(15)	179.4(2)
N(5)-C(7)-C(14)	118.6(4)	F(16)-P(1)-F(15)	89.7(2)
N(5)-C(8)-N(2)	122.0(4)	F(12)-P(1)-F(15)	90.8(2)
N(5)-C(8)-C(9)	125.9(4)	F(11)-P(1)-F(14)	90.4(2)
N(2)-C(8)-C(9)	112.0(4)	F(13)-P(1)-F(14)	90.2(2)
C(10)-C(9)-N(3)	121.6(4)	F(16)-P(1)-F(14)	90.3(2)
C(10)-C(9)-C(8)	123.4(4)	F(12)-P(1)-F(14)	179.7(2)
N(3)-C(9)-C(8)	115.1(4)	F(15)-P(1)-F(14)	89.2(2)
C(9)-C(10)-C(11)	119.2(5)	F(23)-P(2)-F(24)	89.54(19)
C(12)-C(11)-C(10)	118.7(5)	F(23)-P(2)-F(25)	179.5(2)
C(13)-C(12)-C(11)	119.9(5)	F(24)-P(2)-F(25)	89.98(18)
N(3)-C(13)-C(12)	121.5(5)	F(23)-P(2)-F(22)	90.16(19)
C(15)-C(14)-C(19)	120.3(5)	F(24)-P(2)-F(22)	178.96(19)
C(15)-C(14)-C(7)	119.3(5)	F(25)-P(2)-F(22)	90.31(18)
C(19)-C(14)-C(7)	120.4(5)	F(23)-P(2)-F(21)	90.10(18)
C(16)-C(15)-C(14)	120.6(5)	F(24)-P(2)-F(21)	90.48(17)
C(17)-C(16)-C(15)	118.6(5)	F(25)-P(2)-F(21)	90.08(17)
C(18)-C(17)-C(16)	121.9(5)	F(22)-P(2)-F(21)	90.52(17)
C(18)-C(17)-BR1	119.4(4)	F(23)-P(2)-F(26)	90.00(18)
C(16)-C(17)-BR1	118.8(4)	F(24)-P(2)-F(26)	90.08(17)
C(17)-C(18)-C(19)	119.7(5)	F(25)-P(2)-F(26)	89.82(17)
C(18)-C(19)-C(14)	119.0(5)	F(22)-P(2)-F(26)	88.92(17)
N(6)-C(20)-C(21)	121.0(5)	F(21)-P(2)-F(26)	179.44(19)
C(22)-C(21)-C(20)	120.2(5)	F(33)-P(3)-F(34)	94.5(4)
C(21)-C(22)-C(23)	119.3(5)	F(33)-P(3)-F(36)	92.4(3)
C(22)-C(23)-C(24)	118.9(5)	F(34)-P(3)-F(36)	92.1(3)
N(6)-C(24)-C(23)	120.7(5)	F(33)-P(3)-F(35)	175.6(4)
N(6)-C(24)-C(25)	116.1(5)	F(34)-P(3)-F(35)	89.6(4)
C(23)-C(24)-C(25)	123.1(5)	F(36)-P(3)-F(35)	89.2(2)
N(7)-C(25)-C(26)	118.7(5)	F(33)-P(3)-F(32)	87.5(4)
N(7)-C(25)-C(24)	112.8(4)	F(34)-P(3)-F(32)	178.0(4)
C(26)-C(25)-C(24)	128.5(5)	F(36)-P(3)-F(32)	87.9(3)
C(25)-C(26)-C(27)	118.7(5)	F(35)-P(3)-F(32)	88.4(4)
C(28)-C(27)-C(26)	120.9(5)	F(33)-P(3)-F(31)	88.7(3)
C(27)-C(28)-C(29)	118.5(5)	F(34)-P(3)-F(31)	88.4(3)
N(7)-C(29)-C(28)	119.0(5)	F(36)-P(3)-F(31)	178.8(3)
N(7)-C(29)-C(30)	113.4(4)	F(35)-P(3)-F(31)	89.8(3)
C(28)-C(29)-C(30)	127.5(5)	F(32)-P(3)-F(31)	91.6(3)
N(8)-C(30)-C(31)	119.5(5)	N(43)-C(42)-C(41)	178.8(9)
N(8)-C(30)-C(29)	115.4(5)	N(53)-C(52)-C(51)	179.4(8)
C(31)-C(30)-C(29)	125.1(5)	N(63)-C(62)-C(61)	179.4(7)
C(30)-C(31)-C(32)	120.2(5)		

Table 1. Crystal data and structure refinement for **1c, chapter IV.**

Identification code	06srv114
Empirical formula	C39 H30 Br F12 N8 P2 Rh
Formula weight	1083.47
Temperature	120(2)K
Wavelength	0.71073 Å
Crystal system	Monoclinic
Space group	C2/c
Unit cell dimensions	a = 31.5411(17) Å α = 90° b = 11.5912(6) Å β = 96.0320(10)° c = 22.2823(12) Å γ = 90°
Volume	8101.3(7)Å^3
Z	8
Density (calculated)	1.777 g/cm^3
F(000)	4304
Theta range for data collection	1.84 to 30.46°
Index ranges	$-35 \le h \le 44$, $-12 \le k \le 16$, $-31 \le \ell \le 30$
Reflections collected	20606
Independent reflections	11267 [R_{int} = 0.048]
Absorption correction	Semi-empirical from equivalents
Max. and min. transmission	0.5500 and 0.2200
Refinement method	Full-matrix least-squares on F^2
Data / restraints / parameters	11267 / 0 / 626
Goodness-of-fit on F^2	0.969
Final R indices [I>2sigma(I)]	R_1 = 0.0773, wR_2 = 0.1815
R indices (all data)	R_1 = 0.1805, wR_2 = 0.2336
Largest diff. peak and hole	0.877 and -2.567 e/Å^3

Table 2. Atomic coordinates ($x\ 10^4$) and equivalent isotropic displacement parameters ($Å^2\ x\ 10^3$) for **1c, chapter IV.**

U_{eq} is defined as one third of the trace of the orthogonalized Uij tensor.

	Occ.	x	y	z	U_{eq}
Rh(1)	1	1319(1)	7813(1)	930(1)	13(1)
Br	1	-1878(1)	7229(1)	-1238(1)	42(1)
N(6)	1	1646(2)	6814(5)	378(2)	14(1)
C(1)	1	1469(3)	6295(6)	-126(3)	19(2)
C(2)	1	1707(3)	5598(7)	-483(3)	27(2)
C(3)	1	2134(3)	5441(7)	-297(4)	28(2)
C(4)	1	2317(3)	5977(7)	219(4)	29(2)
C(5)	1	2071(2)	6692(6)	557(3)	19(2)
C(6)	1	2227(2)	7379(6)	1099(3)	17(2)
C(7)	1	2643(2)	7523(6)	1382(3)	18(2)
C(71)	1	3024(3)	6866(7)	1208(4)	27(2)
C(8)	1	2702(2)	8311(7)	1844(4)	23(2)
C(9)	1	2378(2)	8965(6)	2072(3)	18(2)
C(91)	1	2496(3)	9803(7)	2575(4)	31(2)
C(10)	1	1957(2)	8778(6)	1813(3)	18(2)
C(11)	1	1550(2)	9251(6)	1981(3)	17(2)
C(12)	1	1494(3)	9970(7)	2465(3)	27(2)
C(13)	1	1101(3)	10276(7)	2600(4)	32(2)
C(14)	1	743(3)	9910(7)	2226(4)	30(2)
C(15)	1	807(3)	9209(6)	1747(4)	25(2)
N(7)	1	1196(2)	8876(5)	1623(3)	16(1)
C(16)	1	1898(2)	8004(6)	1326(3)	17(2)
N(1)	1	1288(2)	9183(5)	335(3)	15(1)
C(17)	1	1595(2)	9940(6)	252(3)	17(2)
C(18)	1	1541(3)	10817(6)	-173(3)	22(2)
C(19)	1	1154(3)	10910(6)	-529(4)	26(2)
C(20)	1	832(3)	10141(6)	-448(3)	21(2)
C(21)	1	902(2)	9297(6)	-8(3)	15(1)
N(2)	1	721(2)	7644(5)	505(3)	16(1)
C(22)	1	578(2)	8423(6)	101(3)	12(1)
C(23)	1	478(2)	6773(6)	638(3)	15(1)
C(24)	1	686(2)	6034(6)	1124(3)	14(1)
C(25)	1	493(3)	5083(6)	1342(3)	19(2)
C(26)	1	704(2)	4456(6)	1808(3)	17(2)
C(27)	1	1113(2)	4796(6)	2040(3)	19(2)
C(28)	1	1296(2)	5747(6)	1791(3)	16(2)
N(3)	1	1099(2)	6360(5)	1342(2)	14(1)
N(5)	1	86(2)	6618(5)	376(3)	15(1)
N(4)	1	183(2)	8393(5)	-169(3)	16(1)
C(29)	1	-48(2)	7475(6)	-24(3)	16(2)
C(30)	1	-487(2)	7376(6)	-330(3)	17(2)
C(31)	1	-622(3)	8085(6)	-812(3)	21(2)
C(32)	1	-1029(3)	8033(7)	-1098(4)	27(2)
C(33)	1	-1303(3)	7260(7)	-871(4)	28(2)
C(34)	1	-1188(3)	6530(7)	-396(4)	26(2)
C(35)	1	-773(2)	6591(6)	-125(3)	21(2)
N(8)	1	9823(2)	8265(7)	1448(3)	38(2)
C(36)	1	9658(3)	7610(8)	1721(4)	32(2)
C(37)	1	9453(3)	6761(10)	2093(6)	60(3)
P(1)	1	585(1)	3141(2)	3468(1)	24(1)

F(1)	1	180(2)	2352(7)	3479(3)	77(2)
F(2)	1	483(2)	3713(5)	4089(2)	48(2)
F(3)	1	986(2)	3960(6)	3458(3)	59(2)
F(4)	1	679(2)	2579(5)	2846(2)	59(2)
F(5)	1	302(2)	4092(5)	3102(2)	45(2)
F(6)	1	871(2)	2199(5)	3842(2)	49(2)

Table 3. Hydrogen coordinates (x 10^4) and isotropic displacement parameters ($Å^2$ x 10^3) for C39 H30 Br F12 N8 P2 Rh.

	Occ.	x	y	z	U_{eq}
H(1)	1	1174	6404	-245	23
H(2)	1	1577	5245	-841	32
H(3)	1	2302	4964	-525	33
H(4)	1	2611	5862	347	34
H(711)	1	3282	7140	1449	41
H(712)	1	3052	6988	779	41
H(713)	1	2986	6041	1283	41
H(8)	1	2985	8424	2026	28
H(911)	1	2384	10569	2458	46
H(912)	1	2807	9842	2657	46
H(913)	1	2374	9547	2939	46
H(12)	1	1738	10253	2707	33
H(13)	1	1070	10736	2945	38
H(14)	1	464	10138	2301	36
H(15)	1	566	8948	1492	29
H(17)	1	1861	9876	493	20
H(18)	1	1765	11345	-220	26
H(19)	1	1112	11498	-826	31
H(20)	1	566	10189	-690	25
H(25)	1	216	4858	1173	22
H(26)	1	572	3804	1969	20
H(27)	1	1264	4383	2363	23
H(28)	1	1575	5970	1950	19
H(31)	1	-427	8624	-949	25
H(32)	1	-1117	8507	-1435	33
H(34)	1	-1387	6001	-258	31
H(35)	1	-683	6094	203	26
H(371)	1	9266	6257	1830	89
H(372)	1	9285	7167	2372	89
H(373)	1	9673	6295	2322	89

Table 4. Anisotropic parameters ($Å^2$ x 10^3) for **1c, chapter IV.**

The anisotropic displacement factor exponent takes the form:

$$-2\pi^2 [h^2 a^{*2} U_{11} + ... + 2 h k a^* b^* U_{12}]$$

	U11	U22	U33	U23	U13	U12
Rh(1)	14(1)	12(1)	11(1)	2(1)	-1(1)	-2(1)
Br	19(1)	49(1)	55(1)	2(1)	-14(1)	-2(1)
N(6)	16(3)	14(3)	11(3)	1(2)	6(2)	-2(2)
C(1)	22(4)	16(4)	19(4)	-2(3)	3(3)	-7(3)
C(2)	34(5)	28(4)	18(4)	-6(3)	3(4)	-3(4)
C(3)	29(5)	24(4)	32(4)	-12(3)	7(4)	5(3)
C(4)	22(4)	29(4)	34(5)	-3(4)	0(4)	-1(4)
C(5)	17(4)	19(4)	23(4)	6(3)	6(3)	-2(3)
C(6)	22(4)	12(3)	19(3)	8(3)	2(3)	0(3)
C(7)	17(4)	19(3)	17(3)	4(3)	0(3)	1(3)
C(71)	21(4)	39(5)	20(4)	6(3)	-5(3)	0(4)
C(8)	15(4)	27(4)	26(4)	6(3)	-3(3)	-4(3)
C(9)	23(4)	19(4)	11(3)	0(3)	-3(3)	-6(3)
C(91)	36(5)	26(4)	29(5)	-3(4)	-5(4)	-18(4)
C(10)	22(4)	16(3)	14(3)	4(3)	-3(3)	-7(3)
C(11)	22(4)	15(3)	12(3)	7(3)	-8(3)	2(3)
C(12)	39(5)	20(4)	21(4)	-4(3)	-4(4)	3(4)
C(13)	51(6)	25(4)	20(4)	-10(3)	5(4)	12(4)
C(14)	25(5)	36(5)	31(5)	4(4)	11(4)	10(4)
C(15)	32(5)	16(4)	25(4)	3(3)	1(4)	4(3)
N(7)	23(3)	12(3)	11(3)	3(2)	-2(2)	-3(2)
C(16)	11(3)	17(4)	23(4)	0(3)	-2(3)	-7(3)
N(1)	20(3)	10(3)	14(3)	3(2)	3(2)	1(2)
C(17)	24(4)	13(3)	14(3)	1(3)	3(3)	-4(3)
C(18)	24(4)	20(4)	23(4)	3(3)	6(3)	-5(3)
C(19)	35(5)	14(4)	29(4)	4(3)	4(4)	-2(3)
C(20)	22(4)	16(3)	23(4)	5(3)	1(3)	-4(3)
C(21)	18(4)	11(3)	15(3)	2(3)	2(3)	1(3)
N(2)	21(3)	14(3)	13(3)	3(2)	2(2)	-3(2)
C(22)	15(4)	14(3)	6(3)	1(3)	1(3)	0(3)
C(23)	18(4)	14(3)	13(3)	4(3)	-2(3)	-4(3)
C(24)	19(4)	12(3)	9(3)	1(3)	0(3)	4(3)
C(25)	26(4)	20(4)	11(3)	8(3)	6(3)	-5(3)
C(26)	24(4)	13(3)	13(3)	4(3)	1(3)	0(3)
C(27)	21(4)	19(4)	17(4)	4(3)	-4(3)	1(3)
C(28)	15(4)	19(3)	11(3)	-1(3)	-6(3)	0(3)
N(3)	20(3)	11(3)	11(3)	-2(2)	-1(2)	0(2)
N(5)	15(3)	16(3)	14(3)	2(2)	-2(2)	-2(2)
N(4)	11(3)	15(3)	20(3)	2(2)	0(2)	0(2)
C(29)	16(4)	15(3)	18(3)	0(3)	0(3)	0(3)
C(30)	19(4)	8(3)	23(4)	-1(3)	2(3)	-3(3)
C(31)	23(4)	14(3)	27(4)	1(3)	5(3)	-1(3)
C(32)	24(4)	30(5)	25(4)	6(3)	-10(3)	4(3)
C(33)	19(4)	34(4)	29(4)	-14(4)	-5(3)	-1(4)
C(34)	18(4)	27(4)	32(4)	0(4)	1(3)	-8(3)
C(35)	22(4)	18(4)	24(4)	2(3)	2(3)	-1(3)
N(8)	28(4)	52(5)	32(4)	8(4)	-4(3)	-7(4)
C(36)	24(5)	34(5)	36(5)	-1(4)	-4(4)	6(4)
C(37)	31(6)	65(7)	82(9)	32(7)	3(6)	-6(5)
P(1)	25(1)	31(1)	18(1)	6(1)	5(1)	7(1)

F(1)	71(5)	107(6)	47(4)	27(4)	-16(3)	-46(4)
F(2)	57(4)	65(4)	23(3)	0(3)	4(3)	28(3)
F(3)	35(3)	80(5)	59(4)	36(3)	-3(3)	-12(3)
F(4)	118(6)	35(3)	28(3)	13(2)	24(3)	37(3)
F(5)	47(3)	62(4)	24(3)	11(2)	0(2)	37(3)
F(6)	64(4)	50(3)	33(3)	23(3)	11(3)	28(3)
P(2)	31(1)	19(1)	20(1)	3(1)	7(1)	1(1)
F(71)	44(6)	61(7)	39(6)	19(5)	-4(5)	0(5)
F(81)	36(6)	24(4)	24(5)	-1(4)	18(4)	0(4)
F(91)	38(5)	30(5)	23(4)	5(4)	0(4)	-2(4)
F(101)	41(6)	33(5)	38(6)	14(5)	19(5)	0(5)
F(111)	81(10)	12(4)	50(7)	9(4)	54(8)	18(6)
F(121)	53(7)	24(5)	26(5)	2(4)	14(5)	-3(5)
F(72)	21(8)	37(8)	52(10)	16(8)	-14(7)	-7(6)
F(82)	54(12)	13(6)	35(9)	0(6)	23(8)	-4(7)
F(92)	55(11)	56(10)	59(12)	12(9)	-3(9)	31(9)
F(102)	72(14)	34(8)	35(9)	8(8)	31(9)	-8(9)
F(112)	49(12)	37(10)	38(9)	-24(7)	19(10)	5(9)
F(122)	53(12)	13(7)	50(10)	6(6)	9(9)	-5(8)

Table 5. Bond lengths [Å] and angles [°] for **1c, chapter IV.**

Rh(1)-C(16)	1.955(7)	N(8)-C(36)	1.132(11)
Rh(1)-N(2)	2.031(6)	C(36)-C(37)	1.477(14)
Rh(1)-N(7)	2.045(6)	P(1)-F(1)	1.573(7)
Rh(1)-N(6)	2.045(6)	P(1)-F(3)	1.583(6)
Rh(1)-N(1)	2.064(5)	P(1)-F(4)	1.588(6)
Rh(1)-N(3)	2.071(6)	P(1)-F(5)	1.589(5)
Br-C(33)	1.910(8)	P(1)-F(6)	1.594(5)
N(6)-C(1)	1.342(9)	P(1)-F(2)	1.597(5)
N(6)-C(5)	1.364(9)	P(2)-F(71)	1.572(9)
C(1)-C(2)	1.403(11)	P(2)-F(122)	1.581(16)
C(2)-C(3)	1.380(12)	P(2)-F(82)	1.581(14)
C(3)-C(4)	1.379(11)	P(2)-F(111)	1.582(11)
C(4)-C(5)	1.406(11)	P(2)-F(92)	1.583(15)
C(5)-C(6)	1.488(10)	P(2)-F(91)	1.587(8)
C(6)-C(16)	1.401(10)	P(2)-F(102)	1.589(15)
C(6)-C(7)	1.406(10)	P(2)-F(101)	1.591(9)
C(7)-C(8)	1.374(11)	P(2)-F(81)	1.605(9)
C(7)-C(71)	1.507(11)	P(2)-F(112)	1.61(2)
C(8)-C(9)	1.408(11)	P(2)-F(72)	1.617(13)
C(9)-C(10)	1.409(10)	P(2)-F(121)	1.632(10)
C(9)-C(91)	1.500(10)	C(16)-Rh(1)-N(2)	178.6(3)
C(10)-C(16)	1.405(10)	C(16)-Rh(1)-N(7)	80.4(3)
C(10)-C(11)	1.481(11)	N(2)-Rh(1)-N(7)	99.7(2)
C(11)-N(7)	1.371(9)	C(16)-Rh(1)-N(6)	80.2(3)
C(11)-C(12)	1.389(10)	N(2)-Rh(1)-N(6)	99.7(2)
C(12)-C(13)	1.353(12)	N(7)-Rh(1)-N(6)	160.6(2)
C(13)-C(14)	1.399(12)	C(16)-Rh(1)-N(1)	100.5(3)
C(14)-C(15)	1.373(11)	N(2)-Rh(1)-N(1)	78.1(2)
C(15)-N(7)	1.342(10)	N(7)-Rh(1)-N(1)	91.2(2)
N(1)-C(17)	1.336(9)	N(6)-Rh(1)-N(1)	92.4(2)
N(1)-C(21)	1.374(9)	C(16)-Rh(1)-N(3)	103.5(3)
C(17)-C(18)	1.388(10)	N(2)-Rh(1)-N(3)	77.9(2)
C(18)-C(19)	1.387(11)	N(7)-Rh(1)-N(3)	93.2(2)
C(19)-C(20)	1.377(10)	N(6)-Rh(1)-N(3)	91.2(2)
C(20)-C(21)	1.387(10)	N(1)-Rh(1)-N(3)	156.0(2)
C(21)-C(22)	1.477(10)	C(1)-N(6)-C(5)	120.4(6)
N(2)-C(23)	1.319(9)	C(1)-N(6)-Rh(1)	124.4(5)
N(2)-C(22)	1.320(8)	C(5)-N(6)-Rh(1)	115.1(5)
C(22)-N(4)	1.326(9)	N(6)-C(1)-C(2)	122.2(7)
C(23)-N(5)	1.324(9)	C(3)-C(2)-C(1)	117.9(7)
C(23)-C(24)	1.479(9)	C(4)-C(3)-C(2)	120.0(8)
C(24)-C(25)	1.372(9)	C(3)-C(4)-C(5)	120.4(8)
C(24)-N(3)	1.396(9)	N(6)-C(5)-C(4)	119.0(7)
C(25)-C(26)	1.380(9)	N(6)-C(5)-C(6)	114.4(7)
C(26)-C(27)	1.397(10)	C(4)-C(5)-C(6)	126.6(7)
C(27)-C(28)	1.386(10)	C(16)-C(6)-C(7)	118.0(7)
C(28)-N(3)	1.327(8)	C(16)-C(6)-C(5)	112.0(7)
N(5)-C(29)	1.370(9)	C(7)-C(6)-C(5)	129.9(7)
N(4)-C(29)	1.348(9)	C(8)-C(7)-C(6)	117.4(7)
C(29)-C(30)	1.482(10)	C(8)-C(7)-C(71)	118.8(7)
C(30)-C(31)	1.383(10)	C(6)-C(7)-C(71)	123.8(7)
C(30)-C(35)	1.391(10)	C(7)-C(8)-C(9)	125.7(7)
C(31)-C(32)	1.373(11)	C(8)-C(9)-C(10)	117.2(7)
C(32)-C(33)	1.377(12)	C(8)-C(9)-C(91)	119.1(7)
C(33)-C(34)	1.374(12)	C(10)-C(9)-C(91)	123.7(7)
C(34)-C(35)	1.385(11)	C(16)-C(10)-C(9)	117.2(7)

C(16)-C(10)-C(11)	112.6(6)	F(3)-P(1)-F(4)	90.5(4)
C(9)-C(10)-C(11)	130.2(7)	F(1)-P(1)-F(5)	89.9(4)
N(7)-C(11)-C(12)	118.8(7)	F(3)-P(1)-F(5)	89.0(3)
N(7)-C(11)-C(10)	114.2(6)	F(4)-P(1)-F(5)	89.0(3)
C(12)-C(11)-C(10)	127.0(7)	F(1)-P(1)-F(6)	90.5(4)
C(13)-C(12)-C(11)	121.5(8)	F(3)-P(1)-F(6)	90.6(3)
C(12)-C(13)-C(14)	119.4(7)	F(4)-P(1)-F(6)	91.6(3)
C(15)-C(14)-C(13)	117.7(8)	F(5)-P(1)-F(6)	179.3(4)
N(7)-C(15)-C(14)	122.9(8)	F(1)-P(1)-F(2)	89.5(4)
C(15)-N(7)-C(11)	119.6(6)	F(3)-P(1)-F(2)	89.8(4)
C(15)-N(7)-Rh(1)	125.4(5)	F(4)-P(1)-F(2)	179.2(4)
C(11)-N(7)-Rh(1)	115.0(5)	F(5)-P(1)-F(2)	90.3(3)
C(6)-C(16)-C(10)	124.4(7)	F(6)-P(1)-F(2)	89.2(3)
C(6)-C(16)-Rh(1)	118.1(5)	F(71)-P(2)-F(122)	67.8(7)
C(10)-C(16)-Rh(1)	117.5(6)	F(71)-P(2)-F(82)	57.8(8)
C(17)-N(1)-C(21)	118.3(6)	F(122)-P(2)-F(82)	92.9(8)
C(17)-N(1)-Rh(1)	127.4(5)	F(71)-P(2)-F(111)	94.1(6)
C(21)-N(1)-Rh(1)	114.3(4)	F(122)-P(2)-F(111)	153.2(8)
N(1)-C(17)-C(18)	122.4(7)	F(82)-P(2)-F(111)	93.5(6)
C(19)-C(18)-C(17)	119.1(7)	F(71)-P(2)-F(92)	137.1(8)
C(20)-C(19)-C(18)	119.4(7)	F(122)-P(2)-F(92)	91.0(9)
C(19)-C(20)-C(21)	119.0(7)	F(82)-P(2)-F(92)	88.2(9)
N(1)-C(21)-C(20)	121.8(7)	F(111)-P(2)-F(92)	115.2(8)
N(1)-C(21)-C(22)	115.4(6)	F(71)-P(2)-F(91)	176.3(6)
C(20)-C(21)-C(22)	122.7(6)	F(122)-P(2)-F(91)	109.1(7)
C(23)-N(2)-C(22)	120.8(6)	F(82)-P(2)-F(91)	121.2(8)
C(23)-N(2)-Rh(1)	120.1(5)	F(111)-P(2)-F(91)	89.5(6)
C(22)-N(2)-Rh(1)	119.1(5)	F(92)-P(2)-F(91)	39.9(7)
N(2)-C(22)-N(4)	121.9(6)	F(71)-P(2)-F(102)	122.8(9)
N(2)-C(22)-C(21)	112.9(6)	F(122)-P(2)-F(102)	91.1(9)
N(4)-C(22)-C(21)	125.2(6)	F(82)-P(2)-F(102)	175.8(8)
N(2)-C(23)-N(5)	122.8(6)	F(111)-P(2)-F(102)	82.3(7)
N(2)-C(23)-C(24)	112.6(6)	F(92)-P(2)-F(102)	93.1(10)
N(5)-C(23)-C(24)	124.5(6)	F(91)-P(2)-F(102)	58.5(8)
C(25)-C(24)-N(3)	121.8(6)	F(71)-P(2)-F(101)	90.7(5)
C(25)-C(24)-C(23)	123.1(7)	F(122)-P(2)-F(101)	69.7(8)
N(3)-C(24)-C(23)	115.1(6)	F(82)-P(2)-F(101)	148.3(8)
C(24)-C(25)-C(26)	119.5(7)	F(111)-P(2)-F(101)	91.9(5)
C(25)-C(26)-C(27)	118.9(7)	F(92)-P(2)-F(101)	117.3(8)
C(28)-C(27)-C(26)	118.9(7)	F(91)-P(2)-F(101)	90.0(5)
N(3)-C(28)-C(27)	123.2(7)	F(102)-P(2)-F(101)	33.1(7)
C(28)-N(3)-C(24)	117.5(6)	F(71)-P(2)-F(81)	89.8(5)
C(28)-N(3)-Rh(1)	128.2(5)	F(122)-P(2)-F(81)	108.6(7)
C(24)-N(3)-Rh(1)	114.3(4)	F(82)-P(2)-F(81)	32.1(6)
C(23)-N(5)-C(29)	113.4(6)	F(111)-P(2)-F(81)	90.2(5)
C(22)-N(4)-C(29)	114.7(6)	F(92)-P(2)-F(81)	61.0(7)
N(4)-C(29)-N(5)	126.2(7)	F(91)-P(2)-F(81)	89.3(5)
N(4)-C(29)-C(30)	117.0(6)	F(102)-P(2)-F(81)	146.8(8)
N(5)-C(29)-C(30)	116.8(6)	F(101)-P(2)-F(81)	177.8(5)
C(31)-C(30)-C(35)	119.1(7)	F(71)-P(2)-F(112)	110.8(8)
C(31)-C(30)-C(29)	120.5(7)	F(122)-P(2)-F(112)	178.6(11)
C(35)-C(30)-C(29)	120.4(7)	F(82)-P(2)-F(112)	86.2(9)
C(32)-C(31)-C(30)	122.0(7)	F(111)-P(2)-F(112)	26.0(6)
C(31)-C(32)-C(33)	116.8(7)	F(92)-P(2)-F(112)	90.0(9)
C(34)-C(33)-C(32)	123.9(7)	F(91)-P(2)-F(112)	72.3(8)
C(34)-C(33)-Br	118.7(6)	F(102)-P(2)-F(112)	89.8(9)
C(32)-C(33)-Br	117.4(6)	F(101)-P(2)-F(112)	110.6(7)
C(33)-C(34)-C(35)	117.7(7)	F(81)-P(2)-F(112)	71.1(7)
C(34)-C(35)-C(30)	120.4(7)	F(71)-P(2)-F(72)	41.8(6)
N(8)-C(36)-C(37)	178.2(10)	F(122)-P(2)-F(72)	90.4(8)
F(1)-P(1)-F(3)	178.7(4)	F(82)-P(2)-F(72)	89.4(8)
F(1)-P(1)-F(4)	90.1(4)	F(111)-P(2)-F(72)	63.8(7)

F(92)-P(2)-F(72)	177.3(8)	F(111)-P(2)-F(121)	176.7(7)
F(91)-P(2)-F(72)	141.4(7)	F(92)-P(2)-F(121)	61.7(8)
F(102)-P(2)-F(72)	89.2(9)	F(91)-P(2)-F(121)	87.3(5)
F(101)-P(2)-F(72)	65.3(6)	F(102)-P(2)-F(121)	96.8(7)
F(81)-P(2)-F(72)	116.3(6)	F(101)-P(2)-F(121)	89.0(5)
F(112)-P(2)-F(72)	88.6(8)	F(81)-P(2)-F(121)	88.9(5)
F(71)-P(2)-F(121)	89.1(5)	F(112)-P(2)-F(121)	151.1(8)
F(122)-P(2)-F(121)	29.7(6)	F(72)-P(2)-F(121)	119.4(6)
F(82)-P(2)-F(121)	87.4(6)		

Appendix 7: Supplementary information for chapter V, part A.

Table 1. Crystal data and structure refinement for **2c, Chapter V, Part A.**

Identification code	gary46
Empirical formula	C38 H24 Br2 Co F^2 N10 P2
Formula weight	1129.36
Temperature	100(2)K
Wavelength	1.54178 Å
Crystal system	Monoclinic
Space group	C2/c
Unit cell dimensions	a = 14.7467(4) Å ? = 90? b = 20.8588(6) Å ? = 96.2640(10)? c = 16.6451(5) Å ? = 90?
Volume	5089.4(3)Å3
Z	4
Density (calculated)	1.474 Mg/m3
Absorption coefficient	5.808 mm-1
F(000)	2228
Crystal size	0.38 x 0.06 x 0.04 mm
Theta range for data collection	3.69 to 55.23?
Reflections collected	22391
Independent reflections	3198 [Rint = 0.043]
Absorption correction	Semi-empirical from equivalents
Max. and min. transmission	0.8400 and 0.4100
Refinement method	Full-matrix least-squares on F^2
Data / restraints / parameters	3198 / 357 / 359
Goodness-of-fit on F^2	0.925
Final R indices [I>2sigma(I)]	R_1 = 0.0428, wR_2 = 0.0783
R indices (all data)	R_1 = 0.0802, wR_2 = 0.0836
Extinction coefficient	0.000011(7)
Largest diff. peak and hole	0.494 and -1.078 e/Å3

Table 2. Bond lengths [Å] and angles [°] for **2c, Chapter V, Part A.**

Co(1)-N(18)	1.986(3)	N(18)-CO1-N(11)#1	100.96(13)
Co(1)-N(18)#1	1.986(3)	N(18)#1-CO1-N(11)#1	75.99(14)
Co(1)-N(114)	2.134(3)	N(114)-CO1-N(11)#1	93.89(12)
Co(1)-N(114)#1	2.134(3)	N(114)#1-CO1-N(11)#1	151.79(13)
Co(1)-N(11)	2.158(4)	N(11)-CO1-N(11)#1	95.96(18)
Co(1)-N(11)#1	2.158(4)	C(12)-N(11)-C(16)	115.8(4)
N(11)-C(12)	1.340(5)	C(12)-N(11)-CO1	128.7(3)
N(11)-C(16)	1.364(4)	C(16)-N(11)-CO1	115.5(3)
C(12)-C(13)	1.374(6)	N(11)-C(12)-C(13)	123.3(4)
C(13)-C(14)	1.398(6)	C(12)-C(13)-C(14)	119.7(4)
C(14)-C(15)	1.383(5)	C(15)-C(14)-C(13)	117.5(5)
C(15)-C(16)	1.356(5)	C(16)-C(15)-C(14)	119.2(4)
C(16)-C(17)	1.484(5)	C(15)-C(16)-N(11)	124.5(4)
C(17)-N(18)	1.319(4)	C(15)-C(16)-C(17)	123.7(4)
C(17)-N(112)	1.338(4)	N(11)-C(16)-C(17)	111.8(4)
N(18)-C(19)	1.355(5)	N(18)-C(17)-N(112)	124.9(4)
C(19)-N(110)	1.327(4)	N(18)-C(17)-C(16)	115.3(4)
C(19)-C(113)	1.465(5)	N(112)-C(17)-C(16)	119.8(4)
N(110)-C(111)	1.359(5)	C(17)-N(18)-C(19)	117.5(3)
C(111)-N(112)	1.345(5)	C(17)-N(18)-CO1	121.4(3)
C(111)-C(119)	1.479(5)	C(19)-N(18)-CO1	121.1(3)
C(113)-N(114)	1.360(4)	N(110)-C(19)-N(18)	123.1(4)
C(113)-C(118)	1.375(5)	N(110)-C(19)-C(113)	123.7(4)
N(114)-C(115)	1.338(5)	N(18)-C(19)-C(113)	113.3(4)
C(115)-C(116)	1.383(5)	C(19)-N(110)-C(111)	114.4(4)
C(116)-C(117)	1.389(5)	N(112)-C(111)-N(110)	126.6(4)
C(117)-C(118)	1.375(5)	N(112)-C(111)-C(119)	117.2(4)
C(119)-C(120)	1.382(5)	N(110)-C(111)-C(119)	116.2(4)
C(119)-C(124)	1.384(5)	C(17)-N(112)-C(111)	113.3(3)
C(120)-C(121)	1.388(5)	N(114)-C(113)-C(118)	123.2(4)
C(121)-C(122)	1.371(6)	N(114)-C(113)-C(19)	113.6(4)
C(122)-C(123)	1.339(5)	C(118)-C(113)-C(19)	123.1(4)
C(122)-Br	1.910(4)	C(115)-N(114)-C(113)	117.0(4)
C(123)-C(124)	1.396(5)	C(115)-N(114)-CO1	127.5(3)
P(1)-F(2)	1.574(10)	C(113)-N(114)-CO1	115.5(3)
P(1)-F(4)	1.586(8)	N(114)-C(115)-C(116)	122.9(4)
P(1)-F(6)	1.596(9)	C(115)-C(116)-C(117)	119.2(4)
P(1)-F(3)	1.596(7)	C(118)-C(117)-C(116)	118.6(4)
P(1)-F(5)	1.600(7)	C(117)-C(118)-C(113)	119.1(4)
P(1)-F(1)	1.603(9)	C(120)-C(119)-C(124)	119.1(4)
P(11)-F(12)	1.574(14)	C(120)-C(119)-C(111)	119.2(4)
P(11)-F(14)	1.575(12)	C(124)-C(119)-C(111)	121.7(4)
P(11)-F(16)	1.594(14)	C(119)-C(120)-C(121)	120.5(4)
P(11)-F(13)	1.603(12)	C(122)-C(121)-C(120)	118.4(4)
P(11)-F(15)	1.609(13)	C(123)-C(122)-C(121)	122.8(4)
P(11)-F(11)	1.614(14)	C(123)-C(122)-BR	118.9(4)
		C(121)-C(122)-BR	118.3(4)
N(18)-CO1-N(18)#1	175.6(2)	C(122)-C(123)-C(124)	119.0(4)
N(18)-CO1-N(114)	76.21(14)	C(119)-C(124)-C(123)	120.2(4)
N(18)#1-CO1-N(114)	107.05(13)	F(2)-P(1)-F(4)	178.9(7)
N(18)-CO1-N(114)#1	107.05(13)	F(2)-P(1)-F(6)	90.4(7)
N(18)#1-CO1-N(114)#1	76.21(14)	F(4)-P(1)-F(6)	89.6(5)
N(114)-CO1-N(114)#1	89.71(18)	F(2)-P(1)-F(3)	88.2(5)
N(18)-CO1-N(11)	75.99(14)	F(4)-P(1)-F(3)	90.8(4)
N(18)#1-CO1-N(11)	100.96(13)	F(6)-P(1)-F(3)	89.0(5)
N(114)-CO1-N(11)	151.79(13)	F(2)-P(1)-F(5)	91.1(7)
N(114)#1-CO1-N(11)	93.89(12)	F(4)-P(1)-F(5)	90.0(7)

F(6)-P(1)-F(5)	89.2(6)	F(14)-P(11)-F(13)	90.4(7)
F(3)-P(1)-F(5)	178.1(8)	F(16)-P(11)-F(13)	90.70(11)
F(2)-P(1)-F(1)	90.9(7)	F(12)-P(11)-F(15)	90.00(12)
F(4)-P(1)-F(1)	89.0(7)	F(14)-P(11)-F(15)	89.40(11)
F(6)-P(1)-F(1)	178.6(7)	F(16)-P(11)-F(15)	90.90(12)
F(3)-P(1)-F(1)	90.9(5)	F(13)-P(11)-F(15)	178.50(14)
F(5)-P(1)-F(1)	90.9(7)	F(12)-P(11)-F(11)	91.7(1)
F(12)-P(11)-F(14)	177.90(13)	F(14)-P(11)-F(11)	90.3(9)
F(12)-P(11)-F(16)	86.60(11)	F(16)-P(11)-F(11)	178.10(11)
F(14)-P(11)-F(16)	91.50(11)	F(13)-P(11)-F(11)	90.1(8)
F(12)-P(11)-F(13)	90.2(8)	F(15)-P(11)-F(11)	88.4(1)

Appendix 8: Supplementary information for chapter V, part B.

Table 1. Crystal data and structure refinement for **L1, Chapter V, Part B.**

Empirical formula	C19 H16 Br N5 O2
Formula weight	426.28
Temperature	150(2)K
Wavelength	1.54178 Å
Crystal system	Monoclinic
Space group	P21/c
Unit cell dimensions	a = 24.9536(10) Å α = 90° b = 3.9351(2) Å β = 110.007(2)° c = 19.0793(8) Å γ = 90°
Volume	1760.43(14)Å^3
Z	4
Density (calculated)	1.608 Mg/m^3
Absorption coefficient	3.406 mm^{-1}
F(000)	864
Crystal size	0.20 x 0.04 x 0.02 mm
Theta range for data collection	1.88 to 68.58°
Index ranges	$-29 \le h \le 29$, $-4 \le k \le 4$, $-22 \le \ell \le 22$
Reflections collected	23442
Independent reflections	3232 [R_{int} = 0.046]
Absorption correction	Semi-empirical from equivalents
Max. and min. transmission	0.9500 and 0.6300
Refinement method	Full-matrix least-squares on F^2
Data / restraints / parameters	3232 / 6 / 256
Goodness-of-fit on F^2	1.048
Final R indices [I>2sigma(I)]	R_1 = 0.0440, wR_2 = 0.1135
R indices (all data)	R_1 = 0.0556, wR_2 = 0.1215
Largest diff. peak and hole	0.963 and -1.145 e/Å^3

Table 2. Bond lengths [Å] and angles [°] for **L1, Chapter V, Part B.**

N(1)-C(5)	1.369(5)	C(2)-C(1)-N(1)	122.6(4)
N(1)-C(1)	1.377(6)	C(1)-C(2)-C(3)	118.0(4)
N(2)-C(6)	1.340(5)	C(4)-C(3)-C(2)	121.0(4)
N(2)-C(8)	1.351(4)	C(3)-C(4)-C(5)	118.7(4)
N(3)-C(13)	1.337(5)	C(4)-C(5)-N(1)	123.0(3)
N(3)-C(9)	1.349(4)	C(4)-C(5)-C(6)	119.0(3)
N(4)-C(7)	1.342(4)	N(1)-C(5)-C(6)	118.0(3)
N(4)-C(6)	1.343(4)	N(2)-C(6)-N(4)	125.1(3)
N(5)-C(7)	1.331(4)	N(2)-C(6)-C(5)	117.0(3)
N(5)-C(8)	1.332(4)	N(4)-C(6)-C(5)	117.8(3)
C(1)-C(2)	1.354(7)	N(5)-C(7)-N(4)	125.1(3)
C(2)-C(3)	1.391(6)	N(5)-C(7)-C(14)	117.3(3)
C(3)-C(4)	1.351(6)	N(4)-C(7)-C(14)	117.6(3)
C(4)-C(5)	1.356(5)	N(5)-C(8)-N(2)	124.6(3)
C(5)-C(6)	1.488(5)	N(5)-C(8)-C(9)	117.7(3)
C(7)-C(14)	1.482(4)	N(2)-C(8)-C(9)	117.7(3)
C(8)-C(9)	1.486(5)	N(3)-C(9)-C(10)	122.6(3)
C(9)-C(10)	1.379(5)	N(3)-C(9)-C(8)	117.3(3)
C(10)-C(11)	1.379(5)	C(10)-C(9)-C(8)	120.1(3)
C(11)-C(12)	1.385(5)	C(11)-C(10)-C(9)	119.0(3)
C(12)-C(13)	1.392(5)	C(10)-C(11)-C(12)	119.5(3)
C(14)-C(19)	1.397(5)	C(11)-C(12)-C(13)	117.7(3)
C(14)-C(15)	1.398(5)	N(3)-C(13)-C(12)	123.4(3)
C(15)-C(16)	1.383(5)	C(19)-C(14)-C(15)	119.0(3)
C(16)-C(17)	1.394(5)	C(19)-C(14)-C(7)	119.9(3)
C(17)-C(18)	1.380(5)	C(15)-C(14)-C(7)	121.1(3)
C(17)-Br(1)	1.899(3)	C(16)-C(15)-C(14)	121.0(3)
C(18)-C(19)	1.383(5)	C(15)-C(16)-C(17)	118.6(3)
C(5)-N(1)-C(1)	116.6(4)	C(18)-C(17)-C(16)	121.6(3)
C(6)-N(2)-C(8)	114.8(3)	C(18)-C(17)-BR1	119.0(2)
C(13)-N(3)-C(9)	117.7(3)	C(16)-C(17)-BR1	119.4(2)
C(7)-N(4)-C(6)	114.7(3)	C(17)-C(18)-C(19)	119.3(3)
C(7)-N(5)-C(8)	115.7(3)	C(18)-C(19)-C(14)	120.6(3)

Table 1. Crystal data and structure refinement for **1a, chapter V, part B.**

Empirical formula	C38 H24 Br2 F12 Fe N10 P2
Formula weight	1126.28
Temperature	100(2)K
Wavelength	1.54178 Å
Crystal system	Monoclinic
Space group	C2/c
Unit cell dimensions	a = 14.4472(6) Å α = 90° b = 21.0450(12) Å β = 99.350(4)° c = 16.4940(9) Å γ = 90°
Volume	4948.2(4)Å^3
Z	4
Density (calculated)	1.512 g/cm^3
Absorption coefficient	5.699 mm^{-1}
F(000)	2224
Crystal size	0.36 x 0.19 x 0.07 mm
Theta range for data collection	3.74 to 73.02°
Index ranges	$-17 \le h \le 17$, $-25 \le k \le 25$, $-19 \le \ell \le 17$
Reflections collected	40326
Independent reflections	4826 [R_{int} = 0.065]
Absorption correction	Semi-empirical from equivalents
Max. and min. transmission	0.7900 and 0.2400
Refinement method	Full-matrix least-squares on F^2
Data / restraints / parameters	4826 / 0 / 361
Goodness-of-fit on F^2	1.089
Final R indices [I>2sigma(I)]	R_1 = 0.0961, wR_2 = 0.2665
R indices (all data)	R_1 = 0.1280, wR_2 = 0.2890
Largest diff. peak and hole	1.439 and -2.241 e/Å^3

Table 2. Bond lengths [Å] and angles [°] for **1a, chapter V, part B.**

Fe-N(2)	1.872(5)	N(2)-FE-N(1)#1	99.7(2)
Fe-N(2)#1	1.872(5)	N(2)#1-FE-N(1)#1	79.3(2)
Fe-N(3)	2.004(6)	N(3)-FE-N(1)#1	93.4(3)
Fe-N(3)#1	2.004(6)	N(3)#1-FE-N(1)#1	159.0(2)
Fe-N(1)	2.006(6)	N(1)-FE-N(1)#1	91.0(4)
Fe-N(1)#1	2.006(6)	C(1)-N(1)-C(5)	117.9(6)
N(1)-C(1)	1.344(9)	C(1)-N(1)-FE	127.3(5)
N(1)-C(5)	1.371(9)	C(5)-N(1)-FE	114.8(5)
N(2)-C(6)	1.338(9)	C(6)-N(2)-C(8)	116.9(5)
N(2)-C(8)	1.356(8)	C(6)-N(2)-FE	122.0(5)
N(3)-C(13)	1.346(9)	C(8)-N(2)-FE	120.9(4)
N(3)-C(9)	1.357(8)	C(13)-N(3)-C(9)	118.4(6)
N(4)-C(6)	1.323(8)	C(13)-N(3)-FE	126.4(5)
N(4)-C(7)	1.370(9)	C(9)-N(3)-FE	115.0(5)
N(5)-C(8)	1.312(8)	C(6)-N(4)-C(7)	114.5(6)
N(5)-C(7)	1.370(9)	C(8)-N(5)-C(7)	115.3(6)
C(1)-C(2)	1.351(13)	N(1)-C(1)-C(2)	122.4(7)
C(2)-C(3)	1.425(13)	C(1)-C(2)-C(3)	119.9(8)
C(3)-C(4)	1.358(11)	C(4)-C(3)-C(2)	118.1(8)
C(4)-C(5)	1.384(10)	C(3)-C(4)-C(5)	119.3(7)
C(5)-C(6)	1.465(10)	N(1)-C(5)-C(4)	122.3(7)
C(7)-C(14)	1.455(9)	N(1)-C(5)-C(6)	112.8(6)
C(8)-C(9)	1.468(9)	C(4)-C(5)-C(6)	124.9(7)
C(9)-C(10)	1.366(10)	N(4)-C(6)-N(2)	124.7(6)
C(10)-C(11)	1.415(10)	N(4)-C(6)-C(5)	124.2(7)
C(11)-C(12)	1.362(11)	N(2)-C(6)-C(5)	111.1(6)
C(12)-C(13)	1.408(10)	N(4)-C(7)-N(5)	124.5(6)
C(14)-C(15)	1.386(10)	N(4)-C(7)-C(14)	117.5(6)
C(14)-C(19)	1.394(11)	N(5)-C(7)-C(14)	118.0(6)
C(15)-C(16)	1.393(10)	N(5)-C(8)-N(2)	124.0(6)
C(16)-C(17)	1.318(12)	N(5)-C(8)-C(9)	125.1(6)
C(17)-C(18)	1.403(12)	N(2)-C(8)-C(9)	110.9(5)
C(17)-Br(1)	1.906(7)	N(3)-C(9)-C(10)	122.9(7)
C(18)-C(19)	1.374(10)	N(3)-C(9)-C(8)	113.2(6)
P(1)-F(15)	1.61(4)	C(10)-C(9)-C(8)	123.8(6)
P(1)-F(13)	1.63(2)	C(9)-C(10)-C(11)	119.1(7)
P(1)-F(11)	1.65(2)	C(12)-C(11)-C(10)	117.9(7)
P(1)-F(14)	1.65(2)	C(11)-C(12)-C(13)	120.5(7)
P(1)-F(16)	1.69(3)	N(3)-C(13)-C(12)	121.1(7)
P(1)-F(12)	1.70(3)	C(15)-C(14)-C(19)	119.9(7)
P(11)-F(116)	1.41(3)	C(15)-C(14)-C(7)	120.9(7)
P(11)-F(114)	1.52(3)	C(19)-C(14)-C(7)	119.1(7)
P(11)-F(115)	1.53(4)	C(14)-C(15)-C(16)	119.3(8)
P(11)-F(113)	1.53(2)	C(17)-C(16)-C(15)	120.4(8)
P(11)-F(111)	1.54(2)	C(16)-C(17)-C(18)	121.7(7)
P(11)-F(112)	1.56(3)	C(16)-C(17)-BR1	120.7(7)
F(113)-F(116)	1.78(6)	C(18)-C(17)-BR1	117.6(6)
N(2)-FE-N(2)#1	178.6(3)	C(19)-C(18)-C(17)	119.1(8)
N(2)-FE-N(3)	79.8(2)	C(18)-C(19)-C(14)	119.4(8)
N(2)#1-FE-N(3)	101.2(2)	F(15)-P(1)-F(13)	166.90(13)
N(2)-FE-N(3)#1	101.2(2)	F(15)-P(1)-F(11)	86.70(15)
N(2)#1-FE-N(3)#1	79.8(2)	F(13)-P(1)-F(11)	86.3(1)
N(3)-FE-N(3)#1	89.7(3)	F(15)-P(1)-F(14)	85.00(12)
N(2)-FE-N(1)	79.3(2)	F(13)-P(1)-F(14)	83.3(9)
N(2)#1-FE-N(1)	99.7(2)	F(11)-P(1)-F(14)	85.10(13)
N(3)-FE-N(1)	159.0(2)	F(15)-P(1)-F(16)	87.10(16)
N(3)#1-FE-N(1)	93.4(3)	F(13)-P(1)-F(16)	98.70(13)

F(11)-P(1)-F(16)	172.10(15)	F(115)-P(11)-F(113)	167(3)
F(14)-P(1)-F(16)	89.30(12)	F(116)-P(11)-F(111)	162(3)
F(15)-P(1)-F(12)	102.30(14)	F(114)-P(11)-F(111)	98.70(18)
F(13)-P(1)-F(12)	88.00(13)	F(115)-P(11)-F(111)	91.50(17)
F(11)-P(1)-F(12)	84.10(13)	F(113)-P(11)-F(111)	91.80(12)
F(14)-P(1)-F(12)	166.60(17)	F(116)-P(11)-F(112)	80.20(19)
F(16)-P(1)-F(12)	102.10(15)	F(114)-P(11)-F(112)	170.60(18)
F(116)-P(11)-F(114)	92.60(19)	F(115)-P(11)-F(112)	74.90(19)
F(116)-P(11)-F(115)	100(2)	F(113)-P(11)-F(112)	92.20(13)
F(114)-P(11)-F(115)	100.50(19)	F(111)-P(11)-F(112)	89.80(13)
F(116)-P(11)-F(113)	74(3)	P(11)-F(113)-F(116)	49.70(14)
F(114)-P(11)-F(113)	91.80(16)	P(11)-F(116)-F(113)	56(2)

Table 1. Crystal data and structure refinement for **1c, chapter V, Part B.**

Empirical formula	C40 H27 Br2 F12 N11 Ni P2
Formula weight	1170.20
Temperature	100(2)K
Wavelength	1.54178 Å
Crystal system	Triclinic
Space group	P-1
Unit cell dimensions	a = 8.5536(2) Å α = 91.0860(10)° b = 13.6850(2) Å β = 102.3480(10)° c = 18.9796(3) Å γ = 91.9730(10)°
Volume	2168.21(7)Å^3
Z	2
Density (calculated)	1.792 g/cm^3
Absorption coefficient	4.392 mm^{-1}
F(000)	1160
Crystal size	0.22 x 0.09 x 0.09 mm
Theta range for data collection	2.38 to 73.11°
Index ranges	$-8 \le h \le 9$, $-16 \le k \le 16$, $-23 \le \ell \le 23$
Reflections collected	26398
Independent reflections	8310 [R_{int} = 0.052]
Absorption correction	Semi-empirical from equivalents
Max. and min. transmission	0.7800 and 0.7700
Refinement method	Full-matrix least-squares on F^2
Data / restraints / parameters	8310 / 2 / 663
Goodness-of-fit on F^2	0.916
Final R indices [I>2sigma(I)]	R_1 = 0.0533, wR_2 = 0.1220
R indices (all data)	R_1 = 0.0899, wR_2 = 0.1343
Largest diff. peak and hole	1.279 and -0.662 e/Å^3

Table 2. Bond lengths [Å] and angles [°] for **1c, chapter V, Part B.**

Ni-N(2)	1.979(3)	C(36)-C(37)	1.403(7)
Ni-N(7)	1.990(4)	C(37)-C(38)	1.382(7)
Ni-N(1)	2.146(4)	C(37)-Br(2)	1.891(4)
Ni-N(3)	2.153(4)	C(38)-C(39)	1.388(6)
Ni-N(6)	2.157(4)	P(1)-F(12)	1.567(7)
Ni-N(8)	2.164(4)	P(1)-F(14)	1.586(7)
N(1)-C(1)	1.330(5)	P(1)-F(13)	1.611(6)
N(1)-C(5)	1.366(5)	P(1)-F(11)	1.621(7)
N(2)-C(8)	1.328(5)	P(1)-F(15)	1.712(5)
N(2)-C(6)	1.352(5)	P(2)-F(25)	1.582(3)
N(3)-C(13)	1.336(5)	P(2)-F(24)	1.590(3)
N(3)-C(9)	1.353(5)	P(2)-F(21)	1.596(3)
N(5)-C(8)	1.310(5)	P(2)-F(26)	1.604(3)
N(5)-C(7)	1.371(6)	P(2)-F(22)	1.604(3)
N(4)-C(6)	1.321(5)	P(2)-F(23)	1.616(3)
N(4)-C(7)	1.344(6)	P(3)-F(32)	1.587(4)
N(6)-C(21)	1.342(5)	P(3)-F(32)#1	1.587(4)
N(6)-C(25)	1.359(5)	P(3)-F(31)	1.595(3)
N(7)-C(26)	1.333(5)	P(3)-F(31)#1	1.595(3)
N(7)-C(28)	1.336(5)	P(3)-F(33)	1.607(3)
N(8)-C(33)	1.328(5)	P(3)-F(33)#1	1.607(3)
N(8)-C(29)	1.363(5)	C(41)-C(42)	1.105(14)
N(10)-C(28)	1.325(5)	C(42)-N(43)	1.247(13)
N(10)-C(27)	1.342(6)	N(43)-C(42)#2	1.247(13)
N(9)-C(26)	1.320(5)	C(51)-C(52)	1.418(12)
N(9)-C(27)	1.360(6)	C(52)-N(53)	1.161(13)
C(1)-C(2)	1.391(6)	N(2)-NI-N(7)	178.72(16)
C(2)-C(3)	1.379(6)	N(2)-NI-N(1)	76.97(14)
C(3)-C(4)	1.374(6)	N(7)-NI-N(1)	103.82(14)
C(4)-C(5)	1.388(6)	N(2)-NI-N(3)	75.96(14)
C(5)-C(6)	1.470(6)	N(7)-NI-N(3)	103.30(15)
C(7)-C(14)	1.462(6)	N(1)-NI-N(3)	152.79(14)
C(8)-C(9)	1.488(6)	N(2)-NI-N(6)	102.24(15)
C(9)-C(10)	1.381(6)	N(7)-NI-N(6)	76.75(14)
C(10)-C(11)	1.406(6)	N(1)-NI-N(6)	92.53(13)
C(11)-C(12)	1.383(7)	N(3)-NI-N(6)	95.84(14)
C(12)-C(13)	1.381(6)	N(2)-NI-N(8)	104.98(15)
C(14)-C(19)	1.385(6)	N(7)-NI-N(8)	76.02(14)
C(14)-C(15)	1.408(6)	N(1)-NI-N(8)	94.40(14)
C(15)-C(16)	1.375(6)	N(3)-NI-N(8)	89.91(14)
C(16)-C(17)	1.366(7)	N(6)-NI-N(8)	152.76(13)
C(17)-C(18)	1.389(7)	C(1)-N(1)-C(5)	118.6(4)
C(17)-Br(1)	1.895(5)	C(1)-N(1)-NI	127.7(3)
C(18)-C(19)	1.371(6)	C(5)-N(1)-NI	113.7(3)
C(21)-C(22)	1.373(6)	C(8)-N(2)-C(6)	116.0(4)
C(22)-C(23)	1.401(6)	C(8)-N(2)-NI	122.8(3)
C(23)-C(24)	1.392(6)	C(6)-N(2)-NI	121.2(3)
C(24)-C(25)	1.367(6)	C(13)-N(3)-C(9)	117.2(4)
C(25)-C(26)	1.482(6)	C(13)-N(3)-NI	128.0(3)
C(27)-C(34)	1.470(5)	C(9)-N(3)-NI	114.5(3)
C(28)-C(29)	1.482(6)	C(8)-N(5)-C(7)	115.1(4)
C(29)-C(30)	1.386(6)	C(6)-N(4)-C(7)	115.3(4)
C(30)-C(31)	1.378(6)	C(21)-N(6)-C(25)	117.0(4)
C(31)-C(32)	1.381(6)	C(21)-N(6)-NI	128.7(3)
C(32)-C(33)	1.398(6)	C(25)-N(6)-NI	114.2(3)
C(34)-C(35)	1.390(6)	C(26)-N(7)-C(28)	116.7(4)
C(34)-C(39)	1.403(6)	C(26)-N(7)-NI	120.8(3)
C(35)-C(36)	1.381(6)	C(28)-N(7)-NI	122.4(3)

C(33)-N(8)-C(29)	117.3(4)	C(31)-C(30)-C(29)	118.6(4)
C(33)-N(8)-NI	128.3(3)	C(30)-C(31)-C(32)	119.4(5)
C(29)-N(8)-NI	114.4(3)	C(31)-C(32)-C(33)	118.6(4)
C(28)-N(10)-C(27)	114.6(4)	N(8)-C(33)-C(32)	123.1(4)
C(26)-N(9)-C(27)	114.5(4)	C(35)-C(34)-C(39)	120.0(4)
N(1)-C(1)-C(2)	122.3(4)	C(35)-C(34)-C(27)	119.8(4)
C(3)-C(2)-C(1)	119.0(4)	C(39)-C(34)-C(27)	120.2(4)
C(4)-C(3)-C(2)	119.5(4)	C(36)-C(35)-C(34)	120.4(5)
C(3)-C(4)-C(5)	118.9(4)	C(35)-C(36)-C(37)	119.0(5)
N(1)-C(5)-C(4)	121.7(4)	C(38)-C(37)-C(36)	121.4(4)
N(1)-C(5)-C(6)	114.7(4)	C(38)-C(37)-BR2	120.2(4)
C(4)-C(5)-C(6)	123.5(4)	C(36)-C(37)-BR2	118.4(4)
N(4)-C(6)-N(2)	124.4(4)	C(37)-C(38)-C(39)	119.2(5)
N(4)-C(6)-C(5)	122.5(4)	C(38)-C(39)-C(34)	120.0(5)
N(2)-C(6)-C(5)	113.0(4)	F(12)-P(1)-F(14)	92.6(4)
N(4)-C(7)-N(5)	124.1(4)	F(12)-P(1)-F(13)	86.9(4)
N(4)-C(7)-C(14)	119.0(4)	F(14)-P(1)-F(13)	178.6(4)
N(5)-C(7)-C(14)	116.9(4)	F(12)-P(1)-F(11)	87.7(4)
N(5)-C(8)-N(2)	125.1(4)	F(14)-P(1)-F(11)	89.2(4)
N(5)-C(8)-C(9)	122.5(4)	F(13)-P(1)-F(11)	89.5(4)
N(2)-C(8)-C(9)	112.4(4)	F(12)-P(1)-F(15)	101.6(3)
N(3)-C(9)-C(10)	124.2(4)	F(14)-P(1)-F(15)	90.0(3)
N(3)-C(9)-C(8)	114.0(4)	F(13)-P(1)-F(15)	91.4(3)
C(10)-C(9)-C(8)	121.8(4)	F(11)-P(1)-F(15)	170.6(4)
C(9)-C(10)-C(11)	118.1(5)	F(25)-P(2)-F(24)	91.7(2)
C(12)-C(11)-C(10)	117.2(5)	F(25)-P(2)-F(21)	91.35(18)
C(13)-C(12)-C(11)	121.1(4)	F(24)-P(2)-F(21)	90.68(19)
N(3)-C(13)-C(12)	122.2(4)	F(25)-P(2)-F(26)	90.34(19)
C(19)-C(14)-C(15)	118.6(4)	F(24)-P(2)-F(26)	90.66(19)
C(19)-C(14)-C(7)	121.3(5)	F(21)-P(2)-F(26)	177.81(19)
C(15)-C(14)-C(7)	120.0(4)	F(25)-P(2)-F(22)	89.79(18)
C(16)-C(15)-C(14)	119.9(5)	F(24)-P(2)-F(22)	178.5(2)
C(17)-C(16)-C(15)	120.1(5)	F(21)-P(2)-F(22)	89.49(17)
C(16)-C(17)-C(18)	121.3(5)	F(26)-P(2)-F(22)	89.12(17)
C(16)-C(17)-BR1	119.8(4)	F(25)-P(2)-F(23)	178.93(18)
C(18)-C(17)-BR1	119.0(4)	F(24)-P(2)-F(23)	89.34(18)
C(19)-C(18)-C(17)	118.7(5)	F(21)-P(2)-F(23)	88.76(16)
C(18)-C(19)-C(14)	121.5(5)	F(26)-P(2)-F(23)	89.52(17)
N(6)-C(21)-C(22)	122.9(4)	F(22)-P(2)-F(23)	89.15(15)
C(21)-C(22)-C(23)	119.3(4)	F(32)-P(3)-F(32)#1	179.997(1)
C(24)-C(23)-C(22)	118.3(4)	F(32)-P(3)-F(31)	90.54(18)
C(25)-C(24)-C(23)	118.3(4)	F(32)#1-P(3)-F(31)	89.46(18)
N(6)-C(25)-C(24)	124.1(4)	F(32)-P(3)-F(31)#1	89.46(18)
N(6)-C(25)-C(26)	113.7(4)	F(32)#1-P(3)-F(31)#1	90.54(18)
C(24)-C(25)-C(26)	122.2(4)	F(31)-P(3)-F(31)#1	180.0(2)
N(9)-C(26)-N(7)	124.3(4)	F(32)-P(3)-F(33)	89.3(2)
N(9)-C(26)-C(25)	121.4(4)	F(32)#1-P(3)-F(33)	90.7(2)
N(7)-C(26)-C(25)	114.3(4)	F(31)-P(3)-F(33)	89.48(16)
N(10)-C(27)-N(9)	125.3(4)	F(31)#1-P(3)-F(33)	90.52(16)
N(10)-C(27)-C(34)	118.6(4)	F(32)-P(3)-F(33)#1	90.7(2)
N(9)-C(27)-C(34)	116.1(4)	F(32)#1-P(3)-F(33)#1	89.3(2)
N(10)-C(28)-N(7)	124.4(4)	F(31)-P(3)-F(33)#1	90.52(16)
N(10)-C(28)-C(29)	122.7(4)	F(31)#1-P(3)-F(33)#1	89.48(16)
N(7)-C(28)-C(29)	112.9(4)	F(33)-P(3)-F(33)#1	179.997(1)
N(8)-C(29)-C(30)	123.0(4)	C(41)-C(42)-N(43)	171.50(12)
N(8)-C(29)-C(28)	114.2(4)	C(42)-N(43)-C(42)#2	180.0(8)
C(30)-C(29)-C(28)	122.8(4)	N(53)-C(52)-C(51)	176.20(19)

Table 1. Crystal data and structure refinement for **1d, Chapter V, Part B.**

Identification code	gary71
Empirical formula	C40 H27 Br2 Cu F12 N11 P2
Formula weight	1175.03
Temperature	100(2)K
Wavelength	1.54178 Å
Crystal system	Triclinic
Space group	P-1
Unit cell dimensions	a = 8.5175(2) Å α = 89.9110(10)° b = 13.7974(3) Å β = 78.4970(10)° c = 18.9148(4) Å γ = 87.8530(10)°
Volume	2176.64(8)Å^3
Z	2
Density (calculated)	1.793 Mg/m^3
Absorption coefficient	4.440 mm^{-1}
F(000)	1162
Crystal size	0.24 x 0.13 x 0.04 mm
Theta range for data collection	2.38 to 67.94°
Index ranges	$-9 \le h \le 10$, $-16 \le k \le 16$, $-22 \le \ell \le 22$
Reflections collected	27217
Independent reflections	7620 [R_{int} = 0.029]
Absorption correction	Semi-empirical from equivalents
Max. and min. transmission	0.8800 and 0.6100
Refinement method	Full-matrix least-squares on F^2
Data / restraints / parameters	7620 / 144 / 790
Goodness-of-fit on F^2	1.023
Final R indices [I>2sigma(I)]	R_1 = 0.0327, wR_2 = 0.0843
R indices (all data)	R_1 = 0.0369, wR_2 = 0.0867
Largest diff. peak and hole	1.472 and -0.714 e/Å^3

Table 2. Bond lengths [Å] and angles [°] for **1d, Chapter V, Part B.**

Cu-N(2)	1.942(2)	C(34)-C(39)	1.396(4)
Cu-N(7)	1.9995(19)	C(35)-C(36)	1.389(4)
Cu-N(5)	2.149(2)	C(36)-C(37)	1.379(4)
Cu-N(1)	2.152(2)	C(37)-C(38)	1.386(4)
Cu-N(6)	2.283(2)	C(37)-Br(2)	1.904(2)
Cu-N(10)	2.320(2)	C(38)-C(39)	1.391(4)
N(1)-C(1)	1.338(3)	P(1)-F(112)	1.54(3)
N(1)-C(5)	1.355(3)	P(1)-F(114)	1.544(15)
N(2)-C(6)	1.339(3)	P(1)-F(111)	1.554(16)
N(2)-C(8)	1.343(3)	P(1)-F(15)	1.558(15)
N(3)-C(6)	1.320(3)	P(1)-F(113)	1.58(3)
N(3)-C(7)	1.354(3)	P(1)-F(116)	1.60(2)
N(4)-C(8)	1.320(3)	P(1)-F(16)	1.61(2)
N(4)-C(7)	1.348(3)	P(1)-F(13)	1.62(3)
N(5)-C(13)	1.333(3)	P(1)-F(14)	1.625(15)
N(5)-C(9)	1.354(3)	P(1)-F(115)	1.647(13)
N(6)-C(21)	1.338(3)	P(1)-F(11)	1.668(16)
N(6)-C(25)	1.347(3)	P(1)-F(12)	1.70(2)
N(7)-C(28)	1.346(3)	F(11)-P(11)	1.667(17)
N(7)-C(26)	1.346(3)	F(12)-P(11)	1.68(2)
N(8)-C(26)	1.318(3)	F(13)-P(11)	1.63(3)
N(8)-C(27)	1.344(3)	F(14)-P(11)	1.653(16)
N(9)-C(28)	1.322(3)	F(15)-P(11)	1.550(15)
N(9)-C(27)	1.351(3)	F(16)-P(11)	1.61(2)
N(10)-C(33)	1.340(3)	P(11)-F(112)	1.51(3)
N(10)-C(29)	1.346(3)	P(11)-F(111)	1.556(17)
C(1)-C(2)	1.386(4)	P(11)-F(114)	1.570(16)
C(2)-C(3)	1.377(4)	P(11)-F(113)	1.59(3)
C(3)-C(4)	1.393(4)	P(11)-F(116)	1.60(2)
C(4)-C(5)	1.373(4)	P(11)-F(115)	1.633(15)
C(5)-C(6)	1.478(3)	P(2)-P(21)#1	0.20(4)
C(7)-C(14)	1.465(3)	P(2)-F(213)#1	1.531(18)
C(8)-C(9)	1.477(4)	P(2)-F(213)	1.531(18)
C(9)-C(10)	1.379(4)	P(2)-F(211)	1.56(2)
C(10)-C(11)	1.385(4)	P(2)-F(211)#1	1.56(2)
C(11)-C(12)	1.378(4)	P(2)-F(22)	1.600(17)
C(12)-C(13)	1.391(4)	P(2)-F(22)#1	1.600(16)
C(14)-C(15)	1.383(4)	P(2)-F(212)	1.606(16)
C(14)-C(19)	1.389(4)	P(2)-F(212)#1	1.606(16)
C(15)-C(16)	1.379(4)	P(2)-F(23)#1	1.649(19)
C(16)-C(17)	1.373(4)	P(2)-F(23)	1.649(19)
C(17)-C(18)	1.373(4)	P(2)-F(21)	1.65(2)
C(17)-Br(1)	1.901(2)	F(21)-P(21)	1.47(5)
C(18)-C(19)	1.386(4)	F(21)-P(21)#1	1.84(4)
C(21)-C(22)	1.387(4)	F(22)-P(21)#1	1.54(5)
C(22)-C(23)	1.380(4)	F(22)-P(21)	1.68(5)
C(23)-C(24)	1.391(4)	F(23)-P(21)#1	1.59(6)
C(24)-C(25)	1.379(3)	F(23)-P(21)	1.73(6)
C(25)-C(26)	1.481(3)	P(3)-F(34)	1.586(7)
C(27)-C(34)	1.468(3)	P(3)-F(33)	1.592(8)
C(28)-C(29)	1.484(3)	P(3)-F(31)	1.611(5)
C(29)-C(30)	1.381(3)	P(3)-F(32)	1.612(4)
C(30)-C(31)	1.386(4)	P(3)-F(35)	1.785(4)
C(31)-C(32)	1.383(4)	N(43)-C(42)#2	1.278(7)
C(32)-C(33)	1.382(4)	N(43)-C(42)	1.278(7)
C(34)-C(35)	1.392(4)	C(42)-C(41)	1.123(8)

C(51)-C(52)	1.42(3)	N(2)-C(6)-C(5)	113.7(2)
C(52)-N(53)	1.07(2)	N(4)-C(7)-N(3)	124.8(2)
C(61)-C(62)	1.446(16)	N(4)-C(7)-C(14)	118.0(2)
C(62)-N(63)	1.113(18)	N(3)-C(7)-C(14)	117.2(2)
P(21)-P(21)#1	0.40(8)	N(4)-C(8)-N(2)	124.0(2)
P(21)-F(211)	1.38(5)	N(4)-C(8)-C(9)	122.5(2)
P(21)-F(213)#1	1.52(6)	N(2)-C(8)-C(9)	113.5(2)
P(21)-F(22)#1	1.54(5)	N(5)-C(9)-C(10)	123.1(2)
P(21)-F(213)	1.57(6)	N(5)-C(9)-C(8)	113.6(2)
P(21)-F(212)#1	1.58(5)	C(10)-C(9)-C(8)	123.3(2)
P(21)-F(23)#1	1.59(6)	C(9)-C(10)-C(11)	118.3(2)
P(21)-F(212)	1.65(5)	C(12)-C(11)-C(10)	119.1(2)
P(21)-F(211)#1	1.74(5)	C(11)-C(12)-C(13)	119.3(3)
F(211)-P(21)#1	1.74(5)	N(5)-C(13)-C(12)	122.1(2)
F(212)-P(21)#1	1.58(5)	C(15)-C(14)-C(19)	118.8(2)
F(213)-P(21)#1	1.52(6)	C(15)-C(14)-C(7)	120.4(3)
N(2)-CU-N(7)	177.57(8)	C(19)-C(14)-C(7)	120.8(3)
N(2)-CU-N(5)	77.10(8)	C(16)-C(15)-C(14)	121.2(3)
N(7)-CU-N(5)	102.94(8)	C(17)-C(16)-C(15)	118.8(3)
N(2)-CU-N(1)	77.21(8)	C(16)-C(17)-C(18)	121.6(2)
N(7)-CU-N(1)	102.93(8)	C(16)-C(17)-BR1	119.1(2)
N(5)-CU-N(1)	153.88(8)	C(18)-C(17)-BR1	119.3(2)
N(2)-CU-N(6)	101.78(8)	C(17)-C(18)-C(19)	119.1(3)
N(7)-CU-N(6)	75.79(7)	C(18)-C(19)-C(14)	120.5(3)
N(5)-CU-N(6)	92.04(7)	N(6)-C(21)-C(22)	122.6(2)
N(1)-CU-N(6)	97.71(7)	C(23)-C(22)-C(21)	119.3(2)
N(2)-CU-N(10)	108.07(8)	C(22)-C(23)-C(24)	119.0(2)
N(7)-CU-N(10)	74.36(7)	C(25)-C(24)-C(23)	117.7(2)
N(5)-CU-N(10)	94.91(7)	N(6)-C(25)-C(24)	124.0(2)
N(1)-CU-N(10)	88.60(7)	N(6)-C(25)-C(26)	114.7(2)
N(6)-CU-N(10)	150.14(7)	C(24)-C(25)-C(26)	121.3(2)
C(1)-N(1)-C(5)	117.8(2)	N(8)-C(26)-N(7)	124.1(2)
C(1)-N(1)-CU	128.41(17)	N(8)-C(26)-C(25)	119.7(2)
C(5)-N(1)-CU	113.68(15)	N(7)-C(26)-C(25)	116.2(2)
C(6)-N(2)-C(8)	116.8(2)	N(8)-C(27)-N(9)	124.4(2)
C(6)-N(2)-CU	121.66(16)	N(8)-C(27)-C(34)	117.1(2)
C(8)-N(2)-CU	121.58(17)	N(9)-C(27)-C(34)	118.5(2)
C(6)-N(3)-C(7)	115.2(2)	N(9)-C(28)-N(7)	124.4(2)
C(8)-N(4)-C(7)	115.2(2)	N(9)-C(28)-C(29)	120.1(2)
C(13)-N(5)-C(9)	118.1(2)	N(7)-C(28)-C(29)	115.5(2)
C(13)-N(5)-CU	128.14(16)	N(10)-C(29)-C(30)	123.5(2)
C(9)-N(5)-CU	113.70(16)	N(10)-C(29)-C(28)	114.5(2)
C(21)-N(6)-C(25)	117.4(2)	C(30)-C(29)-C(28)	122.0(2)
C(21)-N(6)-CU	130.28(16)	C(29)-C(30)-C(31)	118.4(2)
C(25)-N(6)-CU	111.94(15)	C(32)-C(31)-C(30)	118.7(2)
C(28)-N(7)-C(26)	115.92(19)	C(33)-C(32)-C(31)	119.3(2)
C(28)-N(7)-CU	123.07(15)	N(10)-C(33)-C(32)	122.7(2)
C(26)-N(7)-CU	120.99(16)	C(35)-C(34)-C(39)	120.0(2)
C(26)-N(8)-C(27)	115.8(2)	C(35)-C(34)-C(27)	119.4(2)
C(28)-N(9)-C(27)	115.3(2)	C(39)-C(34)-C(27)	120.6(2)
C(33)-N(10)-C(29)	117.4(2)	C(36)-C(35)-C(34)	120.2(3)
C(33)-N(10)-CU	130.20(17)	C(37)-C(36)-C(35)	118.9(3)
C(29)-N(10)-CU	112.38(15)	C(36)-C(37)-C(38)	122.3(2)
N(1)-C(1)-C(2)	122.2(2)	C(36)-C(37)-BR2	118.7(2)
C(3)-C(2)-C(1)	119.6(2)	C(38)-C(37)-BR2	119.0(2)
C(2)-C(3)-C(4)	118.8(3)	C(37)-C(38)-C(39)	118.6(3)
C(5)-C(4)-C(3)	118.3(2)	C(38)-C(39)-C(34)	120.1(3)
N(1)-C(5)-C(4)	123.4(2)	F(112)-P(1)-F(114)	167.6(1)
N(1)-C(5)-C(6)	113.6(2)	F(112)-P(1)-F(111)	90.90(11)
C(4)-C(5)-C(6)	123.0(2)	F(114)-P(1)-F(111)	79.2(7)
N(3)-C(6)-N(2)	124.0(2)	F(112)-P(1)-F(15)	92.70(11)
N(3)-C(6)-C(5)	122.3(2)	F(114)-P(1)-F(15)	80.4(7)

F(111)-P(1)-F(15)	91.8(7)	P(11)-F(12)-P(1)	0.4(4)
F(112)-P(1)-F(113)	95.10(13)	P(1)-F(13)-P(11)	1.0(5)
F(114)-P(1)-F(113)	93.6(1)	P(1)-F(14)-P(11)	0.3(4)
F(111)-P(1)-F(113)	98.1(1)	P(11)-F(15)-P(1)	1.0(5)
F(15)-P(1)-F(113)	167.2(7)	P(11)-F(16)-P(1)	1.0(5)
F(112)-P(1)-F(116)	94.90(13)	F(112)-P(11)-F(15)	94.10(12)
F(114)-P(1)-F(116)	93.8(1)	F(112)-P(11)-F(111)	91.80(11)
F(111)-P(1)-F(116)	168.8(7)	F(15)-P(11)-F(111)	92.1(8)
F(15)-P(1)-F(116)	78.4(7)	F(112)-P(11)-F(114)	168.10(11)
F(113)-P(1)-F(116)	90.9(9)	F(15)-P(11)-F(114)	79.9(8)
F(112)-P(1)-F(16)	90.00(13)	F(111)-P(11)-F(114)	78.3(8)
F(114)-P(1)-F(16)	100.2(9)	F(112)-P(11)-F(113)	95.60(13)
F(111)-P(1)-F(16)	178.2(1)	F(15)-P(11)-F(113)	166.1(8)
F(15)-P(1)-F(16)	89.7(7)	F(111)-P(11)-F(113)	97.5(1)
F(113)-P(1)-F(16)	80.2(1)	F(114)-P(11)-F(113)	92.1(1)
F(116)-P(1)-F(16)	12.2(9)	F(112)-P(11)-F(116)	96.00(13)
F(112)-P(1)-F(13)	88.30(12)	F(15)-P(11)-F(116)	78.6(8)
F(114)-P(1)-F(13)	98.8(1)	F(111)-P(11)-F(116)	168.2(8)
F(111)-P(1)-F(13)	89.4(9)	F(114)-P(11)-F(116)	92.9(1)
F(15)-P(1)-F(13)	178.4(7)	F(113)-P(11)-F(116)	90.5(1)
F(113)-P(1)-F(13)	11.20(11)	F(112)-P(11)-F(16)	91.00(13)
F(116)-P(1)-F(13)	100.3(9)	F(15)-P(11)-F(16)	90.0(8)
F(16)-P(1)-F(13)	89.1(9)	F(111)-P(11)-F(16)	176.40(12)
F(112)-P(1)-F(14)	176.5(1)	F(114)-P(11)-F(16)	99.2(1)
F(114)-P(1)-F(14)	15.6(6)	F(113)-P(11)-F(16)	79.9(1)
F(111)-P(1)-F(14)	90.8(8)	F(116)-P(11)-F(16)	12.2(9)
F(15)-P(1)-F(14)	90.3(7)	F(112)-P(11)-F(13)	88.90(13)
F(113)-P(1)-F(14)	81.6(9)	F(15)-P(11)-F(13)	176.8(9)
F(116)-P(1)-F(14)	83.9(1)	F(111)-P(11)-F(13)	89.0(9)
F(16)-P(1)-F(14)	88.3(1)	F(114)-P(11)-F(13)	97.3(1)
F(13)-P(1)-F(14)	88.6(9)	F(113)-P(11)-F(13)	11.10(11)
F(112)-P(1)-F(115)	80.10(11)	F(116)-P(11)-F(13)	100.0(1)
F(114)-P(1)-F(115)	91.1(7)	F(16)-P(11)-F(13)	88.8(1)
F(111)-P(1)-F(115)	81.2(7)	F(112)-P(11)-F(115)	81.30(11)
F(15)-P(1)-F(115)	16.7(5)	F(15)-P(11)-F(115)	16.8(5)
F(113)-P(1)-F(115)	175.1(9)	F(111)-P(11)-F(115)	81.6(8)
F(116)-P(1)-F(115)	90.3(8)	F(114)-P(11)-F(115)	90.7(7)
F(16)-P(1)-F(115)	100.5(8)	F(113)-P(11)-F(115)	176.8(9)
F(13)-P(1)-F(115)	164.9(7)	F(116)-P(11)-F(115)	90.8(8)
F(14)-P(1)-F(115)	103.2(7)	F(16)-P(11)-F(115)	101.1(9)
F(112)-P(1)-F(11)	80.80(11)	F(13)-P(11)-F(115)	166.1(8)
F(114)-P(1)-F(11)	90.4(7)	F(112)-P(11)-F(14)	175.90(11)
F(111)-P(1)-F(11)	13.5(6)	F(15)-P(11)-F(14)	89.6(7)
F(15)-P(1)-F(11)	101.2(7)	F(111)-P(11)-F(14)	89.8(8)
F(113)-P(1)-F(11)	90.1(9)	F(114)-P(11)-F(14)	15.4(6)
F(116)-P(1)-F(11)	175.60(11)	F(113)-P(11)-F(14)	80.4(1)
F(16)-P(1)-F(11)	166.0(7)	F(116)-P(11)-F(14)	83.1(1)
F(13)-P(1)-F(11)	80.2(8)	F(16)-P(11)-F(14)	87.4(1)
F(14)-P(1)-F(11)	100.4(8)	F(13)-P(11)-F(14)	87.4(1)
F(115)-P(1)-F(11)	88.3(7)	F(115)-P(11)-F(14)	102.6(7)
F(112)-P(1)-F(12)	8.40(16)	F(112)-P(11)-F(11)	81.60(11)
F(114)-P(1)-F(12)	175.8(9)	F(15)-P(11)-F(11)	101.5(7)
F(111)-P(1)-F(12)	98.1(1)	F(111)-P(11)-F(11)	13.5(6)
F(15)-P(1)-F(12)	96.6(1)	F(114)-P(11)-F(11)	89.6(8)
F(113)-P(1)-F(12)	90.00(12)	F(113)-P(11)-F(11)	89.7(9)
F(116)-P(1)-F(12)	88.40(12)	F(116)-P(11)-F(11)	177.60(11)
F(16)-P(1)-F(12)	82.60(11)	F(16)-P(11)-F(11)	166.6(8)
F(13)-P(1)-F(12)	84.30(12)	F(13)-P(11)-F(11)	80.0(9)
F(14)-P(1)-F(12)	168.5(9)	F(115)-P(11)-F(11)	88.8(7)
F(115)-P(1)-F(12)	85.3(9)	F(14)-P(11)-F(11)	99.3(8)
F(11)-P(1)-F(12)	87.4(1)	F(112)-P(11)-F(12)	8.50(16)
P(11)-F(11)-P(1)	1.0(5)	F(15)-P(11)-F(12)	98.0(1)

F(111)-P(11)-F(12)	99.2(1)
F(114)-P(11)-F(12)	176.6(1)
F(113)-P(11)-F(12)	90.50(12)
F(116)-P(11)-F(12)	89.30(12)
F(16)-P(11)-F(12)	83.40(12)
F(13)-P(11)-F(12)	84.90(12)
F(115)-P(11)-F(12)	86.6(1)
F(14)-P(11)-F(12)	168.1(1)
F(11)-P(11)-F(12)	88.2(1)
P(1)-F(111)-P(11)	1.0(5)
P(11)-F(112)-P(1)	0.4(5)
P(1)-F(113)-P(11)	0.9(5)
P(1)-F(114)-P(11)	0.5(5)
P(11)-F(115)-P(1)	0.9(5)
P(11)-F(116)-P(1)	1.0(5)
P(21)#1-P(2)-F(213)#1	98(10)
P(21)#1-P(2)-F(213)	82(10)
F(213)#1-P(2)-F(213)	180.00(17)
P(21)#1-P(2)-F(211)	153(10)
F(213)#1-P(2)-F(211)	104.1(9)
F(213)-P(2)-F(211)	75.9(9)
P(21)#1-P(2)-F(211)#1	27(10)
F(213)#1-P(2)-F(211)#1	75.9(9)
F(213)-P(2)-F(211)#1	104.1(9)
F(211)-P(2)-F(211)#1	180.00(16)
P(21)#1-P(2)-F(22)	69(10)
F(213)#1-P(2)-F(22)	96.3(8)
F(213)-P(2)-F(22)	83.7(8)
F(211)-P(2)-F(22)	92.7(1)
F(211)#1-P(2)-F(22)	87.3(1)
P(21)#1-P(2)-F(22)#1	111(10)
F(213)#1-P(2)-F(22)#1	83.7(8)
F(213)-P(2)-F(22)#1	96.3(8)
F(211)-P(2)-F(22)#1	87.3(1)
F(211)#1-P(2)-F(22)#1	92.7(1)
F(22)-P(2)-F(22)#1	180.00(11)
P(21)#1-P(2)-F(212)	80(10)
F(213)#1-P(2)-F(212)	84.0(7)
F(213)-P(2)-F(212)	96.0(7)
F(211)-P(2)-F(212)	87.4(1)
F(211)#1-P(2)-F(212)	92.6(1)
F(22)-P(2)-F(212)	15.0(7)
F(22)#1-P(2)-F(212)	165.0(7)
P(21)#1-P(2)-F(212)#1	100(10)
F(213)#1-P(2)-F(212)#1	96.0(7)
F(213)-P(2)-F(212)#1	84.0(7)
F(211)-P(2)-F(212)#1	92.6(1)
F(211)#1-P(2)-F(212)#1	87.4(1)
F(22)-P(2)-F(212)#1	165.0(7)
F(22)#1-P(2)-F(212)#1	15.0(7)
F(212)-P(2)-F(212)#1	180.0(9)
P(21)#1-P(2)-F(23)#1	110(10)
F(213)#1-P(2)-F(23)#1	12.20(12)
F(213)-P(2)-F(23)#1	167.80(12)
F(211)-P(2)-F(23)#1	91.9(9)
F(211)#1-P(2)-F(23)#1	88.1(9)
F(22)-P(2)-F(23)#1	97.4(8)
F(22)#1-P(2)-F(23)#1	82.6(8)
F(212)-P(2)-F(23)#1	83.5(8)
F(212)#1-P(2)-F(23)#1	96.5(8)
P(21)#1-P(2)-F(23)	70(10)
F(213)#1-P(2)-F(23)	167.80(12)
F(213)-P(2)-F(23)	12.20(12)
F(211)-P(2)-F(23)	88.1(9)
F(211)#1-P(2)-F(23)	91.9(9)
F(22)-P(2)-F(23)	82.6(8)
F(22)#1-P(2)-F(23)	97.4(8)
F(212)-P(2)-F(23)	96.5(8)
F(212)#1-P(2)-F(23)	83.5(8)
F(23)#1-P(2)-F(23)	180.000(2)
P(21)#1-P(2)-F(21)	162(10)
F(213)#1-P(2)-F(21)	90.7(9)
F(213)-P(2)-F(21)	89.3(9)
F(211)-P(2)-F(21)	13.40(11)
F(211)#1-P(2)-F(21)	166.60(11)
F(22)-P(2)-F(21)	94.0(1)
F(22)#1-P(2)-F(21)	86.0(1)
F(212)-P(2)-F(21)	85.7(9)
F(212)#1-P(2)-F(21)	94.3(9)
F(23)#1-P(2)-F(21)	78.6(8)
F(23)-P(2)-F(21)	101.4(8)
P(21)-F(21)-P(2)	2(2)
P(21)-F(21)-P(21)#1	4(4)
P(2)-F(21)-P(21)#1	1.90(16)
P(21)#1-F(22)-P(2)	6.90(15)
P(21)#1-F(22)-P(21)	13(3)
P(2)-F(22)-P(21)	6.40(14)
P(21)#1-F(23)-P(2)	6.70(14)
P(21)#1-F(23)-P(21)	13(3)
P(2)-F(23)-P(21)	6.20(14)
F(34)-P(3)-F(33)	93.1(5)
F(34)-P(3)-F(31)	90.0(3)
F(33)-P(3)-F(31)	88.9(4)
F(34)-P(3)-F(32)	179.4(4)
F(33)-P(3)-F(32)	87.4(4)
F(31)-P(3)-F(32)	89.6(2)
F(34)-P(3)-F(35)	89.1(3)
F(33)-P(3)-F(35)	176.3(3)
F(31)-P(3)-F(35)	94.1(2)
F(32)-P(3)-F(35)	90.5(2)
C(42)#2-N(43)-C(42)	180.0(5)
C(41)-C(42)-N(43)	172.3(7)
N(53)-C(52)-C(51)	175.90(16)
N(63)-C(62)-C(61)	177.70(17)
P(21)#1-P(21)-F(211)	149(10)
P(21)#1-P(21)-F(21)	159(10)
F(211)-P(21)-F(21)	15.20(13)
P(21)#1-P(21)-F(213)#1	91(10)
F(211)-P(21)-F(213)#1	114(3)
F(21)-P(21)-F(213)#1	99(3)
P(21)#1-P(21)-F(22)#1	104(10)
F(211)-P(21)-F(22)#1	96(3)
F(21)-P(21)-F(22)#1	95(2)
F(213)#1-P(21)-F(22)#1	86(3)
P(21)#1-P(21)-F(213)	75(10)
F(211)-P(21)-F(213)	80(3)
F(21)-P(21)-F(213)	95(3)
F(213)#1-P(21)-F(213)	165(3)
F(22)#1-P(21)-F(213)	97(3)
P(21)#1-P(21)-F(212)#1	93(10)
F(211)-P(21)-F(212)#1	101(3)
F(21)-P(21)-F(212)#1	103(2)
F(213)#1-P(21)-F(212)#1	98(3)
F(22)#1-P(21)-F(212)#1	15.3(8)

F(213)-P(21)-F(212)#1	84(2)	F(213)#1-P(21)-F(23)	154(3)
P(21)#1-P(21)-F(23)#1	103(10)	F(22)#1-P(21)-F(23)	96(3)
F(211)-P(21)-F(23)#1	101(3)	F(213)-P(21)-F(23)	11.20(12)
F(21)-P(21)-F(23)#1	86(3)	F(212)#1-P(21)-F(23)	82(2)
F(213)#1-P(21)-F(23)#1	12.90(13)	F(23)#1-P(21)-F(23)	167(3)
F(22)#1-P(21)-F(23)#1	86(3)	F(212)-P(21)-F(23)	92(3)
F(213)-P(21)-F(23)#1	176(3)	F(22)-P(21)-F(23)	78(2)
F(212)#1-P(21)-F(23)#1	100(3)	P(21)#1-P(21)-F(211)#1	24(10)
P(21)#1-P(21)-F(212)	73(10)	F(211)-P(21)-F(211)#1	173(4)
F(211)-P(21)-F(212)	92(3)	F(21)-P(21)-F(211)#1	169(4)
F(21)-P(21)-F(212)	90(3)	F(213)#1-P(21)-F(211)#1	71(2)
F(213)#1-P(21)-F(212)	83(2)	F(22)#1-P(21)-F(211)#1	88(3)
F(22)#1-P(21)-F(212)	168(4)	F(213)-P(21)-F(211)#1	95(2)
F(213)-P(21)-F(212)	93(3)	F(212)#1-P(21)-F(211)#1	82(2)
F(212)#1-P(21)-F(212)	166(3)	F(23)#1-P(21)-F(211)#1	84(3)
F(23)#1-P(21)-F(212)	84(2)	F(212)-P(21)-F(211)#1	85(2)
P(21)#1-P(21)-F(22)	63(10)	F(22)-P(21)-F(211)#1	79.20(19)
F(211)-P(21)-F(22)	96(3)	F(23)-P(21)-F(211)#1	83(2)
F(21)-P(21)-F(22)	98(3)	P(21)-F(211)-P(2)	4(2)
F(213)#1-P(21)-F(22)	94(2)	P(21)-F(211)-P(21)#1	7(4)
F(22)#1-P(21)-F(22)	167(3)	P(2)-F(211)-P(21)#1	3.00(19)
F(213)-P(21)-F(22)	80(2)	P(21)#1-F(212)-P(2)	7.10(14)
F(212)#1-P(21)-F(22)	154(3)	P(21)#1-F(212)-P(21)	14(3)
F(23)#1-P(21)-F(22)	96(2)	P(2)-F(212)-P(21)	6.80(14)
F(212)-P(21)-F(22)	14.4(7)	P(21)#1-F(213)-P(2)	7.50(15)
P(21)#1-P(21)-F(23)	64(10)	P(21)#1-F(213)-P(21)	15(3)
F(211)-P(21)-F(23)	91(3)	P(2)-F(213)-P(21)	7.20(14)
F(21)-P(21)-F(23)	106(3)		

Table 1. Crystal data and structure refinement for **1d', Chapter V, Part B.**

Empirical formula	C44 H36 Br2 Cu F12 N10 O2 P2
Formula weight	1250.13
Temperature	150(2)K
Wavelength	1.54178 Å
Crystal system	Monoclinic
Space group	C2/c
Unit cell dimensions	a = 14.8156(2) Å α = 90° b = 21.3172(4) Å β = 95.3930(10)° c = 16.7458(3) Å γ = 90°
Volume	5265.37(15)Å^3
Z	4
Density (calculated)	1.577 g/cm^3
Absorption coefficient	3.732 mm^{-1}
F(000)	2492
Crystal size	0.18 x 0.05 x 0.05 mm
Theta range for data collection	3.64 to 68.88°
Index ranges	$-16 \leq h \leq 17$, $-25 \leq k \leq 25$, $-19 \leq \ell \leq 20$
Reflections collected	47594
Independent reflections	4733 [R_{int} = 0.022]
Absorption correction	Semi-empirical from equivalents
Max. and min. transmission	1.0000 and 0.7700
Refinement method	Full-matrix least-squares on F^2
Data / restraints / parameters	4733 / 0 / 425
Goodness-of-fit on F^2	1.043
Final R indices [I>2sigma(I)]	R1 = 0.0613, wR_2 = 0.1782
R indices (all data)	R1 = 0.0684, wR_2 = 0.1889
Largest diff. peak and hole	1.833 and -1.355 e/Å^3

Table 2. Bond lengths [Å] and angles [°] for **1d', Chapter V, Part B.**

Cu(1)-N(2)#1	1.950(3)	N(1)-CU1-N(1)#1	90.00(16)
Cu(1)-N(2)	1.950(3)	N(2)#1-CU1-N(3)#1	76.59(11)
Cu(1)-N(1)	2.205(3)	N(2)-CU1-N(3)#1	101.21(12)
Cu(1)-N(1)#1	2.205(3)	N(1)-CU1-N(3)#1	94.13(11)
Cu(1)-N(3)#1	2.231(3)	N(1)#1-CU1-N(3)#1	152.99(11)
Cu(1)-N(3)	2.231(3)	N(2)#1-CU1-N(3)	101.22(12)
N(1)-C(1)	1.336(5)	N(2)-CU1-N(3)	76.59(11)
N(1)-C(5)	1.346(5)	N(1)-CU1-N(3)	152.99(11)
N(2)-C(8)	1.344(5)	N(1)#1-CU1-N(3)	94.13(11)
N(2)-C(6)	1.347(4)	N(3)#1-CU1-N(3)	94.17(17)
N(3)-C(13)	1.335(5)	C(1)-N(1)-C(5)	117.9(3)
N(3)-C(9)	1.346(5)	C(1)-N(1)-CU1	129.1(3)
N(4)-C(6)	1.319(5)	C(5)-N(1)-CU1	113.0(2)
N(4)-C(7)	1.345(5)	C(8)-N(2)-C(6)	116.2(3)
N(5)-C(8)	1.305(5)	C(8)-N(2)-CU1	122.1(2)
N(5)-C(7)	1.358(5)	C(6)-N(2)-CU1	121.7(2)
C(1)-C(2)	1.381(6)	C(13)-N(3)-C(9)	118.1(4)
C(2)-C(3)	1.377(6)	C(13)-N(3)-CU1	129.7(3)
C(3)-C(4)	1.384(6)	C(9)-N(3)-CU1	112.2(2)
C(4)-C(5)	1.378(5)	C(6)-N(4)-C(7)	115.7(3)
C(5)-C(6)	1.483(5)	C(8)-N(5)-C(7)	115.7(3)
C(7)-C(14)	1.455(6)	N(1)-C(1)-C(2)	122.2(4)
C(8)-C(9)	1.483(5)	C(3)-C(2)-C(1)	119.4(4)
C(9)-C(10)	1.386(6)	C(2)-C(3)-C(4)	119.2(4)
C(10)-C(11)	1.387(6)	C(5)-C(4)-C(3)	118.0(4)
C(11)-C(12)	1.391(8)	N(1)-C(5)-C(4)	123.3(3)
C(12)-C(13)	1.397(8)	N(1)-C(5)-C(6)	114.0(3)
C(14)-C(19)	1.390(6)	C(4)-C(5)-C(6)	122.6(3)
C(14)-C(15)	1.392(6)	N(4)-C(6)-N(2)	123.9(3)
C(15)-C(16)	1.372(6)	N(4)-C(6)-C(5)	121.8(3)
C(16)-C(17)	1.366(7)	N(2)-C(6)-C(5)	114.3(3)
C(17)-C(18)	1.380(7)	N(4)-C(7)-N(5)	124.1(3)
C(17)-Br(1)	1.900(4)	N(4)-C(7)-C(14)	118.9(3)
C(18)-C(19)	1.374(6)	N(5)-C(7)-C(14)	117.0(3)
P(1)-F(11)	1.466(10)	N(5)-C(8)-N(2)	124.4(3)
P(1)-F(15)	1.479(14)	N(5)-C(8)-C(9)	121.2(3)
P(1)-F(112)	1.48(2)	N(2)-C(8)-C(9)	114.5(3)
P(1)-F(116)	1.502(9)	N(3)-C(9)-C(10)	123.7(3)
P(1)-F(113)	1.558(7)	N(3)-C(9)-C(8)	114.6(3)
P(1)-F(14)	1.570(7)	C(10)-C(9)-C(8)	121.7(4)
P(1)-F(115)	1.590(13)	C(9)-C(10)-C(11)	118.0(4)
P(1)-F(12)	1.65(2)	C(10)-C(11)-C(12)	119.0(5)
P(1)-F(16)	1.659(9)	C(11)-C(12)-C(13)	119.2(4)
P(1)-F(111)	1.672(9)	N(3)-C(13)-C(12)	122.1(4)
P(1)-F(114)	1.678(5)	C(19)-C(14)-C(15)	118.5(4)
P(1)-F(13)	1.741(9)	C(19)-C(14)-C(7)	120.2(4)
C(21)-C(22)	1.331(18)	C(15)-C(14)-C(7)	121.3(4)
C(22)-O(24)	1.124(8)	C(16)-C(15)-C(14)	121.0(4)
C(22)-C(23)	1.53(2)	C(17)-C(16)-C(15)	119.3(4)
O(34)-C(32)	1.12(2)	C(16)-C(17)-C(18)	121.4(4)
C(32)-C(31)	1.40(3)	C(16)-C(17)-BR1	119.4(3)
C(32)-C(33)	1.44(2)	C(18)-C(17)-BR1	119.2(3)
N(2)#1-CU1-N(2)	176.86(17)	C(19)-C(18)-C(17)	119.1(4)
N(2)#1-CU1-N(1)	105.70(11)	C(18)-C(19)-C(14)	120.8(4)
N(2)-CU1-N(1)	76.60(11)	F(11)-P(1)-F(15)	99.9(8)
N(2)#1-CU1-N(1)#1	76.59(11)	F(11)-P(1)-F(112)	96.10(11)
N(2)-CU1-N(1)#1	105.70(11)	F(15)-P(1)-F(112)	105.4(1)

F(11)-P(1)-F(116)	146.4(7)	F(116)-P(1)-F(111)	173.0(5)
F(15)-P(1)-F(116)	105.8(6)	F(113)-P(1)-F(111)	86.1(5)
F(112)-P(1)-F(116)	97.6(1)	F(14)-P(1)-F(111)	112.3(5)
F(11)-P(1)-F(113)	56.2(6)	F(115)-P(1)-F(111)	90.5(6)
F(15)-P(1)-F(113)	151.8(6)	F(12)-P(1)-F(111)	79.0(1)
F(112)-P(1)-F(113)	92.9(9)	F(16)-P(1)-F(111)	154.8(5)
F(116)-P(1)-F(113)	92.5(6)	F(11)-P(1)-F(114)	78.4(5)
F(11)-P(1)-F(14)	94.1(5)	F(15)-P(1)-F(114)	68.9(7)
F(15)-P(1)-F(14)	99.4(8)	F(112)-P(1)-F(114)	170.9(8)
F(112)-P(1)-F(14)	151.1(8)	F(116)-P(1)-F(114)	90.9(4)
F(116)-P(1)-F(14)	60.9(6)	F(113)-P(1)-F(114)	89.9(4)
F(113)-P(1)-F(14)	70.7(4)	F(14)-P(1)-F(114)	37.6(4)
F(11)-P(1)-F(115)	119.4(8)	F(115)-P(1)-F(114)	81.9(6)
F(15)-P(1)-F(115)	20.8(7)	F(12)-P(1)-F(114)	155.9(8)
F(112)-P(1)-F(115)	94.8(1)	F(16)-P(1)-F(114)	106.3(4)
F(116)-P(1)-F(115)	89.9(6)	F(111)-P(1)-F(114)	82.3(4)
F(113)-P(1)-F(115)	171.5(6)	F(11)-P(1)-F(13)	87.9(7)
F(14)-P(1)-F(115)	103.6(6)	F(15)-P(1)-F(13)	169.2(7)
F(11)-P(1)-F(12)	92.70(11)	F(112)-P(1)-F(13)	66.1(8)
F(15)-P(1)-F(12)	91.1(1)	F(116)-P(1)-F(13)	70.0(5)
F(112)-P(1)-F(12)	15.60(13)	F(113)-P(1)-F(13)	38.8(4)
F(116)-P(1)-F(12)	107.9(1)	F(14)-P(1)-F(13)	87.3(5)
F(113)-P(1)-F(12)	103.7(9)	F(115)-P(1)-F(13)	149.1(7)
F(14)-P(1)-F(12)	166.4(9)	F(12)-P(1)-F(13)	81.1(8)
F(115)-P(1)-F(12)	83.2(1)	F(16)-P(1)-F(13)	84.2(5)
F(11)-P(1)-F(16)	172.1(7)	F(111)-P(1)-F(13)	112.3(5)
F(15)-P(1)-F(16)	87.8(6)	F(114)-P(1)-F(13)	120.3(4)
F(112)-P(1)-F(16)	80.0(1)	O(24)-C(22)-C(21)	129.80(15)
F(116)-P(1)-F(16)	29.6(4)	O(24)-C(22)-C(23)	111.10(11)
F(113)-P(1)-F(16)	116.9(6)	C(21)-C(22)-C(23)	118.90(15)
F(14)-P(1)-F(16)	86.4(4)	O(34)-C(32)-C(31)	126(2)
F(115)-P(1)-F(16)	68.0(6)	O(34)-C(32)-C(33)	117(2)
F(12)-P(1)-F(16)	85.30(11)	C(31)-C(32)-C(33)	116(2)
F(11)-P(1)-F(111)	30.6(6)		
F(15)-P(1)-F(111)	73.1(6)		
F(112)-P(1)-F(111)	89.3(1)		

Table 1. Crystal data and structure refinement for **2a, Chapter V, Part B.**

Identification code	gar119
Empirical formula	C40 H30 F12 Fe N10 P2
Formula weight	996.53
Temperature	150(2)K
Wavelength	1.54178 Å
Crystal system	Monoclinic
Space group	P21/n
Unit cell dimensions	a = 8.9622(3) Å α = 90° b = 33.0144(8) Å β = 92.053(2)° c = 13.3712(4) Å γ = 90°
Volume	3953.8(2)Å^3
Z	4
Density (calculated)	1.674 g/cm^3
Absorption coefficient	4.763 mm^{-1}
F(000)	2016
Crystal size	0.22 x 0.04 x 0.02 mm
Theta range for data collection	2.68 to 68.97°
Index ranges	$-9 \le h \le 10$, $-39 \le k \le 39$, $-16 \le \ell \le 16$
Reflections collected	54135
Independent reflections	7253 [R_{int} = 0.034]
Absorption correction	Semi-empirical from equivalents
Max. and min. transmission	1.0000 and 0.7500
Refinement method	Full-matrix least-squares on F^2
Data / restraints / parameters	7253 / 0 / 588
Goodness-of-fit on F^2	1.002
Final R indices [I>2sigma(I)]	R1 = 0.0380, wR_2 = 0.0988
R indices (all data)	R1 = 0.0477, wR_2 = 0.1096
Largest diff. peak and hole	0.406 and -0.346 e/Å^3

Table 2. Bond lengths [Å] and angles [°] for **2a, Chapter V, Part B.**

Fe(1)-N(2)	1.8747(18)	C(35)-C(36)	1.384(3)
Fe(1)-N(7)	1.8792(18)	C(36)-C(37)	1.386(4)
Fe(1)-N(1)	2.0059(18)	C(37)-C(38)	1.396(4)
Fe(1)-N(8)	2.0061(19)	C(37)-C(40)	1.513(3)
Fe(1)-N(3)	2.0076(19)	C(38)-C(39)	1.386(3)
Fe(1)-N(6)	2.0093(19)	P(1)-F(15)	1.571(2)
N(1)-C(1)	1.340(3)	P(1)-F(14)	1.5907(18)
N(1)-C(5)	1.373(3)	P(1)-F(11)	1.5912(17)
N(2)-C(8)	1.344(3)	P(1)-F(12)	1.5944(19)
N(2)-C(6)	1.347(3)	P(1)-F(13)	1.598(2)
N(3)-C(13)	1.342(3)	P(1)-F(16)	1.6073(16)
N(3)-C(9)	1.369(3)	P(2)-F(26)	1.5810(17)
N(4)-C(6)	1.317(3)	P(2)-F(25)	1.5836(19)
N(4)-C(7)	1.359(3)	P(2)-F(21)	1.5909(17)
N(5)-C(8)	1.313(3)	P(2)-F(22)	1.5917(17)
N(5)-C(7)	1.355(3)	P(2)-F(23)	1.5986(18)
N(6)-C(21)	1.338(3)	P(2)-F(24)	1.6026(16)
N(6)-C(25)	1.373(3)	N(2)-FE1-N(7)	179.35(8)
N(7)-C(26)	1.338(3)	N(2)-FE1-N(1)	79.70(8)
N(7)-C(28)	1.348(3)	N(7)-FE1-N(1)	99.68(8)
N(8)-C(33)	1.341(3)	N(2)-FE1-N(8)	100.88(8)
N(8)-C(29)	1.366(3)	N(7)-FE1-N(8)	79.29(8)
N(9)-C(26)	1.310(3)	N(1)-FE1-N(8)	92.07(7)
N(9)-C(27)	1.356(3)	N(2)-FE1-N(3)	79.45(8)
N(10)-C(28)	1.324(3)	N(7)-FE1-N(3)	101.17(8)
N(10)-C(27)	1.352(3)	N(1)-FE1-N(3)	159.09(8)
C(1)-C(2)	1.389(3)	N(8)-FE1-N(3)	93.32(7)
C(2)-C(3)	1.378(3)	N(2)-FE1-N(6)	100.07(8)
C(3)-C(4)	1.389(3)	N(7)-FE1-N(6)	79.76(8)
C(4)-C(5)	1.379(3)	N(1)-FE1-N(6)	91.00(7)
C(5)-C(6)	1.473(3)	N(8)-FE1-N(6)	159.04(7)
C(7)-C(14)	1.461(3)	N(3)-FE1-N(6)	91.15(8)
C(8)-C(9)	1.469(3)	C(1)-N(1)-C(5)	117.37(19)
C(9)-C(10)	1.375(3)	C(1)-N(1)-FE1	127.75(15)
C(10)-C(11)	1.386(4)	C(5)-N(1)-FE1	114.88(14)
C(11)-C(12)	1.385(4)	C(8)-N(2)-C(6)	116.68(19)
C(12)-C(13)	1.382(3)	C(8)-N(2)-FE1	121.74(15)
C(14)-C(15)	1.387(3)	C(6)-N(2)-FE1	121.55(15)
C(14)-C(19)	1.393(3)	C(13)-N(3)-C(9)	117.4(2)
C(15)-C(16)	1.380(3)	C(13)-N(3)-FE1	127.63(16)
C(16)-C(17)	1.385(4)	C(9)-N(3)-FE1	114.83(15)
C(17)-C(18)	1.382(4)	C(6)-N(4)-C(7)	115.19(19)
C(17)-C(20)	1.507(3)	C(8)-N(5)-C(7)	115.41(19)
C(18)-C(19)	1.379(4)	C(21)-N(6)-C(25)	117.2(2)
C(21)-C(22)	1.388(4)	C(21)-N(6)-FE1	128.33(16)
C(22)-C(23)	1.375(4)	C(25)-N(6)-FE1	114.50(15)
C(23)-C(24)	1.385(4)	C(26)-N(7)-C(28)	116.77(19)
C(24)-C(25)	1.371(3)	C(26)-N(7)-FE1	121.10(15)
C(25)-C(26)	1.467(3)	C(28)-N(7)-FE1	122.04(15)
C(27)-C(34)	1.472(3)	C(33)-N(8)-C(29)	117.71(19)
C(28)-C(29)	1.474(3)	C(33)-N(8)-FE1	127.17(15)
C(29)-C(30)	1.378(3)	C(29)-N(8)-FE1	115.10(14)
C(30)-C(31)	1.381(4)	C(26)-N(9)-C(27)	115.2(2)
C(31)-C(32)	1.386(3)	C(28)-N(10)-C(27)	115.1(2)
C(32)-C(33)	1.391(3)	N(1)-C(1)-C(2)	122.6(2)
C(34)-C(39)	1.393(4)	C(3)-C(2)-C(1)	119.5(2)
C(34)-C(35)	1.395(4)	C(2)-C(3)-C(4)	119.0(2)

C(5)-C(4)-C(3)	118.7(2)	N(8)-C(29)-C(28)	113.17(19)
N(1)-C(5)-C(4)	122.8(2)	C(30)-C(29)-C(28)	124.3(2)
N(1)-C(5)-C(6)	112.72(19)	C(29)-C(30)-C(31)	119.5(2)
C(4)-C(5)-C(6)	124.5(2)	C(30)-C(31)-C(32)	118.5(2)
N(4)-C(6)-N(2)	124.0(2)	C(31)-C(32)-C(33)	119.5(2)
N(4)-C(6)-C(5)	124.9(2)	N(8)-C(33)-C(32)	122.4(2)
N(2)-C(6)-C(5)	111.14(19)	C(39)-C(34)-C(35)	119.2(2)
N(5)-C(7)-N(4)	124.5(2)	C(39)-C(34)-C(27)	121.3(2)
N(5)-C(7)-C(14)	117.7(2)	C(35)-C(34)-C(27)	119.5(2)
N(4)-C(7)-C(14)	117.8(2)	C(36)-C(35)-C(34)	120.0(2)
N(5)-C(8)-N(2)	124.1(2)	C(35)-C(36)-C(37)	121.5(3)
N(5)-C(8)-C(9)	124.9(2)	C(36)-C(37)-C(38)	118.0(2)
N(2)-C(8)-C(9)	111.01(19)	C(36)-C(37)-C(40)	120.6(3)
N(3)-C(9)-C(10)	123.1(2)	C(38)-C(37)-C(40)	121.3(3)
N(3)-C(9)-C(8)	112.89(19)	C(39)-C(38)-C(37)	121.2(2)
C(10)-C(9)-C(8)	124.0(2)	C(38)-C(39)-C(34)	119.9(2)
C(9)-C(10)-C(11)	118.6(2)	F(15)-P(1)-F(14)	91.12(12)
C(12)-C(11)-C(10)	118.8(2)	F(15)-P(1)-F(11)	90.93(10)
C(13)-C(12)-C(11)	119.8(2)	F(14)-P(1)-F(11)	90.74(10)
N(3)-C(13)-C(12)	122.3(2)	F(15)-P(1)-F(12)	90.50(12)
C(15)-C(14)-C(19)	118.2(2)	F(14)-P(1)-F(12)	177.90(13)
C(15)-C(14)-C(7)	120.9(2)	F(11)-P(1)-F(12)	90.56(10)
C(19)-C(14)-C(7)	120.9(2)	F(15)-P(1)-F(13)	179.74(12)
C(16)-C(15)-C(14)	120.5(2)	F(14)-P(1)-F(13)	88.82(12)
C(15)-C(16)-C(17)	121.5(3)	F(11)-P(1)-F(13)	89.33(10)
C(18)-C(17)-C(16)	117.8(2)	F(12)-P(1)-F(13)	89.55(12)
C(18)-C(17)-C(20)	120.8(3)	F(15)-P(1)-F(16)	89.17(10)
C(16)-C(17)-C(20)	121.3(3)	F(14)-P(1)-F(16)	89.11(9)
C(19)-C(18)-C(17)	121.4(2)	F(11)-P(1)-F(16)	179.83(12)
C(18)-C(19)-C(14)	120.5(2)	F(12)-P(1)-F(16)	89.57(10)
N(6)-C(21)-C(22)	122.1(2)	F(13)-P(1)-F(16)	90.57(10)
C(23)-C(22)-C(21)	120.0(2)	F(26)-P(2)-F(25)	90.03(12)
C(22)-C(23)-C(24)	119.0(2)	F(26)-P(2)-F(21)	179.46(12)
C(25)-C(24)-C(23)	118.3(2)	F(25)-P(2)-F(21)	90.14(11)
C(24)-C(25)-N(6)	123.5(2)	F(26)-P(2)-F(22)	89.58(11)
C(24)-C(25)-C(26)	123.7(2)	F(25)-P(2)-F(22)	92.31(12)
N(6)-C(25)-C(26)	112.8(2)	F(21)-P(2)-F(22)	90.92(10)
N(9)-C(26)-N(7)	124.4(2)	F(26)-P(2)-F(23)	90.98(11)
N(9)-C(26)-C(25)	123.8(2)	F(25)-P(2)-F(23)	178.42(11)
N(7)-C(26)-C(25)	111.76(19)	F(21)-P(2)-F(23)	88.83(11)
N(10)-C(27)-N(9)	124.7(2)	F(22)-P(2)-F(23)	88.90(11)
N(10)-C(27)-C(34)	119.6(2)	F(26)-P(2)-F(24)	90.16(10)
N(9)-C(27)-C(34)	115.7(2)	F(25)-P(2)-F(24)	88.88(10)
N(10)-C(28)-N(7)	123.6(2)	F(21)-P(2)-F(24)	89.33(9)
N(10)-C(28)-C(29)	125.9(2)	F(22)-P(2)-F(24)	178.78(12)
N(7)-C(28)-C(29)	110.38(19)	F(23)-P(2)-F(24)	89.91(10)
N(8)-C(29)-C(30)	122.5(2)		

Table 1. Crystal data and structure refinement for **2b, Chapter V, Part B.**

Identification code	gh10
Empirical formula	C40 H30 Co F12 N10 P2
Formula weight	999.61
Temperature	125(2)K
Wavelength	0.71070 Å
Crystal system	Tetragonal
Space group	I41/acd
Unit cell dimensions	a = 22.1997(19) Å α = 90° b = 22.1997(19) Å β = 90° c = 16.819(3) Å γ = 90°
Volume	8288.7(17)Å^3
Z	8
Density (calculated)	1.602 g/cm^3
Absorption coefficient	0.591 mm^{-1}
F(000)	4040
Crystal size	0.30 x 0.10 x 0.05 mm
Theta range for data collection	1.83 to 28.37°
Index ranges	$-29 \le h \le 29$, $-29 \le k \le 29$, $-22 \le \ell \le 22$
Reflections collected	248860
Independent reflections	2597 [R_{int} = 0.050]
Absorption correction	Semi-empirical from equivalents
Max. and min. transmission	0.7700 and 0.5100
Refinement method	Full-matrix least-squares on F^2
Data / restraints / parameters	2597 / 0 / 152
Goodness-of-fit on F^2	1.073
Final R indices [I>2sigma(I)]	R_1 = 0.0354, wR_2 = 0.0943
R indices (all data)	R_1 = 0.0610, wR_2 = 0.1142
Largest diff. peak and hole	0.778 and -0.511 e/Å^3

Table 2. Bond lengths [Å] and angles [°] for **2b, Chapter V, Part B.**

Co(1)-N(2)#1	1.962(2)	F(2)#4-P(1)-F(2)	180.0
Co(1)-N(2)	1.962(2)	F(2)#4-P(1)-F(1)#4	90.47(9)
Co(1)-N(1)#2	2.2150(19)	F(2)-P(1)-F(1)#4	89.53(9)
Co(1)-N(1)#3	2.2151(19)	F(2)#4-P(1)-F(1)	89.53(9)
Co(1)-N(1)#1	2.2151(19)	F(2)-P(1)-F(1)	90.47(9)
Co(1)-N(1)	2.2151(19)	F(1)#4-P(1)-F(1)	180.0
P(1)-F(2)#4	1.5937(15)	F(2)#4-P(1)-F(3)	90.56(8)
P(1)-F(2)	1.5937(15)	F(2)-P(1)-F(3)	89.44(8)
P(1)-F(1)#4	1.5959(15)	F(1)#4-P(1)-F(3)	90.26(8)
P(1)-F(1)	1.5960(15)	F(1)-P(1)-F(3)	89.74(8)
P(1)-F(3)	1.6090(14)	F(2)#4-P(1)-F(3)#4	89.44(8)
P(1)-F(3)#4	1.6090(14)	F(2)-P(1)-F(3)#4	90.56(8)
C(1)-N(1)	1.332(3)	F(1)#4-P(1)-F(3)#4	89.74(8)
C(1)-C(2)	1.381(4)	F(1)-P(1)-F(3)#4	90.26(8)
C(2)-C(3)	1.373(4)	F(3)-P(1)-F(3)#4	180.0
C(3)-C(4)	1.386(3)	N(1)-C(1)-C(2)	122.6(2)
C(4)-C(5)	1.378(3)	C(3)-C(2)-C(1)	119.5(2)
C(5)-N(1)	1.352(3)	C(2)-C(3)-C(4)	118.9(2)
C(5)-C(6)	1.477(3)	C(5)-C(4)-C(3)	118.2(2)
C(6)-N(3)	1.319(3)	N(1)-C(5)-C(4)	123.1(2)
C(6)-N(2)	1.342(2)	N(1)-C(5)-C(6)	114.41(18)
N(2)-C(6)#2	1.342(2)	C(4)-C(5)-C(6)	122.46(19)
N(3)-C(7)	1.351(2)	N(3)-C(6)-N(2)	124.3(2)
C(7)-N(3)#2	1.351(2)	N(3)-C(6)-C(5)	121.21(18)
C(7)-C(8)	1.459(4)	N(2)-C(6)-C(5)	114.50(18)
C(8)-C(9)#2	1.398(3)	C(1)-N(1)-C(5)	117.63(19)
C(8)-C(9)	1.398(3)	C(1)-N(1)-Co(1)	129.64(15)
C(9)-C(10)	1.379(3)	C(5)-N(1)-Co(1)	112.67(14)
C(10)-C(11)	1.388(3)	C(6)-N(2)-C(6)#2	116.3(3)
C(11)-C(10)#2	1.388(3)	C(6)-N(2)-Co(1)	121.87(13)
C(11)-C(12)	1.504(5)	C(6)#2-N(2)-Co(1)	121.87(13)
N(2)#1-Co(1)-N(2)	180.0	C(6)-N(3)-C(7)	115.37(19)
N(2)#1-Co(1)-N(1)#2	103.54(5)	N(3)-C(7)-N(3)#2	124.4(3)
N(2)-Co(1)-N(1)#2	76.46(5)	N(3)-C(7)-C(8)	117.79(13)
N(2)#1-Co(1)-N(1)#3	76.46(5)	N(3)#2-C(7)-C(8)	117.80(13)
N(2)-Co(1)-N(1)#3	103.54(5)	C(9)#2-C(8)-C(9)	118.7(3)
N(1)#2-Co(1)-N(1)#3	93.12(10)	C(9)#2-C(8)-C(7)	120.66(13)
N(2)#1-Co(1)-N(1)#1	76.46(5)	C(9)-C(8)-C(7)	120.66(13)
N(2)-Co(1)-N(1)#1	103.54(5)	C(10)-C(9)-C(8)	120.3(2)
N(1)#2-Co(1)-N(1)#1	93.16(10)	C(9)-C(10)-C(11)	120.9(2)
N(1)#3-Co(1)-N(1)#1	152.92(9)	C(10)#2-C(11)-C(10)	118.8(3)
N(2)#1-Co(1)-N(1)	103.54(5)	C(10)#2-C(11)-C(12)	120.60(15)
N(2)-Co(1)-N(1)	76.46(5)	C(10)-C(11)-C(12)	120.60(15)
N(1)#2-Co(1)-N(1)	152.92(9)		
N(1)#3-Co(1)-N(1)	93.16(10)		
N(1)#1-Co(1)-N(1)	93.12(10)		

Table 1. Crystal data and structure refinement for **2c, Chapter V, Part B.**

Identification code	gar_120
Empirical formula	C40 H30 F12 N10 Ni P2
Formula weight	999.39
Temperature	150(2)K
Wavelength	1.54178 Å
Crystal system	Tetragonal
Space group	I41/acd
Unit cell dimensions	a = 22.2925(3) Å α = 90° b = 22.2925(3) Å β = 90° c = 16.6862(4) Å γ = 90°
Volume	8292.3(3)Å^3
Z	8
Density (calculated)	1.601 g/cm^3
Absorption coefficient	2.300 mm^{-1}
F(000)	4048
Crystal size	0.20 x 0.04 x 0.01 mm
Theta range for data collection	3.97 to 68.83°
Index ranges	$-26 \le h \le 26$, $-26 \le k \le 26$, $-17 \le \ell \le 19$
Reflections collected	76131
Independent reflections	1928 [R_{int} = 0.033]
Absorption correction	Semi-empirical from equivalents
Max. and min. transmission	1.0000 and 0.8400
Refinement method	Full-matrix least-squares on F^2
Data / restraints / parameters	1928 / 0 / 153
Goodness-of-fit on F^2	1.094
Final R indices [I>2sigma(I)]	R1 = 0.0416, wR_2 = 0.1140
R indices (all data)	R1 = 0.0566, wR_2 = 0.1365
Largest diff. peak and hole	0.275 and -0.472 e/Å^3

Table 2. Bond lengths [Å] and angles [°] for **2c, Chapter V, Part B.**

Ni(1)-N(2)	1.988(3)	C(1)-N(1)-C(5)	117.3(2)
Ni(1)-N(2)#1	1.988(3)	C(1)-N(1)-NI1	128.56(18)
Ni(1)-N(1)	2.154(2)	C(5)-N(1)-NI1	114.11(17)
Ni(1)-N(1)#1	2.154(2)	C(6)-N(2)-C(6)#3	117.0(3)
Ni(1)-N(1)#2	2.155(2)	C(6)-N(2)-NI1	121.52(15)
Ni(1)-N(1)#3	2.155(2)	C(6)#3-N(2)-NI1	121.52(15)
N(1)-C(1)	1.336(3)	C(6)-N(3)-C(7)	115.1(2)
N(1)-C(5)	1.358(3)	N(1)-C(1)-C(2)	122.6(3)
N(2)-C(6)	1.336(3)	C(3)-C(2)-C(1)	119.5(3)
N(2)-C(6)#3	1.336(3)	C(2)-C(3)-C(4)	118.9(3)
N(3)-C(6)	1.317(3)	C(5)-C(4)-C(3)	118.3(3)
N(3)-C(7)	1.354(3)	N(1)-C(5)-C(4)	123.3(2)
C(1)-C(2)	1.383(4)	N(1)-C(5)-C(6)	114.5(2)
C(2)-C(3)	1.376(5)	C(4)-C(5)-C(6)	122.2(2)
C(3)-C(4)	1.385(4)	N(3)-C(6)-N(2)	124.1(2)
C(4)-C(5)	1.380(4)	N(3)-C(6)-C(5)	122.6(2)
C(5)-C(6)	1.478(3)	N(2)-C(6)-C(5)	113.3(2)
C(7)-N(3)#3	1.354(3)	N(3)-C(7)-N(3)#3	124.6(3)
C(7)-C(8)	1.462(5)	N(3)-C(7)-C(8)	117.73(15)
C(8)-C(9)	1.399(3)	N(3)#3-C(7)-C(8)	117.72(15)
C(8)-C(9)#3	1.399(3)	C(9)-C(8)-C(9)#3	118.9(3)
C(9)-C(10)	1.377(4)	C(9)-C(8)-C(7)	120.57(16)
C(10)-C(11)	1.390(3)	C(9)#3-C(8)-C(7)	120.57(16)
C(11)-C(10)#3	1.390(3)	C(10)-C(9)-C(8)	120.1(2)
C(11)-C(12)	1.507(6)	C(9)-C(10)-C(11)	121.4(3)
P(1)-F(11)#4	1.5903(18)	C(10)-C(11)-C(10)#3	118.2(3)
P(1)-F(11)	1.5903(18)	C(10)-C(11)-C(12)	120.89(17)
P(1)-F(13)#4	1.5914(19)	C(10)#3-C(11)-C(12)	120.89(17)
P(1)-F(13)	1.5915(19)	F(11)#4-P(1)-F(11)	180
P(1)-F(12)#4	1.6072(18)	F(11)#4-P(1)-F(13)#4	90.50(11)
P(1)-F(12)	1.6072(18)	F(11)-P(1)-F(13)#4	89.50(11)
N(2)-NI1-N(2)#1	180	F(11)#4-P(1)-F(13)	89.50(11)
N(2)-NI1-N(1)	76.54(6)	F(11)-P(1)-F(13)	90.50(11)
N(2)#1-NI1-N(1)	103.46(6)	F(13)#4-P(1)-F(13)	179.998(1)
N(2)-NI1-N(1)#1	103.47(6)	F(11)#4-P(1)-F(12)#4	89.56(10)
N(2)#1-NI1-N(1)#1	76.53(6)	F(11)-P(1)-F(12)#4	90.44(10)
N(1)-NI1-N(1)#1	93.57(12)	F(13)#4-P(1)-F(12)#4	89.34(11)
N(2)-NI1-N(1)#2	103.47(6)	F(13)-P(1)-F(12)#4	90.66(10)
N(2)#1-NI1-N(1)#2	76.53(6)	F(11)#4-P(1)-F(12)	90.44(10)
N(1)-NI1-N(1)#2	92.64(12)	F(11)-P(1)-F(12)	89.56(10)
N(1)#1-NI1-N(1)#2	153.07(11)	F(13)#4-P(1)-F(12)	90.66(10)
N(2)-NI1-N(1)#3	76.53(6)	F(13)-P(1)-F(12)	89.34(11)
N(2)#1-NI1-N(1)#3	103.47(6)	F(12)#4-P(1)-F(12)	180.00(11)
N(1)-NI1-N(1)#3	153.07(11)		
N(1)#1-NI1-N(1)#3	92.64(12)		
N(1)#2-NI1-N(1)#3	93.57(12)		

Table 1. Crystal data and structure refinement for **2d, Chapter V, Part B.**

Identification code	$gar_1 15$
Empirical formula	C40 H30 Cu F12 N10 P2
Formula weight	1004.22
Temperature	100(2)K
Wavelength	1.54178 Å
Crystal system	Tetragonal
Space group	I41/acd
Unit cell dimensions	a = 22.1672(6) Å α = 90° b = 22.1672(6) Å β = 90° c = 16.8029(10) Å γ = 90°
Volume	8256.7(6)Å^3
Z	8
Density (calculated)	1.616 g/cm^3
Absorption coefficient	2.379 mm^{-1}
F(000)	4056
Crystal size	0.28 x 0.08 x 0.04 mm
Theta range for data collection	3.99 to 59.02°
Index ranges	$-24 \leq h \leq 23$, $-24 \leq k \leq 22$, $-18 \leq \ell \leq 18$
Reflections collected	37122
Independent reflections	1494 [R_{int} = 0.067]
Absorption correction	Semi-empirical from equivalents
Max. and min. transmission	0.9400 and 0.9400
Refinement method	Full-matrix least-squares on F^2
Data / restraints / parameters	1494 / 0 / 153
Goodness-of-fit on F^2	1.049
Final R indices [I>2sigma(I)]	R1 = 0.0302, wR_2 = 0.0830
R indices (all data)	R1 = 0.0435, wR_2 = 0.0983
Largest diff. peak and hole	0.268 and -0.342 e/Å^3

Table 2. Bond lengths [Å] and angles [°] for **2d**, **Chapter V, Part B.**

Cu(1)-N(2)#1	1.963(3)	C(1)-N(1)-C(5)	117.8(2)
Cu(1)-N(2)	1.963(3)	C(1)-N(1)-CU1	129.52(18)
Cu(1)-N(1)#1	2.216(2)	C(5)-N(1)-CU1	112.68(17)
Cu(1)-N(1)#2	2.216(2)	C(6)-N(2)-C(6)#2	116.6(3)
Cu(1)-N(1)#3	2.216(2)	C(6)-N(2)-CU1	121.71(15)
Cu(1)-N(1)	2.216(2)	C(6)#2-N(2)-CU1	121.71(15)
N(1)-C(1)	1.333(4)	C(6)-N(3)-C(7)	115.7(2)
N(1)-C(5)	1.355(3)	N(1)-C(1)-C(2)	122.3(3)
N(2)-C(6)	1.341(3)	C(3)-C(2)-C(1)	119.6(3)
N(2)-C(6)#2	1.341(3)	C(2)-C(3)-C(4)	118.8(3)
N(3)-C(6)	1.319(3)	C(5)-C(4)-C(3)	118.5(2)
N(3)-C(7)	1.355(3)	N(1)-C(5)-C(4)	123.0(2)
C(1)-C(2)	1.381(4)	N(1)-C(5)-C(6)	114.3(2)
C(2)-C(3)	1.374(4)	C(4)-C(5)-C(6)	122.8(2)
C(3)-C(4)	1.384(4)	N(3)-C(6)-N(2)	124.1(2)
C(4)-C(5)	1.376(4)	N(3)-C(6)-C(5)	121.1(2)
C(5)-C(6)	1.473(4)	N(2)-C(6)-C(5)	114.8(2)
C(7)-N(3)#2	1.355(3)	N(3)-C(7)-N(3)#2	123.9(3)
C(7)-C(8)	1.456(5)	N(3)-C(7)-C(8)	118.04(16)
C(8)-C(9)	1.398(3)	N(3)#2-C(7)-C(8)	118.04(16)
C(8)-C(9)#2	1.398(3)	C(9)-C(8)-C(9)#2	118.7(3)
C(9)-C(10)	1.375(4)	C(9)-C(8)-C(7)	120.64(17)
C(10)-C(11)	1.390(3)	C(9)#2-C(8)-C(7)	120.63(17)
C(11)-C(10)#2	1.390(3)	C(10)-C(9)-C(8)	120.4(3)
C(11)-C(12)	1.509(6)	C(9)-C(10)-C(11)	120.9(3)
P(2)-F(12)	1.5920(16)	C(10)#2-C(11)-C(10)	118.8(4)
P(2)-F(12)#4	1.5921(16)	C(10)#2-C(11)-C(12)	120.62(17)
P(2)-F(13)#4	1.5938(16)	C(10)-C(11)-C(12)	120.62(17)
P(2)-F(13)	1.5938(16)	F(12)-P(2)-F(12)#4	180.00(11)
P(2)-F(11)	1.6073(16)	F(12)-P(2)-F(13)#4	89.62(9)
P(2)-F(11)#4	1.6073(16)	F(12)#4-P(2)-F(13)#4	90.38(9)
N(2)#1-CU1-N(2)	180.00(17)	F(12)-P(2)-F(13)	90.38(9)
N(2)#1-CU1-N(1)#1	76.44(5)	F(12)#4-P(2)-F(13)	89.62(9)
N(2)-CU1-N(1)#1	103.56(5)	F(13)#4-P(2)-F(13)	180
N(2)#1-CU1-N(1)#2	103.56(5)	F(12)-P(2)-F(11)	89.66(9)
N(2)-CU1-N(1)#2	76.44(5)	F(12)#4-P(2)-F(11)	90.34(9)
N(1)#1-CU1-N(1)#2	93.28(12)	F(13)#4-P(2)-F(11)	90.14(8)
N(2)#1-CU1-N(1)#3	76.44(5)	F(13)-P(2)-F(11)	89.86(8)
N(2)-CU1-N(1)#3	103.56(5)	F(12)-P(2)-F(11)#4	90.34(9)
N(1)#1-CU1-N(1)#3	152.88(11)	F(12)#4-P(2)-F(11)#4	89.66(9)
N(1)#2-CU1-N(1)#3	93.02(12)	F(13)#4-P(2)-F(11)#4	89.86(8)
N(2)#1-CU1-N(1)	103.56(5)	F(13)-P(2)-F(11)#4	90.14(8)
N(2)-CU1-N(1)	76.44(5)	F(11)-P(2)-F(11)#4	180
N(1)#1-CU1-N(1)	93.02(12)		
N(1)#2-CU1-N(1)	152.87(11)		
N(1)#3-CU1-N(1)	93.28(12)		

Appendix 9: Supplementary information for chapter VI.

Table 1. Crystal data and structure refinement for $[Fe(\mathbf{1a})_2](PF_6)_2$, **Chapter VI.**

Empirical formula	C46 H34 Br2 F12 Fe N8 P2
Formula weight	1204.42
Temperature	100(2)K
Wavelength	1.54178 Å
Crystal system	Triclinic
Space group	P-1
Unit cell dimensions	a = 10.1585(2) Å α = 93.4240(10)° b = 11.4649(2) Å β = 100.5180(10)° c = 22.6626(3) Å γ = 113.1240(10)°
Volume	2361.24(7)Å^3
Z	2
Density (calculated)	1.694 g/cm^3
Absorption coefficient	6.003 mm^{-1}
F(000)	1200
Crystal size	0.34 x 0.07 x 0.05 mm
Theta range for data collection	2.00 to 73.02°
Index ranges	$-12 \le h \le 12$, $-14 \le k \le 14$, $-27 \le \ell \le 28$
Reflections collected	29279
Independent reflections	9061 [R_{int} = 0.040]
Absorption correction	Semi-empirical from equivalents
Max. and min. transmission	0.8100 and 0.5200
Refinement method	Full-matrix least-squares on F^2
Data / restraints / parameters	9061 / 0 / 642
Goodness-of-fit on F^2	1.035
Final R indices [I>2sigma(I)]	R_1 = 0.0515, wR_2 = 0.1294
R indices (all data)	R_1 = 0.0651, wR_2 = 0.1366
Largest diff. peak and hole	0.950 and -0.488 e/Å^3

Table 2. Bond lengths [Å] and angles [°] for $[Fe(\mathbf{1a})_2](PF_6)_2$, **Chapter VI.**

Fe(3)-N(2)	1.876(3)	C(37)-C(38)	1.400(6)
Fe(3)-N(5)	1.877(3)	C(38)-C(39)	1.370(6)
Fe(3)-N(1)	1.970(4)	C(39)-C(40)	1.387(6)
Fe(3)-N(3)	1.972(3)	C(40)-C(41)	1.396(6)
Fe(3)-N(6)	1.974(3)	C(40)-Br(2)	1.894(4)
Fe(3)-N(4)	1.974(3)	C(41)-C(42)	1.388(5)
N(1)-C(1)	1.356(5)	P(1)-F(12)	1.584(3)
N(1)-C(5)	1.361(5)	P(1)-F(13)	1.596(3)
N(2)-C(6)	1.353(5)	P(1)-F(16)	1.598(3)
N(2)-C(10)	1.358(5)	P(1)-F(15)	1.599(3)
N(3)-C(15)	1.340(5)	P(1)-F(11)	1.600(3)
N(3)-C(11)	1.374(5)	P(1)-F(14)	1.611(3)
C(1)-C(2)	1.385(6)	P(2)-F(21)	1.593(3)
C(2)-C(3)	1.385(6)	P(2)-F(25)	1.595(3)
C(3)-C(4)	1.394(6)	P(2)-F(22)	1.597(3)
C(4)-C(5)	1.387(5)	P(2)-F(23)	1.599(3)
C(5)-C(6)	1.470(6)	P(2)-F(24)	1.607(3)
C(6)-C(7)	1.386(5)	P(2)-F(26)	1.615(3)
C(7)-C(8)	1.402(6)	C(51)-C(52)	1.477(7)
C(8)-C(9)	1.410(6)	C(52)-N(53)	1.129(7)
C(8)-C(16)	1.474(5)	C(61)-C(62)	1.447(7)
C(9)-C(10)	1.380(6)	C(62)-N(63)	1.114(7)
C(10)-C(11)	1.464(5)	N(2)-FE3-N(5)	178.83(14)
C(11)-C(12)	1.387(6)	N(2)-FE3-N(1)	81.41(14)
C(12)-C(13)	1.387(6)	N(5)-FE3-N(1)	99.67(14)
C(13)-C(14)	1.392(6)	N(2)-FE3-N(3)	80.75(14)
C(14)-C(15)	1.383(6)	N(5)-FE3-N(3)	98.17(14)
C(16)-C(17)	1.398(6)	N(1)-FE3-N(3)	162.14(14)
C(16)-C(21)	1.402(6)	N(2)-FE3-N(6)	99.45(14)
C(17)-C(18)	1.387(5)	N(5)-FE3-N(6)	81.06(14)
C(18)-C(19)	1.384(6)	N(1)-FE3-N(6)	89.03(14)
C(19)-C(20)	1.391(6)	N(3)-FE3-N(6)	94.59(14)
C(19)-Br(1)	1.899(4)	N(2)-FE3-N(4)	98.36(14)
C(20)-C(21)	1.383(5)	N(5)-FE3-N(4)	81.12(14)
N(4)-C(22)	1.346(5)	N(1)-FE3-N(4)	93.74(14)
N(4)-C(26)	1.362(5)	N(3)-FE3-N(4)	88.14(14)
N(5)-C(31)	1.345(5)	N(6)-FE3-N(4)	162.19(14)
N(5)-C(27)	1.358(5)	C(1)-N(1)-C(5)	117.8(4)
N(6)-C(36)	1.346(5)	C(1)-N(1)-FE3	127.8(3)
N(6)-C(32)	1.376(5)	C(5)-N(1)-FE3	114.2(3)
C(22)-C(23)	1.384(6)	C(6)-N(2)-C(10)	120.5(3)
C(23)-C(24)	1.393(6)	C(6)-N(2)-FE3	119.0(3)
C(24)-C(25)	1.384(6)	C(10)-N(2)-FE3	120.2(3)
C(25)-C(26)	1.392(6)	C(15)-N(3)-C(11)	117.9(4)
C(26)-C(27)	1.470(5)	C(15)-N(3)-FE3	127.5(3)
C(27)-C(28)	1.373(6)	C(11)-N(3)-FE3	114.5(3)
C(28)-C(29)	1.423(5)	N(1)-C(1)-C(2)	122.2(4)
C(29)-C(30)	1.403(6)	C(3)-C(2)-C(1)	119.6(4)
C(29)-C(37)	1.471(5)	C(2)-C(3)-C(4)	118.8(4)
C(30)-C(31)	1.385(5)	C(5)-C(4)-C(3)	118.8(4)
C(31)-C(32)	1.469(5)	N(1)-C(5)-C(4)	122.6(4)
C(32)-C(33)	1.385(6)	N(1)-C(5)-C(6)	113.3(3)
C(33)-C(34)	1.386(6)	C(4)-C(5)-C(6)	124.1(4)
C(34)-C(35)	1.390(5)	N(2)-C(6)-C(7)	120.8(4)
C(35)-C(36)	1.378(6)	N(2)-C(6)-C(5)	111.4(3)
C(37)-C(42)	1.399(6)	C(7)-C(6)-C(5)	127.8(4)

C(6)-C(7)-C(8)	119.8(4)	C(30)-C(31)-C(32)	127.1(4)
C(7)-C(8)-C(9)	118.4(4)	N(6)-C(32)-C(33)	122.1(4)
C(7)-C(8)-C(16)	120.7(4)	N(6)-C(32)-C(31)	113.0(3)
C(9)-C(8)-C(16)	120.9(4)	C(33)-C(32)-C(31)	124.8(4)
C(10)-C(9)-C(8)	119.3(4)	C(32)-C(33)-C(34)	118.9(4)
N(2)-C(10)-C(9)	121.3(4)	C(33)-C(34)-C(35)	119.1(4)
N(2)-C(10)-C(11)	110.7(3)	C(36)-C(35)-C(34)	119.3(4)
C(9)-C(10)-C(11)	128.1(4)	N(6)-C(36)-C(35)	122.7(4)
N(3)-C(11)-C(12)	121.1(4)	C(42)-C(37)-C(38)	117.9(4)
N(3)-C(11)-C(10)	113.6(4)	C(42)-C(37)-C(29)	121.2(4)
C(12)-C(11)-C(10)	125.2(4)	C(38)-C(37)-C(29)	120.9(4)
C(13)-C(12)-C(11)	120.1(4)	C(39)-C(38)-C(37)	121.9(4)
C(12)-C(13)-C(14)	118.7(4)	C(38)-C(39)-C(40)	119.1(4)
C(15)-C(14)-C(13)	118.6(4)	C(39)-C(40)-C(41)	121.1(4)
N(3)-C(15)-C(14)	123.6(4)	C(39)-C(40)-BR2	119.5(3)
C(17)-C(16)-C(21)	118.7(4)	C(41)-C(40)-BR2	119.3(3)
C(17)-C(16)-C(8)	120.1(4)	C(42)-C(41)-C(40)	118.7(4)
C(21)-C(16)-C(8)	121.2(4)	C(41)-C(42)-C(37)	121.2(4)
C(18)-C(17)-C(16)	120.6(4)	F(12)-P(1)-F(13)	90.94(17)
C(19)-C(18)-C(17)	119.3(4)	F(12)-P(1)-F(16)	90.82(19)
C(18)-C(19)-C(20)	121.4(4)	F(13)-P(1)-F(16)	90.83(15)
C(18)-C(19)-BR1	118.8(3)	F(12)-P(1)-F(15)	90.15(15)
C(20)-C(19)-BR1	119.9(3)	F(13)-P(1)-F(15)	178.83(18)
C(21)-C(20)-C(19)	118.8(4)	F(16)-P(1)-F(15)	89.60(15)
C(20)-C(21)-C(16)	121.1(4)	F(12)-P(1)-F(11)	90.55(17)
C(22)-N(4)-C(26)	118.7(4)	F(13)-P(1)-F(11)	89.33(15)
C(22)-N(4)-FE3	126.9(3)	F(16)-P(1)-F(11)	178.62(19)
C(26)-N(4)-FE3	114.3(3)	F(15)-P(1)-F(11)	90.21(15)
C(31)-N(5)-C(27)	120.3(3)	F(12)-P(1)-F(14)	178.65(18)
C(31)-N(5)-FE3	119.8(3)	F(13)-P(1)-F(14)	90.39(17)
C(27)-N(5)-FE3	119.8(3)	F(16)-P(1)-F(14)	89.41(18)
C(36)-N(6)-C(32)	117.7(3)	F(15)-P(1)-F(14)	88.53(16)
C(36)-N(6)-FE3	127.7(3)	F(11)-P(1)-F(14)	89.21(17)
C(32)-N(6)-FE3	114.3(3)	F(21)-P(2)-F(25)	90.43(18)
N(4)-C(22)-C(23)	122.2(4)	F(21)-P(2)-F(22)	90.55(17)
C(22)-C(23)-C(24)	119.2(4)	F(25)-P(2)-F(22)	90.03(17)
C(25)-C(24)-C(23)	119.0(4)	F(21)-P(2)-F(23)	90.49(17)
C(24)-C(25)-C(26)	119.2(4)	F(25)-P(2)-F(23)	178.98(17)
N(4)-C(26)-C(25)	121.7(4)	F(22)-P(2)-F(23)	89.53(16)
N(4)-C(26)-C(27)	114.0(4)	F(21)-P(2)-F(24)	90.14(18)
C(25)-C(26)-C(27)	124.2(4)	F(25)-P(2)-F(24)	90.42(16)
N(5)-C(27)-C(28)	121.1(4)	F(22)-P(2)-F(24)	179.17(19)
N(5)-C(27)-C(26)	110.7(3)	F(23)-P(2)-F(24)	90.00(16)
C(28)-C(27)-C(26)	128.1(4)	F(21)-P(2)-F(26)	179.54(17)
C(27)-C(28)-C(29)	120.0(4)	F(25)-P(2)-F(26)	90.02(16)
C(30)-C(29)-C(28)	117.2(4)	F(22)-P(2)-F(26)	89.56(16)
C(30)-C(29)-C(37)	122.0(4)	F(23)-P(2)-F(26)	89.06(15)
C(28)-C(29)-C(37)	120.8(4)	F(24)-P(2)-F(26)	89.75(16)
C(31)-C(30)-C(29)	120.0(4)	N(53)-C(52)-C(51)	179.3(6)
N(5)-C(31)-C(30)	121.4(4)	N(63)-C(62)-C(61)	177.1(8)
N(5)-C(31)-C(32)	111.6(3)		

Table 1. Crystal data and structure refinement for $[Fe(\mathbf{1b})_2](ClO_4)_2$, **Chapter VI.**

Empirical formula	C44 H33 Br2 Cl2 Fe N13 O8
Formula weight	1158.40
Temperature	100(2)K
Wavelength	1.54178 Å
Crystal system	Triclinic
Space group	P-1
Unit cell dimensions	a = 10.7253(9) Å α = 74.638(5)° b = 15.1165(11) Å β = 73.791(5)° c = 15.5248(10) Å γ = 89.096(5)°
Volume	2326.0(3)Å^3
Z	2
Density (calculated)	1.654 g/cm^3
Absorption coefficient	6.254 mm^{-1}
F(000)	1164
Crystal size	0.34 x 0.21 x 0.12 mm
Theta range for data collection	3.04 to 73.34°
Index ranges	$-12 \leq h \leq 13$, $-18 \leq k \leq 18$, $-19 \leq \ell \leq 19$
Reflections collected	27650
Independent reflections	8842 [R_{int} = 0.069]
Absorption correction	Semi-empirical from equivalents
Max. and min. transmission	0.5300 and 0.2100
Refinement method	Full-matrix least-squares on F^2
Data / restraints / parameters	8842 / 0 / 634
Goodness-of-fit on F^2	1.023
Final R indices [I>2sigma(I)]	R_1 = 0.0711, wR_2 = 0.1894
R indices (all data)	R_1 = 0.0820, wR_2 = 0.2312
Largest diff. peak and hole	1.175 and -1.694 e/Å^3

Table 2. Bond lengths [Å] and angles [°] for $[Fe(\mathbf{1b})_2](ClO_4)_2$, **Chapter VI.**

Fe(1)-N(2)	1.869(4)	C(35)-C(36)	1.396(7)
Fe(1)-N(7)	1.870(4)	C(36)-C(37)	1.377(7)
Fe(1)-N(1)	1.986(4)	C(37)-C(38)	1.398(7)
Fe(1)-N(8)	1.996(4)	C(37)-Br(2)	1.890(4)
Fe(1)-N(3)	2.005(4)	C(38)-C(39)	1.386(7)
Fe(1)-N(6)	2.006(4)	Cl(1)-O(11)	1.437(4)
N(1)-C(1)	1.350(6)	Cl(1)-O(12)	1.441(4)
N(1)-C(5)	1.365(6)	Cl(1)-O(13)	1.444(3)
N(2)-C(8)	1.316(6)	Cl(1)-O(14)	1.446(4)
N(2)-C(6)	1.368(7)	Cl(2)-O(24)	1.433(4)
N(3)-C(13)	1.327(6)	Cl(2)-O(21)	1.439(4)
N(3)-C(9)	1.365(6)	Cl(2)-O(23)	1.443(4)
N(4)-C(6)	1.310(6)	Cl(2)-O(22)	1.444(4)
N(4)-C(7)	1.345(7)	C(51)-C(52)	1.451(8)
N(5)-C(8)	1.334(6)	C(52)-N(53)	1.155(8)
N(5)-C(7)	1.352(7)	C(61)-C(62)	1.463(8)
N(6)-C(21)	1.347(7)	C(62)-N(63)	1.139(7)
N(6)-C(25)	1.370(6)	C(71)-C(72)	1.454(8)
N(7)-C(28)	1.330(7)	C(72)-N(73)	1.141(8)
N(7)-C(26)	1.359(6)	N(2)-FE1-N(7)	175.90(18)
N(8)-C(33)	1.343(6)	N(2)-FE1-N(1)	80.62(18)
N(8)-C(29)	1.370(6)	N(7)-FE1-N(1)	99.66(18)
N(9)-C(26)	1.317(6)	N(2)-FE1-N(8)	96.52(16)
N(9)-C(27)	1.359(6)	N(7)-FE1-N(8)	79.40(16)
N(10)-C(28)	1.323(6)	N(1)-FE1-N(8)	89.35(18)
N(10)-C(27)	1.355(6)	N(2)-FE1-N(3)	79.03(17)
C(1)-C(2)	1.373(8)	N(7)-FE1-N(3)	100.65(17)
C(2)-C(3)	1.380(8)	N(1)-FE1-N(3)	159.64(16)
C(3)-C(4)	1.387(7)	N(8)-FE1-N(3)	93.06(16)
C(4)-C(5)	1.404(7)	N(2)-FE1-N(6)	104.34(17)
C(5)-C(6)	1.451(7)	N(7)-FE1-N(6)	79.74(17)
C(7)-C(14)	1.464(6)	N(1)-FE1-N(6)	93.07(18)
C(8)-C(9)	1.478(7)	N(8)-FE1-N(6)	159.11(16)
C(9)-C(10)	1.386(7)	N(3)-FE1-N(6)	91.84(17)
C(10)-C(11)	1.391(7)	C(1)-N(1)-C(5)	117.2(4)
C(11)-C(12)	1.386(7)	C(1)-N(1)-FE1	128.9(3)
C(12)-C(13)	1.381(8)	C(5)-N(1)-FE1	113.8(3)
C(14)-C(19)	1.383(7)	C(8)-N(2)-C(6)	116.3(4)
C(14)-C(15)	1.419(8)	C(8)-N(2)-FE1	122.9(3)
C(15)-C(16)	1.386(7)	C(6)-N(2)-FE1	119.8(3)
C(16)-C(17)	1.374(8)	C(13)-N(3)-C(9)	117.9(4)
C(17)-C(18)	1.370(8)	C(13)-N(3)-FE1	127.4(3)
C(17)-Br(1)	1.904(5)	C(9)-N(3)-FE1	114.7(3)
C(18)-C(19)	1.392(7)	C(6)-N(4)-C(7)	116.0(4)
C(21)-C(22)	1.389(7)	C(8)-N(5)-C(7)	114.5(4)
C(22)-C(23)	1.372(8)	C(21)-N(6)-C(25)	117.4(4)
C(23)-C(24)	1.398(7)	C(21)-N(6)-FE1	127.7(3)
C(24)-C(25)	1.388(7)	C(25)-N(6)-FE1	114.8(3)
C(25)-C(26)	1.468(7)	C(28)-N(7)-C(26)	116.7(4)
C(27)-C(34)	1.470(6)	C(28)-N(7)-FE1	122.1(3)
C(28)-C(29)	1.469(6)	C(26)-N(7)-FE1	121.2(3)
C(29)-C(30)	1.371(7)	C(33)-N(8)-C(29)	116.7(4)
C(30)-C(31)	1.397(6)	C(33)-N(8)-FE1	128.5(3)
C(31)-C(32)	1.381(7)	C(29)-N(8)-FE1	114.8(3)
C(32)-C(33)	1.377(7)	C(26)-N(9)-C(27)	115.3(4)
C(34)-C(39)	1.393(7)	C(28)-N(10)-C(27)	114.4(4)
C(34)-C(35)	1.401(6)	N(1)-C(1)-C(2)	122.3(5)

C(1)-C(2)-C(3)	121.2(5)	N(9)-C(26)-C(25)	125.3(4)
C(2)-C(3)-C(4)	117.8(5)	N(7)-C(26)-C(25)	111.0(4)
C(3)-C(4)-C(5)	118.8(5)	N(10)-C(27)-N(9)	125.1(4)
N(1)-C(5)-C(4)	122.6(4)	N(10)-C(27)-C(34)	116.9(4)
N(1)-C(5)-C(6)	114.2(4)	N(9)-C(27)-C(34)	117.8(4)
C(4)-C(5)-C(6)	123.2(4)	N(10)-C(28)-N(7)	124.9(4)
N(4)-C(6)-N(2)	123.3(5)	N(10)-C(28)-C(29)	124.2(4)
N(4)-C(6)-C(5)	125.9(5)	N(7)-C(28)-C(29)	110.9(4)
N(2)-C(6)-C(5)	110.7(4)	N(8)-C(29)-C(30)	123.3(4)
N(4)-C(7)-N(5)	124.7(4)	N(8)-C(29)-C(28)	112.7(4)
N(4)-C(7)-C(14)	117.3(5)	C(30)-C(29)-C(28)	124.1(4)
N(5)-C(7)-C(14)	117.9(5)	C(29)-C(30)-C(31)	119.0(4)
N(2)-C(8)-N(5)	124.9(5)	C(32)-C(31)-C(30)	118.0(5)
N(2)-C(8)-C(9)	110.5(4)	C(33)-C(32)-C(31)	120.0(4)
N(5)-C(8)-C(9)	124.5(4)	N(8)-C(33)-C(32)	123.1(4)
N(3)-C(9)-C(10)	123.2(4)	C(39)-C(34)-C(35)	119.3(4)
N(3)-C(9)-C(8)	112.6(4)	C(39)-C(34)-C(27)	120.2(4)
C(10)-C(9)-C(8)	124.2(4)	C(35)-C(34)-C(27)	120.5(4)
C(9)-C(10)-C(11)	117.7(4)	C(36)-C(35)-C(34)	119.9(5)
C(12)-C(11)-C(10)	119.0(5)	C(37)-C(36)-C(35)	119.4(4)
C(13)-C(12)-C(11)	119.7(5)	C(36)-C(37)-C(38)	121.7(4)
N(3)-C(13)-C(12)	122.5(4)	C(36)-C(37)-BR2	119.0(3)
C(19)-C(14)-C(15)	119.0(4)	C(38)-C(37)-BR2	119.2(4)
C(19)-C(14)-C(7)	122.0(5)	C(39)-C(38)-C(37)	118.3(5)
C(15)-C(14)-C(7)	119.0(5)	C(38)-C(39)-C(34)	121.2(4)
C(16)-C(15)-C(14)	119.4(5)	O(11)-CL1-O(12)	110.2(3)
C(17)-C(16)-C(15)	119.8(5)	O(11)-CL1-O(13)	109.6(2)
C(18)-C(17)-C(16)	121.9(5)	O(12)-CL1-O(13)	109.2(2)
C(18)-C(17)-BR1	119.9(4)	O(11)-CL1-O(14)	109.8(2)
C(16)-C(17)-BR1	118.1(4)	O(12)-CL1-O(14)	108.7(2)
C(17)-C(18)-C(19)	118.9(5)	O(13)-CL1-O(14)	109.4(2)
C(14)-C(19)-C(18)	121.0(5)	O(24)-CL2-O(21)	109.0(3)
N(6)-C(21)-C(22)	122.2(5)	O(24)-CL2-O(23)	109.5(3)
C(23)-C(22)-C(21)	120.2(5)	O(21)-CL2-O(23)	109.9(3)
C(22)-C(23)-C(24)	118.7(5)	O(24)-CL2-O(22)	109.6(3)
C(25)-C(24)-C(23)	118.5(5)	O(21)-CL2-O(22)	109.5(3)
N(6)-C(25)-C(24)	122.7(5)	O(23)-CL2-O(22)	109.3(3)
N(6)-C(25)-C(26)	112.8(4)	N(53)-C(52)-C(51)	178.2(6)
C(24)-C(25)-C(26)	124.5(4)	N(63)-C(62)-C(61)	179.3(6)
N(9)-C(26)-N(7)	123.5(5)	N(73)-C(72)-C(71)	178.9(8)

Table 1. Crystal data and structure refinement for $[Fe(\mathbf{1c})_2](PF_6)(ClO_4)$, **chapter VI.**

Identification code	gary81
Empirical formula	C42 H32 Br2 Cl F6 Fe N18 O4 P
Formula weight	1248.95
Temperature	100(2)K
Wavelength	1.54178 $A
Crystal system	Monoclinic
Space group	C2/c
Unit cell dimensions	a = 27.0294(15) Å alpha = 90 ° b = 9.2400(5) Å beta = 106.461(3) ° c = 39.652(2) Å gamma = 90 °
Volume	9497.3(9) $Å^3$
Z	8
Density (calculated)	1.747 g/cm^3
Absorption coefficient	6.135 mm^*1
F(000)	4992
Crystal size	0.48 x 0.14 x 0.06 mm
Theta range for data collection	2.32 to 55.13 °
Index ranges	-28<=h<=28, -9<=k<=9, -42<=l<=41
Reflections collected	38944
Independent reflections	5939 [R(int) = 0.072]
Absorption correction	Semi-empirical from equivalents
Max. and min. transmission	0.7700 and 0.2900
Refinement method	Full-matrix least-squares on F^2
Data / restraints / parameters	5939 / 27 / 641
Goodness-of-fit on F^2	1.012
Final R indices [I>2sigma(I)]	R1 = 0.0779, wR2 = 0.2064
R indices (all data)	R1 = 0.1463, wR2 = 0.2373
Largest diff. peak and hole	1.746 and -1.438 e. $Å^3$

Table 2. Bond lengths [Å] and angles [°] for $[Fe(\mathbf{1c})_2](PF_6)(ClO_4)$, **Chapter VI.**

Fe-N(9)	1.876(9)	C(29)-C(34)	1.393(15)
Fe-N(2)	1.879(9)	C(29)-C(30)	1.419(16)
Fe-N(8)	1.982(9)	C(30)-C(31)	1.378(15)
Fe-N(3)	1.983(8)	C(31)-C(32)	1.446(18)
Fe-N(1)	1.987(8)	C(32)-C(33)	1.367(18)
Fe-N(10)	1.993(9)	C(32)-Br(2)	1.919(13)
N(1)-C(1)	1.344(12)	C(33)-C(34)	1.385(16)
N(1)-C(4)	1.363(12)	P(1)-F(16)	1.547(8)
N(2)-C(7)	1.334(12)	P(1)-F(13)	1.575(8)
N(2)-C(5)	1.346(11)	P(1)-F(12)	1.586(7)
N(3)-C(11)	1.305(12)	P(1)-F(11)	1.602(9)
N(3)-C(8)	1.344(12)	P(1)-F(15)	1.614(9)
N(4)-C(3)	1.306(13)	P(1)-F(14)	1.617(8)
N(4)-C(2)	1.340(13)	Cl-O(11)	1.425(8)
N(5)-C(5)	1.319(12)	Cl-O(14)	1.436(8)
N(5)-C(6)	1.352(13)	Cl-O(12)	1.438(8)
N(6)-C(7)	1.323(12)	Cl-O(13)	1.457(8)
N(6)-C(6)	1.343(12)	C(41)-C(42)	1.52(2)
N(7)-C(10)	1.313(13)	C(42)-N(43)	1.08(2)
N(7)-C(9)	1.337(12)	C(51)-C(52)	1.523(19)
N(8)-C(21)	1.361(13)	C(52)-N(53)	1.132(18)
N(8)-C(18)	1.364(12)	C(61)-C(62)	1.395(19)
N(9)-C(24)	1.337(12)	C(62)-N(63)	1.135(15)
N(9)-C(22)	1.340(13)	C(71)-C(72)	1.491(19)
N(10)-C(28)	1.325(13)	C(72)-N(73)	1.120(16)
N(10)-C(25)	1.369(12)	N(9)-FE-N(2)	178.0(4)
N(11)-C(20)	1.335(13)	N(9)-FE-N(8)	80.5(4)
N(11)-C(19)	1.354(14)	N(2)-FE-N(8)	98.3(4)
N(12)-C(22)	1.336(13)	N(9)-FE-N(3)	98.6(4)
N(12)-C(23)	1.370(13)	N(2)-FE-N(3)	79.7(4)
N(13)-C(24)	1.325(13)	N(8)-FE-N(3)	89.8(3)
N(13)-C(23)	1.353(14)	N(9)-FE-N(1)	101.4(4)
N(14)-C(27)	1.321(14)	N(2)-FE-N(1)	80.2(4)
N(14)-C(26)	1.329(14)	N(8)-FE-N(1)	93.9(3)
C(1)-C(2)	1.391(14)	N(3)-FE-N(1)	159.9(4)
C(3)-C(4)	1.405(13)	N(9)-FE-N(10)	79.0(4)
C(4)-C(5)	1.485(14)	N(2)-FE-N(10)	102.2(4)
C(6)-C(12)	1.450(15)	N(8)-FE-N(10)	159.5(4)
C(7)-C(8)	1.442(13)	N(3)-FE-N(10)	93.3(3)
C(8)-C(9)	1.407(14)	N(1)-FE-N(10)	90.0(3)
C(10)-C(11)	1.401(14)	C(1)-N(1)-C(4)	115.1(9)
C(12)-C(17)	1.369(14)	C(1)-N(1)-FE	130.5(7)
C(12)-C(13)	1.403(14)	C(4)-N(1)-FE	114.4(7)
C(13)-C(14)	1.379(14)	C(7)-N(2)-C(5)	117.0(9)
C(14)-C(15)	1.387(15)	C(7)-N(2)-FE	121.1(7)
C(15)-C(16)	1.356(14)	C(5)-N(2)-FE	121.8(7)
C(15)-Br(1)	1.913(12)	C(11)-N(3)-C(8)	116.7(9)
C(16)-C(17)	1.360(14)	C(11)-N(3)-FE	129.7(8)
C(18)-C(19)	1.368(15)	C(8)-N(3)-FE	113.6(6)
C(20)-C(21)	1.372(15)	C(3)-N(4)-C(2)	116.6(1)
C(21)-C(22)	1.468(14)	C(5)-N(5)-C(6)	115.6(9)
C(23)-C(29)	1.463(15)	C(7)-N(6)-C(6)	116.7(9)
C(24)-C(25)	1.434(15)	C(10)-N(7)-C(9)	113.7(9)
C(25)-C(26)	1.375(15)	C(21)-N(8)-C(18)	116.1(9)
C(27)-C(28)	1.418(15)	C(21)-N(8)-FE	115.3(7)

C(18)-N(8)-FE	128.5(8)	N(12)-C(22)-C(21)	124.10(11)
C(24)-N(9)-C(22)	118.6(9)	N(9)-C(22)-C(21)	112.6(1)
C(24)-N(9)-FE	121.8(8)	N(13)-C(23)-N(12)	125.9(1)
C(22)-N(9)-FE	119.6(7)	N(13)-C(23)-C(29)	116.6(1)
C(28)-N(10)-C(25)	117.4(9)	N(12)-C(23)-C(29)	117.40(11)
C(28)-N(10)-FE	128.3(8)	N(13)-C(24)-N(9)	123.40(11)
C(25)-N(10)-FE	114.3(8)	N(13)-C(24)-C(25)	125.9(1)
C(20)-N(11)-C(19)	116.1(1)	N(9)-C(24)-C(25)	110.7(1)
C(22)-N(12)-C(23)	113.9(1)	N(10)-C(25)-C(26)	121.20(11)
C(24)-N(13)-C(23)	114.7(9)	N(10)-C(25)-C(24)	114.0(1)
C(27)-N(14)-C(26)	117.3(1)	C(26)-C(25)-C(24)	124.7(1)
N(1)-C(1)-C(2)	122.3(1)	N(14)-C(26)-C(25)	121.70(11)
N(4)-C(2)-C(1)	122.00(11)	N(14)-C(27)-C(28)	122.60(11)
N(4)-C(3)-C(4)	122.8(1)	N(10)-C(28)-C(27)	119.60(11)
N(1)-C(4)-C(3)	121.2(1)	C(34)-C(29)-C(30)	118.70(11)
N(1)-C(4)-C(5)	114.2(9)	C(34)-C(29)-C(23)	120.90(11)
C(3)-C(4)-C(5)	124.4(1)	C(30)-C(29)-C(23)	120.30(11)
N(5)-C(5)-N(2)	123.8(9)	C(31)-C(30)-C(29)	120.40(12)
N(5)-C(5)-C(4)	126.7(9)	C(30)-C(31)-C(32)	117.20(13)
N(2)-C(5)-C(4)	109.4(9)	C(33)-C(32)-C(31)	123.90(12)
N(6)-C(6)-N(5)	123.7(1)	C(33)-C(32)-BR2	119.0(1)
N(6)-C(6)-C(12)	117.7(1)	C(31)-C(32)-BR2	117.10(12)
N(5)-C(6)-C(12)	118.6(9)	C(32)-C(33)-C(34)	116.30(13)
N(6)-C(7)-N(2)	123.1(9)	C(33)-C(34)-C(29)	123.40(13)
N(6)-C(7)-C(8)	127.1(1)	F(16)-P(1)-F(13)	91.1(5)
N(2)-C(7)-C(8)	109.8(9)	F(16)-P(1)-F(12)	91.7(5)
N(3)-C(8)-C(9)	120.0(9)	F(13)-P(1)-F(12)	88.9(4)
N(3)-C(8)-C(7)	115.6(9)	F(16)-P(1)-F(11)	177.6(5)
C(9)-C(8)-C(7)	124.3(1)	F(13)-P(1)-F(11)	89.9(5)
N(7)-C(9)-C(8)	123.80(11)	F(12)-P(1)-F(11)	90.5(5)
N(7)-C(10)-C(11)	124.0(1)	F(16)-P(1)-F(15)	89.9(5)
N(3)-C(11)-C(10)	121.8(1)	F(13)-P(1)-F(15)	179.0(5)
C(17)-C(12)-C(13)	117.4(1)	F(12)-P(1)-F(15)	90.9(4)
C(17)-C(12)-C(6)	121.8(1)	F(11)-P(1)-F(15)	89.1(5)
C(13)-C(12)-C(6)	120.8(1)	F(16)-P(1)-F(14)	88.9(4)
C(14)-C(13)-C(12)	122.40(11)	F(13)-P(1)-F(14)	91.0(4)
C(13)-C(14)-C(15)	116.1(1)	F(12)-P(1)-F(14)	179.4(5)
C(16)-C(15)-C(14)	122.70(11)	F(11)-P(1)-F(14)	88.9(4)
C(16)-C(15)-BR1	119.8(9)	F(15)-P(1)-F(14)	89.1(4)
C(14)-C(15)-BR1	117.5(8)	O(11)-CL-O(14)	109.5(5)
C(15)-C(16)-C(17)	119.40(11)	O(11)-CL-O(12)	108.6(5)
C(16)-C(17)-C(12)	121.60(11)	O(14)-CL-O(12)	110.0(5)
N(8)-C(18)-C(19)	119.9(1)	O(11)-CL-O(13)	108.7(5)
N(11)-C(19)-C(18)	123.80(11)	O(14)-CL-O(13)	109.1(5)
N(11)-C(20)-C(21)	121.40(11)	O(12)-CL-O(13)	110.8(5)
N(8)-C(21)-C(20)	122.7(1)	N(43)-C(42)-C(41)	176(4)
N(8)-C(21)-C(22)	112.0(1)	N(53)-C(52)-C(51)	177(3)
C(20)-C(21)-C(22)	125.20(11)	N(63)-C(62)-C(61)	176.10(16)
N(12)-C(22)-N(9)	123.3(1)	N(73)-C(72)-C(71)	162(4)

Table 1. Crystal data and structure refinement for $[Fe(\mathbf{1d})_2](ClO_4)_2$, **chapter VI.**

Identification code	gary91
Empirical formula	C46 H38 Br2 Cl2 Fe N12 O8
Formula weight	1173.45
Temperature	150(2)K
Wavelength	1.54178 Å
Crystal system	Monoclinic
Space group	C2/c
Unit cell dimensions	a = 19.4190(4) Å α = 90° b = 10.2896(2) Å β = 98.8900(10)° c = 24.4899(5) Å γ = 90°
Volume	4834.63(17)Å^3
Z	4
Density (calculated)	1.612 Mg/m^3
Absorption coefficient	6.019 mm^{-1}
F(000)	2368
Crystal size	0.45 x 0.30 x 0.15 mm
Theta range for data collection	3.65 to 58.20°
Index ranges	$-21 \le h \le 21$, $-11 \le k \le 11$, $-26 \le \ell \le 26$
Reflections collected	20606
Independent reflections	3342 [R_{int} = 0.048]
Absorption correction	Semi-empirical from equivalents
Max. and min. transmission	0.5500 and 0.2200
Refinement method	Full-matrix least-squares on F^2
Data / restraints / parameters	3342 / 69 / 387
Goodness-of-fit on F^2	0.951
Final R indices [I>2sigma(I)]	R_1 = 0.0603, wR_2 = 0.1543
R indices (all data)	R_1 = 0.0877, wR_2 = 0.1700
Largest diff. peak and hole	0.520 and -0.412 e/Å^3

Table 2. Bond lengths [Å] and angles [°] for $[Fe(\mathbf{1d})_2](ClO_4)_2$, **chapter VI.**

Fe(1)-N(2)#1	2.084(5)	N(5)-FE1-N(1)#1	146.68(18)
Fe(1)-N(2)	2.084(5)	N(5)#1-FE1-N(1)#1	92.40(15)
Fe(1)-N(5)	2.254(4)	N(2)#1-FE1-N(1)	100.14(17)
Fe(1)-N(5)#1	2.254(4)	N(2)-FE1-N(1)	72.37(17)
Fe(1)-N(1)#1	2.369(4)	N(5)-FE1-N(1)	92.40(15)
Fe(1)-N(1)	2.369(4)	N(5)#1-FE1-N(1)	146.68(18)
N(1)-C(6)	1.341(7)	N(1)#1-FE1-N(1)	96.4(2)
N(1)-C(1)	1.359(6)	C(6)-N(1)-C(1)	116.5(5)
N(2)-C(7)	1.336(7)	C(6)-N(1)-FE1	112.3(3)
N(2)-C(9)	1.350(6)	C(1)-N(1)-FE1	131.2(4)
N(3)-C(7)	1.322(7)	C(7)-N(2)-C(9)	115.0(5)
N(3)-C(8)	1.335(6)	C(7)-N(2)-FE1	122.6(4)
N(4)-C(9)	1.305(8)	C(9)-N(2)-FE1	120.8(4)
N(4)-C(8)	1.348(7)	C(7)-N(3)-C(8)	115.7(5)
N(5)-C(16)	1.341(7)	C(9)-N(4)-C(8)	115.7(5)
N(5)-C(21)	1.362(7)	C(16)-N(5)-C(21)	116.3(5)
C(1)-C(3)	1.389(9)	C(16)-N(5)-FE1	128.9(4)
C(1)-C(2)	1.486(9)	C(21)-N(5)-FE1	114.7(4)
C(3)-C(4)	1.343(9)	N(1)-C(1)-C(3)	121.4(6)
C(4)-C(5)	1.381(8)	N(1)-C(1)-C(2)	119.2(5)
C(5)-C(6)	1.382(8)	C(3)-C(1)-C(2)	119.3(5)
C(6)-C(7)	1.475(7)	C(4)-C(3)-C(1)	120.3(6)
C(8)-C(10)	1.468(9)	C(3)-C(4)-C(5)	120.1(7)
C(9)-C(21)#1	1.493(8)	C(4)-C(5)-C(6)	116.9(7)
C(10)-C(15)	1.375(7)	N(1)-C(6)-C(5)	124.8(5)
C(10)-C(11)	1.386(9)	N(1)-C(6)-C(7)	116.2(5)
C(11)-C(12)	1.388(9)	C(5)-C(6)-C(7)	119.0(6)
C(12)-C(13)	1.378(8)	N(3)-C(7)-N(2)	124.6(5)
C(13)-C(14)	1.373(9)	N(3)-C(7)-C(6)	120.3(5)
C(13)-Br(1)	1.895(6)	N(2)-C(7)-C(6)	115.0(6)
C(14)-C(15)	1.373(8)	N(3)-C(8)-N(4)	124.0(6)
C(16)-C(18)	1.382(8)	N(3)-C(8)-C(10)	118.7(5)
C(16)-C(17)	1.498(9)	N(4)-C(8)-C(10)	117.2(5)
C(18)-C(19)	1.398(9)	N(4)-C(9)-N(2)	124.8(6)
C(19)-C(20)	1.358(9)	N(4)-C(9)-C(21)#1	120.2(5)
C(20)-C(21)	1.386(7)	N(2)-C(9)-C(21)#1	114.7(6)
C(21)-C(9)#1	1.493(8)	C(15)-C(10)-C(11)	119.0(6)
Cl(1)-O(3)	1.332(14)	C(15)-C(10)-C(8)	121.1(6)
Cl(1)-O(1)	1.338(15)	C(11)-C(10)-C(8)	119.8(5)
Cl(1)-O(4)	1.383(15)	C(10)-C(11)-C(12)	120.9(6)
Cl(1)-O(2)	1.390(16)	C(13)-C(12)-C(11)	118.5(7)
Cl(2)-O(7)	1.323(10)	C(14)-C(13)-C(12)	120.9(6)
Cl(2)-O(5)	1.336(9)	C(14)-C(13)-BR1	119.5(4)
Cl(2)-O(8)	1.370(14)	C(12)-C(13)-BR1	119.3(6)
Cl(2)-O(6)	1.421(12)	C(15)-C(14)-C(13)	119.9(6)
C(31)-C(32)	1.422(19)	C(14)-C(15)-C(10)	120.6(6)
C(32)-N(33)	1.131(18)	N(5)-C(16)-C(18)	122.9(7)
C(41)-C(42)	1.43(3)	N(5)-C(16)-C(17)	116.5(5)
C(42)-N(43)	1.13(2)	C(18)-C(16)-C(17)	120.6(6)
N(2)#1-FE1-N(2)	169.1(2)	C(16)-C(18)-C(19)	118.8(6)
N(2)#1-FE1-N(5)	74.46(18)	C(20)-C(19)-C(18)	120.1(5)
N(2)-FE1-N(5)	113.15(18)	C(19)-C(20)-C(21)	117.3(6)
N(2)#1-FE1-N(5)#1	113.15(18)	N(5)-C(21)-C(20)	124.6(6)
N(2)-FE1-N(5)#1	74.46(18)	N(5)-C(21)-C(9)#1	114.7(5)
N(5)-FE1-N(5)#1	97.6(2)	C(20)-C(21)-C(9)#1	120.7(6)
N(2)#1-FE1-N(1)#1	72.37(17)	O(3)-CL1-O(1)	110.20(18)
N(2)-FE1-N(1)#1	100.14(17)	O(3)-CL1-O(4)	107.10(12)

O(1)-CL1-O(4)	113.00(14)	O(7)-CL2-O(6)	110.10(11)
O(3)-CL1-O(2)	105.10(13)	O(5)-CL2-O(6)	87.4(8)
O(1)-CL1-O(2)	100.20(14)	O(8)-CL2-O(6)	107.6(1)
O(4)-CL1-O(2)	120.80(12)	N(33)-C(32)-C(31)	144(5)
O(7)-CL2-O(5)	120.8(1)	N(43)-C(42)-C(41)	139(4)
O(7)-CL2-O(8)	113.8(9)		
O(5)-CL2-O(8)	113.30(12)		

Appendix 10: Supplementary information for chapter VII.

Table 1. Crystal data and structure refinement for **$[CuL1]_2(PF_6)_2$, chapter VII.**

Empirical formula	C58 H36 Br2 Cu2 F12 N14 P2
Formula weight	1505.85
Temperature	220(2)K
Wavelength	1.54178 Å
Crystal system	Monoclinic
Space group	P21/c
Unit cell dimensions	a = 17.2216(15) Å α = 90° b = 27.920(2) Å β = 98.733(4)° c = 13.7457(12) Å γ = 90°
Volume	6532.7(10)Å^3
Z	4
Density (calculated)	1.531 g/cm^3
Absorption coefficient	3.425 mm^{-1}
F(000)	2992
Crystal size	0.35 x 0.25 x 0.06 mm
Theta range for data collection	2.60 to 54.91°
Index ranges	$-18 \le h \le 18$, $-28 \le k \le 27$, $-14 \le \ell \le 14$
Reflections collected	77402
Independent reflections	8070 [R_{int} = 0.072]
Absorption correction	Semi-empirical from equivalents
Max. and min. transmission	0.8600 and 0.5100
Refinement method	Full-matrix least-squares on F^2
Data / restraints / parameters	8070 / 144 / 904
Goodness-of-fit on F^2	1.062
Final R indices [I>2sigma(I)]	R1 = 0.1034, wR_2 = 0.3117
R indices (all data)	R1 = 0.1386, wR_2 = 0.3300
Largest diff. peak and hole	1.900 and -0.647 e/Å^3

To finish the structure, it was decided to use the PLATON (Spek, 2000) facility SQUEEZE to handle the disordered solvent. PLATON identified a remarkably large potential solvent volume of 1057.9Å^3, or 16.1% of the cell volume. The use of PLATON/SQUEEZE resulted in a 2.6% improvement in R1 while correcting for 193 electrons/cell. The reported structure is based on the PLATON/SQUEEZE corrected data. The actual solvent content is unknown, so several quantities reported in table 1 [empirical formula, density, absorption coefficient, F(000)] are incorrect and should be indicated as such in future publications.

Table 2. Atomic coordinates (x 10^4) and equivalent isotropic displacement parameters (Å^2 x 10^3) for **$[CuL1]_2(PF_6)_2$, chapter VII.**

U_{eq} is defined as one third of the trace of the orthogonalized Uij tensor.

	Occ.	x	y	z	U_{eq}
Cu(1)	1	2724(1)	5379(1)	1237(1)	58(1)
N(1)	1	1540(6)	4739(3)	972(7)	62(3)
N(2)	1	3155(5)	4681(3)	1226(5)	45(2)
N(3)	1	3925(5)	5500(3)	1187(6)	45(2)
N(4)	1	3520(4)	6378(2)	1971(6)	39(2)
N(5)	1	3039(5)	6462(3)	3710(7)	52(2)
N(6)	1	5128(5)	5077(3)	1188(5)	41(2)
N(7)	1	5105(5)	5931(3)	1067(6)	43(2)
C(1)	1	784(7)	4785(5)	978(10)	75(4)
C(2)	1	312(7)	4449(5)	1274(10)	75(4)
C(3)	1	645(9)	4028(6)	1618(13)	106(5)
C(4)	1	1427(8)	3968(5)	1618(10)	79(4)
C(5)	1	1873(6)	4316(4)	1292(8)	55(3)
C(6)	1	2727(6)	4262(3)	1290(7)	46(3)
C(7)	1	3096(7)	3838(3)	1354(8)	53(3)
C(8)	1	3907(7)	3806(3)	1368(8)	53(3)
C(9)	1	4337(6)	4218(3)	1322(7)	49(3)
C(10)	1	3934(6)	4644(3)	1245(6)	36(2)
C(11)	1	4368(6)	5110(3)	1201(6)	39(2)
C(12)	1	5490(6)	5520(4)	1140(6)	44(3)
C(13)	1	4356(6)	5916(3)	1125(7)	42(2)
C(14)	1	3909(6)	6366(3)	1196(8)	45(3)
C(15)	1	3893(7)	6734(4)	537(8)	57(3)
C(16)	1	3431(8)	7127(4)	639(10)	72(4)
C(17)	1	3025(6)	7147(3)	1426(9)	58(3)
C(18)	1	3090(5)	6775(3)	2106(7)	42(2)
C(19)	1	2734(6)	6777(3)	3015(8)	48(3)
C(20)	1	2111(7)	7085(4)	3159(10)	67(3)
C(21)	1	1822(8)	7056(4)	4024(11)	72(4)
C(22)	1	2135(9)	6736(5)	4730(10)	84(4)
C(23)	1	2750(8)	6443(4)	4553(9)	67(3)
C(24)	1	6351(6)	5516(4)	1202(7)	47(3)
C(25)	1	6792(7)	5097(4)	1305(8)	59(3)
C(26)	1	7583(7)	5113(5)	1427(10)	74(4)
C(27)	1	7966(7)	5556(5)	1426(9)	72(4)
C(28)	1	7553(7)	5969(4)	1317(9)	64(3)
C(29)	1	6751(7)	5957(4)	1209(8)	55(3)
Br(1)	1	9077(1)	5570(1)	1620(1)	103(1)
Cu(2)	1	3871(1)	6020(1)	3286(1)	64(1)
N(8)	1	4928(6)	6647(3)	3484(7)	70(3)

N(9)	1	4934(5)	5681(3)	3585(6)	44(2)
N(10)	1	3540(5)	5256(3)	3474(6)	50(2)
N(11)	1	2123(4)	5575(3)	2342(6)	43(2)
N(12)	1	2022(5)	5902(3)	528(6)	45(2)
N(13)	1	4142(6)	4509(3)	3833(6)	51(2)
N(14)	1	2748(6)	4581(3)	3677(6)	53(2)
C(30)	1	4878(9)	7107(5)	3337(11)	90(4)
C(31)	1	5492(11)	7378(5)	3081(10)	89(4)
C(32)	1	6180(11)	7172(5)	3032(11)	91(4)
C(33)	1	6249(8)	6672(4)	3205(9)	76(4)
C(34)	1	5610(8)	6426(5)	3436(8)	65(3)
C(35)	1	5647(7)	5898(4)	3587(6)	50(3)
C(36)	1	6350(7)	5646(4)	3705(8)	61(3)
C(37)	1	6327(8)	5157(5)	3808(8)	63(3)
C(38)	1	5635(7)	4929(5)	3813(7)	58(3)
C(39)	1	4943(6)	5203(4)	3695(7)	48(3)
C(40)	1	4163(7)	4973(4)	3666(7)	50(3)
C(41)	1	3418(8)	4330(4)	3827(7)	56(3)
C(42)	1	2834(6)	5040(4)	3465(7)	48(3)
C(43)	1	2146(6)	5346(4)	3193(8)	47(3)
C(44)	1	1552(8)	5388(5)	3755(10)	81(4)
C(45)	1	956(7)	5693(6)	3490(11)	88(4)
C(46)	1	923(7)	5960(4)	2608(10)	69(3)
C(47)	1	1508(6)	5882(4)	2027(8)	47(3)
C(48)	1	1516(6)	6086(3)	1075(8)	46(3)
C(49)	1	1020(7)	6478(4)	704(10)	64(3)
C(50)	1	1060(7)	6659(4)	-181(11)	72(4)
C(51)	1	1592(8)	6474(4)	-731(10)	76(4)
C(52)	1	2067(7)	6103(4)	-344(9)	56(3)
C(53)	1	3338(8)	3786(4)	3985(8)	59(3)
C(54)	1	4012(8)	3518(4)	4058(8)	65(3)
C(55)	1	3954(10)	3015(5)	4210(9)	83(4)
C(56)	1	3214(12)	2837(4)	4301(9)	85(5)
C(57)	1	2539(11)	3111(5)	4213(11)	95(4)
C(58)	1	2620(9)	3595(4)	4067(9)	74(4)
Br(2)	1	3136(2)	2167(1)	4537(1)	134(1)
P(1)	1	6408(2)	3546(1)	2473(2)	69(1)
F(11)	1	6433(7)	3198(3)	3375(6)	129(3)
F(12)	0.50	7150(30)	3377(19)	2280(40)	230(20)
F(13)	0.50	7040(30)	3880(12)	3130(20)	153(15)
F(14)	0.50	5707(19)	3821(15)	2880(30)	133(16)
F(15)	0.50	5780(30)	3221(14)	1860(30)	140(20)
F(16)	1	6351(5)	3904(3)	1551(6)	110(3)
F(122)	0.50	7200(20)	3630(20)	2870(30)	240(30)
F(123)	0.50	6200(40)	3956(11)	3070(30)	163(18)
F(124)	0.50	5591(19)	3404(15)	1980(40)	138(18)
F(125)	0.50	6720(20)	3132(8)	1816(14)	106(9)
P(2)	1	227(3)	7875(2)	1449(4)	109(2)
F(21)	0.30	300(30)	7623(17)	580(30)	138(14)
F(22)	0.30	310(20)	7350(30)	2230(30)	150(20)
F(23)	0.30	-340(30)	7517(19)	810(40)	150(20)
F(24)	0.30	-70(60)	8327(12)	1010(50)	210(30)
F(25)	0.30	1130(30)	7984(11)	1840(40)	150(20)
F(26)	0.30	-700(40)	7760(30)	1800(70)	260(40)
F(211)	0.70	1038(11)	7690(7)	1249(17)	144(6)
F(221)	0.70	40(30)	7361(11)	1580(40)	255(17)
F(231)	0.70	175(18)	8133(16)	430(20)	243(16)
F(241)	0.70	606(18)	8359(11)	1780(30)	255(13)
F(251)	0.70	378(18)	7908(13)	2532(14)	223(11)
F(261)	0.70	-588(12)	8073(11)	1460(20)	187(10)

Table 3. Hydrogen coordinates (x 10^4) and isotropic displacement parameters ($Å^2$ x 10^3) for **$[CuL1]_2(PF_6)_2$, chapter VII.**

	Occ.	x	y	z	U_{eq}
H(1)	1	552	5078	757	90
H(2)	1	-230	4503	1243	90
H(3)	1	342	3786	1850	127
H(4)	1	1665	3679	1850	95
H(7)	1	2803	3556	1391	63
H(8)	1	4156	3506	1409	64
H(9)	1	4885	4208	1341	58
H(15)	1	4193	6718	21	69
H(16)	1	3393	7377	179	86
H(17)	1	2703	7412	1504	70
H(20)	1	1901	7303	2669	80
H(21)	1	1408	7257	4138	87
H(22)	1	1936	6714	5328	101
H(23)	1	2967	6225	5042	80
H(25)	1	6536	4799	1290	71
H(26)	1	7877	4828	1513	88
H(28)	1	7816	6264	1315	76
H(29)	1	6463	6245	1140	66
H(30)	1	4406	7263	3408	108
H(31)	1	5421	7706	2942	107
H(32)	1	6608	7352	2886	109
H(33)	1	6722	6512	3162	91
H(36)	1	6831	5807	3714	73
H(37)	1	6796	4980	3876	76
H(38)	1	5618	4595	3894	69
H(44)	1	1564	5201	4326	97
H(45)	1	562	5731	3889	105
H(46)	1	519	6182	2419	83
H(49)	1	665	6607	1089	77
H(50)	1	727	6911	-428	87
H(51)	1	1631	6598	-1358	91
H(52)	1	2443	5984	-713	67
H(54)	1	4498	3661	4008	78
H(55)	1	4395	2814	4247	100
H(57)	1	2047	2973	4252	114
H(58)	1	2177	3795	4023	89

Table 4. Anisotropic parameters ($Å^2$ x 10^3) for **$[CuL1]_2(PF_6)_2$, chapter VII.**

The anisotropic displacement factor exponent takes the form:

$$-2\pi^2 [h^2 a^{*2} U_{11} + ... + 2 h k a^* b^* U_{12}]$$

	U11	U22	U33	U23	U13	U12
Cu(1)	77(1)	38(1)	60(1)	4(1)	15(1)	24(1)
N(1)	52(7)	38(6)	96(7)	6(5)	8(5)	6(5)
N(2)	63(6)	28(5)	44(5)	-10(4)	11(4)	-4(4)
N(3)	63(6)	25(5)	51(5)	-1(4)	17(4)	22(4)
N(4)	44(5)	20(4)	54(5)	-3(3)	11(4)	5(4)
N(5)	55(6)	35(5)	67(6)	-8(4)	12(5)	4(4)
N(6)	41(5)	31(5)	50(5)	-4(4)	0(4)	1(4)
N(7)	45(6)	33(5)	53(5)	-2(4)	11(4)	8(4)
C(1)	50(9)	59(9)	115(11)	-4(7)	4(7)	2(6)
C(2)	58(8)	59(9)	105(10)	-11(7)	4(7)	-17(7)
C(3)	77(11)	73(11)	179(17)	31(10)	54(10)	-12(8)
C(4)	86(11)	54(9)	96(10)	27(7)	8(8)	0(7)
C(5)	55(8)	48(8)	63(7)	-19(6)	9(6)	-14(6)
C(6)	69(8)	26(6)	42(6)	-8(4)	3(5)	2(5)
C(7)	60(8)	18(6)	79(8)	-9(5)	8(6)	-6(5)
C(8)	75(9)	17(6)	66(7)	-14(5)	6(6)	7(5)
C(9)	63(7)	21(6)	61(7)	-7(5)	10(5)	7(5)
C(10)	42(7)	26(6)	39(6)	-3(4)	0(5)	0(4)
C(11)	46(7)	31(6)	40(6)	-6(4)	9(5)	-6(5)
C(12)	60(7)	42(7)	30(5)	-2(4)	5(5)	10(6)
C(13)	55(7)	28(6)	38(6)	-3(4)	-3(5)	3(5)
C(14)	52(7)	34(6)	49(6)	-7(5)	7(6)	2(5)
C(15)	77(8)	47(7)	54(7)	-9(6)	27(6)	7(6)
C(16)	93(9)	44(8)	82(9)	14(6)	25(8)	27(7)
C(17)	63(7)	21(6)	91(9)	-1(6)	13(7)	7(5)
C(18)	44(6)	34(6)	51(6)	-2(5)	12(5)	4(5)
C(19)	65(7)	19(6)	59(7)	-11(5)	3(6)	5(5)
C(20)	69(8)	40(7)	92(10)	-11(6)	11(7)	13(6)
C(21)	83(9)	48(8)	96(10)	-19(7)	47(8)	12(6)
C(22)	116(11)	63(9)	80(9)	0(7)	39(8)	27(8)
C(23)	94(10)	62(8)	51(7)	-4(6)	30(7)	2(7)
C(24)	48(7)	52(8)	40(6)	-6(5)	2(5)	10(5)
C(25)	63(8)	33(7)	82(8)	-9(5)	14(6)	5(6)
C(26)	56(9)	59(9)	105(10)	-21(7)	13(7)	13(7)
C(27)	75(9)	76(10)	72(8)	-18(7)	33(7)	9(8)
C(28)	58(8)	51(8)	85(9)	-3(6)	21(7)	5(6)
C(29)	54(8)	38(7)	75(8)	6(5)	12(6)	4(5)
Br(1)	55(1)	110(1)	144(2)	-37(1)	13(1)	8(1)
Cu(2)	89(1)	48(1)	56(1)	8(1)	17(1)	29(1)
N(8)	66(7)	34(7)	102(8)	4(5)	-15(6)	-3(5)
N(9)	60(6)	26(5)	48(5)	1(4)	13(4)	-2(4)
N(10)	68(7)	39(5)	44(5)	1(4)	11(5)	14(5)
N(11)	42(5)	22(4)	62(6)	8(4)	-1(4)	3(4)
N(12)	47(5)	32(5)	56(6)	0(4)	6(4)	9(4)
N(13)	74(7)	29(6)	50(5)	-5(4)	11(5)	0(5)
N(14)	73(7)	33(6)	57(6)	4(4)	22(5)	-1(5)
C(30)	82(10)	52(10)	126(12)	-5(8)	-15(9)	6(8)
C(31)	114(13)	46(9)	102(11)	-10(7)	-3(10)	-17(9)
C(32)	122(14)	53(10)	96(10)	-4(7)	14(10)	-20(9)
C(33)	92(10)	51(9)	94(9)	-20(7)	42(8)	-17(7)

C(34)	70(9)	81(10)	41(7)	7(6)	1(6)	-21(8)
C(35)	80(9)	45(7)	20(5)	-3(4)	-4(5)	-1(6)
C(36)	66(8)	56(9)	59(7)	-2(6)	4(6)	4(6)
C(37)	67(9)	58(9)	60(7)	-7(6)	-3(6)	16(7)
C(38)	57(8)	74(8)	40(6)	6(5)	0(5)	12(7)
C(39)	66(8)	39(7)	39(6)	-10(5)	12(5)	8(6)
C(40)	83(9)	27(7)	40(6)	4(4)	7(6)	2(6)
C(41)	91(10)	34(7)	42(6)	-1(5)	7(6)	-3(7)
C(42)	60(8)	39(7)	46(6)	1(5)	16(5)	-9(6)
C(43)	45(7)	43(7)	52(7)	-3(5)	5(5)	2(5)
C(44)	67(9)	106(11)	72(9)	18(7)	20(7)	11(8)
C(45)	49(8)	125(13)	96(11)	5(9)	30(7)	24(8)
C(46)	58(8)	60(8)	90(10)	-5(7)	13(7)	15(6)
C(47)	39(6)	42(7)	58(7)	-17(5)	7(5)	-11(5)
C(48)	46(6)	34(6)	60(7)	-12(5)	12(5)	0(5)
C(49)	56(8)	41(7)	89(9)	14(7)	-8(7)	11(5)
C(50)	58(8)	42(7)	112(11)	20(8)	0(8)	15(6)
C(51)	90(10)	60(9)	77(9)	20(7)	13(8)	18(7)
C(52)	64(8)	34(7)	66(8)	-1(6)	-2(6)	1(5)
C(53)	90(10)	39(7)	48(7)	7(5)	10(6)	4(7)
C(54)	102(10)	39(8)	51(7)	-7(5)	-2(7)	-5(7)
C(55)	122(13)	52(10)	74(9)	-5(7)	8(9)	12(8)
C(56)	166(16)	30(8)	64(8)	-1(6)	30(9)	-6(9)
C(57)	133(14)	53(10)	100(11)	-3(8)	20(10)	-15(9)
C(58)	116(12)	16(7)	92(9)	15(6)	19(8)	-2(6)
Br(2)	247(3)	31(1)	123(1)	7(1)	20(2)	-19(1)
P(1)	77(3)	50(2)	79(2)	2(2)	11(2)	12(2)
F(11)	192(10)	87(6)	106(6)	32(5)	19(6)	37(6)
F(12)	190(40)	240(40)	280(50)	40(30)	140(40)	160(30)
F(13)	210(40)	110(20)	122(19)	-18(16)	-40(20)	-70(20)
F(14)	120(20)	180(30)	109(19)	70(20)	65(15)	75(19)
F(15)	250(60)	80(20)	107(18)	-35(16)	40(30)	-80(30)
F(16)	167(8)	68(5)	103(6)	14(4)	48(6)	-3(5)
F(122)	100(20)	340(50)	280(40)	-240(40)	-10(20)	20(30)
F(123)	280(50)	83(18)	150(20)	-31(14)	100(30)	80(30)
F(124)	72(15)	110(30)	220(40)	30(30)	-15(18)	4(17)
F(125)	170(30)	72(12)	69(10)	-22(9)	10(12)	75(13)
P(2)	106(4)	103(4)	116(4)	-13(3)	6(3)	33(3)
F(21)	140(40)	110(30)	150(30)	-50(30)	20(30)	70(30)
F(22)	90(20)	250(60)	110(30)	90(40)	20(20)	90(30)
F(23)	130(40)	140(40)	170(40)	30(30)	-60(30)	-70(30)
F(24)	350(80)	15(18)	220(50)	20(20)	-110(50)	0(30)
F(25)	240(50)	16(16)	160(30)	-8(17)	-90(30)	-10(20)
F(26)	170(50)	260(70)	350(70)	150(60)	30(50)	140(50)
F(211)	95(12)	155(17)	197(17)	50(14)	78(13)	36(11)
F(221)	320(50)	140(30)	330(50)	-10(30)	130(40)	0(30)
F(231)	250(30)	290(40)	180(20)	90(20)	-2(19)	140(30)
F(241)	200(20)	170(30)	390(40)	-100(30)	10(30)	-48(19)
F(251)	300(30)	270(30)	92(12)	-81(16)	-9(15)	-30(20)
F(261)	102(13)	140(20)	320(30)	30(20)	46(16)	34(14)

Table 5. Bond lengths [Å] and angles [°] for $[CuL1]_2(PF_6)_2$, **chapter VII.**

Cu(1)-N(11)	2.039(8)	C(25)-H(25)	0.9400
Cu(1)-N(12)	2.045(8)	C(26)-C(27)	1.401(17)
Cu(1)-N(2)	2.086(8)	C(26)-H(26)	0.9400
Cu(1)-N(3)	2.108(8)	C(27)-C(28)	1.354(16)
N(1)-C(1)	1.311(14)	C(27)-Br(1)	1.892(13)
N(1)-C(5)	1.357(14)	C(28)-C(29)	1.367(15)
N(2)-C(10)	1.342(12)	C(28)-H(28)	0.9400
N(2)-C(6)	1.393(12)	C(29)-H(29)	0.9400
N(3)-C(11)	1.328(12)	Cu(2)-N(9)	2.047(8)
N(3)-C(13)	1.387(12)	Cu(2)-N(10)	2.234(9)
N(4)-C(14)	1.342(12)	N(8)-C(30)	1.301(15)
N(4)-C(18)	1.360(12)	N(8)-C(34)	1.338(15)
N(4)-Cu(2)	2.073(8)	N(9)-C(39)	1.343(12)
N(5)-C(23)	1.331(13)	N(9)-C(35)	1.370(13)
N(5)-C(19)	1.345(13)	N(10)-C(40)	1.325(13)
N(5)-Cu(2)	2.042(8)	N(10)-C(42)	1.356(13)
N(6)-C(11)	1.314(11)	N(11)-C(43)	1.328(12)
N(6)-C(12)	1.391(12)	N(11)-C(47)	1.379(12)
N(7)-C(13)	1.305(12)	N(12)-C(48)	1.336(12)
N(7)-C(12)	1.323(12)	N(12)-C(52)	1.337(13)
C(1)-C(2)	1.345(17)	N(13)-C(40)	1.317(13)
C(1)-H(1)	0.9400	N(13)-C(41)	1.344(14)
C(2)-C(3)	1.361(18)	N(14)-C(42)	1.327(12)
C(2)-H(2)	0.9400	N(14)-C(41)	1.339(14)
C(3)-C(4)	1.357(18)	C(30)-C(31)	1.387(19)
C(3)-H(3)	0.9400	C(30)-H(30)	0.9400
C(4)-C(5)	1.356(16)	C(31)-C(32)	1.328(19)
C(4)-H(4)	0.9400	C(31)-H(31)	0.9400
C(5)-C(6)	1.478(14)	C(32)-C(33)	1.416(18)
C(6)-C(7)	1.341(14)	C(32)-H(32)	0.9400
C(7)-C(8)	1.397(14)	C(33)-C(34)	1.375(16)
C(7)-H(7)	0.9400	C(33)-H(33)	0.9400
C(8)-C(9)	1.374(14)	C(34)-C(35)	1.488(17)
C(8)-H(8)	0.9400	C(35)-C(36)	1.388(15)
C(9)-C(10)	1.374(13)	C(36)-C(37)	1.375(15)
C(9)-H(9)	0.9400	C(36)-H(36)	0.9400
C(10)-C(11)	1.507(13)	C(37)-C(38)	1.353(16)
C(12)-C(24)	1.473(14)	C(37)-H(37)	0.9400
C(13)-C(14)	1.485(14)	C(38)-C(39)	1.406(14)
C(14)-C(15)	1.367(14)	C(38)-H(38)	0.9400
C(15)-C(16)	1.376(15)	C(39)-C(40)	1.482(15)
C(15)-H(15)	0.9400	C(41)-C(53)	1.541(16)
C(16)-C(17)	1.374(15)	C(42)-C(43)	1.462(14)
C(16)-H(16)	0.9400	C(43)-C(44)	1.377(15)
C(17)-C(18)	1.390(14)	C(44)-C(45)	1.343(18)
C(17)-H(17)	0.9400	C(44)-H(44)	0.9400
C(18)-C(19)	1.472(14)	C(45)-C(46)	1.417(18)
C(19)-C(20)	1.413(14)	C(45)-H(45)	0.9400
C(20)-C(21)	1.359(17)	C(46)-C(47)	1.394(15)
C(20)-H(20)	0.9400	C(46)-H(46)	0.9400
C(21)-C(22)	1.369(17)	C(47)-C(48)	1.430(15)
C(21)-H(21)	0.9400	C(48)-C(49)	1.432(14)
C(22)-C(23)	1.387(17)	C(49)-C(50)	1.328(16)
C(22)-H(22)	0.9400	C(49)-H(49)	0.9400
C(23)-H(23)	0.9400	C(50)-C(51)	1.374(17)
C(24)-C(25)	1.390(14)	C(50)-H(50)	0.9400
C(24)-C(29)	1.411(14)	C(51)-C(52)	1.377(16)
C(25)-C(26)	1.348(15)	C(51)-H(51)	0.9400

C(52)-H(52)	0.9400	C(1)-C(2)-H(2)	121.1
C(53)-C(58)	1.368(17)	C(3)-C(2)-H(2)	121.1
C(53)-C(54)	1.372(16)	C(4)-C(3)-C(2)	118.2(12)
C(54)-C(55)	1.423(17)	C(4)-C(3)-H(3)	120.9
C(54)-H(54)	0.9400	C(2)-C(3)-H(3)	120.9
C(55)-C(56)	1.39(2)	C(5)-C(4)-C(3)	121.6(12)
C(55)-H(55)	0.9400	C(5)-C(4)-H(4)	119.2
C(56)-C(57)	1.38(2)	C(3)-C(4)-H(4)	119.2
C(56)-Br(2)	1.907(12)	C(4)-C(5)-N(1)	119.8(11)
C(57)-C(58)	1.376(17)	C(4)-C(5)-C(6)	122.8(11)
C(57)-H(57)	0.9400	N(1)-C(5)-C(6)	117.3(9)
C(58)-H(58)	0.9400	C(7)-C(6)-N(2)	119.7(10)
P(1)-F(122)	1.42(3)	C(7)-C(6)-C(5)	123.5(10)
P(1)-F(12)	1.43(2)	N(2)-C(6)-C(5)	116.8(9)
P(1)-F(123)	1.48(2)	C(6)-C(7)-C(8)	121.3(9)
P(1)-F(124)	1.52(3)	C(6)-C(7)-H(7)	119.3
P(1)-F(15)	1.55(4)	C(8)-C(7)-H(7)	119.3
P(1)-F(11)	1.569(9)	C(9)-C(8)-C(7)	119.5(9)
P(1)-F(14)	1.60(3)	C(9)-C(8)-H(8)	120.3
P(1)-F(13)	1.60(2)	C(7)-C(8)-H(8)	120.3
P(1)-F(16)	1.605(8)	C(10)-C(9)-C(8)	117.3(10)
P(1)-F(125)	1.612(18)	C(10)-C(9)-H(9)	121.4
P(2)-F(21)	1.41(3)	C(8)-C(9)-H(9)	121.4
P(2)-F(24)	1.46(4)	N(2)-C(10)-C(9)	124.1(9)
P(2)-F(251)	1.475(19)	N(2)-C(10)-C(11)	115.6(8)
P(2)-F(221)	1.49(3)	C(9)-C(10)-C(11)	120.3(9)
P(2)-F(261)	1.51(2)	N(6)-C(11)-N(3)	128.9(8)
P(2)-F(241)	1.54(2)	N(6)-C(11)-C(10)	116.1(8)
P(2)-F(211)	1.553(14)	N(3)-C(11)-C(10)	114.9(9)
P(2)-F(231)	1.56(3)	N(7)-C(12)-N(6)	123.5(9)
P(2)-F(23)	1.57(4)	N(7)-C(12)-C(24)	120.0(9)
P(2)-F(25)	1.60(4)	N(6)-C(12)-C(24)	116.4(9)
P(2)-F(26)	1.77(8)	N(7)-C(13)-N(3)	125.1(8)
P(2)-F(22)	1.80(5)	N(7)-C(13)-C(14)	120.1(9)
F(21)-F(23)	1.23(6)	N(3)-C(13)-C(14)	114.7(9)
F(23)-F(26)	1.72(10)	N(4)-C(14)-C(15)	123.0(9)
F(241)-F(251)	1.71(4)	N(4)-C(14)-C(13)	113.6(9)
N(11)-Cu(1)-N(12)	80.4(3)	C(15)-C(14)-C(13)	123.4(9)
N(11)-Cu(1)-N(2)	118.5(3)	C(14)-C(15)-C(16)	119.0(10)
N(12)-Cu(1)-N(2)	148.1(3)	C(14)-C(15)-H(15)	120.5
N(11)-Cu(1)-N(3)	126.4(3)	C(16)-C(15)-H(15)	120.5
N(12)-Cu(1)-N(3)	112.5(3)	C(17)-C(16)-C(15)	119.0(11)
N(2)-Cu(1)-N(3)	78.3(3)	C(17)-C(16)-H(16)	120.5
C(1)-N(1)-C(5)	117.1(10)	C(15)-C(16)-H(16)	120.5
C(10)-N(2)-C(6)	118.1(8)	C(16)-C(17)-C(18)	120.0(10)
C(10)-N(2)-Cu(1)	115.4(6)	C(16)-C(17)-H(17)	120.0
C(6)-N(2)-Cu(1)	126.2(7)	C(18)-C(17)-H(17)	120.0
C(11)-N(3)-C(13)	112.1(8)	N(4)-C(18)-C(17)	120.4(9)
C(11)-N(3)-Cu(1)	115.7(6)	N(4)-C(18)-C(19)	115.1(8)
C(13)-N(3)-Cu(1)	132.3(6)	C(17)-C(18)-C(19)	124.5(9)
C(14)-N(4)-C(18)	118.5(8)	N(5)-C(19)-C(20)	121.4(10)
C(14)-N(4)-Cu(2)	124.4(6)	N(5)-C(19)-C(18)	115.7(9)
C(18)-N(4)-Cu(2)	111.5(6)	C(20)-C(19)-C(18)	123.0(10)
C(23)-N(5)-C(19)	119.2(9)	C(21)-C(20)-C(19)	118.3(12)
C(23)-N(5)-Cu(2)	126.6(8)	C(21)-C(20)-H(20)	120.9
C(19)-N(5)-Cu(2)	114.0(7)	C(19)-C(20)-H(20)	120.9
C(11)-N(6)-C(12)	113.1(8)	C(20)-C(21)-C(22)	120.1(11)
C(13)-N(7)-C(12)	117.0(8)	C(20)-C(21)-H(21)	120.0
N(1)-C(1)-C(2)	125.4(12)	C(22)-C(21)-H(21)	120.0
N(1)-C(1)-H(1)	117.3	C(21)-C(22)-C(23)	119.4(12)
C(2)-C(1)-H(1)	117.3	C(21)-C(22)-H(22)	120.3
C(1)-C(2)-C(3)	117.8(12)	C(23)-C(22)-H(22)	120.3

N(5)-C(23)-C(22)	121.7(12)	C(35)-C(36)-H(36)	120.8
N(5)-C(23)-H(23)	119.2	C(38)-C(37)-C(36)	120.6(11)
C(22)-C(23)-H(23)	119.2	C(38)-C(37)-H(37)	119.7
C(25)-C(24)-C(29)	118.5(10)	C(36)-C(37)-H(37)	119.7
C(25)-C(24)-C(12)	122.8(10)	C(37)-C(38)-C(39)	118.4(12)
C(29)-C(24)-C(12)	118.6(9)	C(37)-C(38)-H(38)	120.8
C(26)-C(25)-C(24)	120.7(11)	C(39)-C(38)-H(38)	120.8
C(26)-C(25)-H(25)	119.7	N(9)-C(39)-C(38)	123.3(11)
C(24)-C(25)-H(25)	119.7	N(9)-C(39)-C(40)	115.6(9)
C(25)-C(26)-C(27)	119.8(11)	C(38)-C(39)-C(40)	121.1(10)
C(25)-C(26)-H(26)	120.1	N(13)-C(40)-N(10)	125.2(11)
C(27)-C(26)-H(26)	120.1	N(13)-C(40)-C(39)	118.0(10)
C(28)-C(27)-C(26)	120.9(12)	N(10)-C(40)-C(39)	116.8(9)
C(28)-C(27)-Br(1)	120.1(10)	N(14)-C(41)-N(13)	125.6(10)
C(26)-C(27)-Br(1)	119.0(10)	N(14)-C(41)-C(53)	116.4(11)
C(27)-C(28)-C(29)	119.7(11)	N(13)-C(41)-C(53)	118.0(11)
C(27)-C(28)-H(28)	120.1	N(14)-C(42)-N(10)	123.8(10)
C(29)-C(28)-H(28)	120.1	N(14)-C(42)-C(43)	120.5(10)
C(28)-C(29)-C(24)	120.4(10)	N(10)-C(42)-C(43)	115.7(9)
C(28)-C(29)-H(29)	119.8	N(11)-C(43)-C(44)	121.8(10)
C(24)-C(29)-H(29)	119.8	N(11)-C(43)-C(42)	114.9(9)
N(5)-Cu(2)-N(9)	150.1(3)	C(44)-C(43)-C(42)	123.2(10)
N(5)-Cu(2)-N(4)	80.4(3)	C(45)-C(44)-C(43)	120.3(12)
N(9)-Cu(2)-N(4)	122.1(3)	C(45)-C(44)-H(44)	119.9
N(5)-Cu(2)-N(10)	110.0(3)	C(43)-C(44)-H(44)	119.9
N(9)-Cu(2)-N(10)	76.7(3)	C(44)-C(45)-C(46)	119.7(11)
N(4)-Cu(2)-N(10)	121.1(3)	C(44)-C(45)-H(45)	120.2
C(30)-N(8)-C(34)	119.1(12)	C(46)-C(45)-H(45)	120.2
C(39)-N(9)-C(35)	116.4(9)	C(47)-C(46)-C(45)	118.1(11)
C(39)-N(9)-Cu(2)	118.5(7)	C(47)-C(46)-H(46)	121.0
C(35)-N(9)-Cu(2)	124.7(7)	C(45)-C(46)-H(46)	121.0
C(40)-N(10)-C(42)	115.8(9)	N(11)-C(47)-C(46)	120.3(10)
C(40)-N(10)-Cu(2)	112.3(7)	N(11)-C(47)-C(48)	115.0(9)
C(42)-N(10)-Cu(2)	131.9(7)	C(46)-C(47)-C(48)	124.7(10)
C(43)-N(11)-C(47)	119.7(9)	N(12)-C(48)-C(47)	117.3(9)
C(43)-N(11)-Cu(1)	125.2(6)	N(12)-C(48)-C(49)	119.9(10)
C(47)-N(11)-Cu(1)	112.6(6)	C(47)-C(48)-C(49)	122.8(10)
C(48)-N(12)-C(52)	118.4(9)	C(50)-C(49)-C(48)	120.3(12)
C(48)-N(12)-Cu(1)	113.3(7)	C(50)-C(49)-H(49)	119.8
C(52)-N(12)-Cu(1)	127.9(7)	C(48)-C(49)-H(49)	119.8
C(40)-N(13)-C(41)	114.6(9)	C(49)-C(50)-C(51)	119.6(11)
C(42)-N(14)-C(41)	114.8(9)	C(49)-C(50)-H(50)	120.2
N(8)-C(30)-C(31)	122.8(14)	C(51)-C(50)-H(50)	120.2
N(8)-C(30)-H(30)	118.6	C(50)-C(51)-C(52)	118.5(12)
C(31)-C(30)-H(30)	118.6	C(50)-C(51)-H(51)	120.8
C(32)-C(31)-C(30)	119.8(15)	C(52)-C(51)-H(51)	120.8
C(32)-C(31)-H(31)	120.1	N(12)-C(52)-C(51)	123.3(11)
C(30)-C(31)-H(31)	120.1	N(12)-C(52)-H(52)	118.3
C(31)-C(32)-C(33)	118.1(15)	C(51)-C(52)-H(52)	118.3
C(31)-C(32)-H(32)	121.0	C(58)-C(53)-C(54)	123.0(11)
C(33)-C(32)-H(32)	121.0	C(58)-C(53)-C(41)	119.8(11)
C(34)-C(33)-C(32)	118.9(14)	C(54)-C(53)-C(41)	117.1(12)
C(34)-C(33)-H(33)	120.6	C(53)-C(54)-C(55)	118.2(13)
C(32)-C(33)-H(33)	120.6	C(53)-C(54)-H(54)	120.9
N(8)-C(34)-C(33)	121.2(13)	C(55)-C(54)-H(54)	120.9
N(8)-C(34)-C(35)	118.1(11)	C(56)-C(55)-C(54)	116.9(13)
C(33)-C(34)-C(35)	120.6(13)	C(56)-C(55)-H(55)	121.6
N(9)-C(35)-C(36)	122.9(10)	C(54)-C(55)-H(55)	121.6
N(9)-C(35)-C(34)	114.7(10)	C(57)-C(56)-C(55)	124.3(13)
C(36)-C(35)-C(34)	122.4(11)	C(57)-C(56)-Br(2)	118.5(13)
C(37)-C(36)-C(35)	118.4(11)	C(55)-C(56)-Br(2)	117.2(13)
C(37)-C(36)-H(36)	120.8	C(58)-C(57)-C(56)	117.0(15)

C(58)-C(57)-H(57)	121.5
C(56)-C(57)-H(57)	121.5
C(53)-C(58)-C(57)	120.6(14)
C(53)-C(58)-H(58)	119.7
C(57)-C(58)-H(58)	119.7
F(122)-P(1)-F(12)	44(3)
F(122)-P(1)-F(123)	88(2)
F(12)-P(1)-F(123)	131(3)
F(122)-P(1)-F(124)	173(2)
F(12)-P(1)-F(124)	129(3)
F(123)-P(1)-F(124)	100(2)
F(122)-P(1)-F(15)	149(2)
F(12)-P(1)-F(15)	106(3)
F(123)-P(1)-F(15)	123(3)
F(124)-P(1)-F(15)	24(2)
F(122)-P(1)-F(11)	83(2)
F(12)-P(1)-F(11)	91.5(15)
F(123)-P(1)-F(11)	91.2(13)
F(124)-P(1)-F(11)	95.9(19)
F(15)-P(1)-F(11)	90.0(15)
F(122)-P(1)-F(14)	121.7(19)
F(12)-P(1)-F(14)	166(3)
F(123)-P(1)-F(14)	35(2)
F(124)-P(1)-F(14)	65(2)
F(15)-P(1)-F(14)	88(2)
F(11)-P(1)-F(14)	87.4(10)
F(122)-P(1)-F(13)	32.2(17)
F(12)-P(1)-F(13)	75(3)
F(123)-P(1)-F(13)	55.6(19)
F(124)-P(1)-F(13)	155(2)
F(15)-P(1)-F(13)	178(2)
F(11)-P(1)-F(13)	88.9(10)
F(14)-P(1)-F(13)	90(2)
F(122)-P(1)-F(16)	98(2)
F(12)-P(1)-F(16)	90.4(15)
F(123)-P(1)-F(16)	88.0(13)
F(124)-P(1)-F(16)	82.6(18)
F(15)-P(1)-F(16)	89.0(15)
F(11)-P(1)-F(16)	178.1(6)
F(14)-P(1)-F(16)	90.9(10)
F(13)-P(1)-F(16)	92.1(10)
F(122)-P(1)-F(125)	86.8(16)
F(12)-P(1)-F(125)	43(3)
F(123)-P(1)-F(125)	173(2)
F(124)-P(1)-F(125)	86.1(18)
F(15)-P(1)-F(125)	63.0(18)
F(11)-P(1)-F(125)	91.6(9)
F(14)-P(1)-F(125)	151(2)
F(13)-P(1)-F(125)	118(2)
F(16)-P(1)-F(125)	89.4(9)
F(21)-P(2)-F(24)	99(3)
F(21)-P(2)-F(251)	150(2)
F(24)-P(2)-F(251)	111(3)
F(21)-P(2)-F(221)	71(3)
F(24)-P(2)-F(221)	145(4)
F(251)-P(2)-F(221)	87(2)
F(21)-P(2)-F(261)	113(2)
F(24)-P(2)-F(261)	55(4)
F(251)-P(2)-F(261)	89.4(17)
F(221)-P(2)-F(261)	98(2)
F(21)-P(2)-F(241)	127(3)
F(24)-P(2)-F(241)	58(2)
F(251)-P(2)-F(241)	69.2(18)
F(221)-P(2)-F(241)	154(3)
F(261)-P(2)-F(241)	91.6(16)
F(21)-P(2)-F(211)	59(2)
F(24)-P(2)-F(211)	119(5)
F(251)-P(2)-F(211)	100.0(15)
F(221)-P(2)-F(211)	85.4(17)
F(261)-P(2)-F(211)	170.2(15)
F(241)-P(2)-F(211)	89.4(15)
F(21)-P(2)-F(231)	58(2)
F(24)-P(2)-F(231)	42(3)
F(251)-P(2)-F(231)	148(2)
F(221)-P(2)-F(231)	125(3)
F(261)-P(2)-F(231)	84.9(16)
F(241)-P(2)-F(231)	80(2)
F(211)-P(2)-F(231)	85.7(12)
F(21)-P(2)-F(23)	48(3)
F(24)-P(2)-F(23)	100(3)
F(251)-P(2)-F(23)	127(3)
F(221)-P(2)-F(23)	48(2)
F(261)-P(2)-F(23)	75(3)
F(241)-P(2)-F(23)	158(3)
F(211)-P(2)-F(23)	101(3)
F(231)-P(2)-F(23)	81(2)
F(21)-P(2)-F(25)	100(3)
F(24)-P(2)-F(25)	104(4)
F(251)-P(2)-F(25)	69(2)
F(221)-P(2)-F(25)	111(2)
F(261)-P(2)-F(25)	142(2)
F(241)-P(2)-F(25)	52.0(16)
F(211)-P(2)-F(25)	42.6(17)
F(231)-P(2)-F(25)	98(2)
F(23)-P(2)-F(25)	143(3)
F(21)-P(2)-F(26)	110(5)
F(24)-P(2)-F(26)	90(4)
F(251)-P(2)-F(26)	77(3)
F(221)-P(2)-F(26)	64(3)
F(261)-P(2)-F(26)	35.3(16)
F(241)-P(2)-F(26)	116(4)
F(211)-P(2)-F(26)	150(3)
F(231)-P(2)-F(26)	113(2)
F(23)-P(2)-F(26)	62(4)
F(25)-P(2)-F(26)	145(4)
F(21)-P(2)-F(22)	96(3)
F(24)-P(2)-F(22)	160(5)
F(251)-P(2)-F(22)	57(2)
F(221)-P(2)-F(22)	32(3)
F(261)-P(2)-F(22)	106.0(18)
F(241)-P(2)-F(22)	123(3)
F(211)-P(2)-F(22)	81.4(14)
F(231)-P(2)-F(22)	154(3)
F(23)-P(2)-F(22)	79(3)
F(25)-P(2)-F(22)	88(2)
F(26)-P(2)-F(22)	71(2)
F(23)-F(21)-P(2)	73(3)
F(21)-F(23)-P(2)	59(2)
F(21)-F(23)-F(26)	124(5)
P(2)-F(23)-F(26)	65(4)
F(23)-F(26)-P(2)	54(3)
P(2)-F(241)-F(251)	53.6(11)
P(2)-F(251)-F(241)	57.2(14)

Table 1. Crystal data and structure refinement for **[2 x 2] Cu grid Chapter VII with SQUEEZE.**

Empirical formula	C102 H64 Br2 Cu4 F36 N24 O4 P6
Formula weight	2973.57
Temperature	100(2)K
Wavelength	1.54178 Å
Crystal system	Orthorhombic
Space group	Pbcn
Unit cell dimensions	a = 24.630(2) Å α = 90° b = 20.0462(18) Å β = 90° c = 50.870(4) Å γ = 90°
Volume	25116(4)Å^3
Z	8
Density (calculated)	1.573 g/cm^3
Absorption coefficient	3.226 mm^{-1}
F(000)	11808
Crystal size	0.14 x 0.10 x 0.08 mm
Theta range for data collection	1.74 to 58.94°
Index ranges	$-26 \le h \le 26$, $-22 \le k \le 20$, $-56 \le \ell \le 56$
Reflections collected	345839
Independent reflections	17824 [R_{int} = 0.100]
Absorption correction	Semi-empirical from equivalents
Max. and min. transmission	0.8200 and 0.4200
Refinement method	Full-matrix least-squares on F^2
Data / restraints / parameters	17824 / 735 / 1662
Goodness-of-fit on F^2	0.981
Final R indices [I>2sigma(I)]	R1 = 0.0766, wR_2 = 0.1735
R indices (all data)	R1 = 0.2012, wR_2 = 0.1923
Largest diff. peak and hole	1.270 and -0.535 e/Å^3

Table 2. Atomic coordinates (x 10^4) and equivalent isotropic displacement parameters ($Å^2$ x 10^3) for **[2 x 2] Cu grid Chapter VII** with squeeze.

U_{eq} is defined as one third of the trace of the orthogonalized Uij tensor.

	Occ.	x	y	z	U_{eq}
Cu(1)	1	3755(1)	3445(1)	3824(1)	40(1)
Cu(2)	1	4414(1)	6648(1)	4031(1)	44(1)
Cu(3)	1	6148(1)	6868(1)	3403(1)	53(1)
Cu(4)	1	5956(1)	3599(1)	3704(1)	47(1)
N(1)	1	6048(4)	7988(6)	3397(3)	54(4)
N(2)	1	6172(5)	7124(9)	3794(2)	55(4)
N(3)	1	6205(4)	5829(7)	3643(2)	41(3)
N(4)	1	6187(4)	5476(9)	4086(2)	55(4)
N(5)	1	6064(4)	4690(7)	3744(2)	53(4)
N(6)	1	6111(4)	3690(8)	4079(2)	47(3)
N(7)	1	5886(5)	2594(7)	3835(3)	51(4)
N(8)	1	6708(5)	3550(6)	3483(2)	50(4)
N(9)	1	5691(4)	3412(5)	3350(2)	35(3)
N(10)	1	4272(4)	3642(5)	3519(2)	30(3)
N(11)	1	3238(5)	3690(5)	3550(2)	39(3)
N(12)	1	3033(5)	3429(5)	4031(2)	44(3)
N(13)	1	3805(4)	2343(6)	3765(2)	38(3)
N(14)	1	4269(4)	3138(7)	4116(2)	36(3)
N(15)	1	4080(4)	4429(6)	4036(2)	35(3)
N(16)	1	4726(4)	4719(7)	4354(2)	38(3)
N(17)	1	4375(4)	5547(6)	4075(2)	35(3)
N(18)	1	4847(4)	6493(7)	4346(2)	37(3)
N(19)	1	4656(5)	7633(7)	4112(2)	53(4)
N(20)	1	3564(4)	6707(5)	4133(3)	44(3)
N(21)	1	4062(5)	6848(5)	3692(2)	42(3)
N(23)	1	6191(5)	6658(6)	3032(2)	52(3)
N(24)	1	6979(5)	6873(6)	3357(2)	56(4)
O(1)	1	4265(3)	4167(5)	3113(2)	47(3)
O(2)	1	5068(3)	3718(4)	3746(2)	42(3)
O(3)	1	4806(4)	6272(5)	2973(2)	55(3)
O(4)	1	5095(3)	6550(4)	3745(2)	44(3)
C(1)	1	5934(6)	8430(12)	3198(3)	75(6)
C(2)	1	5880(6)	9092(10)	3229(5)	81(6)
C(3)	1	5905(7)	9321(10)	3484(5)	83(6)
C(4)	1	6000(7)	8946(11)	3687(4)	76(6)
C(5)	1	6078(5)	8301(11)	3640(3)	49(4)
C(6)	1	6199(6)	7790(12)	3843(4)	77(6)
C(7)	1	6358(6)	7979(9)	4105(4)	68(5)
C(8)	1	6456(8)	7505(12)	4292(3)	111(8)
C(9)	1	6414(7)	6836(9)	4234(3)	78(6)
C(10)	1	6259(6)	6657(11)	3979(3)	58(5)
C(11)	1	6224(5)	5942(9)	3905(3)	47(4)
C(12)	1	6142(6)	4857(9)	3992(3)	47(4)
C(13)	1	6103(5)	5199(9)	3574(3)	42(4)
C(14)	1	6172(6)	4298(11)	4185(3)	65(5)
C(15)	1	6296(7)	4394(10)	4458(3)	81(6)
C(16)	1	6339(8)	3806(13)	4602(3)	106(8)
C(17)	1	6255(8)	3205(10)	4493(3)	90(7)
C(18)	1	6139(6)	3139(10)	4227(3)	55(5)
C(19)	1	6013(6)	2531(11)	4091(3)	64(5)

C(20)	1	6025(8)	1923(11)	4207(4)	88(7)
C(21)	1	5877(7)	1384(10)	4076(4)	80(6)
C(22)	1	5718(5)	1452(9)	3817(4)	63(5)
C(23)	1	5733(5)	2077(9)	3707(3)	44(4)
C(24)	1	6052(6)	5049(7)	3292(3)	41(4)
C(25)	1	6508(6)	5072(7)	3136(2)	51(4)
C(26)	1	6474(5)	4926(7)	2873(2)	41(4)
C(27)	1	5972(6)	4764(7)	2775(2)	37(4)
C(28)	1	5518(6)	4735(7)	2924(2)	47(4)
C(29)	1	5546(6)	4888(6)	3191(2)	39(4)
C(30)	1	7198(8)	3710(9)	3559(3)	77(6)
C(31)	1	7621(8)	3730(9)	3386(4)	91(7)
C(32)	1	7555(7)	3595(9)	3133(4)	75(6)
C(33)	1	7057(8)	3424(8)	3051(3)	64(5)
C(34)	1	6641(6)	3395(7)	3230(3)	47(4)
C(35)	1	6054(5)	3253(7)	3166(3)	40(4)
C(36)	1	5877(6)	2950(8)	2924(3)	55(5)
C(37)	1	5350(8)	2829(8)	2890(3)	63(5)
C(38)	1	4966(6)	3016(7)	3082(3)	46(4)
C(39)	1	5157(6)	3306(7)	3310(2)	38(4)
C(40)	1	4828(6)	3603(7)	3537(3)	37(4)
C(41)	1	4030(6)	3888(6)	3299(3)	31(3)
C(42)	1	3422(5)	3841(7)	3309(3)	39(4)
C(43)	1	3055(7)	3969(6)	3111(2)	46(4)
C(44)	1	2504(6)	3953(8)	3162(3)	66(5)
C(45)	1	2329(5)	3804(6)	3408(3)	42(4)
C(46)	1	2698(7)	3664(6)	3603(3)	42(4)
C(47)	1	2577(8)	3527(6)	3882(3)	47(4)
C(48)	1	2037(6)	3527(7)	3978(3)	63(5)
C(49)	1	1965(7)	3400(8)	4248(3)	65(5)
C(50)	1	2426(8)	3282(8)	4399(3)	84(7)
C(51)	1	2951(7)	3303(7)	4292(3)	55(4)
C(52)	1	3602(6)	1994(8)	3569(3)	44(4)
C(53)	1	3668(6)	1315(9)	3542(3)	56(5)
C(54)	1	3989(6)	980(7)	3732(3)	60(5)
C(55)	1	4204(5)	1365(8)	3934(2)	47(4)
C(56)	1	4108(6)	2035(8)	3948(3)	42(4)
C(57)	1	4329(6)	2463(8)	4148(3)	40(4)
C(58)	1	4656(7)	2216(7)	4354(3)	63(5)
C(59)	1	4875(6)	2667(9)	4527(3)	64(5)
C(60)	1	4818(6)	3352(8)	4490(3)	52(4)
C(61)	1	4505(5)	3566(9)	4280(2)	41(4)
C(62)	1	4440(6)	4274(8)	4224(2)	31(4)
C(63)	1	4683(5)	5337(8)	4286(3)	31(4)
C(64)	1	4073(5)	5079(8)	3964(2)	30(4)
C(65)	1	4945(6)	5860(8)	4438(3)	39(4)
C(66)	1	5260(5)	5766(8)	4654(3)	45(4)
C(67)	1	5449(6)	6289(10)	4788(3)	63(5)
C(68)	1	5369(6)	6930(9)	4698(3)	66(5)
C(69)	1	5052(6)	7023(9)	4468(3)	46(4)
C(70)	1	4962(6)	7683(9)	4333(3)	58(5)
C(71)	1	5155(7)	8293(8)	4416(3)	81(4)
C(72)	1	5023(7)	8855(8)	4269(3)	81(4)
C(73)	1	4737(6)	8811(9)	4046(3)	69(5)
C(74)	1	4563(7)	8196(10)	3973(3)	62(5)
C(75)	1	3731(6)	5246(6)	3728(2)	34(4)
C(76)	1	3189(6)	5239(6)	3753(3)	40(4)
C(77)	1	2849(6)	5409(7)	3538(3)	45(4)
C(78)	1	3113(7)	5574(7)	3313(2)	43(4)
C(79)	1	3663(6)	5567(6)	3285(2)	37(4)
C(80)	1	3973(5)	5429(6)	3497(2)	33(4)
C(81)	1	3335(7)	6569(7)	4369(3)	63(5)

C(82)	1	2766(8)	6549(8)	4393(3)	66(5)
C(83)	1	2450(6)	6686(8)	4182(4)	61(5)
C(84)	1	2689(7)	6849(7)	3943(3)	60(5)
C(85)	1	3234(7)	6850(7)	3925(3)	42(4)
C(86)	1	3519(6)	6986(6)	3682(3)	35(4)
C(87)	1	3323(6)	7245(7)	3453(3)	47(4)
C(88)	1	3619(7)	7409(7)	3236(3)	49(4)
C(89)	1	4173(6)	7259(6)	3243(2)	43(4)
C(90)	1	4385(6)	6944(6)	3469(2)	37(4)
C(91)	1	4965(6)	6711(7)	3521(3)	43(4)
N(22)	1	5332(4)	6684(5)	3318(2)	42(3)
C(92)	1	5202(7)	6485(8)	3062(3)	48(5)
C(93)	1	5721(6)	6515(8)	2897(3)	55(5)
C(94)	1	5747(6)	6412(8)	2632(3)	68(5)
C(95)	1	6246(7)	6459(8)	2503(3)	73(5)
C(96)	1	6726(6)	6558(7)	2642(3)	58(5)
C(97)	1	6674(6)	6661(7)	2912(3)	54(4)
C(98)	1	7123(6)	6740(8)	3102(3)	59(5)
C(99)	1	7676(8)	6672(8)	3033(3)	81(6)
C(100)	1	8054(6)	6710(8)	3242(4)	78(6)
C(101)	1	7926(7)	6858(10)	3494(3)	104(8)
C(102)	1	7394(7)	6905(8)	3539(3)	74(6)
Br(1)	1	5911(1)	4546(1)	2409(1)	60(1)
Br(2)	1	2669(1)	5816(1)	3020(1)	72(1)
P(1)	1	734(2)	4265(3)	3283(1)	102(2)
F(11)	1	1116(4)	3832(5)	3097(2)	140(4)
F(12)	1	1129(4)	4870(5)	3241(2)	129(4)
F(13)	1	407(4)	4478(6)	3017(2)	143(4)
F(14)	1	329(4)	3633(5)	3316(2)	146(4)
F(15)	1	1041(3)	4033(5)	3536(2)	102(3)
F(16)	1	344(4)	4698(5)	3468(2)	135(4)
P(2)	1	1647(2)	7244(3)	2759(1)	78(2)
F(21)	1	2039(4)	6778(5)	2607(2)	131(4)
F(22)	1	2115(4)	7405(5)	2959(2)	108(3)
F(23)	1	1822(4)	7841(5)	2580(2)	130(4)
F(24)	1	1164(4)	7082(5)	2564(2)	129(4)
F(25)	1	1472(4)	6638(4)	2932(2)	103(3)
F(26)	1	1290(4)	7698(5)	2934(2)	125(4)
P(3)	1	2748(2)	238(3)	1017(1)	99(2)
F(31)	1	2349(4)	49(5)	785(2)	129(4)
F(32)	1	3189(4)	350(6)	797(2)	160(5)
F(33)	1	2922(4)	-520(5)	1037(2)	125(4)
F(34)	1	2285(3)	122(4)	1232(2)	98(3)
F(35)	1	2567(5)	1002(5)	995(2)	165(5)
F(36)	1	3150(4)	433(6)	1239(2)	137(4)
P(4)	1	3442(2)	4850(2)	4782(1)	55(1)
F(41)	1	2882(3)	4507(4)	4735(1)	89(3)
F(42)	1	3478(4)	5085(4)	4490(1)	100(3)
F(43)	1	3143(3)	5519(4)	4863(1)	71(3)
F(44)	1	3439(4)	4627(4)	5082(1)	91(3)
F(45)	1	3760(3)	4178(4)	4700(1)	69(3)
F(46)	1	4012(3)	5191(5)	4834(2)	112(4)
P(5)	1	1063(3)	3143(4)	4899(1)	115(2)
F(51)	1	1034(3)	2874(5)	4605(1)	99(3)
F(52)	1	558(5)	2779(8)	4952(2)	228(6)
F(53)	1	724(6)	3785(7)	4818(3)	232(7)
F(54)	1	1526(5)	3670(6)	4834(2)	164(5)
F(55)	1	1517(6)	2637(7)	4966(3)	224(7)
F(56)	1	1084(4)	3333(6)	5193(2)	150(4)
P(6)	0.685(3)	6439(4)	1876(5)	99(2)	117(3)
F(61)	0.685(3)	6463(5)	1797(7)	398(2)	125(5)
F(62)	0.685(3)	6685(7)	1175(7)	91(3)	166(7)

F(63)	0.685(3)	7030(7)	2157(11)	91(4)	253(11)
F(64)	0.685(3)	6302(9)	2608(8)	81(4)	265(12)
F(65)	0.685(3)	5840(5)	1686(8)	90(3)	140(6)
F(66)	0.685(3)	6402(7)	1743(9)	-197(2)	178(7)
P(7)	0.315(3)	9710(5)	5933(7)	3024(2)	66(4)
F(71)	0.315(3)	9805(13)	5288(12)	2835(5)	201(18)
F(72)	0.315(3)	9501(13)	6291(17)	2777(5)	260(20)
F(73)	0.315(3)	10291(7)	6105(10)	2937(4)	52(7)
F(74)	0.315(3)	9940(11)	5512(13)	3254(4)	159(15)
F(75)	0.315(3)	9137(8)	5645(14)	3090(5)	145(13)
F(76)	0.315(3)	9472(8)	6433(10)	3183(3)	63(7)

Table 3. Hydrogen coordinates (x 10^4) and isotropic displacement parameters ($Å^2$ x 10^3) for **[2 x 2] Cu grid Chapter VII** with squeeze.

	Occ.	x	y	z	U_{eq}
H(1)	1	5891	8255	3025	91
H(2)	1	5827	9384	3084	97
H(3)	1	5849	9784	3513	99
H(4)	1	6012	9123	3860	91
H(7)	1	6394	8438	4149	82
H(8)	1	6556	7638	4465	133
H(9)	1	6488	6505	4363	93
H(15)	1	6344	4823	4535	97
H(16)	1	6431	3831	4783	127
H(17)	1	6275	2817	4600	108
H(20)	1	6140	1884	4384	106
H(21)	1	5879	958	4158	96
H(22)	1	5603	1077	3717	75
H(23)	1	5624	2129	3529	53
H(25)	1	6849	5189	3210	61
H(26)	1	6785	4938	2763	49
H(28)	1	5182	4611	2847	56
H(29)	1	5232	4882	3300	47
H(30)	1	7261	3815	3739	93
H(31)	1	7972	3845	3448	109
H(32)	1	7851	3619	3014	90
H(33)	1	6993	3324	2871	76
H(36)	1	6132	2837	2791	66
H(37)	1	5232	2614	2734	76
H(38)	1	4589	2945	3055	55
H(43)	1	3182	4068	2939	55
H(44)	1	2250	4046	3026	79
H(45)	1	1951	3795	3446	50
H(48)	1	1736	3610	3865	76
H(49)	1	1613	3395	4324	78
H(50)	1	2383	3184	4581	100
H(51)	1	3256	3229	4403	66
H(52)	1	3399	2224	3438	53
H(53)	1	3504	1079	3400	67
H(54)	1	4054	514	3721	72
H(55)	1	4421	1158	4065	56
H(58)	1	4722	1751	4373	76
H(59)	1	5071	2508	4675	77
H(60)	1	4987	3662	4605	62
H(66)	1	5346	5327	4710	54
H(67)	1	5642	6219	4947	76
H(68)	1	5521	7300	4788	79
H(71)	1	5372	8329	4570	97
H(72)	1	5140	9281	4328	97
H(73)	1	4658	9195	3943	83
H(74)	1	4362	8159	3815	74
H(76)	1	3030	5117	3916	48
H(77)	1	2464	5409	3551	54
H(79)	1	3825	5658	3119	44
H(80)	1	4358	5457	3485	40
H(81)	1	3558	6485	4517	76
H(82)	1	2604	6441	4557	79
H(83)	1	2066	6670	4197	73

H(84)	1	2471	6959	3795	71
H(87)	1	2942	7319	3444	57
H(88)	1	3457	7615	3087	59
H(89)	1	4402	7367	3099	51
H(94)	1	5427	6309	2536	82
H(95)	1	6257	6423	2317	87
H(96)	1	7070	6554	2557	69
H(99)	1	7788	6605	2857	97
H(100)	1	8425	6625	3203	94
H(101)	1	8191	6924	3626	125
H(102)	1	7289	6967	3717	88

Table 4. Anisotropic parameters ($Å^2$ x 10^3) for **[2 x 2] Cu grid Chapter VII** with squeeze.

The anisotropic displacement factor exponent takes the form:

$$-2\pi^2 [h^2 a^{*2} U_{11} + ... + 2 h k a^* b^* U12]$$

	U11	U22	U33	U23	U13	U12
Cu(1)	42(1)	41(2)	36(1)	1(1)	4(1)	1(1)
Cu(2)	52(1)	42(2)	38(1)	-5(1)	2(1)	2(1)
Cu(3)	45(2)	70(2)	45(1)	-5(1)	-3(1)	-18(1)
Cu(4)	45(1)	62(2)	36(1)	2(1)	-4(1)	-2(1)
N(1)	30(8)	51(11)	81(9)	-16(9)	4(7)	-16(7)
N(2)	41(9)	63(12)	62(9)	-9(9)	6(7)	-17(9)
N(3)	23(7)	72(11)	27(7)	-18(7)	-4(5)	-1(7)
N(4)	31(8)	85(13)	48(8)	18(9)	0(6)	-20(9)
N(5)	50(9)	86(13)	22(7)	-5(8)	-6(6)	-3(8)
N(6)	56(9)	50(10)	36(7)	7(8)	8(6)	1(8)
N(7)	43(8)	54(11)	55(9)	-10(8)	-8(7)	1(8)
N(8)	47(9)	58(10)	47(8)	4(7)	-14(7)	-1(8)
N(9)	28(7)	43(9)	32(6)	-16(6)	10(5)	-2(7)
N(10)	28(7)	39(8)	23(6)	2(5)	-3(5)	8(6)
N(11)	29(8)	57(10)	29(7)	-6(6)	-9(6)	-4(7)
N(12)	53(9)	39(9)	39(7)	0(7)	11(7)	-7(7)
N(13)	46(8)	37(9)	31(7)	-1(7)	-6(6)	7(7)
N(14)	33(8)	49(10)	26(6)	-10(7)	3(5)	-13(7)
N(15)	36(7)	41(10)	27(6)	7(6)	-4(6)	11(7)
N(16)	48(9)	40(10)	26(7)	2(7)	8(6)	0(8)
N(17)	22(7)	49(10)	34(7)	-1(6)	-1(5)	5(7)
N(18)	49(8)	26(9)	35(7)	-25(7)	8(6)	-3(7)
N(19)	52(9)	61(12)	46(8)	-14(8)	3(7)	1(8)
N(20)	35(8)	26(9)	71(9)	-23(7)	11(7)	18(7)
N(21)	60(9)	42(9)	26(6)	-10(6)	9(6)	2(8)
N(23)	43(9)	68(10)	44(7)	-9(7)	20(7)	-9(8)
N(24)	47(9)	69(11)	54(8)	4(7)	8(7)	-13(7)
O(1)	36(6)	65(8)	39(5)	11(5)	5(4)	4(5)
O(2)	33(6)	61(8)	30(5)	-7(5)	-1(4)	-2(5)
O(3)	39(7)	84(9)	42(6)	-4(5)	-21(5)	-9(6)
O(4)	58(7)	45(7)	30(5)	-4(5)	-8(5)	-5(5)
C(1)	48(12)	93(19)	85(13)	18(14)	-20(10)	23(13)
C(2)	58(13)	28(14)	160(20)	7(14)	-16(13)	12(11)
C(3)	81(15)	45(16)	123(18)	-15(15)	-12(14)	37(12)
C(4)	61(13)	44(16)	123(18)	-33(14)	-10(12)	6(12)
C(5)	29(10)	50(15)	67(12)	-3(12)	-8(8)	-1(10)
C(6)	40(12)	93(19)	96(16)	-9(16)	15(10)	-36(13)
C(7)	79(14)	48(14)	77(13)	-24(12)	-3(11)	-22(11)
C(8)	180(20)	100(20)	53(13)	-24(14)	-10(13)	-42(18)
C(9)	135(17)	58(15)	41(10)	-17(10)	-26(10)	-3(13)
C(10)	56(11)	82(17)	36(10)	1(11)	5(8)	-2(11)
C(11)	35(10)	37(13)	68(13)	-8(11)	0(8)	-11(9)
C(12)	60(12)	22(11)	58(12)	-4(10)	6(9)	-2(9)
C(13)	44(11)	47(13)	36(10)	-11(10)	3(7)	5(10)
C(14)	59(12)	69(16)	69(13)	2(12)	4(9)	6(12)
C(15)	102(15)	104(19)	37(11)	-11(11)	-10(10)	-25(13)
C(16)	145(19)	120(20)	50(12)	13(15)	-38(12)	-25(18)
C(17)	151(19)	63(16)	55(13)	25(11)	-35(12)	-26(14)
C(18)	59(12)	69(15)	38(10)	7(11)	-11(8)	4(11)

C(19)	61(12)	70(17)	62(13)	-5(13)	-12(9)	10(12)
C(20)	102(17)	41(15)	121(18)	-4(15)	-7(13)	4(14)
C(21)	75(14)	67(17)	98(16)	60(14)	36(12)	19(13)
C(22)	40(11)	51(15)	97(15)	7(12)	16(9)	11(10)
C(23)	30(10)	45(13)	55(10)	9(11)	-14(7)	2(9)
C(24)	43(12)	32(11)	48(10)	-4(8)	5(8)	4(9)
C(25)	50(11)	69(13)	33(9)	-10(8)	1(8)	-30(9)
C(26)	34(10)	58(12)	30(8)	-2(8)	5(7)	-9(9)
C(27)	45(11)	52(11)	15(7)	0(7)	2(7)	-4(9)
C(28)	33(10)	67(13)	41(9)	-5(8)	-8(8)	-5(9)
C(29)	34(10)	49(11)	34(8)	7(8)	7(7)	-11(8)
C(30)	63(14)	110(18)	59(12)	-3(11)	-10(11)	24(14)
C(31)	66(16)	93(17)	113(16)	12(15)	-23(14)	17(13)
C(32)	15(11)	70(15)	139(18)	12(14)	32(11)	-6(10)
C(33)	72(14)	50(13)	69(11)	7(9)	47(11)	13(11)
C(34)	31(11)	53(12)	57(10)	-2(9)	-9(9)	3(9)
C(35)	37(11)	46(11)	38(8)	15(8)	8(8)	29(9)
C(36)	24(10)	92(15)	48(10)	-5(9)	-7(8)	9(10)
C(37)	91(15)	55(13)	44(10)	-14(9)	17(10)	20(12)
C(38)	48(11)	33(11)	56(10)	3(9)	-31(9)	5(9)
C(39)	37(10)	37(11)	41(9)	-3(8)	11(8)	-22(9)
C(40)	29(10)	25(11)	58(10)	7(8)	11(8)	7(8)
C(41)	38(10)	16(9)	38(9)	1(7)	-13(8)	0(8)
C(42)	26(10)	56(12)	35(9)	0(8)	7(8)	3(8)
C(43)	72(13)	29(11)	36(9)	11(7)	-6(9)	-1(9)
C(44)	12(10)	75(15)	110(14)	17(11)	-6(9)	5(9)
C(45)	13(9)	40(11)	73(11)	25(9)	3(8)	3(8)
C(46)	54(12)	11(10)	60(11)	-4(8)	-4(9)	6(9)
C(47)	88(15)	9(10)	45(10)	-3(8)	14(10)	-2(10)
C(48)	45(12)	67(14)	77(12)	-9(10)	20(9)	-30(10)
C(49)	53(13)	60(14)	82(13)	-21(11)	9(10)	-9(11)
C(50)	88(16)	65(15)	98(14)	-12(11)	89(13)	-32(13)
C(51)	85(14)	37(11)	43(10)	-9(8)	-15(9)	-6(10)
C(52)	59(11)	18(12)	56(10)	0(9)	9(8)	1(9)
C(53)	81(13)	51(14)	36(9)	15(10)	6(8)	-7(11)
C(54)	82(13)	7(10)	90(12)	-5(10)	21(10)	4(10)
C(55)	55(11)	49(13)	37(9)	-18(9)	-13(7)	2(10)
C(56)	52(11)	13(11)	60(11)	-11(9)	8(9)	8(9)
C(57)	55(11)	15(11)	49(10)	-4(9)	4(8)	-6(9)
C(58)	110(15)	10(11)	70(11)	1(9)	-16(10)	19(10)
C(59)	95(14)	45(14)	52(10)	-4(10)	-34(9)	0(12)
C(60)	92(13)	19(11)	44(9)	-14(9)	-14(9)	-7(10)
C(61)	43(10)	54(14)	27(8)	4(9)	-6(7)	-3(10)
C(62)	45(11)	17(11)	30(9)	-17(8)	15(7)	-14(9)
C(63)	30(9)	31(12)	33(9)	-13(9)	5(7)	-8(9)
C(64)	25(9)	31(11)	35(8)	0(8)	-2(7)	9(9)
C(65)	55(11)	17(11)	45(10)	-7(9)	12(8)	4(9)
C(66)	46(10)	57(13)	33(9)	1(9)	-13(8)	11(9)
C(67)	87(13)	68(15)	35(9)	7(10)	-31(9)	15(12)
C(68)	103(15)	56(14)	38(10)	-10(9)	-32(9)	-19(12)
C(69)	45(11)	48(13)	46(10)	0(10)	6(8)	-15(10)
C(70)	65(13)	42(14)	66(12)	-11(11)	9(9)	-13(10)
C(71)	134(12)	25(10)	84(11)	-16(7)	7(9)	-16(10)
C(72)	134(12)	25(10)	84(11)	-16(7)	7(9)	-16(10)
C(73)	100(15)	48(14)	58(11)	1(10)	-17(10)	-5(12)
C(74)	77(14)	49(14)	58(11)	-2(11)	4(9)	31(12)
C(75)	42(11)	33(11)	28(8)	-2(7)	8(8)	0(8)
C(76)	30(10)	27(10)	63(10)	-2(8)	17(8)	-4(8)
C(77)	38(10)	43(11)	54(10)	0(9)	-12(8)	-9(9)
C(78)	59(12)	32(11)	39(9)	19(8)	-18(8)	-17(9)
C(79)	39(10)	40(11)	32(8)	2(7)	-2(7)	1(9)
C(80)	15(8)	33(10)	51(9)	8(8)	-11(7)	-12(7)

C(81)	60(14)	50(13)	79(12)	-4(10)	22(10)	22(11)
C(82)	87(16)	38(12)	74(13)	6(10)	38(11)	5(12)
C(83)	48(12)	39(12)	94(13)	-21(11)	26(11)	16(10)
C(84)	56(13)	48(13)	75(12)	4(9)	9(10)	12(10)
C(85)	49(12)	19(11)	57(11)	1(8)	9(10)	12(9)
C(86)	30(10)	18(10)	57(10)	3(8)	-8(9)	8(8)
C(87)	26(10)	35(11)	81(12)	-5(10)	-4(9)	14(8)
C(88)	55(13)	24(11)	67(11)	-1(9)	-16(9)	6(9)
C(89)	57(12)	21(10)	51(9)	14(8)	-2(8)	-4(9)
C(90)	56(11)	19(10)	37(9)	-8(7)	-15(8)	20(8)
C(91)	52(12)	13(10)	64(11)	-11(9)	7(10)	-1(9)
N(22)	26(7)	49(9)	51(8)	-6(7)	2(6)	-10(6)
C(92)	62(13)	62(13)	22(9)	-8(8)	-1(8)	10(11)
C(93)	60(12)	72(14)	33(9)	-8(9)	5(8)	-23(10)
C(94)	57(12)	106(16)	42(10)	11(10)	0(8)	-4(11)
C(95)	71(14)	90(15)	58(11)	19(10)	17(11)	8(12)
C(96)	59(13)	67(13)	47(10)	-5(9)	4(9)	-3(10)
C(97)	35(11)	51(12)	75(12)	7(10)	13(10)	-15(9)
C(98)	30(11)	70(14)	79(12)	-3(10)	-1(10)	-22(10)
C(99)	75(15)	83(15)	85(13)	6(11)	27(12)	-16(13)
C(100)	19(10)	91(16)	125(16)	26(14)	-12(11)	-14(10)
C(101)	44(14)	200(20)	70(13)	-2(14)	22(10)	-51(14)
C(102)	66(14)	94(16)	61(11)	2(10)	-20(11)	-63(12)
Br(1)	60(1)	86(2)	34(1)	-9(1)	-2(1)	2(1)
Br(2)	56(1)	91(2)	70(1)	25(1)	-19(1)	-1(1)
P(1)	94(4)	97(5)	116(4)	-2(4)	9(4)	5(4)
F(11)	133(8)	140(8)	147(7)	-13(7)	22(6)	13(7)
F(12)	123(8)	112(8)	152(7)	6(6)	34(6)	-25(7)
F(13)	141(8)	163(9)	124(7)	16(7)	-34(6)	17(7)
F(14)	125(8)	109(8)	204(8)	21(7)	8(7)	-21(7)
F(15)	87(6)	129(8)	89(5)	35(5)	-12(5)	10(6)
F(16)	124(8)	138(8)	143(7)	-16(7)	24(6)	11(7)
P(2)	84(4)	83(4)	67(3)	12(3)	25(3)	27(3)
F(21)	126(8)	149(8)	117(6)	-40(6)	36(6)	23(7)
F(22)	103(7)	107(7)	113(6)	17(6)	-22(6)	13(6)
F(23)	132(8)	141(8)	117(6)	67(6)	3(6)	-1(7)
F(24)	126(8)	138(8)	122(6)	37(6)	-41(6)	-13(7)
F(25)	130(7)	97(7)	81(5)	16(5)	7(5)	12(6)
F(26)	113(7)	105(8)	157(7)	-32(6)	33(6)	24(6)
P(3)	87(4)	107(5)	103(4)	13(4)	-22(4)	-26(4)
F(31)	104(7)	135(8)	148(7)	-39(6)	-29(6)	6(6)
F(32)	151(8)	199(10)	130(7)	28(7)	-16(7)	-66(8)
F(33)	107(7)	116(8)	151(7)	21(6)	33(6)	36(7)
F(34)	72(6)	97(7)	124(6)	8(6)	28(5)	3(5)
F(35)	217(10)	129(9)	149(8)	20(7)	-43(7)	-22(8)
F(36)	114(7)	189(9)	109(6)	19(6)	-29(6)	-30(7)
P(4)	61(3)	56(4)	48(3)	-7(2)	5(2)	-2(3)
F(41)	79(6)	108(7)	79(5)	-33(5)	6(5)	-13(6)
F(42)	130(7)	98(7)	71(5)	13(5)	34(5)	34(6)
F(43)	87(6)	61(6)	64(5)	-15(4)	22(4)	9(5)
F(44)	116(7)	101(7)	57(5)	-10(5)	-5(5)	10(6)
F(45)	90(6)	61(6)	57(5)	-7(4)	-5(4)	12(5)
F(46)	89(7)	100(7)	148(7)	-58(6)	27(6)	-19(6)
P(5)	98(5)	179(6)	67(3)	14(4)	17(3)	-2(5)
F(51)	93(7)	129(8)	75(5)	-5(5)	29(5)	0(6)
F(52)	216(10)	313(11)	154(8)	-19(8)	80(8)	-161(9)
F(53)	249(11)	242(11)	203(10)	-62(9)	-34(9)	78(9)
F(54)	206(9)	172(9)	115(7)	3(7)	34(7)	-30(8)
F(55)	258(11)	204(11)	209(10)	-4(8)	-58(9)	44(9)
F(56)	162(8)	229(10)	60(5)	8(6)	5(6)	-21(8)
P(6)	99(6)	164(8)	89(5)	9(5)	-25(5)	53(6)
F(61)	98(9)	152(10)	124(9)	24(8)	-42(7)	10(8)

F(62)	209(12)	144(11)	146(10)	4(9)	-15(9)	38(10)
F(63)	249(14)	257(15)	254(14)	39(10)	21(10)	6(11)
F(64)	254(15)	238(15)	304(15)	11(11)	-66(10)	-14(11)
F(65)	140(10)	168(11)	112(9)	-12(8)	-9(8)	0(9)
F(66)	187(11)	215(12)	133(9)	45(9)	0(9)	33(9)
P(7)	88(9)	51(8)	58(7)	11(7)	-30(7)	10(7)
F(71)	200(20)	210(20)	190(20)	13(11)	-7(11)	18(11)
F(72)	260(30)	250(30)	270(30)	-14(11)	9(11)	-3(11)
F(73)	50(11)	32(11)	76(11)	9(9)	-1(9)	-19(9)
F(74)	158(17)	162(18)	159(17)	-29(11)	5(11)	-3(11)
F(75)	145(16)	154(17)	137(15)	7(11)	15(11)	45(11)
F(76)	69(11)	78(12)	41(10)	15(9)	-4(9)	16(10)

Table 5. Bond lengths [Å] and angles [°] for **[2 x 2] Cu grid Chapter VII** with squeeze.

Cu(1)-N(11)	1.952(9)	N(17)-C(64)	1.321(14)
Cu(1)-N(14)	2.044(10)	N(17)-C(63)	1.382(15)
Cu(1)-N(10)	2.046(9)	N(18)-C(69)	1.330(15)
Cu(1)-N(12)	2.066(10)	N(18)-C(65)	1.374(15)
Cu(1)-N(13)	2.234(11)	N(19)-C(74)	1.352(16)
Cu(1)-N(15)	2.385(11)	N(19)-C(70)	1.355(16)
Cu(2)-N(18)	1.95(1)	N(20)-C(81)	1.354(15)
Cu(2)-N(21)	1.969(10)	N(20)-C(85)	1.365(15)
Cu(2)-N(19)	2.104(13)	N(21)-C(86)	1.369(14)
Cu(2)-N(20)	2.162(10)	N(21)-C(90)	1.397(14)
Cu(2)-N(17)	2.221(11)	N(23)-C(97)	1.334(15)
Cu(2)-O(4)	2.228(8)	N(23)-C(93)	1.376(15)
Cu(3)-N(23)	1.938(10)	N(24)-C(98)	1.371(16)
Cu(3)-N(2)	2.055(12)	N(24)-C(102)	1.381(15)
Cu(3)-N(24)	2.061(11)	O(1)-C(41)	1.243(13)
Cu(3)-N(22)	2.088(10)	O(2)-C(40)	1.241(14)
Cu(3)-N(1)	2.259(13)	O(3)-C(92)	1.158(15)
Cu(3)-N(3)	2.421(12)	O(4)-C(91)	1.226(14)
Cu(4)-N(6)	1.953(11)	C(1)-C(2)	1.34(2)
Cu(4)-N(9)	1.953(9)	C(2)-C(3)	1.38(2)
Cu(4)-N(7)	2.129(13)	C(3)-C(4)	1.30(2)
Cu(4)-N(8)	2.169(12)	C(4)-C(5)	1.327(19)
Cu(4)-O(2)	2.209(8)	C(5)-C(6)	1.48(2)
Cu(4)-N(5)	2.212(13)	C(6)-C(7)	1.44(2)
N(1)-C(1)	1.377(17)	C(7)-C(8)	1.37(2)
N(1)-C(5)	1.388(17)	C(8)-C(9)	1.38(2)
N(2)-C(10)	1.344(17)	C(9)-C(10)	1.396(17)
N(2)-C(6)	1.360(19)	C(10)-C(11)	1.486(19)
N(3)-C(13)	1.334(16)	C(12)-C(14)	1.490(19)
N(3)-C(11)	1.352(16)	C(13)-C(24)	1.473(17)
N(4)-C(11)	1.314(16)	C(14)-C(15)	1.438(18)
N(4)-C(12)	1.335(16)	C(15)-C(16)	1.39(2)
N(5)-C(12)	1.318(15)	C(16)-C(17)	1.34(2)
N(5)-C(13)	1.343(16)	C(17)-C(18)	1.391(18)
N(6)-C(18)	1.338(16)	C(18)-C(19)	1.44(2)
N(6)-C(14)	1.342(17)	C(19)-C(20)	1.36(2)
N(7)-C(23)	1.280(15)	C(20)-C(21)	1.32(2)
N(7)-C(19)	1.344(16)	C(21)-C(22)	1.383(19)
N(8)-C(30)	1.309(18)	C(22)-C(23)	1.370(18)
N(8)-C(34)	1.337(14)	C(24)-C(25)	1.378(16)
N(9)-C(35)	1.336(13)	C(24)-C(29)	1.384(15)
N(9)-C(39)	1.346(14)	C(25)-C(26)	1.369(14)
N(10)-C(41)	1.362(13)	C(26)-C(27)	1.371(15)
N(10)-C(40)	1.374(14)	C(27)-C(28)	1.352(15)
N(11)-C(42)	1.341(13)	C(27)-Br(1)	1.919(11)
N(11)-C(46)	1.356(15)	C(28)-C(29)	1.396(15)
N(12)-C(51)	1.367(14)	C(30)-C(31)	1.37(2)
N(12)-C(47)	1.372(16)	C(31)-C(32)	1.323(19)
N(13)-C(52)	1.317(14)	C(32)-C(33)	1.340(19)
N(13)-C(56)	1.342(15)	C(33)-C(34)	1.371(17)
N(14)-C(61)	1.332(15)	C(34)-C(35)	1.507(17)
N(14)-C(57)	1.371(15)	C(35)-C(36)	1.439(17)
N(15)-C(62)	1.341(15)	C(36)-C(37)	1.330(17)
N(15)-C(64)	1.353(15)	C(37)-C(38)	1.410(17)
N(16)-C(63)	1.292(15)	C(38)-C(39)	1.383(15)
N(16)-C(62)	1.313(14)	C(39)-C(40)	1.528(16)

C(41)-C(42)	1.500(16)	P(1)-F(11)	1.595(9)
C(42)-C(43)	1.378(15)	P(1)-F(16)	1.598(9)
C(43)-C(44)	1.384(17)	P(1)-F(14)	1.621(9)
C(44)-C(45)	1.358(16)	P(1)-F(13)	1.632(9)
C(45)-C(46)	1.372(16)	P(2)-F(26)	1.546(8)
C(46)-C(47)	1.477(17)	P(2)-F(21)	1.552(8)
C(47)-C(48)	1.417(18)	P(2)-F(25)	1.559(8)
C(48)-C(49)	1.408(17)	P(2)-F(23)	1.564(8)
C(49)-C(50)	1.39(2)	P(2)-F(22)	1.569(8)
C(50)-C(51)	1.406(18)	P(2)-F(24)	1.584(9)
C(52)-C(53)	1.377(17)	P(3)-F(36)	1.548(8)
C(53)-C(54)	1.417(17)	P(3)-F(32)	1.576(9)
C(54)-C(55)	1.392(16)	P(3)-F(33)	1.582(9)
C(55)-C(56)	1.366(17)	P(3)-F(31)	1.585(8)
C(56)-C(57)	1.439(17)	P(3)-F(34)	1.597(8)
C(57)-C(58)	1.412(17)	P(3)-F(35)	1.60(1)
C(58)-C(59)	1.372(17)	P(4)-F(41)	1.559(8)
C(59)-C(60)	1.394(17)	P(4)-F(42)	1.564(7)
C(60)-C(61)	1.386(16)	P(4)-F(46)	1.583(8)
C(61)-C(62)	1.455(17)	P(4)-F(43)	1.584(7)
C(63)-C(65)	1.452(17)	P(4)-F(44)	1.587(7)
C(64)-C(75)	1.505(16)	P(4)-F(45)	1.612(7)
C(65)-C(66)	1.361(16)	P(5)-F(52)	1.468(10)
C(66)-C(67)	1.333(17)	P(5)-F(56)	1.546(8)
C(67)-C(68)	1.378(18)	P(5)-F(55)	1.549(11)
C(68)-C(69)	1.416(17)	P(5)-F(53)	1.586(11)
C(69)-C(70)	1.509(19)	P(5)-F(51)	1.589(8)
C(70)-C(71)	1.379(18)	P(5)-F(54)	1.59(1)
C(71)-C(72)	1.391(19)	P(6)-F(64)	1.508(13)
C(72)-C(73)	1.339(18)	P(6)-F(65)	1.526(12)
C(73)-C(74)	1.356(19)	P(6)-F(62)	1.530(12)
C(75)-C(76)	1.342(15)	P(6)-F(66)	1.531(12)
C(75)-C(80)	1.369(14)	P(6)-F(61)	1.531(11)
C(76)-C(77)	1.417(16)	P(6)-F(63)	1.559(13)
C(77)-C(78)	1.360(16)	P(7)-F(76)	1.415(13)
C(78)-C(79)	1.361(16)	P(7)-F(72)	1.534(15)
C(78)-Br(2)	1.911(12)	P(7)-F(73)	1.536(13)
C(79)-C(80)	1.350(14)	P(7)-F(74)	1.551(14)
C(81)-C(82)	1.406(19)	P(7)-F(75)	1.560(15)
C(82)-C(83)	1.356(18)	P(7)-F(71)	1.627(15)
C(83)-C(84)	1.387(17)	N(11)-CU1-N(14)	176.5(5)
C(84)-C(85)	1.347(17)	N(11)-CU1-N(10)	79.4(4)
C(85)-C(86)	1.444(17)	N(14)-CU1-N(10)	102.8(4)
C(86)-C(87)	1.364(16)	N(11)-CU1-N(12)	78.8(5)
C(87)-C(88)	1.367(16)	N(14)-CU1-N(12)	99.2(4)
C(88)-C(89)	1.396(17)	N(10)-CU1-N(12)	157.7(4)
C(89)-C(90)	1.413(15)	N(11)-CU1-N(13)	100.9(4)
C(90)-C(91)	1.527(17)	N(14)-CU1-N(13)	76.5(5)
C(91)-N(22)	1.374(15)	N(10)-CU1-N(13)	93.1(4)
N(22)-C(92)	1.397(15)	N(12)-CU1-N(13)	95.8(4)
C(92)-C(93)	1.531(18)	N(11)-CU1-N(15)	109.5(4)
C(93)-C(94)	1.365(16)	N(14)-CU1-N(15)	73.4(5)
C(94)-C(95)	1.396(18)	N(10)-CU1-N(15)	88.5(4)
C(95)-C(96)	1.391(18)	N(12)-CU1-N(15)	94.1(4)
C(96)-C(97)	1.399(17)	N(13)-CU1-N(15)	149.4(4)
C(97)-C(98)	1.478(18)	N(18)-CU2-N(21)	172.7(5)
C(98)-C(99)	1.412(19)	N(18)-CU2-N(19)	80.3(5)
C(99)-C(100)	1.416(19)	N(21)-CU2-N(19)	96.1(5)
C(100)-C(101)	1.349(19)	N(18)-CU2-N(20)	109.9(5)
C(101)-C(102)	1.333(19)	N(21)-CU2-N(20)	76.9(5)
P(1)-F(15)	1.559(8)	N(19)-CU2-N(20)	100.1(4)
P(1)-F(12)	1.572(9)	N(18)-CU2-N(17)	77.5(5)

N(21)-CU2-N(17)	105.7(4)	C(39)-N(9)-CU4	119.7(8)
N(19)-CU2-N(17)	157.7(5)	C(41)-N(10)-C(40)	120.70(11)
N(20)-CU2-N(17)	89.3(4)	C(41)-N(10)-CU1	114.9(9)
N(18)-CU2-O(4)	96.3(4)	C(40)-N(10)-CU1	124.1(8)
N(21)-CU2-O(4)	77.2(4)	C(42)-N(11)-C(46)	121.30(11)
N(19)-CU2-O(4)	89.9(4)	C(42)-N(11)-CU1	119.2(9)
N(20)-CU2-O(4)	153.1(4)	C(46)-N(11)-CU1	119.3(9)
N(17)-CU2-O(4)	90.6(3)	C(51)-N(12)-C(47)	116.40(12)
N(23)-CU3-N(2)	174.8(5)	C(51)-N(12)-CU1	128.70(11)
N(23)-CU3-N(24)	80.6(5)	C(47)-N(12)-CU1	114.9(9)
N(2)-CU3-N(24)	94.6(5)	C(52)-N(13)-C(56)	119.50(13)
N(23)-CU3-N(22)	79.2(5)	C(52)-N(13)-CU1	127.4(1)
N(2)-CU3-N(22)	105.8(4)	C(56)-N(13)-CU1	113.0(1)
N(24)-CU3-N(22)	159.0(5)	C(61)-N(14)-C(57)	120.90(12)
N(23)-CU3-N(1)	102.1(5)	C(61)-N(14)-CU1	122.10(11)
N(2)-CU3-N(1)	76.5(6)	C(57)-N(14)-CU1	116.8(1)
N(24)-CU3-N(1)	95.9(4)	C(62)-N(15)-C(64)	115.10(12)
N(22)-CU3-N(1)	93.9(4)	C(62)-N(15)-CU1	110.6(9)
N(23)-CU3-N(3)	107.6(5)	C(64)-N(15)-CU1	132.1(9)
N(2)-CU3-N(3)	74.0(6)	C(63)-N(16)-C(62)	118.30(13)
N(24)-CU3-N(3)	90.2(4)	C(64)-N(17)-C(63)	115.10(12)
N(22)-CU3-N(3)	90.5(4)	C(64)-N(17)-CU2	133.4(1)
N(1)-CU3-N(3)	150.3(5)	C(63)-N(17)-CU2	110.9(1)
N(6)-CU4-N(9)	169.7(5)	C(69)-N(18)-C(65)	120.70(13)
N(6)-CU4-N(7)	78.3(6)	C(69)-N(18)-CU2	117.80(11)
N(9)-CU4-N(7)	94.5(5)	C(65)-N(18)-CU2	121.5(1)
N(6)-CU4-N(8)	110.1(5)	C(74)-N(19)-C(70)	117.70(15)
N(9)-CU4-N(8)	78.4(5)	C(74)-N(19)-CU2	129.30(12)
N(7)-CU4-N(8)	100.8(4)	C(70)-N(19)-CU2	113.00(11)
N(6)-CU4-O(2)	95.1(4)	C(81)-N(20)-C(85)	118.90(12)
N(9)-CU4-O(2)	77.2(4)	C(81)-N(20)-CU2	127.30(11)
N(7)-CU4-O(2)	89.5(4)	C(85)-N(20)-CU2	113.6(1)
N(8)-CU4-O(2)	154.1(4)	C(86)-N(21)-C(90)	119.90(11)
N(6)-CU4-N(5)	78.2(5)	C(86)-N(21)-CU2	120.3(9)
N(9)-CU4-N(5)	108.4(4)	C(90)-N(21)-CU2	119.1(9)
N(7)-CU4-N(5)	156.4(5)	C(97)-N(23)-C(93)	121.70(12)
N(8)-CU4-N(5)	89.5(4)	C(97)-N(23)-CU3	119.40(11)
O(2)-CU4-N(5)	90.2(4)	C(93)-N(23)-CU3	118.9(9)
C(1)-N(1)-C(5)	112.20(14)	C(98)-N(24)-C(102)	116.80(13)
C(1)-N(1)-CU3	132.10(13)	C(98)-N(24)-CU3	111.3(1)
C(5)-N(1)-CU3	115.60(13)	C(102)-N(24)-CU3	131.30(11)
C(10)-N(2)-C(6)	123.20(16)	C(40)-O(2)-CU4	111.7(8)
C(10)-N(2)-CU3	120.60(12)	C(91)-O(4)-CU2	112.7(9)
C(6)-N(2)-CU3	115.00(13)	C(2)-C(1)-N(1)	124.60(18)
C(13)-N(3)-C(11)	115.20(13)	C(1)-C(2)-C(3)	116(2)
C(13)-N(3)-CU3	132.0(9)	C(4)-C(3)-C(2)	124(2)
C(11)-N(3)-CU3	110.80(11)	C(3)-C(4)-C(5)	117(2)
C(11)-N(4)-C(12)	114.50(14)	C(4)-C(5)-N(1)	126.20(17)
C(12)-N(5)-C(13)	114.40(14)	C(4)-C(5)-C(6)	125(2)
C(12)-N(5)-CU4	110.90(11)	N(1)-C(5)-C(6)	108.40(18)
C(13)-N(5)-CU4	134.5(1)	N(2)-C(6)-C(7)	116.10(18)
C(18)-N(6)-C(14)	121.20(14)	N(2)-C(6)-C(5)	122.90(19)
C(18)-N(6)-CU4	118.90(12)	C(7)-C(6)-C(5)	121(2)
C(14)-N(6)-CU4	119.80(12)	C(8)-C(7)-C(6)	120.60(18)
C(23)-N(7)-C(19)	118.80(15)	C(7)-C(8)-C(9)	120.90(17)
C(23)-N(7)-CU4	129.20(12)	C(8)-C(9)-C(10)	118.10(17)
C(19)-N(7)-CU4	111.90(14)	N(2)-C(10)-C(9)	121.00(17)
C(30)-N(8)-C(34)	117.20(13)	N(2)-C(10)-C(11)	119.00(15)
C(30)-N(8)-CU4	128.50(11)	C(9)-C(10)-C(11)	119.80(17)
C(34)-N(8)-CU4	113.9(1)	N(4)-C(11)-N(3)	124.60(15)
C(35)-N(9)-C(39)	120.80(11)	N(4)-C(11)-C(10)	120.90(16)
C(35)-N(9)-CU4	118.0(9)	N(3)-C(11)-C(10)	114.40(15)

N(5)-C(12)-N(4)	126.20(15)	C(45)-C(46)-C(47)	126.60(15)
N(5)-C(12)-C(14)	116.50(16)	N(12)-C(47)-C(48)	125.30(13)
N(4)-C(12)-C(14)	117.30(16)	N(12)-C(47)-C(46)	113.10(14)
N(3)-C(13)-N(5)	124.20(13)	C(48)-C(47)-C(46)	121.50(16)
N(3)-C(13)-C(24)	117.90(14)	C(49)-C(48)-C(47)	117.10(15)
N(5)-C(13)-C(24)	117.90(15)	C(50)-C(49)-C(48)	118.00(16)
N(6)-C(14)-C(15)	122.30(16)	C(49)-C(50)-C(51)	122.00(16)
N(6)-C(14)-C(12)	114.40(15)	N(12)-C(51)-C(50)	121.20(14)
C(15)-C(14)-C(12)	123.10(19)	N(13)-C(52)-C(53)	123.70(14)
C(16)-C(15)-C(14)	114.30(17)	C(52)-C(53)-C(54)	117.80(14)
C(17)-C(16)-C(15)	122.20(17)	C(55)-C(54)-C(53)	117.00(14)
C(16)-C(17)-C(18)	121.20(18)	C(56)-C(55)-C(54)	121.10(14)
N(6)-C(18)-C(17)	118.80(17)	N(13)-C(56)-C(55)	120.80(14)
N(6)-C(18)-C(19)	114.60(15)	N(13)-C(56)-C(57)	115.30(14)
C(17)-C(18)-C(19)	126.50(18)	C(55)-C(56)-C(57)	123.80(15)
N(7)-C(19)-C(20)	120.90(19)	N(14)-C(57)-C(58)	119.80(13)
N(7)-C(19)-C(18)	115.90(19)	N(14)-C(57)-C(56)	117.60(14)
C(20)-C(19)-C(18)	123.20(18)	C(58)-C(57)-C(56)	122.20(15)
C(21)-C(20)-C(19)	121(2)	C(59)-C(58)-C(57)	118.00(14)
C(20)-C(21)-C(22)	118.50(18)	C(58)-C(59)-C(60)	121.60(14)
C(23)-C(22)-C(21)	118.00(17)	C(61)-C(60)-C(59)	117.70(14)
N(7)-C(23)-C(22)	122.90(15)	N(14)-C(61)-C(60)	121.80(15)
C(25)-C(24)-C(29)	122.00(12)	N(14)-C(61)-C(62)	117.30(13)
C(25)-C(24)-C(13)	119.00(13)	C(60)-C(61)-C(62)	120.90(14)
C(29)-C(24)-C(13)	119.00(13)	N(16)-C(62)-N(15)	123.70(14)
C(26)-C(25)-C(24)	120.20(13)	N(16)-C(62)-C(61)	120.30(15)
C(25)-C(26)-C(27)	117.50(12)	N(15)-C(62)-C(61)	116.00(13)
C(28)-C(27)-C(26)	123.40(11)	N(16)-C(63)-N(17)	122.90(13)
C(28)-C(27)-BR1	118.00(11)	N(16)-C(63)-C(65)	121.00(14)
C(26)-C(27)-BR1	118.6(1)	N(17)-C(63)-C(65)	116.00(15)
C(27)-C(28)-C(29)	119.70(12)	N(17)-C(64)-N(15)	124.20(12)
C(24)-C(29)-C(28)	117.00(12)	N(17)-C(64)-C(75)	119.60(13)
N(8)-C(30)-C(31)	121.30(16)	N(15)-C(64)-C(75)	115.90(13)
C(32)-C(31)-C(30)	121.90(19)	C(66)-C(65)-N(18)	120.20(14)
C(31)-C(32)-C(33)	117.80(17)	C(66)-C(65)-C(63)	125.70(16)
C(32)-C(33)-C(34)	119.20(15)	N(18)-C(65)-C(63)	114.10(14)
N(8)-C(34)-C(33)	122.50(14)	C(67)-C(66)-C(65)	120.20(15)
N(8)-C(34)-C(35)	111.80(13)	C(66)-C(67)-C(68)	120.80(14)
C(33)-C(34)-C(35)	125.50(14)	C(67)-C(68)-C(69)	118.40(14)
N(9)-C(35)-C(36)	119.80(13)	N(18)-C(69)-C(68)	119.40(15)
N(9)-C(35)-C(34)	116.50(12)	N(18)-C(69)-C(70)	115.40(14)
C(36)-C(35)-C(34)	123.70(12)	C(68)-C(69)-C(70)	125.00(16)
C(37)-C(36)-C(35)	119.00(14)	N(19)-C(70)-C(71)	120.80(16)
C(36)-C(37)-C(38)	121.00(15)	N(19)-C(70)-C(69)	113.30(14)
C(39)-C(38)-C(37)	117.80(14)	C(71)-C(70)-C(69)	125.90(17)
N(9)-C(39)-C(38)	121.50(12)	C(70)-C(71)-C(72)	118.10(17)
N(9)-C(39)-C(40)	110.10(12)	C(73)-C(72)-C(71)	121.80(17)
C(38)-C(39)-C(40)	128.10(14)	C(72)-C(73)-C(74)	117.10(17)
O(2)-C(40)-N(10)	121.30(12)	N(19)-C(74)-C(73)	124.40(16)
O(2)-C(40)-C(39)	117.80(12)	C(76)-C(75)-C(80)	121.10(12)
N(10)-C(40)-C(39)	120.20(12)	C(76)-C(75)-C(64)	118.70(12)
O(1)-C(41)-N(10)	125.70(12)	C(80)-C(75)-C(64)	120.20(13)
O(1)-C(41)-C(42)	121.40(12)	C(75)-C(76)-C(77)	120.90(13)
N(10)-C(41)-C(42)	112.70(12)	C(78)-C(77)-C(76)	115.20(13)
N(11)-C(42)-C(43)	119.30(12)	C(77)-C(78)-C(79)	124.10(12)
N(11)-C(42)-C(41)	112.60(12)	C(77)-C(78)-BR2	116.50(12)
C(43)-C(42)-C(41)	128.00(13)	C(79)-C(78)-BR2	119.40(11)
C(42)-C(43)-C(44)	120.10(13)	C(80)-C(79)-C(78)	118.90(12)
C(45)-C(44)-C(43)	119.30(14)	C(79)-C(80)-C(75)	119.60(12)
C(44)-C(45)-C(46)	120.00(13)	N(20)-C(81)-C(82)	119.90(14)
N(11)-C(46)-C(45)	120.00(13)	C(83)-C(82)-C(81)	119.70(15)
N(11)-C(46)-C(47)	113.30(13)	C(82)-C(83)-C(84)	119.90(16)

C(85)-C(84)-C(83)	118.90(15)	F(23)-P(2)-F(22)	90.9(6)
C(84)-C(85)-N(20)	122.60(14)	F(26)-P(2)-F(24)	93.1(6)
C(84)-C(85)-C(86)	122.90(15)	F(21)-P(2)-F(24)	91.7(6)
N(20)-C(85)-C(86)	114.50(15)	F(25)-P(2)-F(24)	89.2(6)
C(87)-C(86)-N(21)	117.00(13)	F(23)-P(2)-F(24)	89.8(5)
C(87)-C(86)-C(85)	129.00(15)	F(22)-P(2)-F(24)	178.6(6)
N(21)-C(86)-C(85)	113.90(13)	F(36)-P(3)-F(32)	92.3(6)
C(86)-C(87)-C(88)	126.40(14)	F(36)-P(3)-F(33)	91.4(6)
C(87)-C(88)-C(89)	116.60(13)	F(32)-P(3)-F(33)	89.6(7)
C(88)-C(89)-C(90)	118.60(13)	F(36)-P(3)-F(31)	178.2(7)
N(21)-C(90)-C(89)	120.80(13)	F(32)-P(3)-F(31)	86.0(6)
N(21)-C(90)-C(91)	110.50(12)	F(33)-P(3)-F(31)	89.1(6)
C(89)-C(90)-C(91)	128.50(14)	F(36)-P(3)-F(34)	89.7(5)
O(4)-C(91)-N(22)	121.10(14)	F(32)-P(3)-F(34)	177.9(6)
O(4)-C(91)-C(90)	119.00(13)	F(33)-P(3)-F(34)	90.6(5)
N(22)-C(91)-C(90)	119.90(13)	F(31)-P(3)-F(34)	92.0(6)
C(91)-N(22)-C(92)	124.10(12)	F(36)-P(3)-F(35)	89.4(6)
C(91)-N(22)-CU3	118.0(9)	F(32)-P(3)-F(35)	90.3(7)
C(92)-N(22)-CU3	117.6(9)	F(33)-P(3)-F(35)	179.2(7)
O(3)-C(92)-N(22)	131.60(14)	F(31)-P(3)-F(35)	90.2(6)
O(3)-C(92)-C(93)	120.20(13)	F(34)-P(3)-F(35)	89.4(6)
N(22)-C(92)-C(93)	107.90(13)	F(41)-P(4)-F(42)	92.0(5)
C(94)-C(93)-N(23)	118.90(13)	F(41)-P(4)-F(46)	179.1(6)
C(94)-C(93)-C(92)	125.10(14)	F(42)-P(4)-F(46)	88.8(5)
N(23)-C(93)-C(92)	116.00(12)	F(41)-P(4)-F(43)	90.1(5)
C(93)-C(94)-C(95)	119.70(14)	F(42)-P(4)-F(43)	91.0(5)
C(96)-C(95)-C(94)	121.30(14)	F(46)-P(4)-F(43)	90.2(5)
C(95)-C(96)-C(97)	116.20(14)	F(41)-P(4)-F(44)	91.2(5)
N(23)-C(97)-C(96)	121.90(14)	F(42)-P(4)-F(44)	176.8(6)
N(23)-C(97)-C(98)	111.80(14)	F(46)-P(4)-F(44)	88.0(5)
C(96)-C(97)-C(98)	126.20(15)	F(43)-P(4)-F(44)	89.2(4)
N(24)-C(98)-C(99)	120.20(14)	F(41)-P(4)-F(45)	91.3(5)
N(24)-C(98)-C(97)	116.40(14)	F(42)-P(4)-F(45)	88.8(4)
C(99)-C(98)-C(97)	123.40(16)	F(46)-P(4)-F(45)	88.5(5)
C(98)-C(99)-C(100)	116.30(15)	F(43)-P(4)-F(45)	178.6(5)
C(101)-C(100)-C(99)	124.70(16)	F(44)-P(4)-F(45)	91.0(4)
C(102)-C(101)-C(100)	114.20(17)	F(52)-P(5)-F(56)	88.3(6)
C(101)-C(102)-N(24)	127.40(16)	F(52)-P(5)-F(55)	104.2(1)
F(15)-P(1)-F(12)	92.4(6)	F(56)-P(5)-F(55)	85.5(7)
F(15)-P(1)-F(11)	92.4(6)	F(52)-P(5)-F(53)	90.4(9)
F(12)-P(1)-F(11)	88.4(6)	F(56)-P(5)-F(53)	93.9(7)
F(15)-P(1)-F(16)	88.3(6)	F(55)-P(5)-F(53)	165.4(1)
F(12)-P(1)-F(16)	91.9(6)	F(52)-P(5)-F(51)	88.2(6)
F(11)-P(1)-F(16)	179.3(7)	F(56)-P(5)-F(51)	174.3(8)
F(15)-P(1)-F(14)	88.9(6)	F(55)-P(5)-F(51)	91.0(7)
F(12)-P(1)-F(14)	178.0(7)	F(53)-P(5)-F(51)	90.6(6)
F(11)-P(1)-F(14)	90.0(6)	F(52)-P(5)-F(54)	167.8(1)
F(16)-P(1)-F(14)	89.7(6)	F(56)-P(5)-F(54)	90.8(6)
F(15)-P(1)-F(13)	177.9(7)	F(55)-P(5)-F(54)	87.8(8)
F(12)-P(1)-F(13)	89.4(6)	F(53)-P(5)-F(54)	77.6(8)
F(11)-P(1)-F(13)	86.5(6)	F(51)-P(5)-F(54)	93.6(5)
F(16)-P(1)-F(13)	92.8(6)	F(64)-P(6)-F(65)	91.4(1)
F(14)-P(1)-F(13)	89.2(6)	F(64)-P(6)-F(62)	168.50(13)
F(26)-P(2)-F(21)	174.8(7)	F(65)-P(6)-F(62)	98.80(11)
F(26)-P(2)-F(25)	88.8(5)	F(64)-P(6)-F(66)	95.5(1)
F(21)-P(2)-F(25)	89.2(6)	F(65)-P(6)-F(66)	82.5(8)
F(26)-P(2)-F(23)	92.3(6)	F(62)-P(6)-F(66)	80.6(9)
F(21)-P(2)-F(23)	89.8(6)	F(64)-P(6)-F(61)	99.80(11)
F(25)-P(2)-F(23)	178.6(6)	F(65)-P(6)-F(61)	92.3(8)
F(26)-P(2)-F(22)	85.7(5)	F(62)-P(6)-F(61)	85.3(8)
F(21)-P(2)-F(22)	89.4(6)	F(66)-P(6)-F(61)	164.00(11)
F(25)-P(2)-F(22)	90.0(5)	F(64)-P(6)-F(63)	81.70(11)

F(65)-P(6)-F(63)	172.50(12)	F(76)-P(7)-F(75)	76.40(12)
F(62)-P(6)-F(63)	87.8(1)	F(72)-P(7)-F(75)	92.60(14)
F(66)-P(6)-F(63)	95.3(1)	F(73)-P(7)-F(75)	170.60(15)
F(61)-P(6)-F(63)	91.7(9)	F(74)-P(7)-F(75)	88.20(13)
F(76)-P(7)-F(72)	89.80(14)	F(76)-P(7)-F(71)	163.70(15)
F(76)-P(7)-F(73)	113.00(13)	F(72)-P(7)-F(71)	86.40(14)
F(72)-P(7)-F(73)	88.30(14)	F(73)-P(7)-F(71)	82.80(12)
F(76)-P(7)-F(74)	96.00(12)	F(74)-P(7)-F(71)	87.80(14)
F(72)-P(7)-F(74)	174.20(17)	F(75)-P(7)-F(71)	87.90(13)
F(73)-P(7)-F(74)	90.00(12)		

Table 1. Crystal data and structure refinement for **$[CuL2]_2^{2+}$ chapter VII.**

Empirical formula	C50 H40 Cu2 F12 N12 O5 P2
Formula weight	1305.96
Temperature	100(2)K
Wavelength	1.54178 Å
Crystal system	Triclinic
Space group	P-1
Unit cell dimensions	a = 11.4580(12) Å α = 96.286(4)° b = 11.8380(12) Å β = 103.165(4)° c = 21.346(2) Å γ = 110.023(4)°
Volume	2592.6(4)Å^3
Z	2
Density (calculated)	1.673 g/cm^3
Absorption coefficient	2.530 mm^{-1}
F(000)	1320
Crystal size	0.30 x 0.10 x 0.04 mm
Theta range for data collection	2.17 to 59.02°
Index ranges	$-12 \le h \le 12$, $-12 \le k \le 13$, $-23 \le \ell \le 23$
Reflections collected	35310
Independent reflections	7246 [R_{int} = 0.058]
Absorption correction	Semi-empirical from equivalents
Max. and min. transmission	0.6300 and 0.3900
Refinement method	Full-matrix least-squares on F^2
Data / restraints / parameters	7246 / 2 / 754
Goodness-of-fit on F^2	0.992
Final R indices [I>2sigma(I)]	R1 = 0.0543, wR_2 = 0.1458
R indices (all data)	R1 = 0.0721, wR_2 = 0.1579
Largest diff. peak and hole	0.972 and -0.770 e/Å^3

Table 2. Atomic coordinates (x 10^4) and equivalent isotropic displacement parameters ($Å^2$ x 10^3) for C50 H40 Cu2 F12 N12 O5 P2.

U_{eq} is defined as one third of the trace of the orthogonalized Uij tensor.

	x	y	z	U_{eq}
Cu(1)	2582(1)	4014(1)	2408(1)	29(1)
Cu(2)	3775(1)	1724(1)	2520(1)	29(1)
P(2)	5720(1)	2225(1)	9087(1)	36(1)
F(26)	7019(3)	3083(2)	8947(1)	44(1)
F(21)	4415(3)	1384(3)	9220(2)	65(1)
F(24)	4984(3)	3014(2)	8734(1)	46(1)
N(8)	4746(3)	3598(3)	2922(2)	28(1)
F(25)	5327(3)	1317(2)	8397(1)	41(1)
N(3)	1551(3)	2125(3)	2228(2)	29(1)
N(1)	3480(3)	5808(3)	2906(2)	28(1)
N(7)	3615(3)	4195(3)	1745(2)	27(1)
N(5)	5409(3)	1617(3)	2179(2)	31(1)
N(2)	2070(3)	3873(3)	3213(2)	27(1)
F(23)	6124(3)	3137(2)	9781(1)	54(1)
O(4)	6627(3)	5143(3)	2876(2)	43(1)
F(22)	6473(4)	1449(3)	9433(1)	63(1)
O(3)	5602(1)	4909(2)	3960(1)	36(1)
O(2)	-179(3)	829(3)	1349(2)	41(1)
C(29)	3670(4)	4230(4)	640(2)	29(1)
N(6)	1229(3)	4175(3)	1527(2)	28(1)
C(32)	4878(4)	4357(4)	1918(2)	28(1)
C(4)	3849(4)	7135(4)	3920(2)	33(1)
N(9)	3717(3)	1753(3)	3424(2)	30(1)
N(10)	2723(4)	-114(3)	2468(2)	30(1)
C(11)	941(4)	1755(4)	2705(2)	32(1)
N(4)	3114(3)	1520(3)	1511(2)	26(1)
C(5)	3325(4)	5995(4)	3515(2)	29(1)
C(39)	3039(4)	716(4)	3590(2)	29(1)
C(18)	5205(4)	1487(4)	1518(2)	27(1)
C(19)	6160(5)	1441(4)	1231(2)	35(1)
C(41)	1697(4)	-1536(4)	3084(2)	37(1)
C(27)	1643(4)	4056(4)	985(2)	27(1)
C(17)	3911(4)	1368(4)	1146(2)	28(1)
C(38)	2890(4)	730(4)	4216(2)	34(1)
C(16)	3467(5)	1101(4)	463(2)	34(1)
C(12)	979(5)	1395(4)	1602(2)	29(1)
C(6)	2531(4)	4855(4)	3697(2)	31(1)
C(31)	5586(4)	4484(4)	1464(2)	30(1)
C(2)	4714(5)	7963(4)	3078(2)	36(1)
C(26)	820(5)	3812(4)	359(2)	34(1)
C(14)	1422(5)	1093(4)	516(2)	34(1)
C(1)	4157(4)	6784(4)	2695(2)	31(1)
C(35)	4280(4)	2815(4)	3860(2)	31(1)
C(22)	6555(5)	1703(4)	2550(3)	42(1)
C(10)	1328(4)	2770(4)	3288(2)	31(1)
C(13)	1896(4)	1365(4)	1195(2)	29(1)
C(33)	5511(4)	4412(4)	2624(2)	30(1)
C(23)	12(4)	4079(4)	1447(2)	33(1)
C(44)	2249(5)	-1034(4)	1945(2)	35(1)
C(30)	4943(4)	4387(4)	811(2)	32(1)

C(28)	3007(4)	4171(4)	1120(2)	28(1)
C(21)	7520(5)	1606(5)	2278(3)	47(1)
C(40)	2458(4)	-358(4)	3043(2)	30(1)
C(3)	4560(5)	8131(4)	3698(2)	36(1)
C(7)	2260(5)	4762(4)	4295(2)	37(1)
C(15)	2234(5)	980(4)	148(2)	35(1)
C(20)	7319(5)	1482(4)	1611(3)	41(1)
C(43)	1490(5)	-2227(4)	1956(2)	38(1)
C(24)	-865(5)	3844(4)	834(2)	37(1)
C(9)	998(5)	2614(4)	3860(2)	35(1)
C(36)	4180(4)	2891(4)	4502(2)	35(1)
C(8)	1490(4)	3630(4)	4374(2)	35(1)
C(25)	-440(5)	3700(4)	285(2)	39(1)
C(34)	4982(4)	3897(4)	3595(2)	31(1)
C(42)	1210(5)	-2470(4)	2539(2)	40(1)
C(37)	3462(5)	1830(4)	4673(2)	39(1)
P(1)	7280(1)	1603(1)	4547(1)	38(1)
F(14)	6936(3)	2795(2)	4526(2)	54(1)
F(12)	7565(3)	389(3)	4551(2)	64(1)
F(16)	8349(3)	2150(3)	4182(2)	58(1)
F(15)	6194(3)	974(3)	3849(1)	65(1)
F(11)	6169(3)	1042(2)	4897(1)	50(1)
F(13)	8277(3)	2241(3)	5247(2)	64(1)
O(1)	231(3)	716(3)	2704(2)	37(1)
N(53)	9646(4)	4786(4)	2970(2)	50(1)
C(51)	9012(5)	5122(4)	4051(2)	42(1)
C(52)	9361(5)	4929(4)	3440(2)	37(1)
N(63)	1889(5)	3421(5)	8994(2)	61(1)
C(62)	1916(5)	2711(5)	8599(3)	46(1)
C(61)	1965(6)	1814(5)	8087(3)	68(2)
O(73)	7595(1)	7219(2)	4153(2)	67(1)
C(73)	9281(6)	8949(6)	4024(4)	77(2)
C(72)	8128(7)	7870(6)	3686(3)	73(2)

Table 3. Hydrogen coordinates (x 10^4) and isotropic displacement parameters ($Å^2$ x 10^3) for **$[CuL2]_2^{2+}$ chapter VII.**

	x	y	z	U_{eq}
H(29)	3230	4160	194	35
H(4)	3727	7239	4345	40
H(19)	6012	1380	770	42
H(41)	1516	-1693	3486	44
H(38)	2403	-3	4331	41
H(16)	4025	1002	212	41
H(31)	6485	4633	1595	36
H(2)	5191	8637	2916	44
H(26)	1123	3722	-16	41
H(14)	554	987	308	41
H(1)	4258	6664	2266	37
H(22)	6718	1834	3014	50
H(23)	-272	4176	1827	40
H(44)	2439	-865	1546	42
H(30)	5392	4431	486	39
H(21)	8310	1626	2552	57
H(3)	4940	8927	3972	43
H(7)	2597	5462	4643	45
H(15)	1943	820	-319	42
H(20)	7970	1426	1417	49
H(43)	1170	-2862	1575	45
H(24)	-1728	3784	793	45
H(9)	451	1835	3904	42
H(36)	4592	3647	4813	42
H(8)	1295	3546	4780	42
H(25)	-1018	3525	-142	47
H(42)	685	-3276	2561	47
H(37)	3361	1856	5103	47
H(51A)	8768	4352	4210	64
H(51B)	8280	5389	3968	64
H(51C)	9755	5755	4383	64
H(61A)	2165	2205	7723	102
H(61B)	1123	1126	7927	102
H(61C)	2637	1509	8269	102
H(73)	6990(20)	6529(14)	4080(20)	80
H(73A)	9065	9483	4324	116
H(73B)	9611	9397	3701	116
H(73C)	9944	8697	4276	116
H(72A)	7474	8121	3414	88
H(72B)	8349	7320	3391	88

Table 4. Anisotropic parameters ($Å^2$ x 10^3) for **$[CuL2]_2^{2+}$ chapter VII.**

The anisotropic displacement factor exponent takes the form:

$$-2\pi^2 [h^2 a^{*2} U_{11} + ... + 2 h k a^* b^* U_{12}]$$

	U11	U22	U33	U23	U13	U12
Cu(1)	27(1)	31(1)	26(1)	0(1)	10(1)	9(1)
Cu(2)	29(1)	32(1)	28(1)	4(1)	13(1)	10(1)
P(2)	49(1)	30(1)	32(1)	3(1)	18(1)	14(1)
F(26)	35(2)	47(2)	42(2)	3(1)	10(1)	10(1)
F(21)	81(2)	51(2)	58(2)	5(2)	48(2)	3(2)
F(24)	42(2)	41(2)	54(2)	4(1)	13(1)	19(1)
N(8)	21(2)	32(2)	27(2)	3(2)	8(2)	8(2)
F(25)	47(2)	36(1)	35(2)	-1(1)	17(1)	11(1)
N(3)	25(2)	31(2)	29(2)	2(2)	9(2)	11(2)
N(1)	24(2)	33(2)	25(2)	2(2)	6(2)	11(2)
N(7)	24(2)	23(2)	30(2)	-1(2)	9(2)	6(2)
N(5)	23(2)	37(2)	32(2)	6(2)	11(2)	9(2)
N(2)	23(2)	30(2)	27(2)	-1(2)	5(2)	13(2)
F(23)	76(2)	46(2)	38(2)	-5(1)	23(2)	21(2)
O(4)	26(2)	54(2)	37(2)	4(2)	8(2)	4(2)
F(22)	102(3)	47(2)	41(2)	7(1)	7(2)	38(2)
O(3)	34(2)	38(2)	31(2)	-3(2)	9(2)	9(2)
O(2)	26(2)	47(2)	41(2)	-7(2)	3(2)	11(2)
C(29)	35(3)	26(2)	25(2)	1(2)	8(2)	11(2)
N(6)	28(2)	27(2)	27(2)	0(2)	7(2)	9(2)
C(32)	24(3)	25(2)	30(3)	-1(2)	8(2)	5(2)
C(4)	30(3)	41(3)	24(2)	-4(2)	4(2)	14(2)
N(9)	23(2)	38(2)	27(2)	4(2)	6(2)	12(2)
N(10)	29(2)	34(2)	33(2)	7(2)	13(2)	16(2)
C(11)	22(3)	39(3)	35(3)	2(2)	8(2)	13(2)
N(4)	27(2)	23(2)	28(2)	2(2)	11(2)	8(2)
C(5)	27(3)	37(3)	26(3)	1(2)	6(2)	18(2)
C(39)	24(3)	38(3)	32(3)	10(2)	11(2)	16(2)
C(18)	27(3)	24(2)	28(3)	5(2)	11(2)	6(2)
C(19)	39(3)	31(2)	36(3)	3(2)	21(2)	8(2)
C(41)	35(3)	42(3)	42(3)	16(2)	20(2)	18(2)
C(27)	30(3)	22(2)	28(3)	5(2)	8(2)	8(2)
C(17)	34(3)	21(2)	32(3)	5(2)	15(2)	10(2)
C(38)	25(3)	46(3)	33(3)	14(2)	8(2)	15(2)
C(16)	47(3)	29(2)	31(3)	3(2)	18(2)	15(2)
C(12)	28(3)	29(2)	29(3)	1(2)	4(2)	14(2)
C(6)	23(3)	38(3)	31(3)	2(2)	7(2)	15(2)
C(31)	27(3)	28(2)	35(3)	5(2)	13(2)	9(2)
C(2)	31(3)	37(3)	39(3)	9(2)	8(2)	11(2)
C(26)	36(3)	39(3)	29(3)	11(2)	14(2)	13(2)
C(14)	36(3)	28(2)	32(3)	0(2)	3(2)	9(2)
C(1)	30(3)	31(2)	30(3)	3(2)	8(2)	13(2)
C(35)	27(3)	39(3)	32(3)	7(2)	8(2)	18(2)
C(22)	35(3)	51(3)	44(3)	12(2)	12(3)	20(3)
C(10)	27(3)	32(3)	40(3)	7(2)	12(2)	17(2)
C(13)	26(3)	25(2)	31(3)	-1(2)	4(2)	8(2)
C(33)	24(3)	34(2)	32(3)	0(2)	5(2)	13(2)
C(23)	30(3)	38(3)	36(3)	8(2)	12(2)	17(2)
C(44)	38(3)	38(3)	35(3)	6(2)	14(2)	20(2)
C(30)	33(3)	30(2)	38(3)	6(2)	23(2)	11(2)

C(28)	32(3)	22(2)	26(3)	-1(2)	8(2)	9(2)
C(21)	28(3)	52(3)	69(4)	17(3)	15(3)	22(3)
C(40)	25(3)	39(3)	34(3)	14(2)	14(2)	19(2)
C(3)	38(3)	35(3)	32(3)	-6(2)	4(2)	17(2)
C(7)	39(3)	43(3)	29(3)	0(2)	13(2)	15(2)
C(15)	46(3)	32(2)	23(2)	3(2)	5(2)	14(2)
C(20)	35(3)	35(3)	61(4)	7(2)	29(3)	14(2)
C(43)	36(3)	32(3)	47(3)	6(2)	16(2)	13(2)
C(24)	30(3)	46(3)	40(3)	11(2)	10(2)	19(2)
C(9)	34(3)	42(3)	37(3)	13(2)	19(2)	17(2)
C(36)	30(3)	47(3)	25(3)	1(2)	5(2)	16(2)
C(8)	32(3)	47(3)	33(3)	8(2)	15(2)	19(2)
C(25)	32(3)	51(3)	30(3)	10(2)	0(2)	15(2)
C(34)	23(3)	44(3)	26(3)	3(2)	6(2)	15(2)
C(42)	34(3)	35(3)	55(3)	13(2)	18(3)	14(2)
C(37)	35(3)	56(3)	26(3)	9(2)	6(2)	21(3)
P(1)	48(1)	35(1)	35(1)	6(1)	21(1)	14(1)
F(14)	51(2)	46(2)	74(2)	19(2)	31(2)	20(2)
F(12)	89(3)	56(2)	81(2)	31(2)	54(2)	43(2)
F(16)	60(2)	60(2)	74(2)	25(2)	47(2)	27(2)
F(15)	71(2)	58(2)	41(2)	9(1)	11(2)	-2(2)
F(11)	55(2)	43(2)	53(2)	10(1)	32(2)	10(1)
F(13)	45(2)	71(2)	56(2)	9(2)	2(2)	6(2)
O(1)	30(2)	31(2)	45(2)	3(1)	16(2)	5(2)
N(53)	53(3)	58(3)	47(3)	13(2)	23(2)	25(2)
C(51)	44(3)	47(3)	35(3)	5(2)	16(2)	15(3)
C(52)	33(3)	39(3)	38(3)	7(2)	11(2)	11(2)
N(63)	55(3)	75(3)	43(3)	-4(3)	17(2)	15(3)
C(62)	28(3)	54(3)	38(3)	4(3)	4(2)	-2(3)
C(61)	55(4)	61(4)	62(4)	-18(3)	7(3)	4(3)
O(73)	72(3)	61(2)	68(3)	17(2)	35(2)	17(2)
C(73)	65(5)	63(4)	98(5)	-6(4)	32(4)	19(4)
C(72)	66(5)	83(5)	69(4)	12(4)	24(4)	23(4)

Table 5. Bond lengths [Å] and angles [°] for **$[CuL2]_2^{2+}$ chapter VII.**

Cu(1)-N(2)	1.943(4)	C(38)-C(37)	1.386(6)
Cu(1)-N(7)	2.027(3)	C(16)-C(15)	1.370(7)
Cu(1)-N(1)	2.051(3)	C(12)-C(13)	1.513(6)
Cu(1)-N(3)	2.083(3)	C(6)-C(7)	1.390(6)
Cu(1)-N(6)	2.221(4)	C(31)-C(30)	1.392(6)
Cu(2)-N(9)	1.943(4)	C(2)-C(3)	1.376(6)
Cu(2)-N(4)	2.071(4)	C(2)-C(1)	1.387(6)
Cu(2)-N(10)	2.071(4)	C(26)-C(25)	1.375(7)
Cu(2)-N(8)	2.086(3)	C(14)-C(15)	1.376(7)
Cu(2)-N(5)	2.194(4)	C(14)-C(13)	1.387(6)
P(2)-F(22)	1.593(3)	C(35)-C(36)	1.397(6)
P(2)-F(21)	1.595(3)	C(35)-C(34)	1.506(6)
P(2)-F(25)	1.596(3)	C(22)-C(21)	1.390(7)
P(2)-F(24)	1.598(3)	C(10)-C(9)	1.371(6)
P(2)-F(23)	1.603(3)	C(23)-C(24)	1.389(7)
P(2)-F(26)	1.604(3)	C(44)-C(43)	1.389(6)
N(8)-C(34)	1.381(5)	C(21)-C(20)	1.373(7)
N(8)-C(33)	1.384(6)	C(7)-C(8)	1.383(6)
N(3)-C(12)	1.388(5)	C(43)-C(42)	1.390(7)
N(3)-C(11)	1.389(6)	C(24)-C(25)	1.383(7)
N(1)-C(1)	1.342(5)	C(9)-C(8)	1.390(6)
N(1)-C(5)	1.355(5)	C(36)-C(37)	1.384(7)
N(7)-C(32)	1.349(6)	P(1)-F(13)	1.579(3)
N(7)-C(28)	1.349(6)	P(1)-F(12)	1.579(3)
N(5)-C(22)	1.334(6)	P(1)-F(16)	1.591(3)
N(5)-C(18)	1.359(5)	P(1)-F(14)	1.592(3)
N(2)-C(6)	1.329(5)	P(1)-F(11)	1.607(3)
N(2)-C(10)	1.342(5)	P(1)-F(15)	1.614(3)
O(4)-C(33)	1.225(5)	N(53)-C(52)	1.137(6)
O(3)-C(34)	1.227(5)	C(51)-C(52)	1.466(7)
O(2)-C(12)	1.220(5)	N(63)-C(62)	1.136(6)
C(29)-C(30)	1.361(6)	C(62)-C(61)	1.463(8)
C(29)-C(28)	1.402(6)	O(73)-C(72)	1.443(7)
N(6)-C(23)	1.329(6)	C(73)-C(72)	1.451(8)
N(6)-C(27)	1.357(5)	N(2)-CU1-N(7)	163.17(15)
C(32)-C(31)	1.388(6)	N(2)-CU1-N(1)	79.71(14)
C(32)-C(33)	1.500(6)	N(7)-CU1-N(1)	95.79(13)
C(4)-C(5)	1.372(6)	N(2)-CU1-N(3)	79.83(14)
C(4)-C(3)	1.386(7)	N(7)-CU1-N(3)	103.08(13)
N(9)-C(35)	1.334(5)	N(1)-CU1-N(3)	159.38(14)
N(9)-C(39)	1.343(5)	N(2)-CU1-N(6)	119.42(14)
N(10)-C(44)	1.335(5)	N(7)-CU1-N(6)	77.31(14)
N(10)-C(40)	1.368(6)	N(1)-CU1-N(6)	101.40(13)
C(11)-O(1)	1.220(5)	N(3)-CU1-N(6)	90.91(13)
C(11)-C(10)	1.499(6)	N(9)-CU2-N(4)	158.82(15)
N(4)-C(13)	1.344(6)	N(9)-CU2-N(10)	79.33(14)
N(4)-C(17)	1.370(5)	N(4)-CU2-N(10)	91.51(14)
C(5)-C(6)	1.495(6)	N(9)-CU2-N(8)	79.35(14)
C(39)-C(38)	1.383(6)	N(4)-CU2-N(8)	107.82(13)
C(39)-C(40)	1.472(6)	N(10)-CU2-N(8)	158.57(14)
C(18)-C(19)	1.382(6)	N(9)-CU2-N(5)	123.65(15)
C(18)-C(17)	1.464(6)	N(4)-CU2-N(5)	76.68(14)
C(19)-C(20)	1.371(7)	N(10)-CU2-N(5)	101.24(13)
C(41)-C(42)	1.372(6)	N(8)-CU2-N(5)	92.37(13)
C(41)-C(40)	1.393(6)	F(22)-P(2)-F(21)	90.86(19)
C(27)-C(26)	1.384(6)	F(22)-P(2)-F(25)	90.19(15)
C(27)-C(28)	1.478(6)	F(21)-P(2)-F(25)	89.56(15)
C(17)-C(16)	1.392(6)	F(22)-P(2)-F(24)	178.96(19)

F(21)-P(2)-F(24)	90.14(18)	C(26)-C(27)-C(28)	123.6(4)
F(25)-P(2)-F(24)	89.52(15)	N(4)-C(17)-C(16)	119.9(4)
F(22)-P(2)-F(23)	89.53(17)	N(4)-C(17)-C(18)	116.2(4)
F(21)-P(2)-F(23)	90.73(16)	C(16)-C(17)-C(18)	123.9(4)
F(25)-P(2)-F(23)	179.59(17)	C(39)-C(38)-C(37)	119.0(4)
F(24)-P(2)-F(23)	90.76(16)	C(15)-C(16)-C(17)	120.8(4)
F(22)-P(2)-F(26)	90.10(18)	O(2)-C(12)-N(3)	125.9(4)
F(21)-P(2)-F(26)	179.0(2)	O(2)-C(12)-C(13)	118.4(4)
F(25)-P(2)-F(26)	90.40(14)	N(3)-C(12)-C(13)	115.7(4)
F(24)-P(2)-F(26)	88.91(15)	N(2)-C(6)-C(7)	120.7(4)
F(23)-P(2)-F(26)	89.31(15)	N(2)-C(6)-C(5)	112.9(4)
C(34)-N(8)-C(33)	118.3(3)	C(7)-C(6)-C(5)	126.5(4)
C(34)-N(8)-CU2	114.2(3)	C(32)-C(31)-C(30)	118.1(4)
C(33)-N(8)-CU2	123.3(3)	C(3)-C(2)-C(1)	118.5(4)
C(12)-N(3)-C(11)	116.5(4)	C(25)-C(26)-C(27)	119.1(4)
C(12)-N(3)-CU1	123.4(3)	C(15)-C(14)-C(13)	118.7(5)
C(11)-N(3)-CU1	113.3(3)	N(1)-C(1)-C(2)	122.5(4)
C(1)-N(1)-C(5)	118.1(4)	N(9)-C(35)-C(36)	121.3(4)
C(1)-N(1)-CU1	127.9(3)	N(9)-C(35)-C(34)	114.6(4)
C(5)-N(1)-CU1	114.0(3)	C(36)-C(35)-C(34)	124.1(4)
C(32)-N(7)-C(28)	120.3(4)	N(5)-C(22)-C(21)	122.1(5)
C(32)-N(7)-CU1	121.7(3)	N(2)-C(10)-C(9)	121.6(4)
C(28)-N(7)-CU1	118.0(3)	N(2)-C(10)-C(11)	113.9(4)
C(22)-N(5)-C(18)	118.6(4)	C(9)-C(10)-C(11)	124.4(4)
C(22)-N(5)-CU2	127.0(3)	N(4)-C(13)-C(14)	122.8(4)
C(18)-N(5)-CU2	114.3(3)	N(4)-C(13)-C(12)	118.2(4)
C(6)-N(2)-C(10)	121.0(4)	C(14)-C(13)-C(12)	118.8(4)
C(6)-N(2)-CU1	119.3(3)	O(4)-C(33)-N(8)	126.6(4)
C(10)-N(2)-CU1	119.6(3)	O(4)-C(33)-C(32)	118.5(4)
C(30)-C(29)-C(28)	120.1(4)	N(8)-C(33)-C(32)	114.8(4)
C(23)-N(6)-C(27)	118.6(4)	N(6)-C(23)-C(24)	123.1(4)
C(23)-N(6)-CU1	127.9(3)	N(10)-C(44)-C(43)	122.9(4)
C(27)-N(6)-CU1	111.4(3)	C(29)-C(30)-C(31)	119.9(4)
N(7)-C(32)-C(31)	121.7(4)	N(7)-C(28)-C(29)	119.6(4)
N(7)-C(32)-C(33)	117.9(4)	N(7)-C(28)-C(27)	116.4(4)
C(31)-C(32)-C(33)	120.4(4)	C(29)-C(28)-C(27)	124.0(4)
C(5)-C(4)-C(3)	118.7(4)	C(20)-C(21)-C(22)	119.3(5)
C(35)-N(9)-C(39)	120.9(4)	N(10)-C(40)-C(41)	121.0(4)
C(35)-N(9)-CU2	119.5(3)	N(10)-C(40)-C(39)	114.1(4)
C(39)-N(9)-CU2	119.4(3)	C(41)-C(40)-C(39)	124.8(4)
C(44)-N(10)-C(40)	118.6(4)	C(2)-C(3)-C(4)	119.7(4)
C(44)-N(10)-CU2	127.8(3)	C(8)-C(7)-C(6)	118.6(4)
C(40)-N(10)-CU2	113.5(3)	C(16)-C(15)-C(14)	119.1(4)
O(1)-C(11)-N(3)	126.8(4)	C(19)-C(20)-C(21)	118.7(4)
O(1)-C(11)-C(10)	120.2(4)	C(44)-C(43)-C(42)	118.4(4)
N(3)-C(11)-C(10)	112.8(4)	C(25)-C(24)-C(23)	117.8(5)
C(13)-N(4)-C(17)	118.6(4)	C(10)-C(9)-C(8)	118.0(4)
C(13)-N(4)-CU2	123.3(3)	C(37)-C(36)-C(35)	118.0(4)
C(17)-N(4)-CU2	117.5(3)	C(7)-C(8)-C(9)	120.2(4)
N(1)-C(5)-C(4)	122.4(4)	C(26)-C(25)-C(24)	119.8(4)
N(1)-C(5)-C(6)	113.9(4)	O(3)-C(34)-N(8)	127.8(4)
C(4)-C(5)-C(6)	123.7(4)	O(3)-C(34)-C(35)	120.5(4)
N(9)-C(39)-C(38)	120.7(4)	N(8)-C(34)-C(35)	111.5(4)
N(9)-C(39)-C(40)	113.4(4)	C(41)-C(42)-C(43)	119.4(4)
C(38)-C(39)-C(40)	125.9(4)	C(36)-C(37)-C(38)	120.0(4)
N(5)-C(18)-C(19)	121.1(4)	F(13)-P(1)-F(12)	92.3(2)
N(5)-C(18)-C(17)	115.1(4)	F(13)-P(1)-F(16)	92.36(18)
C(19)-C(18)-C(17)	123.8(4)	F(12)-P(1)-F(16)	91.71(17)
C(20)-C(19)-C(18)	120.1(5)	F(13)-P(1)-F(14)	89.64(18)
C(42)-C(41)-C(40)	119.6(4)	F(12)-P(1)-F(14)	177.7(2)
N(6)-C(27)-C(26)	121.5(4)	F(16)-P(1)-F(14)	89.36(16)
N(6)-C(27)-C(28)	115.0(4)	F(13)-P(1)-F(11)	89.22(17)

F(12)-P(1)-F(11)	88.66(16)	F(14)-P(1)-F(15)	88.04(18)
F(16)-P(1)-F(11)	178.37(19)	F(11)-P(1)-F(15)	88.01(17)
F(14)-P(1)-F(11)	90.21(16)	N(53)-C(52)-C(51)	179.2(6)
F(13)-P(1)-F(15)	176.4(2)	N(63)-C(62)-C(61)	179.1(6)
F(12)-P(1)-F(15)	89.96(19)	O(73)-C(72)-C(73)	110.5(5)
F(16)-P(1)-F(15)	90.40(17)		